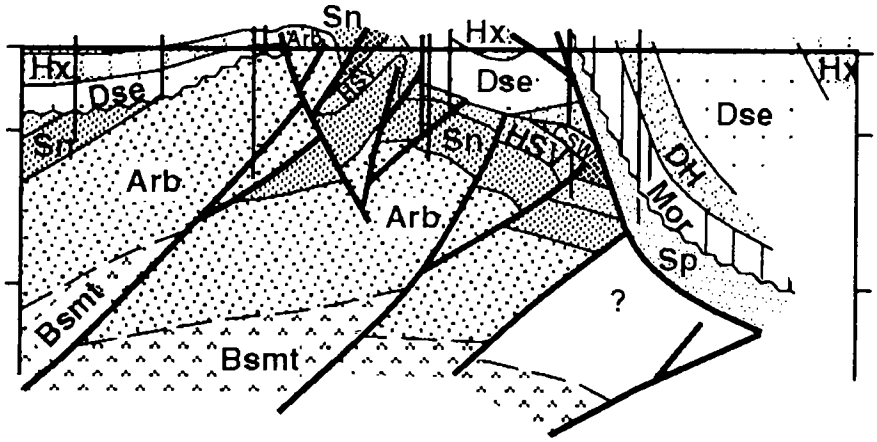
OKLAHOMA GEOLOGICAL SURVEY
Charles J. Mankin, *Director*

CIRCULAR 97

ISSN 0078-4397

STRUCTURAL STYLES IN THE SOUTHERN MIDCONTINENT, 1992 SYMPOSIUM

KENNETH S. JOHNSON
Editor



Proceedings of a symposium held March 31–April 1, 1992, in Norman, Oklahoma.

Co-sponsored by:
Oklahoma Geological Survey
and
Bartlesville Project Office,
U.S. Department of Energy

The University of Oklahoma
Norman
1995

OKLAHOMA GEOLOGICAL SURVEY

CHARLES J. MANKIN, *Director*
KENNETH S. JOHNSON, *Associate Director*

SURVEY STAFF

JAMES H. ANDERSON, *Cartographic Draftsperson II*
BETTY D. BELLIS, *Word-Processing Operator II / Technical Typist*
TOM L. BINGHAM, *Geologist III*
MITZI G. BLACKMON, *Clerk-Typist I*
JOCK A. CAMPBELL, *Petroleum Geologist IV*
BRIAN J. CARDOTT, *Geologist III*
JAMES R. CHAPLIN, *Geologist IV*
JANISE COLEMAN, *Chief Clerk, Publication Sales*
CHRISTIE L. COOPER, *Editor*
TAMMIE K. CREEL, *Secretary II*
CHARLES DYER III, *Drilling Technician*
KIM EDWARDS, *Office Assistant II*
WALTER C. ESRY, *Manager, Core and Sample Library*
ROBERT O. FAY, *Geologist IV*
SAMUEL A. FRIEDMAN, *Senior Coal Geologist IV*
T. WAYNE FURR, *Manager of Cartography*
L. JOY HAMPTON, *Petroleum Geologist III*
PATRONALIA HANLEY, *Chemist*
LEROY A. HEMISH, *Coal Geologist IV*
SHIRLEY A. JACKSON, *Research Specialist I*
PRISCILLA A. JOHNSON, *Office Assistant IV*
RUTH KING, *Research Specialist I*
JAMES E. LAWSON, JR., *Chief Geophysicist*
CHARLOTTE C. LLOYD, *Cartographic Draftsperson II*
KENNETH V. LUZA, *Engineering Geologist IV*
TODD MCCORMICK, *Electronic Technician*
MICHAEL MERCER, *Manager, Log Library*
RICHARD G. MURRAY, *Copy Center Operator*
LINDA NERO, *Senior Receptionist-Clerk*
TRACY PEETERS, *Editorial Assistant*
DAVID O. PENNINGTON, *Operations Assistant*
JUDY A. SCHMIDT, *Office Manager*
CONNIE G. SMITH, *Promotion and Information Specialist*
PAUL E. SMITH, *Supervisor, Offset Press Copy Center*
MICHELLE J. SUMMERS, *Technical Project Coordinator*
NEIL H. SUNESON, *Stratigrapher / Geologist IV*
DANNY L. SWINK, *Drilling Technician*
JANE L. WEBER, *Organic Chemist*
STEPHEN J. WEBER, *Chief Chemist*

Title-Page Illustration

Geologic cross section across the Criner Hills trend in south-central Oklahoma (from p. 150 of this volume).

♻ *printed on recycled paper*

This publication, printed by the Oklahoma Geological Survey, is issued by the Oklahoma Geological Survey as authorized by Title 70, Oklahoma Statutes, 1981, Sections 231–238. 1,050 copies have been prepared for distribution at a cost of $8,040 to the taxpayers of the State of Oklahoma. Copies have been deposited with the Publications Clearinghouse of the Oklahoma Department of Libraries.

PREFACE

The transfer of technical information will aid in the search for, and production of, our oil and gas resources. To facilitate this technology transfer, the Oklahoma Geological Survey (OGS) and the Bartlesville Project Office of the U.S. Department of Energy (BPO-DOE) co-sponsored a symposium dealing with structural geology, petroleum geology, and reservoir characterization in the southern Midcontinent. The symposium was held on March 31–April 1, 1992, at the Oklahoma Center for Continuing Education, The University of Oklahoma, Norman. This volume contains the proceedings of that symposium.

Research reported upon at the symposium focused on structural geology, tectonic evolution, petroleum reservoirs in various structural settings, development of oil and gas resources, geophysics, and neotectonics. In describing the various structural styles and related petroleum reservoirs in the southern Midcontinent, the researchers have increased our understanding of how the tectonic history of an area can affect reservoir heterogeneity and our ability to efficiently recover the hydrocarbons they contain. We hope that the symposium and these proceedings will bring such research to the attention of the geoscience and energy-research community, and will help foster exchange of information and increased research interest among industry, university, and government workers.

Twenty papers were presented orally at the symposium, and they are presented here as full papers or abstracts. An additional 15 reports were given as posters, and they are presented here as short reports or abstracts. About 260 persons attended the symposium. Stratigraphic nomenclature and age determinations used by the various authors in this volume do not necessarily agree with those of the OGS.

This is the fifth symposium in as many years dealing with topics of major interest to geologists and others involved in petroleum-resource development in Oklahoma and adjacent states. These symposia are intended to foster the exchange of information that will improve our ability to find and recover our nation's oil and gas resources. Earlier symposia subjects were: the Anadarko basin (published as OGS Circular 90); Late Cambrian–Ordovician geology of the southern Midcontinent (OGS Circular 92); Source rocks in the southern Midcontinent (OGS Circular 93); and Petroleum-reservoir geology in the southern Midcontinent (OGS Circular 95).

Persons involved in the organization and planning of the structural-styles symposium include: Kenneth Johnson, Jock Campbell, and Charles Mankin of the OGS; Tom Wesson, Michael Ray, and Bob Lemmon of BPO-DOE; and David Stearns of the School of Geology and Geophysics at The University of Oklahoma. Other personnel who contributed include: Michelle Summers and Tammie Creel, Registration Co-Chairs; Brian Cardott, Poster Session Chair; Connie Smith, Publicity Chair; and Gwen Williamson and Judy Schmidt, Exhibits Coordinators. Appreciation is expressed to each of them and to the many authors who worked toward a highly successful symposium.

KENNETH S. JOHNSON
General Chairman

CONTENTS

iii **Preface**

PART I — Papers Presented Orally at the Symposium

3 **The Paradox Transcontinental Fault Zone**
William A. Thomas and D. L. Baars

13 **Basement Influence on the Structural Geology of Southern Oklahoma Inferred from Residual Aeromagnetic Maps**
Thomas L. Thompson, Bronson W. Hawley, James R. Howe, and S. Parker Gay

15 **Structural Styles in the Ouachita Mountains and Southern Arkoma Basin, Arkansas**
Boyd R. Haley and Charles G. Stone

16 **Origin of Disharmonic Folding, Central Ouachita Mountains, Oklahoma**
George W. Viele

26 **Interpretation of Structure from Surface Geology, Frontal Ouachitas, Southeastern Oklahoma**
Colin Mazengarb

32 **The Dyer Mountain Fault Zone: Southerly Directed Thrusting in the Broken Bow Uplift**
Kent C. Nielsen and Qingming Yang

45 **Tectonic and Stratigraphic Synthesis of Events in the Region of the Intersection of the Arbuckle and Ouachita Structural Systems, Oklahoma**
William McBee, Jr.

82 **Seismic Investigation of the Ouachita Trend from Western Arkansas to North Texas**
Richard E. Schneider

83 **Ablative Subduction and Its Structural Effects Upon the Midcontinent During the Pennsylvanian**
Raymon L. Brown

99 **Regional Sedimentation Patterns Associated with the Passive- to Active-Margin Transition, Ouachita Orogeny, Southern Midcontinent, U.S.A.**
Paula J. Noble

113 **Inversion Model for the Structural Style of the Arbuckle Region**
Bryan Tapp

119 **Significance of Air-Photograph Linears in the Basement Rocks of the Arbuckle Mountains**
Rodger E. Denison

132 **The Collings Ranch Conglomerate of the Oklahoma Arbuckles: Its Origin and Tectonic Significance**
Kevin Pybas, Ibrahim Cemen, and Zuhair Al-Shaieb

144 **Geological Evolution of the Criner Hills Trend, Ardmore Basin, Oklahoma**
J. Calvin Cooper

161 **Thermal Evolution of the Harper Field, Central Basin Platform, Ector County, Texas**
Jack G. Elam

174 **Connections Between Laramide Foreland Arches**
Eric A. Erslev and Philipp Molzer

178 **The Slick Hills of Oklahoma and Their Regional Tectonic Setting**
R. Nowell Donovan

187 **Structural Framework of the Meers Fault and Slick Hills Area, Southwestern Oklahoma, Based on Magnetic Data**
Meridee Jones-Cecil, R. Nowell Donovan, and Lee-Ann Bradley

208 **Structural Development of the Nemaha Tectonic Zone in Kansas**
Pieter Berendsen and Kevin P. Blair

215 **Neotectonic Relations of the Nemaha Uplift in Oklahoma**
Kenneth V. Luza

PART II — Abstracts and Short Reports Related to Poster Presentations

233 **Structural Analysis of the Potato Hills, Ouachita Mountains, Oklahoma**
Mark W. Allen

236 **Reconnaissance Study of Womble Formation, Broken Bow Uplift**
Steve Erickson and Bryan Tapp

240 **Structural and Stratigraphic Framework of the Wapanucka Formation (Pennsylvanian), Southeastern Oklahoma**
Victoria L. French and Robert C. Grayson, Jr.

244 **Relationships of Southern Midcontinent Structures to a Postulated Late Precambrian Transcontinental Fault**
Gary L. Kinsland

249 **Wapanucka Formation (Morrowan): Facies and Fractures, Frontal Ouachita Mountains**
Darrell L. Mauldin and Robert C. Grayson, Jr.

259 **Structural Interpretations of the Arkoma Basin–Ouachita Mountains Transition Zone, Southeastern Oklahoma: A Review**
Neil H. Suneson

264 **Evidence for Recurrent Left-Lateral Deformation from the Vicinity of the Depew Field, Creek County, Oklahoma**
Dorothy L. Swindler

265 **Stratigraphy and Structural Styles of the Lower Stanley Tuffs: Northwest Flank of the Broken Bow Uplift, McCurtain County, Oklahoma**
Charles A. O. Titus and Thomas E. Legg

277 **Surface to Subsurface Study of the Northwest Plunge of the Arbuckle Anticline**
Christopher P. Saxon

280 **Significance of Fault Dip to Angle of Bedding in Determination of Structural Styles: Examples from Southern Oklahoma**
Christopher P. Saxon

283 **Structural Control of the Reagan and Mill Creek Faults on the Sedimentary Environments of the Deese Conglomerate, Arbuckle Mountains, Southern Oklahoma**
Craig Stafford, Ibrahim Cemen, and Zuhair Al-Shaieb

288 **Surface Structures in Permian Strata of Southwestern Oklahoma as Indicators of Deep-Seated Structures**
Kenneth S. Johnson

293 **Imaging of Basement-Block Configuration in the Wichita Mountain Frontal Zone**
Roger A. Young

297 **Structure, Timing, and Tectonic Interpretation of Ancestral Rocky Mountain Deformation within Central New Mexico**
William C. Beck and Charles E. Chapin

PART I

PAPERS PRESENTED ORALLY AT THE SYMPOSIUM

The Paradox Transcontinental Fault Zone

William A. Thomas
University of Kentucky
Lexington, Kentucky

D. L. Baars
Kansas Geological Survey
Lawrence, Kansas

ABSTRACT.—An alignment of well-documented basement-fault systems, herein named the Paradox transcontinental fault zone, extends northwestward across the North American continent, from the Bahamas fracture zone of the western Atlantic Ocean to Vancouver Island on the Pacific margin, and perhaps beyond. The Paradox transcontinental fault zone includes continuous, mappable fault systems (for example, faults of the Ancestral Rockies, the Southern Oklahoma fault system, and the Alabama-Arkansas fault system); it also includes laterally discontinuous faults, displacement transfer zones, and cross faults. Deep sedimentary basins (for example, the Paradox, Anadarko, and Oquirrh basins) are distributed along the Paradox transcontinental fault zone. Part of the Paradox transcontinental fault zone defines the margin of continental crust (the Alabama-Oklahoma transform fault along the late Precambrian–Cambrian continental margin of North America). The Black Warrior and Arkoma orogenic foreland basins reflect thrust loading (late Paleozoic Ouachita thrust belt) of the continental margin along the Paradox transcontinental fault zone.

Different elements of the Paradox transcontinental fault zone were active at different times, mainly during the (1) Precambrian before ~1 Ga (billion years), (2) late Precambrian–Cambrian, (3) late Paleozoic, and (4) early Mesozoic. The range of ages of activity is so great that some rocks involved in the later stages of movement at both ends of the system either had not been accreted to North America or had not been formed when the central older elements of the system were initiated and reactivated. The Paradox transcontinental fault zone propagated upward into younger rocks and extended lengthwise through geologic time.

INTRODUCTION

An alignment of basement-fault systems extends northwestward across the North American continent, from the Bahamas fracture zone of the western Atlantic Ocean to Vancouver Island on the Pacific margin, and perhaps beyond (Fig. 1). Northwest-striking systems of basement faults have been mapped in Florida, from Alabama to southern Arkansas, across Oklahoma and the Panhandle of Texas, in northern New Mexico, and across southwestern Colorado and eastern Utah. The alignment extends along an exceptionally deep sedimentary basin in north-central Utah and through northwest-striking faults in Cenozoic volcanic rocks in southwestern Idaho. Northwestward from Idaho, the regional alignment continues as the Olympic-Wallowa lineament (Wise, 1963) and possibly from Vancouver Island to the Kodiak seamount chain. We propose the name "Paradox transcontinental fault zone" for this transcontinental fracture zone of crustal scale.

The northwest-trending alignment of fault systems includes numerous individual faults. Different elements along the Paradox transcontinental fault zone were active at different times, mainly during the (1) Precambrian before ~1 Ga (billion years), (2) late Precambrian–Cambrian, (3) late Paleozoic, and (4) early Mesozoic (Fig. 2). Parts of the alignment are well-known, continuous, mappable faults; but other parts include laterally discontinuous faults, displacement transfer zones, and cross faults that together constitute a more-or-less continuous zone of distinct fault systems. The long, northwest-trend-

Thomas, W. A.; and Baars, D. L., 1995, The Paradox transcontinental fault zone, *in* Johnson, K. S. (ed.), Structural styles in the southern Midcontinent, 1992 symposium: Oklahoma Geological Survey Circular 97, p. 3–12.

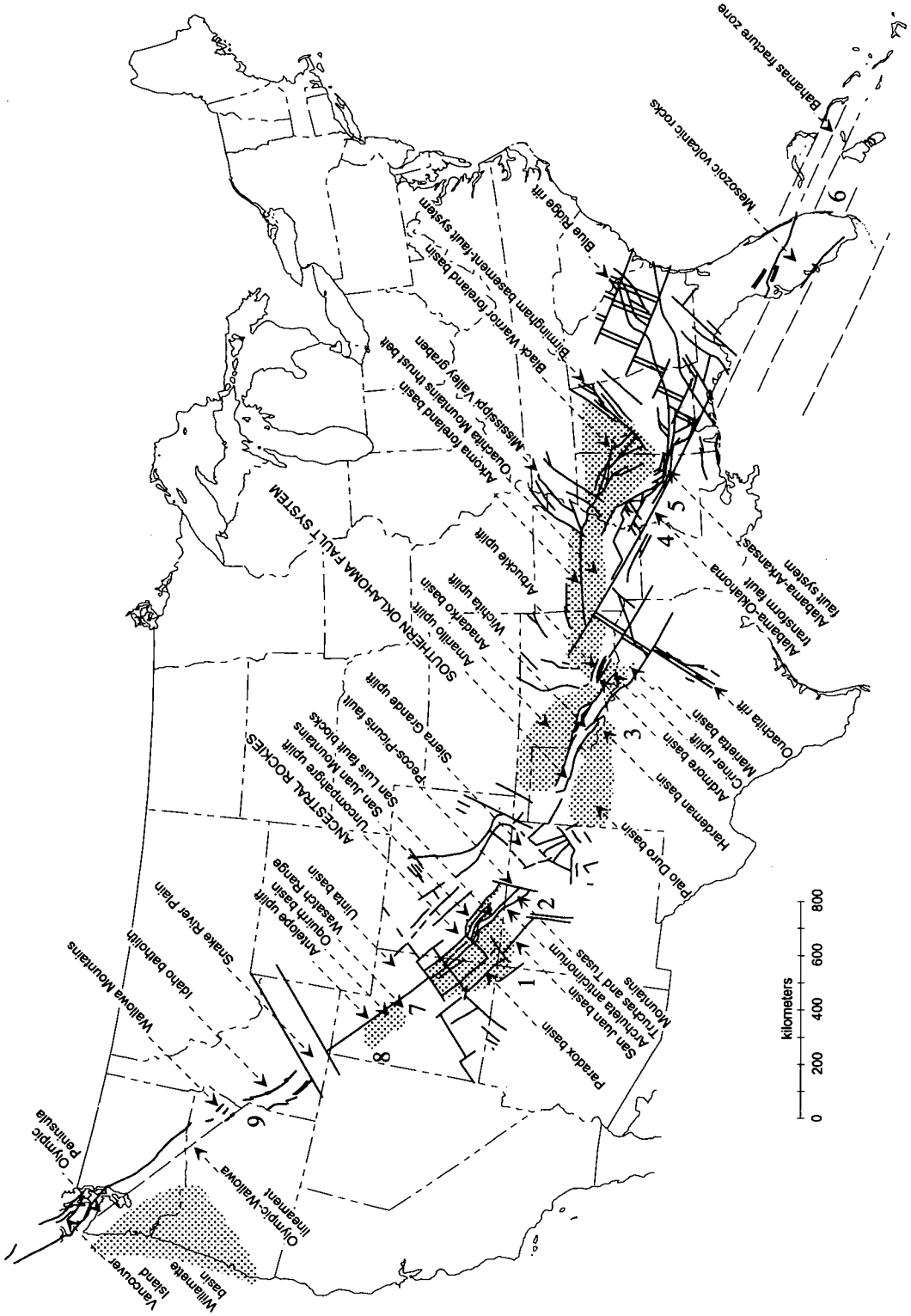


Figure 1. Map of the Paradox transcontinental fault zone (compiled from references cited in text). Large numerals designate regions discussed in text. Deep sedimentary basins are shown by stipple pattern.

ing alignment of fault systems is intersected and offset locally by sets of northeast-striking faults. Displacement varies along the fault systems, and sense of slip varied through time.

In addition to the characteristic basement faults, deep sedimentary basins of several different types are scattered along the Paradox transcontinental fault zone. Basement faults with large vertical separation bound some deep intracratonic basins; erosion of intracratonic uplifts supplied large volumes of sediment to the yoked basins. Parts of the Paradox transcontinental fault zone constitute segments of rifted continental margins, especially transform-fault margins; and synrift sedimentary accumulations fill rift-related grabens. Where an older continental margin has been overridden by a thin-skinned thrust belt, flexural subsidence of the crust in response to the thrust load has produced a foreland basin that is filled with synorogenic deposits. Some basement-fault movement accompanied thrusting.

DISCUSSION OF DATA

The history of fault movement, as well as sense of slip, is documented with variable precision at different places along the Paradox transcontinental fault zone. The following sections summarize the available data for each of the distinctive segments of the transcontinental fault zone. In this discussion, each segment is identified by a number that is keyed to a location on Figure 1.

1. Outcrops in the San Juan Mountains: Uncompahgre Uplift and Paradox Basin

Excellent outcrops in the San Juan Mountains in southwestern Colorado and abundant drill data from the Paradox basin provide detailed resolution of movement history of the basement faults that bound the southwest side of the well-known Uncompahgre uplift of the Ancestral Rocky Mountains and the adjacent Paradox basin (Fig. 1). Several faults are exposed, and the high relief of the San Juan Mountains permits the preparation of thoroughly constrained cross sections that illustrate stratigraphy and structure. Several episodes of fault movement are documented. We selected the name "Paradox" for the transcontinental fault zone because (1) well-exposed, mappable faults displace basement rocks and bound the northeastern side of the Paradox basin; (2) an episodic movement history, characteristic of the entire Paradox transcontinental fault zone, is well documented here; and (3) the oldest known movement along the Paradox transcontinental fault zone is recorded here.

The oldest documented episode of fault movement was during Early to Middle Proterozoic time. Metamorphic basement rocks of the Twilight Gneiss (1.75 ± 0.01 Ga), as well as the Whitehead Granite (1.69 ± 0.01 Ga), are juxtaposed against the "younger Precambrian" Uncompahgre Formation of quartzites and metapelites (Barker, 1969; Barker and others, 1969; Bickford and others, 1969; ages recalculated by Harris and others, 1987). The contacts are interpreted to be contact-parallel shears associated with cuspate infolding of cover strata (Uncompahgre) into basement (Harris and others, 1987; Gibson, 1990) or, alternatively, to be thrust faults (Tewksbury, 1985). The Precambrian metasedimentary rocks and the bounding faults are intruded by the Eolus Granite (1.43 ± 0.02 Ga), thereby constraining the time of fault movement between ~1.69 and ~1.43 Ga (Fig. 2A).

The bounding faults between gneiss and metasedimentary rocks, as well as faults within the metasedimentary sequence, were reactivated episodically from Cambrian (Fig. 2B) to Mississippian time. Vertical separation along the faults is indicated by thickness and clast-size distribution in Upper Cambrian sandstone and quartzite-clast conglomerate, which onlap against some of the fault scarps and locally overstep some of the faults (Baars, 1966; Baars and See, 1968; Block, 1986). Although the paleorelief on the sub-Cambrian surface might be interpreted simply as paleotopography expressed on dormant fault blocks, distribution of thickness and sediment-dispersal patterns in the sandstone and conglomerate favor synsedimentary fault reactivation and tilting of some fault blocks. Similarly, thickness and facies distributions, as well as onlap and overstep patterns, in Upper Devonian and Lower Mississippian strata indicate synsedimentary reactivation of the same faults. Stratigraphic variations suggest small-magnitude fault movements during the Cambrian through Early Mississippian, and the sense of vertical separation generally represents an inversion of Precambrian movement.

Although basement faults across the San Juan Mountains had moved earlier, the most spectacular movements occurred during the Ancestral Rockies phase of deformation during Pennsylvanian and Permian time (Fig. 2C). Pennsylvanian-Permian strata >4,500 m thick fill the eastern part of the Paradox basin; sediment-dispersal patterns indicate transport of clastic detritus from the Uncompahgre uplift (Fig. 1) (Baars, 1962; Baars and Stevenson, 1982). The oldest clastic deposits associated with rapid rise of the Uncompahgre uplift were derived from the San Luis fault blocks and are of Atokan age (Baars and Stevenson, 1982,1984). Coarse detritus continued to be supplied to the basin into Early Permian time. Synsedimentary movement of some of the faults during Pennsylvanian-Permian time is indicated by local angular unconformities and locally derived clastic detritus (Baars and See, 1968). Some faults displace the youngest preserved Permian strata. Most of the vertical displacement along the Uncompahgre-Paradox segment of the Paradox transcontinental fault zone is associated with the

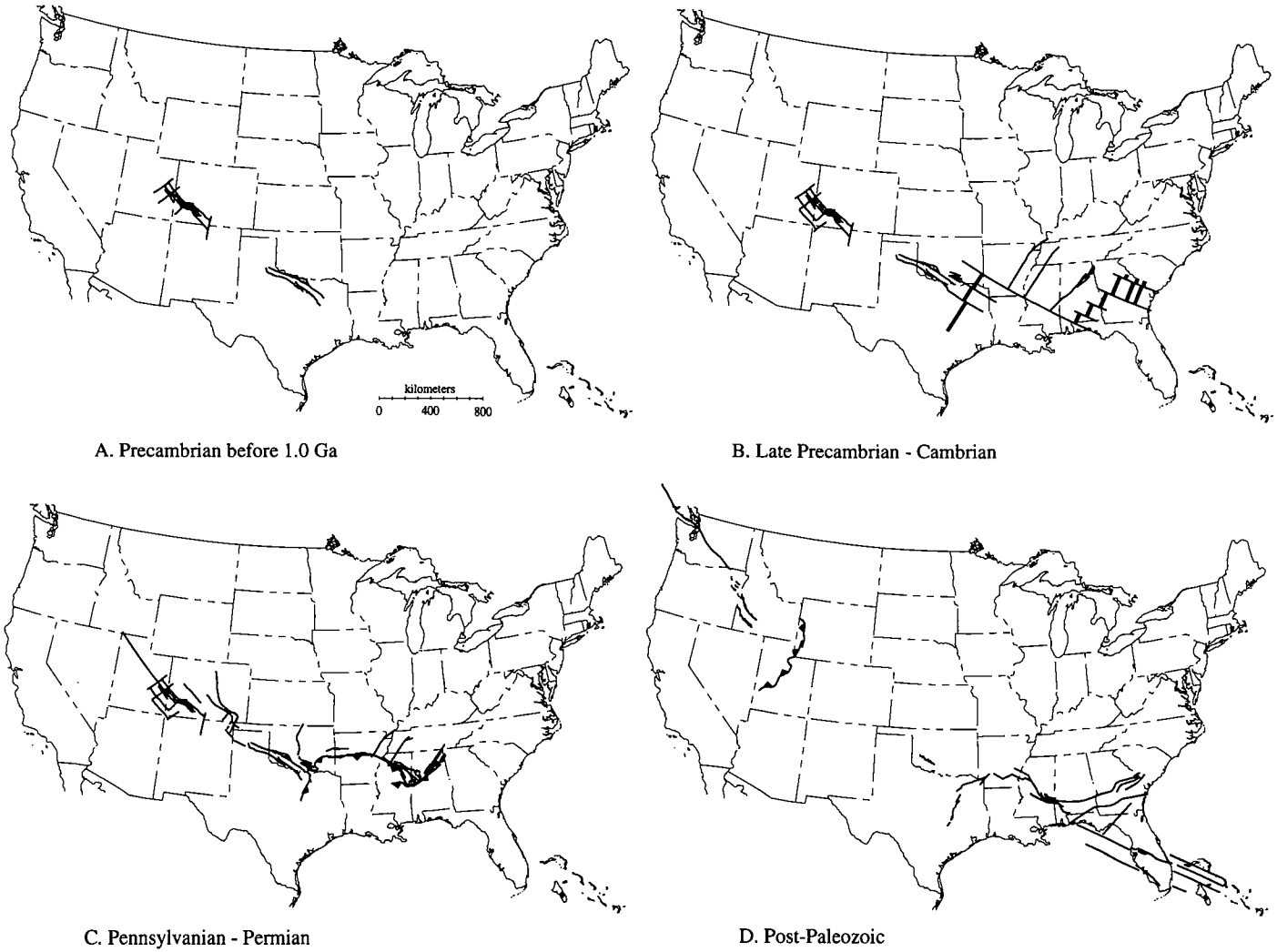


Figure 2. Sequence of maps showing successive elements of the Paradox transcontinental fault zone, organized according to times of fault movement. *A*—Precambrian before 1.0 Ga. *B*—Late Precambrian–Cambrian. *C*—Pennsylvanian-Permian (Ouachita-Appalachian thrust belt shown by barbed line.) *D*—Post-Paleozoic (Cordilleran thrust belt shown by barbed line).

Ancestral Rockies phase of deformation, but possible reactivation of that segment during Laramide deformation (Late Cretaceous and early Tertiary) cannot be eliminated from consideration.

2. Southeastward from the San Juan Mountains

Fault blocks extend from the San Juan Mountains southeastward beneath the northeastern bounding monocline of the Mesozoic San Juan basin and the Archuleta anticlinorium in north-central New Mexico (Fig. 1) (Baars and Stevenson, 1984). Northwest-striking faults in late Precambrian metasedimentary rocks of the Truchas and Tusas Mountains in New Mexico are interpreted as extensions of the Uncompahgre boundary-fault system. Continuity of the northwesterly structural alignment is disrupted by the north-striking Pecos-Picuris fault system of north-central New Mexico and the northeasterly-striking Sierra Grande uplift. Farther east, faults of the Amarillo uplift in the Panhandle of Texas strike northwest (Fig. 1). Numerous northwest-striking diabase dikes (~570 to 495 Ma [million years]) are scattered from Colorado to Oklahoma (Larson and others, 1985; Denison, 1989), suggesting regional-scale continuity of the northwest-striking fracture system.

3. Southern Oklahoma Fault System

The Southern Oklahoma fault system bounds the late Paleozoic Arbuckle, Wichita, Amarillo, and Criner basement uplifts and the Anadarko, Ardmore, Marietta, Hardeman, and Palo Duro basins (Fig. 1). Some of the basement faults have vertical separation of >12 km and probably have larger strike-slip separation (review by Perry, 1989; McConnell, 1989). Rock associations along the fault system indicate at least three episodes of large-scale fault movement and some Holocene reactivation.

The oldest Precambrian crystalline basement rocks in the region are dated at 1.2 to 1.4 Ga (Bickford and Lewis, 1979; Denison, *in* Johnson and others, 1988). The Tillman Metasedimentary Group, which has been penetrated in wells south and southwest of the Wichita uplift, is as old as 1.0 to 1.2 Ga (Muehlberger and others, 1967; Denison and others, 1984; Coffman and others, 1986). COCORP seismic-reflection profiles show a thick succession (7–10 km) of layered reflectors that represent the Tillman metasedimentary rocks south of the Wichita uplift, but the layered reflectors are absent to the north (Brewer and others, 1981,1983). The abrupt northward termination of the Tillman reflectors suggests a Precambrian fault, the oldest dated episode of movement along the Southern Oklahoma fault system (Fig. 2A).

An alignment of Cambrian igneous rocks along the Southern Oklahoma fault system records a second phase of fault movement (Fig. 2B), a phase that was associated with rifting of the southeastern margin of North America and opening of the Iapetus Ocean (Thomas, 1991). Cambrian igneous rocks include a layered gabbro complex, gabbro plutons, basalt-spilite, granite, and rhyolite; the lithologic association suggests a continental-rift environment (Ham and others, 1964; Gilbert, 1983a). Crystallization ages of the gabbros range from 577 Ma (Rb-Sr and Sm-Nd) to 552 ± 7 Ma (U-Pb zircon) (Bowring and Hoppe, 1982; Lambert and Unruh, 1986). The granite and rhyolite are interpreted to be 525 ± 25 Ma (Rb-Sr) (Ham and others, 1964) and are intruded by diabase dikes. Fault displacements indicate vertical separation of ~1 km along a zone ~65 km wide (Ham and others, 1964; Coffman and others, 1986; McConnell and Gilbert, 1986). Regionally, Precambrian crystalline basement and the Cambrian igneous rocks are overlain nonconformably by a transgressive Upper Cambrian sandstone (Ham and others, 1964; Gilbert, 1983a; Coffman and others, 1986). The age of fault movement is bracketed between the oldest gabbros (577 Ma) and the Late Cambrian transgression.

Upper Cambrian and Lower Ordovician carbonate rocks thicken regionally into an elongate basin, the axis of which coincides with the alignment of Cambrian igneous rocks (Johnson and others, 1988; Perry, 1989). Middle Paleozoic rocks also reflect differential subsidence of the elongate basin, but the rate of subsidence decreased after Middle Ordovician (Johnson and others, 1988). Subsidence evidently was a result of loading by the dense mafic igneous rocks at a shallow crustal level.

Thick accumulations of coarse clastic sediments indicate late Paleozoic fault movement along the Southern Oklahoma fault system (Fig. 2C), which bounds the Amarillo, Wichita, Arbuckle, and Criner uplifts (Fig. 1) (extensive literature reviewed by Johnson and others, 1988; Perry, 1989). Progradation of locally derived clastic sediments began as early as Late Mississippian, but most of the structural relief was produced in the Late Pennsylvanian (Johnson and others, 1988). Thick accumulations of Pennsylvanian clastic rocks characterize the Anadarko, Ardmore, Marietta, Hardeman, and Palo Duro basins. The late Paleozoic episode of movement along the Southern Oklahoma fault system was associated with compression during the Ouachita orogeny, but reactivation of basement faults extended far into the craton from the Ouachita thrust front (Fig. 2C) (Hoffman and others, 1974; Kluth and Coney, 1981; Kluth, 1986).

Late Holocene movement along some faults of the Southern Oklahoma system has been documented recently (Fig. 2D) (Gilbert, 1983b; Ramelli and Slemmons, 1990; Slemmons, 1991). The potential seismicity along faults that bound the deepest intracratonic basin (Anadarko basin) within the North American craton further attests to the long-term and large-scale nature of this system of basement faults.

4. Alabama-Oklahoma Transform Fault and the Late Precambrian–Cambrian Rifted Margin of North American Crust

The northwest-striking Alabama-Oklahoma transform fault (Fig. 1) defines part of the Cambrian rifted margin of southeastern North America (Fig. 2B) (Thomas, 1991). Recognition of the nature and location of the transform margin of continental crust is based on the trace and composition of the late Paleozoic Ouachita thrust belt, on the distribution of early and middle Paleozoic passive-margin carbonate-shelf facies, and on geophysical data. The southern margin of continental crust is documented beneath southward-dipping thrust sheets of the southern part of the Ouachita Mountains in Arkansas by a velocity model derived from PASSCAL wide-angle reflection and refraction seismic data (Keller and others, 1989). That location is consistent with COCORP seismic-reflection data and with gravity models (Nelson and others, 1982; Lillie and others, 1983; Mickus and Keller, 1992). Continental crust thins abruptly southward within ~25 km to thin transitional crust or oceanic crust. The narrow zone of transition from continental crust to oceanic crust is typical of a transform margin (Keen, 1982; Scrutton, 1982; Keen and Haworth, 1985), and it contrasts with the broad zone of attenuated continental crust that characterizes an extensional rifted margin.

A boundary between regions of contrasting magnetic signatures (Zietz, 1982; Hinze and Braile, 1988) extends northwest and southeast from the seismically defined edge of continental crust beneath the southern Ouachita thrust belt to intersections with northeast-striking rift segments of the continental margin on the northwest in Oklahoma (Ouachita rift) and on the southeast in Alabama (Blue Ridge rift) (Fig. 1) (Thomas, 1991). The Alabama-Oklahoma transform fault is parallel to, but not aligned with, the Southern Oklahoma fault system; the alignment is offset at the northeast-striking Ouachita rift in southeastern Oklahoma. In addition to intersections with northeast-striking rift segments of the continental margin, the transform fault also intersects two northeast-striking intracratonic fault systems, the Mississippi Valley graben and the Birmingham basement-fault system (Fig. 1). In the context of diachronous rifting of the southeastern margin of North America, the Alabama-Oklahoma transform fault reflects a shift in the spreading center from the Blue Ridge rift to the Ouachita rift at about the beginning of the Cambrian Period (Thomas, 1991). A passive margin evolved along the transform fault during Late Cambrian time and persisted until Mississippian time, as indicated by an extensive passive-margin carbonate-shelf facies (Thomas, 1988a).

During the late Paleozoic Ouachita orogeny, off-shelf facies were thrust over the old shelf edge as a result of arc-continent collision at a south-dipping subduction zone (Viele and Thomas, 1989). The Black Warrior and Arkoma foreland basins (Fig. 1) formed on continental crust adjacent to the older Alabama-Oklahoma transform fault as a result of flexural subsidence in response to the Ouachita thrust load on the edge of North American continental crust (Fig. 2C), and the foreland basins were filled with Mississippian (Meramecian) to Middle Pennsylvanian synorogenic clastic-wedge deposits. A northwest- to west-striking system of down-to-southwest to down-to-south basement faults parallels the Ouachita thrust front along both the Black Warrior and Arkoma foreland basins (Houseknecht, 1986; Thomas, 1988a), and synsedimentary movement of the basement faults occurred during flexural subsidence and sedimentary filling of the foreland basins. The northwest- to west-striking fault system is approximately parallel to the Alabama-Oklahoma transform fault, and some of the faults possibly had a Cambrian phase of movement in association with the active Alabama-Oklahoma transform. Available data are not adequate to define the possible early history of these faults.

5. Alabama-Arkansas Fault System and the Mesozoic Rifted Margin of North American Crust

The early Mesozoic Alabama-Arkansas fault system (Thomas, 1988b) coincides spatially with part of the Cambrian Alabama-Oklahoma transform fault and extends farther to the southeast into the Gulf of Mexico (Figs. 1,2D). From Arkansas to southern Alabama, the Mesozoic fault system is overprinted on the late Precambrian–Cambrian Alabama-Oklahoma transform fault along the margin of Precambrian continental crust. The Mesozoic fault system extends southeastward beyond the rifted margin of North American Precambrian continental crust in southern Alabama (Fig. 1); to the southeast in Florida, the Mesozoic faults extend into a terrane that was accreted onto the margin of North America during the late Paleozoic Alleghanian orogeny along the Appalachian orogenic belt (Thomas and others, 1989). The northwest-striking Mesozoic fault system is dominated by down-to-southwest faults and some cross faults that bound rhombic grabens. Synsedimentary fault-bounded basins are filled with thick accumulations of clastic sedimentary rocks of Late Triassic and Jurassic age; the Jurassic succession includes evaporites.

Volcanic rocks in western Mississippi (Thomas, 1988b) and in southern Alabama (Guthrie and Raymond, 1992) are clustered along the fault system. The faults, in part, define the limits of the Jurassic Louann Salt, and salt structures protrude upward into post-Jurassic strata above buried basement faults. Like older elements of the Paradox transcontinental fault zone, the Mesozoic Alabama-Arkansas fault system is intersected by northeast-striking

faults (Fig. 1). The Alabama-Arkansas fault system is approximately parallel to the margin of North American continental crust to the south in the Gulf of Mexico and is interpreted to be part of parallel systems of faults associated with opening of the Gulf of Mexico and Atlantic Ocean (Klitgord and others, 1984).

6. South Florida and the Bahamas Fracture Zone

A wide northwest-trending band of Mesozoic volcanic rocks extends in the subsurface across southern Florida (Fig. 1) (Chowns and Williams, 1983; Klitgord and others, 1983; Mueller and Porch, 1983; Thomas and others, 1989). The band of volcanic rocks is aligned with the Bahamas fracture zone of the western Atlantic Ocean, and a continuous trace from Florida across the northeastern Gulf of Mexico to connect with the Alabama-Arkansas fault system is interpreted from gravity and aeromagnetic map patterns (Klitgord and others, 1984). Alignment of the Alabama-Arkansas fault system with Mesozoic volcanic rocks in Florida and, farther southeast, with the Bahamas fracture zone suggests a system of transform and continental transfer faults associated with early Mesozoic opening of the Atlantic Ocean and Gulf of Mexico (Thomas, 1988b). Coincidence of the Mesozoic transform-transfer system with the transform offset of the late Precambrian–Cambrian margin of North America indicates an inherited tectonic control on the shape of the Mesozoic continental margin, even though the Mesozoic faults on the southeast are in rocks that were not part of North America during the Precambrian-Cambrian rifting event (Fig. 2).

7. Northwesterly Extension of the Uncompahgre Uplift

From the San Juan Mountains in southwestern Colorado, where timing and displacement of episodic fault movements are well documented, basement faults extend northwestward, forming the boundary between the Uncompahgre uplift and Paradox basin (Fig. 1). Deep drilling and seismic surveys show clearly that the late Paleozoic Uncompahgre uplift continues northwestward and separates the post-Paleozoic Uinta basin from the northern end of the Paradox basin (Woodward, 1988). The northwest-trending structural alignment extends as far as the Wasatch Range in north-central Utah, where the basement structures pass beneath the Cordilleran thrust front (Fig. 1).

8. Oquirrh Basin

Although not closely constrained by deep drilling and geophysical studies, the Oquirrh basin and associated Antelope uplift are positioned along the northwestward projection of the system of northwest-striking basement faults between the Paradox basin and Uncompahgre uplift (Fig. 1) (Bissell, 1962; Welsh, 1976; Stokes, 1979). In latest Devonian to Mississippian time, the Oquirrh basin became a separate basin on the Cordilleran shelf east (cratonward) of a foreland basin associated with the Antler orogenic belt (Sloss, 1988). A sedimentary fill of 7,900 m of Pennsylvanian-Permian strata characterizes this as a rapidly subsiding basin, contemporaneous with large-scale movement along faults in the Ancestral Rockies (Fig. 2C). Finer grain size and substantial carbonate components in the Oquirrh basin contrast with the coarse proximal fill of the Paradox basin. The Oquirrh basin is now part of the younger Cordilleran thrust belt and has been translated some distance eastward; however, unless substantial rotation occurred during thrusting, a palinspastic restoration would maintain the northwesterly orientation.

9. Northwest of the Oquirrh Basin, the Snake River Plain, and the Olympic-Wallowa Lineament

A northwest-trending magnetic anomaly (Zietz, 1982) extends from the Oquirrh basin to the southeastern side of the Snake River Plain in southern Idaho, suggesting a northwest-striking basement structure (Fig. 1). The northeast-trending arm of the Snake River Plain and an accompanying northeast-trending magnetic anomaly define a northeast-striking structure that intersects the Paradox transcontinental fault zone in southern Idaho. Farther northwest, northwesterly structural continuity is reflected in mapped faults in Cenozoic volcanic rocks across the western part of the Snake River Plain (Fig. 1) (King and Beikman, 1974).

The Olympic-Wallowa lineament extends from the western part of the Snake River Plain (southwest of the Idaho batholith), through the Wallowa Mountains, and northwestward to the Olympic Peninsula (Wise, 1963). The Olympic-Wallowa lineament is interpreted to represent a basement structure, and it is reflected in a variety of tectonic offsets, discontinuities, and terminations (Wise, 1963). Several northwest-striking faults are mapped across the Columbia Plateau (King, 1969; King and Beikman, 1974). The trace of the lineament is spectacularly displayed by a computer-processed shaded-relief image (Thelin and Pike, 1991). Although Precambrian and Paleozoic rocks are not exposed along the lineament from Idaho through Washington, the trace separates exposures of late Precambrian (Belt) and Paleozoic rocks in eastern Washington and northern Idaho from younger rocks to the southwest. The lineament marks the northern limit of a very thick accumulation of Eocene volcanic and sedimentary rocks in western Washington (Cook and Bally, 1975).

The rocks of Vancouver Island are cut by northwest-striking faults that define the shape of the island (Fig. 1) (King, 1969). The Olympic-Wallowa

lineament and the structure of Vancouver Island define the northwestern trace of the Paradox transcontinental fault zone. Farther northwest, along the same northwesterly alignment, the Kodiak seamount chain has a similar alignment (Wise, 1963) and possibly reflects control by the Paradox transcontinental fault zone.

CONCLUSIONS

An alignment of basement faults extends across the North American continent from the Bahamas fracture zone to Vancouver Island. The Paradox transcontinental fault zone forms the boundaries of numerous deep sedimentary basins of a variety of tectonic styles, indicating that large-scale vertical movements of the crust accompanied some of the fault movement. Various segments of the fault system were reactivated with various senses of movement at various times, and the northwest-trending alignment of basement-fault systems documents a persistent zone of crustal-scale faulting through a long span of geologic time. The oldest elements of the Paradox transcontinental fault zone are in the central part of the craton. The range of ages of movements is so great that some rocks involved in the youngest stages of movement at both ends of the system either had not been accreted to North America or had not been formed when the central older elements of the system were initiated and reactivated. Movement along the fault system generally propagated upward (into younger rocks) and lengthwise through time. Lengthwise propagation extended into rocks that were accreted to North America or that were formed by igneous petrogenesis long after the older elements of the fault system had been initiated in the central part of the North American Precambrian craton. Propagation lengthwise into younger rocks, as well as repeated reactivation of faults in the older rocks, indicates the importance of tectonic inheritance in localization of fault movement. Recent seismicity along some parts of the Paradox transcontinental fault zone demonstrates continuing tectonic inheritance and suggests the importance of old fracture zones to modern seismic risk.

ACKNOWLEDGMENTS

Reviews of the manuscript by J. L. Allen, J. C. Mars, and J. M. Montgomery, Jr., are gratefully acknowledged.

REFERENCES CITED

Baars, D. L., 1962, Permian System of the Colorado Plateau: American Association of Petroleum Geologists Bulletin, v. 46, p. 149–218.

_____ 1966, Pre-Pennsylvanian paleotectonics: key to basin evolution and petroleum occurrences in Paradox basin, Utah and Colorado: American Association of Petroleum Geologists Bulletin, v. 50, p. 2082–2111.

Baars, D. L.; and See, P. D., 1968, Pre-Pennsylvanian stratigraphy and paleotectonics of the San Juan Mountains, southwestern Colorado: Geological Society of America Bulletin, v. 79, p. 333–349.

Baars, D. L.; and Stevenson, G. M., 1982, Subtle stratigraphic traps in Paleozoic rocks of Paradox basin: American Association of Petroleum Geologists Memoir 32, p. 131–158.

_____ 1984, The San Luis uplift, an enigma of the Ancestral Rockies: Mountain Geologist, v. 21, no. 2, p. 57–67.

Barker, F., 1969, Precambrian geology of the Needle Mountains, southwestern Colorado: U.S. Geological Survey Professional Paper 644-A, 33 p.

Barker, F.; Peterman, Z. E.; and Hildreth, R. A., 1969, A rubidium-strontium study of the Twilight Gneiss, West Needle Mountains, Colorado: Contributions to Mineralogy and Petrology, v. 23, p. 271–282.

Bickford, M. E.; and Lewis, R. D., 1979, U-Pb geochronology of exposed basement rocks in Oklahoma: Geological Society of America Bulletin, v. 90, p. 540–544.

Bickford, M. E.; Wetherill, G. W.; Barker, F.; and Lee-Hu, C.-N., 1969, Precambrian Rb-Sr chronology in the Needle Mountains, southwestern Colorado: Journal of Geophysical Research, v. 74, p. 1660–1676.

Bissell, H. J., 1962, Pennsylvanian and Permian rocks of Cordilleran area, *in* Branson, C. C. (ed.), Pennsylvanian System in the United States: American Association of Petroleum Geologists, Tulsa, p. 188–263.

Block, T. C., 1986, Tectonic controls on facies relationships and deposition of the Cambrian Ignacio and Devonian Elbert Formations, San Juan Mountains, Colorado: University of Alabama, Tuscaloosa, unpublished M.S. thesis, 142 p.

Bowring, S. A.; and Hoppe, W. J., 1982, U/Pb zircon ages from Mount Sheridan Gabbro, Wichita Mountains, *in* Gilbert, M. C.; and Donovan, R. N. (eds.), Geology of the eastern Wichita Mountains, southwestern Oklahoma: Oklahoma Geological Survey Guidebook 21, p. 54–59.

Brewer, J. A.; Brown, L. D.; Steiner, D.; Oliver, J. E.; Kaufman, S.; and Denison, R. E., 1981, Proterozoic basin in the southern Midcontinent of the United States revealed by COCORP deep seismic reflection profiling: Geology, v. 9, p. 569–575.

Brewer, J. A.; Good, R.; Oliver, J. E.; Brown, L. D.; and Kaufman, S., 1983, COCORP profiling across the southern Oklahoma aulacogen: overthrusting of the Wichita Mountains and compression within the Anadarko basin: Geology, v. 11, p. 109–114.

Chowns, T. M.; and Williams, C. T., 1983, Pre-Cretaceous rocks beneath the Georgia Coastal Plain—regional implications, *in* Gohn, G. S. (ed.), Studies related to the Charleston, South Carolina, earthquake of 1886—tectonics and seismicity: U.S. Geological Survey Professional Paper 1313, p. L1–L42.

Coffman, J. D.; Gilbert, M. C.; and McConnell, D. A., 1986, An interpretation of the crustal structure of the southern Oklahoma aulacogen satisfying gravity data, *in* Gilbert, M. C. (ed.), Petrology of the Cambrian Wichita Mountains igneous suite: Oklahoma Geological Survey Guidebook 23, p. 1–10.

Cook, T. D.; and Bally, A. W. (eds.), 1975, Stratigraphic atlas of North and Central America: Princeton University Press, 272 p.

Denison, R. E., 1989, Foreland structure adjacent to the Ouachita foldbelt, *in* Hatcher, R. D., Jr.; Thomas, W. A.; and Viele, G. W. (eds.), The Appalachian-Ouachita orogen in the United States: Geological Society of America, The Geology of North America, v. F-2, p. 681–688.

Denison, R. E.; Lidiak, E. G.; Bickford, M. E.; and Kisvarsanyi, E. B., 1984, Geology and geochronology of Precambrian rocks in the Central Interior region of the United States: U.S. Geological Survey Professional Paper 1241-C, 20 p.

Gibson, R. G., 1990, Proterozoic contact relationships between gneissic basement and metasedimentary cover in the Needle Mountains, Colorado, U.S.A.: Journal of Structural Geology, v. 12, p. 99–111.

Gilbert, M. C., 1983a, Timing and chemistry of igneous events associated with the southern Oklahoma aulacogen: Tectonophysics, v. 94, p. 439–455.

_____ 1983b, The Meers fault of southwestern Oklahoma: evidence for possible strong Quaternary seismicity in the Midcontinent [abstract]: EOS (Transactions, American Geophysical Union), v. 64, p. 313.

Guthrie, G. M.; and Raymond, D. E.; 1992, Pre-Middle Jurassic rocks beneath the Alabama Gulf Coastal Plain: Alabama Geological Survey Bulletin 150, 155 p.

Ham, W. E.; Denison, R. E.; and Merritt, C. A., 1964, Basement rocks and structural evolution of southern Oklahoma: Oklahoma Geological Survey Bulletin 95, 302 p.

Harris, C. W.; Gibson, R. G.; Simpson, C.; and Eriksson, K. A., 1987, Proterozoic cuspate basement-cover structure, Needle Mountains, Colorado: Geology, v. 15, p. 950–953.

Hinze, W. J.; and Braile, L. W., 1988, Geophysical aspects of the craton: U.S., *in* Sloss, L. L. (ed.), Sedimentary cover—North American craton; U.S.: Geological Society of America, The Geology of North America, v. D-2, p. 5–24.

Hoffman, P.; Dewey, J. F.; and Burke, K., 1974, Aulacogens and their genetic relation to geosynclines, with a Proterozoic example from Great Slave Lake, Canada: Society of Economic Paleontologists and Mineralogists Special Publication 19, p. 38–55.

Houseknecht, D. W., 1986, Evolution from passive margin to foreland basin: the Atoka Formation of the Arkoma basin, south-central U.S.A.: International Association of Sedimentologists Special Publication 8, p. 327–345.

Johnson, K. S.; Amsden, T. W.; Denison, R. E.; Dutton, S. P.; Goldstein, A. G.; Rascoe, Bailey, Jr.; Sutherland, P. K.; and Thompson, D. M., 1988, Southern Midcontinent region, *in* Sloss, L. L. (ed.), Sedimentary cover—North American craton; U.S.: Geological Society of America, The Geology of North America, v. D-2, p. 307–359.

Keen, C. E., 1982, The continental margins of eastern Canada: a review: American Geophysical Union Geodynamics Series, v. 6, p. 45–58.

Keen, C. E.; and Haworth, R. T., 1985, D-2 Transform margin south of Grand Banks: offshore eastern Canada: Geological Society of America Centennial Continent/Ocean Transect #2.

Keller, G. R.; Braile, L. W.; McMechan, G. A.; Thomas, W. A.; Harder, S. H.; Chang, W.-F.; and Jardine, W. G., 1989, Paleozoic continent-ocean transition in the Ouachita Mountains imaged from PASSCAL wide-angle seismic reflection-refraction data: Geology, v. 17, p. 119–122.

King, P. B. (compiler), 1969, Tectonic map of North America: U.S. Geological Survey, scale 1:5,000,000.

King, P. B.; and Beikman, H. M. (compilers), 1974, Geologic map of the United States: U.S. Geological Survey, scale 1:2,500,000.

Klitgord, K. D.; Dillon, W. P.; and Popenoe, P., 1983, Mesozoic tectonics of the southeastern United States Coastal Plain and continental margin, *in* Gohn, G. S. (ed.), Studies related to the Charleston, South Carolina, earthquake of 1886—tectonics and seismicity: U.S. Geological Survey Professional Paper 1313, p. P1–P15.

Klitgord, K. D.; Popenoe, P.; and Schouten, H., 1984, Florida: a Jurassic transform plate boundary: Journal of Geophysical Research, v. 89, p. 7753–7772.

Kluth, C. F., 1986, Plate tectonics of the Ancestral Rocky Mountains: American Association of Petroleum Geologists Memoir 41, p. 353–369.

Kluth, C. F.; and Coney, P. J., 1981, Plate tectonics of the Ancestral Rocky Mountains: Geology, v. 9, p. 10–15.

Lambert, D. D.; and Unruh, D. M., 1986, Isotopic constraints on the age and source history of the Glen Mountains layered complex, Wichita Mountains, *in* Gilbert, M. C. (ed.), Petrology of the Cambrian Wichita Mountains igneous suite: Oklahoma Geological Survey Guidebook 23, p. 53–59.

Larson, E. E.; Patterson, P. E.; Curtis, G.; Drake, R.; and Mutschler, F. E., 1985, Petrologic, paleomagnetic, and structural evidence of a Paleozoic rift system in Oklahoma, New Mexico, Colorado, and Utah: Geological Society of America Bulletin, v. 96, p. 1364–1372.

Lillie, R. J.; Nelson, K. D.; de Voogd, B.; Brewer, J. A.; Oliver, J. E.; Brown, L. D.; Kaufman, S.; and Viele, G. W., 1983, Crustal structure of Ouachita Mountains, Arkansas: a model based on integration of COCORP reflection profiles and regional geophysical data: American Association of Petroleum Geologists Bulletin, v. 67, p. 907–931.

McConnell, D. A., 1989, Determination of offset across the northern margin of the Wichita uplift, southwest Oklahoma: Geological Society of America Bulletin, v. 101, p. 1317–1332.

McConnell, D. A.; and Gilbert, M. C., 1986, Calculations for Cambrian extension of the southern Oklahoma aulacogen, *in* Gilbert, M. C. (ed.), Petrology of the Cambrian Wichita Mountains igneous suite: Oklahoma Geological Survey Guidebook 23, p. 11–20.

Mickus, K. L.; and Keller, G. R., 1992, Lithospheric structure of the south-central United States: Geology, v. 20, p. 335–338.

Muehlberger, W. R.; Denison, R. E.; and Lidiak, E. G., 1967, Basement rocks in continental interior of United States: American Association of Petroleum

Geologists Bulletin, v. 51, p. 2351–2380.
Mueller, P. A.; and Porch, J. W., 1983, Tectonic implications of Paleozoic and Mesozoic igneous rocks in the subsurface of peninsular Florida: Gulf Coast Association of Geological Societies Transactions, v. 33, p. 169–173.
Nelson, K. D.; Lillie, R. J.; de Voogd, B.; Brewer, J. A.; Oliver, J. E.; Kaufman, S.; Brown, L. D.; and Viele, G. W., 1982, COCORP seismic reflection profiling in the Ouachita Mountains of western Arkansas: geometry and geologic interpretation: Tectonics, v. 1, p. 413–430.
Perry, W. J., Jr., 1989, Tectonic evolution of the Anadarko basin region, Oklahoma: U.S. Geological Survey Bulletin 1866-A, 19 p.
Ramelli, A. R.; and Slemmons, D. B., 1990, Implications of the Meers fault on seismic potential in the central United States, *in* Krinitzski, E. L.; and Slemmons, D. B. (eds.), Neotectonics in earthquake evaluation: Geological Society of America Reviews in Engineering Geology, v. 8, p. 59–75.
Scrutton, R. A., 1982, Crustal structure and development of sheared passive continental margins: American Geophysical Union Geodynamics Series, v. 6, p. 133–140.
Slemmons, D. B., 1991, Introduction, *in* Slemmons, D. B.; Engdahl, E. R.; Zoback, M. D.; and Blackwell, D. D. (eds.), Neotectonics of North America: Geological Society of America, Decade Map, v. 1, p. 1–20.
Sloss, L. L., 1988, Tectonic evolution of the craton in Phanerozoic time, *in* Sloss, L. L. (ed.), Sedimentary cover—North American craton; U.S.: Geological Society of America, The Geology of North America, v. D-2, p. 25–51.
Stokes, W. L., 1979, Stratigraphy of the Great Basin region, *in* Newman, G. W.; and Goode, H. D. (eds.), Basin and Range symposium: Rocky Mountain Association of Geologists and Utah Geological Association, p. 195–219.
Tewksbury, B. J., 1985, Revised interpretation of the age of allochthonous rocks of the Uncompahgre Formation, Needle Mountains, Colorado: Geological Society of America Bulletin, v. 96, p. 224–232.
Thelin, G. P.; and Pike, R. J., 1991, Landforms of the conterminous United States—a digital shaded-relief portrayal: U.S. Geological Survey Miscellaneous Investigations Series Map I-2206, scale 1:3,500,000.
Thomas, W. A., 1988a, The Black Warrior basin, *in* Sloss, L. L. (ed.), Sedimentary cover—North American craton; U.S.: Geological Society of America, The Geology of North America, v. D-2, p. 471–492.
_____ 1988b, Early Mesozoic faults of the northern Gulf Coastal Plain in the context of opening of the Atlantic Ocean, *in* Manspeizer, W. (ed.), Triassic-Jurassic rifting: Developments in Geotectonics 22, Elsevier, Amsterdam, p. 463–476.
_____ 1991, The Appalachian-Ouachita rifted margin of southeastern North America: Geological Society of America Bulletin, v. 103, p. 415–431.
Thomas, W. A.; Chowns, T. M.; Daniels, D. L.; Neathery, T. L.; Glover, L., III; and Gleason, R. J., 1989, The subsurface Appalachians beneath the Atlantic and Gulf Coastal Plains, *in* Hatcher, R. D., Jr.; Thomas, W. A.; and Viele, G. W. (eds.), The Appalachian-Ouachita orogen in the United States: Geological Society of America, The Geology of North America, v. F-2, p. 445–458.
Viele, G. W.; and Thomas, W. A., 1989, Tectonic synthesis of the Ouachita orogenic belt, *in* Hatcher, R. D., Jr.; Thomas, W. A.; and Viele, G. W. (eds.), The Appalachian-Ouachita orogen in the United States: Geological Society of America, The Geology of North America, v. F-2, p. 695–728.
Welsh, J. E., 1976, Relationships of Pennsylvanian-Permian stratigraphy to the late Mesozoic thrust belt in the eastern Great Basin, Utah and Nevada, *in* Hill, J. G. (ed.), Geology of the Cordilleran hingeline: Rocky Mountain Association of Geologists, Denver, p. 153–160.
Wise, D. U., 1963, An outrageous hypothesis for the tectonic pattern of the North American Cordillera: Geological Society of America Bulletin, v. 74, p. 357–362.
Woodward, L. A., 1988, Tectonic map of the Rocky Mountain region of the United States, *in* Sloss, L. L. (ed.), Sedimentary cover—North American craton; U.S.: Geological Society of America, The Geology of North America, v. D-2, pl. 2.
Zietz, I. (compiler), 1982, Composite magnetic anomaly map of the United States: U.S. Geological Survey Geophysical Investigations Map GP-954-A.

Basement Influence on the Structural Geology of Southern Oklahoma Inferred from Residual Aeromagnetic Maps

Thomas L. Thompson
James R. Howe
Consulting Geologists
Boulder, Colorado

Bronson W. Hawley
S. Parker Gay
Applied Geophysics, Inc.
Salt Lake City, Utah

INTRODUCTION

Discontinuities in the crystalline basement of cratonic sedimentary basins commonly control the geologic structure of the overlying sedimentary sequence. Whereas new faults may form at any time, ancient breaks along discontinuities in the basement often are the sites of recurrent faulting before, during, and after deposition of the basin fill. The geologic structure of the platform rocks of southern Oklahoma dramatically exhibits such basement involvement because intense foreland deformation associated with late Paleozoic orogenic activity has created high structural relief.

Aeromagnetic techniques allow interpretation of the location, strike, and lateral extent of basement faults. The utility of magnetics in accomplishing this type of interpretation comes from application of two concepts: (1) old basement faults have dissected the basement into a set of distinct blocks, and (2) these blocks often have different magnetic susceptibilities because of differing lithologies. Consequently, residual magnetic maps often have magnetic highs and lows over adjacent blocks. The faults occur along the gradients between the magnetic highs and lows.

High-resolution residual aeromagnetic mapping provides a particularly useful display of areal continuity of basement-block patterns that (when considered in the context of regional stress fields) allows predictions of specific fault reactivation, sense of displacement, and deformation in the overlying sedimentary-rock sequence. Visualizing the dynamic interplay between basement blocks, defined by magnetics, provides very useful guidance to subsurface structural mapping based on well and seismic control.

OUACHITA STRUCTURAL SYSTEM

Basement-involved movements characterize the structural style of the foreland and subthrust platform sequence of the entire Ouachita system. Aeromagnetic mapping in southeastern Oklahoma (and elsewhere along the Ouachita trend) clearly reveals the foreland and subthrust basement-fault-block pattern that was largely established before or during the Cambrian rifting of the early Paleozoic continental margin. Late Paleozoic orogenic activity reactivated many of these basement faults to accentuate the preexisting fault-block pattern and cut upward through the platform sedimentary sequence.

Magnetic techniques greatly aid the subsurface mapping of this horst-and-graben system and in the delineation of exploration targets. Many basement-rooted horst-block structures have been mapped, including structures at the Wilburton, Red Oak, and Bonanza gas fields.

WICHITA–ARBUCKLE STRUCTURAL SYSTEM

Transpression, in several episodes during the Late Mississippian to Permian assembly of Pangaea, acting across rifted Precambrian basement blocks, seems to account for the dominant structural styles indicated along the Wichita–Marietta block, the Ardmore basin block, and the several blocks of the Arbuckle Mountains. Although complex in detail, the various structures and their mechanical linkages find common explanation in context of east–west to northeast–southwest compression and reactivation of northwest-trending basement blocks. During rifting, graben apparently were filled with rhyolite before the region accumulated 20,000–40,000 ft of sediment during the Cambrian to Late Mississippian.

The dynamic interplay among basement blocks under transpression apparently caused structural inversion of rhyolite-filled graben and the formation of several types of mechanically linked structures as follows. (1) North–northwest to west–northwest trending, left-reverse, oblique-slip faults (including high-angle faults and low-angle faults). Variation in fault orientation in many cases reflects variation in the orientation of reactivated block interfaces, with stronger uplift and downwarp pairs

Thompson, T. L.; Hawley, B. W.; Howe, J. R.; and Gay, S. P., 1995, Basement influence on the structural geology of southern Oklahoma inferred from residual aeromagnetic maps, *in* Johnson, K. S. (ed.), Structural styles in the southern Midcontinent, 1992 symposium: Oklahoma Geological Survey Circular 97, p. 13–14.

and imbricate faulting at confining bends in the basement-block pattern (i.e., the Wichita uplift–Cyril basin pair and the Criner Hills–Ardmore deep basin pair). (2) En echelon folds and thrusts generally trend northwest–southeast, oblique to the basement blocks, apparently controlled by slippage along basement-block boundaries. (3) Northeast-trending basement fractures (made obvious by the magnetic pattern) apparently provided antithetic adjustment to the dominant northwest-trending folds and faults, and commonly influenced the plunge of folds and caused confining bends during slippage along basement-block boundaries. (4) Left-reverse, oblique-slip flower structures formed at several scales (including the complex Cumberland anticline and faulting above the Criner, the Tishomingo, and the Wichita–Marietta basement blocks).

Structural Styles in the Ouachita Mountains and Southern Arkoma Basin, Arkansas

Boyd R. Haley and Charles G. Stone
Arkansas Geological Commission
Little Rock, Arkansas

ABSTRACT.—This display represents a variety of geologic maps of the Ouachita Mountains/southern Arkoma basin, Arkansas. These maps largely were made through an intensive 5½-year field and aerial photographic project—COGEOMAP, a cooperative venture with the Oklahoma Geological Survey and the U.S. Geological Survey designed to generate geologic maps and reports providing information on the complex structure, stratigraphy, and mineral resources in the Ouachita Mountain orogen. To date, in Arkansas, 151 geologic maps have been completed at a scale of 1:24,000 and then reduced and compiled at scales of 1:100,000 and 1:250,000. The remaining 26 maps currently are being field checked or are in various stages of preparation. Biostratigraphic evaluation of the early Paleozoic strata also has been very important and includes evaluations by Ray Ethington, Jim Stitt, John Repetski, and others.

A few geological features that are newly illustrated include: (1) décollements in middle Stanley shales between Potter and Hatfield in Polk County and near Gillham Dam in Howard County; (2) the duplex, triangle, or "tepee" nature of the structure in Atokan rocks along Dutch Creek in Scott and Yell Counties; (3) extensive belts of Lower Ordovician and Early Cambrian strata in Garland and Saline Counties of the eastern Benton uplift; (4) several additional tear and thrust faults in the vicinity of Amity in Pike and Montgomery Counties; (5) exposures of Jackfork Sandstone in the Mazarn basin southwest of Hot Springs in Garland County; and (6) lineaments trending northwest and northeast at several sites in western Polk and Howard Counties.

Haley, B. R.; and Stone, C. G., 1995, Structural styles in the Ouachita Mountains and southern Arkoma basin, Arkansas, *in* Johnson, K. S. (ed.), Structural styles in the southern Midcontinent, 1992 symposium: Oklahoma Geological Survey Circular 97, p. 15.

Origin of Disharmonic Folding, Central Ouachita Mountains, Oklahoma

George W. Viele
University of Missouri
Columbia, Missouri

ABSTRACT.—As Miser (1929) noted, the central Ouachita Mountains of Oklahoma comprise two structural decks: a lower deck of tight, cleaved folds in pre–middle Mississippian strata generally records multiple folding and low-grade metamorphism; an upper deck forms broad synclines in post–middle Mississippian to Atokan strata. Folding in the upper deck is harmonic. Folding in the lower deck is polyharmonic. The two decks are disharmonically folded relative to one another. Measurements of linear strain made from cross sections indicate that shortening of the lower deck is about five times greater than shortening of the upper deck. The differences in fold style have been attributed to rheological differences between a stiff upper deck and a ductile lower deck, but variations in thickness and spacing of rigid versus ductile beds are roughly comparable from deck to deck. Thrust faulting in the upper deck cannot account for the difference in shortening, because the faults equally displace lower-deck strata and have tip lines in lower-deck strata. The hypothesis is offered that the disharmonic folding is related to the unconformable deposition of the upper-deck strata in a fore-arc basin across the tightly folded strata of an accretionary wedge, the lower deck.

INTRODUCTION

Several large synclines, the Tuskohoma, Lynn Mountain, Boktukola, and Bethel synclines, are among the most visible features of the central Ouachita Mountains of Oklahoma (Fig. 1). All are easily identified on small-scale (1:250,000) topographic maps, on radar imagery of the same scale (Fig. 2A,B), and on even smaller-scale Landsat imagery. The synclines lie in Carboniferous strata extending upward from the approximate middle of the Mississippian Stanley Group through the Pennsylvanian Jackfork Group and the Johns Valley and Atoka Formations. Stratigraphic units younger than the Atoka are eroded away. The synclines overlie tightly folded older Paleozoic strata, which include Cambrian through Devonian strata (Ethington and others, 1989) and the lower part of the Stanley Group. The two fold systems appear to be disharmonic with respect to one another. In this paper, I will describe the geometry of this disharmonic folding and examine several hypotheses for the origin of the disharmonic folds.

TERMINOLOGY OF DISHARMONIC FOLDS

The terminology describing the stacking of a fold system is taken from Ramsay and Huber (1987); it provides precise definitions of the terms "harmonic," "polyharmonic," and "disharmonic." For example, if fold amplitudes and wavelengths are the same throughout a stack of buckled multilayers, the folding is said to be "harmonic" (Fig. 3). Generally, this type of folding is associated with multilayers of strata of about the same thickness and spacing from one another. In addition, the contrast in stiffness between the rigid and ductile layers is essentially constant throughout the stack. Other factors controlling the geometry of buckle folds include changing of rheological properties with changing temperature and pressure, orientation of mineral grains during folding, mechanical properties of the interfaces between layers, boundary constraints on the multilayers being folded, and the scale of the multilayer stack being folded (Ramsay and Huber, 1987).

A stratigraphic packet made up of beds of different thicknesses and spacings generally folds into a "polyharmonic" stack (Fig. 3). Each competent bed has its own characteristic wavelength, depending upon the thickness and stiffness of the bed and upon the mechanical properties of the bedding interfaces. In addition, each sideways buckling of a competent bed displaces the adjacent, relatively ductile material within a "zone of contact strain"

Viele, G. W., 1995, Origin of disharmonic folding, central Ouachita Mountains, Oklahoma, *in* Johnson, K. S. (ed.), Structural styles in the southern Midcontinent, 1992 symposium: Oklahoma Geological Survey Circular 97, p. 16–25.

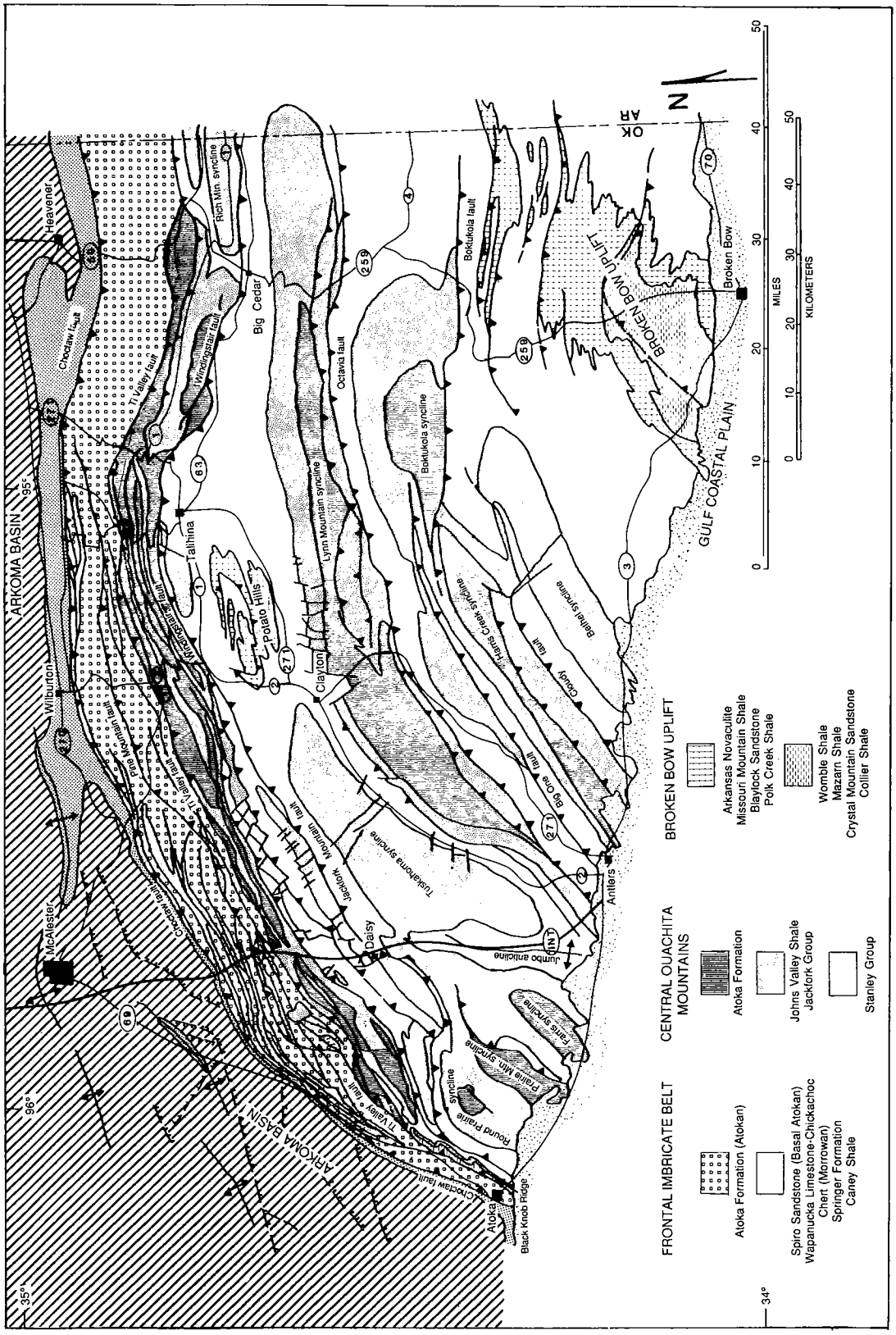


Figure 1. Index map of the Ouachita Mountains of southeastern Oklahoma. The central Ouachitas lie between the Windingstair thrust fault and the Broken Bow uplift.

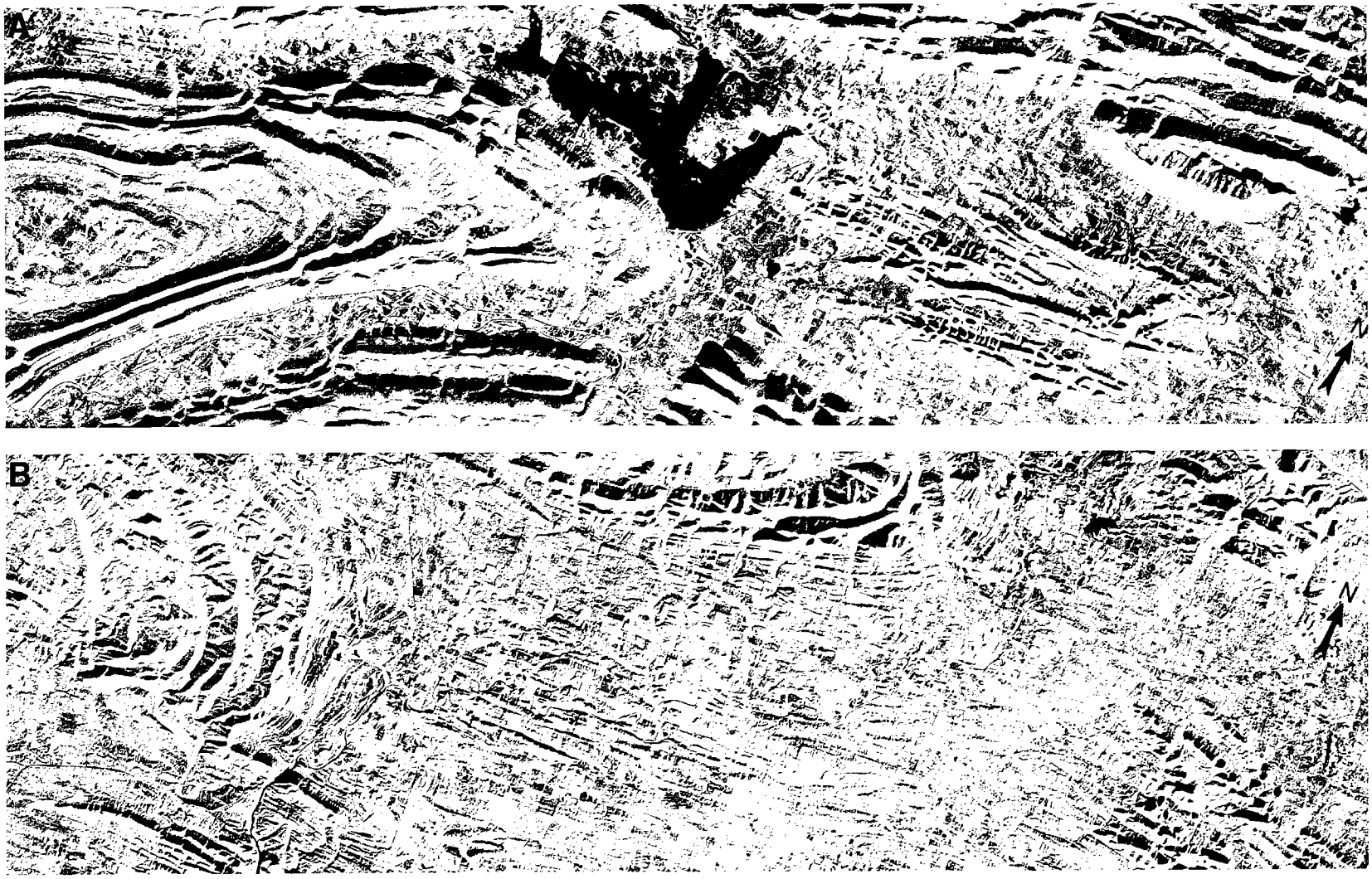


Figure 2. Parts of radar image mosaic, McAlester, NI 15-4. *A*—Eastern end of Tuskahoma syncline to the left and Potato Hills to the right. *B*—Eastern end of Boktukola syncline to the left; Lynn Mountain syncline in the upper central part of image; and Cossatot Mountains (western end of the Benton uplift) in the lower right.

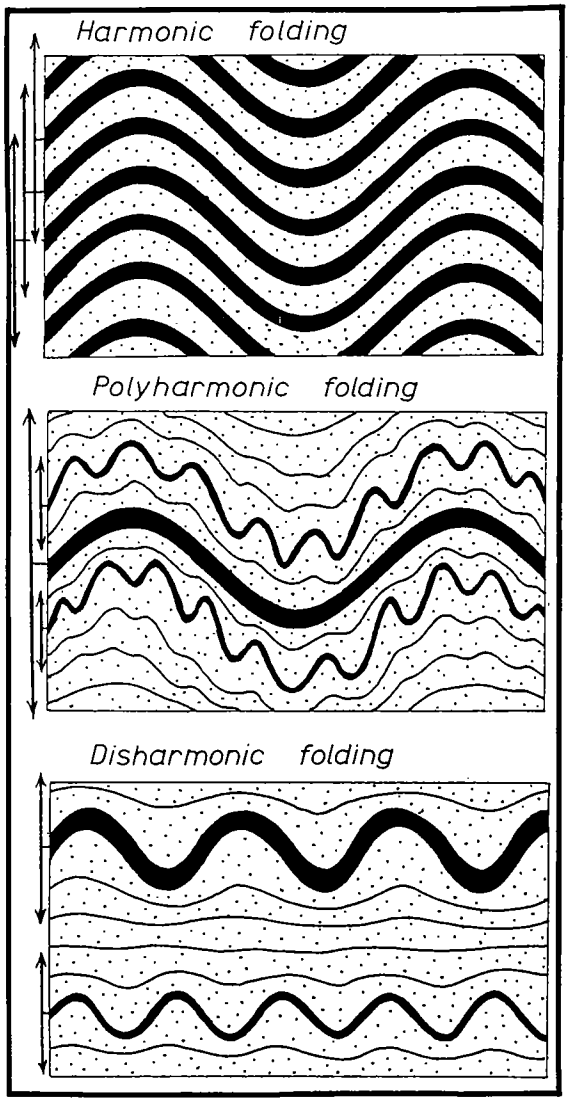


Figure 3. Stacking of strata into harmonic folds, polyharmonic folds, and disharmonic folds. Vertical arrows indicate zones of contact strain. Modified from Ramsay and Huber (1987).

extending out to one-half the fold wavelength of the buckled competent bed (Ramberg, 1961,1964). When the zones of contact strain overlap one another, folds of different wavelength may form, but the anticlinal culminations and depressions throughout the stack are coincident. In other words, the folding is anticlinorial and synclinorial.

If, however, two competent layers are widely separated from one another so that the zones of contact strain do not overlap (Fig. 3), the beds fold independently of one another. Fold wavelengths reflect the thicknesses and mechanical properties of the rigid beds, but anticlines and synclines throughout the stack are not coincident with one another. This is specifically what is meant by the term "disharmonic folding."

OUACHITA FOLD STYLES

Figures 4 and 5 show, respectively, an older interpretation of Ouachita folding (Miser, 1929) and a more recent interpretation (Arbenz, 1989b). Two properties of the cross sections are worth noting. Both show clearly the contrast between the tightly folded Ordovician through lower Stanley strata and the broadly folded upper Stanley through Atokan strata. On both, the change in fold wavelength takes place within the middle part of the Stanley Group. Moreover, on each cross section, the anticlines and synclines are broadly coincident throughout the entire stratigraphic section. The folding shown on the sections is polyharmonic in the sense of the previously stated definitions.

The radar imagery of the central Ouachita Mountains of Oklahoma (Fig. 2A,B) and the structural data of numerous workers confirms the variation in the tightness of folding. Folds in the older strata in the western end of the Benton uplift (Fig. 1,2B) have wavelengths of 200–1,800 m and limb dips of 40°–60° (Babaei and Viele, 1992). Folds in the older strata in the Cossatot Mountains (Fig. 2B) have an average macrofold wavelength of 1.2 km, and limb dips on the balanced cross section are generally 45°–65° (Weber and Zimmerman, 1988, Fig. 5). In the lower part of the Stanley Group on the east of the Boktukola syncline (Fig. 1), north-dipping fold limbs dip 40°–70° and south-dipping limbs dip 45°–80° (Briggs, 1973). To the north, in the pre-Mississippian strata of the Potato Hills, the distance between the major anticlinal hinges is generally 2–3 km and limb dips, compiled from Arbenz (1968), are typically 50°–70° (Fig. 6).

Within the large synclines, wavelengths and limb dips are different. The distance between the map traces of the axial surfaces of the Boktukola and Lynn Mountain synclines, for example, is ~15 km in some locations. Most bedding dips within the Boktukola syncline are <40°, although locally, along the northern limb, dips are as high as 60°–70°, and on the southern limb, close to the trace of the north-verging Boktukola thrust fault, dips are steep to vertical to southward and overturned. In the Lynn Mountain syncline, most beds dip southward at <30°, although to the west, along the northern flank of the syncline, some beds dip steeply southward or even northward, depending on the degree of south-directed folding and overturning. Data for limb dips of the Tuskahoma syncline are sparse, but an inspection of the radar imagery (Fig. 2) indicates shallow dips. To summarize: in Ordovician to lower Stanley strata, dips are generally steep, and wavelengths of the folds are short, whereas in the upper Stanley and Pennsylvanian strata, dips are low and wavelengths are long.

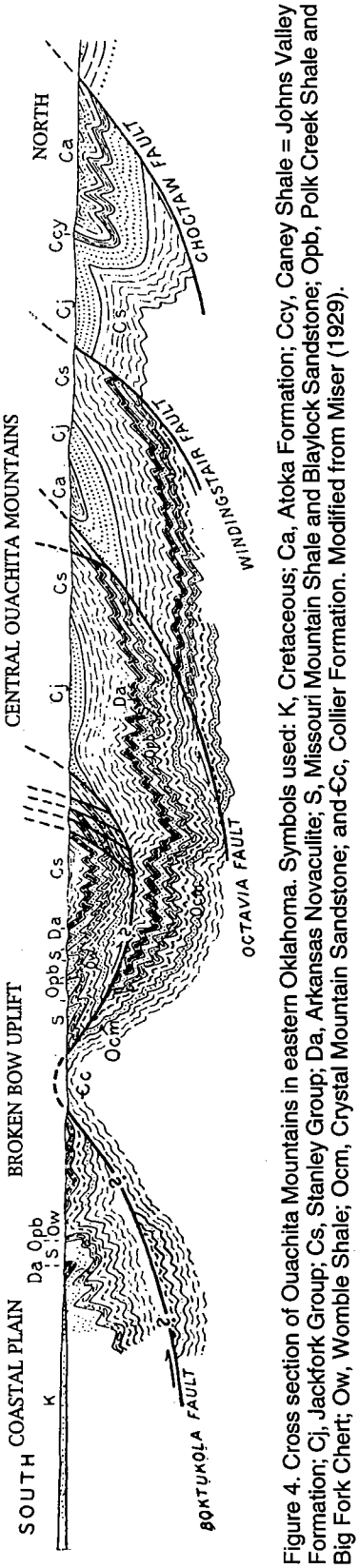


Figure 4. Cross section of Ouachita Mountains in eastern Oklahoma. Symbols used: K, Cretaceous; Ca, Atoka Formation; Ccy, Caney Shale = Johns Valley Formation; Cj, Jackfork Group; Cs, Stanley Group; Da, Arkansas Novaculite; S, Missouri Mountain Shale and Blaylock Sandstone; Opb, Polk Creek Shale and Big Fork Chert; Ow, Womble Shale; Ocm, Crystal Mountain Sandstone; and Cc, Collier Formation. Modified from Miser (1929).

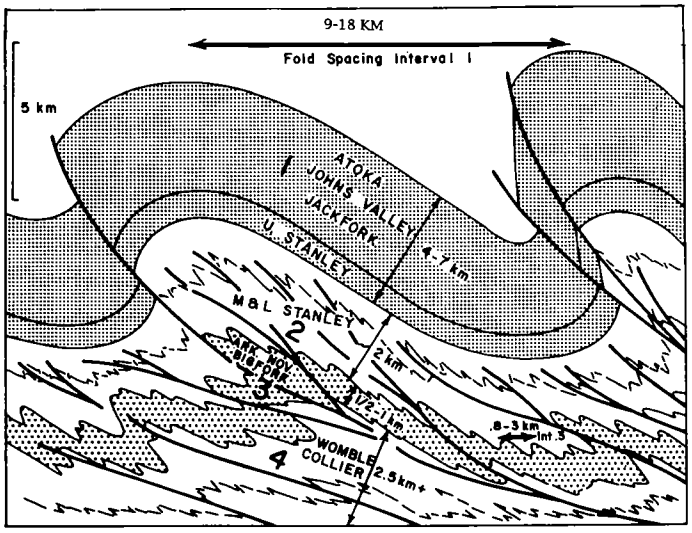


Figure 5. Cross-sectional diagram, approximately scaled, depicting the vertical distribution and contrasts of structural styles caused by the lithology-controlled variations of relative ductility and strength. Copied from Arbenz (1989b).

Folding is not polyharmonic throughout the central Ouachita Mountains. It is true that in the uplifts of older strata—Benton, Broken Bow, and Potato Hills uplifts—polyharmonic folds predominate, for folds in the Cambrian through Lower Mississippian strata form regional anticlinoria and synclinoria (Honess, 1923; Purdue and Miser, 1927; Miser and Purdue, 1923; Miser, 1954; Haley and others, 1976). Fold wavelengths and amplitudes vary from formation to formation, but the hingelines of anticlines and synclines collect into large anticlinoria and synclinoria. The fold hinges and axial surfaces are penetrative from formation to formation.

These polyharmonic folds are not penetrative into the upper Stanley Group; instead, they plunge beneath the eastern end of several of the larger synclines. The anticlinorial culmination of the Potato Hills, for example, plunges southwestward beneath the broad Tuskahoma syncline (Fig. 2A). Tightly folded strata of the lower part of the Stanley Group extend westward from the Cossatot Mountains and plunge beneath the Boktukola syncline (Fig. 2B). On the eastern end of the Boktukola syncline, tightly folded and strongly cleaved beds of the lower Stanley Group lie, at the most, 100 m downhill from broadly folded, noncleaved beds of the upper Stanley Group. Vegetation covers the interval between, so the exact nature of the contact is not visible. These upper Stanley beds lie well within a half wavelength of the underlying folds. Similar relations between the upper and lower Stanley Group may be seen at the eastern end of the Lynn Mountain syncline, although here the covered interval is wider.

Therefore, folding within the Ouachita Mountains is truly disharmonic. The tightly folded anticlinorial culminations plunge westward beneath the broad synclines without evidence of flattening into synclinoria. Moreover, the fold hinges of the "lower-deck" strata are not evident within the "upper-deck" synclines, despite the close proximity of the two decks to one another—within a half wavelength. If the decks were folded

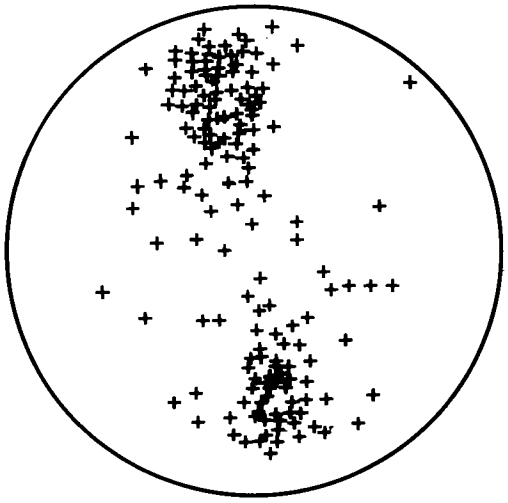


Figure 6. Pole points to bedding in the area of the Potato Hills. Compiled from geologic mapping by Arbenz (1968).

simultaneously, the zones of contact strain of the lower-deck folds should extend into the upper-deck beds, but they do not. What is the cause of this disharmonic folding?

CAUSES OF DISHARMONY

Previous workers (Miser, 1929; Arbenz, 1989a) attributed the disharmonic folding of the Ouachita strata to variations of ductility and strength between beds of quartzose sandstone, massive novaculite, and shale. Bed thickness and bed spacing were also viewed as important factors. The lower-deck strata were shown on cross sections as being tightly folded and as the more ductile of the two decks of strata.

Within the lower-deck anticlinoria—the Benton, Broken Bow, and Potato Hills uplifts—beds of sandstone and thick beds of novaculite compose slightly more than 45% of the stratigraphic section and range in thickness from <50 to >450 m (Fig. 7). Most of these beds contain shale intervals too thin to show at the scale of Figure 7. Interstratified with the rigid sandstones and novaculites are shales, thin-bedded micrites, and thin-bedded cherts, all viewed as being relatively ductile. The spacing between ductile and rigid beds ranges from <1 to >400 m. With this much variation in thickness and spacing, polyharmonic folding could be predicted, and indeed, it is the dominant style of fold stacking within the lower-deck strata.

Within the harmonically folded, upper-deck synclines, sandstones lie against shales. The sandstones compose slightly more than 54% of the strata and are generally viewed as rigid (Fig. 7). The stratigraphic thicknesses of rigid strata range from <50 to 700 m, although they too contain numerous interbeds of shale too thin to show in Figure 7. The thickness of some beds of sandstone, however, does approach 50 m. Thick beds of sandstone are concentrated in the Jackfork Group and in the lower part of the upper Stanley Group. Beds of sandstone are thinner in the lower part of the Stanley Group and within the Atoka Formation. The spacing between sandstone beds ranges from <1 to slightly >840 m.

The upper-deck synclines contain a higher ratio of rigid to ductile beds, but differences in bed thickness and spacing are substantial and of the same order of magnitude as in the lower-deck strata. The similarities are puzzling, for if these Carboniferous strata were shortened as much as the strata in the lower deck, one would expect to find polyharmonic folds within them, especially in the Atoka Formation. But, notwithstanding the large variations in thickness and spacing of rigid and ductile beds, the Carboniferous synclines lie in harmonic stacks of strata dominated by the wavelength and amplitude of folds in the rigid sandstones of the Jackfork Group.

DIFFERENCES IN LINEAR STRAIN

The lower-deck strata appear to be shortened much more than the upper-deck strata. Using simple line-length methods, Babaei and Viele (1992) suggested that strata in the Potato Hills were shortened by at least 97%. Our calculations deliberately omitted thrust imbrications of fold limbs and estimates of tangential longitudinal strain (Ramsay and Huber, 1987), for including these factors would have increased the shortening even more.

Measurements of changes of line lengths from other areas show similar results. On the balanced cross section of the Cossatot Mountains (Weber and Zimmerman, 1988, fig. 5), where the structural style of upright uncleaved folds is similar to that of the Potato Hills, the total shortening is in the range of 69%. The strain is partitioned into approximately 67% folding and 2% thrust faulting. Thrust faulting in the Cossatot Mountains plays only a minor role in the calculation of horizontal shortening on this cross section, because at the level of the cross section, listric bending of the faults has turned them to vertical or even steep north dips. These north-dipping thrust faults exhibit normal separation and extend, rather than shorten, the cross section. The shortening of strata in the Potato Hills and Cossatot Mountains is about five times greater than the shortening of Carboniferous strata in the upper-deck synclines.

Measurements of changes of line lengths on cross sections were not attempted for either the Benton or the Broken Bow uplifts. The rocks of these regions are strongly cleaved and exhibit mul-

tiple periods of deformation (Feenstra and Wickham, 1975; Nielsen and others, 1989). In addition, substantial volumes of rock were probably lost during the formation of multiple cleavages and ubiquitous quartz veins. The shortening of strata in the Benton and Broken Bow uplifts is even greater than the shortening in the Cossatot Mountains and Potato Hills.

Figure 5, although diagrammatic, illustrates a regional problem associated with the partitioning of strain. Measurements of line lengths made on a 200% enlargement of Figure 5 showed a shortening of ~41.8% for the base of the upper Stanley Group, of which 32.8% was due to folding and 9% was due to thrust faulting. The top of the Arkansas Novaculite, however, was shortened by 108.4%: folding accounts for 94% and thrusting accounts for 14.4%. Yet if the deformation of the upper and lower decks was simultaneous, the total amount of shortening of the two decks must somewhere be the same. Somewhere, the upper-deck synclines must have lost length by bulk flattening or lost volume perhaps by the formation of solution cleavage or by the imbrication of numerous small thrust faults. To my knowledge, none of these features has been reported in the literature, nor have I seen such features in the field in the upper-deck synclines.

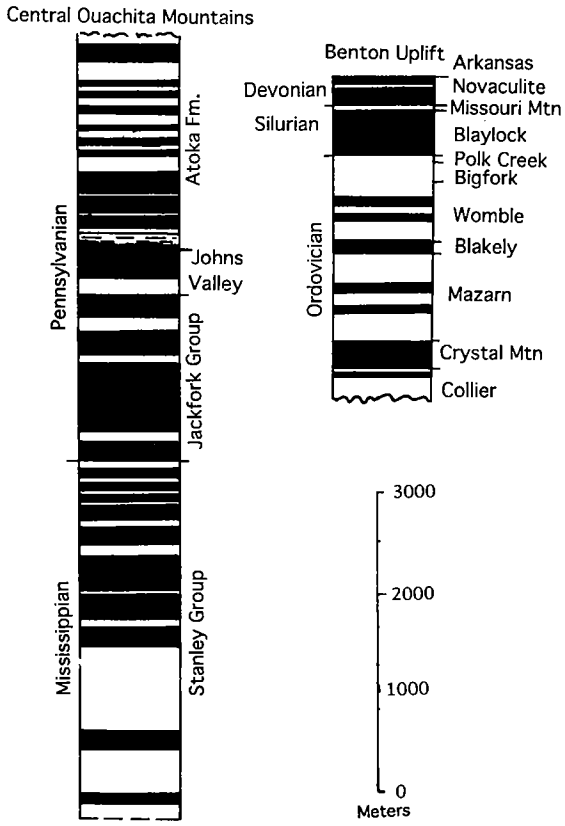


Figure 7. Distribution of relatively rigid beds (in black) within the stratigraphic column of the Ouachita Mountains. Modified from Arbenz (1989a, figs. 5,6).

Displacements by Thrust Faulting

Several large, south-dipping thrust faults—Windingstair, Octavia, and Boktukola faults—transect the central Ouachitas and possibly account for the discrepancy in shortening between the upper and lower decks (Figs. 1,4). They account for the discrepancy, however, only if the thrusts do not root within, or displace, the lower-deck strata. On Figure 4, for example, the shortening of the lower deck by thrust faulting appears to be fully as great as the shortening of the upper deck. Figure 5 also shows thrust faults displacing both the upper- and lower-deck beds. On both cross sections, the fault separations balance, shortening the upper and lower decks by approximately equal amounts; therefore, thrust faulting cannot be used to explain the difference in shortening.

Perhaps a major décollement underlies the Upper Mississippian and Pennsylvanian strata. In this model, the trace of the Windingstair thrust fault could be the leading edge of a large thrust sheet containing all the upper-deck synclines. The Octavia and Boktukola thrust faults could be south-dipping splays off the Windingstair fault, which would be the floor thrust. The separations of the base of the Jackfork Group by the Octavia and Boktukola thrusts could thus be balanced on cross sections without extending the separations into the lower deck. Indeed, Miser (1929) showed the Potato Hills as a window in the Windingstair thrust sheet, and he suggested that the central part of the Broken Bow uplift was a window in the Boktukola thrust fault (Fig. 4). Arbenz (1968) showed the Potato Hills as a window in the Jackfork Mountain thrust sheet, which has a mapped trace between the northern edge of the Potato Hills and the Windingstair thrust fault. A recent worker in the Potato Hills, however, has rejected the window hypothesis (Allen, 1992).

There are three-dimensional problems associated with the hypothesis of shortening by thrust faulting. On all published maps, the eastern tip lines of the Octavia and Boktukola faults extend and disappear into the tightly folded strata of the lower Stanley Group, where folding apparently takes up the displacement on the thrust. This interpretation does not help the aforementioned shortening problem. If the trace of the Windingstair fault is projected eastward, without an abrupt change of strike, its eastern tip line must lie in the highly deformed rocks on the north of the Benton uplift, which would then necessarily lie within the thrust sheet. Instead, one can hypothesize that, in Arkansas, the Windingstair fault passes to the south of the Benton uplift and, in Oklahoma, it bends upward from beneath the southernmost synclines of the

central Ouachitas and rims the Broken Bow uplift. The upper thrust sheet might then root far to the south in a region now covered by the Gulf Coastal Plain. No published maps show this configuration, nor is there any hint of a root zone on seismic lines extending southward over the coastal plain.

A second problem with the hypothesis that thrust faults account for the discrepancy in shortening of the decks is that the structural geometry necessarily calls for thrusting younger strata over older. In many places the dip of the thrusts would be less than the dip of the footwall strata, yet there are no known outcrops of footwall cutoffs in the upper-deck strata. The regional décollement would necessarily exactly follow the beds within the Stanley Group, where the style of folding changes. It would be fortuitous if a major thrust sheet of younger rocks over older took place without a single footwall cutoff.

Finally, gravity modeling of the central Ouachitas suggests that the Octavia and Boktukola faults are young, steeply dipping faults, possibly reactivated basement faults that cut all older structures (Ragland, 1991). If so, these late, high-angle faults would do little to resolve the problem of difference in shortening between the upper and lower decks.

THE UNCONFORMITY MODEL

An extensive literature exists (King, 1937,1975; Thomas, 1976,1991; Graham and others, 1975; Wickham and others, 1976; Viele, 1977,1979; Lillie and others, 1983; Lillie, 1985; Viele and Thomas, 1989) that argues for deposition of the Ouachita sediments off the North American craton in slope, rise, and abyssal sea-floor environments. The stratigraphic section formed from these sediments includes all formations from the Upper Cambrian Collier Formation to the lower Stanley Group. In earlier papers (Viele and Thomas, 1989), these strata have been designated as "preorogenic" because they were deposited prior to structural deformation of the Ouachita strata. It is emphasized here that the lower part of the Stanley Group, containing extensive deposits of barite (Hanor and Baria, 1977) and submarine ash falls (Niem, 1977), is viewed as preorogenic.

Authors of the post-1975 literature have further argued that the Ouachita ocean was closed by south-directed subduction of the North American plate beneath a growing accretionary wedge. Graham and others (1975) compared the Ouachita orogenic belt to the Bengal fan and the Indoburman-Sunda subduction zone; Welland and others (1985) compared the Ouachita belt to the Makran accretionary wedge of Iran; and Viele and Thomas (1989) compared it to the subduction of Australia beneath Timor. Seismic profiling has confirmed the presence of deeply buried, strongly attenuated continental crust or oceanic crust on the south side of the Ouachita Mountains (Keller and others, 1989).

Strata deposited on transitional and oceanic crust of the southern part of the North American plate were transferred to the upper plate by thrust faults propagating northward from the toe of the accretionary wedge. Yet even as the preorogenic strata were being stacked into the growing wedge, sediments of the upper Stanley Group and younger Pennsylvanian sediments were being deposited at ever-increasing rates across the top and flank of the wedge (see Viele and Thomas, 1989, fig. 18). At the front of the wedge, Carboniferous sediments were subducted and intensely deformed, but in the region of the central Ouachita Mountains of Oklahoma, sediments were deposited in a Late Mississippian and Pennsylvanian fore-arc basin formed across the quiescent top and southern flank of the accretionary wedge. The abrupt thinning of the Stanley Group from south to north (Cline, 1960) probably records the prograding of fore-arc basin strata over the wedge. The unconformity would be time transgressive, becoming younger toward the north.

The multiple episodes of folding of lower-deck strata, described by many authors (Comstock, 1888; Viele, 1966,1973; Feenstra and Wickham, 1975; Underwood and Viele, 1985; Nielsen and others, 1989), are attributed to deformation within the accretionary wedge as it grew off the flank of the North American craton. The broad folds of Carboniferous strata, however, formed during or after thrusting of Ouachita strata onto the southern margin of North America in Atokan time (Houseknecht, 1986). The thrust faults and folds of Carboniferous strata in the central Ouachita Mountains represent a partial collapse of the fore-arc basin.

If an unconformity does separate the lower and upper parts of the Stanley Group, the problem of the disharmonic folding disappears. The tight folds and multiple deformations of the lower deck formed in the accretionary wedge before deposition of the higher Carboniferous strata. The broad folds and thrust faults in the Carboniferous strata formed after these strata were deposited across the wedge. The two-decked structure of the Ouachita Mountains primarily records the formation of an unconformity developed as fore-arc basin sediments prograded across a quiescent accretionary wedge. Interpreters of seismic profiles should be careful about extending the prominent surface structures of the central Ouachita Mountains to any great depth.

At the time this paper was presented orally in Norman, Oklahoma, I was unaware of the work of Paula Noble of The University of Texas at Austin. I was surprised and delighted when, a few minutes after my presentation, she presented paleontological evidence for a major hiatus within the Tesnus Formation of the Marathon uplift (Noble, 1993), for the Tesnus is the equivalent of the Stanley Group in the Ouachitas. The hiatus lies at the level of the unconformity hypothesized in this paper.

REFERENCES CITED

Allen, M. W., 1992, Structural analysis of the western Potato Hills, Ouachita Mountains, Oklahoma: Oklahoma Geology Notes, v. 52, p. 173–183.

Arbenz, J. K., 1968, Structural geology of the Potato Hills, Oklahoma, *in* Cline, L. M. (ed.), Guidebook to the geology of the western Arkoma basin and Ouachita Mountains, Oklahoma: Oklahoma City Geological Guidebook, p. 109–121.

_____ 1989a, The Ouachita system, *in* Bally, A. W.; and Palmer, A. R. (eds.), The geology of North America; an overview: Geological Society of America, The Geology of North America, v. A, p. 371–396.

_____ 1989b, Ouachita thrust belt and Arkoma basin, *in* Hatcher, R. D., Jr.; Thomas, W. A.; and Viele, G. W. (eds.), The Appalachian-Ouachita orogen in the United States: Geological Society of America, The Geology of North America, v. F-2, 621–634.

Babaei, A.; and Viele, G. W., 1992, Two-decked nature of the Ouachita Mountains, Arkansas: Geology, v. 20, p. 995–998.

Briggs, Garrett, 1973, Geology of the eastern part of the Lynn Mountain syncline, Le Flore County, Oklahoma: Oklahoma Geological Survey Circular 75, 34 p.

Cline, L. M., 1960, Stratigraphy of the Late Paleozoic rocks of the Ouachita Mountains, Oklahoma: Oklahoma Geological Survey Bulletin 85, 113 p.

Comstock, T. B., 1888, Report upon the geology of western central Arkansas with especial reference to gold and silver, *in* Branner, J. C., Annual report for 1888: Arkansas Geological Survey, v. 1, p. 1–299.

Ethington, R. L.; Finney, S. C.; and Repetski, J. E., 1989, Biostratigraphy of the Paleozoic rocks of the Ouachita orogen, Arkansas, Oklahoma, West Texas, *in* Hatcher, R. D., Jr.; Thomas, W. A.; and Viele, G. W. (eds.), The Appalachian-Ouachita orogen in the United States: Geological Society of America, The Geology of North America, v. F-2, p. 563–574.

Feenstra, R.; and Wickham, J., 1975, Evolution of folds around Broken Bow uplift, Ouachita Mountains, southeastern Oklahoma: American Association of Petroleum Geologists Bulletin, v. 59, p. 974–985.

Graham, S. A.; Dickinson, W. R.; and Ingersoll, R. V., 1975, Himalayan-Bengal model for flysch dispersal in the Appalachian-Ouachita system: Geological Society of America Bulletin, v. 86, p. 273–286.

Haley, B. R.; Glick, E. E.; Bush, W. V.; Clardy, B. F.; Stone, C. G.; Woodward, M. B.; and Zachry, D. L., 1976, Geological map of Arkansas: Arkansas Geological Commission and U.S. Geological Survey, scale 1:500,000.

Hanor, J. S.; and Baria, L. R., 1977, Controls on distribution of barite deposits in Arkansas, *in* Stone, C. G. (ed.), Symposium on the geology of the Ouachita Mountains, v. 2: Arkansas Geological Commission, p. 42–49.

Honess, C. W., 1923, Geology of the southern Ouachita Mountains of Oklahoma: Oklahoma Geological Survey Bulletin 32, part 1, 278 p.

Houseknecht, D. W., 1986, Evolution from passive margin to foreland basin: the Atoka Formation of the Arkoma basin, south-central U.S.A.: International Association of Sedimentologists Special Publication 8, p. 327–345.

Keller, G. R.; Braile, L. W.; McMechan, G. A.; Thomas, W. A.; Harder, S. H.; Chang, W. F.; and Jardine, W. G., 1989, Paleozoic continent-ocean transition in the Ouachita Mountains imaged from PASSCAL wide-angle seismic reflection-refraction data: Geology, v. 17, p. 119–122.

King, P. B., 1937, Geology of the Marathon region: U.S. Geological Survey Professional Paper 187, 148 p.

_____ 1975, Ancient southern margin of North America: Geology, v. 3, p. 732–734.

Lillie, R. J., 1985, Tectonically buried continent/ocean boundary, Ouachita Mountains, Arkansas: Geology, v. 13, p. 18–21.

Lillie, R. J.; Nelson, K. D.; de Voogd, B.; Brewer, J. A.; Oliver, J. E.; Brown, L. D.; Kaufman, S.; and Viele, G. W., 1983, Crustal structure of Ouachita Mountains, Arkansas: a model based on integration of COCORP reflection profiles and regional geophysical data: American Association of Petroleum Geologists Bulletin, v. 67, p. 907–931.

Miser, H. D., 1929, Structure of the Ouachita Mountains of Oklahoma and Arkansas: Oklahoma Geological Survey Bulletin 50, 30 p.

_____ 1954, Geologic map of Oklahoma: U.S. Geological Survey in cooperation with Oklahoma Geological Survey, scale 1:500,000.

Miser, H. D.; and Purdue, A. H., 1929, Geology of the DeQueen and Caddo Gap Quadrangles, Arkansas: U.S. Geological Survey Bulletin 808, p. 195 p.

Nielsen, K. C.; Viele, G. W.; and Zimmerman, J., 1989, Structural setting of the Benton–Broken Bow uplifts, *in* Hatcher, R. D., Jr.; Thomas, W. A.; and Viele, G. W. (eds.), The Appalachian-Ouachita orogen in the United States: Geological Society of America, The Geology of North America, v. F-2, p. 635–660.

Niem, A. R., 1977, Mississippian pyroclastic flow and ash-fall deposits in the deep-marine Ouachita flysch basin, Oklahoma and Arkansas: Geological Society of America Bulletin, v. 88, p. 49–61.

Noble, P. J., 1993, Paleoceanographic and tectonic implications of a regionally extensive Early Mississippian hiatus in the Ouachita system, southern midcontinental United States: Geology, v. 21, p. 315.

Purdue, A. H.; and Miser, H. D., 1923, Hot Springs Folio, Arkansas: U.S. Geological Survey Geologic Atlas of the United States, Folio 215, 12 p.

Ragland, B. C. S., 1991, Gravity investigation of a portion of the Ouachita central zone, southeastern Oklahoma and western Arkansas [abstract]: Oklahoma Geology Notes, v. 51, p. 207–208.

Ramberg, H., 1961, Contact strain and folding instability of a multilayered body under compression: Geologische Rundschau, v. 51, p. 405–439.

_____ 1964, Selective buckling of composite layers with contrasted rheological properties, a theory for simultaneous formation of several orders of folds: Tectonophysics, v. 1. p. 307–341.

Ramsay, J. G.; and Huber, M. I., 1987, The techniques of modern structural geology, vol. 2: Academic Press, London, p. 309–700.

Thomas, W. A., 1976, Evolution of Ouachita-Appalachian continental margin: Journal of Geology, v. 84, p. 323–324.

_____ 1991, The Appalachian-Ouachita rifted margin of southeastern North America: Geological Society of America Bulletin, v. 103, p. 415–431.

Underwood, M. B.; and Viele, G. W., 1985, Early Pennsylvanian tectonic transition within the frontal Ouachitas of Arkansas [abstract]: Geological Society of America Abstracts with Programs, v. 17, p. 195.

Viele, G. W., 1966, The regional structure of the Ouachita Mountains of Arkansas, a hypothesis, *in* Flysch facies and structure of the Ouachita Mountains: Kansas Geological Society 29th Field Conference Guidebook, p. 245–278.

_____ 1973, Structure and tectonic history of the Ouachita Mountains, Arkansas, *in* DeJong, K.; and Scholten, R. (eds.), Gravity and tectonics: John Wiley and Sons, New York, p. 361–377.

_____ 1977, A plate tectonic model, Ouachita Mountain folded belt [abstract]: Geological Society of America Abstracts with Programs, v. 9, p. 661–662.

_____ 1979, Geological map and cross section eastern Ouachita Mountains, Arkansas: map summary: Geological Society of America Bulletin, v. 90, p. 1096–1099.

Viele, G. W.; and Thomas, W. A., 1989, Tectonic synthesis of the Ouachita orogenic belt, *in* Hatcher, R. D., Jr.; Thomas, W. A.; and Viele, G. W. (eds.), The Appalachian-Ouachita orogen in the United States: Geological Society of America, The Geology of North America, v. F-2, p. 695–728.

Weber, J. C.; and Zimmerman, J., 1988, Macroscopic structural geology of the central Cossatot Mountains and surrounding areas, Benton uplift, Arkansas, *in* McFarland, J. D., III (ed.), Contributions to the Geology of Arkansas: Arkansas Geological Commission, Little Rock, p. 85–94.

Welland, M.; Cambray, F. W.; and Voight, D. S., 1985, Structural and stratigraphic fabric of the Ouachita thrustbelt, Ok. and Ark.: a Paleozoic accretionary complex [abstract]: Geological Society of America Abstracts with Programs, v. 17, p. 746.

Wickham, J.; Roeder, D. R.; and Briggs, G., 1976, Plate tectonic models for the Ouachita fold belt: Geology, v. 4, p. 173–176.

Interpretation of Structure from Surface Geology, Frontal Ouachitas, Southeastern Oklahoma

Colin Mazengarb
Institute of Geological and Nuclear Sciences
Lower Hutt, New Zealand

ABSTRACT.—Complexly folded and faulted turbidite sequences (Atoka Formation) dominate the surface geology of the Ouachita frontal imbricate zone near Heavener, in southeastern Oklahoma. Because of patchy exposures, few marker beds, and extremely poor biostratigraphic and lithostratigraphic control, it is difficult to interpret the structural relations from surface geology alone. The keys to understanding the geology are an areally exhaustive field-mapping program, formline construction, and applying thrust-belt principles. Ideally, subsurface information should be included in this project, but few wells have been drilled in the area and seismic data were not freely available.

The interpreted geologic map of the Hontubby 7.5′ Quadrangle and part of the Loving 7.5′ Quadrangle reveals a significantly imbricated stack of moderately to steeply dipping thrust slices containing numerous folds and tear faults. Folds are typically tight to isoclinal and are generally modeled as fault-propagation folds. Geologic cross sections made for the area were cut off at shallow depth and were not balanced, because of the many uncertainties (both stratigraphic and structural) that still remain.

The boundary between the Ouachita frontal imbricate zone and the Arkoma fold belt is complex and probably is very different from the traditional concept of a single south-dipping thrust fault (the Choctaw fault). Instead, a series of thrusts forming a passive roof duplex could be a better alternative concept in some parts, in which case the boundary fault is a backthrust. This hypothesis needs to be tested.

INTRODUCTION

This paper serves (1) to document the techniques used to map and interpret the geology of the Hontubby 7.5′ Quadrangle and the Oklahoma part of the Loving 7.5′ Quadrangle of southeastern Oklahoma (Mazengarb and Hemish, 1993), and (2) to comment on important problems and findings. The map with cross sections has been published separately (Mazengarb and Hemish, 1993).

The mapping program was carried out by Mazengarb and Hemish in the autumn of 1991, as part of the cooperative geologic mapping project COGEOMAP between the U.S. Geological Survey (USGS), Oklahoma Geological Survey (OGS), and Arkansas Geological Commission (AGC). The study area is situated immediately west of Arkansas and south of the town of Heavener (Fig. 1). Forested hills of the Ouachita Mountains dominate the quadrangles, whereas broad alluvial flats occur in valley floors, which are commonly in pasture. Outcrops of rock are generally sparse, but a surprising amount of data was obtained from an areally exhaustive field-mapping program. Satellite images and aerial photography were also useful. To date, there has been comparatively little subsurface investigation of the area (for hydrocarbon exploration) to assist the surface interpretation. Logs of holes drilled by Arkla Exploration and Hunt Oil in nearby Arkansas were used, but proprietary seismic data could be examined only briefly.

Although some existing surface maps were available (oil-company studies, university theses, OGS bulletins), the area was completely remapped. Recent COGEOMAP mapping by OGS staff provides important control to the west, and less-detailed work in nearby Arkansas, by Charles Stone and Boyd Haley (AGC), was also valuable.

GEOLOGIC SETTING

The stratigraphy of the study area (Fig. 2) comprises two sequences of contrasting facies that subsequently have been structurally juxtaposed. Shallow-water (Arkoma facies) Atokan sequences currently lie beside deep-water (Ouachita facies) sequences of the same age, but the original basin configuration, distances, and relations (in space and

Mazengarb, Colin, 1995, Interpretation of structure from surface geology, frontal Ouachitas, southeastern Oklahoma, *in* Johnson, K. S. (ed.), Structural styles in the southern Midcontinent, 1992 symposium: Oklahoma Geological Survey Circular 97, p. 26–31.

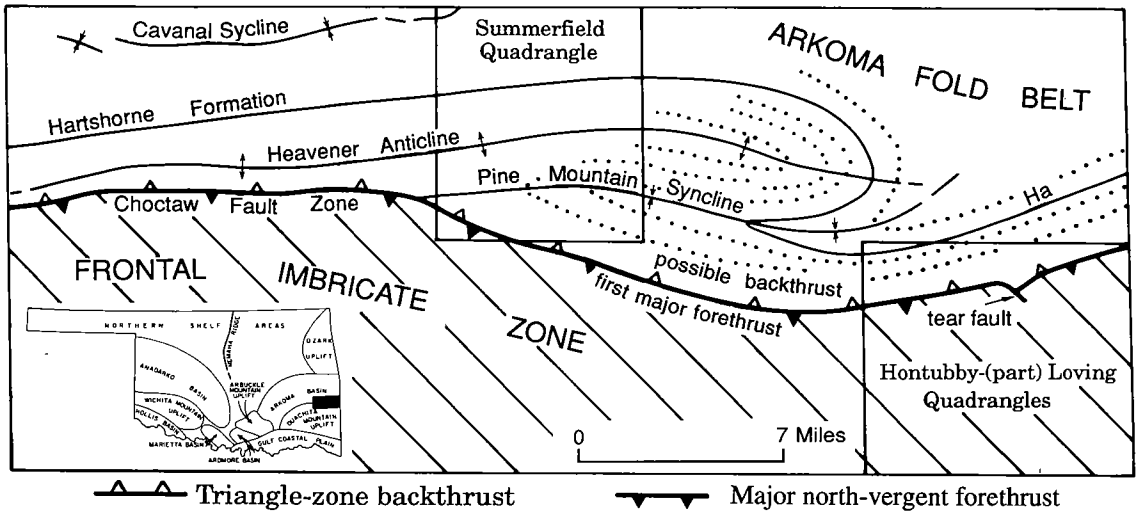


Figure 1. Location of study area (Hontubby and Loving Quadrangles) in the Ouachita frontal imbricate zone and Arkoma fold belt. Ha = Hartshorne Formation.

time) between the two facies realms is not well understood. Biostratigraphic control for both sequences is poor, and the Ouachitas facies cannot be subdivided lithostratigraphically. Growth faulting was an important controlling factor in the development of the Atokan sequences (Arbenz, 1989), so it is reasonable to invoke faults of this nature when attempting to reconstruct basin geometry (Fig. 2).

During the Carboniferous, a major collision and/or subduction event formed the Ouachita thrust belt, pushing the rocks of the Ouachita facies northward against the Arkoma facies rocks. The Choctaw fault, which now separates the two depositional suites, has traditionally been considered as the thrust front (i.e., the northern limit of compressional, detached structures), but this interpretation is not correct. Although a strong contrast in structural styles occurs here (the Arkoma facies being structurally simpler and less disrupted), it has been previously realized that thin-skinned deformation is also present in the Arkoma facies (e.g., Arbenz, 1989); thus, technically, the thrust front is some distance farther north. I accept the Arbenz (1989) description of the Arkoma basin as a mildly compressed and detached fold belt (Arkoma fold belt) and the frontal Ouachitas as the location of emergence and onset of major north-vergent thrusting (Ouachita frontal imbricated zone).

STRUCTURAL TECHNIQUES

This discussion is largely confined to the structurally complex Atoka Formation south of the Choctaw fault. North of the fault, the lithostratigraphic relations are obvious, within the sequences represented; but to the south, where complex structure and absence of markers are typical, the sequences are poorly understood. A goal of the field program was to attempt to get as even a spread of outcrop data over the map as possible. Some sandstone beds could be traced short distances, but generally all that could be determined was orientation and facing direction (tops of beds), plus lithological description. Some minor folds are exposed, and they were measured taking into account their style and vergence. Many reversals of facing direction were identified during the field program, but as the structure was not visible, it was often impossible to determine whether the structure is a fault or fold. Such information forms the raw data for the structural interpretation.

The two most important interpretive techniques used were formline constructions and thrust-belt principles.

Formline Construction

Formlines are lines constructed parallel to the intersection of bedding planes with the land surface; they should parallel any marker beds. One attempts first to draw and recognize formline sets, taking into account facing directions; then structures are drawn at the set intersections, be they folds or faults. For instance, faults may be detected where one formline set is truncated by another.

The drawing of formlines is somewhat an intuitive artform (akin to seismic interpretation). One tries to honor all the data, but sometimes the odd data point is assumed to be "noise" if it cannot be satisfactorily explained. Formlines can be drawn relatively quickly, because the lines will not be significantly affected by topographic variations in an area of typically subdued relief and steep bedding. It is reassuring that the results of this approach create geometric patterns similar to obvious structures seen on satellite imagery.

Thrust-Belt Principles

In the mapping, we aimed to provide realistic structural interpretations in terms of relevant published thrust-belt geometries. For instance, where thrust intersections were ambiguous, we assumed a normal imbrication sequence, so the forward thrust is younger and truncates or folds faults to the rear. This assumption appears to work well in many instances. Where the truncation rule does not work, however, it is uncertain whether the thrust in question is truly out of sequence or whether it is a younger, deeper thrust breaking back through the pile.

Most observed and inferred folds are tight, north-verging structures, and we modeled these structures as fault-propagation folds. Thrust faults were drawn to only cut up-section within the hanging wall.

CROSS SECTIONS

The cross sections of Mazengarb and Hemish (1993) do not show much of the deeper structure and are unbalanced because the structural and stratigraphic uncertainties are so great. The available subsurface information did permit the drawing of a detachment surface that, although probably overly simplistic, shows a major buried ramp approximately below the trace of the Choctaw fault. The fault, which dips ~45° south, was probably initially a growth fault and later was exploited as a ramp during the northward thrusting.

The importance of gathering dip information from a wide zone on either side of the cross-section line is stressed here, because of observed lateral variations of dip value along strike (even though facing and strike directions are constant) in individual thrust slices. Significant differences in geom-

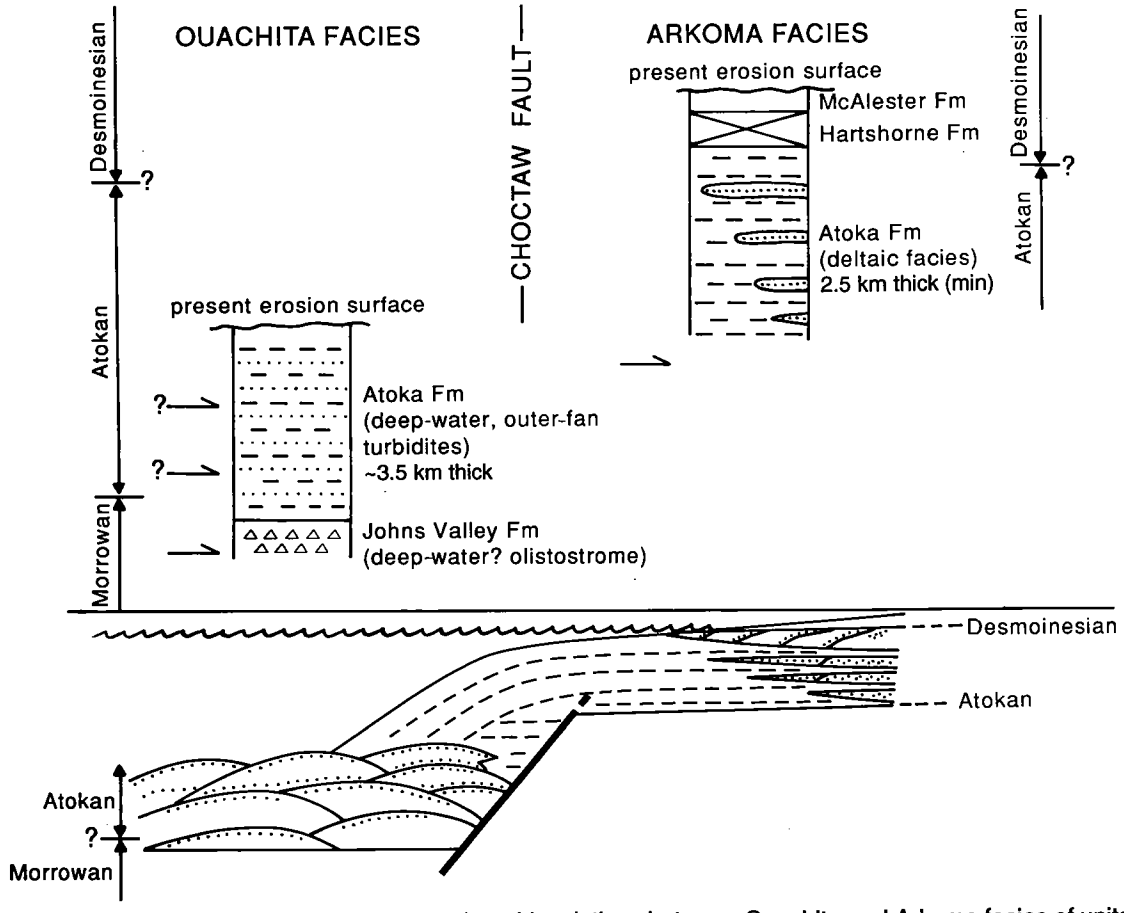


Figure 2. Upper diagram shows chronostratigraphic relations between Ouachita and Arkoma facies of units exposed in study area. The uncertainties in this diagram are considerable because of the poor stratigraphic control. Thrust arrows emphasize tectonic dismembering process that occurred subsequent to deposition. Lower diagram shows hypothetical basin cross section (no scale intended) to demonstrate relation between Atoka Formation of Arkoma facies and Atoka Formation of Ouachita facies. Here I suggest that the two were separated by one or more growth faults that controlled the position of the shelf edge. It is purely speculative whether the shelf facies prograded over the deep basin as shown, because syn- or postorogenic erosion has removed that part of the section.

etry would be apparent between closely spaced cross sections, even in relatively simple areas if the dips were not averaged out. I have seen this well displayed on a shore platform involving identical rock types near East Cape, New Zealand. The rocks there are incorporated in a thrust belt that has some structural similarities to the Ouachitas. In the New Zealand example, although the stratigraphy is grossly intact, there are many minor faults, commonly disguised in shale interbeds, that produce local structural complications.

The core areas of many Ouachita folds are tight, complex structures that, if one disregarded the outlying limbs and along-strike information, would produce unusual geometries; e.g., an anticline with both limbs overturned would have a mushroom-shaped profile. In an example of disharmonic folding involving contrasting rock types, a 1-m-thick sandstone bed is moderately folded into an archlike anticline, whereas the thinner-bedded rocks underneath are tightly folded into at least two or more fold pairs. It would seem reasonable to draw cross sections with simplified fold forms in this case.

INTERPRETED STRUCTURAL STYLE

The map and cross sections of Mazengarb and Hemish (1993) show an imbricate stack of thrust slices containing many folds and tear faults. An imbricate fan-type geometry is restricted to the very front, whereas the majority of thrusts are steep and are stacked parallel to each other.

Tear faults are a necessary interpretation in a number of instances. There is a particularly complex zone (including backthrusts) along the Blackfork River west of Haw Creek settlement, and one wonders if a deep-seated structure (e.g., a dip-parallel ramp on the basal detachment) is affecting the overlying thrust geometry. A north-south line at about this point does seem to separate two areas of contrasting complexity, with the west side being much more complex.

CHOCTAW FAULT: THRUST, BACKTHRUST, FACIES BOUNDARY, ANTICLINE, TRIANGLE ZONE, OR WHAT?

The Choctaw fault is a difficult feature to accurately locate, as evidenced by its varying positions on published maps, probably because the fault is not exposed at the surface. Furthermore, at outcrop scale, it is often difficult to decide whether one is looking at Arkoma or Ouachita facies. Some mappers (e.g., Marcher and Bergman, 1983), assuming that the gross lithologic difference between the two facies has a geomorphic expression, have placed the fault on the topographic boundary between the Ouachita Mountain foothills and the Quaternary floodplain; the Oklahoma Geological Survey COGEOMAP mappers have instead used mainly structural criteria (diverging facing directions) to place it farther north between Wilburton and Le Flore. Our most recent mapping in the Summerfield 7.5′ Quadrangle (Hemish and Mazengarb, 1992) indicates that the area of diverging facing directions is probably at the western end of the Heavener anticline, in which case the Choctaw fault must lie farther south.

The Choctaw fault has been traditionally regarded as a single, south-dipping, leading thrust fault; however, because the fault is never exposed, the traditional view may be based on assumptions that are wrong. First, it is evident from previous OGS COGEOMAP maps that the so-called Choctaw fault is not a single fault, but an array of splaying faults, in which case a name change to "Choctaw fault zone" may be a better way of referring to the structure. This fault zone is further complicated in the Hontubby 7.5′ Quadrangle where it is offset by a tear fault (Fig. 1). As previously discussed, the Choctaw fault is not the true thrust front; the basal detachment is in fact buried beneath the Arkoma fold belt (Arbenz, 1989) and is probably a Morley (1986) type 1a buried thrust front, in large part.

What then is the Choctaw fault? For a start, it is certainly a fault and not merely a sedimentary contact between different facies. Structural relations, including differences in tectonic shortening between the two structural belts (Arbenz, 1989), require faults to be invoked somewhere in the vicinity of the boundary, but does the facies boundary necessarily have to be the exact position of the fault in all cases? Could the original sedimentary contact between the Arkoma and Ouachita facies be preserved locally, in which case it may lead to the incorrect positioning of the fault? In most places, however, a fault of some orientation is a reasonable assumption close to, or on, the facies boundary, although seldom is the geometry of the fault known.

The traditional assumption that the Choctaw fault is a south-dipping fault, along which the Ouachita facies was thrust over the Arkoma facies before being eroded back to its present position (similar to Morley's [1986] emergent-type thrust-front model) must be challenged in light of the above-described unclear geometry of the fault. I propose an alternative model; in doing so, I am not rejecting outright the traditional south-dipping thrust model, but merely provoking further discussion and, I hope, scientific testing. It could be argued that the Choctaw fault is, at most, only a weakly emergent thrust (Morley, 1986) because (1) the Arkoma sequence shows no corresponding increase in vitrinite/coal rank (Brian Cardott [OGS], personal communication, 1992) indicative of tectonic burial and (2) there is no evidence of synorogenic conglomerates (erosion of the emerging thrusts). I agree, along with others (e.g., Arbenz, 1989), that the Ouachita/Arkoma boundary is in fact a triangle zone, which is a structure bounded by thrust surfaces involving a component of backthrusting. The kinematics and geometry of Ouach-

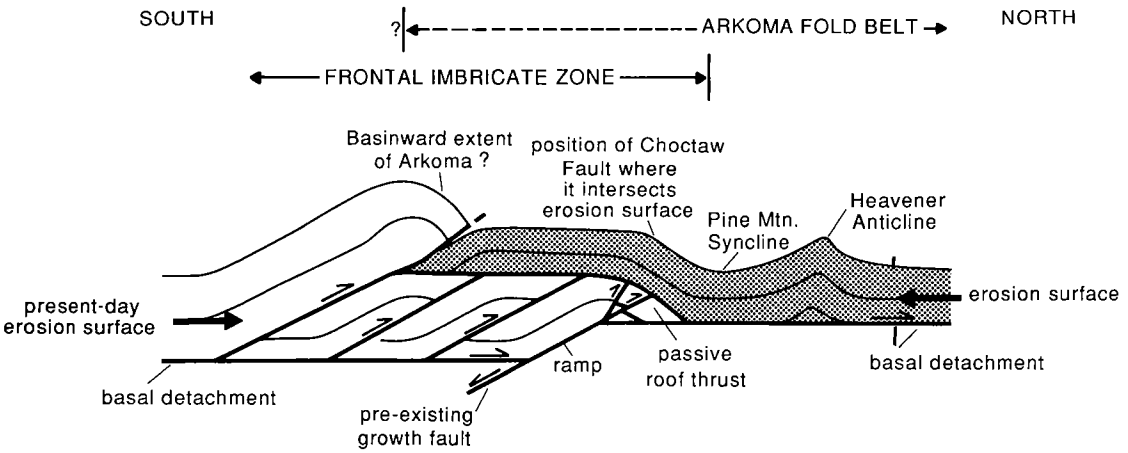


Figure 3. Hypothetical model (adapted from Washington, 1987) of the Arkoma fold belt and the Ouachita frontal imbricate zone, represented as a passive roof duplex. There may be other equally valid models, but this one at least allows a partial decoupling between sequences of the shelf (in gray) and basin (in white) so that only a small portion of the forward movement is transferred into the Arkoma basin: this interpretation supports a nonemergent geometry. The model assumes that the shelf margin prograded beyond the growth fault so as to provide a structural roof during the later thrusting. Beyond the extent of the original shelf margin the structures may have been roofless, but there is no evidence to support a strongly emergent thrusting style at this point.

ita triangle zones are not well understood, as few published cross sections have dared to project geology above the present erosion surface (Hardie [1988] is one exception). Commonly one sees the convergence of the forethrust and the backthrust coinciding approximately with the present erosion surface on published sections (e.g., Arbenz, 1989, fig. 3), but what is the intersection relation of the two faults. Does the forethrust offset or terminate the backthrust (e.g., Hardie, 1988)? Alternatively, is the backthrust a roof thrust (Fig. 3), or has a complex interaction process formed a fishtail structure? (A fishtail structure is analogous to two partially interleaved packs of cards, and, although I am not aware of a formal reference, it is an accepted term at the geology department of Rice University, Houston [Joan Flinch, personal communication, 1992]). Whatever model is chosen affects the map pattern; e.g., on what side of the thrust should the fault ticks be placed? Southward-verging structures along the Choctaw fault zone in the Hodgen 7.5′ Quadrangle (Suneson and Hemish, 1993) may be telling us that a backthrust is present locally; consequently, I have placed fault ticks on both sides of the fault to represent the ambiguity (Fig. 1).

CONCLUSIONS

1. Formline construction and thrust-belt principles are powerful tools for resolving the complexly deformed rock sequences of the Ouachita frontal imbricated zone.

2. Detailed surface mapping by the COGEOMAP participants has greatly improved the positioning of the Ouachita/Arkoma facies boundary and structural boundaries (Choctaw fault zone), although the fundamental question, "What is it?" is still unanswered. Traditional views on the geometry of the Choctaw fault are based on conceptual models that may be too simplistic.

ACKNOWLEDGMENTS

I am grateful to Arkla Exploration Ltd. for providing subsurface information and welcome advice. Jim Anderson prepared the figures. Neil Suneson, William Perry, and Kaspar Arbenz reviewed the manuscript, prompting significant revision. Thanks to all who helped make my visit possible and to all those Okies who made this Kiwi feel welcome.

REFERENCES CITED

Arbenz, J. K., 1989, Ouachita thrust belt and Arkoma basin, in Hatcher, R. D., Jr.; Thomas, W. A.; and Viele, G. W. (eds.), The Appalachian-Ouachita orogen in the United States: Geological Society of America, The Geology of North America, v. F-2, p. 621–634.

Hardie, W. E., 1988, Structural style of the frontal thrust belt of the Ouachita Mountains, southern Pittsburg County, Oklahoma: Oklahoma Geology Notes, v. 48, p. 232–246.

Hemish, L. A.; and Mazengarb, Colin, 1992, Geologic map of the Summerfield Quadrangle, Le Flore County, Oklahoma: Oklahoma Geological Survey COGEOMAP Geologic Quadrangle Map, scale 1:24,000.

Marcher, M. V.; and Bergman, D. L., 1983, Reconnaissance of the water resources of the McAlester and Texarkana Quadrangles, southeastern Oklahoma: Oklahoma Geological Survey Hydrologic Atlas 9, scale 1:250,000.

Mazengarb, Colin; and Hemish, L. A., 1993, Geologic map of the Hontubby and Loving Quadrangles, Le Flore County, Oklahoma: Oklahoma Geological Survey COGEOMAP Geologic Quadrangle Map, 2 sheets, scale 1:24,000.

Morley, C. K., 1986, A classification of thrust fronts: American Association of Petroleum Geologists Bulletin, v. 70, p. 12–25.

Suneson, N. H.; and Hemish, L. A., 1993, Geologic map of the Hodgen Quadrangle, Le Flore County, Oklahoma: Oklahoma Geological Survey COGEOMAP Geologic Quadrangle Map, scale 1:24,000.

Washington, P. A., 1987, A classification of thrust fronts: discussion: American Association of Petroleum Geologists Bulletin, v. 71, p. 737–738.

The Dyer Mountain Fault Zone: Southerly Directed Thrusting in the Broken Bow Uplift

Kent C. Nielsen and Qingming Yang
The University of Texas at Dallas
Richardson, Texas

ABSTRACT.—Late Carboniferous deformation in the Ouachita Mountains of Oklahoma is characterized by northerly directed thrusts. To the north of the Broken Bow uplift are the large-scale, northerly verging folds and thrust faults of the central zone; however, within the Broken Bow uplift, southerly verging structures dominate. The Broken Bow uplift has been subdivided into four structural domains: Hochatown dome, Carter Mountain anticlinorium (CTMA), Linson Creek synclinorium, and Cross Mountain anticlinorium. The Dyer Mountain fault zone (DMFZ) separates the Hochatown dome, on the south, from the Carter Mountain anticlinorium, on the north. The DMFZ has been traced from the western flank of the uplift to the Broken Bow Reservoir (6 mi). The DMFZ is characterized by a complex pattern of faults, imbricate slices, and rootless folds. The faults dip steeply to the north. Refolded mesoscopic first-generation folds in the footwall of the DMFZ indicate southerly directed thrusting associated with the second stage of folding. The first-generation folds are tight to isoclinal, subhorizontal, with sharp hinges and planar limbs. The second-generation folds are coaxial with the first and are open to tight, inclined, and southerly verging. A megascopic second-generation syncline (wavelength 1.2 mi) has been outlined just south of the DMFZ in the Arkansas Novaculite. Northerly dipping faults truncate the south-facing limbs of the second-generation folds, and flattening associated with the faults modifies both first- and second-generation folds. Steeply dipping limbs are folded into recumbent buckles, whereas gently dipping limbs are thinned. The early slaty cleavage is rotated, and a new locally developed rough cleavage is associated with pencil structures. First-generation folds trend east–west and are subhorizontal in the footwall of the DMFZ; but in the hanging wall, they are dispersed about a great circle, which suggests rotation associated with simple shear. These mesoscopic data suggest initial southerly directed thrusting along the DMFZ. North of CTMA, faults reorienting the slaty cleavage and cutting across early fold structures dip toward the south, forming a fan-like distribution south of the Boktukola fault of the central zone. The second-generation folds and associated faults are interpreted to be related to northerly translation of the Ouachita sequence. The earliest folds are interpreted as deformation related to initial collapse of the Ouachita basin.

INTRODUCTION

The Ouachita Mountains represent the deformed Paleozoic margin of the North American craton. These shelf, continental-slope, and abyssal-plain sediments were deposited from Late Cambrian to Late Pennsylvanian time. During Early Mississippian time the Ouachita basin deepened rapidly, and deposition changed from slow sedimentation of shale- and chert-dominated successions, to rapid turbidite accumulation. During Middle to Late Pennsylvanian deformation, the entire sequence underwent detachment and large-scale translation to the north. The resulting fold and thrust belt extends ~1,200 mi, from Alabama through Arkansas and Oklahoma, and on into Texas (Fig. 1).

On a regional scale, the structural style is characterized by northerly verging folds and thrust faults (Fig. 2). Data from extensive hydrocarbon exploration in Oklahoma indicates that the fault geometry is listric (i.e., steeply dipping near the surface, becoming more gently dipping at depth) (Hendricks and others, 1947; Suneson and others, 1990). The Ouachita fold and thrust belt has many structural features in common with other thrust belts, including a triangular zone, an imbrication fan, and a pos-

Nielsen, K. C.; and Yang, Qingming, 1995, The Dyer Mountain fault zone: southerly directed thrusting in the Broken Bow uplift, *in* Johnson, K. S. (ed.), Structural styles in the southern Midcontinent, 1992 symposium: Oklahoma Geological Survey Circular 97, p. 32–44.

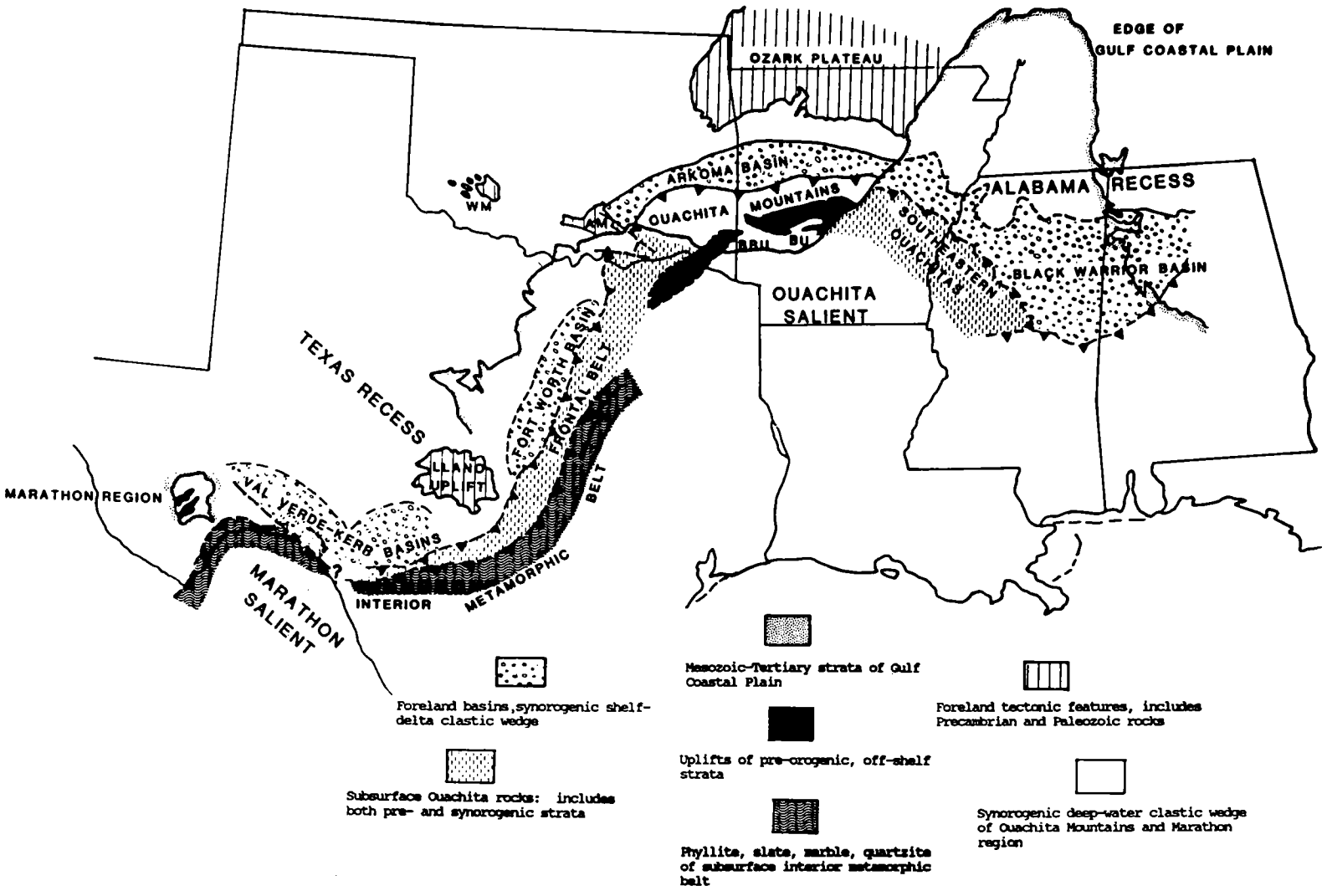


Figure 1. Distribution of the Ouachita System across southern North America (after Viele, 1989). Benton uplift (BU), Broken Bow uplift (BBU), Arbuckle Mountains (AM), and Wichita Mountains (WM).

sible duplex zone in the Potato Hills. The spacing of the thrust faults also follows a pattern seen in other thrust belts; very closely spaced at the leading edge, and more broadly spaced in the interior areas (Bally and others, 1966; Price, 1981).

Feenstra and Wickham (1975) subdivide the Ouachita Mountains in Oklahoma. The frontal zone represents the imbrication fan (between the Choctaw and Windingstair thrusts) (Fig. 2). The central zone consists of the widely spaced reverse faults cutting the thick Carboniferous turbidites. The Broken Bow uplift (Fig. 2) contains the oldest, highest metamorphic grade, most intensely deformed rocks. The Appalachian and Rocky Mountains have similar subdivisions and there is a rough parallelism with the Ouachita mountain belt. However, whereas the Appalachian and Rocky Mountain belts show a consistent increase in metamorphic grade and intensity of deformation toward the hinterland, the highest grade of metamorphism is only lower greenschist in the Ouachita Mountains (Flawn and others, 1961; Denison and others, 1977). Southeast of the Broken Bow uplift, the grade of metamorphism decreases and the style of deformation is similar to the central and frontal zones (Walthall, 1967).

Within both the Broken Bow and Benton uplifts, a polyphase deformational history has been established (Viele, 1973; Feenstra and Wickham, 1975; Nielsen and others, 1989). Although the succession of events varies, depending on location, the southerly verging structures developed relatively early in the deformation history of both uplifts. This opposing sense of vergence has stimulated many discussions and is the focus of this paper. The area of interest is the Broken Bow uplift in southeastern Oklahoma.

BROKEN BOW UPLIFT

The Broken Bow uplift was originally mapped by Honess (1923). Building on his efforts, the uplift was subdivided into four large structures: three large folds (Cross Mountain anticlinorium, Linson Creek synclinorium, and Carter Mountain anticlinorium) in the northern half of the uplift and the Hochatown dome in the southern part of the uplift (Nielsen, 1985; Nielsen and others, 1989) (Fig. 3). The folds are doubly plunging with upright or slightly inclined axial surfaces. In general, from north to south, the folds are progressively more overturned toward the south (Feenstra and Wickham, 1975). These folds have a core of the Ordovician Womble Shale and Bigfork Chert. The southern half of the uplift is a large domal structure, the Hochatown dome (Nielsen and others, 1989). The flank of this dome is defined by a middle-Paleozoic sequence, including the Bigfork Chert, Blaylock Sandstone, and Arkansas Novaculite (Fig. 3). The trend of the dome and of the overall Broken Bow uplift is northeast–southwest. Detailed mapping in this area has led to re-evaluation of the deformational history and contact relationships between the Carter Mountain anticlinorium (CTMA) and the Hochatown dome. The remainder of this paper will focus on the deformation history with particular attention to the Dyer Mountain fault zone (DMFZ) as a major tectonic contact between the CTMA and the Hochatown dome.

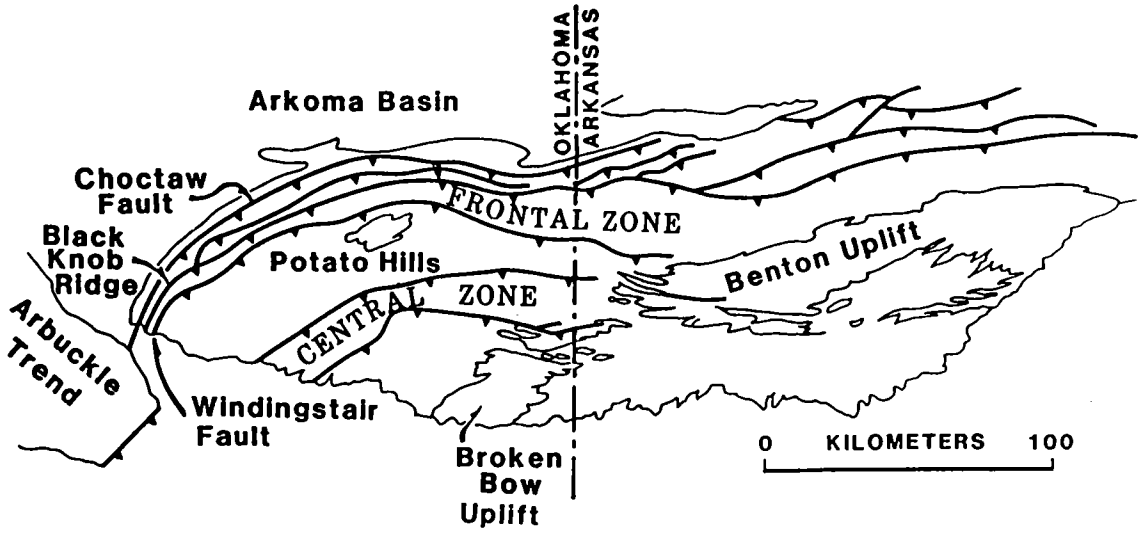


Figure 2. Principal structural elements of the Ouachita Mountains of Arkansas and Oklahoma.

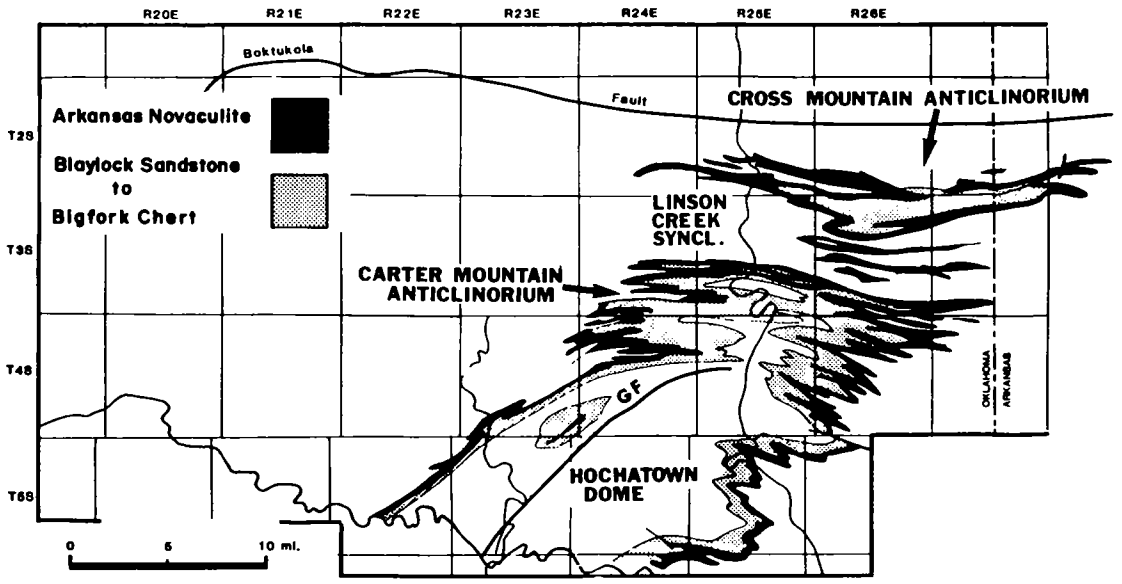


Figure 3. Subdivisions of the Broken Bow uplift in southeastern Oklahoma (modified from Honess, 1923). GF is the Glover fault. The dotted pattern (Blaylock Sandstone) represents the interval from the top of the Bigfork Chert to the base of the Arkansas Novaculite.

Hochatown Dome

The oldest rocks of the Ouachita Mountains crop out in the core of the Hochatown dome. For example, the oldest unit, the Collier Formation, has been identified as Late Cambrian to Early Ordovician age by Ethington and others (1989). This old sequence is shale-dominated and, therefore, is very poorly exposed. Mapping in this area includes the initial work of Honess (1923), followed by another general analysis by Pitt (1955) and several more-recent detailed studies (Dunagan, 1981; Hubert, 1984; Dix, 1985; Erickson and Tapp, 1995). Common to all of the recent studies is the observation that the oldest rocks are repeated by closely spaced, low-angle faults developed in the shales. The result is a stack of shales (Womble and Mazarn Formations). The sense of motion on these low-angle faults has been difficult to constrain. The only lithologically distinctive units are the Collier Formation, the Crystal Mountain Sandstone, and the Lukfata Sandstone. However, Dunagan (1981) argued that the Lukfata Sandstone (Pitt, 1955; Flawn and others, 1961) was in fact a repeated section of Crystal Mountain Sandstone.

Hubert (1984) outlined at least three thrust nappes that repeat the Crystal Mountain Sandstone as well as part of the underlying Collier Formation. Relying on mesoscopic folds and boudinage patterns, Hubert (1984) proposed a dominant southeasterly vergence. Dix (1985) found a fold history consistent with this southeasterly vergence, and Erickson and Tapp (1995) examined kinematic indicators within the Womble Shale to conclude a southeasterly sense of motion. Drilling in this area has also revealed the same repetition of shale and sandstone to a depth of ~12,000 ft (Leander and Legg, 1988). Below this tectonically thickened sequence, the drilling records indicate a metamorphosed carbonate succession which has been correlated with the Arbuckle Group to the west. Therefore, the Hochatown dome surface exposures down to ~12,000 ft appear to be allocthonous, in fault contact with and overlying coeval Arbuckle facies. This geometry is similar to that proposed for the deep seismic profile obtained across the Benton uplift of Arkansas (Nelson and others, 1982).

The flanks of the Hochatown dome are commonly defined by the middle Paleozoic sequence which is characterized by cherts and sandstones. Consequently, there is a more pronounced relief, as well as better exposures. The deformational history of these rocks has been the focus of several workers since Honess (1923). Feenstra (1974) and Feenstra and Wickham (1975) documented variation in fold geometry from north to south in this flank sequence. They also pointed out unusual fold patterns and a locally developed cleavage that transected the dominant fold system. Nielsen (1982, 1988) and Nielsen and others (1989) have emphasized the polyphase history seen in these rocks.

The structural style seen along the eastern flank of the Broken Bow uplift is significantly different from that of the underlying core sequence (Nielsen

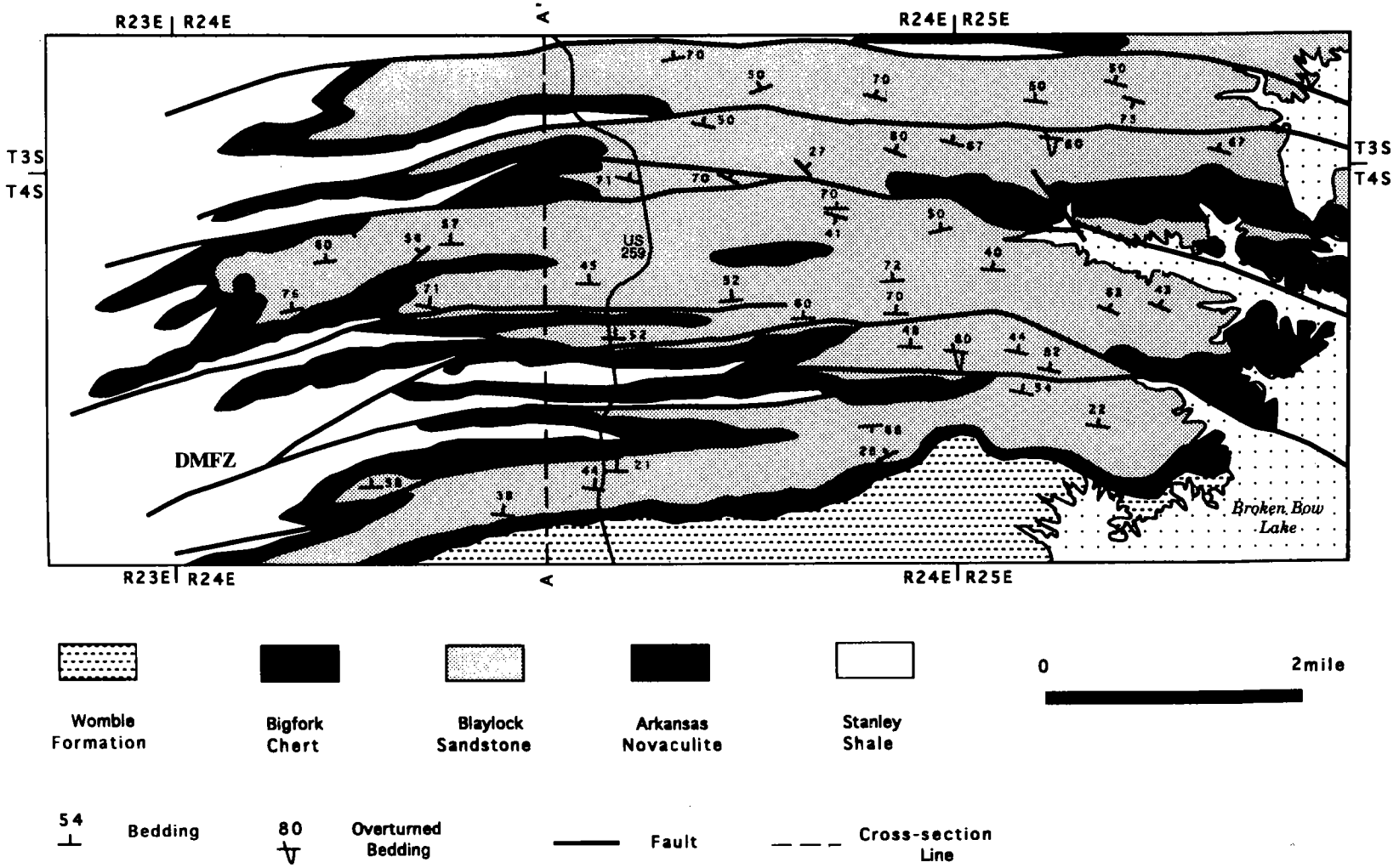


Figure 4. Western flank of the Broken Bow uplift illustrating the fault and fold relationships in the Carter Mountain anticlinorium. U.S. Highway 259 is the irregular line trending north–south just east of the dashed cross-section line A–A′. DMFZ = Dyer Mountain fault zone.

and others, 1989). Honess (1923) had originally suggested an unconformity within the core and mapped a younger fault, the Glover fault, trending in a northeasterly direction (Fig. 3). Miser (1929) used the mapping of Honess (1923) and proposed that the flank sequence was detached from the core. He believed that the Glover fault was the folded equivalent of the Boktukola fault to the north (Fig. 3). The resulting fenster is shown on the Oklahoma State Geologic Map, and represents a younger-over-older fault system. This fundamental question has remained unresolved; but recent work by Dix (1985) drew attention to the structural contrast. Colson (1992) made a detailed map across a portion of the proposed detachment, along the eastern flank, and agreed with the earlier map of Nielsen (1988). At this point, it appears that the eastern-flank sequence is detached from the underlying core sequence. On the other hand, on the west side of the uplift, the structural style and orientation of the flank sequence is more coherent with that of the underlying core sequence (Hubert, 1984). There is not general agreement about the detachment along the west flank (Dix, 1985; Hubert, 1984); however, the flank sequence is infolded with the Womble (and Mazarn) Formations in the Old Glory Mountain syncline (T. 4 S., R. 23 E.) (Fig. 3).

Carter Mountain Anticlinorium

North of the Hochatown dome, the Carter Mountain anticlinorium (CTMA) (Fig. 3) is characterized by the middle Paleozoic sequence, with the oldest exposed rocks being the Womble Formation. Honess (1923) mapped this area as a sequence of east–west trending, doubly plunging, tight folds. He also showed this fold sequence as continuous with the flanks of the Hochatown dome. His cross sections for this area show consistently southward verging folds and a few northerly dipping faults. Several of these northerly dipping faults were interpreted to have normal separation; however, an element of thrust offset was also inferred (Honess, 1923, p. 232–236). Johnson (1990) mapped the northeastern part of the CTMA and outlined a fold pattern similar to that of Honess (1923). He also documented various generations of faults. Although he indicated normal separation, he attributed the normal separation to reactivation of older thrust faults.

Mapping along the western side of the CTMA has revealed a more complex fold system than initially envisioned by Honess (1923) (Shore and Nielsen, 1987; Nielsen and others, 1989; Yang and Nielsen, 1992). Rather than being a continuous series of folds, the folds within the CTMA are dismembered (Fig. 4). On the north side of Carter Mountain, a major fault (northernmost fault in Fig. 4) truncates a westerly plunging anticline. This fault dips to the north and places Mississippian Stanley Shale against the Silurian Blaylock Sandstone. This fault, which was originally mapped by Honess (1923), led to his discussion of normal faults in the area. To the south, three more faults cut across successive anticlinal structures (Fig. 4). These faults all trend east–west in this area, approximately parallel to the trend of the folds, and also appear to be dipping to the north.

Dyer Mountain Fault Zone

Another fault zone is at the boundary between the CTMA and the Hochatown dome. This zone has been named the Dyer Mountain fault zone (DMFZ), because of the significant ridge by that name located near the reservoir in sec. 7, T. 4 S., R. 25 E. Within the fault zone, slices of the novaculite section are isolated by the fault splays and a few tight fold hinges have been identified. The sequence is generally facing towards the north. These faults can be followed from the western flank of the anticlinorium to the reservoir (6 mi). At the reservoir, the Bigfork Chert is in fault contact with upright Blaylock Sandstone (Fig. 4). The Bigfork Chert cropping out in the Hochatown dome can also be traced to the reservoir where it is possibly truncated by the DMFZ; unfortunately, however, this critical contact is located under the reservoir. The extension of the DMFZ to the east will be discussed later, and is the focus of current mapping. In the footwall of the DMFZ, the novaculite section is folded into a large syncline with a small anticlinal hinge truncated on the north side (Fig. 4). A cross section through the CTMA illustrates the imbricated nature of the folds, and particularly the DMFZ (Fig. 5). In summary, the CTMA contains a succession of faulted folds that are in tectonic contact with rocks of the Hochatown dome.

The history of movement along the DMFZ is assumed to be complex, reflecting the initial formation of the fault, as well as reactivation related to later stages of deformation. A detailed examination of mesoscopic structures, particularly in the footwall of the DMFZ, provides a consistent sense of rotation related to the second-generation folds. This southerly vergence is interpreted to reflect the initial motion on this fault zone. In other words, the first-generation folds apparently predate the DMFZ; whereas the second-generation folds are directly related to the development of the fault zone. Consequently, a review of the early fold generation is necessary.

The earliest folding documented in the flank sequence was accompanied by the development of regional slaty cleavage. These folds are tight to isoclinal, overturned, and southerly verging (Fig. 6). Characteristically, these folds have planar limbs and angular hinges. Data collected from outcrops along U.S. Highway 259 show that the upright limbs of the folds dip gently and the overturned limbs dip moderately toward the north (Fig. 7). The slaty cleavage is oriented nearly parallel to the

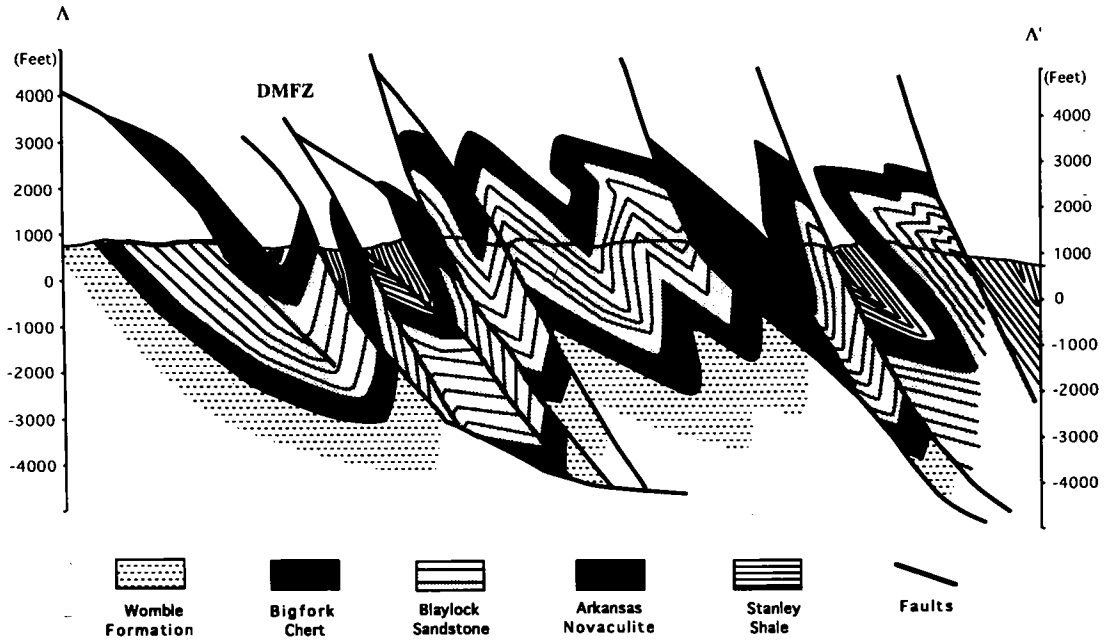


Figure 5. Cross section A–A′ across the Carter Mountain anticlinorium (right two-thirds of diagram), the northern Hochatown dome (far left), and the Dyer Mountain fault zone (DMFZ). Location is shown in Figure 4.



Figure 6. First-generation folds developed in the flank sequence of the Hochatown dome. Photograph taken along U.S. Highway 259, looking east.

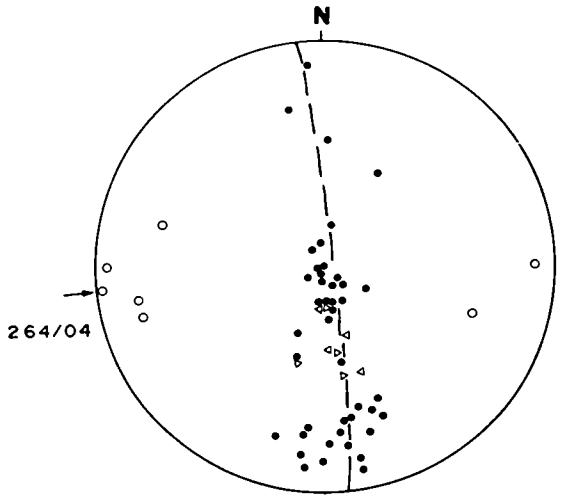


Figure 7. Orientation data for first-generation folds along the northwestern boundary of the Hochatown dome. Solid dots are poles to bedding, triangles are poles to cleavage, and open circles are mesoscopic fold axes.

upright limb, making these folds overturned and asymmetric. The fold axes plunge gently toward the west.

The second-generation folds are coaxial with the early folds, have more-rounded limbs and hinges, and are southerly verging as well (Fig. 8A). Their identification is based principally on the presence of folded slaty cleavage. In Figure 8A,B, the slaty cleavage can be followed around the hinge, dipping to the north in the southern limb and dipping to the south in the northern limb. Orientation data illustrates the more-open nature of the younger folds as well as the rotated cleavage (Fig. 9). In places, the early folds can be seen to be folded about the younger fold axes. A small anticline is exposed in the hinge area of the syncline discussed above (Fig. 8). The slaty cleavage is axial planar to this small anticline and is folded around the synclinal hinge. In many cases the axial surfaces of the early folds are clearly curviplanar. Other modifications to the earlier folds include development of recumbent buckles on the steeply dipping limbs, thinning of the upright limbs, and local development of pencil structures (Fig. 10) and a new subhorizontal rough cleavage. Commonly the north limbs of the second-generation synclines are truncated by northerly dipping faults (Fig. 11). These faults appear to repeat the section in the upright limbs and generate zones of disrupted folds in the overturned limbs of first-generation folds.

A larger-scale second-generation fold is located in the footwall of DMFZ (Fig. 4). The Arkansas Novaculite exposed along the margin of the Hochatown dome has been mapped across U.S. Highway 259 and into a large syncline just south of the DMFZ fault trace. The half-wavelength of this syncline is ~0.6 mi, and is illustrated in the cross section (Fig. 5). This fold rotates the slaty cleavage, has a gently north-dipping rough cleavage in the novaculite, has a well-developed zone of pencil structures in the underlying shale unit, and the northern limb is truncated by the DMFZ. In other words, the elements associated with the mesoscopic second-generation folds are also associated with this larger-scale second-generation fold.

In addition to the overall sense of rotation associated with mesoscopic structures, shear is indicated by the distribution of early fold axes. North of the DMFZ, the orientations of early fold axes approximate a planar distribution (Fig. 12). While the orientations plotted in Figure 12 are characterized by a concentration trending in a west–northwest direction, the data are clearly scattered with orientations trending due north, as well as moderately to the east. It is this rotation of fold axes that is believed to account for the unusual lithological pattern seen in the cross section (Fig. 5). North of the DMFZ, a horse block is developed around a thick sequence of Arkansas Novaculite (right of center, Fig. 5). Field data indicate that this is a fold hinge with a trend of 350°/45° isolated within the horse. The line of cross section (Fig. 5) intersects the fold approximately parallel to the fold axis. The best-fit great circle for the rotated fold axis data has an orientation of 95°/55°N. We currently are interpreting this data distribution as indicative of passive rotation of the fold axes by distributive simple shear within the CTMA (Ramsay and Graham, 1970; Sanderson, 1982). This calculated plane would represent the plane of flattening associated with the simple shear system. The average orientation of fault planes is difficult to determine, but in general these faults dip between 50° and 60° northward. Clearly, more analysis will be necessary before a complete model can be proposed, but the planar distribution of fold axes supports the idea that faulting postdated early folding, and the faults reoriented and modified the early folds.

DISCUSSION

The field observations cited above indicate that the DMFZ developed initially during the second phase of deformation. The slaty cleavage is rotated generally into synforms; the faults truncate the northern limbs and cut out the associated antiforms (Fig. 11). These synforms are southerly verging, and although similar to the first-generation folds, they are more open and do not have an axial cleavage. A much more complicated pattern is developed in the overturned sections. These zones tend to be more chaotic, having dismembered folds in which the dominant bedding orientation is overturned (Fig. 11). At the south end of the long road cut along U.S. Highway 259 (south of the DMFZ), three second-

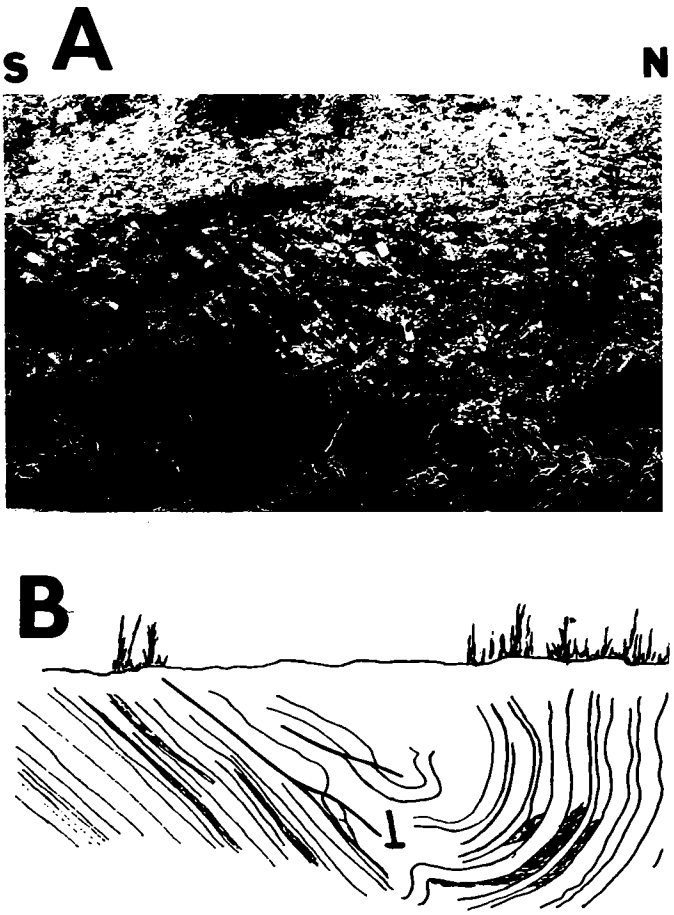


Figure 8. (A) A second-generation fold identified principally by the presence of folded slaty cleavage. Outcrop is located along U.S. Highway 259; view is toward the west. (B) Sketch of a second-generation fold emphasizing the orientation of slaty cleavage around the hinge. Note small anticline in the hinge of the larger syncline. The slaty cleavage is axial planar to the smaller fold.

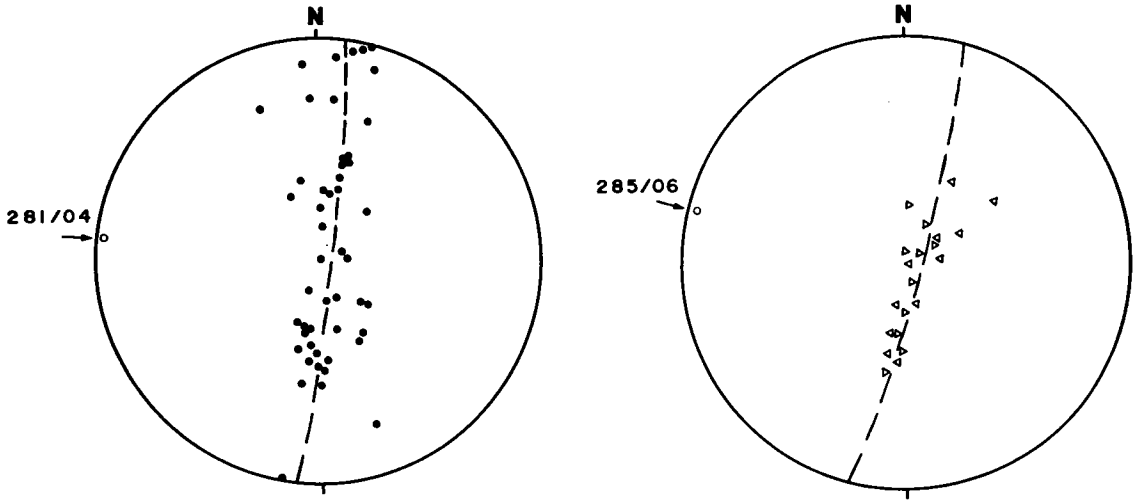


Figure 9. Orientation data for second-generation folds. Poles to bedding are plotted in the upper diagram (solid dots). Poles to the rotated slaty cleavage are plotted in the lower diagram (triangles). The fold axis orientation calculated from bedding and cleavage data (281°/04° and 285°/06°, respectively) is approximately coaxial with the fold axis of the first-generation folds (264°/04°, Fig. 7).

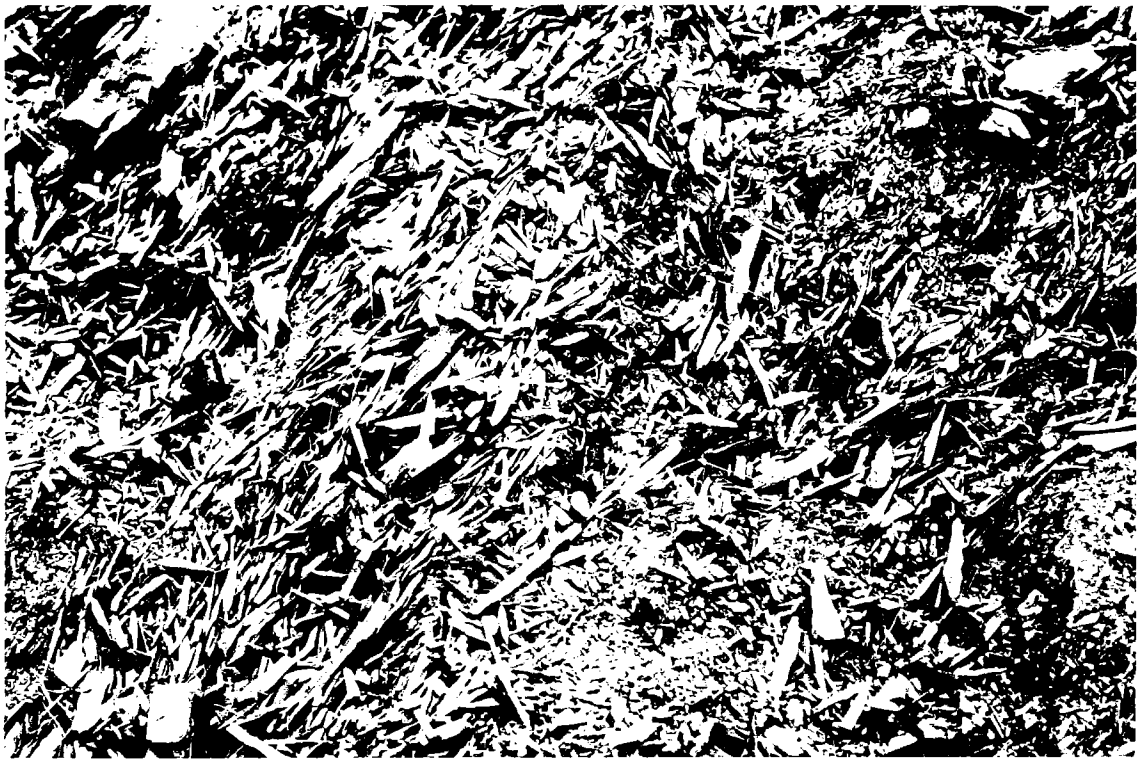


Figure 10. Pencil structures developed in association with second-generation deformation. Pencil in lower central portion of photograph is 16 cm long.

generation folds have been identified (labeled 2, Fig. 11). Each is associated with a fault or apparent local bedding-plane slip. North of this zone, a section of the Blaylock Sandstone is characteristically overturned. The folds in this area are more chaotic, having dismembered limbs and very curviplanar axial surfaces. The faults commonly cut out the synclinal folds and consequently stack the anticlines. Beds in the northern third of the outcrop are again upright, and the folds verge consistently southward.

The Blaylock Sandstone outcrop along U.S. Highway 259 provides a mesoscopic analog with which to examine the CTMA and the DMFZ. Extending these mesoscopic observations to the DMFZ, we conclude that the DMFZ developed in the north limb of a second-generation syncline, and that the zone contains dismembered elements of the overturned limb of a large-scale first-generation fold. North of the fault zone, the CTMA may be the upright limb of this first-generation fold nappe.

Earlier workers have debated the contact relationships between the flank and core of the Hochatown dome (Honess, 1923; Miser, 1929; Pitt, 1955; Hubert, 1984; Dix, 1985; Nielsen and others, 1989; Colson, 1992). On the west side of the Hochatown dome, flank sequences and the core are folded together into large-scale structures, exemplified by the Old Glory Mountain syncline. The strong cleavage development and consistent structural orientation between the flank and core suggest that the flank and core may have deformed together. The style of deformation is different in the shale-dominated core sequence. Characteristically, low-angle faults separate repeated sections of shale (Dunagan, 1981; Hubert, 1984; Dix, 1985; Erickson and Tapp, 1995). However, where folds are observed, they trend consistently northeast–southwest and verge to the southeast (Hubert, 1984; Dix, 1985). Interestingly, Hubert (1984) concluded that these earliest folds in the core area were later folded about an east–west axis.

In contrast, a pronounced structural discontinuity is present between the east flank and core of the Hochatown dome (Miser, 1929; Dix, 1985; Nielsen, 1988; Nielsen and others, 1989; Colson, 1992). Within the flank sequence at Beavers Bend State Park (T. 5 S., R. 24 E., Fig. 3), the dominant fold set trends 95°/14°; whereas, just to the north and west, tight recumbent folds in the older shales reveal a strong northeast-trending fabric. Deformed clasts within the Womble Shale, near the Bigfork Chert contact, have a well-developed southeast-trending finite extension direction. Detailed mapping has identified a detachment surface between the Bigfork Chert and the Womble Shale along the southern

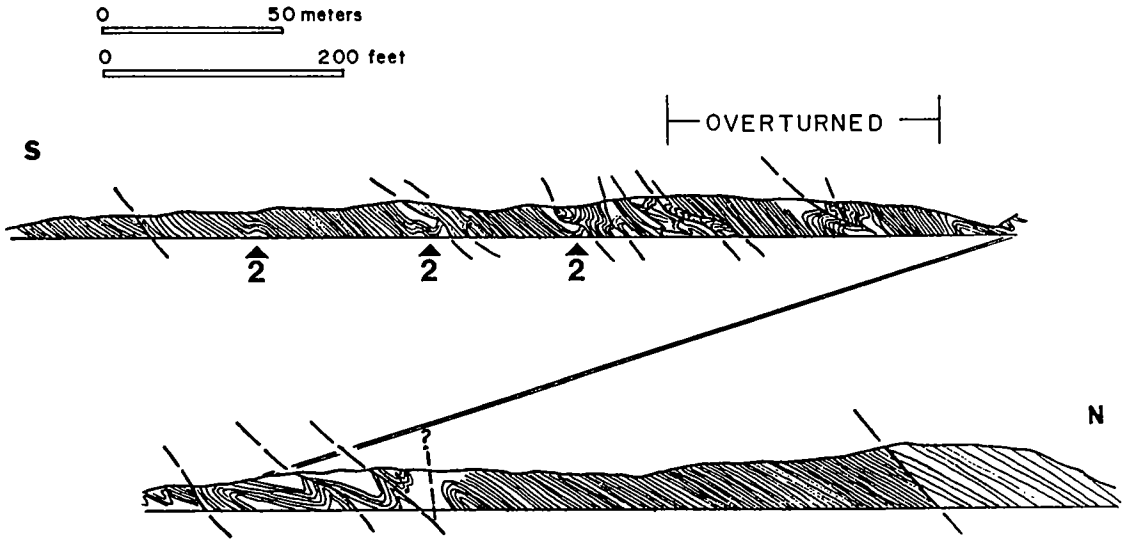


Figure 11. Sketch of the Blaylock Sandstone outcrop in the footwall of the Dyer Mountain fault zone along U.S. Highway 259. A large-scale first-generation fold is interpreted to include upright limbs on the south and north, with an overturned limb (labeled) in between. Arrows labeled 2 point to second-generation folds in the upright limb. Figure 8 is a photograph and sketch of the middle second-generation fold. Second-generation deformation created a chaotic pattern in the overturned limb.

shoreline of Broken Bow Reservoir (Nielsen, 1988; Colson, 1992).

The eastward extension of the DMFZ is of primary importance to understanding the evolution of the Broken Bow uplift. The DMFZ truncates a second-generation syncline along the northwestern margin of the Hochatown dome (Fig. 4). To the east, this fault zone cuts down section and appears to cut out the Bigfork Chert near the western shoreline of the reservoir (Fig. 4). The eastward extension of the DMFZ has not been established beyond this area. However, the deformational sequence, style, and orientation seen in the flank sequence along the east side of Hochatown dome are very similar to those observed in the CTMA. We would propose that the detachment mapped along the southern shoreline of the reservoir (Fig. 13) is in fact the extension of the DMFZ. Therefore, the flank sequence on the east side of the dome is in the hanging wall, and the flank sequence on the west side of the dome is in the footwall of this southerly directed thrust. The contact zone developed on the north side of the dome is a deformed ramp, and the DMFZ in this area is compared to a duplex structure developed in association with this ramp (Boyer and Elliot, 1982). Younger faults such as the Glover fault, possibly related to the northeast-trending uplift associated with Mesozoic rifting, are interpreted as cutting the DMFZ (Fig. 13).

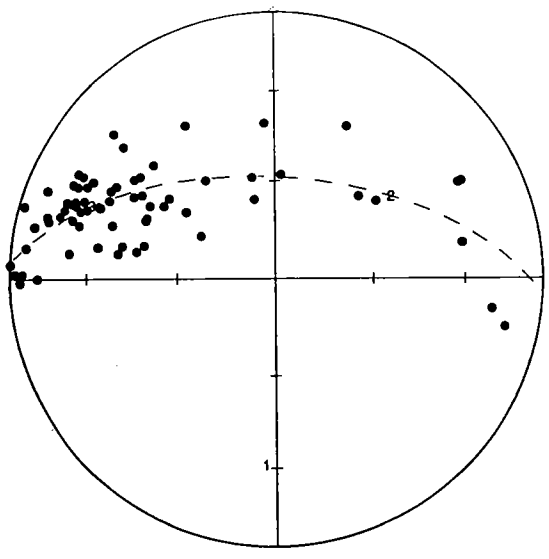


Figure 12. Distribution of early fold axes (solid dots) north of the Dyer Mountain fault zone.

The relationship between the structures and the dominant northerly directed thrusts has been discussed in another paper (Nielsen and others, 1989). Our current data indicate that the relationship between first- and second-generation structures can be carried north to the Boktukola fault. Northward, the orientation of second-generation faults changes from northerly dipping to southerly dipping, and the sense of motion changes from southerly to northerly directed. The conceptual model to incorporate these observations is that of a structural fan or large box-like structure with opposing vergence

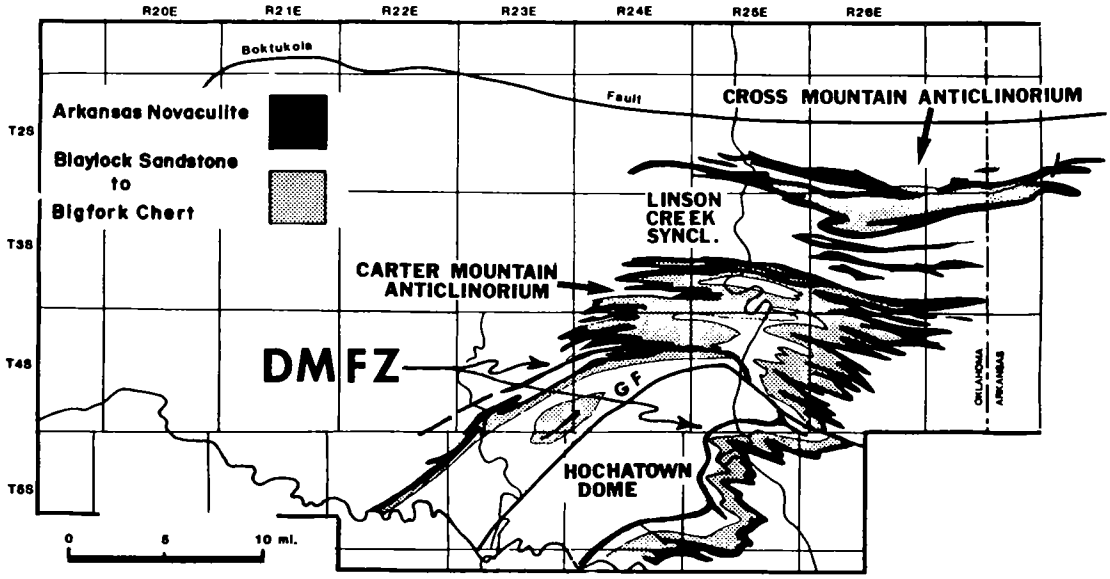


Figure 13. Proposed extension along the eastern flank of the Broken Bow uplift of the Dyer Mountain fault zone (DMFZ). The Glover fault (GF) and the southeasterly trending fault that offsets the eastern flank of the uplift in the northern part of T. 5 S., R. 26 E. are interpreted to be younger than the DMFZ.

in the hanging wall of the Boktukola fault. Most importantly, this fan is viewed as a second-generation structure directly related to emplacement of the northerly directed thrusts. The earliest folds of the Broken Bow uplift consistently verge southward, and are interpreted as structures related to the initial stages of deformation in the Ouachita basin.

REFERENCES CITED

Bally, A. W.; Gordy, P. L.; and Stewart, G. A., 1966, Structure, seismic data, and orogenic evolution of southern Canadian Rockies: Canadian Association of Petroleum Geologists Bulletin, v. 14, p. 337–381.

Boyer, S. E.; and Elliott, D., 1982, Thrust systems: American Association of Petroleum Geologists Bulletin, v. 66, p. 1196–1230.

Colson, R., 1992, Strain distribution and low angle faulting on the eastern flank of the Broken Bow uplift, Oklahoma: Stephen F. Austin State University unpublished M.S. thesis, 144 p.

Denison, R. E.; Burke, W. H.; Otto, J. B.; and Heatherington, E. A., 1977, Age of igneous and metamorphic activity affecting the Ouachita foldbelt, *in* Stone, C. G. (ed.), Symposium on the geology of the Ouachita Mountains: Arkansas Geological Commission, v. 1, p. 25–40.

Dix, M. C., 1985, Sequential deformation of Ordovician slates in the Stephens Gap area, eastern Broken Bow uplift, Oklahoma, Ouachita Mountains [abstract]: Geological Society of America Abstracts with Programs, v. 17, p. 156.

Dunagan, J. F., 1981, Geology of the Lower Ordovician rocks of the Choctaw anticlinorium, southeastern Oklahoma: Shale Shaker, v. 32, no. 11, p. 33–54.

Erickson, Steve; and Tapp, Bryan, 1995 [this volume], Reconnaissance study of Womble Formation, Broken Bow uplift, *in* Johnson, K.S. (ed.), Structural styles in the southern Midcontinent, 1992 symposium: Oklahoma Geological Survey Circular 97, p. 236-239.

Ethington, R. L.; Finney, S. C.; and Repetski, J. E., 1989, Biostratigraphy of the Paleozoic rocks of the Ouachita orogen, Arkansas, Oklahoma, West Texas, *in* Hatcher, R. D.; Thomas, W. A.; and Viele, G. W. (eds.), The Appalachian–Ouachita orogen in the United States: Geological Society of America, The Geology of North America, v. F-2, p. 563–574.

Feenstra, R. E., 1974, Evolution of folds in the Blaylock Formation (Silurian), Ouachita Mountains, southeastern Oklahoma: University of Oklahoma unpublished M.S. thesis, 77 p.

Feenstra, R. E.; and Wickham, J., 1975, Evolution of folds around the Broken Bow uplift, Ouachita Mountains, southeastern Oklahoma: American Association of Petroleum Geologists Bulletin, v. 59, p. 975–985.

Flawn, P. T.; Goldstein, A., Jr.; King, P. B.; and Weaver, C. E., 1961, The Ouachita system: University of Texas, Bureau of Economic Geology Publication No. 6120, 401 p.

Hendricks, T. A.; Gardner, L. S.; Knechtel, M. M.; and Averitt, P., 1947, Geology of the western part of the Ouachita Mountains in Oklahoma: U.S. Geological Survey Oil and Gas Investigation Series, Preliminary Map 66, scale 1:42,240.

Honess, C. W., 1923, Geology of the southern Ouachita Mountains of Oklahoma: Oklahoma Geological Survey Bulletin 32, part 1, 278 p.

Hubert, L. M., 1984, Structure and lithologic variation in the central core of the Broken Bow uplift: University of Texas at Dallas, Richardson, unpublished M.S. thesis, 112 p.

Johnson, L. A., 1990, Geology, structure, and strain distribution on the eastern flank of the Carter Mountain anticlinorium, McCurtain County, Oklahoma: Stephen F. Austin State University unpublished M.S. thesis, 213 p.

Leander, M. H.; and Legg, T. E., 1988, Potential for subthrust as fields; results of recent deep drilling in the Ouachitas [abstract]: American Association of Petroleum Geologists Bulletin, v. 72, p. 211.

Miser, H. D., 1929, Structure of the Ouachita Mountains of Oklahoma and Arkansas: Oklahoma Geological Survey Bulletin 50, 30 p.

Nelson, K. D.; Lillie, R. J.; de Voogd, B.; Brewer, J. A.; Oliver, J.; Kaufman, S.; Brown, L.; and Viele, G. W., 1982, COCORP seismic reflection profiling in the Ouachita Mountains of western Arkansas: geometry and geological interpretations: Tectonics, v. 1, p. 413–430.

Nielsen, K. C. (ed.), 1982, Structural styles of the Ouachita Mountains, southeastern Oklahoma: Geological Society of America, South-Central Section Guidebook, Field Trip No. 3, 124 p.

Nielsen, K.C., 1985, Integrated structural model for the Broken Bow uplift, southeastern Oklahoma [abstract]: Geological Society of America Abstracts with Programs, v. 14, p. 134.

Nielsen, K. C., 1988, Beavers Bend State Park, Broken Bow uplift, Oklahoma, *in* Hayward, O. T. (ed.), South-Central Section: Geological Society of America Centennial Field Guide, v. 4, p. 195–202.

Nielsen, K. C.; Viele, G. W.; and Zimmerman, J., 1989, Structural setting of the Benton–Broken Bow uplifts, *in* Hatcher, R. D.; Thomas, W. A.; and Viele, G. W. (eds.), The Appalachian–Ouachita orogen in the United States: Geological Society of America, The Geology of North America, v. F-2, p. 635–660.

Pitt, W. D., 1955, Geology of the core of the Ouachita Mountains of Oklahoma: Oklahoma Geological Survey Circular 34, 34 p.

Price, R. A., 1981, The Cordillera fold and thrust belt in the southern Canadian Rocky Mountains, *in* McClay, K. R.; and Price, N. J. (eds.), Thrust and nappe tectonics: Geological Society of London Special Publication 9, p. 427–448.

Ramsay, J. G.; and Graham, R. H., 1970, Strain variation in shear belts: Canadian Journal of Earth Sciences, v. 7, p. 786–813.

Sanderson, D. J., 1982, Models of strain variation in nappes and thrust sheets: a review: Tectonophysics, v. 88, p. 201–233.

Shore, P. S.; and Nielsen, K. C., 1987, Pencil lineations and coaxial deformation, Broken Bow uplift, southeastern Oklahoma [abstract]: Geological Society of America Abstracts with Programs, v. 19, p. 843.

Suneson, N. H.; Campbell, J. A.; and Tilford, M. J. (eds.), 1990, Geology and resources of the frontal belt of the western Ouachita Mountains, Oklahoma: Oklahoma Geological Survey Special Publication 90-1, 196 p.

Viele, G. W., 1973, Structure and tectonic history of the Ouachita Mountains, Arkansas, *in* DeJong, K. A.; and Scholten, R. (eds.), Gravity and tectonics: John Wiley and Sons, New York, p. 361–377.

_____ 1989, The Ouachita orogenic belt, *in* Hatcher, R. D.; Thomas, W. A.; and Viele, G. W. (eds.), The Appalachian–Ouachita orogen in the United States: Geological Society of America, The Geology of North America, v. F-2, p. 555–561.

Walthall, B. H., 1967, Stratigraphy and structure, part of the Athens Plateau, southern Ouachitas: American Association of Petroleum Geologists Bulletin, v. 51, p. 504–528.

Yang, Qingming; and Nielsen, K. C., 1992, The Dyer Mountain fault zone, Broken Bow uplift, southeastern Oklahoma [abstract]: Geological Society of America Abstracts with Programs, v. 24, p. 51–52.

Tectonic and Stratigraphic Synthesis of Events in the Region of the Intersection of the Arbuckle and Ouachita Structural Systems, Oklahoma

William McBee, Jr.
Geological Consultant
Tulsa, Oklahoma

ABSTRACT.— The term Oklahoma megashear (OM) is proposed as a more appropriate name for the intensely folded and faulted, WNW-trending tectonic belt in southern Oklahoma. It is a 50- to 120-mi-wide zone of anastomosing, left-oblique faults with as much as 55 mi of left-lateral offset. It is only one of several major WNW-trending wrench-fault systems that transect the North American craton. They originated as compressional shear fractures with associated dike swarms during Middle Proterozoic time; many became sinistral faults, some with very large displacements. During the separation of Laurentia from Pangaea (~525 Ma), a local pull-apart basin formed in a releasing bend of the OM in southwestern Oklahoma and became filled with the Wichita igneous complex. The Wichita complex was submerged in Late Cambrian time and remained buried until Morrowan time, when it emerged during the Wichita orogeny. Laurentia was being pushed and carried eastward by the Ruby and Antler subduction orogenies in the west. The pulsating stresses that propagated the OM originated in a "squeeze play" between eastward-directed subduction of Laurentia's west margin and the several collisions of Laurentia's east margin with Africa and South America (Gondwana). The OM became increasingly active as a simple oblique-slip fault zone during early Paleozoic time. Activity climaxed in Desmoinesian time but did not end. Some movement occurred as recently as Holocene.

The OM apparently was not affected by the northward-directed forces of the Ouachita orogeny which were only active during Mississippian through Middle Pennsylvanian time. Each pulse of the Ouachita orogeny produced uplift with accelerated erosion in the hinterland, vigorous northward thrusting, progressive sagging of the foreland basin, and deposition of tremendous volumes of flysch. The two sets of surging stresses that caused the two orogenies did not always act concurrently.

The Ouachita allochthon probably extended further north and west of the present-day trace of the Choctaw fault. The folds in the Arkoma basin, north of the Choctaw fault, are interpreted to be exhumed subthrust folds. These extend from the Tishomingo block eastward to the Cretaceous overlap in central Arkansas. That part of the buried allochthon south of the Muenster uplift in Texas (the southern extension of the outcropping Ouachita Mountains) appears to have been almost completely removed from the shelf by the peneplanation. Only the master sole fault separates the shelf from the overriding flysch deposits, as it does on the Tishomingo block.

The OM system was structurally dominant over the thin-skinned Ouachita system. The Oklahoma megashear was active long before, during, and after the Ouachita orogeny. In all likelihood, the Ouachita orogeny had little, if any, effect on the OM structures. However, OM activity caused uplift and differential erosion of the Ouachita allochthon and the Choctaw fault; buried Ouachita faults may also have been offset.

INTRODUCTION

This paper is a review of the chronology of events relating to the Arbuckle and Ouachita orogenic systems. Their histories are revealed largely in the stratigraphic and erosional record of the several basins that are part of this complex. The Arbuckle and Ouachita orogenic systems have different structural styles and independent histories, although for a short time their activities overlapped.

The Arbuckle system is part of a WNW-trending intensely broken and deformed multi-fault zone in southern Oklahoma that is herein called the Oklahoma megashear (OM) (Fig. 1). The OM has been

McBee, William, Jr., 1995, Tectonic and stratigraphic synthesis of events in the region of the intersection of the Arbuckle and Ouachita structural systems, *in* Johnson, K. S. (ed.), Structural styles in the southern Midcontinent, 1992 symposium: Oklahoma Geological Survey Circular 97, p. 45–81.

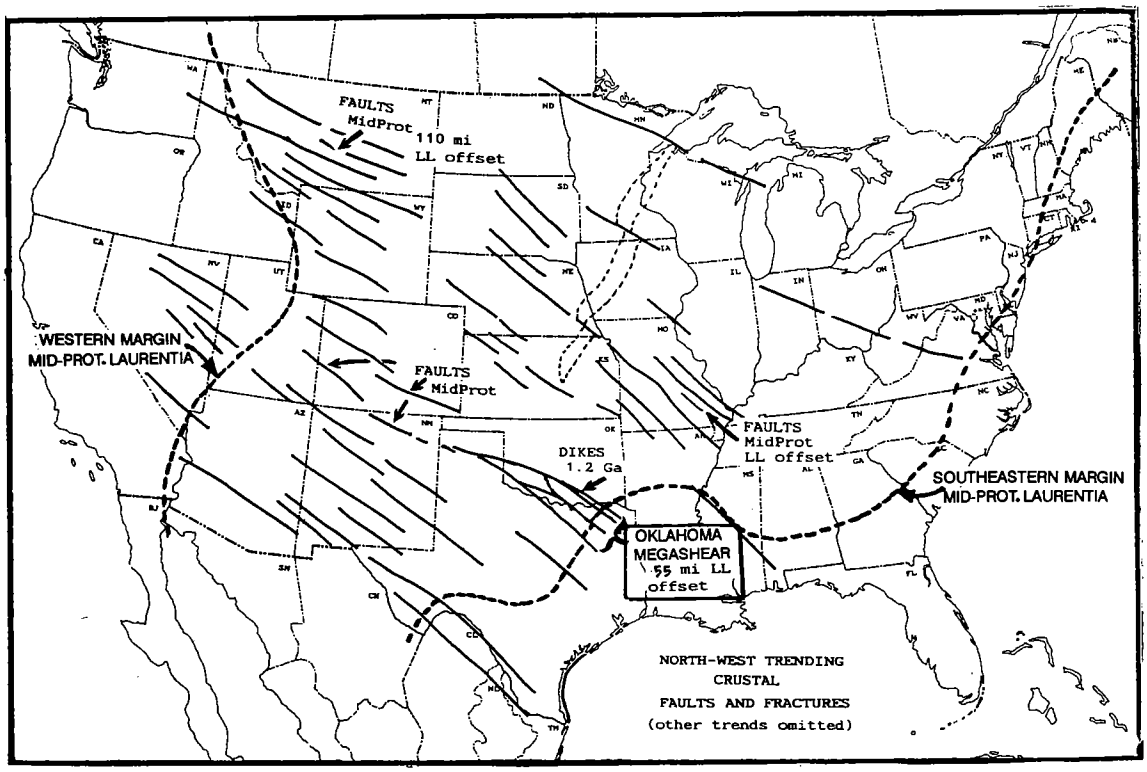


Figure 1. The margins of Laurentia, relative to present geography and the location of the Oklahoma megashear. Only the dominant, WNW-trending faults are depicted. Most, perhaps all, are left-lateral; several have large amounts of horizontal displacement. These originated in Middle Proterozoic time and some are still active.

given many names, often dictated by the prevailing tectonic fad. Geological evidence presented here will show that the southern Oklahoma "disturbed belt" is a very active, long-lived, transcratonic, convergent, shear-fault (wrench) system. It was probably not an aulacogen. An aulacogen is a rifted but failed arm of a triple junction. A plume-generated triple junction is the intersection of three rifts, two of which continue to widen, eventually forming a rifted margin. The third rift (the aulacogen) fails to spread (Burke and Dewey, 1973) and is merely a graben bounded by normal faults. The OM is not bounded by normal faults and was formed in an entirely different way.

The OM system formed from a primal crustal fracture as early as Middle Proterozoic time. Intermittent activity occurred thereafter, climaxing in Middle Pennsylvanian, and waning, but not ending, in Late Pennsylvanian time. Minor action has occurred as recently as the Holocene (Ramelli and Slemmons, 1986; Lawson and Luza, 1993). The complexity, width, length, long life, and the amount of movement involved, are consistent with the definition of the term "megashear" (Carey, 1958; DeSitter, 1956; Walper, 1956). In a megashear (or wrench) system, structural style typically varies along the length of the fault zone, ranging from extension to compression (pseudo-thrusting). Reversals of fault throw are also common.

The Ouachita system is the product of southward plunging subduction of the southern margin of Laurentia (Texas, Oklahoma, Arkansas, and Mississippi) beneath Amazonia (also known as Llanoria) and their eventual collision. The Ouachita orogeny, which started before the actual collision of the two cratons, and ceased soon afterward, was relatively short. It began in Late Mississippian time, peaked in Middle Pennsylvanian, and ended, for the most part, in Late Pennsylvanian time. Diminishing orogenic pulses continued on into Early Permian time.

This chronology is accompanied by a series of maps that are pictorial hybrids, but largely paleogeographic in aspect. The maps have been palinspastically restored to reflect the geography and the structural and depositional patterns that characterized particular intervals of geological time. Average environments and lithofacies noted on the maps are described in Table 1. Formation or group names are spotted in bold type, and isopachous (thickness) lines are shown on several maps. Figure 2 is a skeletal index to the stratigraphic names used herein.

TABLE 1. — KEY TO LITHOFACIES

Prograding systems	Regressive sequences grade upward from deeper-water shale and thin limestone into coarser shallow-marine, delta, and coastal-plain sediments.
Carbonate shelves	Broad sheet-like carbonates, with some shale and sands.
Shale basins	Shale-dominated cratonic depressions, regardless of thickness; possibly with small amounts of sandstone or limestone.
Abyssal sediments	Deep water, very fine grained deposits off of the craton.
Flysch	Thick accumulations of interbedded shale and sandstone deposited in relatively deep water adjacent to a rapidly rising and eroding land mass.

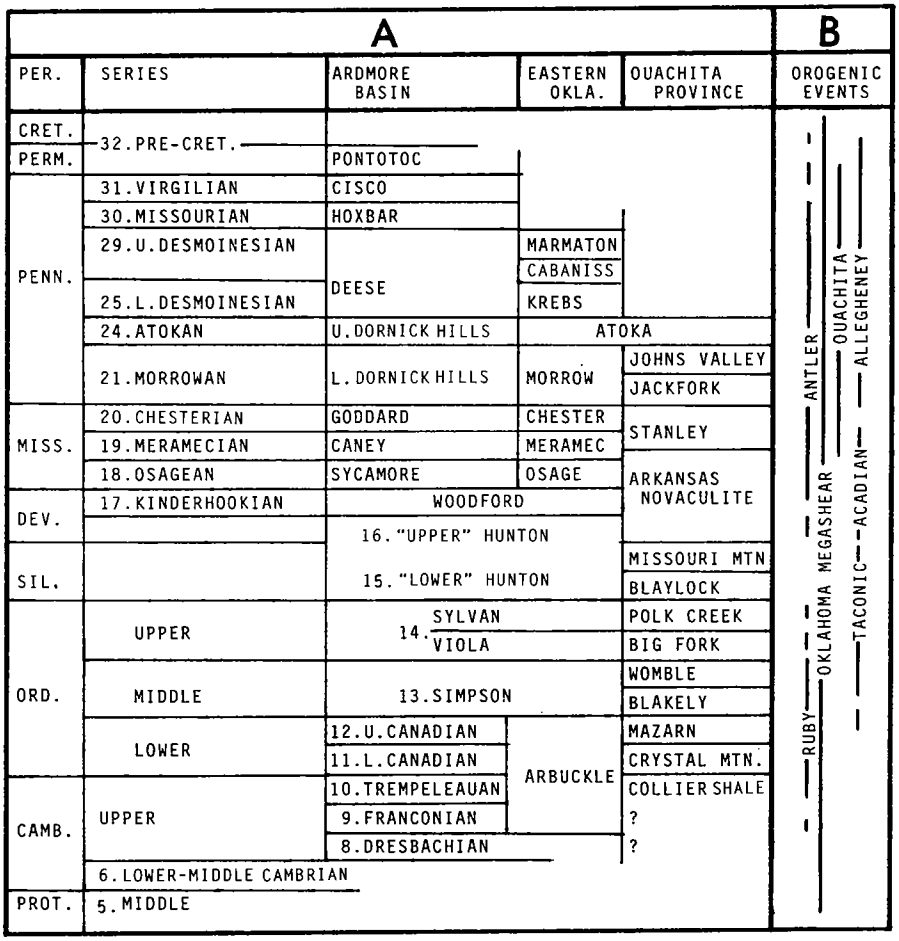


Figure 2. Column A: Index to the stratigraphic names used in the report; numbers refer to relevant figures in text. Column B: Relative timing and duration of orogenies that affected the North American craton—the Ruby and Antler orogenies in the west, the Taconic, Acadian, and Allegheny orogenies in the east, and the Ouachita orogeny in relation to activity of the QM.

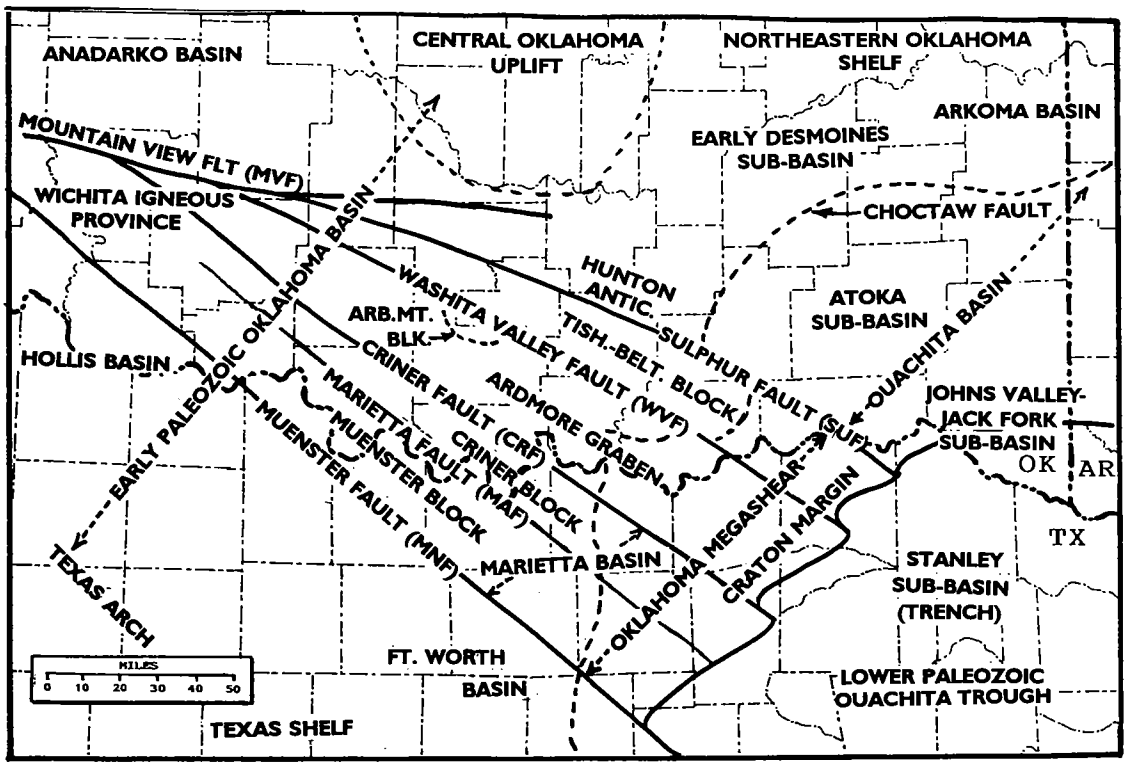


Figure 3. Index to tectonic elements mentioned in this study.

Faults that were active during each specified period are shown in bold lines. The fault traces have been smoothed to facilitate palinspastic restorations. Most of the major faults are actually anastomosing complexes of associated breaks, reminiscent of the San Andreas system in California. Figure 3 is a location map and key to the various structural features and provinces discussed in this work. The compilation of these maps was begun in 1954, and has been in progress ever since. Most of the work is original, although data from a myriad of sources were considered.

IN THE BEGINNING . . .

A NW-trending diorite dike swarm in the eastern Arbuckle province (Fig. 3) dated at 1,350 Ma (Denison, 1982) indicates that the OM was active at least as early as Middle Proterozoic time. The OM is only one of several northwest-trending transpressional shear zones that transected the Proterozoic Laurentian craton (Fig. 1). The Lewis and Clark lineament in Montana is a cluster of six NW-trending, left-lateral slip faults, one of which has been dated at 1,250 Ma (Middle Proterozoic). The offset of two of them is estimated to be 110 mi (Smith, 1965). Another series of NW-trending strike-slip faults extends across Wyoming and northern Colorado: the Owl Creek, Fish Creek, Wind River, King Soloman Creek, Douglas Creek, and Garmesa faults (Stone, 1969). The Uncompahgre lineament in southwestern Colorado and northern New Mexico which has been dated between 1,780 and 1,460 Ma (Barrs and Stevenson, 1982) is a western extension of the OM. The 150-mi-wide tectonic system between the Ste. Genevieve and Bolivar–Mansfield faults in southeast Missouri includes at least six NW-trending, near-vertical faults with considerable left-oblique displacement. These faults formed in Precambrian time and were reactivated in the Phanerozoic (Clendenin and others, 1989). They describe the St. Francis Mountain uplift, at the core of this system, as a "positive flower structure." Howe (1993) stated: "The Pennsylvanian history of the Ozark uplift is complex, reflecting major late Mississippian or early Pennsylvanian reactivation along prominent NW-trending tectonic zones." Berendsen and Wilson (1993) point out: "Orogenic events in and around the Midcontinent in Proterozoic time were responsible for the formation of the dominant set of younger NE- and older NW-trending faults that dominate the [eastern Kansas and western Missouri] area today." Sims (1988) describes several NW-trending, left-slip faults of Proterozoic age: the Lake Superior belt; southern Wisconsin fault zone; the Reservation fault in northeastern Nebraska; a 65-mi offset in southeastern Minnesota and a 35-mi left offset in southeastern Nebraska of the 1,000–1,200-Ma Midcontinent rift. Paulsen and Marshak (1994) present

evidence for a NW-trending tectonic zone (the Dakota–Carolina corridor) that extends from South Carolina to South Dakota that apparently originated during Middle Proterozoic time along an old zone of cratonic weakness. Later movements were propagated upward into Phanerozoic strata. At least three of these NW-trending megashears experienced early, minor local rifting that resulted in the emplacement of narrow, datable dikes. Small-scale rifting along release bends in transpressional systems are not uncommon. Many of these primal fractures became left-slip faults, some remained frozen.

Lateral displacement across the OM system is estimated to be ~55 mi. The evidence for about half of this displacement is the apparent left-lateral offset of the gravity-defined cratonic margin where it is intersected by the Muenster fault (Fig 4). Tanner (1967) demonstrated 37–40 mi of offset of several Lower Paleozoic formations across the Washita Valley fault. The writer made the same observation in a very detailed proprietary study in 1954. Displacements of the same order of magnitude are not uncommon on the craton. Several examples of left-lateral displacement were cited by Sylvester (1988): 110 mi in the TransMexican volcanic belt; 625 mi in western Mexico; 750 mi at Baja California. Brookfield (1993) cited several other large displacements on Middle Proterozoic left-lateral fault systems: 310 mi in the western extension of the Olympic–Wichita system; 1,000 mi along the Tintinia fault in western Canada; and 190 mi along the Texas–Walker lineament.

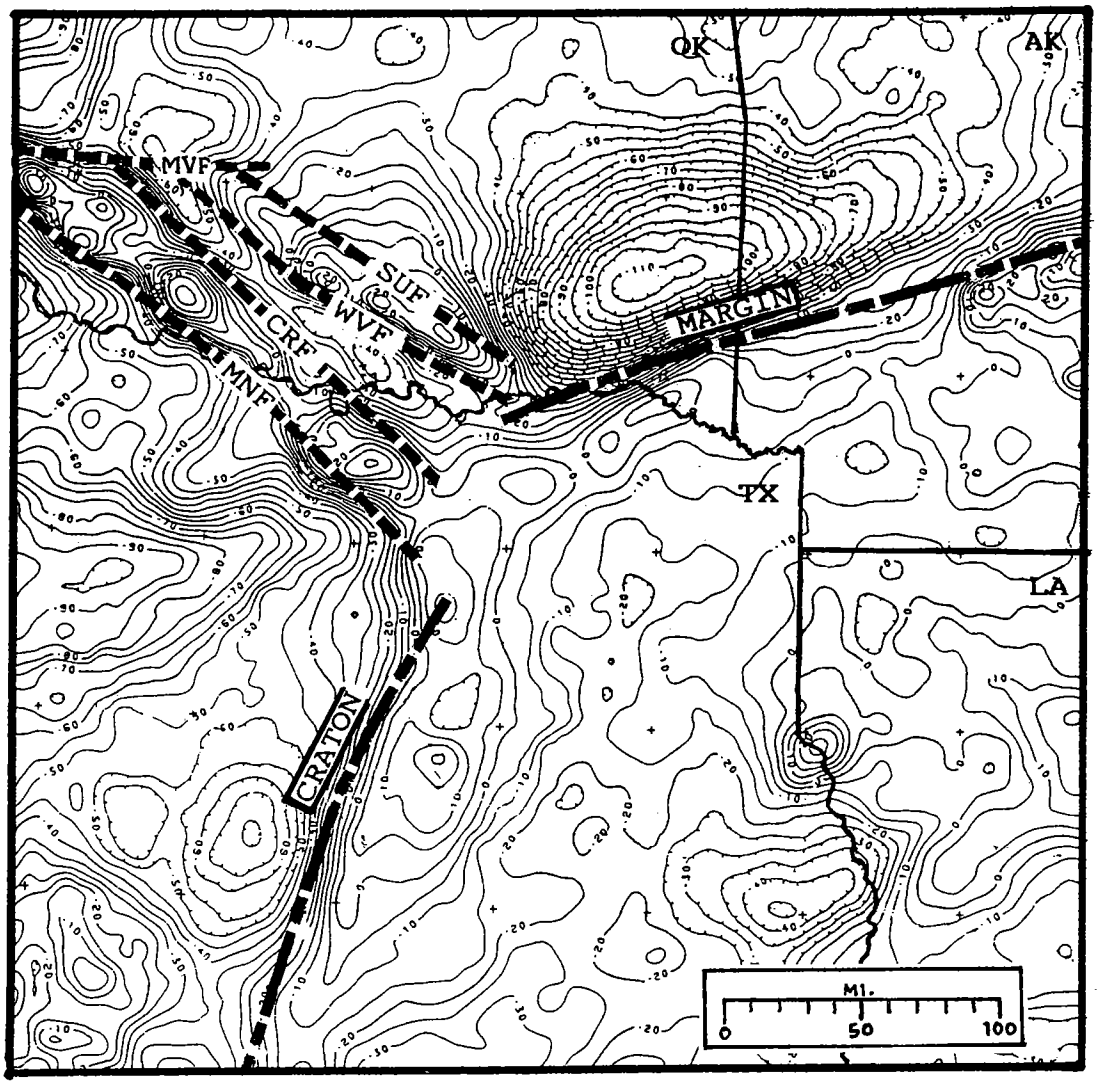


Figure 4. Bouger gravity map showing apparent left-lateral offset across the OM of the anomalously steep gradient that is considered to represent the craton margin. SUF = Sulphur fault; WVF = Washita Valley fault; CRF = Criner fault; MAF = Marietta fault; MNF = Muenster fault.

These NW-trending transcratonic megashears formed during Middle Proterozoic time. At that time, Laurentia was central in the supercontinent, Pangaea (Fig. 5), which apparently overlay a descending mantle convection cell (Hoffman, 1991). This would explain the inwardly directed stresses from the outer ring of cratons that impinged on Laurentia, setting up the shear fracture systems there. Pangaea apparently remained fairly intact following the dike emplacement (~1,250 Ma) until ~600 Ma, when the break-up started (Hoffman, 1991). The down-welling movement of the mantle convection cell that previously held the supercontinent together in a geoidal depression evidently reversed to become an upwelling plume which led to the break-up of Pangaea. The breaks probably formed along old lines of weakness at boundaries between the pre-Pangean cratons (Fig. 5). This process was similar to the breaking up of a large shelf-ice floe. It is in contrast to the hot-spot and triple-junction concept of rifting. Possible forces responsible for keeping the major faults active after the break-up include differential resistance to cratonic drifting, active undulations and varying rates of movement of the mantle beneath the cratons, cratonic collisions, and earth tides.

LOWER AND MIDDLE CAMBRIAN

During and following the break-out of Laurentia from Pangaea about 570–550 Ma (Williams and Hiskott, 1987) several of the older fracture zones, including the OM, experienced reactivation. NW-trending dike swarms dated 525–500 Ma are found in the OM (Ham and others, 1964; Denison, 1982), in the Sangre de Cristo area (Reed, 1984), and in southwestern Colorado (Larson and others, 1985). During this same period of time, the OM underwent its first major left-slip movement and the block between the Muenster and Washita Valley faults (Fig. 6) became a deep graben in which the Tillman sediments were deposited. This graben probably was not the result of regional rifting. A more reasonable explanation, and one that is compatible with all the nearby tectonic features, is illus-

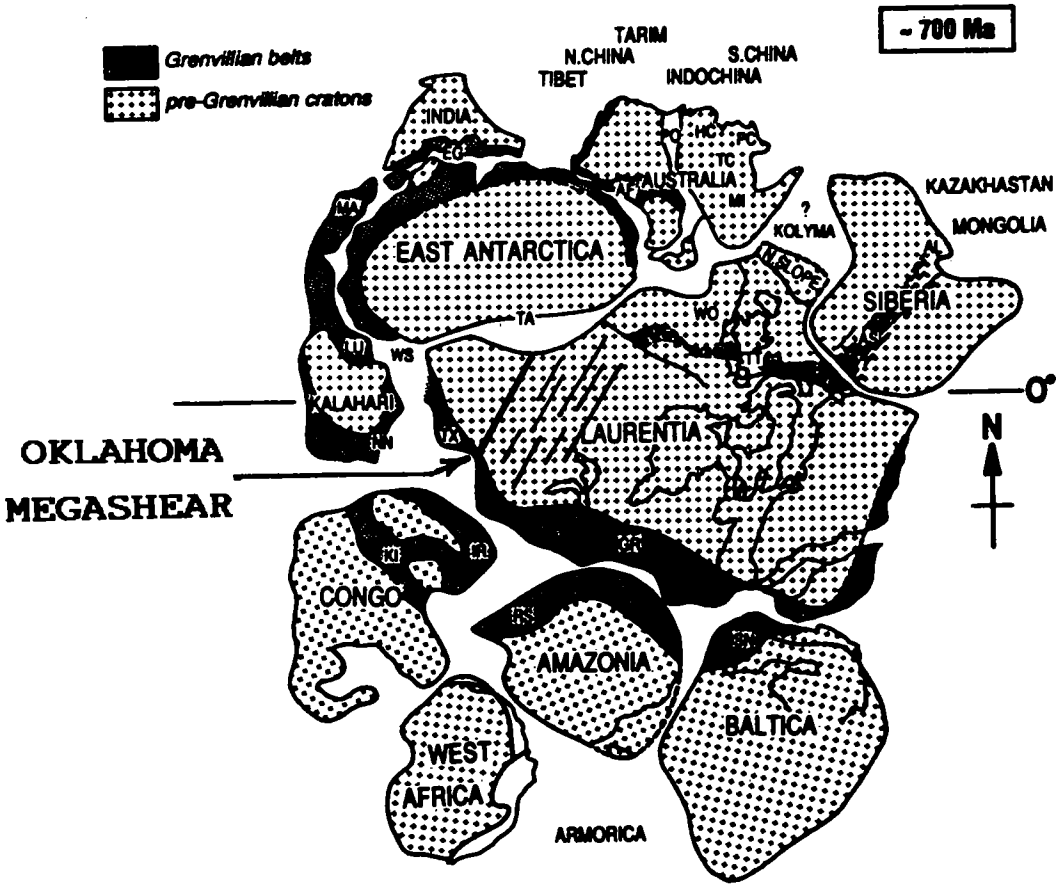


Figure 5. Reconstruction of Middle Protozoic Pangaea based on the juxtaposition of Grenville orogenic belts and paleomagnetic data (after Hoffman, 1991). The convergent actions of the cratons surrounding Laurentia may have imposed the primal shear-fracture pattern on Laurentia. Amazonia in this figure and text is also known as Llanoria.

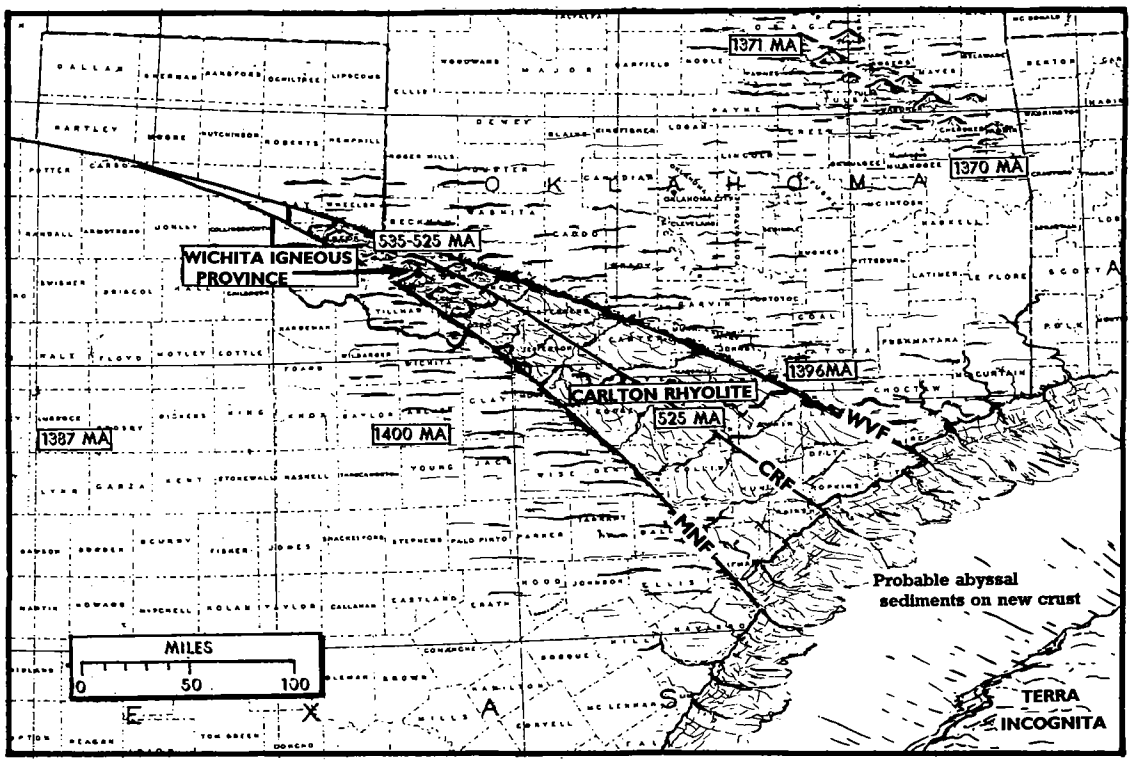


Figure 6. Early–Middle Cambrian aspects of the study area shortly after Laurentia rifted from Pangaea, with radiometric ages of basement rocks. MNF = Muenster fault; CRF = Criner fault; WVF = Washita Valley fault.

trated in Figure 7. The Muenster and Washita Valley faults converge to the northwest, where their combined left-lateral movements were transferred and diverted ~20° into the Mountain View fault. This change in direction resulted in a large release bend that quickly opened into a local pull-apart basin during left-lateral movement (Fig. 7C). The resulting rupture of the crust allowed the effusion of the Wichita igneous complex which filled the pull-apart basin and poured several thousand feet of rhyolite into the graben (Fig. 7D). The effusion was apparently restricted to the Wichita Mountain area and the Wichita–Ardmore graben (Figs. 3,6).

There is no irrefutable evidence of a hot-spot or triple junction having been present where the OM intersects the craton margin. The graben was merely a down-dropped block bounded by primal vertical faults in a megashear system and was most likely formed while under transpression. Elsewhere along the extended OM, essentially identical crustal ruptures and igneous effusions occurred at about the same time: one in the Sangre de Cristo range, New Mexico (Reed, 1984), and another in the Uncompahgre range, southwestern Colorado (Larson and others, 1984). Here too, evidence for triple junctions is lacking.

A classic example of this type of igneous emplacement is the Mortagne granite pluton. The Mortagne granite pluton is an igneous-filled crustal rift resulting from a pull-apart in the transpressional South Amorican shear zone of northwestern France (Guineberteau and others, 1987). Similar settings have also been described in Saudi Arabia (Davies, 1982), northwest Ireland (Hutton, 1982), and in the Hercynian belt in central Europe (Castro, 1985).

Even though the Wichita activity produced several thousand cubic miles of volcanic material, topographic relief was not significant, because the entire area experienced severe erosion, thermal contraction and subsidence, and was buried very shortly thereafter.

Beyond the margin of the craton, Lower and Middle Cambrian clastics were probably being deposited as a rifted margin prism on the deep, new ocean crust (Dickinson, 1974) (Fig. 6).

LATE CAMBRIAN

Dresbachian

Thermal subsidence of the craton margin following the rifting of Laurentia from Pangaea resulted in the slow submergence of the Texas shelf south of the OM where >1,000 ft of westward-prograding marine strata were deposited. The shelf was terminated abruptly on the north by the uplifted scarp of the Muenster fault. Igneous activity had long

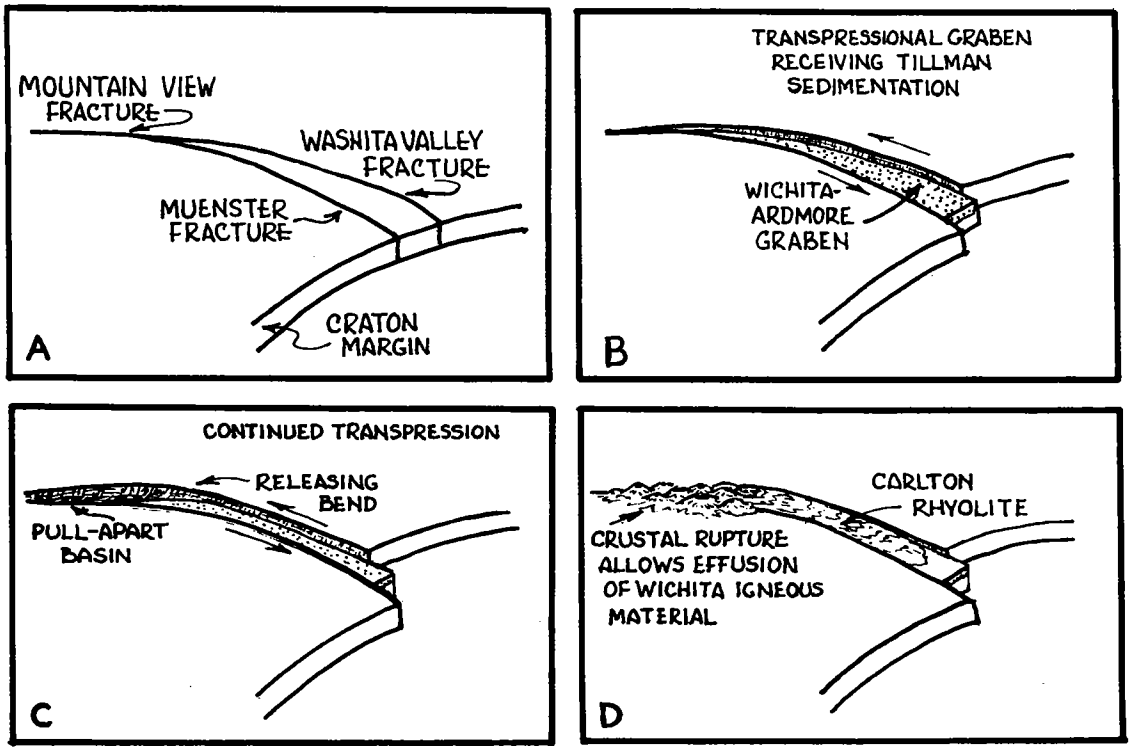


Figure 7. The origin and development of the Wichita igneous field: (A) The original Middle Proterozoic fracture system (OM). (B) Left-lateral transpression during the break-up of Pangaea caused subsidence of the Wichita–Ardmore graben in which the thick Tillman sediments (now meta-sediments) were deposited. (C) The change in fault direction where the Washita Valley and Muenster faults merge into the Mountain View fault resulted in a releasing bend under left-lateral transpression and became the site of a pull-apart basin. (D) The pull-apart basin widened, resulting in rupturing of the crust and emplacement of the Wichita igneous complex in Early–Middle Cambrian time. The extrusive Carlton Rhyolite flowed southeastward and filled the previously formed graben.

ceased in the Wichita area, which was undergoing intense tropical weathering.

Although not yet documented, abyssal clastics were probably deposited off the trailing edge of the craton in the new Ouachita oceanic trough (Fig. 8).

Franconian

The region between the Muenster and Washita Valley faults was submerged and became contiguous with the Texas shelf where >1,000 ft of Arbuckle Group shelf carbonates were deposited (Fig. 9). During this time the Wichita igneous complex was eroded and finally submerged and covered. The Ozark shelf began a slow subsidence leading to the deposition of sands and shallow-water carbonates overlapping the Proterozoic basement. Much of Oklahoma was a broad, slightly arched, peninsula between the Ozark shelf on the northeast and the Texas shelf on the southwest.

Trempeleauan

An east–west compressional stress imposed on the area resulted in emergence of the new Texas arch (Figs. 3,10). Faulting was minimal. The Oklahoma peninsula began to submerge slowly, and a broad, but steadily sinking symmetrical basin centered over the OM received >1,000 ft of Arbuckle Group carbonates (Fig. 10). Fine-grained clastics were probably deposited in the deep Ouachita trough.

EARLY ORDOVICIAN

Early Canadian

A broad area on the southern margin of Laurentia continued its slow subsidence. The Texas arch submerged, as did the Oklahoma peninsula (Fig. 11). About 1,500 ft of syntectonic shallow-water carbonates were deposited near the margin of the Texas shelf. The broad, shallow symmetrical basin of the previous epoch (Trempeleauan, Fig. 10) was broken up by vigorous, oblique-slip movements in the megashear.

This tectonic event was probably the result of a shear couple created by the Taconic orogeny on the east margin of Laurentia, and an opposing force

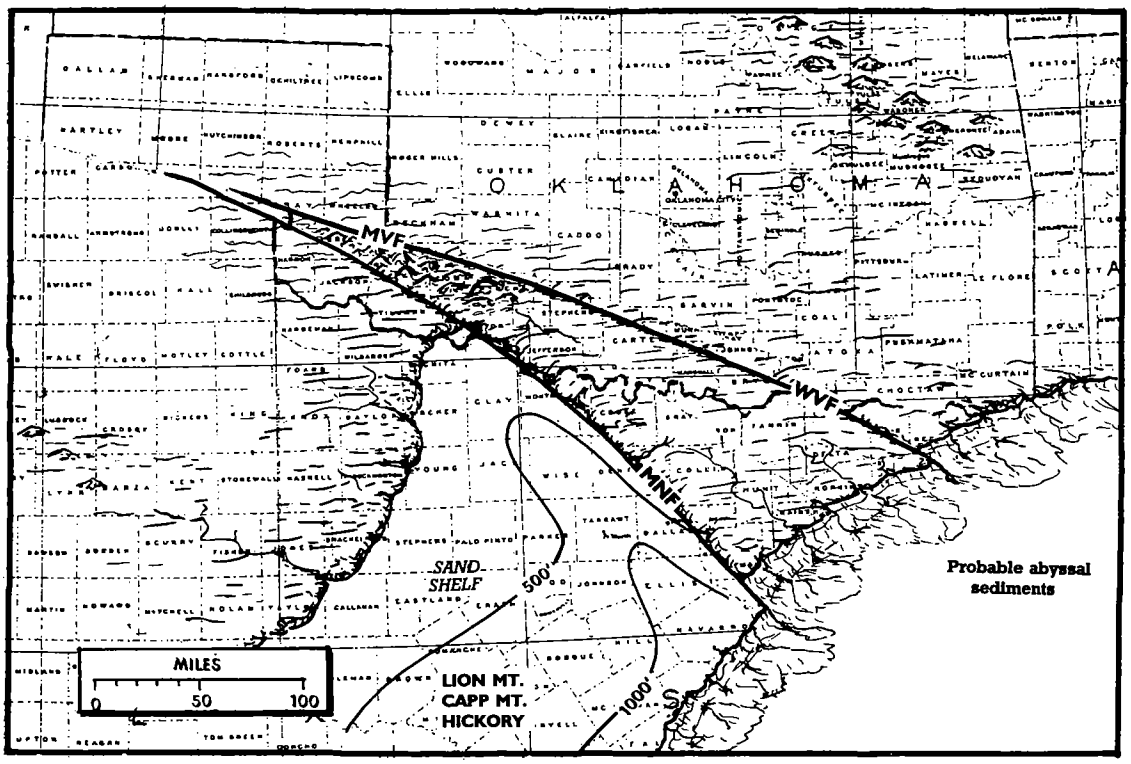


Figure 8. Late Cambrian (Dresbachian) reconstruction. Post-rift subsidence of the Texas shelf south of the OM where the first marine sediments on this part of the craton were deposited. MNF = Muenster fault; WVF = Washita Valley fault.

acting on the west margin, the Ruby orogeny, an eastward-directed subduction event (Willden, 1979). The regional dip and thickening in the area north of the OM was now toward the shear zone instead of toward the ocean basin, as was the pattern previously. More than 2,000 ft of shallow-water carbonates were deposited along the axis of the basin which has been called the proto-Anadarko–Ardmore "half basin," or taphrogeosyncline (Kay, 1951). The oldest known pre-flysch Ouachita unit, the Collier Shale, was deposited as part of the rifted margin prism in the deep oceanic trough (Fig. 11).

Late Canadian

The Texas shelf continued to subside toward the Ouachita trough, with steadily transgressing seas depositing shallow-water carbonates (Fig. 12). The Texas arch, on the other hand, began a slow emergence. The proto-Anadarko–Ardmore basin continued to subside; >3,000 ft of shallow-water carbonates and evaporites accumulated just north of the Washita Valley fault and thinned onto the northeastern Oklahoma shelf. The shelf south of the OM apparently did not sag as much; receiving only ~1,500 ft of carbonates. Several periods of emergence and submergence of broad areas during this time resulted in widespread karstification. The Mazarn Shale was deposited in the deep oceanic trough.

MIDDLE ORDOVICIAN

A disturbance of great proportion (possibly the climax of the Taconic and Ruby orogenies) resulted in the first massive influx of terrigenous clastics into the several epeiric basins in southern Laurentia (Fig. 13). Rebound shocks from these orogenies gave rise to the transmission of undulatory waves across the somewhat pliable crust of Laurentia (Gurnis, 1992) and initiated the Simpson style of cyclic sedimentation. The waves caused certain broad areas to become depressed (the Oklahoma, West Texas, Illinois–Indiana, Colorado, Williston, and western Great basins). Other areas were uplifted and subjected to erosion (e.g., Texas arch, Ozarkia, Siouxia). In the study area, the Simpson consists of five stacked and essentially identical prograding cyclothems (parasequences) that reflect very rapid transgressions and slow regressions. These cyclothems are interpreted to be the direct result of five transpressional surging shock waves that emanated from Laurentia's impacts with South America during the Taconic–Ruby orogeny. Semi-starved basin, restricted-marine shales, and thin, shallow-water, fossiliferous limestones make up

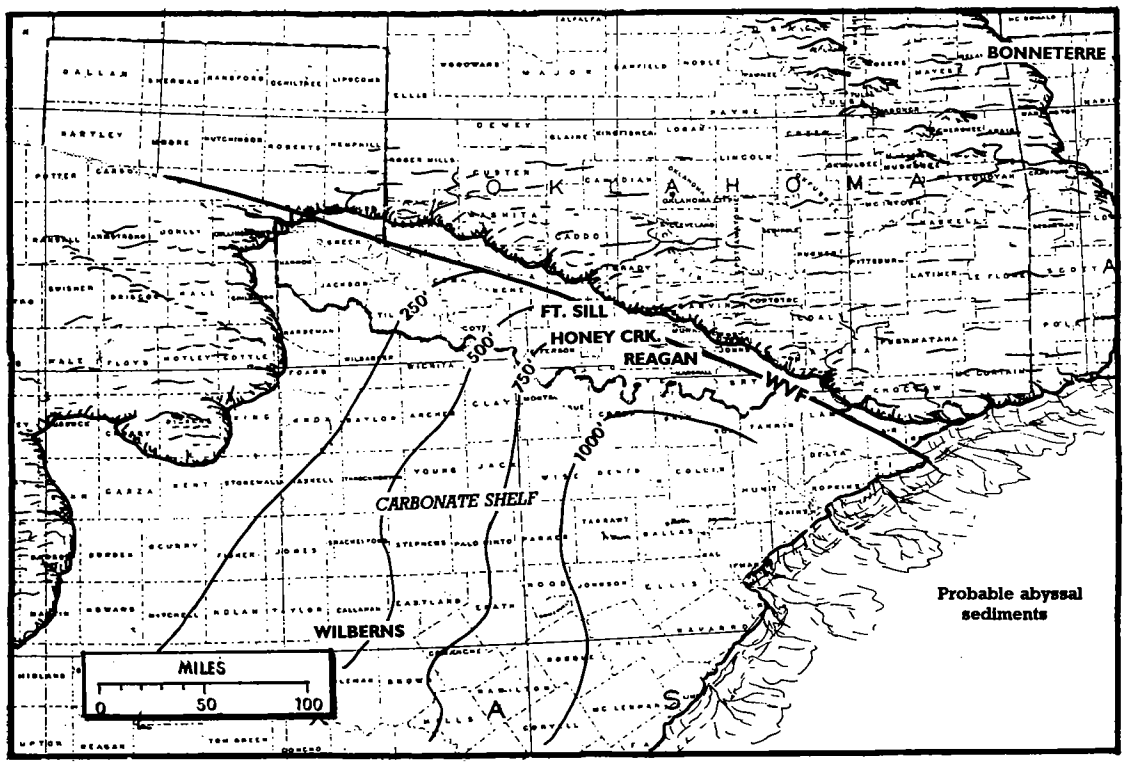


Figure 9. Late Cambrian (Franconian) reconstruction. Wichita igneous complex and the OM south of the Washita Valley fault (WVF) were submerged and became continuous with the Texas shelf.

the bulk of each cyclothem. The upper member of each cyclothem is characterized by extensive and thick progradational beds of orthoquartzite sandstone, many of which are prolific reservoirs for oil and gas. The entire Simpson Group thickens to >2,200 ft into the Ardmore graben, the axis of the OM. The Simpson section is much thinner and contains no sandstone south of the Muenster fault. The Womble and Blakely clastic sequences were deposited in the adjacent Ouachita oceanic trough (Fig. 13).

The end of Simpson time was marked by the cessation of clastic deposition and a return to clear shallow-marine conditions as indicated by the widespread deposition of the fairly thick Bromide dolomite. The "short period," collision-induced sequence of submergences and emergences that characterized the Simpson had also ceased.

UPPER ORDOVICIAN

The shallow-marine environment of the Bromide carried over into the overlying Viola carbonate (Fig. 14). The OM activity continued. The Viola Limestone and overlying Sylvan Shale thicken into the OM; the Ardmore graben received ~900 ft of Viola Limestone and ~300 ft of Sylvan Shale. Very little, if any, were deposited south of the OM. Ozarkia and the Texas arch remained emergent. The 700-ft-thick Big Fork Chert was deposited in the Ouachita trough.

The Viola carbonate deposition was ended by a fairly sudden influx of mud (Sylvan Shale), most likely a wash-over from the Ouachita and Allegheny troughs. A drastic tectonic event, probably the Taconic orogeny, initiated this action. The Sylvan shale and its correlatives which are found in several epeiric basins is >300 ft thick in the Ardmore graben, and laps out near the edge of the Viola.

SILURIAN

Lower Hunton

The late surge of the Taconic–Ruby convergence continued into Silurian time. The squeeze caused regional warping to occur, raising some areas to emerge and be eroded and causing others to submerge. Shallow-water carbonate deposition was interrupted by periods of slight emergence and erosion. Deformation during this period of unrest resulted in several miles of left-oblique movement on the OM. Compare the palinspastic offsets in Figures 14 and 15. Only ~300 ft of Lower Hunton carbonate, representing only a small part of Silurian time, is preserved. A new, or rejuvenated, shear fault striking northward across north-central Oklahoma be-

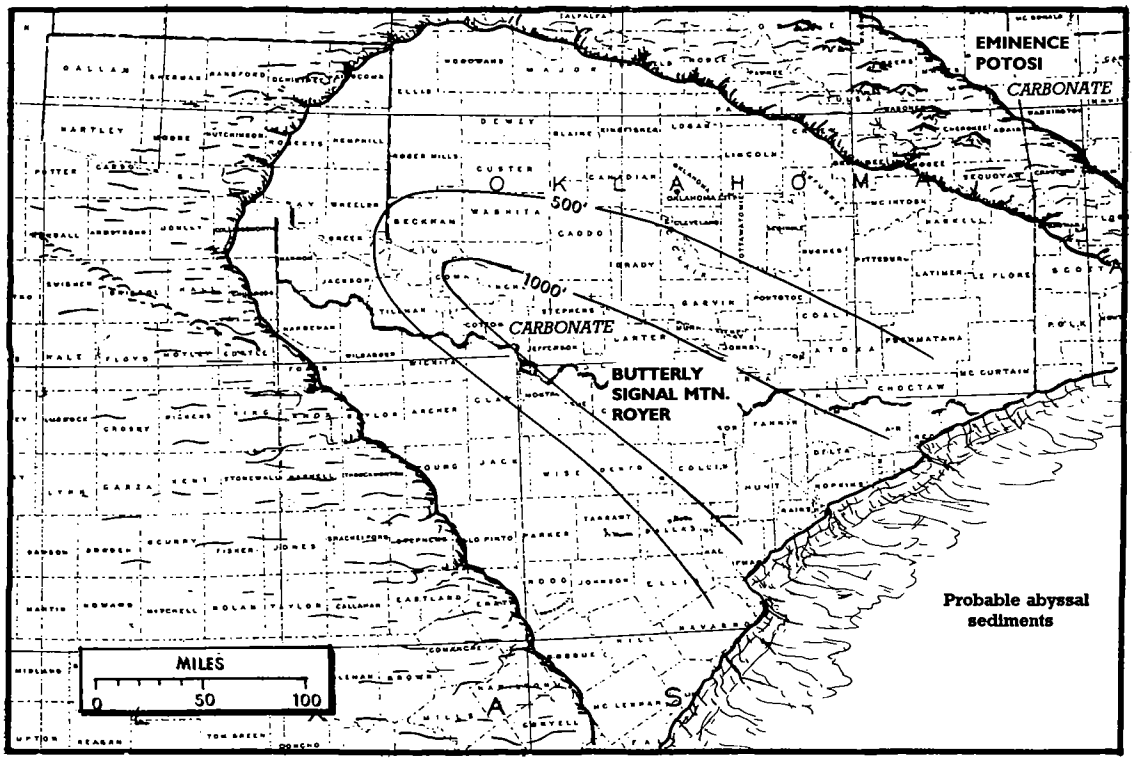


Figure 10. Late Cambrian (Trempeleauan) reconstruction. A broad symmetrical basin centered over the OM received >1,000 ft of Arbuckle Group carbonates.

came apparent. It has been called the Nemaha arch, ridge, uplift, or fault. It is not an arch, ridge, or uplift in Oklahoma, because regional dip on both sides of the fault is fairly low and uniform to the west and southwest. Here it will be referred to as the Nemaha fault. It is an extension of the Humboldt fault in southcentral Kansas, and is not the same fault as the original Nemaha fault of northeastern Kansas. Evidence for strike-slip movement on the Nemaha fault includes several reversals of throw along strike, uplifts at constraining bends, and grabens at release bends. Of special interest is the fact that this extensive fault, which is not apparent in strata older than Silurian, does not disrupt the much older Oklahoma megashear. To the southeast, off the cratonic margin, abyssal clastic deposition continued with the Missouri Mountain and Blaylock sequences.

DEVONIAN

Upper Hunton

The areal extent and lithological facies of the upper Hunton strata (Fig. 16) are very similar to those of the lower Hunton (Silurian). Shallow-water limestones dominated. Syntectonic deposition kept pace with subsidence with >1,000 ft of strata accumulating in the Anadarko basin. Upper Hunton strata pinch out to the northwest and to the northeast against the south flank of the Chautauqua arch (Bennison, 1993). Upper Hunton is absent and was probably not deposited immediately south of the OM.

A series of pulses from the Acadian orogeny in the east (the successor to the Taconic) elevated parts of the megashear and the eastern part of the northern shelf resulting in some erosion and thinning (0–400 ft, Fig. 16). The remaining strata represent only a small part of Devonian time. On the shelf, the end of Devonian time was marked by the development of a basin-wide carbonate-surfaced peneplain over which many rivers carved out channels that became choked with sand. These sand deposits became the prolific Misener sandstone oil and gas reservoirs. The lower Arkansas Novaculite was deposited in the slowly filling, deep Ouachita trough. Deposition of the novaculite was continuous into Mississippian time.

MISSISSIPPIAN

Kinderhookian

The post-Hunton peneplain extended well beyond the northern limit of the Hunton Group; rocks as old as Arbuckle and the granite basement were exposed on the northern shelf. The OM and the

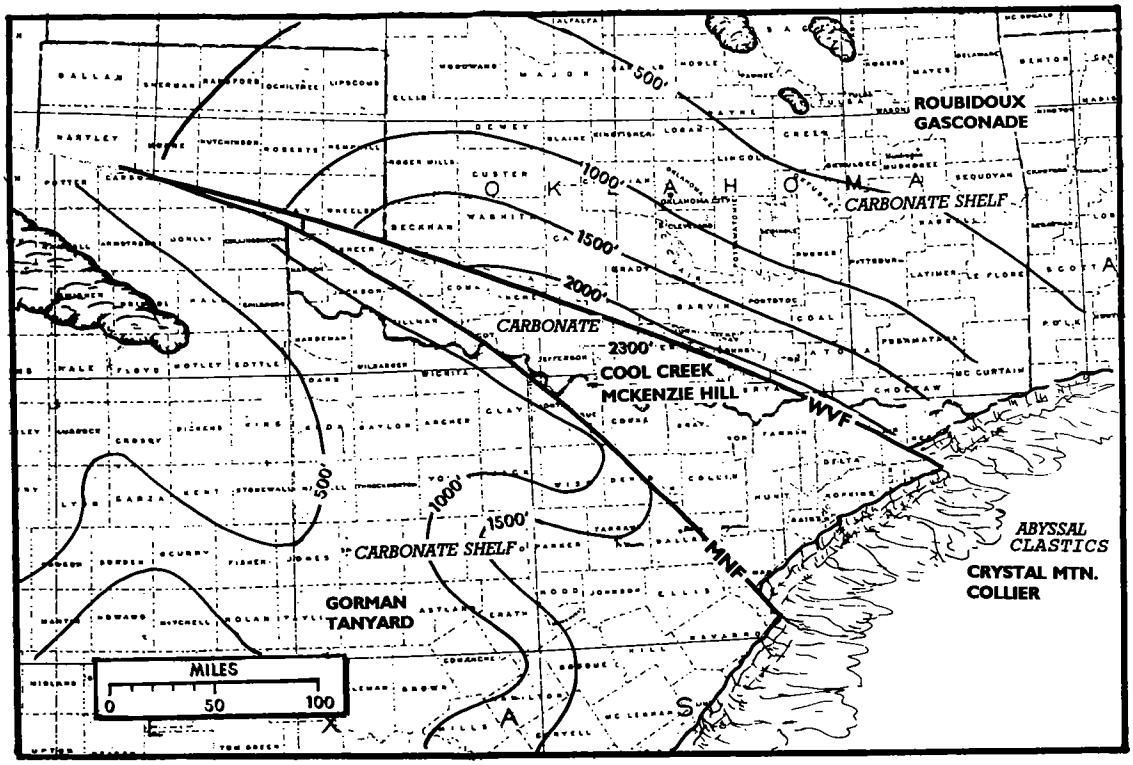


Figure 11. Early Ordovician reconstruction (lower Canadian). Regional sagging accompanied by shallow-water carbonate deposition (Arbuckle Group). The oldest known unit (Collier Shale) was deposited offshore in the Ouachita trough. MNF = Muenster fault; WVF = Washita Valley fault.

shelf north of the OM sagged and received a widespread veneer of black, organic-rich, radioactive Woodford Shale that thickens southward into the OM attesting to contemporaneous activity there (Fig. 17). Deposition of Arkansas Novaculite in the Ouachita trough continued into Osagean time.

Osagean

Depositional conditions changed drastically as open-marine circulation was restored over the very flat surface of the craton (Fig. 18). Shallow-water carbonates dominated there, and novaculite continued to be deposited in the trough. Tectonically, this was a relatively quiet time on the craton. However, things were about to change.

During Kinderhookian and Osagean deposition, continental drifting of Laurentia was smooth, as stratigraphically recorded tectonic activity was minimal. The eastward drift eventually brought Laurentia and its sutured east-bounding oceanic crust toward the irregular west margin of Gondwana, a much larger and less mobile cratonic assemblage. That part of Gondwana later collided with the eastern margin of Laurentia to become the Allegheny orogeny. Although Laurentia was still some distance away, the Ouachita trough oceanic crust, which carried the Early Paleozoic abyssal sediments, began an offshore subduction action beneath Amazonia, a possible component of Gondwana (Fig. 18). With this action, the Ouachita trough (a reverse-trapped margin basin [Dickinson, 1977]) became the Ouachita trench, and the Ouachita orogeny was initiated offshore from Laurentia. This offshore subduction continued as Laurentia's eastern margin sutured with Africa early in Pennsylvanian time, and, shortly thereafter, its south margin collided with Amazonia.

Meramecian

Figure 19 shows that the only structural element active on this part of the craton was the broad sag inherited from the Osagean that lay across the OM. North of the OM, shallow-water carbonates grade to the southwest into shale which is >1,000 thick in places (Fig. 19). On parts of the shelf, Meramecian strata are thin or absent due to erosion. Meramecian carbonates of the northern shelf contain millions of barrels of oil, possibly billions, most of which is not economically recoverable because of very low porosity and permeability.

As Laurentia drifted nearer to Amazonia, subduction continued, the Ouachita trench deepened,

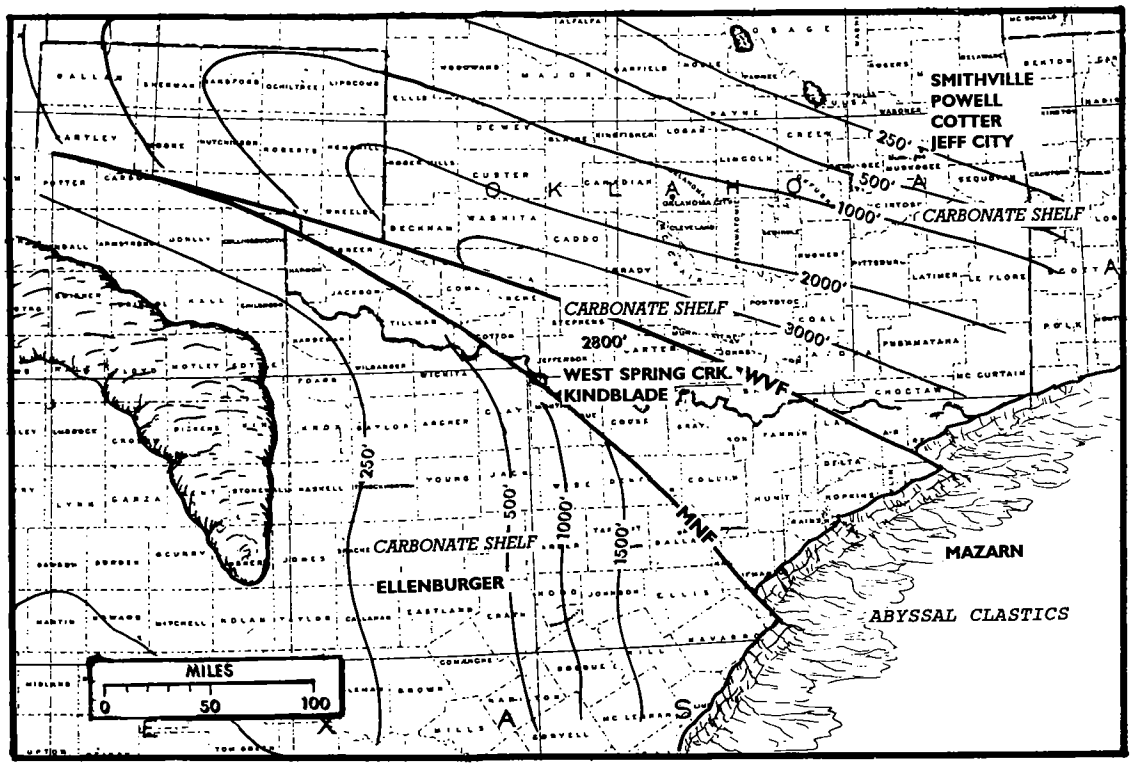


Figure 12. Early Ordovician (upper Canadian). Subsidence of the proto-Anadarko–Ardmore basin continued; south of the OM, the Texas arch began a slow emergence. WVF = Washita Valley fault; MNF = Muenster fault.

and a volcanic island arc formed offshore. According to Loomis and others (1994), the tuffs in the Stanley Group (Hatton Tuffs) in the Ouachita trough are geochemically comparable to "... continentarc silicic volcanic rocks. Because the tuffs are non-welded and were deposited as volcanic turbidite flows, they may have been deposited at a great distance (hundreds of kilometers) from their southern source." In the humid and hot tropical climate, the arc and the highly elevated Amazonian margin were subjected to intense erosion which provided tremendous amounts of siliciclastics (Stanley) that were deposited in the Ouachita trough. In Pennsylvanian time, some of the Stanley Shale and the older formations were thrust northward onto the craton. Figure 19 is a reconstruction showing the Ouachita trough (Stanley Shale and Hatton Tuff) before thrusting.

Stratigraphic and structural evidence indicate that subduction and convergence did not proceed smoothly. Instead, episodic activity (i.e., surges) occurred over millions of years. With each surge, the trench deepened, the margin of Amazonia was uplifted, thrusting extended further northward, and thousands of feet of prograding clastics flooded into the ever-narrowing trough. Northward-directed floods of coarser clastics were followed by finer sequences. Each thick sand-shale pair, a flysch and molasse couplet (or a parasequence) was the result of a major subductional impulse. This cyclic pattern of subduction, northward thrusting, uplift of Amazonia, intense erosion, and prograding deposition into and across the forearc basin is reflected in the Stanley and the three succeeding flysch formations.

The stresses that activated the north–northwestward Ouachita thrusts were from an entirely different source (Amazonia) and direction (south–southeast) than those that produced and sustained OM activity. OM activity was caused by eastward-directed stresses from the Ruby and Antler subductional orogenies on Laurentia's west margin that pushed the east margin of Laurentia into several collisional events (the Allegheny, Acadian, and Taconic orogenies). The end of Meramecian time was marked on the craton when most of the carbonate shelf was slightly elevated and moderately eroded.

Chesterian

The Texas shelf emerged, as did the Muenster and Criner blocks and the Wichita uplift (Figs. 3,20). As much as 1,500 ft of shallow-water carbon-

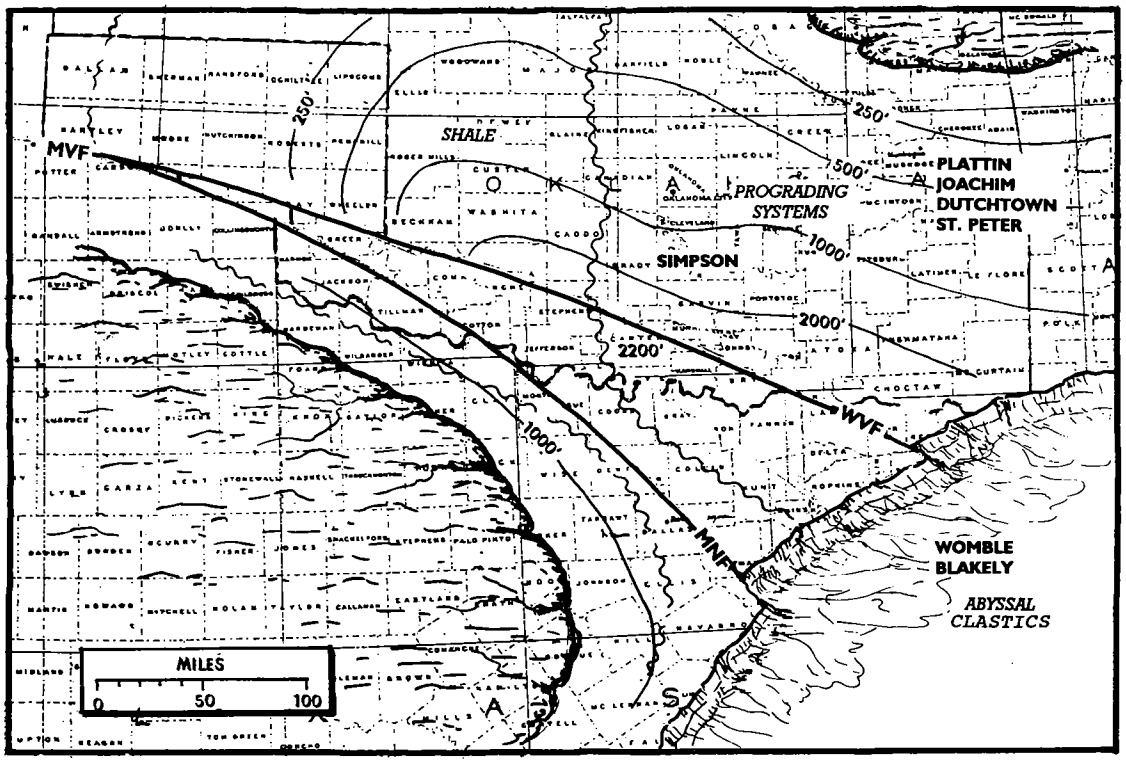


Figure 13. Middle Ordovician (Simpson Group) reconstruction. Emergence of the Texas arch; the first major influx of terrigenous clastics were deposited as five cyclothems. The cyclic pattern was likely the result of Taconic collisions on the east margin of Laurentia. MVF = Mountain View fault. Wavy lines mark boundaries between dominant lithofacies.

ate was deposited on the shelf. Basinward, the shelf carbonates give way to shale. More than 1,500 ft of Springer Shale was deposited in the Anadarko basin and as much as 2,300 ft was deposited in the Ardmore graben. These shales were probably circulated from the narrowing Ouachita forearc basin. The deep Stanley sub-basin (Fig. 3) received 8,000–10,000 ft of turbidites (flysch), probably derived from the arc and Amazonia.

EARLY PENNSYLVANIAN

Morrowan

Movement during this time was the earliest of several very intense Pennsylvanian tectonic events. Resurgent Alleghenian collisional pulses continued to jostle the OM in a sinistral transpressional manner. In this paper, "Alleghenian" surge or orogeny refers to the east–west stresses that activated the megashear, even though the actual driving forces may have originated in the west.[1] Laurentia responded to the collisional impacts with some movement along interior zones of crustal weakness, i.e., fractures, faults, and megashears. It is in and adjacent to these zones that the most intense deformation occurred on the craton. A local uplift that popped-up, the fairly small Criner Hills (Fig. 21), led Van Waterschoot Van der Gracht (1931) to conclude that the Criner Hills were part of the larger Wichita Mountains, so he introduced the term Wichita orogeny for the Early Pennsylvanian deformation.

Laurentia maintained its spasmodic, but incessant, southeasterly collision course with Amazonia. The north–northwest-directed compressional stresses associated with subduction and the collision of Laurentia and Amazonia lasted only from

[1]I have been cautioned by several structural geologists that the cratonic crust is physically incapable of transmitting stresses from the margins of a craton to its deep interior to effect deformation there. However, Craddock and others (1993) present compelling evidence from crystal fabric analysis that compressive orogenic stresses were transmitted as much as 1,100 mi through carbonates of the foreland during the Appalachian–Ouachita orogeny. Stevenson and Cloetingh (1991) point out that large changes in the intraplate stress field may cause extensive deformation of the entire lithosphere on a scale of hundreds of kilometers.

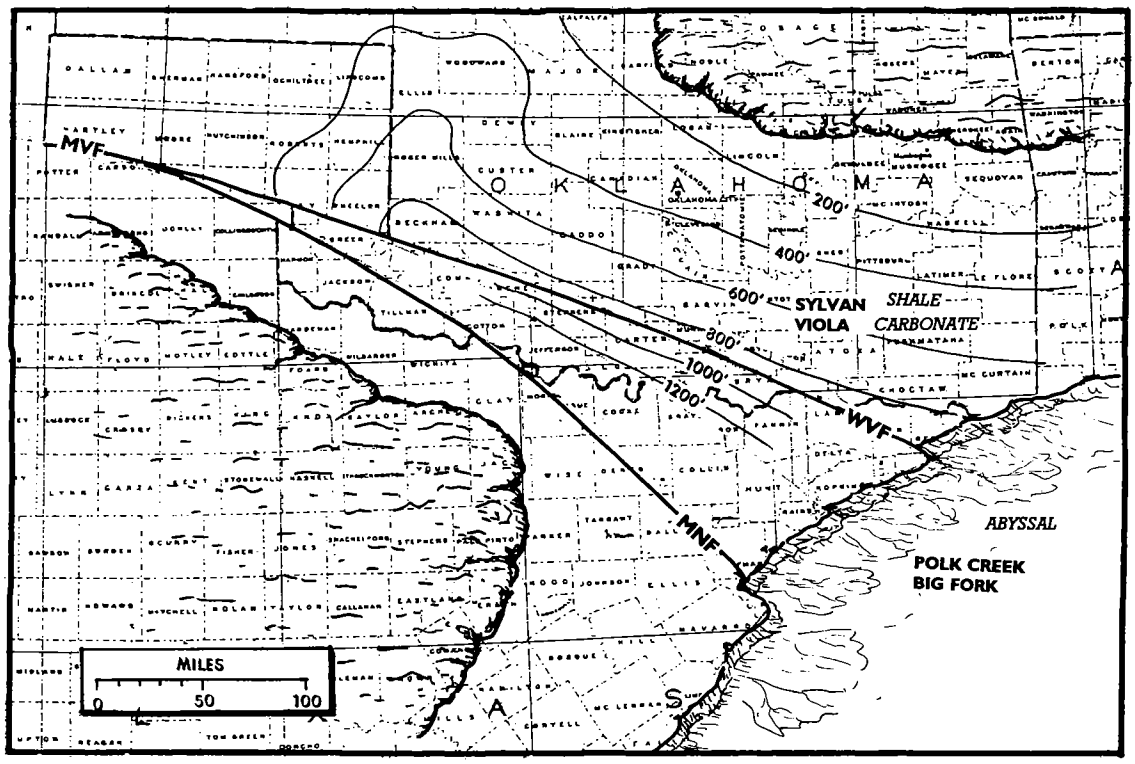


Figure 14. Late Ordovician reconstruction. Overall configuration of the study area was the same as in the previous epoch. Thick Viola shelf carbonates are overlain by basinal shale (Sylvan). WVF = Washita Valley fault; MNF = Muenster fault.

Middle Mississippian to Middle Pennsylvanian time, and were entirely separate from the west–east shear stresses that reactivated the OM.

The Texas shelf, south of the Muenster fault (Fig. 21), tilted southeast toward the trench and received >500 ft of westward-prograding shales and thin sands. The block between the Muenster and Criner faults (Fig. 3) remained emergent, and its southeastern end was eroded down into the Arbuckle Group. The Ardmore graben was depressed further while receiving ~3,000 ft of sediment, mostly shale (locally called the Lower Dornick Hills Group), carried in from the Ouachita trench.

More than 5,000 ft, mostly shale, was deposited in the southwestern part of the Anadarko basin as it continued to sag. Most of the surrounding land masses had carbonates exposed. Perhaps most of the mud came from the Ouachita area, although some came from the Wichita uplift and some was delivered by rivers from the northwest. A broad low-relief arch emerged across northcentral Oklahoma, effectively separating the Anadarko basin from the relatively stable northeastern Oklahoma shelf with its shallow-water sands and carbonates (Fig 21). Many of the littoral and channel sandstones in the northwestern Anadarko basin and on the northeastern shelf are important oil and gas reservoirs.

As the Ardmore graben was being depressed, it was subjected to strong transpression between the Washita Valley and Criner faults. This led to the formation of many tightly folded and faulted en echelon uplifts in the Ardmore graben. Similar uplifts formed in the Anadarko basin. These uplifts have been called *flower structures* (Harding and others, 1983) or *buckle structures*. The term *squeeze-up structure* is used herein, as it clearly describes the origin of the features. Squeeze-up structures are commonly found in thick, pliable, shale-filled basins, where, upon the application of transpressional forces, deformation is by plastic flow into en echelon, rootless, faulted, and tightly folded anticlines with upward-branching axial faults (Fig. 22A). Each belt of en echelon folds is the shallow manifestation of a single strike-slip fault at depth. The shallow aspects of these structures give the appearance of a great deal of horizontal shortening, when, in fact, there is little, if any, at the basement level. Seismic sections across squeeze-ups, or flower structures, show the deep strata to be relatively unfolded (Fig.

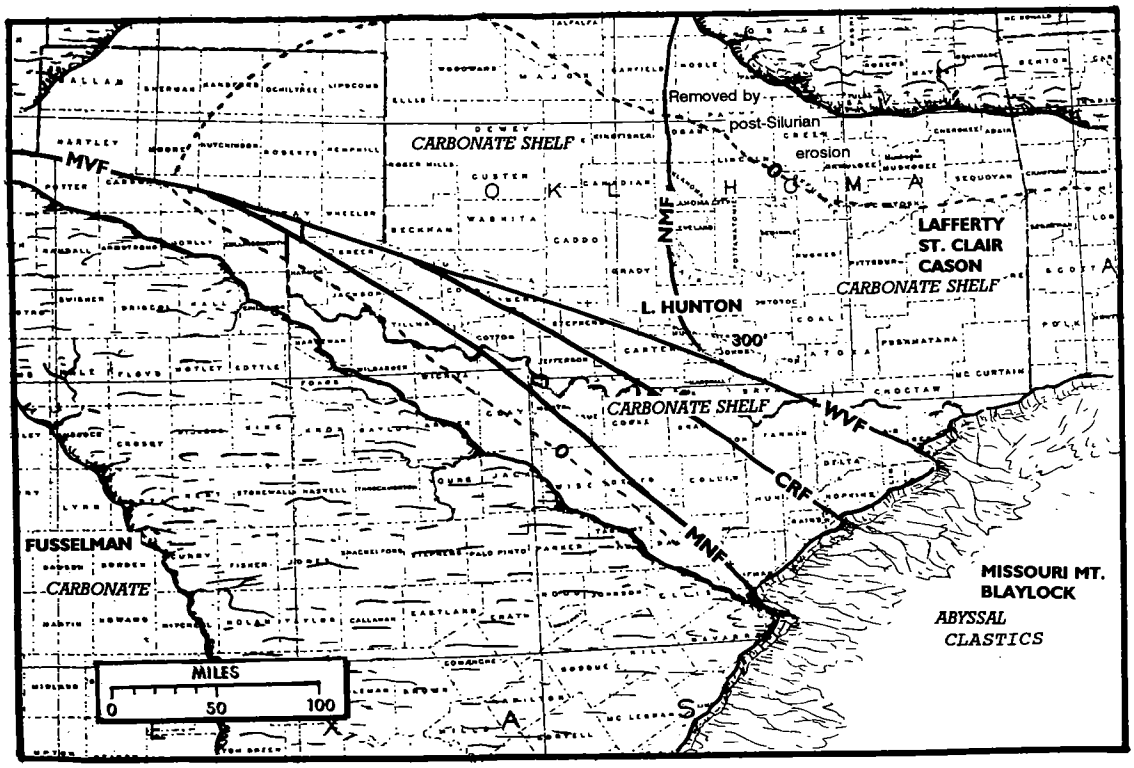


Figure 15. Silurian (lower Hunton Group) reconstruction shows several miles of left-oblique movement on the OM (compare to Fig. 14); and first appearance of the Nemaha fault zone (NMF) which is interpreted to be a right-lateral strike-slip fault. Deformation and the development of several extensive unconformities are attributed to the Taconic orogeny. CRF = Criner fault.

23). Clay model studies show that as strike-slip movement of the basement (i.e., the boards on which the clay is mounted) progresses, en echelon folds and faults form in the clay above the fault. The near-surface clay deforms into diagonal uplifts (squeeze-ups) and depressions, giving the appearance of horizontal shortening at the surface but with none perpendicular to the basement fault. A factor often overlooked in attempting to balance cross sections perpendicular to strike-slip faults is that strata may have moved laterally into or out of the plane of the cross section. For this reason, two-dimensional balanced cross sections of these structures are meaningless.

A few miles north of the Washita Valley fault, and sub-parallel to and converging with it to the west, the Sulphur fault came into existence (Fig. 21). Left-lateral transpressional movement resulted in uplift of the Tishomingo–Belton block between the two faults (Figs. 3,21). As used herein, the term *pop-up structure* refers to uplifts that resemble ordinary horst blocks. Unlike horst blocks, they are bounded by strike-slip faults that extend well beyond the uplift (through-going faults) and converge downward (Fig. 22B). Pop-ups are diamond- or lens-shaped in areal aspect and are composed mostly of competent strata. They are very common in intricate shear fault systems and "pop up" as strike-slip movement progresses.

The Ouachita trough narrowed as Laurentia approached Amazonia. The oceanic plate was being pushed down into the subduction zone by mantle convection currents and by tectonic loading by the 3–5-mi-thick overriding allochthon. The cratonic margin, part of the subducting plate, with its veneer of older shelf sediments was also carried downward. The competent (brittle) nature of the shelf deposits (mostly thick carbonates underlain by granite) resulted in their being broken by down-to-the-basin normal faults of large magnitude. These faults may have originated by crustal attenuation and thermal subsidence associated with the Cambrian break-up of Pangea and were later propagated upward into the concurrently deposited sedimentary prism to become large-scale synsedimentary faults. How thick would the allochthon have to be to cause a competent shelf margin to sag 20,000–30,000 ft? It must have been several miles thick at least. The relative abundance of shelf-derived olistostromes in the Johns Valley Shale (and,

to a lesser extent, in the Stanley and Jackfork Formations) suggests that the craton margin had finally been overridden by the thrust-faulted flysch wedges. The olistostromes that were carried northward by the resurgent thrust faults were either fragments ripped from the shelf edge or talus from submarine fault scarps. Convergence of the two cratons continued with Laurentia's deeply depressed shelf margin beginning to underplate the thrusted flysch wedge. As much as 7,000 ft of flysch (Johns Valley and Jackfork Formations) were deposited in the Ouachita trough. The Morrowan depocenter of the Ouachita trough (the Johns Valley–Jackfork sub-basin, Fig. 3) had shifted northward onto the deeply depressed cratonic margin. The intermittent surges of the subduction resulted in uplift of Amazonia and its sedimentary apron. The highly elevated allochthon and hinterland were essentially barren of protective vegetation, as only aquatic and swamp plants had evolved. Vigorous erosion provided thousands of feet of interbedded sandstone and shale which were deposited in the progressively northward shifting basin. Northward thrusting, which now extended well inland from the deeply depressed shelf margin was renewed.

MIDDLE PENNSYLVANIAN

Atokan

The Texas shelf maintained its steady, gentle, basinward subsidence. Now, instead of subsidence being entirely caused by rift-related attenuation, it was also caused by the tectonic loading imposed on it by the highly elevated overriding allochthon. The degree of loading and subsidence of the Texas shelf margin was not as great as that of the Oklahoma margin because of the low-angle oblique approach of the allochthon onto the Texas margin. More than 5,000 ft of fluvial and coastal sediments derived from the rising Ouachita Mountains were deposited near the margin in several prograding sequences that thinned abruptly toward the northwest (Fig. 24).

With renewed lateral movement of the OM, the block between the Muenster and Criner faults was split by the new Marietta fault (Fig. 24). The Criner block (north of the Marietta fault) subsided southeastward to form the Marietta basin which received >3,000 ft of shales and thin sands. The Muenster block (immediately north of the Muenster fault) was considerably elevated and deeply eroded, giving rise to the extensive Bendian carbonate con-

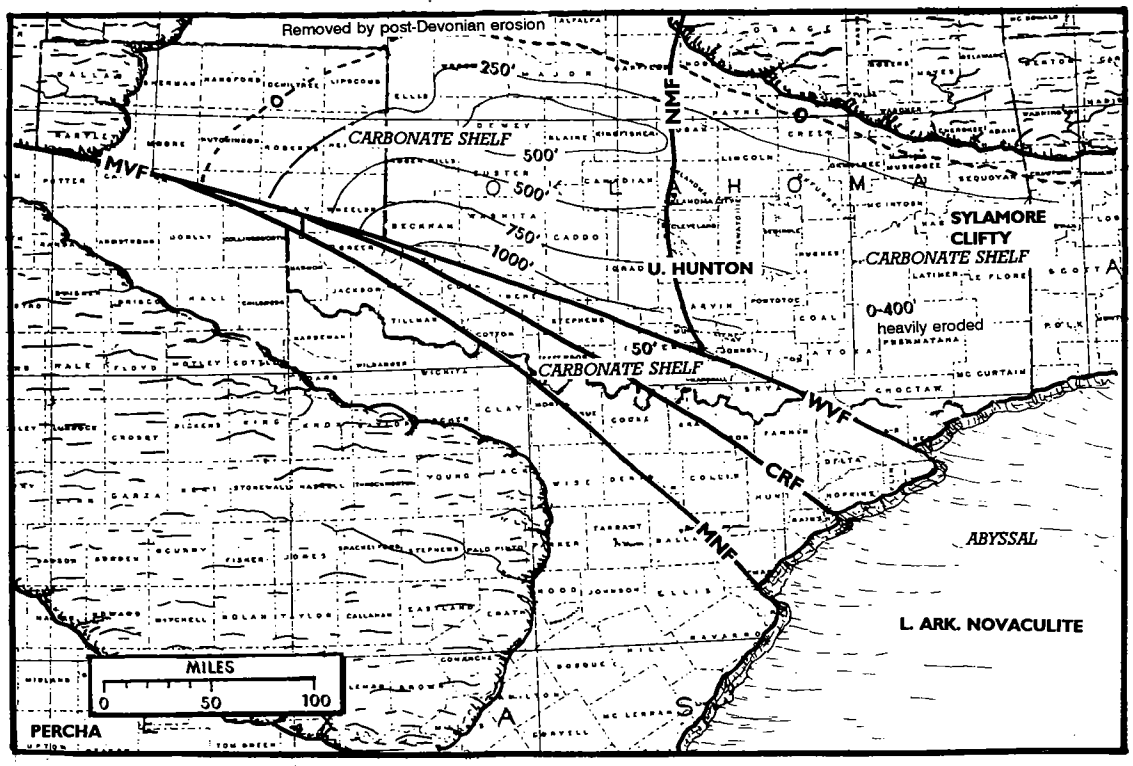


Figure 16. Early Devonian (upper Hunton Group) reconstruction. Upper Hunton carbonates are thin to absent east of the NMF (0–400 ft) and thin in the OM due to uplift and erosion associated with the Acadian orogeny.

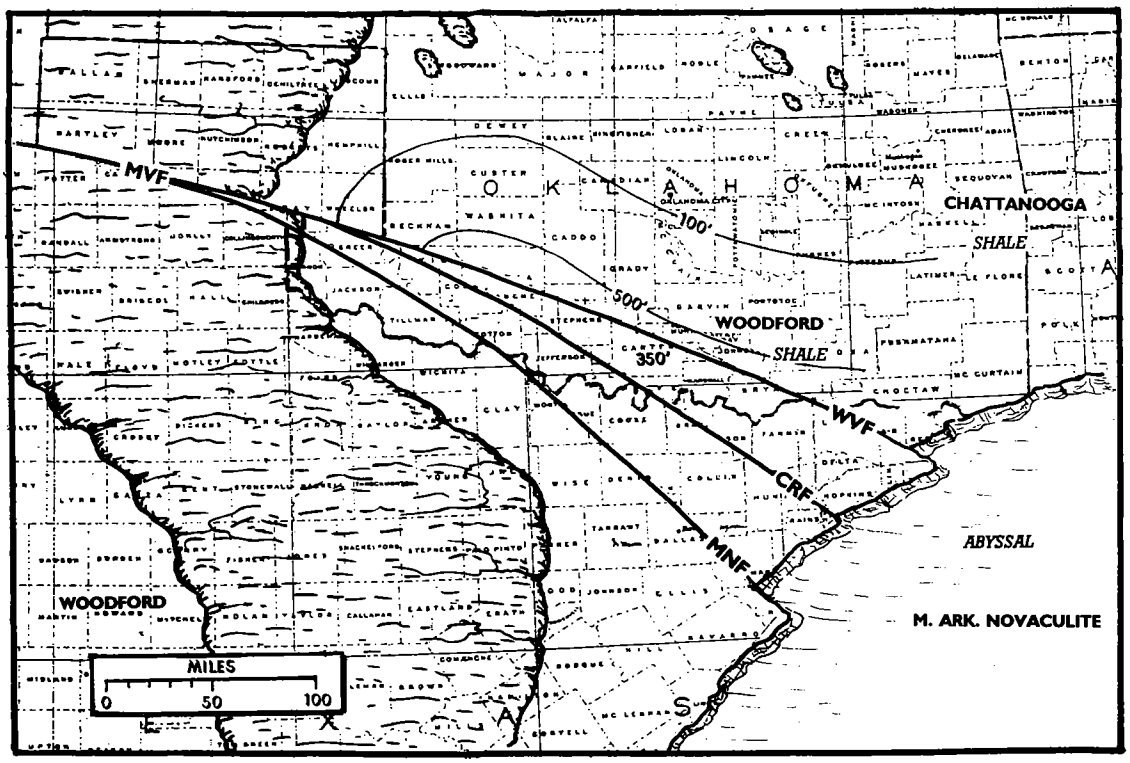


Figure 17. Kinderhookian reconstruction. Black, organic-rich, radioactive shale (Woodford and Chattanooga) thicken into the graben. Arkansas novaculite was deposited in deep water of the Ouachita trough.

glomerates to the south (McBee and Vaughan, 1956). Intense erosion of the Criner Hills uplift resulted in the Bostwick carbonate conglomerates being deposited around its submerged flanks (Fig. 24). Transpression, still acting on the narrow shale-filled Ardmore graben, further folded the earlier-formed squeeze-up structures, some of which had emerged and were partially beheaded by erosion. The incessant down-warping of the Anadarko basin impounded 4,000 ft of shale and thin sands. Most of the clastics probably came from the rising Ouachita allochthon, through the Ardmore graben, where the 4,000-ft-thick Upper Dornick Hills Group was deposited. The seaway between the Atoka sub-basin and the Ardmore–Marietta basin was restricted, but had not yet been blocked by the emerging thrust front.

The central Oklahoma uplift remained a low-relief peninsula with an exposed carbonate terrain, as did the Wichita block (Fig. 24). The central Oklahoma uplift separated the southwesterly sagging Anadarko basin from the gently southeasterly sloping and submerged northeastern Oklahoma shelf. Erosion of landmasses to the north and northeast provided great volumes of terrestrial siliciclastics to the northeastern Oklahoma shallow-marine shelf and to the sagging Atoka sub-basin (Figs. 3,24). Western Appalachia was the source of similar clastic suites deposited in both the eastern part of the Arkoma basin and the Black Warrior basin (Nicholas and others, 1989). (The Arkoma basin is that part of the Atoka sub-basin that lies between the present trace of the Choctaw fault and the Ozark uplift).

As in the immediately preceding epochs, southward subduction continued. Regional thrust faults moved blocks that were thousands of feet thick northward onto the shelf. Flexural downwarping of the shelf, caused by the encroaching allochthon, developed new and reactivated old down-to-the-basin normal faults in the Atoka sub-basin. Floods of sediments from the north cascaded down over these blocks, forming locally perched, as well as abyssal, submarine fans. Porous sands trapped in these structures were to become prolific gas reservoirs. In addition to the sediments from the north, thousands of cubic miles of sediments rapidly eroded from the high-relief allochthon were deposited in the trench where >16,000 ft of sediments accumulated (Fig. 24). From Morrowan to Atokan time, the allochthon and the foredeep moved northward as a result of an active period of subduction, hence the Johns Valley–Jackfork sub-basin (Figs.

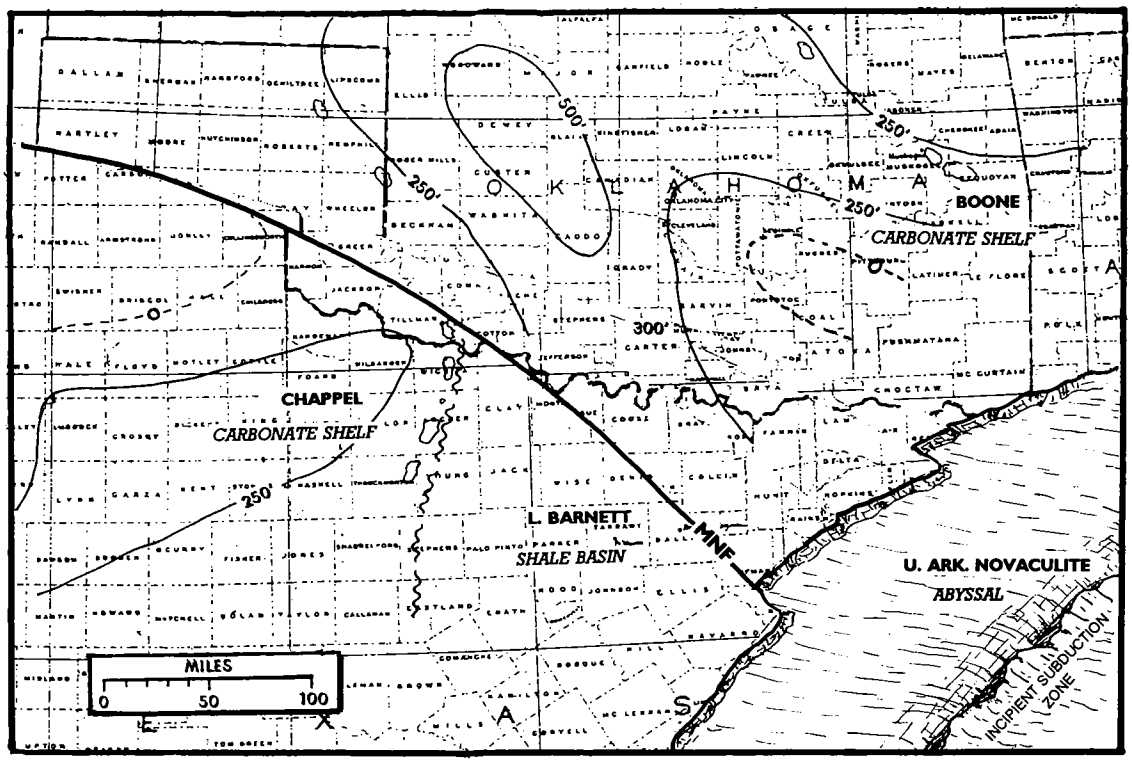


Figure 18. Osagean reconstruction. Broad carbonate banks on the shelves with little evidence of deformation on the craton. An incipient subduction zone offshore probably formed as Laurentia and Amazonia converged. Wavy line shows the boundary between lithofacies. MNF = Muenster fault.

3,21) evolved into the Atoka sub-basin (Figs. 3,24). The southwestern reach of the very deep Atoka sub-basin terminated abruptly at the emergent Tishomingo block.

The end of Atokan time came about when the thrust front in the Arkansas sector encountered the buttressing effect of Ozarkia which resisted further sagging. With the cessation of sagging and the ramping effect of subsequent thrusts, abyssal trench deposits were raised above sea level. This action also marked the end of the Ouachita basin, as that term is generally used. However, it was not the end of the Ouachita collisional orogeny, which persisted into Early Permian time when the aftershocks of the suturing ceased.

Early Desmoinesian

Probably the most intense and widespread taphrogenic event since the Middle Proterozoic shattered and re-shattered Laurentia during early Desmoinesian time (Fig. 25). Extremely strong shock waves were projected westward from the surging impacts of Laurentia's pre-climactic lock-up with Africa (Gondwana), during the Allegheny orogeny. These surges were generated by the subduction of the Pacific oceanic plate beneath the west margin of Laurentia (Antler orogeny) (Wilson and Laule, 1979). At the same time Laurentia was being pushed/carried eastward into collision with Amazonia. However, the actual suturing of the two did not happen until middle Desmoinesian time.

Nearly every fault on the craton was activated by this disturbance. Most experienced syntectonic sedimentation. Along the extended trend of the OM, the Marietta, Ardmore, Hollis, Anadarko, Dalhart, Apishapa, Taos, Paradox, Eagle, Uinta, and Oquirrh basins subsided and received thousands of feet of clastics from adjacent contemporaneous uplifts during this period. Similar tectonic events occurred along Laurentia's other megashear zones. Figure 26 shows a rather detailed interpretation by Ferrebee (1991a,b) of a portion of the intensely faulted Ardmore and Marietta basins. Many pop-up and squeeze-up structures occur in this system.

The Washita Valley fault was described by Tomlinson (1952) as a structural "oddity" which he called a "propeller fault." Immediately north of the West Timbered Hills area of the Arbuckle block, the Washita Valley fault is known to dip ~50°S. (back under the popped-up Arbuckle block.) Fifteen miles to the east–southeast, at the town of Crusher,

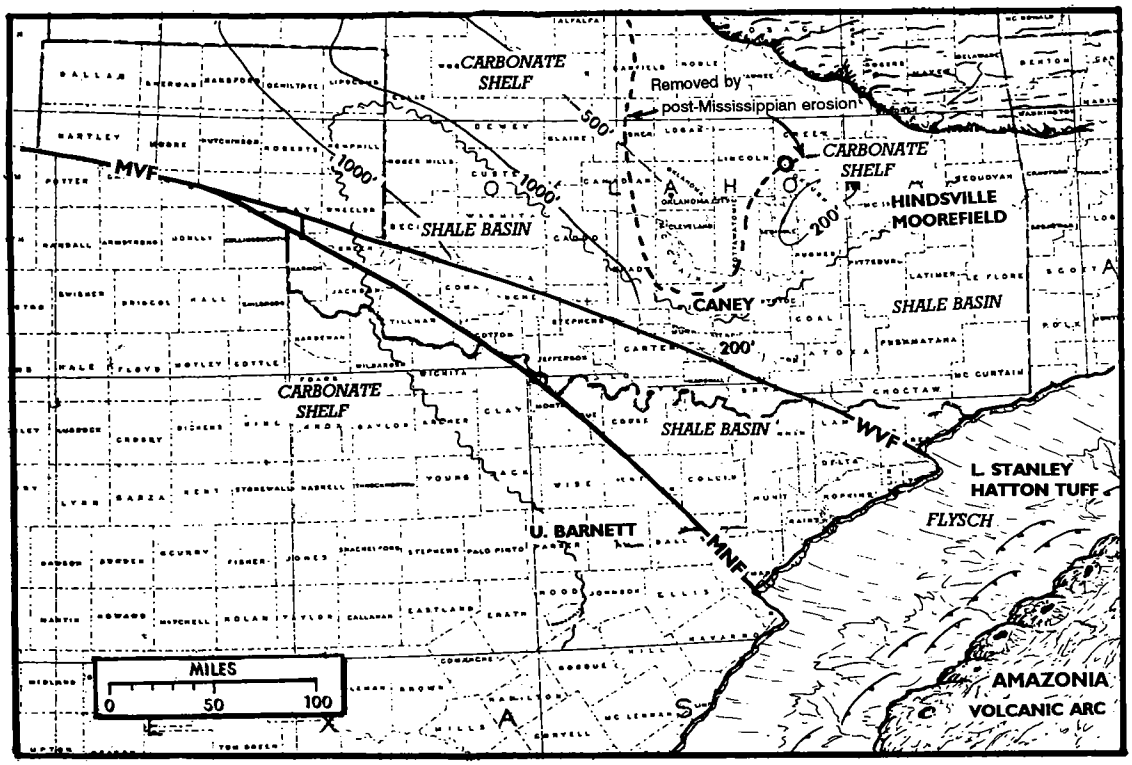


Figure 19. Meramecian reconstruction. Broad symmetrical sag on the stable shelf, with carbonate banks and a central shale basin. Southeast of the craton, southward subduction of oceanic crust beneath Amazonia resulted in formation of a volcanic arc (source of the Hatton tuff), and uplift of the margin of Amazonia which was the source of floods of flysch (Lower Stanley Shale) deposited in the newly formed trench. Wavy line shows boundaries between lithofacies.

the same fault is essentially vertical, and 15 mi farther to the east–southeast, the fault has flipped over and dips ~55°N. (back under the popped-up Tishomingo block) (Fig. 3). The presence of throw-reversals along strike is one of the most diagnostic features of strike-slip faults (Sylvester, 1988). The rigid "hanging" walls of both dipping fault segments are merely leaning out (not thrusted) over the less-competent shale-filled basins.

The Anadarko basin and Wichita Mountain blocks are separated by the Mountain View fault (Fig. 3). The rigid Wichita block, which consisted of thick lower Paleozoic carbonates and older igneous rocks began to pop up and spread out laterally. At the same time, the shale-filled Anadarko basin was subsiding rapidly. Part of the basin's subsidence may have been caused by its having been drawn down into the deep space formerly occupied by the rising Wichita block. Isostasy? As the basin subsided, the Wichita block continued to rise and spread laterally. As left-lateral movement continued, the outer blocks and their bounding faults tended to rotate (lean, not move) out over toward the subsiding basin. Figure 27 shows how this process might have worked. The outer blocks now lean ~45°, dipping back southward under the main Wichita block.

In discussing the Anadarko basin–Wichita Mountain COCORP seismic profiles 2 and 2a, Brewer and others (1983) conclude that "the COCORP data could be consistent with oblique slip along the Wichita trend. Some degree of left-lateral slip is suggested by the en echelon (Burch and Muenster) faults flanking the south side of the Wichita Mountains, and those in the northern frontal system." Although they were uncertain as to how to project the downward-converging bounding faults into the deeper zones, Brewer and others (1983, fig. 4) present an excellent illustration of a pop-up block.

The older-rock-over-younger aspect gives the illusion of thrusting. However, considering the facts known about the Washita Valley fault, and other faults in the OM, these structures could not have been produced by a simple northward compressional force, as advocated by some workers. Far too many "analytical studies" have been made of this structural feature in which only the local aspects were considered, without putting it into the perspective of being a very small part of a craton-

wide tectonic system. Only large-scale, left-lateral transpression can explain the complicated structures just described. The distinction between reverse faults associated with pop-up structures (i.e., pseudo-thrusts) and those formed during tectonic thrusting can be easily perceived when the circumambience is understood.

Oblique subduction of the Texas shelf led to additional tectonic loading and subsidence of the shelf margin; syntectonic deposition of westward-prograding coastal plains kept pace with subsidence. As before, the source of these thousands of cubic miles of shale and fine-grained sand was the uplands to the east. In central Texas, a carbonate shelf developed in an open-marine environment, and a vast and long-lived, reef-fringed carbonate bank began to form (Fig. 25).

By Desmoinesian time, Laurentia had moved far enough to the south–southeast, so that the southeastern ends of the Muenster and Tishomingo island blocks had collided with the emergent thrust front thereby cutting off free-marine circulation between the Arkoma, Ardmore, and Fort Worth basins (Fig. 25). Each basin then received its own unique sedimentary sequence, making inter-basin lithologic correlations difficult. The western end of the Criner–Muenster block was sufficiently uplifted and eroded to unroof the long-buried Wichita igneous pile. Granite wash (arkose) was deposited in the surrounding sedimentary apron. The submerged southeastern end of the Criner block (the Ardmore basin and the northeast part of the Marietta basin) received >1,200 ft of westward-prograding deltaic deposits which included several thick beds of chert conglomerate derived from pre-flysch strata exposed in the nearby Ouachita provenance (Fig. 25). The very thick, shale-filled Ardmore graben was continually subjected to left-lateral transpression between the Criner and Washita Valley faults. The earlier-formed, en echelon squeeze-up structures were further folded, faulted, and elevated once again to become islands. The soft sediments were quickly eroded and redeposited in the surrounding shallow waters (Tomlinson and McBee, 1959,1988). Lenticular sandstones in these structures subsequently became reservoirs for prolific oil and gas fields.

In the Anadarko basin, >1,100 ft of new sediments were added. Left-lateral transpression renewed large squeeze-up structures (Fort Cobb, Cordell, and Elk City anticlines) with axes oriented ~30° clockwise from the basin axis (Fig. 25). Great quantities of granite wash and carbonate conglomerate were deposited in extensive submarine fans along the very steep escarpment on the north edge of the Wichita uplift. Beds of porous granite wash

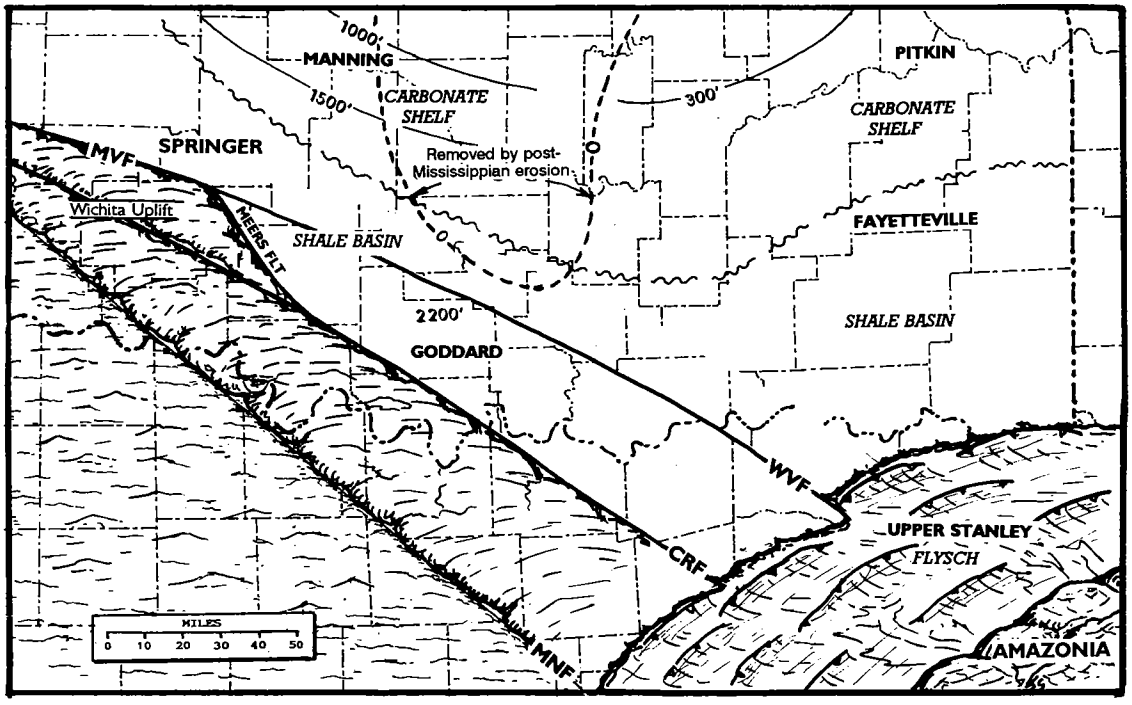


Figure 20. Chesterian reconstruction. The area south of the megashear, the Muenster and Criner blocks, and the Wichita block were uplifted. On the shelf north of the OM, carbonates grade southward into shale. Mud was probably washed in from the Ouachita trough where Upper Stanley Shale was being deposited. Wavy line shows boundaries between lithofacies.

that were deposited over the syndepositional squeeze-up structures became hosts to important hydrocarbon accumulations.

Following the filling and uplift of the Atoka sub-basin, much of the Ouachita frontal area had been reduced to a very flat, intermittently emergent and submergent coastal and delta plain. Anastomosing channel systems carried sediment westward into a shallow epeiric sea; thus, the Hartshorne Formation of the Krebs Group was deposited. Immediately afterward, a compressional surge from the south began to form a syndepositional sag at the west end of the Arkoma basin in which coastal plain and neritic sediments of the McAlester, Savanna, and Bog-

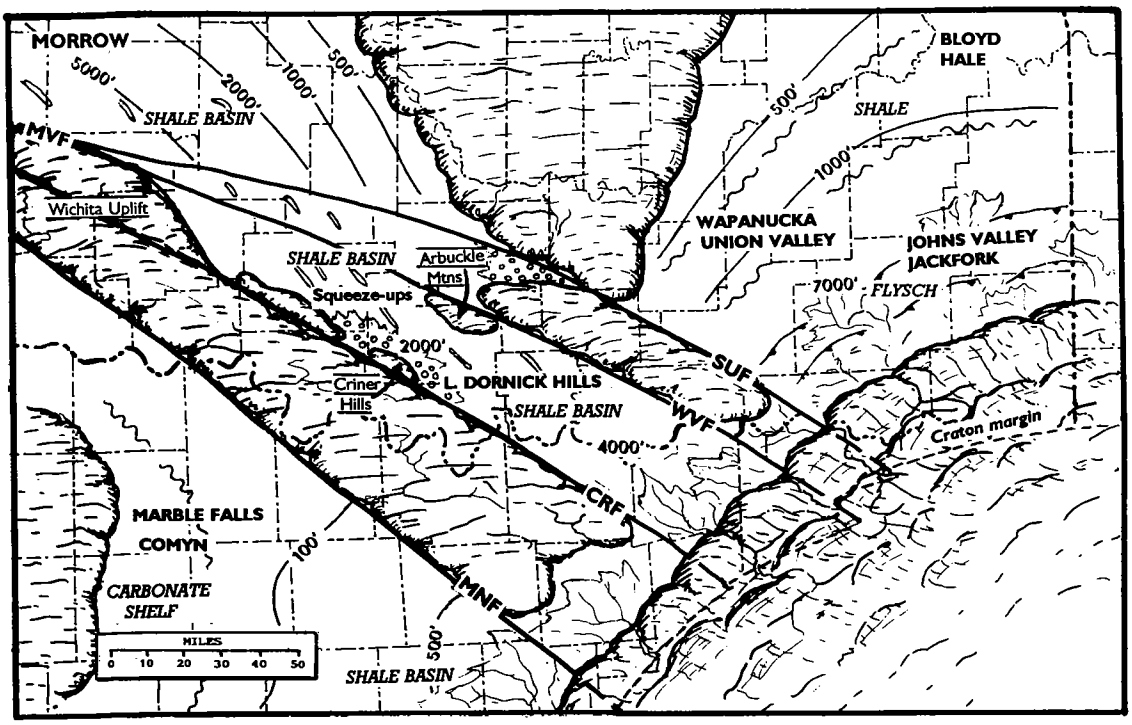


Figure 21. Morrowan reconstruction. Emergence of the Criner Hills, Arbuckle Mountains, the Muenster–Criner arch, the Tishomingo block (between WVF and SUF), and the central Oklahoma uplift. The Ouachita thrust front encroached onto the craton as Laurentia's southern margin was subducted beneath Amazonia. Johns Valley–Jackfork sub-basin (Fig. 3) is a foreland basin formed by tectonic loading of the shelf. Wavy lines show boundaries between lithofacies.

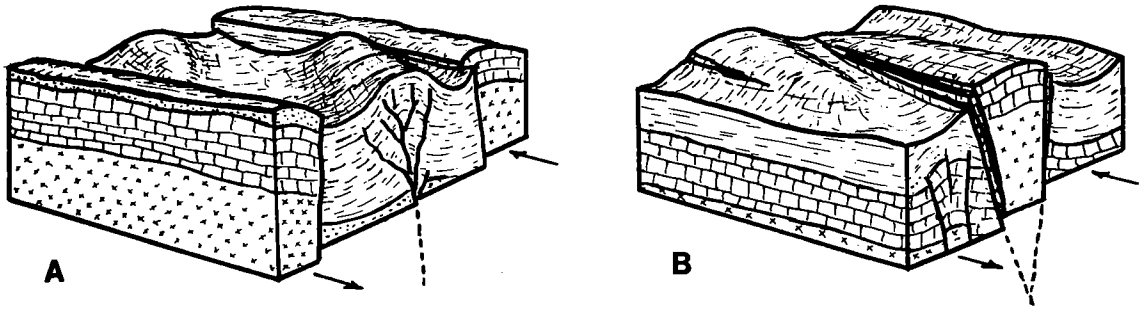


Figure 22. Two entirely different uplifts that are formed by strike-slip deformation, and commonly referred to as "flower structures" (Harding and others, 1983). (A) Squeeze-up structures are steep-sided folds with internal faults that converge downward into a single strike-slip fault. The fold axes are ~30° to the strike-slip fault at depth. Squeeze-ups form under transpression in thick accumulations of incompetent shale in basins or grabens bounded by relatively competent blocks. (B) Pop-up structures are uplifts bounded by downward-converging through-going faults. They form in competent, fairly rigid strata in active strike-slip fault zones.

gy Formations of the Krebs Group were deposited. The maximum Krebs Group thickness preserved is >8,000 ft (Fig. 25) in the Early Desmoinesian sub-basin just north of the Choctaw fault (Fig. 3). Therefore, this basin must have extended at least 20–30 mi beyond its present southern limit which is located in steeply dipping outcrops parallel to and immediately north of the present trace of the Choctaw fault (which did not exist at that time). The southern part of the Early Desmoinesian sub-basin has long since been uplifted and removed by erosion.

The central Oklahoma uplift had become a faulted peninsula that essentially blocked marine circulation between the Anadarko basin and the northeastern shelf (Fig. 25). Clastics eroded from uplifts to the north and east prograded westward into the shallow epeiric sea of the northeastern Oklahoma shelf and southward into the deep Early Desmoinesian sub-basin (Figs 3,25). Intermittent small-scale subsidence of the shelf, caused by minor shocks from the Ouachita collision, resulted in cyclic deposition of progradational clastic suites (cyclothems or parasequences). The upper surfaces of many of these suites were dissected by very widespread, anastomosing fluvial systems. Sandstones in these channel deposits, which are as much as 100 ft thick and 1 mi wide, contain some very important (but elusive) oil and gas reservoirs (e.g., Booch and Bartlesville).

The northward thrusting of the Ouachita allochthon bore directly onto that area of the craton that lay between the central Oklahoma and Ozark up-

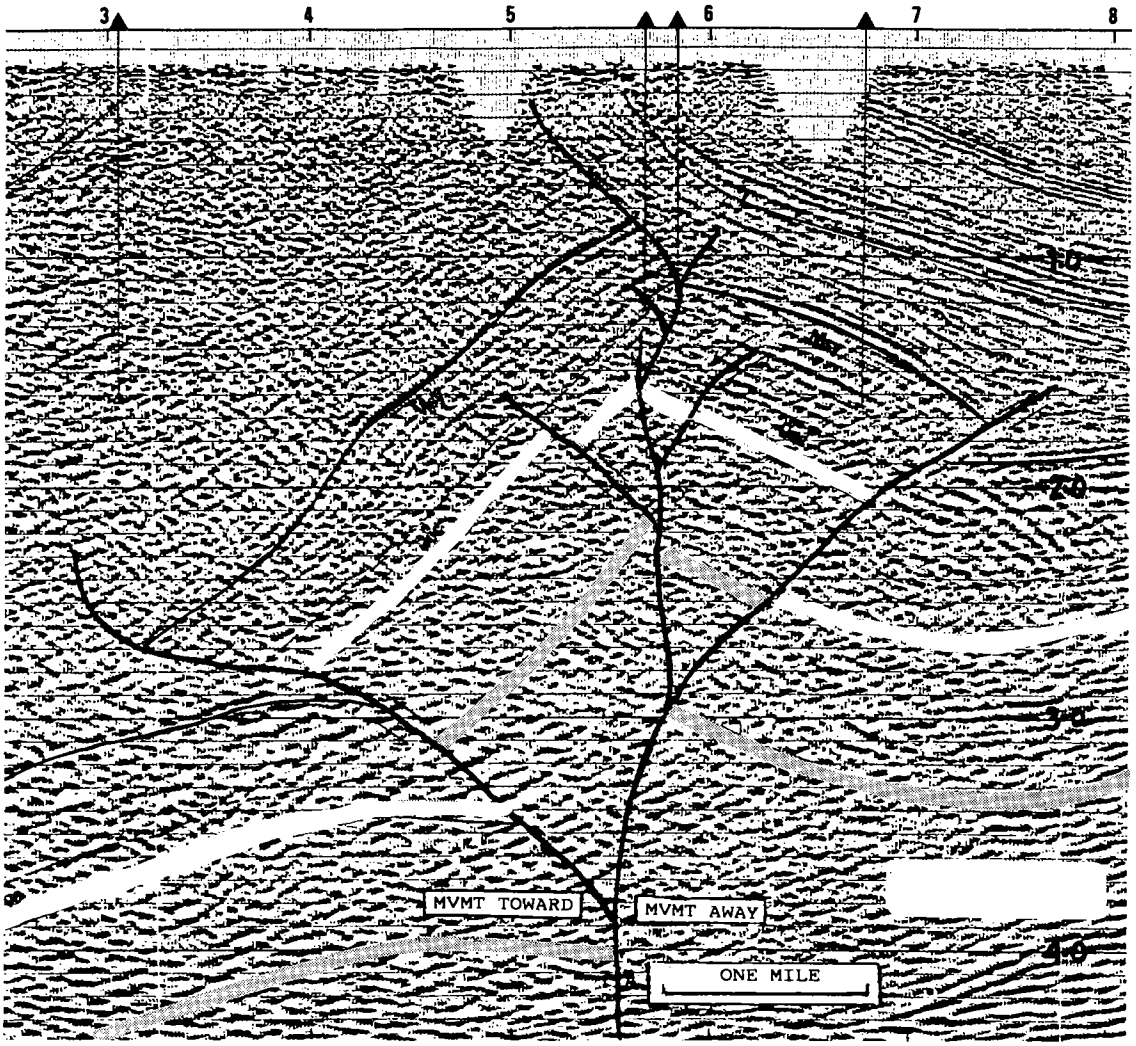


Figure 23. Seismic section across the Caddo anticline, a squeeze-up structure in the Ardmore graben (modified from Harding and others, 1983). Squeeze-ups form by rotation and uplift of incompetent strata overlying a strike-slip fault. This section demonstrates the illusion of a great deal of horizontal shortening in the shallow strata, with little shortening of deeper strata. (Permission to use granted by AAPG.)

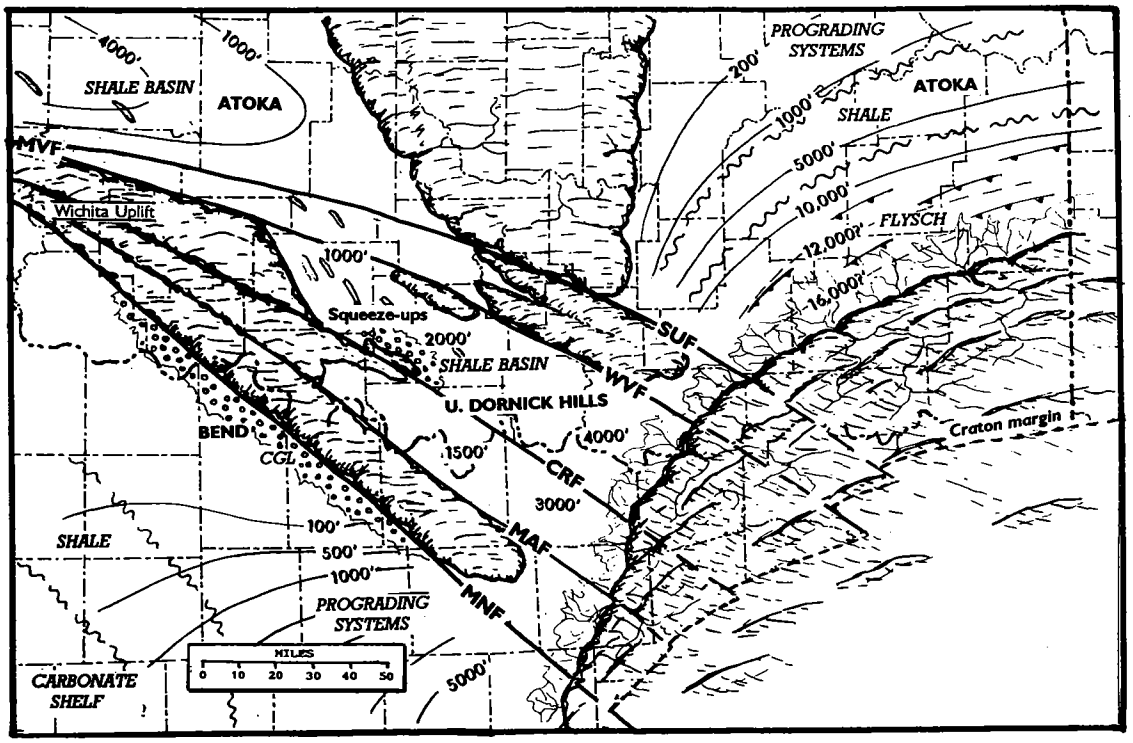


Figure 24. Atokan reconstruction. Transpression of the OM continued to deform existing structures. The axis of the Ouachita foreland basin had shifted northward since Morrowan time (Atoka sub-basin in Fig. 3). A series of strong subductional surges from the south raised the Atoka sub-basin above sea level, thus eliminating the Ouachita depositional basin. CGL = conglomerate. Wavy lines show boundaries between lithofacies.

lifts. The surges were so strong that a series of parallel, NNE-trending basement shear faults on the east flank of the central Oklahoma uplift were formed or reactivated. Left-lateral movement along these basement faults is indicated at the surface by the several belts (50–120 mi long) of en echelon, NW-trending, synthetic faults (Fig. 28). A set of N-trending, right-lateral crustal faults were formed or reactivated on the west flank of the Ozark uplift, as evidenced by the presence of a number of NE-trending, en echelon, synthetic surface faults there. Limited northward movement of the area between the two faulted areas is suggested by this fault configuration. This movement persisted in surges from early Desmoinesian time into early Missourian time. Syndepositional movement on these faults is indicated by thickening of Desmoinesian and younger strata by as much as 30% on the downthrown sides of many of the en echelon faults, particularly in the western swarm. Many oil and gas fields are associated with these structures.

Late Desmoinesian

Later in Desmoinesian time, surge-induced deformation and thrusting resulted in uplift and considerable erosion of Boggy and older strata around the edges of the Early Desmoinesian sub-basin. The western part of the basin subsided into a closed depression (Fig. 29). Several episodes of thrusting and crustal sagging resulted in syntectonic deposition of ~2,600 ft of prograding cyclothems of the Cabaniss Group (Fig. 29). Here again, the upper parts of these cyclothems contain extensive fluvial and deltaic sandstones which include Red Fork, Skinner, and Prue oil and gas reservoirs.

During deposition of the Cabaniss Group, Ouachita tectonic surges pushed farther northward, crumpling the overridden axis of the Early Desmoinesian sub-basin. The area lying between the Ozark and Ouachita uplifts (the Arkoma basin) was elevated, so that marine circulation from the east was cut off. Thus, a new provenance was established that added more clastics to the westward retreating epeiric sea. This was probably the time of the climactic suturing of the two cratons. During this event, the Choctaw thrust fault was emplaced, and long, narrow, subparallel folds of considerable magnitude were formed by the advancing thrust front. Originally the leading edge of the allochthon was probably 15–25 mi farther to the north and northwest than its present limit at the Choctaw fault. Evidence for this has been largely, but not

entirely, removed by the subsequent very long period of erosion. This will be discussed in a later paragraph.

Laurentia continued its southward subduction under the Ouachita thrust front, which by this time was well up on the shelf (Fig. 29). The constantly advancing and rising allochthon, coupled with torrential tropical rainfalls, produced vast amounts of terrigenous clastics. Widespread fluvial and delta-plain deposits prograded westward onto the easterly sagging Texas shelf and Marietta basin which were separated by the Muenster peninsula (Figs. 3,29). About 2,000 ft of shale and sand were deposited in the Ardmore graben, which was being further depressed by transpression within the OM. The squeeze-up structures, formed earlier here and in the Anadarko basin, were again compressed, uplifted, partially beheaded by erosion, and then re-submerged. The Wichita Mountain pop-up continued to shed floods of granite wash into the surrounding basins (Fig. 29). More than 1,200 ft of shale was deposited along the axis of the Anadarko basin. With the waning of the Ouachita orogeny, the sediment load delivered to the central and northeastern shelf area was considerably diminished, leading to clearing of the marine waters and southward (basinward) progradation of the short-lived Marmaton carbonate shelf.

LATE PENNSYLVANIAN

Missourian

The Allegheny orogeny was winding down, so activity in the OM was diminishing. The Texas shelf received >800 ft of westerly prograding coastal plain sediments. The Muenster–Marietta–Criner block and the Ardmore graben subsided through action of the OM and received 1,200 ft of similar deposits. The Wichita Mountains continued to shed granite wash into the immediate surroundings. The Anadarko basin continued to subside and received >2,200 ft of fine clastics (Fig. 30). Slow regional uplift of eastern Oklahoma, including the Ozark and Ouachita uplifts, and westward progradation of successive cyclothems drove the epeiric sea ever westward. Uplifts parallel to and associated with the Nemaha fault zone affected the pattern of clastic deposition. Most of the coarser clastics were trapped east of the Nemaha fault zone. To the north, the wide stable platform received a succes-

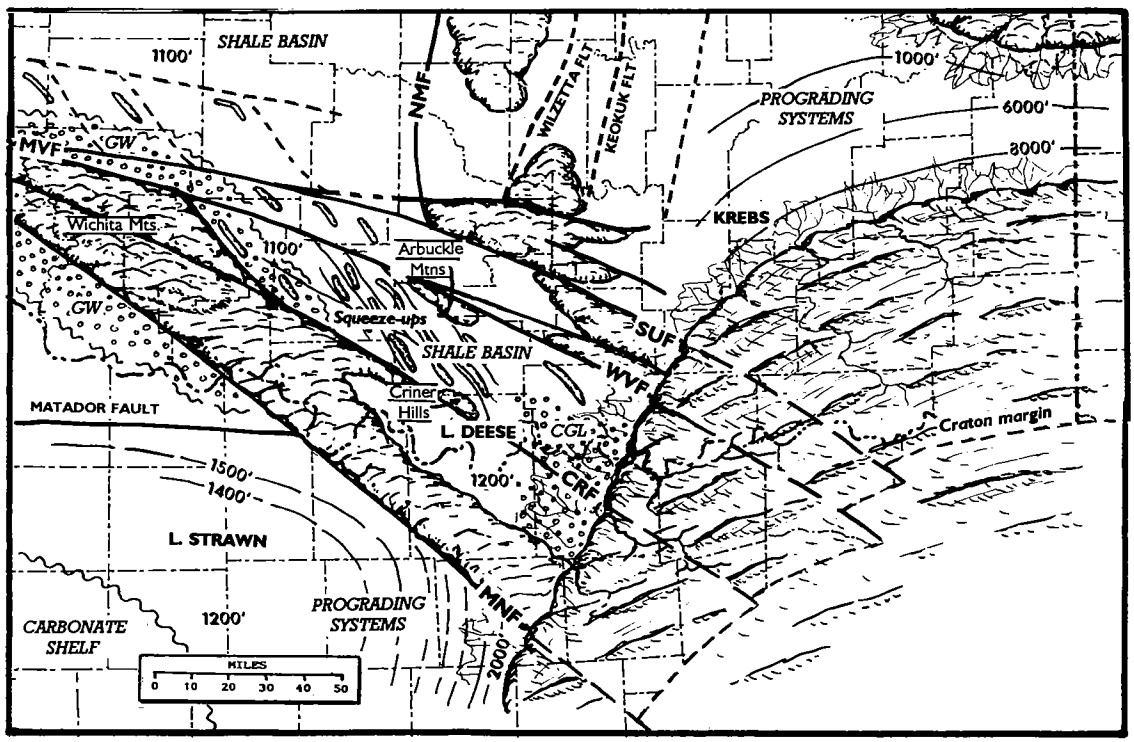


Figure 25. "Lower" Desmoinesian reconstruction (Krebs Group and equivalents). Intense transpression caused the formation or deformation of at least 11 structural basins and related uplifts across the craton. A broad arch appeared at the junction of the OM and the western Arkoma basin. Cyclic sedimentation became prominent on both the stable and depressed cratonic shelves as a result of episodic surges from the subduction processes. Dashed lines represent small antithetic strike-slip faults. GW = granite wash; CGL = conglomerate. Wavy lines show boundaries between lithofacies.

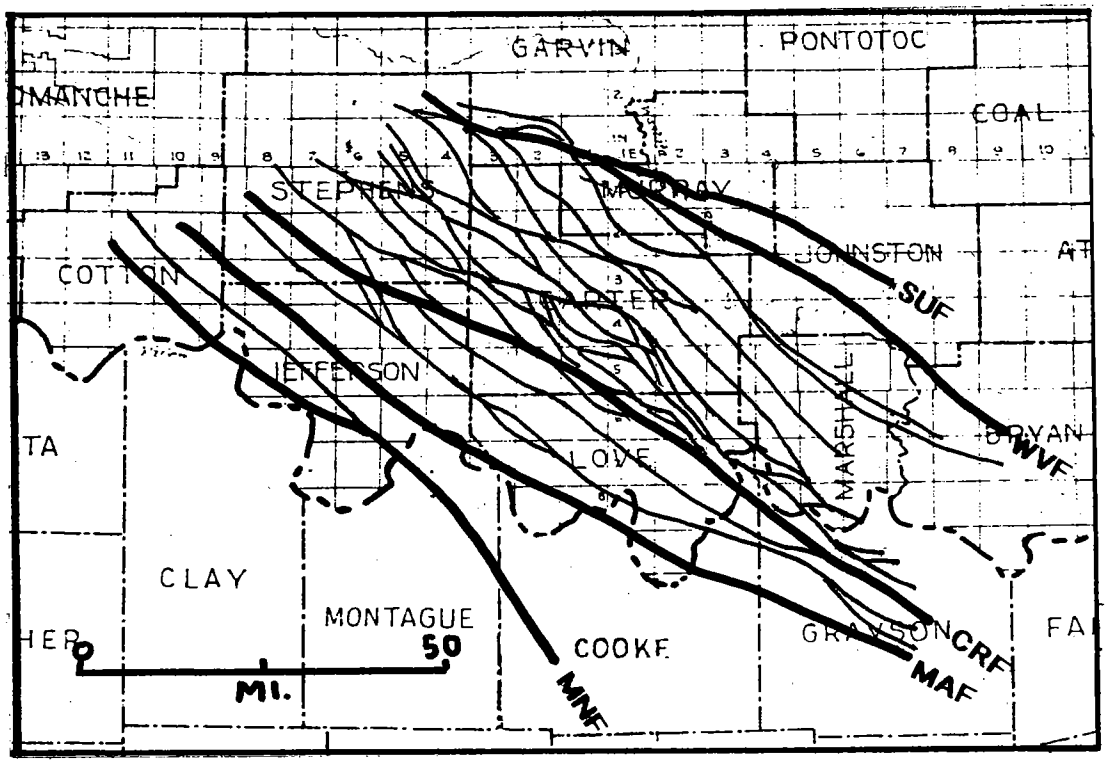


Figure 26. An interpretation of the intense, anastomosing, fault complex in the Ardmore basin, from Ferrebee (1991a). Most of the fault-bounded uplifts are pop-ups or squeeze-ups. Such patterns are found only in wide belts of large-scale, extensive, strike-slip fault systems (compare this with the San Andreas system). They could not have been formed by simple thrusting.

sion of carbonate-dominated cyclothems that can be correlated with clastic-dominated cyclothems that were clearly controlled by movements of the Ouachita orogeny, and, to a lesser extent, by those of the OM.

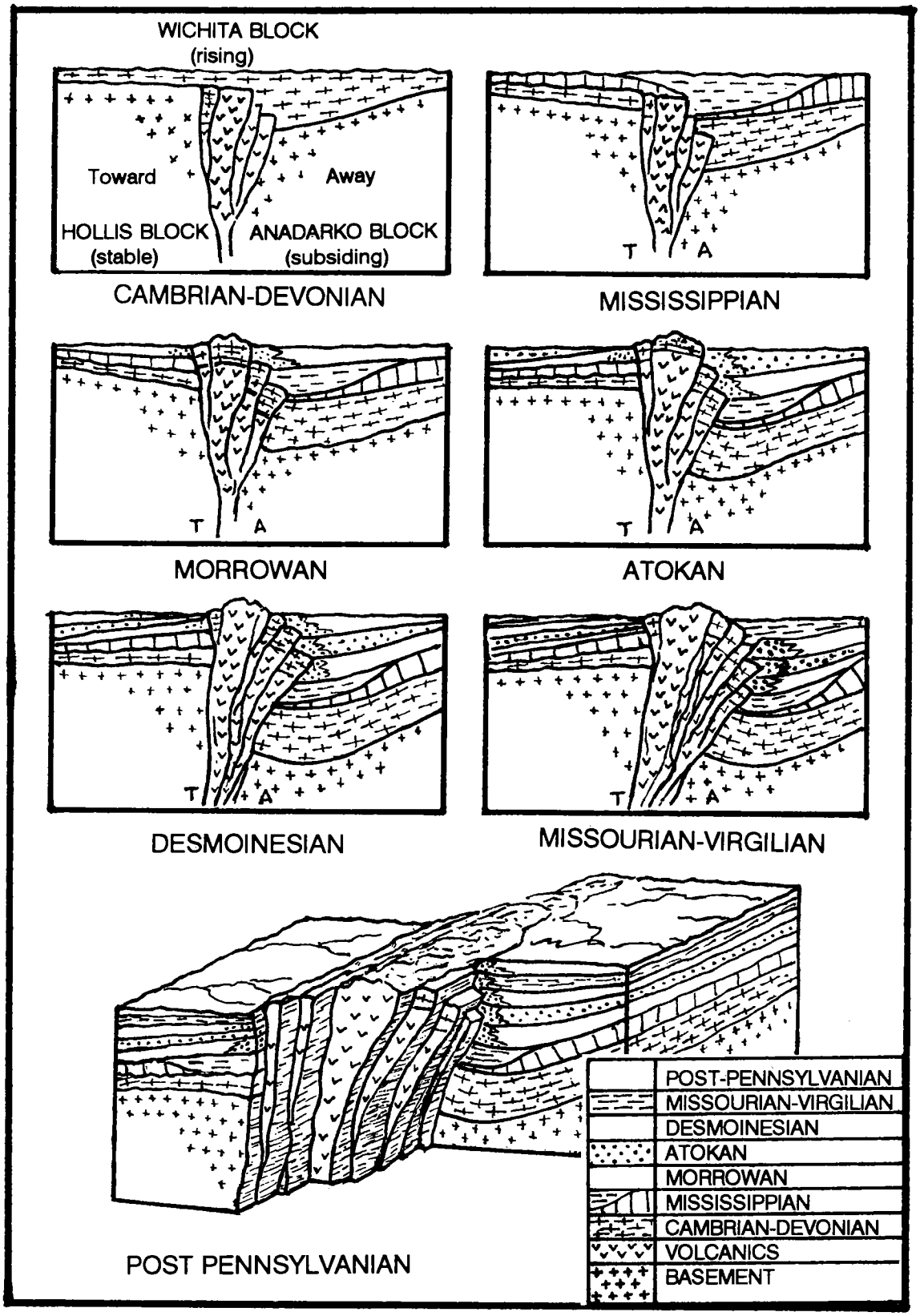
Deformation in the OM resulted in uplift of the Arbuckle Mountain block (sensu stricto) and the Tishomingo block (Fig. 3). This relatively minor tectonic event has been called the Arbuckle orogeny (Tomlinson and McBee, 1959,1988).

Virgilian

The basal deposits of the Virgilian Series in the immediate vicinity of the Arbuckle and Tishomingo blocks (which were uplifted during the previous epoch) contain thick, coarse conglomerates and abundant arkose (Fig. 31). Middle Cambrian rhyolite basement was unroofed in the Arbuckle block and a large area of the Middle Proterozoic granite core of the Tishomingo block was also unroofed. Both blocks became buried in their own erosional debris.

The land in the eastern part of the study area continued its slow elevation as a forebulge. Several faults within the OM were still active. The Wichita Mountain block continued to rise and was the source of the thick granite wash that surrounds it (Fig. 31). At the same time, the Anadarko basin sagged further to receive >2,600 ft of fine clastics. Subsidence of the Anadarko basin continued as the underlying basement moved to replace material beneath the rising and obliquely pseudo-thrusting Wichita pop-up block.

Figure 27 *(opposite page).* A schematic representation of psuedo-thrusting. The Sulphur, Washita Valley, and Criner faults converge into the Mountain View fault which separates the Wichita block from the Anadarko basin. Left-lateral transpression of the OM caused progressive uplift of the Wichita block and subsidence of the Anadarko basin. The stable, basement-rock-cored Hollis block prevented the formation of new faults to the south, whereas the sagging shale-filled Anadarko block yielded readily to new faults which caused segments of the rising Wichita block to fan out and lean over the basin, creating the illusion of thrusting. This process, pseudo-thrusting continued as long as lateral movement resulted in oblique uplift of the Wichita block.


WICHITA BLOCK
(rising)
Toward
Away
HOLLIS BLOCK
(stable)
ANADARKO BLOCK
(subsiding)
CAMBRIAN-DEVONIAN
T
A
MISSISSIPPIAN
MORROWAN
ATOKAN
DESMOINESIAN
MISSOURIAN-VIRGILIAN
POST PENNSYLVANIAN
POST-PENNSYLVANIAN
MISSOURIAN-VIRGILIAN
DESMOINESIAN
ATOKAN
MORROWAN
MISSISSIPPIAN
CAMBRIAN-DEVONIAN
VOLCANICS
BASEMENT

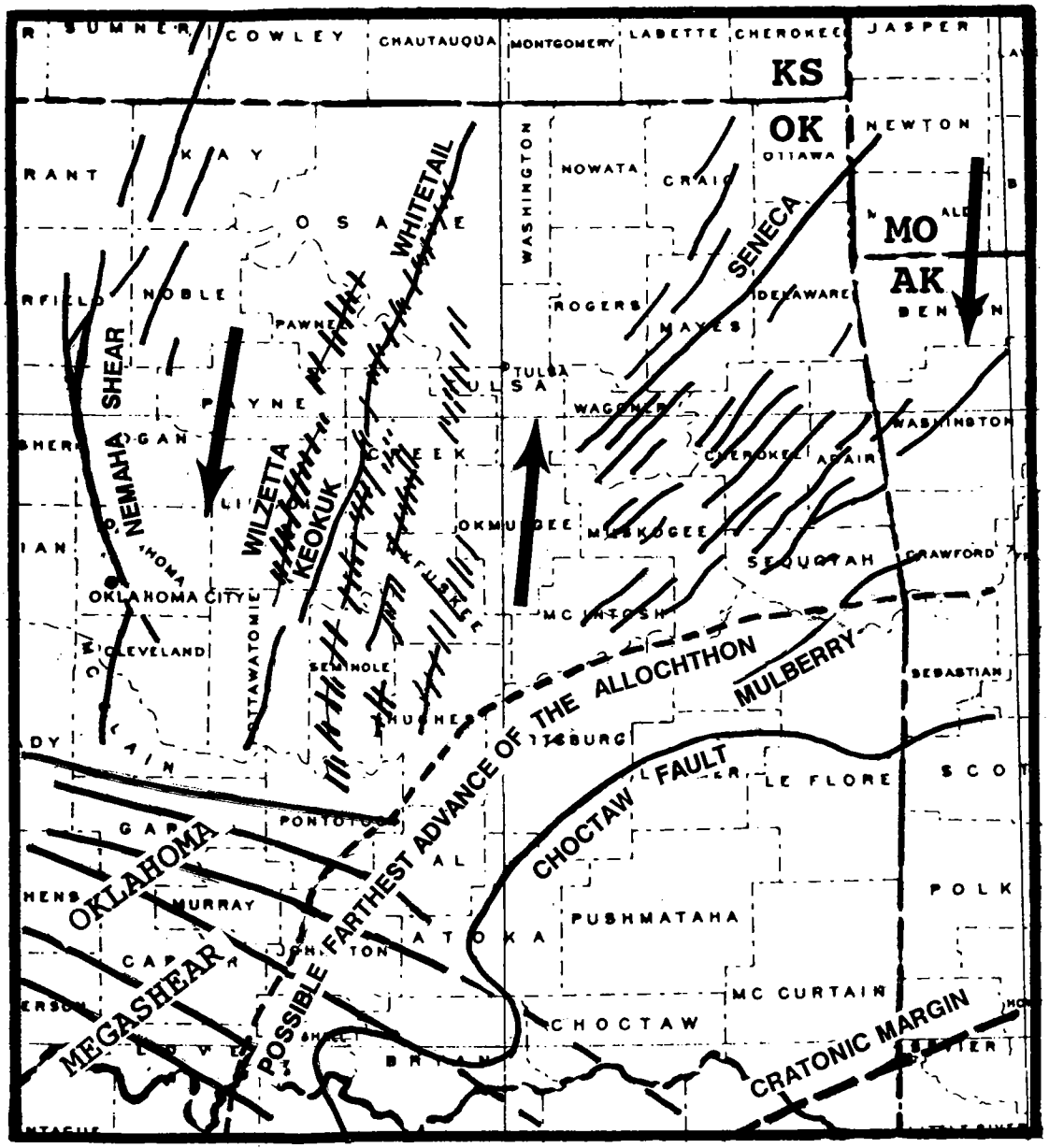


Figure 28. Shear faults and associated en echelon faults in eastern Oklahoma formed or were reactivated by the collision of Laurentia and Amazonia during Desmoinesian time. Arrows indicate the relative sense of motion.

POST VIRGILIAN

Uplift and intense erosion of the eastern part of the study area continued. Central and western Oklahoma, the Texas Panhandle, and eastern New Mexico became a vast marsh land in which red beds and thick evaporites were deposited as the open seaway receded southward into the Midland–Delaware (Tobosa) basin. Many large, high-energy rivers flowed west and northwest out of the highly elevated Ouachita Mountains and across the marsh lands in Late Pennsylvanian and Early Permian times.

Tectonically, this was a relatively quiet time for the OM and the Ouachita Mountains. The only stratigraphic evidence of tectonics during this time is in the immediate vicinity of the Arbuckle and Wichita Mountain blocks. The presence of chert cobbles as much as 3 in. in diameter in many Upper Pennsylvanian and Lower Permian fluvial channel outcrops

in central and northern Oklahoma has been interpreted as evidence for contemporaneous vigorous uplift of the Ouachitas. However, a more plausible explanation is that erosion had finally cut down through the thousands of feet of flysch, to expose the once deeply buried Mississippian–Devonian Arkansas Novaculite or Ordovician Big Fork Chert in the core areas of the Ouachita Mountains.

MESOZOIC–CENOZOIC

During the Jurassic rifting of Laurentia from Amazonia, lithospheric attenuation and, probably, thermal contraction caused a general southward sag to develop along the southern margin of the craton. What had started out as an intra-cratonic rift during Cambrian time, later to be involved in a suture belt in Pennsylvanian time, had once again become a rift zone. What had been Laurentia had now become North America. Once again, rifting occurred without the benefit of a triple-junction, but, rather, along the weak zone that marked the margin of the old craton. As the rift deepened and widened to form the proto-Gulf of Mexico, the central and southern North American shelves tilted southward into the sag. This resulted in all the previously westward-flowing rivers in the area to be redirected to the southeast. In northeastern Texas and southeastern Oklahoma, a number of rivers and streams are incised into Cretaceous strata, along zones of weakness (fractures?) that overlie buried OM faults.

A new and nearly continuous series of prograding coastal-plain and shelf deposits began to fill the new Gulf basin. This lasted from Jurassic to the present. As the progradation progressed southward, the northern area began a slow, isostatic rebound that raised the upper surfaces of the Mesozoic and Cenozoic sequences to several hundred feet above sea level, where they are today.

INTERACTION BETWEEN THE OUACHITA SYSTEM AND THE OKLAHOMA MEGASHEAR

Generalized Outcrop and Cretaceous Subcrop Map

Present-day structural aspects are important, but must be considered in proper perspective. Outcrops in the Ouachita province are the residual erosional terrane not far above the sole fault at the base of the Ouachita allochthon; in places the allochthon has been entirely removed by erosion.

Figure 32 is based on the geologic map of the study area. It shows the general configuration of outcrops Precambrian through Cretaceous. The

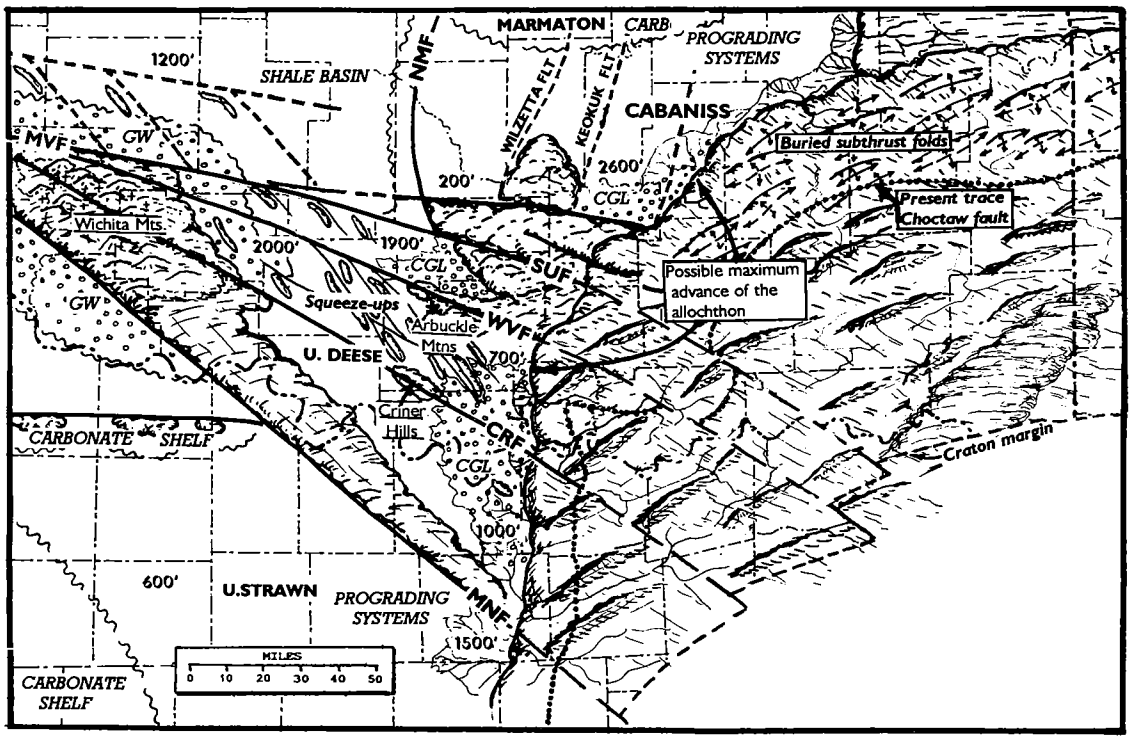


Figure 29. "Late" Desmoinesian reconstruction (Cabaniss and Marmaton Group equivalents). The possible maximum advance of the Ouachita allochthon and the present trace of the Choctaw fault are also shown. Orogenically initiated cyclic sedimentation continued over the marginal basins and interior shelves. CGL = conglomerate; GW = granite wash.

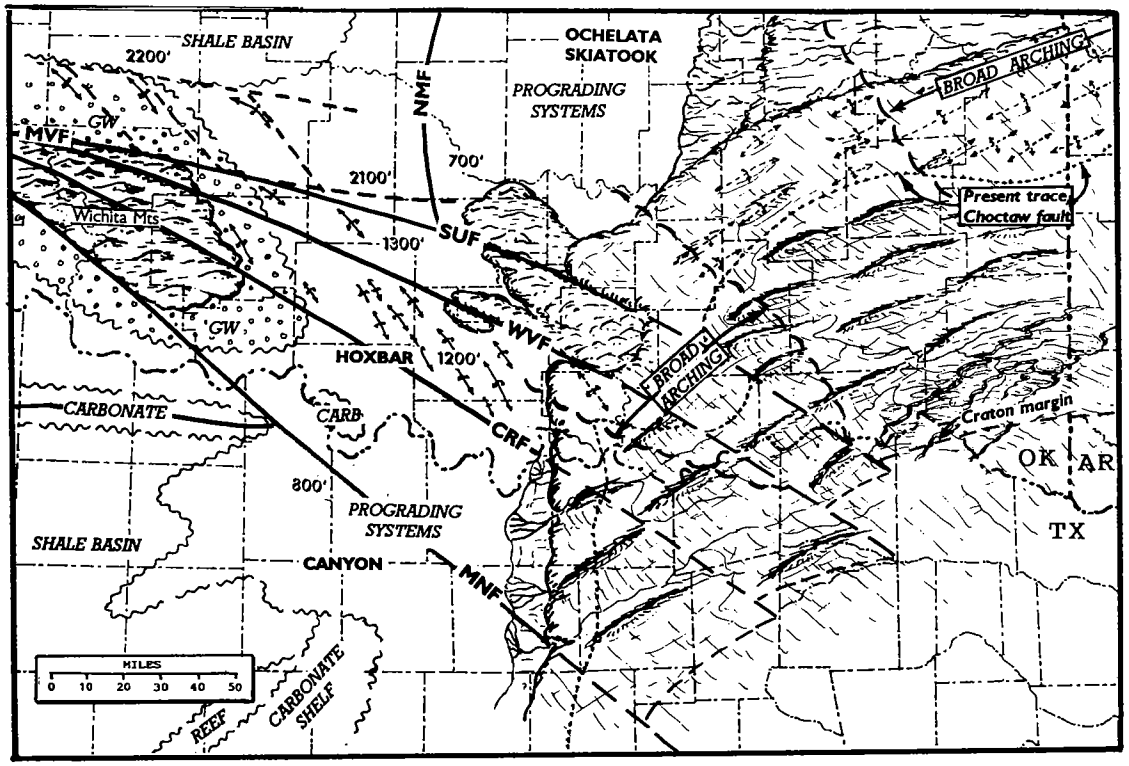


Figure 30. Missourian reconstruction. Several faults in the OM were still active. Although crustal suturing had been effected, periodic aftershocks maintained the previously established pattern of cyclic sedimentation. A broad NW-trending uplift is centered over the Tishomingo block.

deeply eroded remnant of Cretaceous strata crops out in the southeastern quadrant of the study area (south and east of the dashed line, Fig. 32). The Precambrian and Paleozoic subcrops beneath the Cretaceous reflect the erosion that occurred from Desmoinesian to Early Cretaceous time, ~170 m.y. North and west of the Cretaceous overlap the present outcrop pattern and the orientations of folds in the Arkoma basin north of the Choctaw fault are shown. Parts of this area may have been exposed from Desmoinesian to the present, ~315 m.y. Assuming an average erosion rate of 0.1 in. per 1,000 yr, a total of 31,500 ft of sediments could have been removed.

Location and Orientation of the Choctaw Fault

In thin-skinned thrusting, such as occurred in the Ouachitas, the vertical stratigraphic sequence above the thrust fault remains relatively intact. Older strata just above the sole fault remain buried until exposed by erosion. Along the buried Ouachita front in the Fort Worth basin (Flawn and others, 1961, pl. 4) and the Ardmore basin (Hardie, 1990), pre-flysh strata in the thrust sheet are overlain by Cretaceous rocks (Fig. 32). This suggests that several thousand feet of flysch, strata and structures equivalent to those in the Ouachita Mountain outcrops, had been eroded and the entire area reduced to a near-peneplain prior to the Cretaceous transgression.

Uplift of the Tishomingo–Hunton arch and the southern flank of the Ozark uplift in Missourian time, after thrusting (Fig. 30), also raised the overlying allochthon and the Choctaw fault. As a consequence, erosion has exposed stratigraphically deeper horizons in the two uplifted areas than in the area in between (i.e., Atoka, Pittsburg, and Latimer Counties in Oklahoma). With increased depth of erosion, the trace of a thrust fault shifts in the direction of fault dip. As a result, the curvilinear trace of the Choctaw fault is a function of not only thrust direction but differences in stratigraphic depth of erosion (Fig. 32).

Considering the amount of time between emplacement and burial (Desmoinesian–Early Cretaceous, ~170 m.y.), it is very possible that the maximum extent of the thrust sheet in the Ardmore basin was originally 15–20 mi northwest of its current position. The proposed maximum advance of the allochthon and the original position of the Choctaw fault is shown by the wavy line in Figure 32.

The position of the Choctaw fault in the Arkoma basin just prior to the Cretaceous transgression can

be projected from the westernmost thrust in the Ardmore basin, following the general Ouachita structural grain. This projection is ~18 mi northwest of the present trace. In other words, post-Cretaceous erosion stripped the Choctaw fault and the superjacent thrust sheet southeast ~18 mi.

If the Ouachita allochthon had extended another 15–20 mi north or northwest, it would have covered most of the folds now exposed in the Arkoma basin. Nearly all of these folds are subparallel, not to the arcuate Choctaw fault, but to the craton margin well to the south (Fig. 32). Several of these folds appear to plunge beneath the Choctaw fault suggesting their presence beneath the Ouachita allochthon (Hendricks and others, 1937–39) (Figs. 30,32). These folds are interpreted to have been formed as normal subthrust folds during thrusting.

Many studies have attempted to explain the stress orientation(s) responsible for Ouachita thrusting. Most agree on a northerly direction, with variations from northeast to west. A number of these studies were based on orientations of the surface trace of the Choctaw fault (Fig. 32). All neglected the fact that the surface configuration offers nothing but general information about thrust direction. Therefore, the most meaningful evidence for determining the direction of maximum compressive stress is the orientation of the undisturbed, and once deeply buried, subthrust folds. The average axial orientation of folds in the Arkoma basin is approximately N.50°E. and is the result of N.40°W. thrusting plus or minus a few degrees. This unidirectional thrust direction can account for all structural deformation associated with the Ouachita orogeny. Is it a coincidence that the axes of the complex folds in the Marathon area have the same bearing and lie at a considerable angle to the deeply eroded thrust fault bounding the area?

The Choctaw Fault and the Tishomingo Uplift

The Choctaw fault over the Tishomingo block is much further southeast than it is in the Ardmore and Arkoma basins (Fig. 32). This configuration suggests *right-lateral* offset of the Choctaw fault across the Washita Valley fault and left-lateral offset across the Sulphur fault. However, right-lateral movement is not compatible with the overwhelming evidence of left-lateral slip throughout the OM. This configuration can be explained by uplift of the Tishomingo block. In Missourian time, a broad WNW-trending arch formed in the area which now

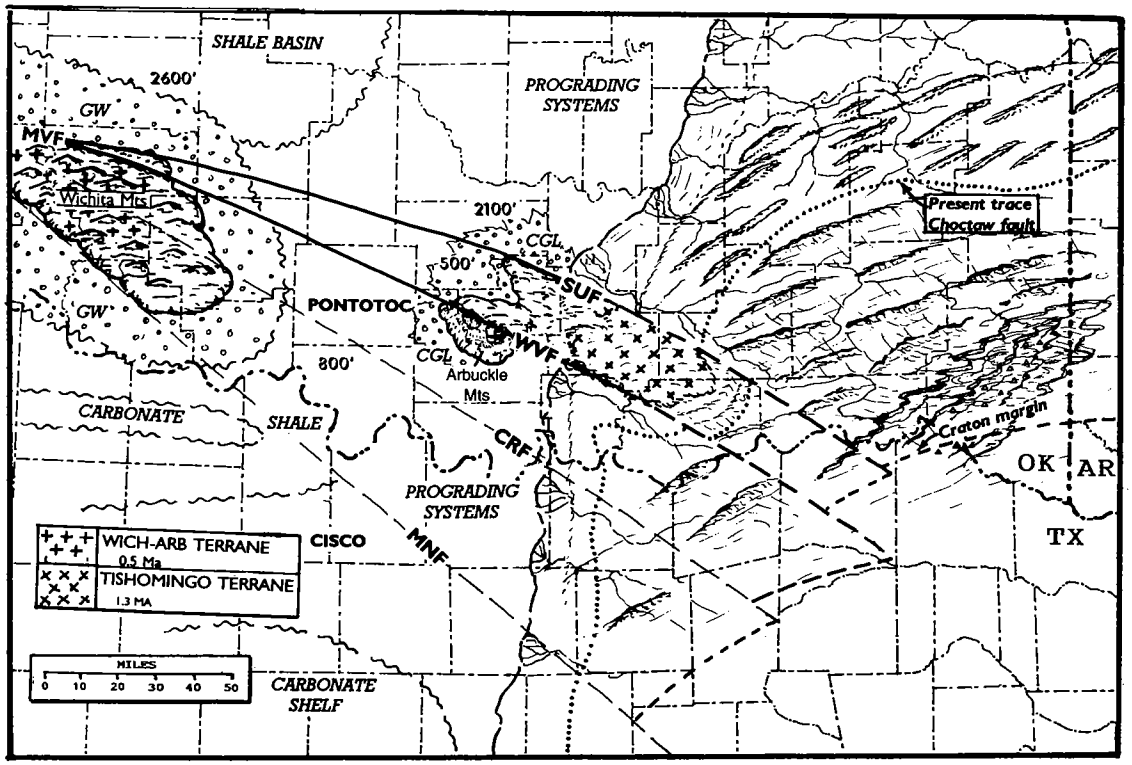


Figure 31. Virgilian reconstruction. The Allegheney orogeny still affected the OM. The Tishomingo and Arbuckle blocks and the Wichita Mountains were uplifted and eroded sufficiently to expose their igneous cores. The Ardmore and Anadarko grabens were further depressed and filled with syntectonic clastics. CGL = conglomerate; GW = granite wash. Wavy lines show boundaries between lithofacies.

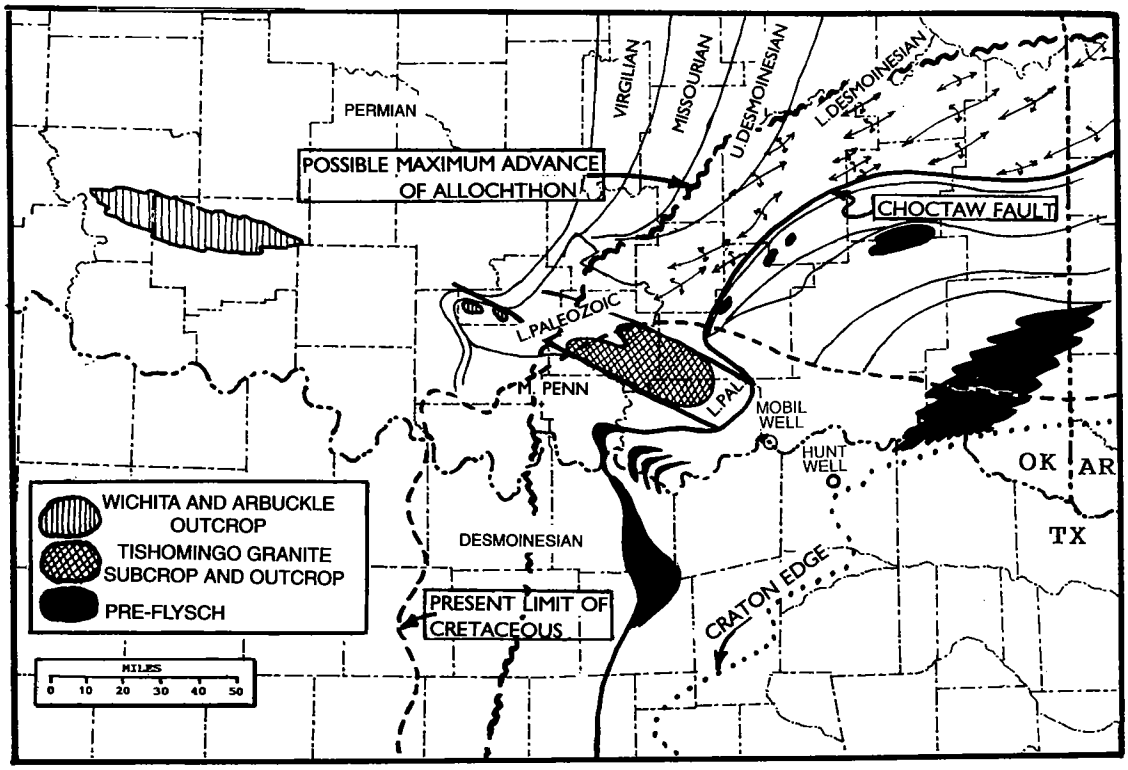


Figure 32. Outcrop map of the study area with Cretaceous subcrops and select structural features. The dashed line represents the northern and western erosional limit of Cretaceous rocks in the study area. The Choctaw fault at the surface and beneath the Cretaceous is indicated by a dark line. Other outcropping thrust faults are shown by thin lines south of the Choctaw fault. The wavy broken line indicates proposed maximum extent of the allochthon (i.e., the original trace of the Choctaw fault) 20–25 mi north and west of the modern trace. The west–northwest trending block is the Tishomingo uplift bounded by the Sulfur fault on the north and the Washita Valley fault on the south.

includes the Tishomingo block, the Hunton anticline, the southwestern Arkoma basin, and the Lawrence uplift (Fig. 30). As deformation and uplift proceeded, the faults bounding the Tishomingo block (Sulphur fault on the north, Washita Valley fault on the south) sliced up through the arching flysch wedge stranding the north and south flanks of the arch on the downthrown sides of the faults. The Tishomingo block itself continued to "pop up" under transpression, carrying its sedimentary veneer and the overlying thrust sheet(s) which were undergoing concomitant weathering. The ensuing erosion from late Desmoinesian until Cretaceous time is estimated to have removed several thousand feet of the overlying Ouachita thrust sheet(s), >10,000 ft of Paleozoic sedimentary rocks, and an unknown amount of Middle Proterozoic granite (Figs. 31,32). The stratigraphic depth of the Choctaw fault trace over the Tishomingo block is much greater than in the adjacent basins, and, with increasing depth, the fault trace shifts in the direction of dip.

Ouachita Thrust Faults and the Tishomingo Uplift

Beyond ~30 mi northeast of the Tishomingo block, several thrust faults are south of and fairly parallel to the Choctaw fault. Beginning ~30 mi northeast of the Tishomingo block, these faults converge southwestward toward the Choctaw fault then disappear beneath Cretaceous outcrops (Fig. 32). Fault projections beneath the Cretaceous cover appear to merge into one zone (Fig. 33). Cross sections across thrust belts show frontal thrusts that converge downward and merge with a basal thrust fault. The area just described is interpreted to be a cross section across the Ouachita frontal thrust belt that was rotated upward to a more-or-less horizontal position and exposed by erosion (Fig. 33A–D). Thus, we can now "see" the convergence of the frontal thrust faults into one sole fault, the Choctaw fault. Another indication that the frontal faults merge into a basal sole fault in this area is that only one thrust sheet was apparent in the deep Mobil

test well in southeastern Bryan County, Oklahoma, and in the deep Hunt test in central Lamar County, Texas, which is not far from the craton margin (Fig. 32). Both tests, which were located on the east–southeast projection of the Tishomingo block, drilled through Cretaceous strata into flysch and, at great depths, into Arbuckle shelf facies (Denison, 1989; Nicholas and Waddell, 1989).

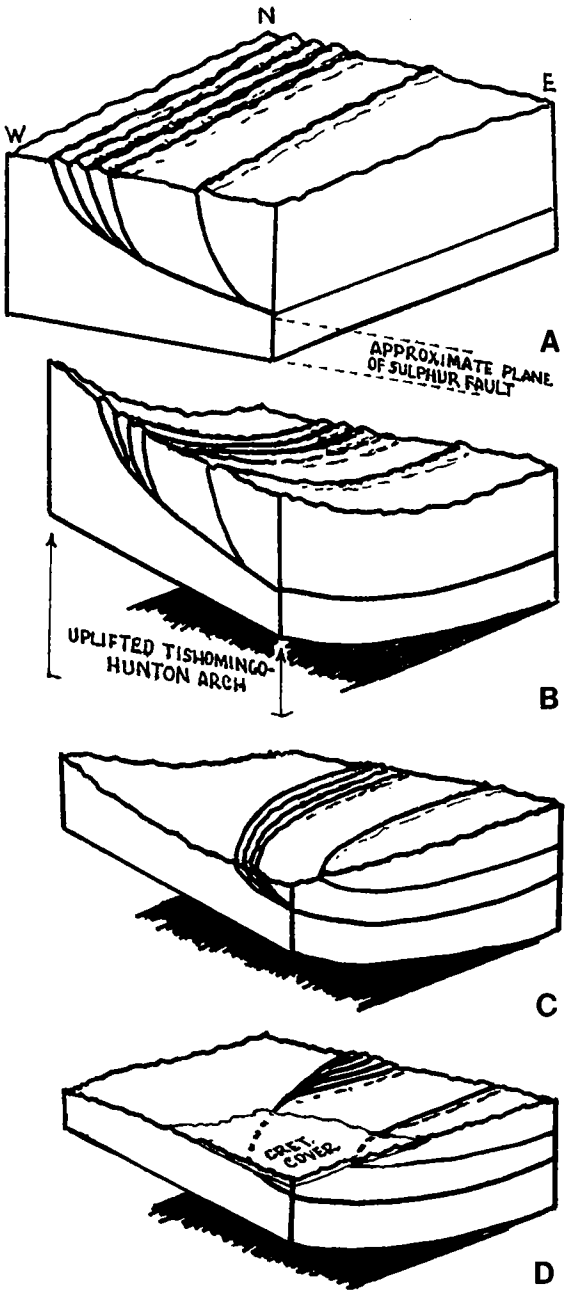


Figure 33. Schematic representation of the effects of uplift and erosion at the intersection of the Ouachita frontal fault zone and the OM during (A) Desmoinesian time, before uplift (see Fig. 29); (B) Missourian time, after uplift (see Fig. 30); (C) just prior to burial by Cretaceous strata; (D) present configuration. The westernmost fault is the Choctaw fault.

Ouachita Frontal Folds and the Hunton Anticline

Structures on the northeast flank of the Hunton anticline (Fig. 34) present an interesting structural enigma (Ham and others, 1954). The overall trend of the Hunton anticline is parallel to that of the OM, but the similarity ends there. The en echelon configuration of the sigmoidal Franks and Clarita fault zones suggests the possibility of a right-lateral fault at depth. This, of course, is incompatible with the mechanics of the entire OM system. The Franks fault zone curves into the Jessie nose, a feature that forms a slight eastward divergence from the general west–northwest trend. The Jessie Nose is bounded by the Coal Creek fault that strikes northeast for ~15 mi at the surface and is colinear with the buried Ashland anticline in the Arkoma basin (Fig. 34). The WNW-trending Clarita fault zone veers to the northeast on the north side of the NE-plunging Clarita anticline which is colinear with the long, narrow Coalgate anticline in the Arkoma basin. Both the Ashland and Coalgate anticlines are interpreted to be normal subthrust folds (Fig. 32), as described earlier. The Jessie nose and the Clarita anticline on the north flank of the Hunton anticline are interpreted to be subthrust folds that were uplifted with the broad Tishomingo–Hunton arch in Missourian time (Fig. 30). The sigmoidal Franks and Clarita fault zones (Fig. 34) are interpreted to be upturned flexural-slip (bedding-plane) faults which are common on the flanks of parallel folds. The folds may be, or may be related to, triangle structures which are common beneath thrust faults in thin-skinned tectonics.

The complexly faulted northeast flank of the Hunton arch and the disruption of the Ouachita front by the Tishomingo block may be the only indications of interference between the Arbuckle and Ouachita systems.

SUMMARY

The Arbuckle and Ouachita orogenic systems are the results of two separate and genetically independent structural events. The Arbuckle system, which is part of the WNW-trending Oklahoma megashear, began as a crustal shear-fracture zone while Laurentia was imbedded in the center of Middle Proterozoic Pangaea. As Laurentia broke loose from Pangaea and entered a drifting phase, it was subjected to intermittent, west–east transpression that originated with the Ruby and Antler subductional orogenies acting on its western margin. These forces were opposed by inertial resistance created by the contemporaneous Taconic, Acadian, and Allegheny collisional orogenies along its east-

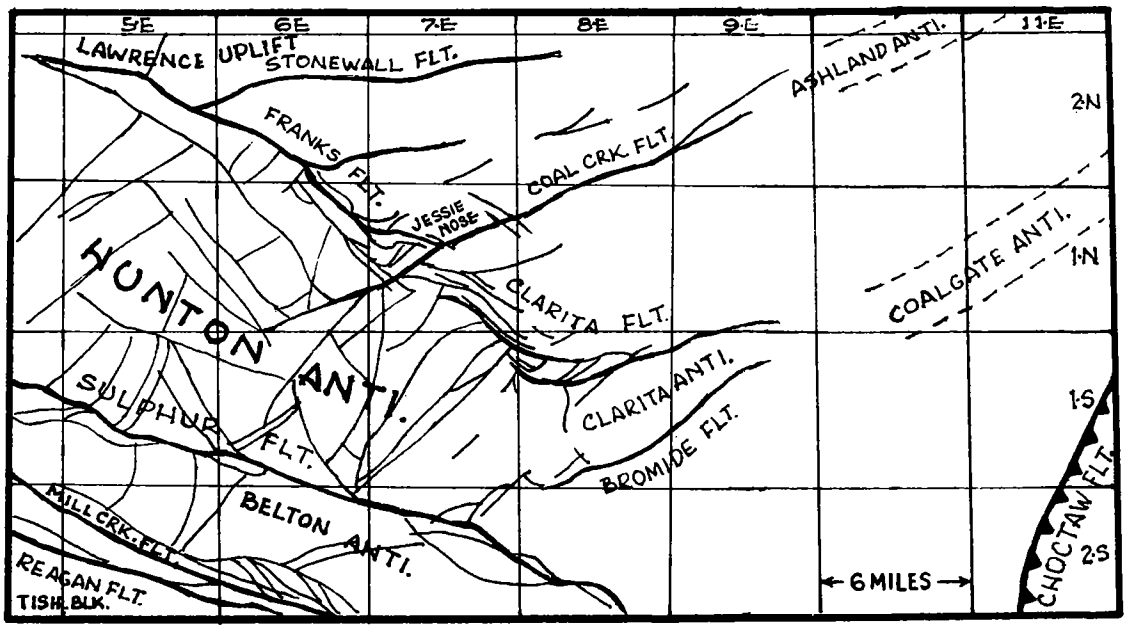


Figure 34. Surface structure in vicinity of the intersection of the Oklahoma megashear and the Ouachita and frontal fold belt (modified from Ham, 1954). The dashed lines show the location and orientation of subsurface subthrust folds in the Arkoma basin. The Jessie nose and Clarita anticline are interpreted to be extensions of the subsurface Coalgate and Ashland anticlines that have been uplifted and exposed by erosion.

ern margin. The first major movement of the OM was probably on the Muenster fault on the south side of the OM in Early Cambrian time. The latest major movement was probably on the Sulphur fault on the north side in Middle Pennsylvanian time. Minor activity occurred as recently as Holocene. The total left-lateral displacement may be as much as 55 mi. The OM has apparently been under transpression since inception. The few places where rifting has been suspected in the OM may be attributed to the local development of releasing bends, which are common in convergent shear systems.

The north–northwestward Ouachita thrusting began in Mississippian time as Laurentia drifted into proximity with Amazonia. As Laurentia drifted ever closer, a subduction zone and volcanic island arc formed offshore, and the hinterland (Amazonia) was uplifted. The volcanic arc and Amazonia were the source of the Hatton Tuff and several thousand cubic miles of flysch deposited in the Ouachita trough and basins associated with the OM. Convergence continued and great volumes of older basinal deposits were thrust northward toward and onto (in Morrowan time) the depressed cratonic margin. Deep depocenters (foreland basins) were formed by tectonic loading in front of the highly elevated allochthon that was now tens of thousands of feet thick. As thrusting pushed northward, the depocenters migrated northward. The actual cratonic collision occurred during Desmoinesian time. During the Allegheny orogeny, collision of the eastern margin of Laurentia with Africa caused a series of surges that created new faults and affected virtually every existing fault in the southern part of the craton. Most experienced syntectonic cyclic sedimentation.

In the area of the intersection of the two systems, the short-lived, thin-skinned Ouachita event had very little, if any, influence on the OM or the Arbuckle system. It did provide, however, most of the thousands of cubic miles of siliciclastics deposited in the basins associated with the OM. Depositional basins must be formed by structural events before, or during the time of sedimentary filling. Sedimentation, by itself, cannot cause the crust to subside.

The Ouachita and Arbuckle Mountains and Arkoma basin have been subjected to uninterrupted severe erosion for the past 315 m.y. Many thousands of feet of overburden have been removed from these areas. The wide Oklahoma megashear zone exhibits very intense and complicated deformation, including as much as 55 mi of left-lateral offset of the cratonic margin, caused by transpression, acting over a very long period of time. In a completely separate tectonic event, the Ouachita orogeny resulted in as much as 120 mi of north–northwestward, straight-forward, low-angle, thin-skinned thrusting that occurred in a comparatively short period of time. These facts must be considered in making any definitive study of either area.

ACKNOWLEDGMENTS

I wish to recognize with gratitude the time and efforts expended by John Shelton and Norman Hyne in reviewing this manuscript, and for their helpful suggestions; to Patricia Lufholm for editing and typing early versions of the manuscript; to Peter Lufholm for making available his extensive geological reference library; and to Dorothy Swindler for organizing my random thoughts and for final editing. The writings of a very large number of Ouachita and Arbuckle workers have been read over the years and many have been informative and influential in one way or another; to the authors, I express my appreciation. I am especially grateful for the inspirations provided by the following pioneers, with whom I have spent hundreds of hours in discussions on Oklahoma geology, and many weeks in the field: John Emery Adams, Carl Branson, Lewis Cline, Max Elias, Bill Ham, Bruce Harlton, and C. W. Tomlinson, all of whom are now deceased. This presentation was made possible by funds provided by an agency of the Federal Government, the SSA, augmented by a retirement pension from ARCO Oil and Gas Co.

REFERENCES CITED

Barrs, D. L.; and Stevenson, G. M., 1982, Subtle stratigraphic traps in Paleozoic rocks of Paradox basin, *in* Halbouty, M. T. (ed.), The deliberate search for the subtle trap: American Association of Petroleum Geologists Memoir 32, p. 131–158.

Bennison, A. P., 1993, Pennsylvanian history of the Chautauqua arch [abstract]: Geological Society of America Abstracts with Programs, v. 25, p. 7.

Berendsen, P.; and Wilson, F. W., 1993, Tectonic history and analysis of structures in eastern Kansas and western Missouri [abstract]: Geological Society of America Abstracts with programs, v. 25, p. 7.

Brewer, J. A.; Good, R.; Oliver, J. E.; Brown, L. D.; and Kaufman, S., 1983, COCORP profiling across the southern Oklahoma aulacogen: overthrusting of the Wichita Mountains and compression within the Anadarko basin: Geology, v. 11, p. 109–114.

Brookfield, M. E., 1993, Neoproterozoic Laurentia–Australia fit: Geology, v. 21, p. 683–686.

Burke, K.; and Dewey, J. F., 1973, Plume generated triple junctions: key indicators in applying plate tectonics to old rocks: Journal of Geology, v. 81, p. 217–220.

Carey, S. W., 1958, The tectonic approach to continental drift, *in* Carey, S. W. (ed.), Continental drift: University of Tasmania Geology Department Symposium no. 2, p. 188–355.

Castro, A., 1985, The Central Extremadua batholith: geotectonic implications (European Hercynian Belt): Tectonophysics, v. 120, p. 57–68.

Clendenin, C. W.; Nieuwendorp, C. A.; and Lowell, G. R., 1989, Reinterpretation of faulting in southeast Missouri: Geology, v. 17, p. 217–220.

Craddock, J. P.; Jackson, M.; van der Pluijm, B. A.; and Versical, R. T., 1993, Regional shortening fabrics in eastern North America: far-field stress transmission from the Appalachian–Ouachita orogenic belt: Tectonics, v. 12, p. 257–264.

Davies, F. B., 1982, Pan-African granitic intrusion in response to tectonic volume changes in a ductile shear zone from northern Saudi Arabia: Journal of Geology, v. 90, p. 467–483.

Denison, R. E., 1982, Geologic cross section from the Arbuckle Mountains to the Muenster arch, southern Oklahoma and Texas: Geological Society of America, Map and Chart Series MC-28R.

_____ 1989, Foreland structure adjacent to the Ouachita foldbelt, *in* Hatcher, R. D.; Thomas, W. A.; and Viele, G. W. (eds.), The Appalachian Ouachita orogen in the United States: Geological Society of America, The Geology of North America, v. F-2, p. 681–688.

Deratmiroff, G. N., 1971, Late Cenozoic imbricate thrusting in Venezuelan Andes: American Association of Petroleum Geologists Bulletin, v. 55, p. 1336–1355.

DeSitter, L. U., 1956, Structural geology: McGraw-Hill Book Co., New York, 552 p.

Dickinson, W. R., 1974, Plate tectonics and sedimentation, *in* Dickinson, W. R. (ed.), Tectonics and sedimentation: Society of Economic Paleontologists and Mineralogists Special Publication 22, p. 1–27.

_____ 1977, Paleozoic plate tectonics and the evolution of the Cordilleran continental margin, *in* Stewart, J. H.; Stevens, C. H.; and Fritsche, A. E. (eds.), Paleozoic paleogeography symposium I: Pacific Section, Society of Economic Paleontologists and Mineralogists, p. 137–156.

Ferebee, C. D., 1991a, Subsidence and basin development in the southern Oklahoma aulacogen: University of Tulsa unpublished M.S. thesis, 121 p.

_____ 1991b, Subsidence and basin development in the southern Oklahoma aulacogen [abstract]: American Association of Petroleum Geologists Bulletin, v. 75, p. 572.

Flawn, P. T.; Goldstein, A., Jr.; King, P. B.; and Weaver, C. E., 1961, The Ouachita System: Bureau of Economic Geology, The University of Texas at Austin, Publication 6120, 401 p.

Gastil, R. G.; and Jensky, W., 1973, Evidence for strike-slip displacement beneath the transMexico volcanic belt, *in* Conference on tectonic problems of the San Andreas fault system: Stanford University Publications in the Geological Sciences, v. 13, p. 171–180.

Guineberteau, B.; Bouchez, L. L.; and Vignaresse, J. L., 1987, The Mortagne granite pluton emplaced by pull-apart along a shear zone, France: Geological Society of America Bulletin, v. 99, p. 763–770.

Gurnis, M., 1992, Long term controls on eustatic and epeirogenic motions by mantle convection: Geological Society of America Today, v. 2, p. 141; 144–145; 156–157.

Ham, W. E., 1969, Regional geology of the Arbuckle Mountains, Oklahoma: Oklahoma Geological Survey Guidebook 17, 52 p.

Ham, W. E.; McKinley, M. E.; and others, 1954, Geological map and sections of the Arbuckle Mountains, Oklahoma: Oklahoma Geological Survey Map A-2.

Ham, W. E.; Denison, R. E.; and Merritt, C. A., 1964, Basement rocks and structural evolution of southern Oklahoma: Oklahoma Geological Survey Bulletin 95, 302 p.

Hardie, W. E., 1990, Subsurface structural study of the buried Ouachita thrust front, southeastern Oklahoma: Oklahoma City Geological Society Shale Shaker, v. 41, p. 32–55.

Harding, T. P.; Gregory, R. F.; and Stephens, L. H., 1983, Convergent wrench-fault and positive flower structure, Ardmore basin, Oklahoma, *in* Bally, A. W. (ed.), Seismic expressions of structural styles: American Association of Petroleum Geologists Studies in Geology, series 15, v. 3, p. 4.2-13 to 4.2-15.

Hendricks, T. A.; Knechtel, M. M.; Dane, C. H.; Rothrock, H. E.; and Williams, J. S., 1937–1939, Geology and fuel resources of the southern part of the Oklahoma coal field: U.S. Geological Survey Bulletin 874-A–D, 90 p.

Hoffman, P. F., 1991, Did the breakout of Laurentia turn Gondwanaland inside out?: Science, v. 252, p. 1409–1412.

Howe, W. B., 1993, Principal elements of Ozark uplift during the Pennsylvanian [abstract]: Geological Society of America Abstracts with Programs, v. 25, p. 27.

Hutton, D. H. W., 1982, A tectonic model for the emplacement of the Main Donegal Granite, Northwest Ireland: Geological Society of London Journal, v. 139, p. 615–631.

Kay, M., 1951, North American geosynclines: Geological Society of America Memoir 48, 143 p.

Keller, G. R.; Braile, L. W.; McMechan, G. A.; Thomas, W. A.; Harder, S. H.; Chang, W. F.; and Jardine, W. G., 1989, Paleozoic continent-ocean transition in the Ouachita mountains imaged from PASSCAL wide-angle seismic reflection-refraction data: Geology, v. 17, p. 119–122.

Loomis, J.; Weaver, B.; and Blatt, H., 1994, Geochemistry of Mississippian tuffs from the Ouachita Mountains, and implications for the tectonics of the Ouachita orogen, Oklahoma and Arkansas: Geological Society of America Bulletin, v. 106, p. 1158–1171.

Larson, E. E.; Patterson, P. E.; Curtis, G.; Drake, R.; and Mutschler, F. E., 1985, Petrologic, paleomagnetic, and structural evidence of a Paleozoic rift system in Oklahoma, New Mexico, Colorado, and Utah: Geological Society of America Bulletin, v. 96, p. 1364–1372.

Lawson, J. E.; and Luza, K. V., 1993, Oklahoma earthquakes, 1992: Oklahoma Geology Notes, v. 53, p. 51–56.

Lowell, J. D., 1972, The Spitzbergen orogenic belt: Geological Society of America Bulletin, v. 83, p. 3091–3102.

_____ 1985, Structural styles in petroleum exploration: Oil and Gas Consultants International, Tulsa, Oklahoma, 460 p.

McBee, W., Jr.; and Vaughan, L. G., 1956, Oil fields of the central Muenster Waurika arch, Jefferson County, Oklahoma and Montague County, Texas, *in* Petroleum geology of southern Oklahoma, v. 1, a symposium, Ardmore Geological Society: American Association of Petroleum Geologists, Tulsa, p. 355–372.

Nicholas, R. L.; and Waddell, D. E., 1989, The Ouachita system in the subsurface of Texas, Arkansas, and Louisiana, *in* Hatcher, R. D.; Thomas, W. A.; and Viele, G. W. (eds.), The Appalachian Ouachita orogen in the United States: Geological Society of America, The Geology of North America, v. F-2, p. 661–672.

Paulsen, T.; and Marshak, S., 1994, Cratonic weak zone in the U.S. continental interior: the Dakota–Carolina corridor: Geology, v. 22, p. 15–18.

Ramelli, A. R.; and Slemmons, D. B., 1986, Neotectonic activity of the Meers fault, *in* Donovan, R. N. (ed.), The Slick Hills of southwestern Oklahoma—fragments of an aulacogen?: Oklahoma Geological Survey Guidebook 24, p. 45–54.

Reed, J. C., 1984, Proterozoic rocks of the Taos Range, Sangre de Cristo Mountains, New Mexico, *in* Rio Grande rift: New Mexico, Geological Society 35th Field Conference Guidebook, p. 179–185.

Sims, P. K., 1988, Precambrian basement map of the northern Mid-Continent, U.S.A., *in* Rascoe, Bailey, Jr.; and Hyne, N. J. (eds.), Petroleum geology of the Mid-Continent: Tulsa Geological Society Special Publication no. 3, p. 10–11.

Smith, J. G., 1965, Fundamental transcurrent faulting in northern Rocky Mountains: American Association of Petroleum Geologists Bulletin, v. 49, p. 1398–1404.

Stevenson, R. A.; and Cloetingh, S., 1991, Some examples and mechanical aspects of continental folding: Tectonophysics, v. 188, p. 27–37.

Stocklin, J., 1968, Structural history and tectonics of Iran, a review: American Association of Petroleum Geologists Bulletin, v. 52, p. 1229–1258.

Stone, D. S., 1969, Wrench faulting and Rocky Mountain tectonics: Mountain Geologist, v. 6, p. 67–69.

Sylvester, A. G., 1988, Strike-slip faults: Geological Society of America Bulletin, v. 100, p. 1666–1703.

Tanner, J. H., 1967, Wrench-fault movements along the Washita Valley fault, Arbuckle Mountain area, Oklahoma: American Association of Petroleum Geologists Bulletin, v. 51, p. 126–141.

Tomlinson, C. W., 1952, Odd geologic structures in southern Oklahoma: American Association of Petroleum Geologists Bulletin, v. 36, p. 1820–1840.

Tomlinson, C. W.; and McBee, W., Jr., 1959, Pennsylvanian sediments and orogenies of the Ardmore district, Oklahoma, *in* Petroleum geology of southern Oklahoma, v. II, a symposium, Ardmore Geological Society: American Association of Petroleum Geologists, Tulsa, p. 460–500.

_____ 1988, Pennsylvanian sediments and orogenies of the Ardmore district, Oklahoma, *in* Rascoe, Bailey, Jr.; and Hyne, N. J. (eds.), Petroleum geology of the Mid-continent: Tulsa Geological Society Special Publication no. 3, p. 85–89.

Walper, J. L., 1956, Basement control of the structural evolution of southern Oklahoma [abstract]: American Association of Petroleum Geologists Bulletin, v. 48, p. 551.

Willden, R. D., 1979, The Ruby orogeny, a major tectonic event, *in* Newman, G. W.; and Goode, H. D.

(eds.), Basin and range symposium: Rocky Mountain Association of Geologists and Utah Geological Association, p. 54–74.
Williams, H.; and Hiscott, R. H., 1987, Definition of the Iapetus rift-drift transition in western Newfoundland: Geology, v. 15, p. 1044–1047.
Wilson, B. R.; and Laule, S. W., 1979, Tectonics and sedimentation along the Antler orogenic belt of central Nevada, *in* Newman, G. W.; and Goode, H. D. (eds.), Basin and range symposium: Rocky Mountain Association of Geologists and Utah Geological Association, p. 81–92.
Van Waterschoot van der Gracht, W. A. J. M., 1931, Permo–Carboniferous orogeny of the south-central United States: American Association of Petroleum Geologists Bulletin, v. 15, p. 991–1057.

Seismic Investigations of the Ouachita Trend from Western Arkansas to North Texas

Richard E. Schneider
Schneider Strata Science, Inc.
Oklahoma City, Oklahoma

ABSTRACT.—The Ouachita trend has been the location of discoveries of large gas reserves in recent years. Since 1986 it has been estimated that >5 Tcf of gas has been added to existing reserves from Arkansas to north Texas along this trend. Developing an understanding of both the structure model and the reservoir characteristics is key to exploring the potential of Ordovician through Pennsylvanian rocks along the trend. A series of seismic lines have been shot from western Arkansas to north Texas in an effort to unravel the structural picture. A sampling along a 200-mi-long fairway reveals that there are three main targets for exploring along this trend: (1) The deformable Pennsylvanian sedimentary units shoved forward into décollement structures by the Ouachita thrust. (2) The thrusted Spiro-Wapanucka-Cromwell strata that lie beneath, and sometimes within or in front of, the Choctaw fault. (3) The block-faulted structures in lower Paleozoic rocks that typically underlie the Choctaw fault, with the Arbuckle Group being a prime target.

The structural styles have strong similarity along the entire extent of the Ouachita trend from the Wilburton area, to features east of Wilburton into Arkansas, and finally from Wilburton southwest to the Red River and into north Texas. Some of the data are older-vintage seismic records that were shot during the 1950s—but still they are of good quality if they are redisplayed after removal of NMO (normal moveout). Much of the seismic data are of recent vintage, and incorporate high-fold stack and modern processing techniques.

Repeatable structures and complex anomalies can be seen along the entire trend area.

Schneider, R. E., 1995, Seismic investigations of the Ouachita trend from western Arkansas to north Texas, *in* Johnson, K. S. (ed.), Structural styles in the southern Midcontinent, 1992 symposium: Oklahoma Geological Survey Circular 97, p. 82.

Ablative Subduction and Its Structural Effects Upon the Midcontinent During the Pennsylvanian

Raymon L. Brown
Oklahoma Geological Survey
Norman, Oklahoma

ABSTRACT.—Subduction on the border of North America acted to initiate tectonic movements and influence the structural styles associated with Midcontinent tectonics during the Pennsylvanian. However, regardless of the assumed directions of plate convergence, the Wichita and Arbuckle uplifts were building at right angles to any compressive stresses that might be transferred from the prescribed collisional front (the Ouachita thrust). The relationship between subduction and Midcontinent tectonics does not appear to be a simple one in which forces applied to the boundary of a plate act to transmit stresses to the interior of the plate.

This paper uses a speculative model for subduction to interpret the tectonic history of the Midcontinent during the Pennsylvanian. The subduction model described can be used to explain the timing, distribution, and sense of tectonic motion within the Midcontinent. The paper concludes with a brief discussion pointed toward the style of subduction-related structures in the Midcontinent. Evidence supporting the classic fold-thrust model of Berg (1962) appears to be ubiquitous throughout the Midcontinent, and Berg's model should be used as a tool for exploration.

INTRODUCTION

Exploration in southern Oklahoma has been difficult because of the complex structures and the difficulty of acquiring good seismic data. One of the keys to defining the structural style of a region is an understanding of the tectonic environment responsible for creating the structures. This paper describes a model for the subduction-related processes that could have acted to influence the structural development of the Midcontinent. The model can be used to account for the spatial and temporal distribution of events that occurred during the Pennsylvanian. The structural style best characterizing many of the tectonic features created during the Pennsylvanian is that of the fold-thrust (Berg, 1962). Exploration in the Midcontinent requires a thorough understanding of the evolution of fold-thrust structures.

ABLATIVE MODEL FOR SUBDUCTION

The relationship of interior continental structures to subduction on the boundaries of a continent can be explained by using one of two assumptions: (1) the Earth's crust and part of the upper mantle—the lithosphere—are capable of transferring stresses over long distances like an elastic plate or (2) much of the Earth's lower crust and part of the upper mantle—again, the lithosphere—acts more like a fluid than an elastic solid over geologic time scales. According to assumption 2, the structures observed on the surface and in the upper crust occur within a thin elastic veneer that forms the top of the lithosphere. In this paper, the word "crust" will be used as an approximation to this veneer, with the understanding that its dimensions may be thicker or thinner than the crust as usually defined. As such, the crust deforms elastically and is basically along for the ride on top of the lower part of the lithosphere with its fluidlike motion.

The first assumption has certainly been the popular one since early workers on the topic of plate tectonics introduced the idea of "rigid plates." Nevertheless, the timing, spatial distribution, and diversity of stresses applied to the Midcontinent during the Pennsylvanian cannot be explained by the simple idea of plate-collision stresses transmitted from the edges of the plates to the interior of the continent. For example, the Arbuckle and Wichita uplifts were constructed with compressive forces that had to be at right angles to those building the Ouachita thrust; i.e., the directions of crustal shortening for these structures are at right angles. In addition to the problems of explaining tectonic movements in the Midcontinent by using the first assumption, the localization and tectonic length

Brown, R. L., 1995, Ablative subduction and its structural effects upon the Midcontinent during the Pennsylvanian, *in* Johnson, K. S. (ed.), Structural styles in the southern Midcontinent, 1992 symposium: Oklahoma Geological Survey Circular 97, p. 83–98.

scales are not easily explained. The second assumption appears to explain many phenomena that cannot be explained by using rigid-plate concepts (Tao and O'Connell, 1992).

Because of the more applied, as opposed to theoretical, emphasis of the workshop (the understanding of the structural styles of the Midcontinent), the second assumption is used in this paper without any further justification. The point will be to illustrate how many facets of the Pennsylvanian tectonic history of the Midcontinent can simply be explained by using the assumption that the lithosphere behaves predominantly as a fluid, while the crust is just along for the ride. First, a fluid model for subduction is discussed, along with some of the issues related to tectonic movements that are simplified by using this model. The counterflow associated with those movements is portrayed in the next section as the mechanism responsible for transferring stresses to the interior of the continent. Finally, a map notation for representing subduction is introduced that will be used in the discussion on the Midcontinent.

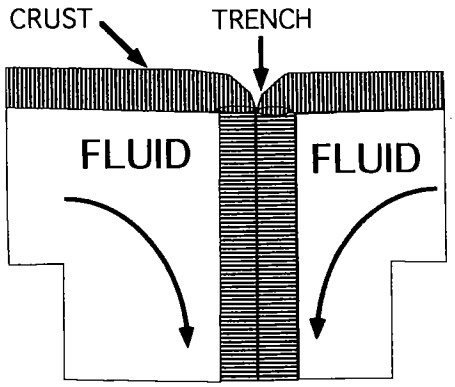


Figure 1. Illustration of equally ablative plate subduction and the two-sided nature of subduction processes. When the crustal densities are the same, equal amounts are ablated from each plate and subducted. The subduction is vertical in this case since the position of the trench is determined by the ablation rate from each of the crusts.

Fluid Model for Subduction—Ablative Subduction

The subduction model used here to explain the timing of events in the Midcontinent during the Pennsylvanian has been proposed in a paper by Tao and O'Connell (1992). The reader is referred to that paper for a more detailed description of the fluid model of subduction.

The basic idea, called ablative subduction, proposed by Tao and O'Connell (1992) is that the upper, more elastic portion of the lithosphere (i.e., the crust) is passively riding on top of the lower lithosphere, which is moving like a fluid. Surprisingly, the possibility of detachments between the crust and the fluid movement of the lower lithosphere can be used to simply explain many tectonic environments previously seen as complicated.

One of the definitions of ablative is "a separation or direction away from" the main body (sometimes used in a surgical reference). Geologists use the term "ablation" to refer to the totality of all processes by which a glacier is reduced. "Ablative" is descriptive of this model of subduction because crust is ablated from both lithospheric "plates" during subduction.

Figure 1 illustrates the convergence of two plates experiencing equal amounts of ablative subduction. A fluid instability exists in the upper mantle, causing (in the case shown) a downward vertical motion in the upper mantle. The crust of each plate (remember the special usage of the term "crust") is simply along for the ride and can even become detached from the lower lithosphere.

At the trench where the crusts of the two plates meet, equal amounts of each of the crusts are ablated and subducted. Tao and O'Connell (1992) have argued that buoyancy plays a major role in determining the amount of crust that is ablated from each of the plates. Figure 1, then, might be a model of two oceanic plates with crusts that have the same density, since the same amount of crust from each plate is going down with the fluid. Admittedly, there are not too many examples of vertical subduction, but consider the small probability of having two plates converge whose crusts have identical densities. For example, oceanic crusts become more dense with age, so that the convergence of oceanic crusts usually implies a situation in which crusts with slightly different densities converge at a trench.

When the crustal densities are different, the ablation rate of the lightest crust is reduced (owing to increased buoyancy) as shown in Figure 2. Since the ablation rate of the lighter crust is reduced, the trench moves toward the plate with the heavier crust while the fluid is still dropping vertically. The result is the steeply dipping subduction that is so typical of converging oceanic plates. If the upper mantle has some motion relative to the position of the density instability, then some relativistic arguments need to be considered. Tao and O'Connell (1992) have given a complete discussion of this issue. The results are the same, regardless of the circumstances: relative crustal densities determine the dip of the subduction (in this model).

Much of the paper by Tao and O'Connell (1992) is written for a general audience. Most of the mathematics associated with the numerical simulation is reserved for the appendix. The paper mentions a number of complex tectonic processes (e.g., double subduction and subduction polarity reversal) that are easily understood in terms of the ablative model of subduction. The Earth's crust (or whatever part

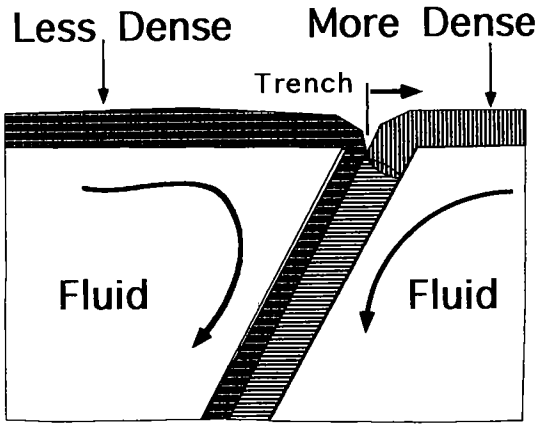


Figure 2. Illustration of unequally ablative plate subduction, which causes the absolute position of the trench to move with respect to the downward-moving fluid. The steeply dipping geometry of the subduction is typical of converging oceanic plates of different ages (and therefore buoyancy).

represents the elastic upper portion in Figs. 1 and 2) can be modeled as though it is resting on a series of conveyor belts (fluid motion in the upper mantle). When two of the conveyor belts converge, buoyancy acts to reduce the ablation rate of the lighter crust. The sediments deposited during this process are squeezed into smaller spaces acting to build the orogenic belts associated with continents. Many plate-tectonic concepts are more easily explained when there is some detachment between the crusts and the "conveyor belts" upon which they are carried (e.g., the subduction of Asia beneath Tibet) (Willett and others, 1994). In addition to its simplicity, Tao and O'Connell (1992) have shown that their ablative model for subduction exhibits most of the desirable features of the rigid-plate models.

Counterflow—The Driving Mechanism

An old adage, "whatever goes up must come down," can be applied to subduction. In fluid mechanics, the rule is called conservation of mass. When fluid begins to move downward because of density instabilities, additional fluid begins to move upward to compensate for the downward motion. I will refer to this movement as a counterflow. The counterflow acts to make subduction zones even more interesting than described above. In fact, perhaps Tao and O'Connell (1992) should be freed from any association with what is said below concerning the importance of the counterflow, and I as author of this paper will take the responsibility for the following speculations on its importance.

In Figure 3 the counterflow associated with the convergence of two oceanic plates is illustrated rising to delaminate the plate. Ultimately, the delamination leads to volcanism over the subduction zone. The origin of the magmas is still a topic of debate. Note that the thicknesses of the crusts are drawn out of proportion to the thicknesses of the plates for the sake of clarity.

Figure 4 illustrates a circumstance in which two plates with large density differences in their crusts are converging. This figure is an example of what can happen when a continent and an oceanic plate converge. The ablation is practically one-sided in this case because of the buoyancy of the continental

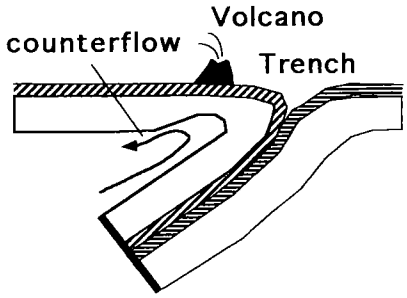


Figure 3. Illustration of unequally ablative plate subduction typical of convergence between oceanic plates. The plate on the right has a denser crust that, on the basis of the ablative model for subduction, is ablated and subducted at a faster rate than the plate on the left. The relative thicknesses of the crusts, with respect to the plate thickness, are not drawn to scale. The counterflow associated with subduction is responsible for volcanism over the dipping subduction zone.

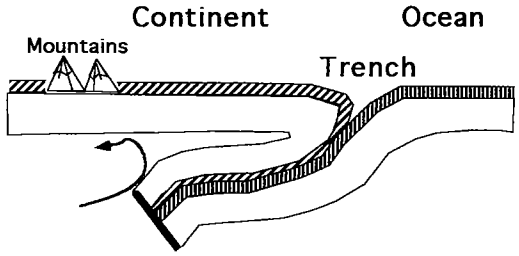


Figure 4. Illustration showing a convergence between continental and oceanic plates. The upper portions of the plates (e.g., the crusts) control the geometry of the subduction zone and, ultimately, the geometry of the counterflow. In practice, two-sided subduction is the rule for the lower portions of the lithospheric plates as shown in Figure 3. Because of the almost one-sided nature of the ablation for continent/ocean convergence, the subduction zone exhibits a shallow dip beneath the continent that acts to push the counterflow toward the continental interior. When a continent/ocean convergence zone lies along one part of a trench and an ocean/ocean convergence zone lies along another part, a transition zone is required between the two types of convergence zones.

crust. Note that the counterflow is now predominantly affecting the continent. When subduction is shallow beneath a continent, the mountain-building processes are thought to be in action (Barazangi and Isacks, 1976). Unfortunately, there is not a unanimous opinion on how shallow-dipping subduction is related to mountain building within the interior of a continent. One early idea assumed that the subducted plate was dragging along the underside of the continent, acting to build a mountain range, such as the Rocky Mountains (Dickinson and Snyder, 1978). A more recent paper by Bird (1988) suggested that the counterflow (rather than a physical contact or viscous drag) acted to build the Rocky Mountains during the Laramide orogeny. Although Bird's (1988) modeling and treatment of the counterflow are outstanding, the plates used in his model are rigid, and the subduction angles are defined by him. For the Pennsylvanian Midcontinent, both the bottom-drag hypothesis (Dickinson and Snyder, 1978) and the counterflow model (Bird, 1988) seem equally plausible, until the distribution and sense of tectonic movements within the Midcontinent are considered. The distribution, timing, and orientation of stresses in the Midcontinent during the Pennsylvanian are all best explained in terms of the counterflow related to subduction beneath the continents. The question of how counterflow acts to transfer stresses to the crust will be asked in a later discussion. Before considering that problem, the sequence of Pennsylvanian events responsible for creating many of Oklahoma's geologic features will be reviewed. In order to simplify the discussion, a map notation for representing subduction geometry is described in the next section.

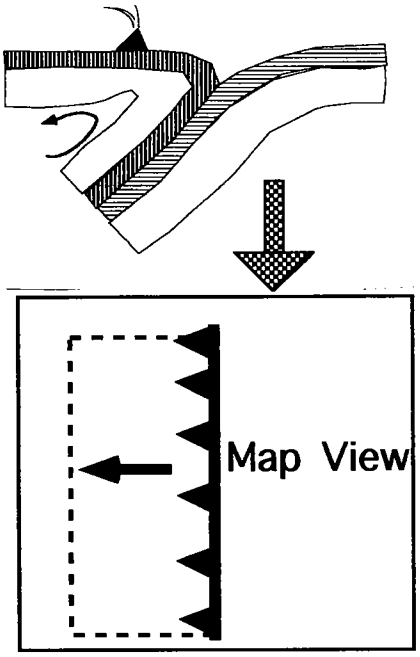


Figure 5. Map symbols shown in this figure are used to indicate the subduction geometry and the counterflow related to the geometry. The trench axis and the direction of dip for the trench are indicated by the solid line with triangles pointing in the direction of the dip. The projection of the subducted plate (above a specified depth) is indicated by the dashed line. The dashed projection of the plate will be used to indicate the propellerlike shape of a subduction zone that has different types of convergence along the strike of the trench. The important variable in this paper is the direction of the counterflow that acts to determine the direction of forces applied to the underside of the continental plate when subduction occurs on the boundary of the continent.

Map Representation of Counterflow Directions

Since crustal buoyancy is assumed in this paper to be one of the factors controlling the geometry of subduction, the direction and amount of dip of a subduction zone will vary along a trench if different types of crusts are converging along the trench. This circumstance occurred along the southern border of North America during the Pennsylvanian, when one part of the trench was associated with shallow-dipping subduction (continent/ocean) while another part was associated with steeply dipping subduction (ocean/ocean). Where subduction occurred between ocean plates, the direction of subduction could have been either toward North America (as is usually shown) or away from it, depending on the relative densities of the oceanic crusts involved. However, where the trench was bounded by continental crust on one side and oceanic crust on the other, the buoyancy of the continental crust is assumed to have forced shallow subduction of the oceanic plate beneath the continent. A gradual transition is assumed to have taken place between these two extremes. The map symbols used to discuss the subduction with respect to North America are shown in Figure 5.

Midcontinent Tectonic Features

The map shown in Figure 6 illustrates some of the major tectonic features created during the Pennsylvanian. The uplifts on this map are named in Figure 7, and the basins are named in Figure 8. One of the striking features of the Midcontinent is the frequent association of tectonic movements with those regions that have a history of intrusion, extrusion, and/or rifting. The Ozark uplift, the Midcontinent rift (a failed rift), the southern Oklahoma aulacogen (a failed rift), and the Delaware aulacogen all appear to have influenced the subsequent tectonics of their respective regions.

The Delaware aulacogen and the southern Oklahoma aulacogen are not indicated on these maps for the sake of clarity. The Delaware aulac-

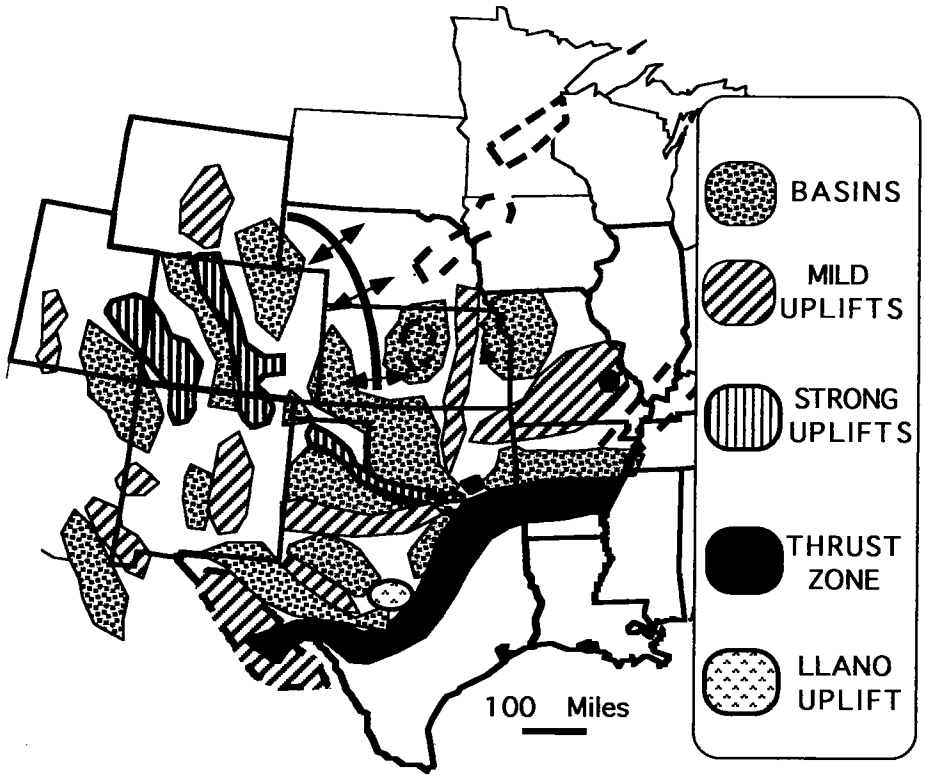


Figure 6. Major tectonic features of the Midcontinent. Most of the basins and uplifts in this map were formed during the Pennsylvanian. These features are identified in Figures 7 and 8.

ogen (Walper, 1977) is in the approximate location of the Delaware basin (Fig. 8), whereas the southern Oklahoma aulacogen (Johnson and others, 1989) is beneath the Amarillo-Wichita uplift (Fig. 7).

There are many excellent reviews and references for the Midcontinent. The papers by Mallory (1972), Moore (1979), Kluth and Coney (1981), Gilbert and Donovan (1982), Budnik (1986), and Johnson and others (1989) were useful in constructing the maps shown in Figures 7–9. Although they are interesting, it is rather difficult to get any sense of what was happening by looking at these maps. Only when the relative timing of events is considered does the Midcontinent tectonic map shown in Figure 6 begin to make sense.

INTERPRETATION OF THE TIMING AND DISTRIBUTION OF MIDCONTINENT TECTONIC EVENTS USING AN ABLATIVE-SUBDUCTION MODEL

Early Mississippian—The Beginning of Movement

The timing of Midcontinent tectonic movements is discussed in some of the classic references (e.g., Tomlinson, 1952; Tomlinson and McBee, 1962; Moore, 1979; Budnik, 1986). The first movement came when an Early Mississippian jolt, so to speak, struck the Midcontinent and initiated movements along the Ancestral Rockies (ancestral Front Range and the Uncompahgre uplift) and the Amarillo-Wichita uplift, shown in Figure 9. The central Kansas uplift and the Chadron-Cambridge arch, collectively referred to as the central Kansas uplift in this paper, also began rising during this time (Figs. 7,9). This first movement has been referred to as a jolt because there is no evidence to indicate any kind of spatial and temporal progression of events.

This Early Mississippian jolt may have occurred when the trench shown in Figure 9 first made contact with the continent, or it may have been related to the turning of the subduction trend from southwestward (from the Appalachian orogeny) to westward in its progression toward Oklahoma. On the basis of the assumed importance of the counterflow from subduction, this initial jolt to the Midcontinent was probably caused by counterflow in the direction of the arrow shown in Figure 9. The major features that were initiated during this first jolt are indicated in Figure 9. This figure gives the reader a clear picture of the first movements within the

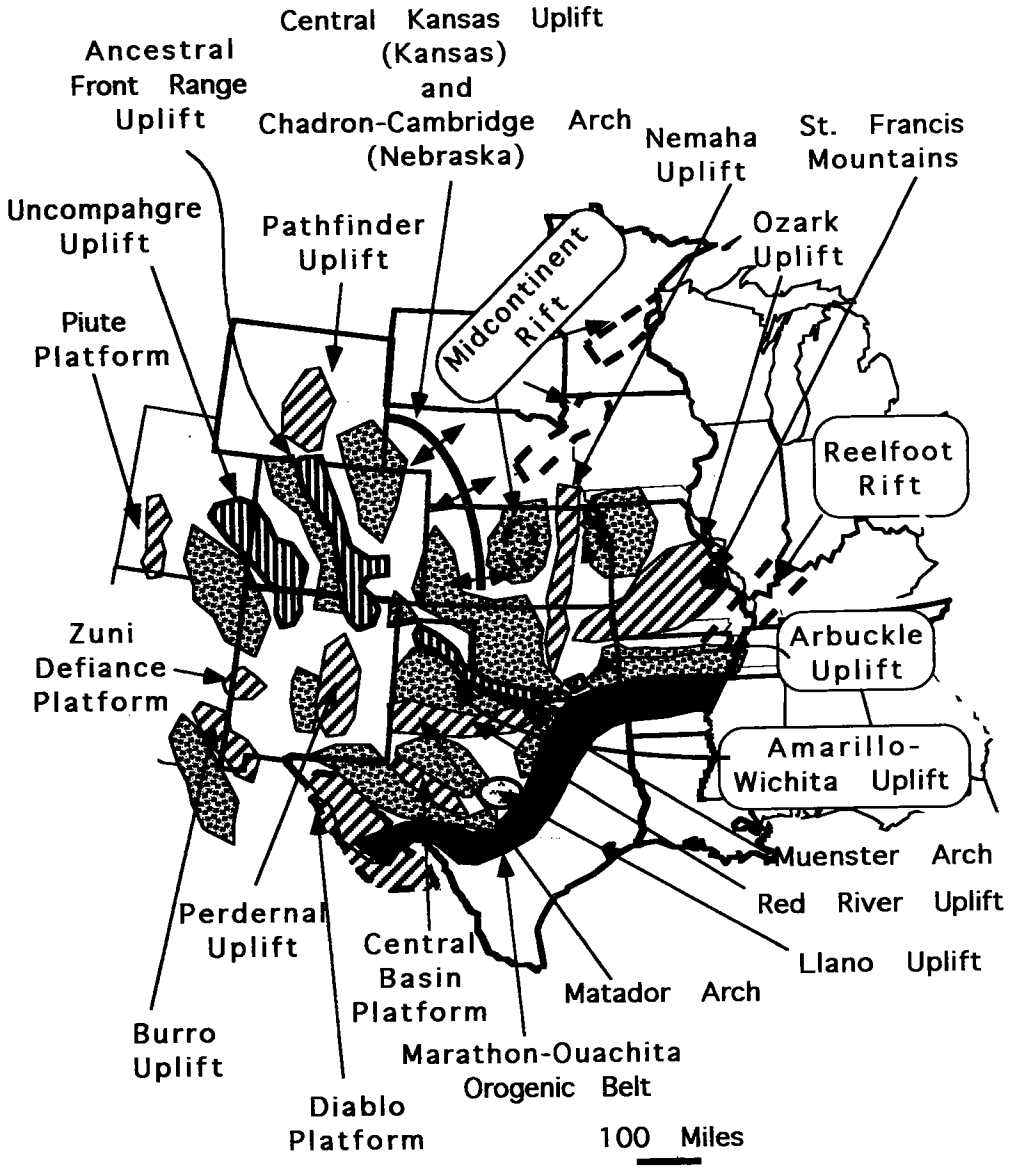


Figure 7. Major tectonic uplifts created during the Pennsylvanian and associated with subduction on the southern border of North America. The Marathon–Ouachita orogenic belt represents the thrust belt associated with the collision front. The Llano uplift is not a Pennsylvanian feature, but is used here as a landmark.

Midcontinent that were associated with the approaching subduction zone. In Oklahoma, this activity was responsible for uplifting the Amarillo-Wichita Mountains, the Criner uplift (an eastward extension of the Amarillo-Wichita Mountains not shown in Fig. 9), and the associated basins.

Mississippian—The Nemaha Uplift

During the middle and latter parts of the Mississippian, the Midcontinent tectonics seemed to be predominantly focused in the vicinity of the central Kansas, Nemaha, and Ozark uplifts shown in Figure 10. At this time, shallow-dipping subduction is interpreted (continent/ocean) for the eastern portion of the trench, whereas steeply dipping subduction (ocean/ocean) occurred in the west off the coast of Texas. The map symbols given in Figure 5 are used to illustrate the approximate geometry of the subduction and the direction of the counterflow. This counterflow is assumed to be responsible for the construction of the Nemaha uplift, the contin-

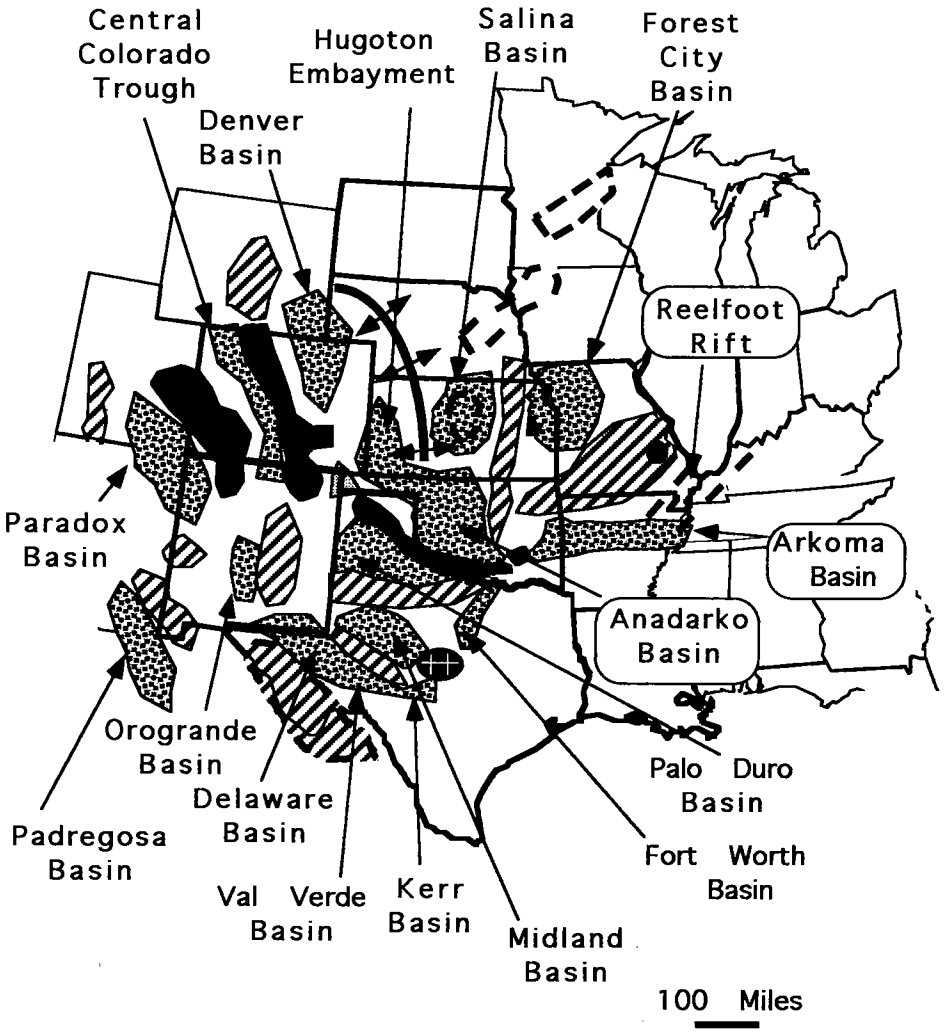


Figure 8. Major tectonic basins created during the Pennsylvanian and associated with subduction on the southern border of North America.

ued warping of the central Kansas uplift, and a reactivated uplift of the Ozarks. The counterflow is interpreted to have been restricted from moving to the east because of the restricted flow regime over the region characterized by shallow-dipping subduction. The resulting flow was forced out at an angle determined by the propeller shape of the subduction zone in which the steeply dipping subduction offshore of Mexico and Texas changes to shallow-dipping subduction under the continent.

Note that the Nemaha uplift is parallel to the southern extension of the Midcontinent rift (Figs. 7,10). This feature is apparently the result of localized compression (east-west), which I believe is directly related to the presence of the Midcontinent rift. The central Kansas uplift is not exactly parallel to the Midcontinent rift, but it is not too difficult to imagine that it was also influenced by the rift and may be the result of large-scale anomalies in the lower crust or upper mantle associated with the rift. The Ozark uplift has also exhibited some igneous activity in the past; therefore, the Ozark uplift may have some characteristics in common with failed rifts that allow it to become active during periods of subduction along the borders of the continent. If the alignment of rifts with Midcontinent tectonics only occurred here, it would not have been mentioned. However, the association of Midcontinent tectonics with a prior history of rifting and/or intrusion is the rule rather than the exception.

Before leaving the picture of Mississippian tectonics (Fig. 10), note that if the relative geometry of the subduction is rotated counterclockwise ~30°, the counterflow during the Early Mississippian could be explained (Fig. 9) as resulting from the suture zone's turning the corner from the East

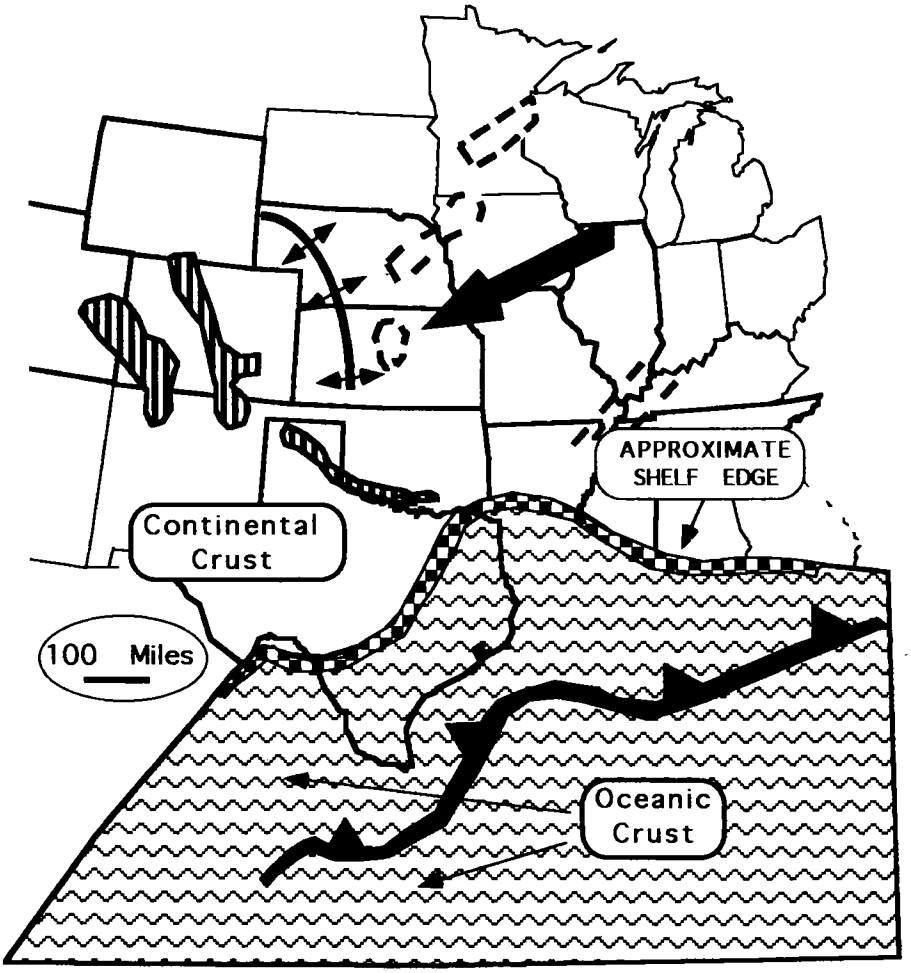


Figure 9. The illustrated Ancestral Rockies, Amarillo-Wichita uplift, and central Kansas uplift were the first structures to begin rising during the Early Mississippian jolt that seemed to hit the Midcontinent. The arrow represents the direction of the counterflow from subduction near the East Coast that started building these major Midcontinent structures.

Coast (the Appalachian thrust) to the southern boundary of the continent.

Wichita Orogeny

As the continent/ocean portion of the trench moved toward Oklahoma and around the corner of the shelf toward Texas, the subduction zone shown in Figure 10 (the Mississippian) rotated so as to give the Ancestral Rockies and the Amarillo-Wichita system a broadside shot of the counterflow (Fig. 11). This process was responsible for what is called the Wichita orogeny.

The actual counterflow, shown in Figure 11, should not be interpreted to be a simultaneous blast all along the length of the Ancestral Rockies and the Amarillo-Wichita systems. Instead, the first blast of a counterflow (A), as the subduction system began to turn the corner, acted to create the Ancestral Rockies (Fig. 11). As the subduction system migrated farther around the turn toward Texas (B), the Amarillo-Wichita system continued active building while the Ancestral Rockies were nearly completed. Figure 11 represents a condensation of the countermotion, so the different subduction configurations are left to the imagination of the reader. Note that the sequence of tectonic movements in the subduction model moves toward the plate boundaries, i.e., toward the trench. This sense of structural progression is exactly that noted by several authors (e.g., McConnell, 1987). Stresses transferred from the boundary of an elastic plate by pushing cannot explain this migration of events from Colorado toward Oklahoma. In addition, the direction of the counterflow changes as the subduction moves around the corner in general agreement with the direction of the structures created. However, I do not want to claim that this counterflow is directly related to the principal-stress direction re-

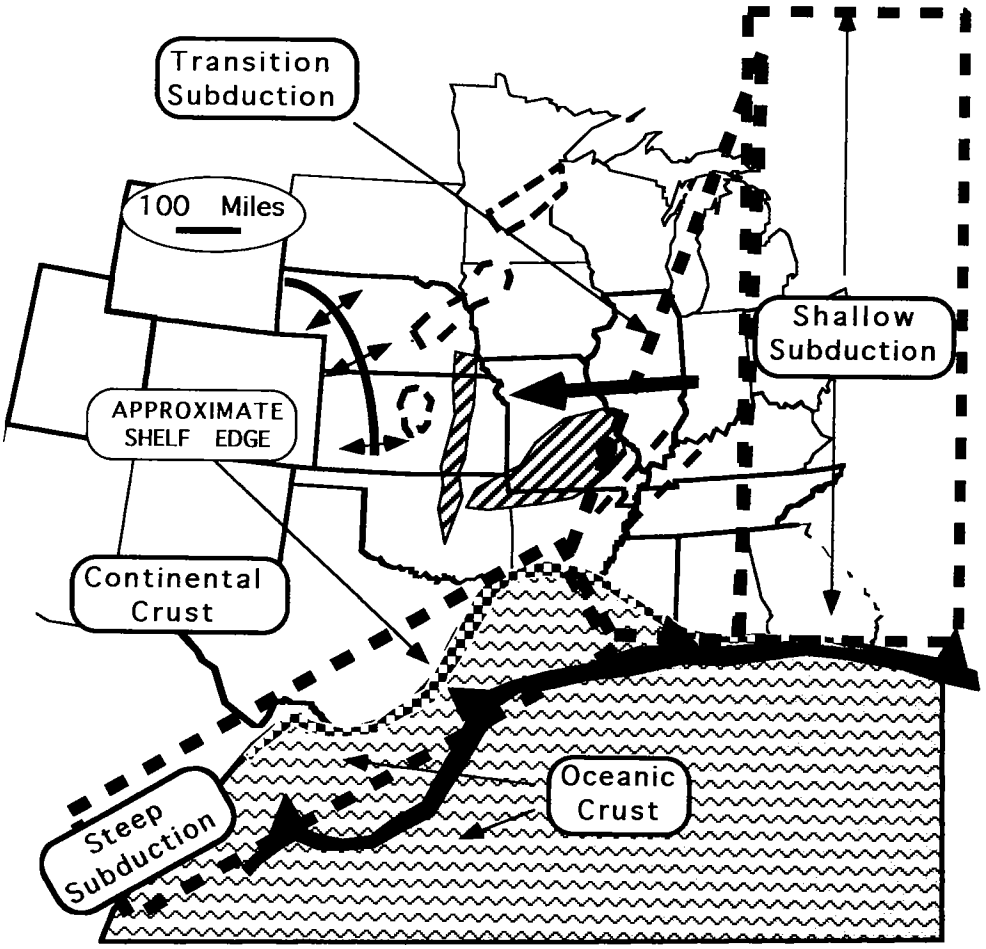


Figure 10. Mississippian tectonic movements. During the Mississippian, shallow-dipping subduction occurred beneath the eastern United States while steeply dipping subduction took place offshore Texas and Louisiana. The transition in subduction geometry formed a zone that acted to focus the counterflow from the deep-seated subduction toward the Ozark uplift, the Nemaha uplift, and the central Kansas uplift, which continued its Early Mississippian movement. All of these features are associated with some intrusive history.

sponsible for any structures that develop in the crust (even though the match with the structures created does look promising). Since the role of prior igneous activity and/or rifting seems to also affect what happens, the stress distribution that results from a counterflow appears to be the combined result of prior geologic events and the direction of counterflow.

Arbuckle Orogeny

The Arbuckle orogeny represents the last stage of movement in Oklahoma (Fig. 12) as the subduction zone completed the turn around the corner and moved toward Texas. Although the details of the counterflow are not shown in Figure 13, the almost simultaneous building of the shallow portion of the more northerly striking Carter-Knox structure, a feature on the northeast shelf edge of the Anadarko basin, and the more easterly striking Arbuckle thrust (Saxon, 1994) can be explained by the rotation of the counterflow as the suture zone began migrating toward Texas.

The rift-related features in Texas appear to have been activated during this time. The Delaware and Midland basins were subsiding, while the Central Basin platform and Diablo platform were rising.

New Mexico Orogeny

By now, the idea of what was happening (as far as this model is concerned) is becoming familiar. As the subduction turned the corner in Texas around the Llano uplift, the counterflow (D) was redirected toward New Mexico (Fig. 13). The result was the building of the structures shown in New Mexico. Thus, the timing of Midcontinent events during the Pennsylvanian can easily be explained by the counterflow associated with the ablative model of subduction. The question that remains is how the

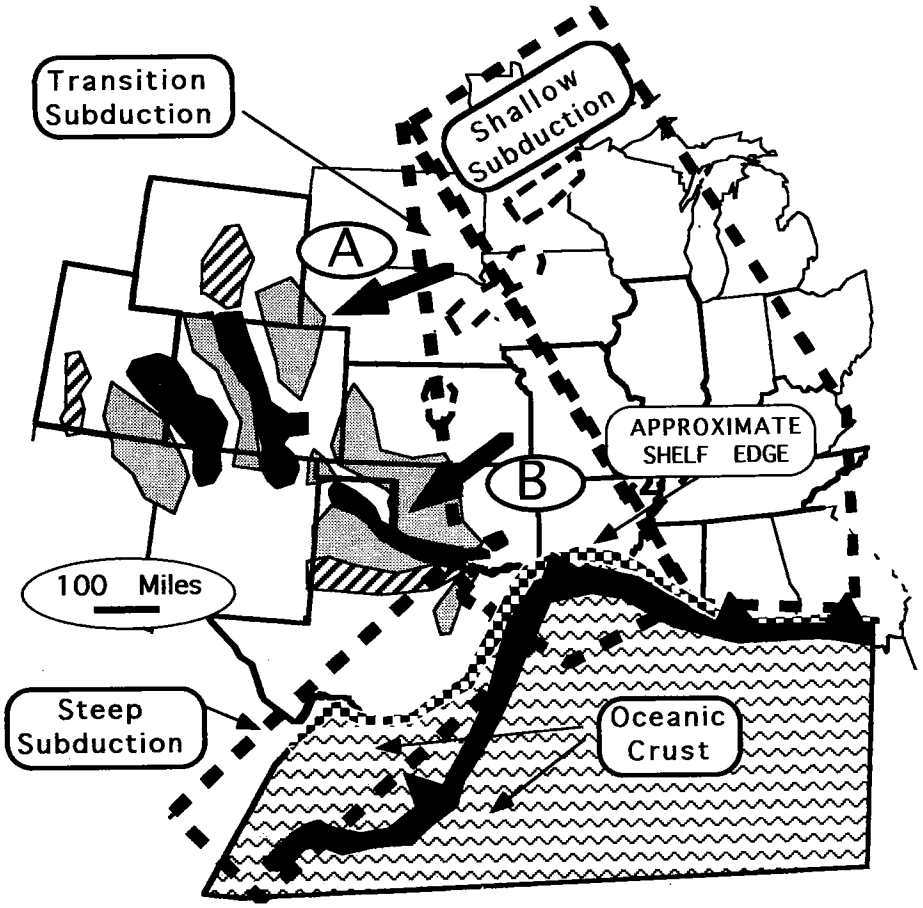


Figure 11. Wichita orogeny. As the subduction geometry changed so that the trench began to turn the corner near Oklahoma, the counterflow acted very much like a fire hose, spraying almost in a continuous motion first (A) in the direction of the Ancestral Rockies and then (B) moving toward the Amarillo-Wichita uplift. This rotation of the counterflow (and the tectonic movements) from the Ancestral Rockies toward the trench explains the apparent building of structures toward the trench. The transfer of elastic stresses through a plate cannot explain this behavior, since the structures would have been formed in the other direction—i.e., from the trench inland.

stresses created in the continental crust are related to the counterflow. Some of the ideas I have regarding these matters are discussed in the next section.

STRESS TRANSFER AND THE INFLUENCE OF CONTINENTAL RIFTS

How does a counterflow transfer stress to the crust of the Earth? Does a history of prior rifting affect the possibility of Midcontinent tectonics? If so, how? A brief discussion of these questions can be used to give some insight into the types of structures expected for the Midcontinent.

Stress Transfer without Prior Rifting

The discussion can begin by considering how a counterflow might be solely responsible for transferring stresses to the continental crust. Consider first the oceanic-oceanic subduction shown in Figure 3. The counterflow from deep subduction in this case causes volcanism and is expected to be less viscous than the fluids making up the plate. The depth of penetration of the subduction zone seems to cause a counterflow capable of delaminating the underside of a plate and, if sustained long enough, to eventually allow venting above the zone of delamination. When shallow-dipping subduction occurs, however, the counterflow may consist of a more viscous fluid except where the subduction becomes deeper under the Midcontinent. In this way, the shallow-dipping subduction could act to apply a viscous drag on the bottom of the continent. I do not believe that this process happened because the nature of forces were at right angles to the drag over the regions of shallow-dipping subduction (Figs. 10–13). Instead, much of the tectonic move-

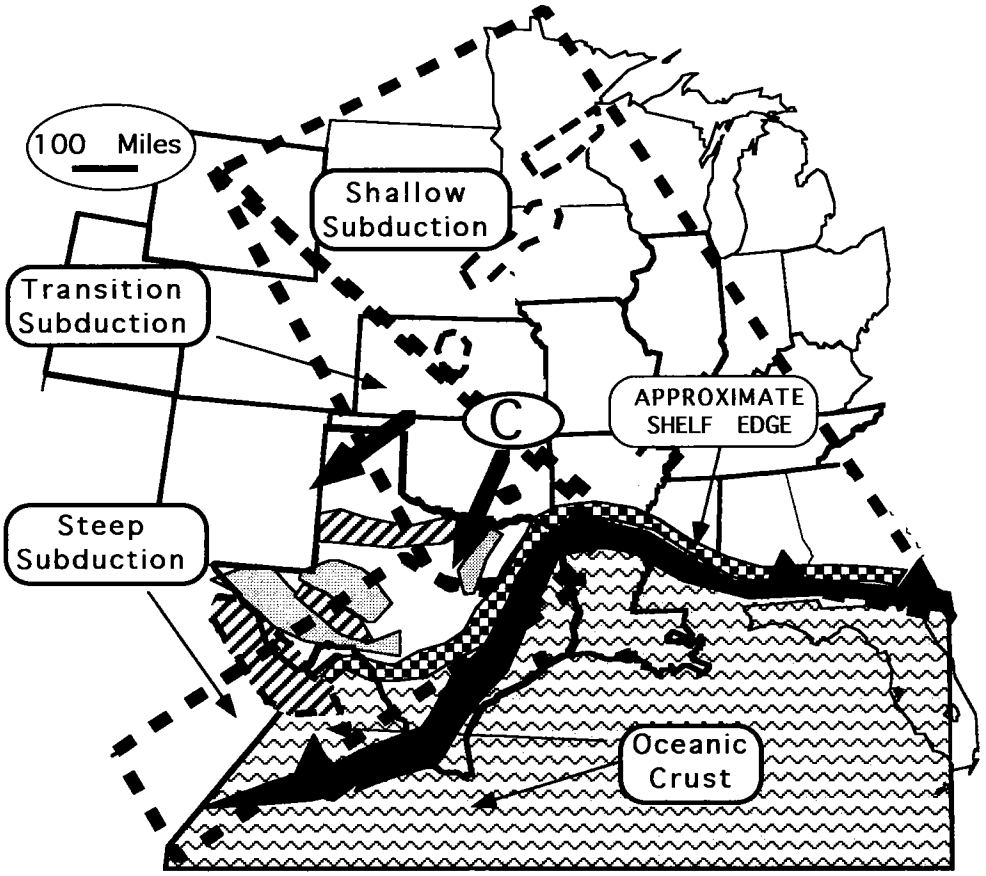


Figure 12. Arbuckle orogeny. The last remnants of tectonic movement associated with the subduction occurred during the Arbuckle orogeny, as the transition zone began to move into Texas. The counterflow (C) may have been oriented more north-south than the stresses that caused the Wichita uplift, but counterflow is not expected to be the only factor governing the sense of tectonic movement.

ment appears to have taken place above the deep-related subduction, i.e., where the subduction geometry hit a critical depth, as it shifted positions beneath the Midcontinent. If the deep-seated counterflow acted to transfer stress to portions of the Midcontinent (as shown in Fig. 3, beneath an oceanic plate), the timing and localization of stresses can be explained by the changing geometry of the subduction zone. The deep-seated counterflow seems to be at least a part of the story of how stresses can be transferred to the continental crust (Griggs, 1939; Bird, 1988). Another part may be the history of prior rifting.

Stress Transfer Associated with Prior Rifting and/or Intrusive History

In this section, I will discuss some possible explanations of why Midcontinent tectonic events may be related to regions that have some prior history of rifting and/or intrusion. There are some very interesting questions than can be asked in this section. For example, why would the Rocky Mountains be built twice in the same location? Is it fortuitous that the central Kansas uplift and the Nemaha uplift seem to be associated with the Midcontinent rift? Why does the Amarillo-Wichita uplift align with the southern Oklahoma aulacogen? Is it just a coincidence that the West Texas features align with the Delaware aulacogen? There is a hint that the southern Oklahoma aulacogen extended into Colorado. These ancestral features of the Midcontinent have been reactivated when subduction on the borders of the continent has reactivated them. Anyone who has viewed the thrust faults over the Midcontinent rift is immediately forced to admit that extension occurred when the rift was active, but that some later phase of compression acted to cause the thrusting. Has anyone asked why the thrusting is localized about the failed rift (Brown and Morgan, 1991)? Pick a region of the Midcontinent that was active (see Fig. 6), and you can most likely find a nearby history of rifting and/or intrusion (e.g., the Ozark uplift–Saint Francis Moun-

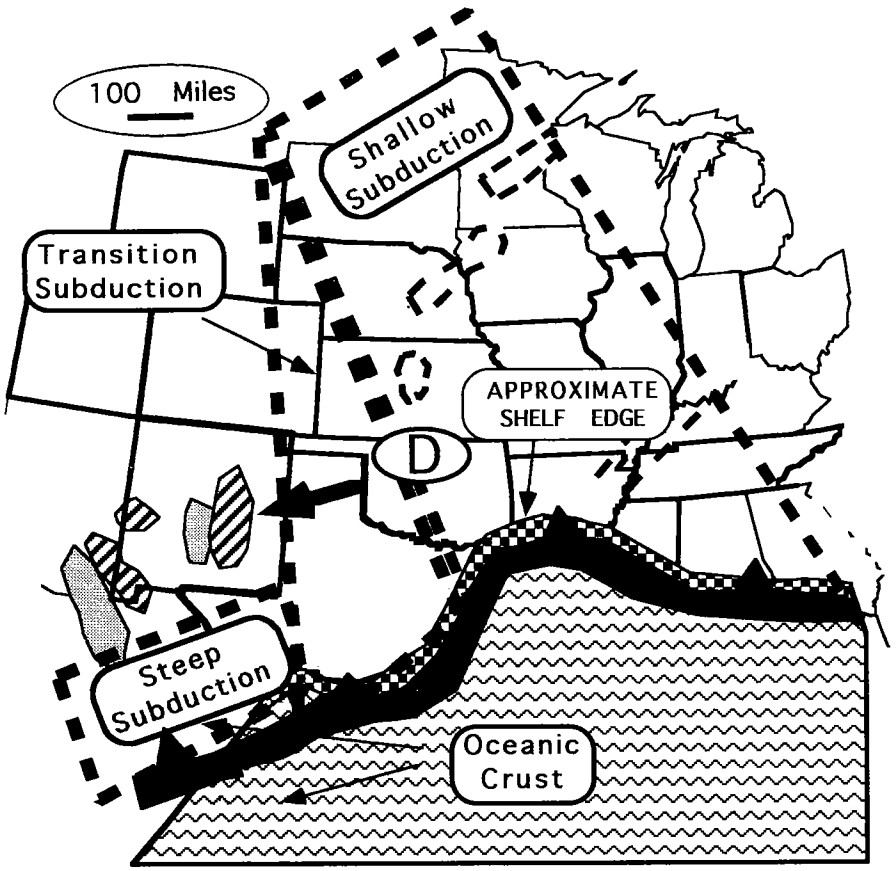


Figure 13. New Mexico orogeny. The last stages of Midcontinent movement (and counterflow D) in the United States, as the structures in New Mexico, Arizona, and Mexico began forming.

tains). The degree of the movement associated with these features seems to vary all the way from simple folds to large-scale mountain building. Some ideas for how these features can interact with the counterflow to create localized compression are described below.

Zones of Weakness or Strength?

Applying stresses to the crust can focus the stresses in the weaker portions of the crust. Since rifting represents an attempt to break the crust, it is natural to assume that the rift represents a zone of weakness when stresses are applied later. However, the results of recent work in the Canning basin (Braun, 1992) argue that a region of prior rifting actually becomes fortified by the injection of ultramafic bodies into the crust and upper mantle. Admittedly, having a stronger crustal region will also focus the stresses, but both explanations share the same problem: the scale of the regional events will have to match the scale of the heterogeneities.

Increased Counterflow Drag

Another explanation for how prior rifting can act to transfer stress to the continental plate is shown in Figure 14. The prior rifting may leave a root that acts to increase the drag of the counterflow in localized regions. The result will be a combined horizontal and vertical push in the lower crust that should manifest itself as horizontal compression in the near-surface.

Paleo–Upper-Mantle Effect—Faster Sinking Creates More Vigorous Counterflow

In the last suggestion of possible relations between rifts and the counterflow associated with subduction, a paleoroot with a different, lower density may exist beneath these failed rifts. Steeples (1982) has suggested the possibility for such a feature below the Midcontinent rift. In the discussion of the ablative-subduction model, the upper mantle was assumed to have constant properties. Suppose the upper mantle beneath these ancestral rifts retained its low-density characteristics for long periods after the rifting phase. Then, as shown in Figure 15, when the subduction zone began to change its geometry to a steeper dip (the heavier lithospheric fluid sinks faster in the less-dense portion of the mantle), the deep-seated counterflow would be exaggerated near regions of prior rifting.

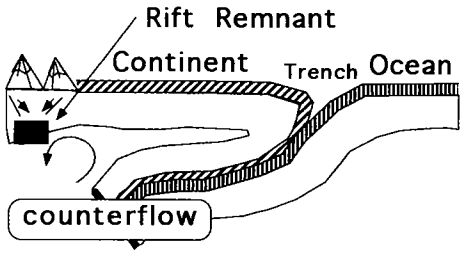


Figure 14. Plate heterogeneity associated with ancestral rift. Counterflow across the bottom of the continental plate may not transfer much stress, unless a heterogeneity acts to perturb the flow and cause a downward pull on the plate as shown.

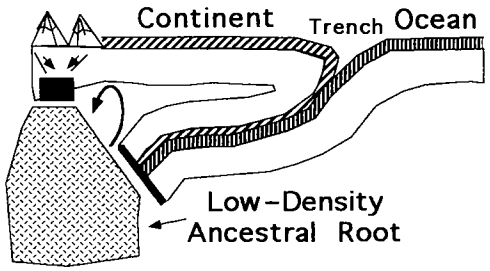


Figure 15. Upper-mantle heterogeneity associated with ancestral rift. Low-density roots beneath ancestral rifts act to steepen the subduction geometry and increase the counterflow beneath the continent. This process would act to locally exaggerate the counterflow shown in Figures 11–13. Once the subducted lithosphere pushes through these local mantle anomalies, the increased buoyancy of the lithosphere in the neighboring regions revives the shallow geometry and reduced counterflow.

Rift Summary

In summary, rifts seem to play a critical role in the history of the Midcontinent. This conclusion is surprising since they are so old, geologically. They should be dead and gone. Instead, they seem to be reactivated every time subduction occurs near the borders of the continent.

Contrary to popular opinion, rifts do not exist for just one geologic instant (Braun, 1992). Instead, they are quite capable of activation and deactivation for periods of several hundreds of millions of years. Their shifting from one spot to the next to create distinct basins has been observed in Australia and can be the explanation of some of the Proterozoic basins around the Midcontinent. For Oklahoma, a popular consideration of the southern Oklahoma aulacogen is that it represents an instant in time (at ~520 Ma). However, observations by Denison (1995) indicate that the southern Oklahoma aulacogen was active to some extent long before the estimated age of 520 Ma. What is it about a rift that makes it reactivate in a compressive mode? Some possibilities include (1) heterogeneous weakness or strength, (2) increased counterflow drag due to a root, and (3) a paleo–upper-mantle effect.

Deciding which of the mechanisms is most important should be the subject of another study. The structural style of some of the mechanisms should differ slightly. In fact, studying the structural styles of the Midcontinent may be the key to unraveling the relationship of the counterflow to the rifts. All of the rift-related stress-transfer mechanisms, except perhaps the structural-weakness mechanism, should basically create horizontal compression with a downward component of movement over most of a region. Since the zones affected are localized, the edges of these thrust zones will be characterized by strike-slip movement. Some exceptions to these rules may occur where sections of the crust are being pulled down into the upper mantle, rather than horizontally. Admittedly, the model is speculative from top to bottom, and not all of the details have been explained. However, the ablative model and the effects of the counterflow can be used as a hypothesis during the examination of the structural styles found in the Midcontinent.

STRUCTURAL STYLES FOR SOUTHERN OKLAHOMA

Suture Zone—Normal and Thrust Faults Working Together

Since the subduction process has been the central theme of this paper, it is natural to include a side note on the structures directly related to the trench. The Ouachita thrust and the Arkoma basin are examples of subduction-related features that occur near a trench. Now with the ablative model of subduction, some new ideas concerning the structures near the trench can be proposed. The primary predictions for an ablative trench would be that (1) the upper crust is primarily under compression (as are the sediments in the trench) and (2) the lower crust (both sides) is under tension as it is pulled downward.

In essence, the effects of the counterflow in the Midcontinent are basically the same as those at the trench: a two-sided pull on the crust toward the area where the counterflow is pushed downward. Thus, trenches might be considered as cousins to the mechanisms responsible for building mountains (Griggs, 1939).

Consider the illustration of a trench in which the sediments fill the trench (Fig. 16). Assume that both crusts are participating (ablative subduction), but that most of the movement is associated with the *crust* on the right-hand side of the trench. Those sediments on the right are then forced gradually down and toward the bottom of the trench. The sediments will be thrust up and out of the trench as indicated in Figure 17, where the top of the sedi-

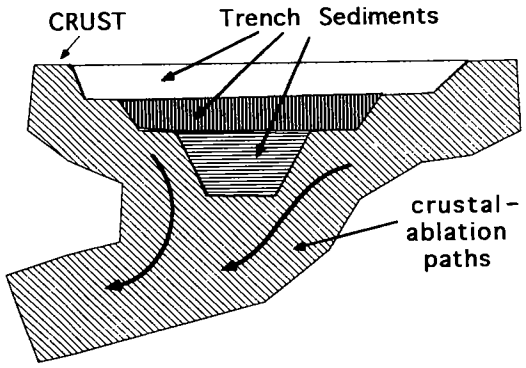


Figure 16. Illustration of crustal portion of trench and sediment fill at an instant in time. The left side represents continental crust, and the right side represents oceanic crust ablating at a more rapid rate. The downward contraction within the trench acts to force sediments out of the trench, forming the cores of thrust zones (see Fig. 17).

ment mass (or core complex) is compared to the Broken Bow uplift in the Ouachita Mountains. In an ablative model for the subduction process, the trench shifts beneath the upper crust and acts to compress sediments that are much older than any trench sediments expected to be deformed during rigid-plate subduction. Figure 17 also shows some foreland deformation (a triangle zone), associated with the crustal pull toward the trench and the compression due to the sediments' being squeezed out of the trench. Note the thickening of the continental crust toward the trench. The thicker crust, combined with the thick accumulation of sediments, can explain the large negative-gravity anomaly over the Ouachita Mountains (the largest in North America). The normal or growth faults in the Arkoma basin do not have to be related to the earlier rifting event in this area because they are now seen to be an expected part of the ablative-subduction model. The crust was being stretched toward the trench. Since there was some crowding within the trench, some compression features should develop over the trench. The triangle zone is the result of (1) the dominant compression of the sediments as they were pushed from the trench and (2) the pull on the crust toward the trench in the foreland. The triangle zone or zones may represent a transition between the dominance of these two forces.

The structures within the Arkoma basin are controlled by detachments within the weaker sedimentary units. Since the thrust zone is basically an analogue to the Midcontinent story, the rest of the paper is devoted to structural styles within the Midcontinent.

The Midcontinent—Rift-Related Structures

In this section the structural style expected for the Midcontinent, as the result of subduction-related tectonics, is discussed. Understanding these structures is the key to exploration in the Midcontinent.

Simple horizontal shortening of a bed with a detachment zone at the base of the bed is likely to produce an initial pop-up feature (Butler, 1982) of the type shown in Figure 18. As shortening continues, one of the two ramps developed begins to dominate, and a one-sided fold with a simple fault on one side is developed (see the paper by Chester and Chester, 1990, on fault-propagation folds). Some features of this model may apply to basement structures. However, there is an element to this model that is missing from most of the one-sided structures observed in the Midcontinent: the stair-stepped pattern of faults down the steep flank of an uplift.

Figure 19 illustrates the structural development and style that best characterizes Midcontinent tectonics: the fold-thrust model that Berg (1962) has used to describe the structures in the Rocky Mountains. In terms of the subduction-related ideas discussed earlier, the likelihood of folding and localized uplift is increased by the localized downward motion of the lower crust, thus creating an instabil-

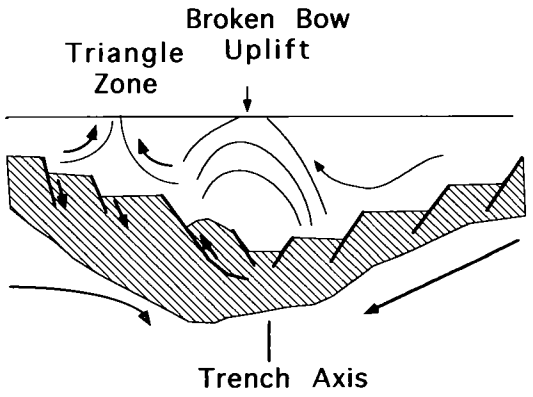


Figure 17. Illustration of the structural styles expected near the trench (continent to the left). The core complexes along the Ouachita thrusts are interpreted to be the result of sediments' being bunched over the axis of the trench. Two-sided ablation caused the trench axis to (1) move under and (2) deform sediments that were deposited long before the trench arrived on the scene. The core complexes transferred compressive stresses within the sedimentary column into the foreland. The foreland deformation within the sediments is the result of the continental crusts being pulled toward the trench; this process caused tension and normal faulting in the basement, whereas compression ruled in the sedimentary section; the result created the triangle zone. Not shown are the compressive features that must have occurred in the vicinity of the throat of the trench as a result of crustal crowding. The crustal crowding is expected to cause a thickening of the continental crust toward the trench.

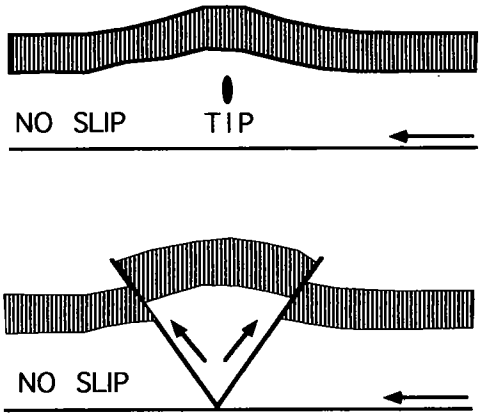


Figure 18. Pop-up structure. Simple horizontal compression along a bed with a detachment surface along the bottom is likely to form an initial pop-up structure such as the one shown (after Butler, 1982).

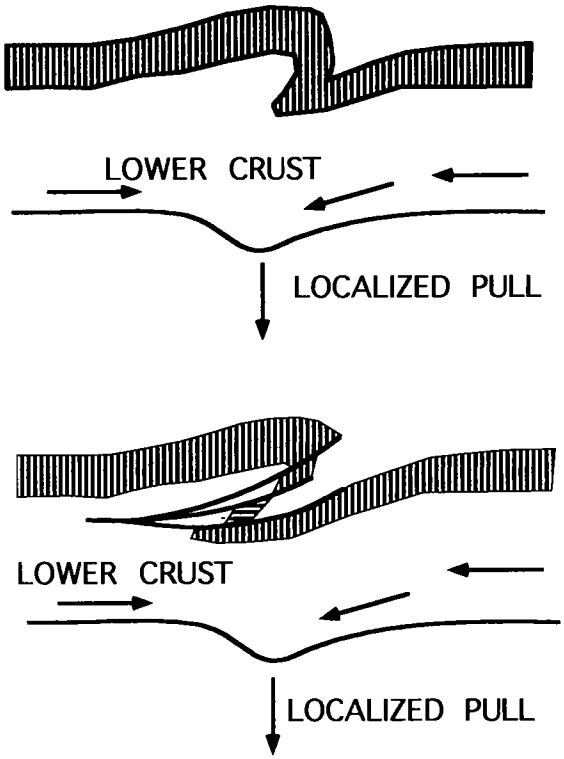


Figure 19. Fold-thrust structure. Berg (1962) wrote a classic paper defining the fold-thrust structure that develops first as an uplift and then as a fold (above). The fold is then cut by a series of thrusts (below). This figure illustrates the basic structural style of the Midcontinent: an overturned fold with stair-stepped faulting down the flank. The origin of the folding is most likely related to the localized downward movement of the lower crust. This structural style is compared to the Nemaha uplift, the Wichita Mountain uplift, and the Arbuckle uplift in the text.

ity that more easily leads to folding. As the fold matures, a series of faults develops with overturned beds along one side. Thus, what would have developed into a single fault surface, with the model shown in Figure 18, becomes a fault zone in Figure 19. This frontal fault zone is a characteristic style that appears to be associated with many of the structures formed during the Pennsylvanian—e.g., the Nemaha uplift, the Wichita Mountains, and Arbuckle Mountains.

The fold-thrust style seems to occur at all scales, which makes it an important model for exploration purposes. Exploration in these types of structures requires an understanding of where the detachments are likely to occur as the folds develop. In addition, methods of cross-section and three-dimensional balancing are required to account for changes in fold geometry associated with hidden detachment faults. One approach to balancing fold-thrust structures has been described by Spang and others (1985). Exploring these structures without any effort to account for all the parts (i.e, balancing) is asking for trouble.

SUMMARY AND CONCLUSIONS

In summary, subduction-related processes can be used to explain the Pennsylvanian tectonic history of the Midcontinent. The ablative-subduction model of Tao and O'Connell (1992) and the counterflow associated with the subduction offer an easy explanation of the timing and distribution of tectonic events. The regions most strongly affected by the counterflow usually have had a rift or intrusive history. Several mechanisms have been considered in order to explain why localized stresses develop over these regions with a prior rift history. They are all capable of producing localized compressional tectonics resulting in the type of fold-thrusts described by Berg (1962).

One of the surprising aspects of the model proposed is that there is now an explanation for why the Rockies could have been created twice in the same location. Ancestral roots of the sort described by Steeples (1982) are likely to have a long-lived effect upon the upper mantle, such as those described by Braun (1992). When subduction occurs on the borders of a continent, those areas of the continent that have the anomalous upper mantle are reactivated. The building of the Rocky Mountains in the same place twice can now be explained in terms of an anomalous mantle capable of inducing a steeper dip to the subduction zone and a strong counterflow. The counterflow produces the convective motion responsible for building mountains in the interior of a continent in the manner described by Griggs (1939).

ACKNOWLEDGMENTS

I learned much of the geologic history of Oklahoma while working on a project, funded by the

Gas Research Institute, directed toward compiling a gas atlas for the Midcontinent. Geologists working on that project who were constantly open for discussion were Robert Northcutt, Jock Campbell, and Tom Bingham. Although he has not published much of his work, W. (Bill) Brown at Baylor (no relation) has guided and directed several graduate students from whom I have learned a great deal. In a lengthy telephone conversation with Bill Brown, he told me of an ancestral lineament associated with the Rocky Mountains. This conversation, along with the observation by Denison (1995) and the paper by Braun (1992), pointed toward the ancestral influence of rifts and the potential for creating mountains twice in the same location, e.g., the Rockies. Chris Saxon and James Willis, who studied under Bill Brown at Baylor, introduced me to Berg's work on the fold-thrust model. Serving on Chris Saxon's Ph.D. thesis committee has been a learning experience, rather than one of teaching. Appreciation is expressed to Mary Eberle for her technical and editorial input to this paper.

REFERENCES CITED

Barazangi, M.; and Isacks, B. L., 1976, Spatial distribution of earthquakes and subduction of the Nazca plate beneath South America: Geology, v. 4, p. 686–692.

Berg, R. R., 1962, Mountain flank thrusting in Rocky Mountain foreland, Wyoming and Colorado: American Association of Petroleum Geologists Bulletin, v. 46, p. 2019–2032.

Bird, P., 1988, Formation of the Rocky Mountains, western United States: a continuum computer model: Science, v. 239, p. 1501–1507.

Braun, J., 1992, Postextensional mantle healing and episodic extension in the Canning basin: Journal of Geophysical Research, v. 97 (B6), p. 8927–8936.

Brown, R. L.; and Morgan, George, 1991, Aulacogen collapse: model for the compressive stage of aulacogen evolution, *in* Johnson, K. S. (ed.), Late Cambrian–Ordovician geology of the southern Midcontinent: Oklahoma Geological Survey Circular 92, p. 185–188.

Budnik, R. T., 1986, Left-lateral intraplate deformation along the Ancestral Rocky Mountains: implications for Late Paleozoic plate reconstructions: Tectonophysics, v. 132, p. 195–214.

Butler, R. W. H., 1982, The terminology of structures in thrust belts: Journal of Structural Geology, v. 4, p. 239–245.

Chester, J. S.; and Chester, F. M., 1990, Fault-propagation folds above thrusts with constant slip: Journal of Structural Geology, v. 12, p. 903–910.

Dickinson, W. R.; and Snyder, W. S., 1978, Plate tectonics of the Laramide orogeny: Geological Society of America Memoir 151, p. 355–366.

Denison, R. E., 1995 [this volume], Significance of airphotograph linears in the basement rocks of the Arbuckle Mountains, *in* Johnson, K. S. (ed.), Structural styles in the southern Midcontinent, 1992 Symposium: Oklahoma Geological Survey Circular 97, p. 119–131.

Gilbert, M. C.; and Donovan, R. N. (eds.), 1982, Geology of the eastern Wichita Mountains, southwestern Oklahoma: Oklahoma Geological Survey Guidebook 21, 160 p.

Griggs, David, 1939, A theory of mountain-building: American Journal of Science, v. 237, p. 611–650.

Johnson, K. S.; Amsden, T. W.; Denison, R. E.; Dutton, S. P.; Goldstein, A. G.; Racoe, Bailey, Jr.; Sutherland, P. K.; and Thompson, D. M., 1989, Geology of the southern Midcontinent: Oklahoma Geological Survey Special Publication 89-2, 53 p.

Kluth, C. F.; and Coney, P. J., 1981, Plate tectonics of the Ancestral Rocky Mountains: Geology, v. 9, p. 10–15.

Mallory, W. M., 1972, Regional synthesis of the Pennsylvanian System, *in* Geologic atlas of the Rocky Mountain region: Rocky Mountain Association of Geologists, Denver, p. 111–127.

McConnell, D. A., 1987, Paleozoic structural evolution of the Wichita uplift, southwest Oklahoma: Texas A&M University Ph.D. dissertation, 219 p.

Moore, G. E., 1979, Pennsylvanian paleogeography of the southern Midcontinent, *in* Hyne, N. D. (ed.), Pennsylvanian sandstones of the Mid-continent: Tulsa Geological Society Special Publication 1, p. 2–12.

Saxon, C. P., 1994, Thrust displacement transfer zone, southern Oklahoma [abstract]:American Association of Petroleum Geologists, 1994 Annual Convention Official Program, p. 25.

Spang, J. H.; Evans, J. P.; and Berg, R. R., 1985, Balanced cross sections of small fold-thrust structures: The Mountain Geologist, v. 22, p. 41–46.

Steeples, D. W., 1982, Structure of the Salina–Forest City interbasin boundary from seismic studies: UMR Journal (University of Missouri, Rolla), v. 3, p. 55–81.

Tao, W. C.; and O'Connell, R. J., 1992, Ablative subduction: a two-sided alternative to the conventional subduction model: Journal of Geophysical Research, v. 97 (B6), p. 8877–8904.

Tomlinson, C. W., 1952, Odd geologic structures of southern Oklahoma: American Association of Petroleum Geologists Bulletin, v. 36, p. 1820–1840.

Tomlinson, C. W.; and McBee, William, Jr., 1962, Pennsylvanian sediments and orogenies of Ardmore district, Oklahoma, *in* Branson, C. C. (ed.), Pennsylvanian system of the United States: American Association of Petroleum Geologists, Tulsa, v. 2, p. 461–500.

Walper, J. L., 1977, Paleozoic tectonics of the southern margin of North America: Gulf Coast Association of Geological Societies, Transactions, v. 27, p. 230–241.

Willett, S. D.; Beaumont, C.; and Fulsack, P., 1994, Subduction of Asian lithospheric mantle beneath Tibet inferred from models of continental collision: Nature, v. 369, p. 642–645.

Regional Sedimentation Patterns Associated with the Passive- to Active-Margin Transition, Ouachita Orogeny, Southern Midcontinent, U.S.A.

Paula J. Noble
The University of Texas
Austin, Texas

ABSTRACT.—Recent biostratigraphic studies have allowed for the recognition of a regionally extensive Early Mississippian hiatus, which marks the transition from passive- to active-margin sedimentation associated with the onset of the Ouachita orogeny. In the basinal-facies strata of the Ouachita orogenic belt, Radiolaria and conodonts recovered from measured sections that straddle the pre-flysch to flysch boundary show that no strata of late Kinderhookian through Osagean age are present, a period of roughly 10 m.y. (million years). The lithologic change is most commonly gradational, with few signs of erosion. The presence of glauconite and maroon shales at the horizon of the hiatus indicates that the absence of Early Mississippian strata is more likely a result of prolonged nondeposition, rather than erosion.

The Early Mississippian section is also shown to be thin to absent in the Ouachita foreland throughout parts of Texas, New Mexico, and Oklahoma, where detailed biostratigraphic control exists. On both the shelf and in the basin, early Kinderhookian- and Devonian-age strata are overlain by late Meramecian-age strata. This constrains the minimum age of shelf erosion and shows it to be coeval with the period of basin nondeposition. It should be noted that thin, discontinuous Early Mississippian strata are present in parts of central Texas and Oklahoma; however, nondeposition and erosion were the dominant sedimentary processes along the paleo-continental margin of North America during the Early Mississippian.

The onset of regional tectonic activity provides a mechanism for this regional unconformity. Whereas erosion can be caused by a relatively short-lived event, 10 m.y. of nondeposition must be explained by a long-lasting change in basin-sedimentation patterns. In the Early Mississippian, tectonic activity associated with the onset of the Ouachita orogeny may have altered bottom circulation and established contour currents, accelerated by passage through a narrow strait, which prevented sediment accumulation in the basin and on the shelf. In the Late Mississippian, increased constriction of this passage may have eventually cut off trans-equatorial bottom-water circulation, allowing for deposition to resume uniformly on both the shelf and in the basin. These data suggest that major changes in both shelf- and basin-sedimentation patterns occurred ~10 m.y. prior to the onset of flysch deposition. They also suggest that the onset of widespread Ouachita orogenic activity began at least as early as Early Mississippian.

INTRODUCTION

The Ouachita orogeny is a late Paleozoic event caused by the collision of Laurasia and Gondwana. Paleozoic basinal rocks now constituting the Ouachita orogenic belt were deformed and thrust onto the shelf margin as a result of this collision (Flawn and others, 1961). They form a sinuous, mainly subsurface belt that extends from the Big Bend region of West Texas to the Ouachita Mountains of Arkansas and Oklahoma, and eastward to the southern termination of the Appalachian Mountains. The basinal rocks are exposed only in the Marathon and Solitario uplifts of West Texas, and in the Ouachita Mountains (Fig. 1).

The Ouachita orogeny dramatically changed the depositional regime along the southern paleo-continental margin of North America. From the Cambrian through earliest Mississippian, this margin existed as a rifted passive margin (Arbenz, 1989) with slowly accumulating limestone, shale, and chert. As a result of Late Paleozoic orogenic activity, sedimentation rates increased by more than an order of magnitude over the slow accumulation rates of the preceding 200 m.y. (McBride, 1989) and thick progradational packages of flysch rapidly

Noble P. J., 1995, Regional sedimentation patterns associated with the passive- to active-margin transition, Ouachita orogeny, southern Midcontinent, *in* Johnson, K. S. (ed.), Structural styles in the southern Midcontinent, 1992 symposium: Oklahoma Geological Survey Circular 97, p. 99–112.

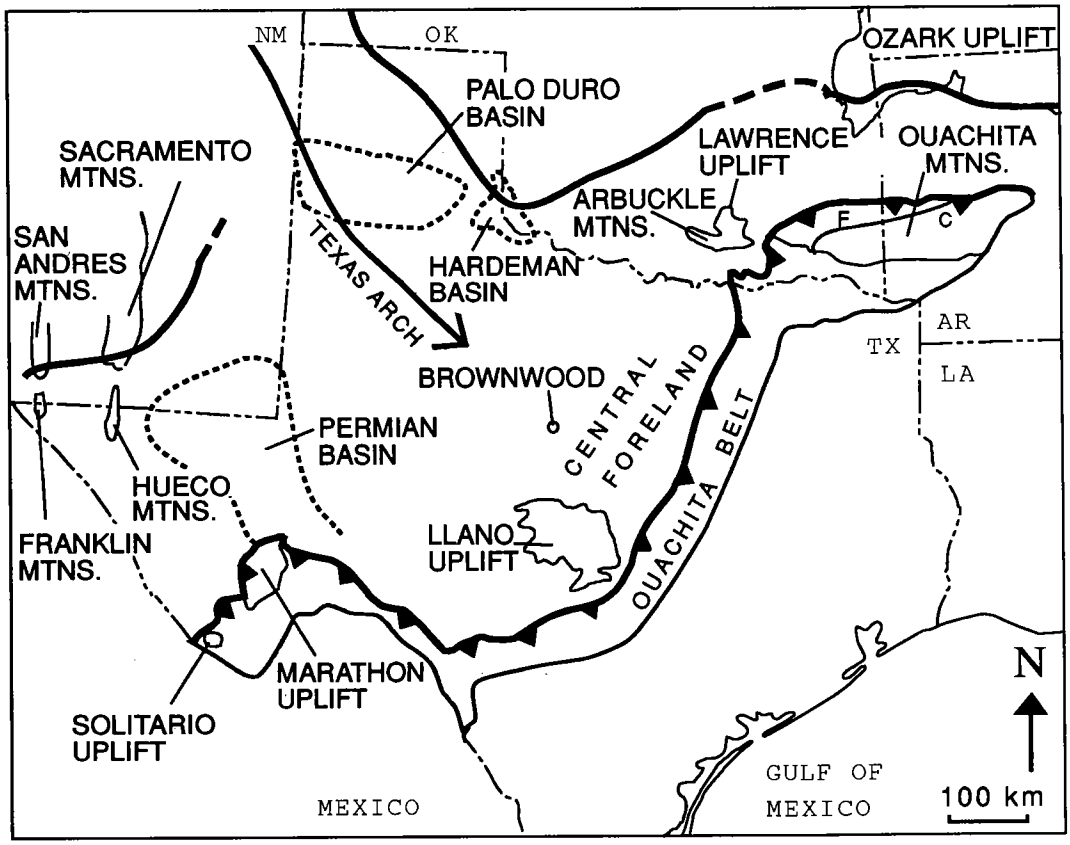


Figure 1. Locality map showing major geographic provinces referred to in the text. Thin solid lines surround surface features and outcrop areas referred to in the text. Black dotted lines surround subsurface areas referred to in the text. Heavy black line delineates boundary between the Ouachita foreland region and the region with Osagean deposits >5 m thick.

filled the Ouachita trough and foreland basins. The pre-flysch to flysch transition rocks are highly condensed biosiliceous units which are commonly devoid of most fossils traditionally employed for biostratigraphy. However, they contain abundant Radiolaria, which have recently proven useful for high-resolution biostratigraphy (Jones and Murchey, 1986). Radiolarian and conodont biostratigraphy, combined with detailed field sedimentology, have provided a wealth of information concerning the onset of Ouachita deformation and the accompanying changes in sedimentation patterns.

Recent biostratigraphic studies employing conodonts and Radiolaria show that the passive- to active-margin transition was marked by a prolonged period of nondeposition or extremely slow sediment accumulation. In the Ouachita orogenic belt, a regional hiatus equivalent to much of the Early Mississippian, a period of roughly 10 m.y., is recognized (Cheng, 1986; Noble, 1990,1992). This hiatus corresponds to a period of erosion, nondeposition, or extremely slow sediment accumulation coeval throughout the Ouachita foreland in Texas, New Mexico, and southeastern Oklahoma (Fig. 2) (Wilson, 1975; Ruppel and Lemmer, 1986; Schwartzapfel, 1990; Haywa-Branch and Barrick, 1990). This regional Early Mississippian unconformity was previously unrecognized, because it commonly occurs in gradational sections of shale with no erosional signature. Until recently, the biostratigraphic control in these sections was not sufficiently detailed to allow for its recognition.

Improved biostratigraphic control and recognition of an Early Mississippian unconformity at the pre-flysch to flysch transition has significance to the regional geology for the following reasons:

1) Sections of Ouachita foreland strata once thought to be Osagean (late Early Mississippian) in age are actually younger, indicating that there was substantially less sediment accumulation along the southern paleocontinental margin of North America during the Early Mississippian than previously thought. In light of these new data, it is necessary to reevaluate existing interpretations of the Early Mississippian depositional history in the southern Midcontinent.

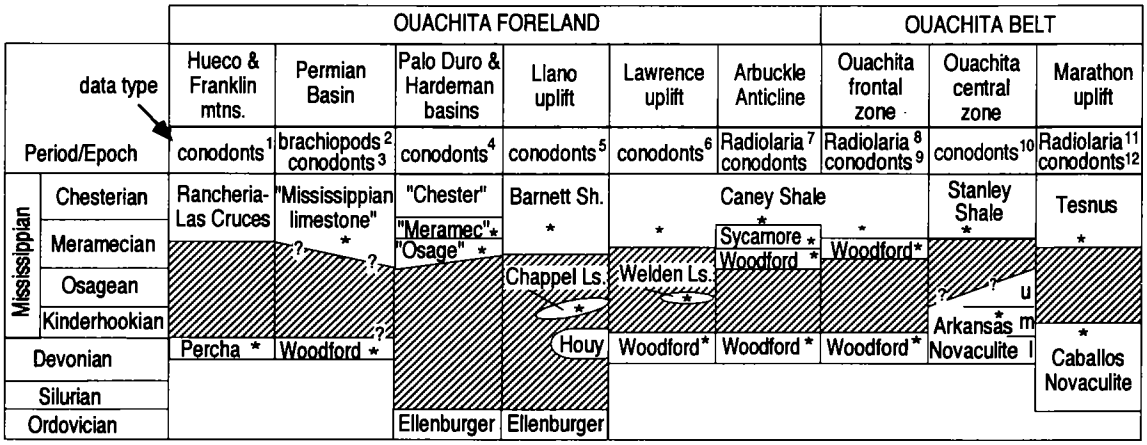


Figure 2. Correlation of lithostratigraphic units that straddle the pre-flysch to flysch transition in the Ouachita orogenic belt and foreland. Detailed biostratigraphy of these units reveals an Early Mississippian unconformity. Asterisk (*) denotes units with biostratigraphic control based on conodonts or Radiolaria, as discussed in text. Patterned areas = missing strata. Superscripts = sources of biostratigraphic data: (1) Lane, 1975; (2) Lloyd, 1949; (3) Ellison, 1950; (4) Ruppel and Lemmer, 1986; (5) Hoyle, 1978; Ellison, 1989; (6) Haywa-Branch and Barrick, 1990; (7) Schwartzapfel, 1990; (8) Cheng, 1986; (9) Hass and Huddle, 1965; (10) Hass, 1951; (11) Noble, 1990; (12) Barrick, 1987; Ellison and Powell, 1989. Age control for Ellenburger is not discussed in text, but is well established as Ordovician with invertebrate fossils (Barnes and others, 1959).

2) The hiatus is interpreted as the first widespread effect of tectonic activity and pushes the age of the onset of Ouachita deformation back at least 10 m.y. prior to the onset of flysch deposition.

3) Regionally extensive nondeposition may be explained by changes in basin circulation and the subsequent closing of a trans-equatorial seaway caused by the collision of Laurasia and Gondwana. A model is presented which attempts to relate this hiatus to the governing tectonic and paleoceanographic parameters.

STRATIGRAPHY

To facilitate discussion, the southern Midcontinent region is subdivided into three provinces (Fig. 1): the Ouachita orogenic belt, the Ouachita foreland, and regions of significant (>5 m) Osagean deposits. Although the Texas Panhandle is several hundred kilometers from the Ouachita orogenic belt, it is included herein as part of the foreland region because its Mississippian sedimentation patterns are the same as on parts of the shelf closer to the Ouachita belt. A summary of the stratigraphic data in each region is discussed in the following sections, and particular emphasis is placed on chronostratigraphic interpretations published in the past six years.

Ouachita Orogenic Belt

Marathon Uplift, West Texas

The Caballos Novaculite, a radiolarian and sponge-spicule chert, is the youngest of the pre-flysch units. It grades upward into the fine-grained flysch of the lower Tesnus Formation (Figs. 2,3). King (1937) speculated that the Caballos/Tesnus boundary may be unconformable and that most of the Mississippian is not represented in the Marathon uplift. Subsequent workers have interpreted the boundary to be conformable because erosional signs, such as conglomerates, are rare, and the lithologic change is most commonly gradational (McBride and Thomson, 1970). However, conodont and radiolarian biostratigraphy across the boundary between these units confirms King's speculation. Within an apparently conformable sequence of siliceous shale (Fig. 3), Radiolaria equivalent to the *Albaillella* 2a through *Albaillella* 3 zone are absent (Noble, 1990), and the basal Tesnus beds contain lag deposits of Late Mississippian-age conodonts (Ellison, 1987) (Fig. 4). The hiatus is equivalent to much of the Early Mississippian. In two of the studied sections that straddle the boundary, the sampling resolution is <1 m, leaving little doubt that late Kinderhookian- through Osagean-age strata are absent.

Three of the four Marathon uplift sections studied (Fig. 3) grade from chert to siliceous mudstone with no visible signs of erosion. The only visible evidence that suggests a break in sedimentation at these localities is a 20-cm to 6-m interval of maroon shale directly underlying the horizon of the hiatus. This shale may represent a zone that was oxidized through prolonged exposure to bottom waters. It is interpreted to be analogous to slowly accumulating red clays in the abyssal regions of modern oceans, and it indicates extremely slow accumulation as opposed to erosion (McBride and Thomson, 1970). At one locality (Monument Creek), the upper meters

of the Caballos Formation have been eroded and Frasnian (early Late Devonian) chert is unconformably overlain by Meramecian shale.

Other interesting features that may have a relationship to the transition from passive- to active-margin sedimentation occur in the western basin margin, the area closest to the North American paleo-continental shelf. At several localities, Late Devonian to Early Mississippian strata are thin or absent (Barrick, 1987; Noble, 1990). Locally, in the Payne Hills, an olistostrome directly underlies the hiatus (Noble 1990) (Fig. 3). The interpreted transport direction for the olistoliths is southward, off the North American shelf margin (McBride, 1978). Local destabilization of the shelf edge and basin margin could have deposited the olistoliths and stripped off some of the Late Devonian sediments, indicating that Ouachita-related tectonic activity may have started as early as Late Devonian–earliest Mississippian.

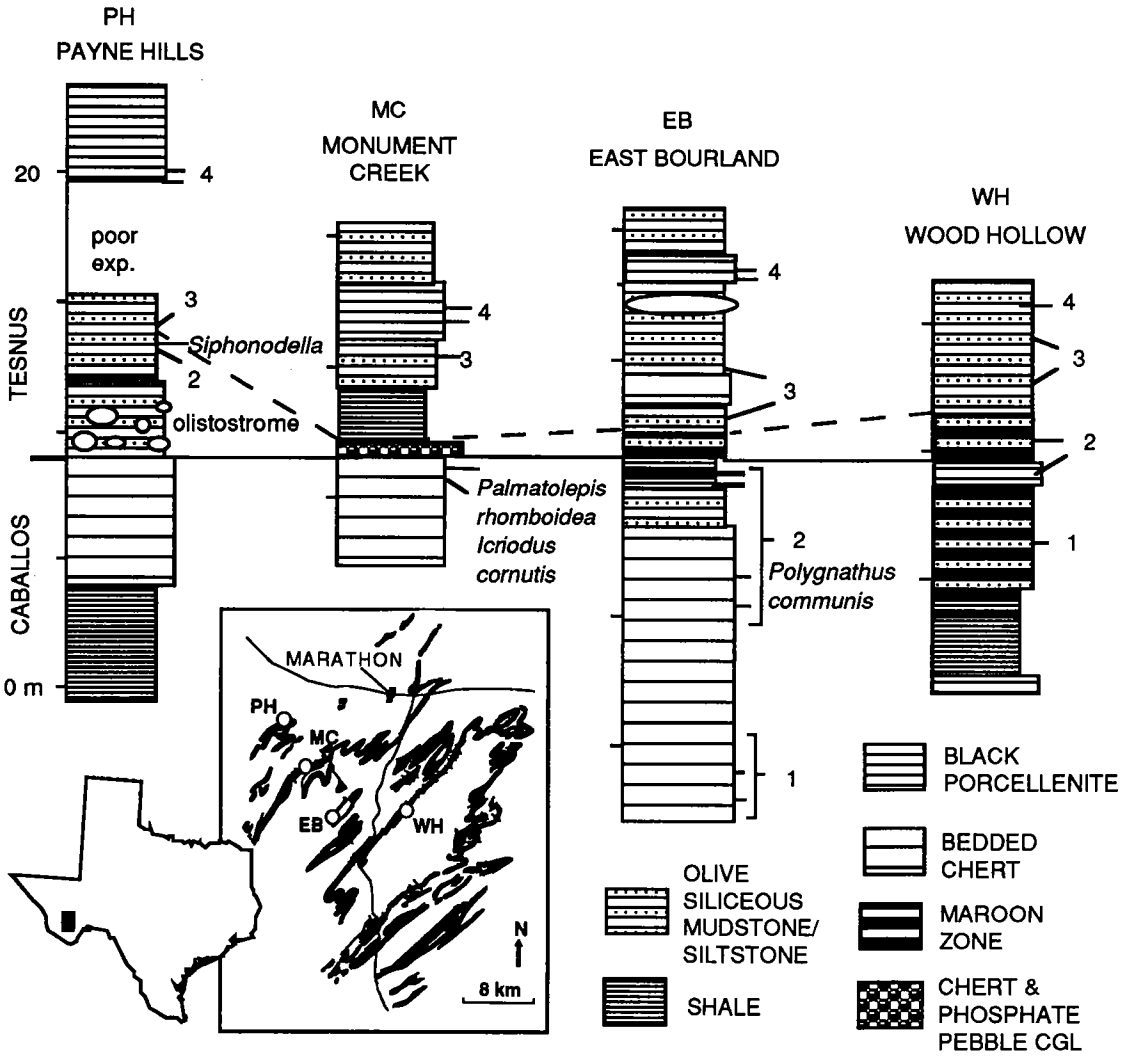


Figure 3. Measured sections across the Caballos/Tesnus boundary, showing lithology and location of fossil sample horizons (modified from Noble, 1992). Numbers 1–4 correspond to the local radiolarian zones (Noble, 1990). Datum (solid line) is the contact between the Caballos and Tesnus Formations. See Figure 5 for the chronostratigraphic calibration of the local radiolarian zones. Dashed line marks horizon of hiatus between local radiolarian zones 2 and 3. At Monument Creek, an unconformity is present; Late Devonian chert is unconformably overlain by Late Mississippian siliceous mudstone. Inset map (after King, 1937) shows the outcrop pattern of the Caballos Novaculite (black) and locations of sections in the Marathon uplift.

Ouachita Frontal Zone, Oklahoma

Cheng (1986) sampled the Woodford Formation at the Turnpike section (Fig. 4), near Pinetop, Oklahoma, for Radiolaria, and recognized a hiatus equivalent in magnitude to the one recognized in the Marathon uplift (Fig. 5). He recovered a late Meramecian fauna containing *Albaillella cartalla* from the base of a green shale in the upper Woodford, 1 m above an early Kinderhookian fauna that includes *Huasha* spp. and *Protoalbaillella* spp. Cheng's Kinderhookian fauna was collected from a horizon 0.4 m below the conodont horizon 21910-PC of Hass and Huddle (1965), which yielded Kinderhookian conodonts, including *Siphonodella duplicata.*

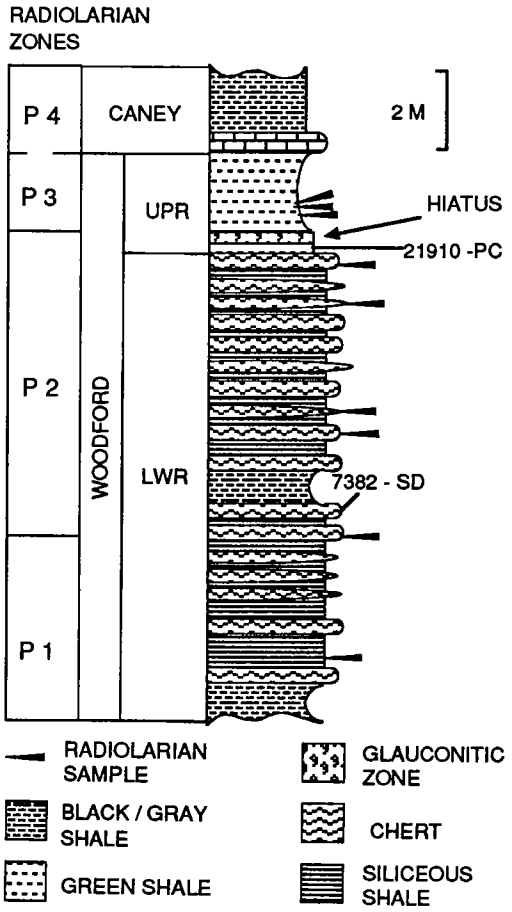


Figure 4. Measured section across the Woodford/ Caney boundary at the Turnpike section near Pinetop, Oklahoma (after Cheng, 1986) showing distribution of local radiolarian zones. See Figure 5 for chronostratigraphic calibration of these zones. Location of this section (labeled "Pinetop") is shown on inset map of Figure 6. Sample numbers 21910-PC and 7382-SD refer to conodont samples of Hass and Huddle (1965).

The lithologic contact between the upper and lower parts of the Woodford is described as a change from black, phosphatic siliceous shale to greenish-gray shale. Cheng describes a 15-cm-thick glauconite zone between his samples at the hiatus horizon. Glauconite and phosphate are commonly found on nondeposition surfaces and in condensed sections (Goldman, 1922; Odin and Fullagar, 1988), and their presence is consistent with the interpretation that the absence of Early Mississippian strata are a result of an extended period of nondeposition, rather than erosion.

Central Ouachita Mountains

The presence and extent of a hiatus in the central Ouachita Mountains cannot be confirmed at this point, due to the lack of chronostratigraphic control. The pre-flysch and early flysch equivalent units in the central Ouachitas are the Arkansas Novaculite and the overlying Stanley Shale (Fig. 2). The boundary between these formations is gradational over several meters (Hass, 1951). The basal 4 m of the Stanley has been dated at various localities as late Meramecian, based on conodonts and Radiolaria (Hass, 1956; Cheng, 1986). The underlying novaculite is not well dated. At Caddo gap, Kinderhookian conodonts recovered from the middle division of the Arkansas Novaculite, ~9 m below the Stanley contact, led Hass (1951,1956) to suggest that the upper division is Osagean. No age-diagnostic fossils have been recovered from the upper division to confirm this. Hass (1951) described a small conodont fauna from a sample collected from the upper division, but it contained *Gnathodus*, *Hindeodella*, and several bar-like genera, none of which are restricted to the Osagean. Further biostratigraphic work is needed to determine if Osagean strata are actually present in the upper part of the Arkansas Novaculite, and, if so, how regionally extensive they are.

Ouachita Foreland

Arbuckle Mountains, Oklahoma

The pre-flysch equivalent in the Arbuckle Mountains is the Woodford Shale, a siliceous phosphatic shale, which is overlain by the Sycamore Limestone (Fig. 2). A hiatus equivalent to the one in the Ouachita orogenic belt is recognized within the Woodford (Schwartzapfel ,1990) that locally coincides with a glauconitic interval several meters below the contact with the Sycamore Limestone (Fig. 5). Schwartzapfel (1990) recovered Kinderhookian Radiolaria from below the glauconitic interval, and Radiolaria no older than latest Osagean (*Latentifistula* [Scharfenbergia] *plenospongiosa*) from directly above the interval (Fig. 6). In Schwartzapfel's measured section on the southern flank of the anticline, the glauconitic interval is thicker and the sampling resolution is ~6 m. However, in his north-

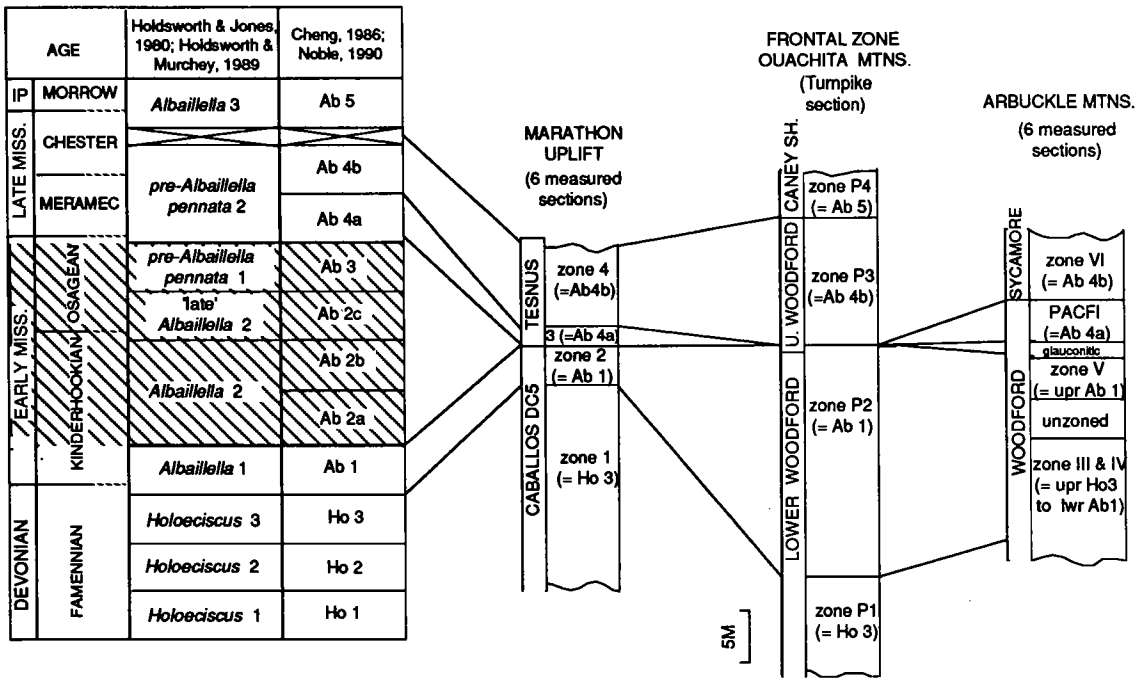


Figure 5. Correlation of local radiolarian zones from the Marathon uplift, Ouachita frontal zone, and Arbuckle Mountains to established radiolarian zonal schemes. Zonal abbreviations in text follow those of Cheng (1986). Ruled area on left represents radiolarian zones missing at hiatus. Data from Noble (1990), Cheng (1986), and Schwartzapfel (1990).

ern-flank section, the sampling resolution is ~60 cm. The overlying Sycamore Limestone is well dated as late Meramecian–Chesterian based on conodonts and Radiolaria (Schwartzapfel, 1990). Osagean conodonts were identified in the Sycamore Limestone (Ormiston and Lane, 1976), but were later shown to be in rip-up clasts (Schwartzapfel, 1990). Glauconite associated with the hiatus indicates nondeposition at the Arbuckle localities, yet the presence of Osagean rip-up clasts in the Sycamore Limestone is significant, as it indicates that there was active erosion of Osagean sediments in the region.

Lawrence Uplift, Oklahoma

The Welden Limestone, a 1- to 1.5-m-thick fossiliferous wackestone, contains the only Osagean documented in the region (Haywa-Branch and Barrick, 1990). Stratigraphically, it occurs between the Woodford Shale and the Caney Shale. The outcrop forms a thin belt which can be traced along strike over a distance of no more than 8 km before it pinches out (Decker and others, 1931). Osagean strata are absent throughout the remainder of the Lawrence uplift. Shaley or limey beds of the late Meramecian Caney Shale directly overlie the uppermost beds of Kinderhookian Woodford Shale (Over and Barrick, 1990).

Central Texas Foreland

The Devonian through Mississippian section in the central Texas foreland is a thin (≤5 m) condensed sequence of chert, shale, and limestone which lies unconformably on the Ordovician Ellenburger Group (Fig. 2). In the Llano uplift, the entire Devonian is represented by chert, siliceous phosphatic shales, and cherty carbonates of the Houy and Stribling Formations (Cloud and others, 1957). The Early Mississippian is represented by the Chappel Limestone, a crinoidal packstone, ranging from 20 cm to 14 m thick, which is overlain by the Meramecian Barnett Shale (Hoyle, 1978; Ellison, 1989). The Chappel is thin and discontinuous and commonly rests unconformably on the Ellenburger Group. In the subsurface to the north of the Llano uplift, the Chappel is extremely condensed. In cores recovered near Brownwood, Texas, a 70-cm to 3.5-cm-thick Chappel Limestone interval contains three conodont zones calibrated as late Kinderhookian through early Osagean (Fig. 7) (Hoyle, 1978). Reworked Ordovician–Devonian conodonts are present in zone 1 (*Siphonodella cooperi* zone), indicating pre-Mississippian erosion. The abundance of reworked conodonts decreases in zones 2 and 3, both of Osagean age (Hoyle, 1978), indicating that these thin zones (locally as thin as 2 cm) are condensed zones representing extremely low-accumulation

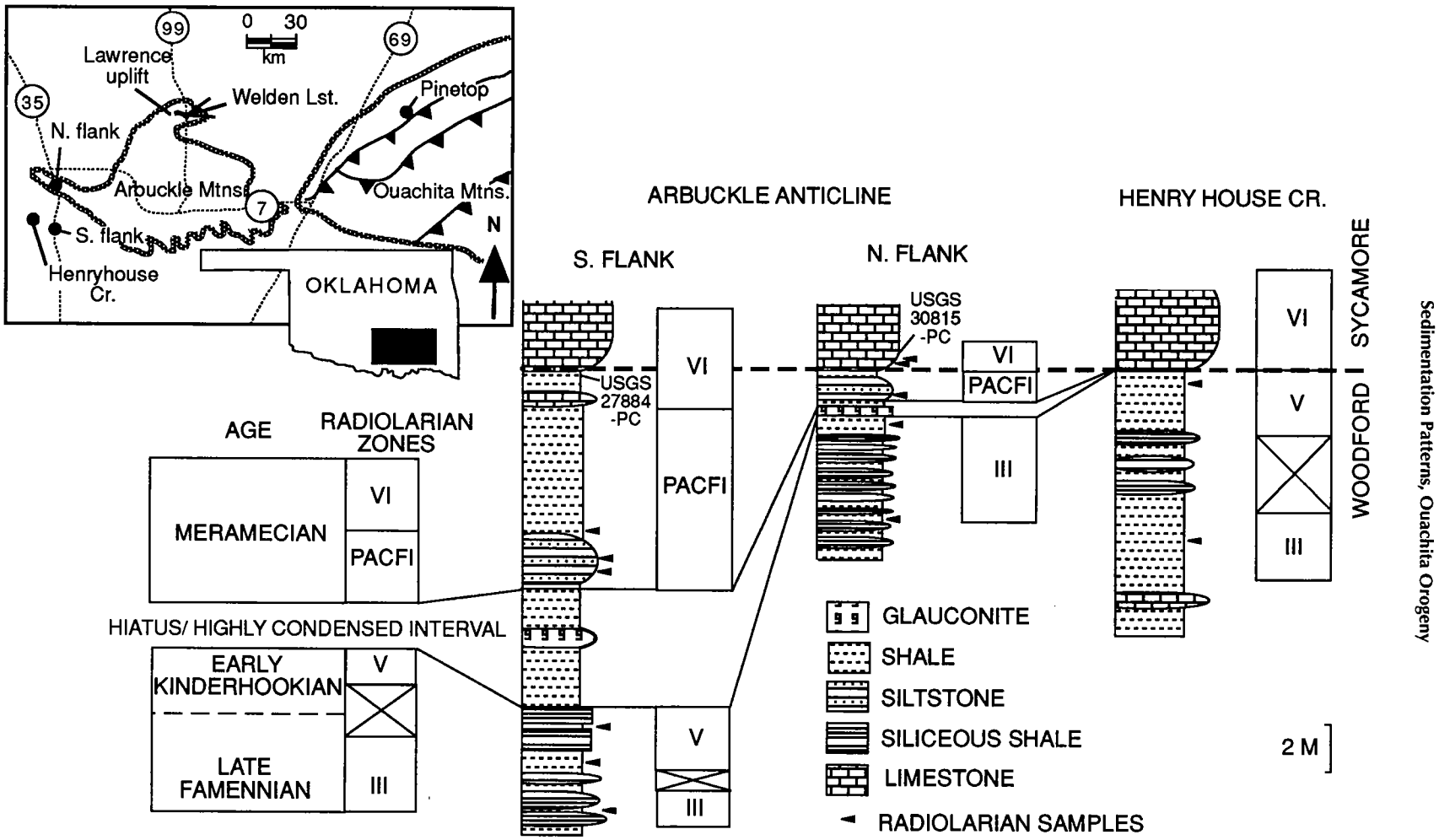


Figure 6. Measured sections across the Woodford/Sycamore boundary in the Arbuckle Mountains, showing lithology and distribution of local radiolarian zones (III, V, VI) (after Schwartzapfel, 1990). Samples 27884-PC and 30815-PC are conodont samples reported to contain *Cavusgnathus* spp. See Schwartzapfel (1990) for a more detailed discussion of the conodont and radiolarian faunas.

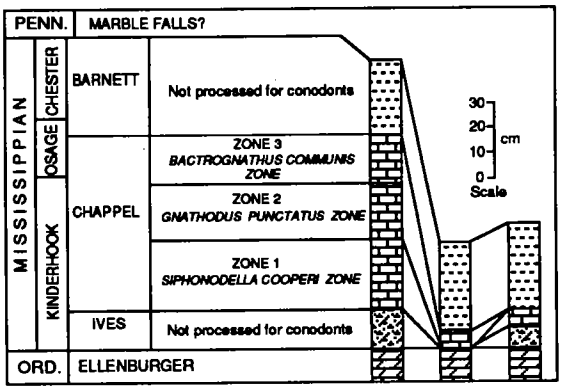


Figure 7. Mississippian conodont occurrences from cores in Brown County, Texas. After Hoyle (1978) and Ellison (1989).

rates with little erosion and reworking of older sediments during Osagean time.

Palo Duro and Hardeman Basins, Texas Panhandle

Ruppel and Lemmer (1986) describe late Meramecian conodonts from the cherty limestones of the "Osage group," which unconformably overlies the Ordovician Ellenburger Group (Figs. 2,8). Their conclusion was that Mississippian deposition did not begin until the late Meramecian in all but the northern extremes of the Palo Duro and Hardeman basins. Their study has great significance, as it provides some of the first chronostratigraphic control of Mississippian subsurface units in West Texas. Prior to their study, all units were correlated on the basis of lithostratigraphy, and their ages inferred from lithologic similarity to the Mississippi Valley deposits. The absence of Osagean rocks in the subsurface of the southern Texas Panhandle suggest that there may be considerably less Osagean strata present in other parts of the subsurface of north and West Texas (Ruppel and Lemmer, 1986).

Permian Basin, Texas and New Mexico

Most of the Mississippian strata of the Permian basin are in the subsurface; however, many of the units can be studied in outcrop in the Hueco and Franklin Mountains located to the west. Here, the Rancheria or Las Cruces Formation rests unconformably on the Devonian Percha Formation (Wilson, 1975; Lane, 1975). Conodonts recovered from the Rancheria and Las Cruces are interpreted to be no older than late Osagean (Lane, 1975). In the subsurface, biostratigraphic resolution of Mississippian strata is poor. The Late Devonian Percha Shale or Woodford Shale is interpreted to be overlain disconformably by Meramecian-age "Mississippian limestone" (Comer, 1991). The Meramecian age is based on the presence of *Leiorhynchus carboniferum*, a Meramecian brachiopod, found ~37 m above the contact with the Woodford Shale in a well in southern Lea County, New Mexico (Lloyd, 1949). Ellison (1950) described Late Devonian conodonts from the middle unit of the Woodford, but was unsuccessful in recovering conodonts from the upper unit. Although no Early Mississippian strata have been identified in the Permian basin subsurface, biostratigraphic control is sparse and Early Mississippian strata may be present in either the upper part of the Woodford or in the basal section of the "Mississippian limestone." As in the central Ouachita Mountains, more work is needed to conclusively determine if Early Mississippian strata are present.

Extent of Osagean Deposition in the Southern Midcontinent

The southernmost extent of significant Osagean deposits can be traced from the southern San Andres and Sacramento Mountains, New Mexico, through the Anadarko basin to the southern Ozark uplift (Fig. 9). The Lake Valley Group comprises the Osagean units in the New Mexico region (Kottlowski, 1975; Wilson, 1975). It reaches a maximum thickness of 75 m, pinches out to the south, and is absent in the Hueco and Franklin Mountains (Wilson, 1975). Osagean strata are reported in the subsurface of the Anadarko basin and in the northern part of the Hardeman basin, just south of the Amarillo uplift (Ruppel, 1985; Lane and De Keyser, 1980). In the Ozark uplift, the Osagean is represented by the Boone Group, consisting of the St. Joe, Reeds Spring, and Keokuk Formations. The Boone Group pinches out along the southern flank of the Ozark uplift, and the overlying Moorefield Formation unconformably overlies the Late Devonian–early Kinderhookian Chattanooga Shale (Huffman, 1958).

The thinning of Early Mississippian strata in the southern part of the Ozark uplift is a result of slow accumulation, rather than erosion. Nine conodont zones, calibrated as mid-Kinderhookian through

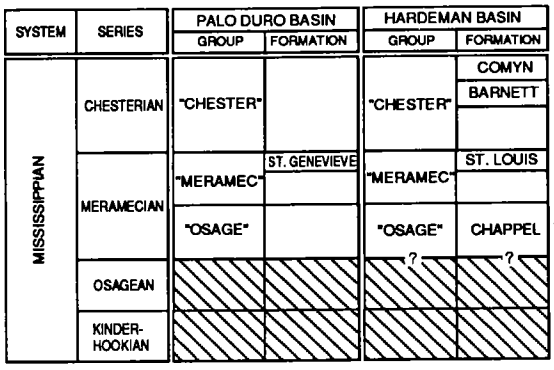


Figure 8. Revised Mississippian stratigraphy in the Palo Duro and Hardeman basins. Osagean rocks may be present in the eastern Hardeman basin. From Ruppel (1985).

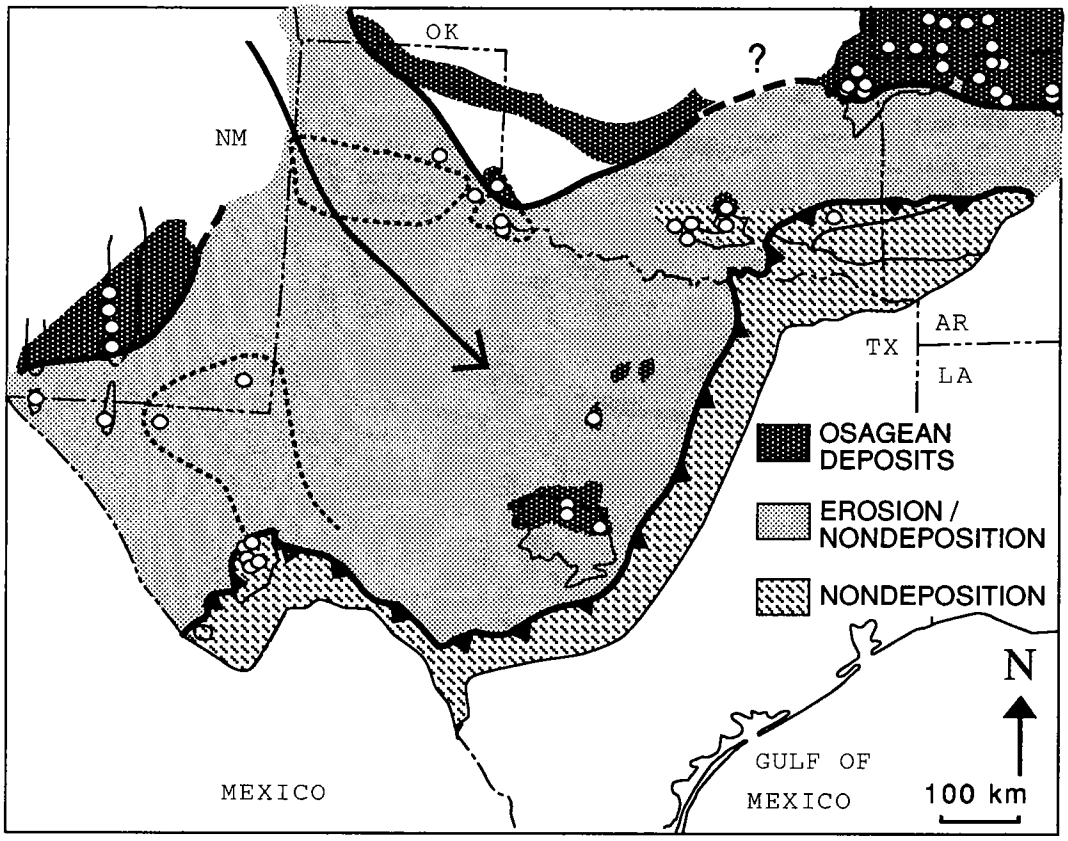


Figure 9. Map showing interpreted distribution of depositional patterns during the Osagean. Heavy black line represents southern limit of significant Osagean deposits >5 m thick. South and east of this line, erosion and nondeposition were the dominant processes. White circles show locations of biostratigraphic data referred to in text. Depositional patterns are interpreted from these data and from data synthesized in Huffman (1958), Thompson and Fellows (1969), Wilson (1975), Craig and others (1979), Lane and De Keyser (1980), Gutschick and Sandberg (1983), and Comer (1991).

late Osagean, are recognized in the Ozark uplift (Thomson and Fellows, 1969). No early Kinderhookian strata are recognized and the mid-Kinderhookian Bachelor Sandstone disconformably overlies the Chattanooga Shale. The lower eight conodont zones (*S. sandbergi–S. duplicata* through *Gnathodus bulbosus* zones) occur in the Bachelor Sandstone and overlying St. Joe Limestone, and are condensed into <1 m of section along the southern flank of the uplift in Cherokee County, Oklahoma (Thomson and Fellows, 1969). This indicates extremely slow accumulation rates along the southern flank of the Ozark uplift until late Osagean time.

Stratigraphic Summary

Biostratigraphic data show that little or no deposition occurred in the Ouachita orogenic belt and Ouachita foreland during mid-Kinderhookian through late Osagean time (*Siphonodella lobata–S. crenulata* through *Taphrognathus varians–Apatognathus* conodont zones of Collinson and others [1971], and Radiolaria of the *Albaillella* 2a through *Albaillella* 3 zone of Holdsworth, as summarized in Cheng [1986]). In light of these data, the southern limit of Osagean strata deposits >5 m thick is farther to the north and west than had been indicated by previous stratigraphic syntheses (i.e., Craig and others,1979; Lane and De Keyser, 1980; Gutschick and Sandberg, 1983) (Fig. 9). All areas to the south and east of this line are interpreted to be areas where erosion and nondeposition were the dominant processes.

In the Ouachita belt, nondeposition is interpreted to have been the dominant process based on three major lines of evidence: (1) The hiatus occurs in a gradational sequence of siliceous chert and shale with no physical signs of erosion. (2) Maroon shale or glauconite at the horizon of the hiatus indicates nondeposition or extremely slow accumulation as opposed to erosion. (3) The regularity in the age of the underlying surface; four out of five sec-

tions in the Ouachita belt have a thin, 1–2-m layer of early Kinderhookian strata preserved below the disconformity. If the hiatus were caused by erosion, more variation in the age of the units directly below the disconformity would seem likely.

Both nondeposition and active erosion are interpreted to have occurred on the shelf. Nondeposition, or extremely slow accumulation, is indicated locally by (1) the glauconitic interval associated with an Early Mississippian hiatus in the Arbuckle Mountains, (2) the highly condensed section of Osagean Chappel Limestone near Brownwood, Texas, and (3) the highly condensed Boone Group along the southern flank of the Ozark uplift. Active erosion on the shelf is indicated by the presence of Osagean rip-up clasts in the overlying Sycamore Limestone, reworked conodonts in Hoyle's zone 1 of the Chappel Limestone, and the patchy distribution and irregular thickness of the Chappel Limestone. The Chappel commonly rests unconformably on the Ellenburger Group, filling sinkholes and local paleo-topographic depressions. Crossbedding and sorting indicate that the Chappel may represent storm deposits or current-swept sediments which accumulated in local depressions near the strandline (Hoyle, 1978). In the Texas Panhandle, late Meramecian strata unconformably rest on Ordovician platform carbonates. However, the overlying Meramecian strata can only constrain the minimum age of erosion. It is not clear how much of the post-Ordovician strata may have been eroded prior to the Early Mississippian.

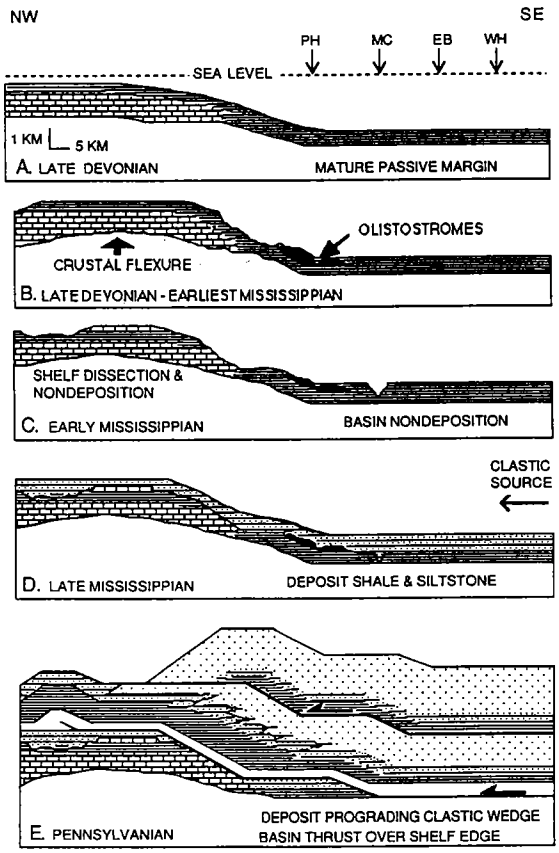


Figure 10. Schematic shelf-to-basin cross sections reconstructing the sequence of events leading up to the Ouachita orogeny, based on data from the Marathon uplift. PH, MC, EB, and WH are four localities shown in Figure 3. See text for a detailed explanation.

RECONSTRUCTION OF EVENTS

The improved chronostratigraphic control in both the Ouachita orogenic belt and the Ouachita foreland allow for a more precise reconstruction of events leading up to the Ouachita orogeny. Schematic shelf-to-basin profiles showing the sequence of events (Fig. 10) are based largely on the data from the Marathon uplift, yet these profiles can be used to illustrate shelf-to-basin events from the Arbuckle Mountains to the Ouachita Mountains.

Stage 1 (Late Devonian).—Siliceous biogenous sediments were deposited in the basin and on much of the shelf (Fig. 10A). These sediments formed the chert and siliceous shales of the upper Caballos and Arkansas Novaculites, and the Woodford and Percha Shales.

Stage 2 (latest Devonian through Kinderhookian).—The first manifestations of tectonic activity caused local destabilization of the shelf edge and slope, resulting in deposition of olistostromes in the Marathon uplift and local erosion on the shelf and in the basin (McBride, 1978) (Fig. 10B). Slope destabilization can be attributed to an increased slope grade caused by crustal flexure, such as proposed during the Cretaceous in Oman (Robertson, 1987).

Stage 3 (Osagean–Meramecian).—Sedimentary bypass was the dominant process throughout the Ouachita basin, with possible local buildup of winnowed siliceous ooze (novaculite) in the Arkansas region. Currents scoured the outer shelf, allowing for thin local buildups of reworked skeletal packstone (Fig. 10C).

Stage 4 (late Mississippian).—Deposition resumed throughout the region, covering the shelf and the basin with shale and limestone (Fig. 10D).

Stage 5 (Pennsylvanian–Early Permian).—Thick packages of clastic sediment prograded into the basin. Basinal sequences were, in turn, folded and thrusted onto the continental margin into the configuration seen today (Fig. 10E).

This reconstruction raises two questions which need further explanation. First, what processes could account for such a prolonged period of nondeposition? There is strong evidence that there was widespread nondeposition throughout parts of the shelf and basin for ~10 m.y. Whereas an unconformity produced by erosion can be caused by a relatively short-lived event, an unconformity pro-

duced by nondeposition requires a long-lived mechanism. The absence of Osagean strata in the basin is particularly puzzling because there is evidence for active erosion and scouring of the shelf during this time. One would expect that eroded shelf sediments would be redeposited in the basin. Instead, there is a hiatus. Second, why did deposition resume throughout the shelf and the basin in the Meramecian after such a prolonged period of nondeposition? Late Meramecian shales consistently overlie the unconformity throughout the shelf and basin. A mechanism is proposed in the following section which attempts to address these questions in a regional tectonic and paleoceanographic context.

PALEOGEOGRAPHIC AND PALEOCEANOGRAPHIC HISTORY

Late Paleozoic paleogeographic reconstructions depict the convergence of two major land masses, Laurasia and Gondwana (Fig. 11A). In the earliest Mississippian, the southern paleo-continental margin of North America delineated the northern boundary of a trans-equatorial passage connecting the Iapetus and Panthalassic seas. The convergence of Laurasia and Gondwana closed off the trans-equatorial passage in the Late Carboniferous, forming a series of borderland basins which filled with clastic sediments that were subsequently overlain by Permian carbonates and evaporites.

The late Paleozoic paleoceanographic history can be summarized as a change from open-ocean circulation in the Late Devonian–earliest Mississippian to increasingly restricted circulation resulting in compartmentalization of the shelf margin throughout the remainder of the Paleozoic. Although our ability to resolve the basin geometry from paleogeographic models is still limited, the initial restriction of open-marine circulation must have occurred during the Mississippian, prior to the compartmentalization of the continental margin into borderland basins during the Pennsylvanian (Ross, 1978,1986; Wuellner and others, 1986).

I propose that Early Mississippian compression, caused by the onset of Ouachita deformation, al-

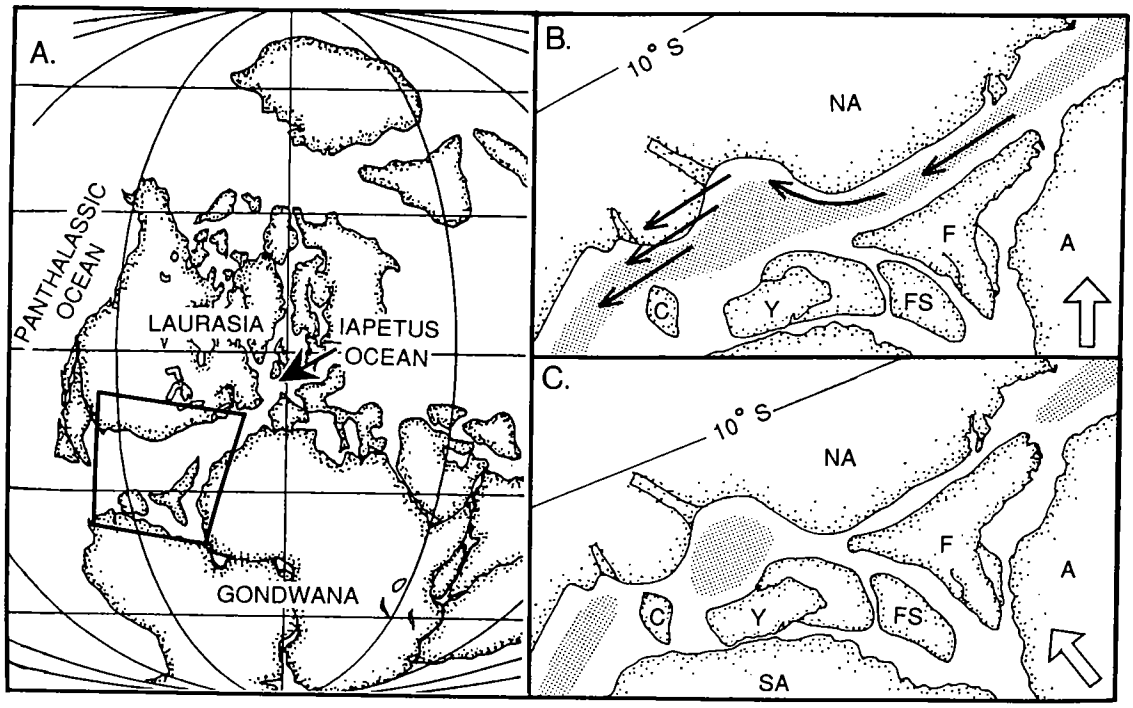


Figure 11. Paleogeographic reconstructions for Late Devonian through Late Mississippian time. (*A*) General reconstruction showing configuration of continents at the end of the Late Devonian (after Scotese and McKerrow, 1990). Boxed area shows location of maps *B* and *C*. (*B*) Onset of tectonic activity constricts seaway, establishing contour currents and allowing for sedimentary bypass. (*C*) Increased constriction cuts off bottom circulation, allowing deposition to resume uniformly. Shaded area = bathymetric lows; black arrows = bottom-current pathways; white arrows = direction of plate movement; NA = North America; C = Coahuila platform; F = Florida block; FS = Florida straits block; Y = Yucatan block; A = Africa; SA = South America. Maps *B* and *C* are modified from the Alleghenian reconstruction of Pindell (1985), using the kinematic model of Sacks and Secor (1990) to reconstruct plate positions in the Mississippian.

tered bottom-circulation patterns by narrowing the trans-equatorial passage. Stricture of the trans-equatorial passage may have increased the velocity of bottom currents circulating throughout the Ouachita trough, and may have established contour currents across the shelf in the central Texas foreland (Fig. 11B). The Late Mississippian lag concentrates in the basal Tesnus Formation and Chappel Limestone are interpreted to be a result of density-driven currents (Ellison, 1987). Similar lag concentrates in Late Devonian beds of the Canutillo Formation in the Hueco Mountains, and the Houy Formation of the Llano uplift, indicate that density-driven currents were acting locally on the shelf prior to the Early Mississippian (Ellison, 1987). The widespread establishment of high-velocity bottom currents would provide a long-term mechanism for preventing the accumulation of sediments on a regional scale. In the Late Mississippian, increased restriction and blockage of the trans-equatorial passageway would have eventually cut off bottom-water circulation, allowing for deposition to resume uniformly on both the shelf and in the basin (Fig. 11C).

Prolonged marine hiatuses of 3 m.y. or longer have been shown to develop in paths or regions of significant bottom-current movement and can be associated with tectonically controlled closing of major seaways (Moore and others, 1978; Keller and Barron, 1984). For example, dramatic changes in circulation patterns are associated with the emergence of the Isthmus of Panama in the late Cenozoic (Keller and Barron, 1984). Initial uplift of Central America deflected preexisting circulation patterns, generating an increased frequency and magnitude of hiatuses in the regions of maximum constriction. Progressive silling of this passage cut off the high-velocity bottom currents, isolated the basins, and established Recent sedimentation patterns.

Hiatuses produced by bottom-current activity may show few physical signs. Lag deposits, or contourites, are commonly considered to be physical evidence of hiatuses produced in this fashion (Stow and Lovell, 1979). However, in regions that were extremely sediment starved, or that lacked any coarse-grained component, lag deposits are not always found (Oczlon, 1990). Contour currents have played a more significant role in preventing sediment accumulation, rather than actively eroding sediment or reworking it into contourites (Barusseau, 1979). Oczlon (1990) describes a hiatus in Middle Devonian shales throughout Europe and North Africa which he attributes to the establishment of the Northern Gondwana boundary current. He notes the presence of lag deposits or contourites in only a few areas. Commonly, there are no physical signs of erosion or nondeposition associated with the hiatus. The lack of contourites or scarcity of lag deposits associated with a regional unconformity therefore does not preclude the possibility of its formation by contour currents.

CONCLUSIONS

1. Biostratigraphic data published over the past six years indicates that substantially less early Mississippian strata were deposited throughout Texas and southern Oklahoma than had been suspected. These studies have shown that units once considered to be Osagean are, in fact, younger. This implies that subsurface units in adjacent areas of West Texas may also lack Osagean strata.

2. A regional unconformity occurs at the passive- to active-margin transition and is interpreted to be evidence of widespread Early Mississippian tectonic activity. This pushes back the onset of Ouachita deformation to at least 10 m.y. before the onset of flysch deposition.

3. Alteration of bottom-circulation patterns and increased bottom-current velocities may explain the prolonged episode of nondeposition in the basin that occurred during the Early Mississippian erosional phase on the shelf. Increased velocities are attributed to increased constriction of the trans-equatorial passageway connecting the Iapetus and Panthalassic seas during the collision of Laurasia and Gondwana.

4. A change in sedimentation patterns allowed a blanket of Late Meramecian strata to be deposited uniformly both on the shelf and in the basin. This change in sedimentation patterns may be explained by the compartmentalization of the continental margin by formation of synorogenic foreland basins which progressively blocked the trans-equatorial passageway. High-velocity bottom-water currents would have been cut off, and deposition would have resumed on the shelf and in the basin.

ACKNOWLEDGMENTS

This study was funded by grants from the Geological Society of America, Sigma Xi, Gulf Coast Association of Geological Societies, and the Geology Foundation at The University of Texas at Austin. Thanks to Jim Hayne and Ike Roberts, of the Paisano Cattle Co., and Gage Holland and Ann and Mark Daugherty, of the Gage Ranch, for graciously allowing access for field studies. This manuscript was improved by helpful discussions and reviews by P. Carpenter, M. Cloos, R. L. Folk, M. B. Lagoe, E. F. McBride, and W. R. Muehlberger. Thanks to Laura Brock who assisted me in the field and P. Carpenter who assisted with drafting the text figures.

REFERENCES CITED

Arbenz, J. K., 1989, The Ouachita system, *in* Bally, A. W.; and Palmer, A. R. (eds.), The geology of North America—an overview: Geological Society of America, Boulder, The Geology of North America, v. A, p. 371–396.

Barrick, J. E., 1987, Conodont biostratigraphy of the Caballos Novaculite (Early Devonian–Early Mississippian), northwestern Marathon uplift, West

Texas, *in* Austin, R. L. (ed.), Conodonts: investigative techniques and applications; British micropaleontology series: John Wiley and Sons, New York, p. 120–135.

Barnes, V. E.; Cloud, P. E., Jr.; Dixon, L. P.; Folk, R. L.; Jonas, E. C.; Palmer, A. R.; and Tynan, E. J., 1959, Stratigraphy of the pre-Simpson Paleozoic subsurface rocks of Texas and southeast New Mexico: University of Texas, Austin, Bureau of Economic Geology Publication 5924, v. 1, 294 p.

Barusseau, J. P., 1979, Le role geologique des courants profonds: Oceanis, v. 5, p. 735–752.

Cheng, Y. N., 1986, Taxonomic studies on Upper Paleozoic Radiolaria: National Museum of Natural History Special Publication 1, Taiwan, R.O.C., 311 p.

Cloud, P. E., Jr.; Barnes, V. E.; and Hass, W. H., 1957, Devonian–Mississippian transition in central Texas: Geological Society of America Bulletin, v. 68, p. 807–816.

Collinson, C.; Rexroad, C. B.; and Thompson, T. L., 1971, Conodont zonation of the North American Mississippian: Geological Society of America Memoir 127, p. 353–394.

Comer, J. B., 1991, Stratigraphic analysis of the Upper Devonian Woodford Formation, Permian basin, West Texas and southeastern New Mexico: University of Texas, Austin, Bureau of Economic Geology Report of Investigations 201, 63 p.

Craig, L. C.; Connor, C. W., and others, 1979, Paleotectonic investigations of the Mississippian System in the United States: U.S. Geological Survey Professional Paper 1010, parts I–III, 559 p., 15 pls.

Decker, C. E.; Cooper, C. L.; and McGehee, R., 1931, Geological map of the Arbuckle Mountains, Oklahoma [Plate 1], *in* Decker, C. E.; and Merritt, C. A. (eds.), The stratigraphy and physical characteristics of the Simpson Group: Oklahoma Geological Survey Bulletin 55, 112 p.

Ellison, S. P., Jr., 1950, Subsurface Woodford black shale, West Texas and southeast New Mexico: University of Texas, Austin, Bureau of Economic Geology Report of Investigations 7, 20 p.

_____ 1987, Examples of Devonian and Mississippian conodont lag concentrates from Texas, *in* Austin, R. L. (ed.), Conodonts: investigative techniques and applications; British micropaleontology series: John Wiley and Sons, New York, p. 77–93.

_____ 1989, Mississippian conodont zonations, central Texas, *in* Geology of Mississippian carbonates in north-central Texas: Fort Worth Geological Society and Texas Christian University Symposium, p. 57–65.

Ellison, S. P., Jr.; and Powell, J. D., 1989, Tesnus (Mississippian) conodonts, Brewster County, Texas: Courier Forsh.-Inst. Senkenberg, v. 117, p. 359–373.

Flawn, P. T.; Goldstein, A.; King, P. B.; and Weaver, C. E., 1961, The Ouachita System: University of Texas Publication 6120, 401 p.

Goldman, M. I., 1922, Basal glauconite and phosphate beds: Science, v. 56, p. 171–173.

Gutschick, R. C.; and Sandberg, C. A., 1983, Mississippian continental margins of the conterminous United States, *in* Stanley, D. J.; and Moore, G. T. (eds.), The shelfbreak: critical interface on continental margins: Society of Economic Paleontologists and Mineralogists Special Publication 33, p. 79–96.

Hass, W. H., 1951, The Arkansas Novaculite: American Association of Petroleum Geologists Bulletin, v. 35, p. 2525–2541.

_____ 1956, Conodonts from the Arkansas Novaculite, Stanley Shale, and Jackfork Sandstone: Ardmore Geological Society Guidebook for Ouachita Mountains field conference, p. 25–33.

Hass, W. H.; and Huddle J. W., 1965, Late Devonian and early Mississippian age of the Woodford Shale in Oklahoma, as determined from conodonts: U.S. Geological Survey Professional Paper 525-D, p. D125–D132.

Haywa-Branch, J. N.; and Barrick, J. E., 1990, Conodont biostratigraphy of the Welden Limestone (Osagean, Mississippian), Lawrence uplift, southern Oklahoma, *in* Ritter, S. M. (ed.), Early to Middle Paleozoic conodont biostratigraphy of the Arbuckle Mountains, southern Oklahoma: Oklahoma Geological Survey Guidebook 27, p. 75–84.

Holdsworth, B. K.; and Jones, D. L., 1980, Preliminary radiolarian zonation for Late Devonian through Permian time: Geology, v. 8, p. 281–285.

Holdsworth, B. K.; and Murchey, B. L., 1989, Paleozoic radiolarian biostratigraphy of the northern Brooks Range, Alaska: U.S. Geological Survey Professional Paper 1399, p. 777–797.

Hoyle, B. L., 1978, Lower Mississippian conodont biostratigraphy of the Chappel Limestone, central Texas and Welden Limestone, southern Oklahoma: University of Texas, Austin, unpublished M.A. thesis, 290 p.

Huffman, G. G., 1958, Geology of the flanks of the Ozark uplift, northeastern Oklahoma: Oklahoma Geological Survey Bulletin 77, 281 p.

Jones, D. L.; and Murchey, B., 1986, Geologic significance of Paleozoic and Mesozoic radiolarian chert: Annual Revue of Earth and Planetary Science, v. 14, p. 455–492.

Keller, G.; and Barron, J. A., 1984, Paleoceanographic implications of Miocene deep-sea hiatuses: Geological Society of America Bulletin, v. 94, p. 590–613.

King, P. B., 1937, Geology of the Marathon region, Texas: U.S. Geological Survey Professional Paper 187, 148 p.

Kottlowski, F. E., 1975, Mississippian strata of the San Andres Mountains, *in* Pray, L. C. (ed.), Mississippian shelf-edge and basin facies carbonates, Sacramento Mountains and southern New Mexico region: Dallas Geological Society Guidebook, p. 119–123.

Lane, R., 1975, Correlation of the Mississippian rocks of southern New Mexico and West Texas using conodonts, *in* Pray, L. C. (ed.), Mississippian shelf-edge and basin facies carbonates, Sacramento Mountains and southern New Mexico region: Dallas Geological Society Guidebook, p. 87–98.

Lane, H. R.; and De Keyser, T. L., 1980, Paleogeography of the late early Mississippian (Tournaisian 3) in the central and southwestern United States, *in* Fouch, T. D.; and Magathan, E. R. (eds.), Paleozoic paleogeography of the west-central United States,

Rocky Mountain paleogeography symposium 1: Society of Economic Paleontologists and Mineralogists, Rocky Mountain Section, Denver, p. 149–162.

Lloyd, E. R., 1949, Pre-San Andres stratigraphy and oil-producing zones in southeastern New Mexico: New Mexico Bureau of Mines and Mineral Resources Bulletin 29, 87 p.

McBride, E. F., 1978, Olistostrome in the Tesnus Formation (Mississippian–Pennsylvanian), Payne Hills, Marathon region, Texas: Geological Society of America Bulletin, v. 89, p. 1550–1558.

_____ 1989, Stratigraphy and sedimentary history of pre-Permian Paleozoic rocks of the Marathon uplift, *in* Hatcher, R. D., Jr.; Thomas, W. A.; and Viele, G. W. (eds.), The Appalachian–Ouachita orogen in the United States: Geological Society of America, Boulder, The Geology of North America, v. F-2, p. 603–620.

McBride, E. F.; and Thomson, A., 1970, The Caballos Novaculite, Marathon region, Texas: Geological Society of America Special Paper 22, 129 p.

Moore, T. C., Jr.; van Andel, Tj. H.; Sancetta, C.; and Psias, N., 1978, Cenozoic hiatuses in marine sediments: Micropaleontology, v. 24, p. 113–138.

Noble, P. J., 1990, Radiolarian biostratigraphy: evidence for an early Mississippian basin-wide hiatus at the Caballos–Tesnus boundary, Marathon basin, Texas, *in* Laroche, T. M.; and Higgins, L. (eds.), Marathon thrust belt: structure, stratigraphy, and hydrocarbon potential: West Texas Geological Society and Society of Economic Paleontologists and Mineralogists, Permian Basin Section, Field Seminar, Midland, Texas, May 10–12, 1990, p. 83–91.

Noble, P. J., 1992, Biostratigraphy of the Caballos Novaculite–Tesnus Formation boundary, Marathon basin, Texas: Palaeogeography, palaeoclimatology, paleoecology, v. 96, p. 141–153.

Oczlon, M. S., 1990, Ocean currents and unconformities: the North Gondwana Middle Devonian: Geology, v. 18, p. 509–512.

Odin, G. S.; and Fullagar, P. D., 1988, Geological significance of the glaucony facies, *in* Odin, G. S. (ed.), Green marine clays: developments in sedimentology: Elsevier, Amsterdam, v. 45, p. 295–332.

Ormiston, A. R.; and Lane, H. R., 1976, A unique radiolarian fauna from the Sycamore Limestone (Mississippian) and its biostratigraphic significance: Palaeontographica, Abteilung, v. 154, p. 158–180.

Over, D. J.; and Barrick, J. E., 1990, The Devonian/Carboniferous boundary in the Woodford Shale, Lawrence uplift, south-central Oklahoma, *in* Ritter, S. M. (ed.), Early to Middle Paleozoic conodont biostratigraphy of the Arbuckle Mountains, southern Oklahoma: Oklahoma Geological Survey Guidebook 27, p. 63–74.

Pindell, J. L., 1985, Alleghenian reconstruction and subsequent evolution of the Gulf of Mexico, Bahamas, and proto-Caribbean: Tectonics, v. 4, p. 1–39.

Robertson, A., 1987, The transition from a passive margin to an Upper Cretaceous foreland basin related to ophiolite emplacement in the Oman Mountains: Geological Society of America Bulletin, v. 99, p. 633–653.

Ross, C. A., 1978, Late Pennsylvanian and Early Permian sedimentary rocks and tectonic setting of the Marathon geosyncline, *in* Mazzullo, S. J. (ed.), Tectonics and Paleozoic facies in the Marathon geosyncline, West Texas: Society of Economic Paleontologists and Mineralogists, Permian Basin Section, Field Conference Guidebook 78-17, p. 89–94.

_____ 1986, Paleozoic evolution of southern margin of Permian basin: Geological Society of America Bulletin, v. 97, p. 536–554.

Ruppel, S. C., 1985, Stratigraphy and petroleum potential of pre-Pennsylvanian rocks, Palo Duro basin, Texas Panhandle: University of Texas, Austin, Bureau of Economic Geology Report of Investigations 147, 81 p.

Ruppel, S. C.; and Lemmer, T. C., 1986, Mississippian conodonts from the southern Texas Panhandle: University of Texas, Austin, Bureau of Economic Geology Circular 86-7, 36 p.

Sacks, P. E.; and Secor, D. T., Jr., 1990, Kinematics of Late Paleozoic continental collision between Laurentia and Gondwana: Science, v. 250, p. 1702–1705.

Schwartzapfel, J. A., 1990, Biostratigraphic investigations of Late Paleozoic (Upper Devonian to Mississippian) Radiolaria within the Arbuckle Mountains and Ardmore basin of south-central Oklahoma: University of Texas, Dallas, unpublished Ph.D. dissertation, 475 p.

Scotese, C. R.; and McKerrow, W. S., 1990, Revised World maps and introduction, *in* McKerrow, W. S.; and Scotese, C. R. (eds.), Palaeozoic palaeogeography and biogeography: Geological Society of London Memoir 12, p. 1–21.

Stow, D. A. V.; and Lovell, J. P. B., 1979, Contourites: their recognition in modern and ancient sediments: Earth Science Reviews, v. 14, p. 251–291.

Thompson, T. L.; and Fellows, L. D., 1969, Stratigraphy and conodont biostratigraphy of Kinderhookian and Osagean rocks of southwestern Missouri and adjacent areas: Missouri Geological Survey and Water Resources Report of Investigations 45, 261 p.

Wilson, J. L., 1975, Regional Mississippian facies thickness in southern New Mexico and Chihuahua, *in* Pray, L. C. (ed.), Mississippian shelf-edge and basin facies carbonates, Sacramento Mountains and southern New Mexico region: Dallas Geological Society Guidebook, p. 124–128.

Wuellner, D. E.; Lehtonen, L. R.; and James, W. C., 1986, Sedimentary-tectonic development of the Marathon and Val Verde basins, West Texas, U.S.A.: a Permo–Carboniferous migrating foredeep: International Association of Sedimentologists Special Publications, v. 8, p. 347–368.

Inversion Model for the Structural Style of the Arbuckle Region

Bryan Tapp
University of Tulsa
Tulsa, Oklahoma

ABSTRACT.—The structural style of the Arbuckle region is controversial. The region contains a wide range of structures that have been used to support structural models, including pure compression, pure strike slip, transpression, and polyphase deformation. Detailed field and subsurface analysis provide data supporting an alternative interpretation for the structural style of the region. These data suggest that the region is a partially inverted asymmetric half-graben. Inversion took place in left-lateral transpression. All of the inconsistencies that have caused the controversies of the past fit into the new model of the region. The evidence for inversion includes such disparate features as the allochthonous nature of the northern limb of the Arbuckle anticline, and the Cumberland–Ravia nappe. These features are interpreted as a rollover anticline, and as a room-accommodation backthrust that formed in positive inversion. Previous models are flawed in that they do not fit all of the data preserved in the field area. The contractional inversion model provides the best-fit model for the various structures seen in the area.

INTRODUCTION

The structural style of the Arbuckle Mountain area has been the topic of heated debate over the past 50+ years. Much of the reason for the debate is the abundance of seemingly inconsistent structural features in both outcrops and the subsurface. These include wrench-related positive flower structures (Tapp, 1991b), and low-angle thrusts and "rabbit ear" anticlines exposed in road cuts on I-35 (Brown and others, 1985; Tapp, 1991c). Other inconsistencies include thrusts in the Southwest Davis field, overthrusting of the northern limb of the Arbuckle anticline on the Washita Valley fault in the vicinity of the West Timbered Hills, while the Washita Valley fault is nearly vertical along the southern boundary of the Tishomingo uplift. While showing evidence of thrusting, the Washita Valley fault also shows irrefutable evidence of left-lateral strike-slip motion, offsetting strata of the Simpson Group as much as 64 km (Tanner, 1967), and the Hunton Group by as much as 32 km (Carter, 1979). The subsurface of the Ardmore basin does not add data that serve to resolve the inconsistency; rather, the subsurface of the Ardmore basin shows thrust-nappe development along the Cumberland–Ravia trend, where thrusting is to the south, and thrust development along the Criner–Overbrook trend, with thrusting to the north.

These inconsistencies of structural style have resulted in proposal of a variety of models—pure strike-slip deformation, pure compressional thrusting, polyphase episodes of strike slip and compression, and transpression—to interpret the geological and tectonic history of the Arbuckle region. Several authors have suggested strike-slip offset as the dominant mode of deformation in the Arbuckle region. The strike-slip interpretation is based on a variety of field data, including orientation of folds and secondary faults in the uplift relative to the master through-going faults, orientation and slip directions of slickensides, and offset of stratigraphic units (Tanner, 1967; Wickham and Dennison, 1978; Wiltse, 1973; Carter, 1979; Booth, 1981; Haas, 1981). Compressional models proposed are based on subsurface data, and on the interpretation of surface features as regional through-going thrusts and "rabbit ear" anticlines (Brown, 1984; Brown and others, 1985). Transpressional models suggested are based on regional basinal analysis (Brewer and others, 1983; Granath, 1988), and a polyphase interpretation is based on calcite twin lamellae in the Wapanucka Limestone (Islam and Nielsen, 1984). Recent seismic and drilling data suggest that the Arbuckle complex is, at least in part, allochthonous. These models use a combination of outcrop, subsurface, and some strain data, but do not incorporate all aspects of the regional geology. Each model can explain the structures in a local region, but, to date, no single model has satisfactorily resolved all of the inconsistencies of structural style into a simple geologic and tectonic history.

Tapp, Bryan, 1995, Inversion model for the structural style of the Arbuckle region, *in* Johnson, K. S. (ed.), Structural styles in the southern Midcontinent, 1992 symposium: Oklahoma Geological Survey Circular 97, p. 113–118.

The purpose of the investigations presented in this paper was to determine whether the variety of structures in the Arbuckle uplift and Ardmore basin could be explained by a simple geologic model. The process of developing a model requires evaluation of all geological factors that could influence, or control, the structural style. The following interdependent factors affect structural style of any area. (1) The original basin geometry, including the presence and configuration (or absence) of basin-bounding faults, controls not only sediment distribution and supply, but also the types and locations of structures that develop during deformation. (2) During the deformation process, the load geometry will strongly affect the localization of structures and the regional structural style. The types of loading geometries that can produce structures seen in the Arbuckle region include pure compression, pure strike slip, and transpression. (3) A significant factor that is often ignored in the formulation of structural models is the characteristics of the rock package that is being deformed. Mechanical stratigraphy of a region will strongly affect the localization of structures, and, to a lesser degree, can affect the development of structures that are characteristic of particular structural styles. (4) The structural style can vary significantly, depending on whether the dominant deformation mechanism is brittle or ductile.

Any model describing the structural style of the region is incomplete if it does not incorporate all aspects of the deformation. To my knowledge, no model proposed to explain the geologic/tectonic history of the Arbuckle region has considered all of the above points. In this paper I examine all aspects of the historical development of the region in an attempt to formulate a simple geologic model that satisfies all of the data available, both in the field, at the surface, and in the subsurface. To that end, investigations into the deformation mechanism(s) that acted to accumulate the strain preserved in the area, fracture-orientation studies, and a subsurface study on the basinal history of the area are used to formulate an alternative model for the structural style of the Arbuckle region.

DOMINANT DEFORMATION MECHANISM

In structural analysis, it is imperative to determine what deformation mechanisms acted during the formation of the structures seen in the field. The dominant mode of deformation will control, to a large degree, the style of structures, and, to a lesser degree, the variety of structures that develop in a region. The mode of deformation can range from purely brittle to purely ductile, with a continuum between of hybrid modes of deformation. The determination of deformation mode hinges largely on the recognition of deformation-induced rock fabrics. The mechanical stratigraphy of the Arbuckle region is dominated by thick, competent carbonate units separated by thinner shales and sandstones. To determine the dominant mode of deformation, more than 250 oriented samples were collected on traverses that crossed perpendicular to the Washita Valley fault. Samples were collected from all of the rock units in the Arbuckle uplift area, including basement rocks of the Tishomingo blocks and upward through the section into the Sycamore Formation. The samples were oriented relative to the fault, and cut on three orthogonal planes with the primary plane being parallel to the plane of the fault. The results of the investigation into the dominant deformation mechanisms have been reported before (Tapp, 1991a) and are here only briefly summarized.

The dominant mechanism of deformation is brittle. All units in the area show deformation fabrics at the crystalline scale that are characteristic of brittle, cataclastic failure. The carbonates of the Arbuckle Group, Viola, Hunton, and Sycamore are extensively fractured at both macroscopic and microscopic scales. At the microscopic scale, the carbonates deformed by a combination of cataclastic failure, microcracking, and pressure solution. Basement rocks in the Tishomingo blocks deformed primarily by cataclastic failure and microcracking. Simpson sandstones deformed primarily by microcracking and macroscopic fracture. Deformation of the Woodford Shale was largely by microcracking and macroscopic fracture. The results of the study on deformation mode of the major stratigraphic units in the Arbuckle region support the conclusion that all of the strain was accumulated through brittle processes, with some pressure solution and only minor twinning. The results suggest that the structures seen in the field and in the subsurface developed in the brittle field, eliminating any interpretation of the structures as ductile-domain features. For example, as a consequence, folding in the area was accomplished by brittle flexural slip rather than flexural flow or ductile buckling. This result significantly narrows the interpretation of the origin of several structures seen in outcrop in the Arbuckle uplift.

FRACTURE DATA

Fracture orientations were measured along seven traverses across the Washita Valley fault. The orientation of each fracture within a 1-m-square area was measured at stations that were 30 m apart along each traverse. These data are shown in Figure 1 in the form of unweighted azimuthal diagram of numbers of fractures measured per orientation. Only one entry was made for each fracture orientation at each field location. The similarity of the fracture-orientation data strongly suggest that the major component of deformation in this region is strike slip rather than being compressional to the expected Reidel fracture pattern for simple shear (Fig. 1). The field character of the fractures also fits

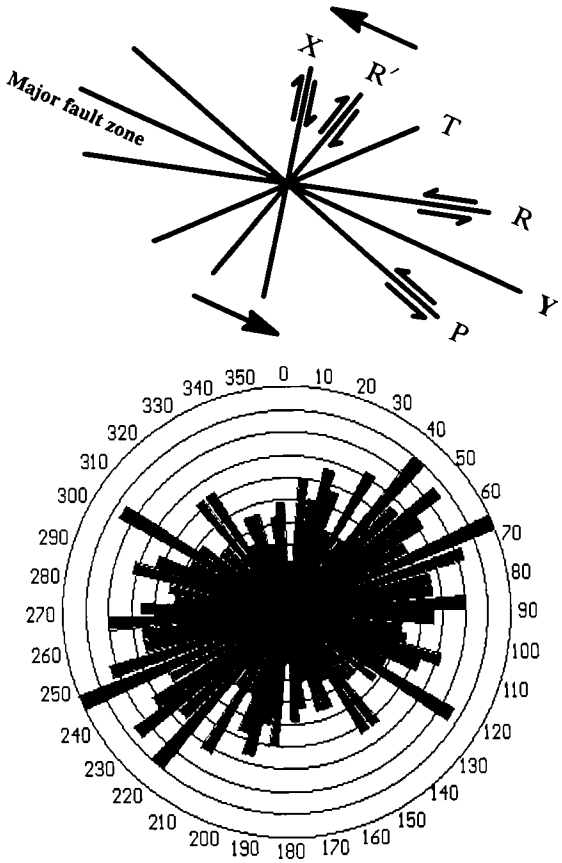


Figure 1. Comparison of unweighted azimuthal plot (below) of all fracture data collected on four traverses across the Washita Valley fault to Reidel shear pattern (above) expected for left-lateral strike-slip deformation. The fracture data are in right-hand-rule azimuth orientation. The Reidel shear pattern is after Bartlett and others (1981), where Y is the fault zone, R is the Reidel shear, R′ is the conjugate Riedel shear, T is the extensional fracture orientation, and X is a high-angle shear fracture.

within the general character of strike-slip related fractures. The shear sets of fractures in most cases had slickensides, and most were healed with calcite. Very few fracture sets were open in the field; although T-direction fractures are dominant in the open-fracture dataset. Fracture sets that correspond to R, R′, and P usually have associated stylolites or solution activity along the fractures. Timing of these fractures cannot be interpreted from the field data, and cannot be compared with the idealized relative timing of the Riedel model.

In addition, fracture-density was studied from samples collected on one traverse using the counting technique of Hilliard (1968). Fracture intersections were counted for at least six concentric circles on each orthogonal face of a sample, where the faces are parallel with the Washita Valley fault, vertical and perpendicular to the fault, and horizontal. The fracture-density data show, as expected, a marked increase in fracture density approaching the Washita Valley fault, but also point out several associated shear zones that were identified in the field (Tapp, 1991a). Removal of data from the fault zone and from the associated shear zones reveals that the fracture density in the southern block is greater than in the northern block of the Arbuckle uplift (Tapp, 1991a). The difference in density seems to indicate that the associated shear zones subdivided the region into distinct strain systems.

BASINAL GEOMETRY

Recent studies in the subsurface of the Ardmore basin suggest that the original basin was asymmetric, with the steepest side to the south (Ferebee, 1991). The significance of this is that, like many modern rifts, the initial geometry of the southern Oklahoma aulacogen was that of an asymmetric half-graben rather than a symmetric graben as depicted in most cross sections of the region. Figure 2 shows a more reasonable schematic of the basin prior to deformation.

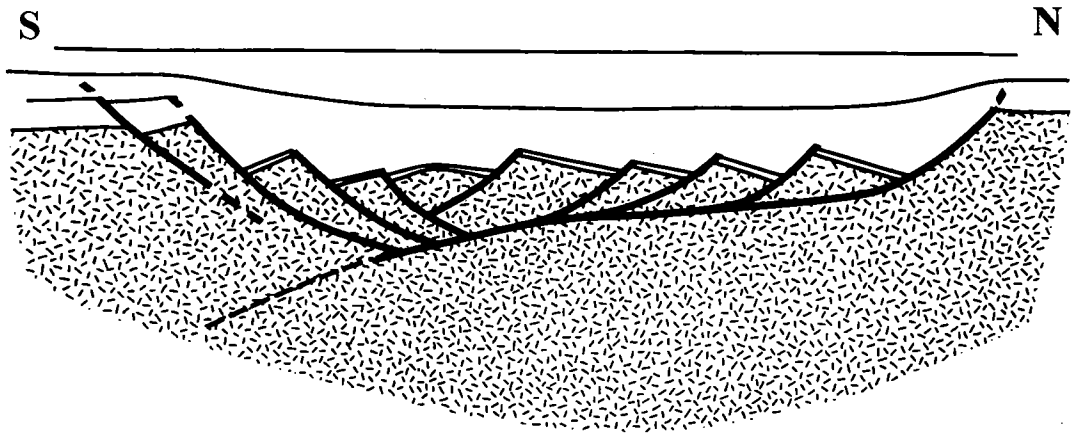


Figure 2. Diagrammatic cross section of southern Oklahoma aulacogen as an asymmetric half-graben prior to inversion, based on subsurface work of Ferebee (1991). Diagram is modified after Morley (1989).

DISCUSSION

The dominant mode of deformation in the region is brittle, largely fracturing, microfaulting, and cataclasis. This mode of deformation was pervasive in the region and strongly affected the style of structures in the area. The structural features seen in the field include folds and faults related to strike-slip deformation. The faults in the region mimic positive flower structures at most scales of observation. Many of the faults formed small gouge zones, and most of the faults have associated secondary shear zones developed through localization of cataclasite zones.

The behavior of rocks in the region of the Washita Valley fault is only slightly affected by lithology. The history of development of cataclasites along the fault shows identical paths for both limestone and tectonic dolomites, with only minor exceptions. The field data indicate that the dolomitization occurred early in the fault history. In the field, fractures related to the Washita Valley fault are concentrated in a relatively narrow band, suggesting that cataclasis and the formation of secondary cataclastic-shear zones partitioned strain related to the fault. As a consequence, structures directly related to slip along the fault are concentrated within a few kilometers of the fault. This suggests that the larger structures are part of the overall wrench setting rather than local features attributable to fault movement.

All of the folding in the region is flexural slip in nature. In many cases the bedding-plane slips die out into thrust faults in the inner arc of the fold hinges. Thrust faults in the hinges of folds can be seen at several locations, including the Hunton anticline, at the Hunton quarry near Arbuckle Lake (both in the larger anticline and in the smaller folds in the lower bench of the quarry; the Sycamore Creek anticline and associated smaller scale folds along the Washita Valley fault; small-scale folds at the crest of the Arbuckle anticline; and small folds in the Viola Formation on the north flank of the Arbuckle uplift. Thrusting in the hinges of brittle flexural slip folds formed in thick competent units is common (Ramsay, 1967, p. 401; Ramsay and Huber, 1987, p. 458). The fact that conjugate thrusts in the hinge zones of folds are common over the uplift, and present in all formations suggests that flexural slip is the folding mechanism for the Arbuckle anticline (Tapp, 1991c). The folds described also possess fold-related fractures around the outer arcs of the folds, and in some folds, cataclastic textures and tectonic pressure-solution surfaces are preserved in the hinge zones.

None of the models proposed to date for the Arbuckle region adequately address the diversity of structures seen in the area. Pure strike-slip models do not account for the overthrust character of the Arbuckle anticline in the West Timbered Hills, or for the emplacement of the Ravia nappe. Compressional models cannot account for the paucity of low-angle thrusts on the Arbuckle uplift and fail to explain the emplacement of the Ravia nappe. Furthermore, all thrusts described in outcrops are the result of flexural slip folding rather than regional thrusting. Transpressional models, while best fitting the observed structural data in the region, do not address the presence of both north- and south-directed thrusts in the region. These problems can be adequately addressed by evaluating the region using fundamental ideas from inversion tectonics.

INVERSION MODEL FOR ARBUCKLE REGION

Inversion occurs when basin-controlling faults reverse their offset in deformation. Inversion of extensional half-grabens results in a set of apparently contradictory structures, depending on the configuration of the bounding faults and the loading directions (Williams and others, 1989). Contractional, positive inversion can form under any conditions that result in compression across the original basinal faults (Williams and others, 1989). Transpression of basin-bounding faults will result in contractional inversion of the basin. Contractional inversion of a basin can result in asymmetric rollover anticlines with the limb of the fold closer to the fault dipping more steeply than the limb farther away from the fault (Williams and others, 1989) (Fig. 3A). In partial inversion, only the steep limb of the rollover anticline may be allochthonous (Cooper and others, 1989). When the basin-bounding faults are steep, rollover anticlines may not develop in favor of backthrusts, footwall shortcuts, and horse formation (Bally, 1984; Hayward and Graham, 1989) (Fig. 3B–D).

The structures in the Arbuckle region are best fit by contractional inversion of the original asymmetric half-graben. The inversion model encompasses all of the apparently contradictory features preserved in the Arbuckle region, including the allochthonous character of the northern limb of the Arbuckle anticline and the southward directed thrusts of the Ravia nappe. The Arbuckle anticline is an asymmetric anticline with a truncated and steep northern limb of thick Cambrian–Ordovician syn-rift deposits thrust over a thinner section of the same syn-rift units. The Arbuckle anticline is best interpreted as a rollover anticline formed in contractional inversion. The Ravia nappe is a southward-directed thrust fault in the southeastern part of the Arbuckle region. The nappe places Ordovician deposits on younger basin fill. The nappe can be interpreted as a backthrust that resulted from inversion of a steep segment of the Washita Valley fault (Fig. 4). Although investigation of the application of inversion tectonics to the Ardmore basin is not complete, the initial results are promising. The interpretation of the region using the inversion model resolves problem areas that were unex-

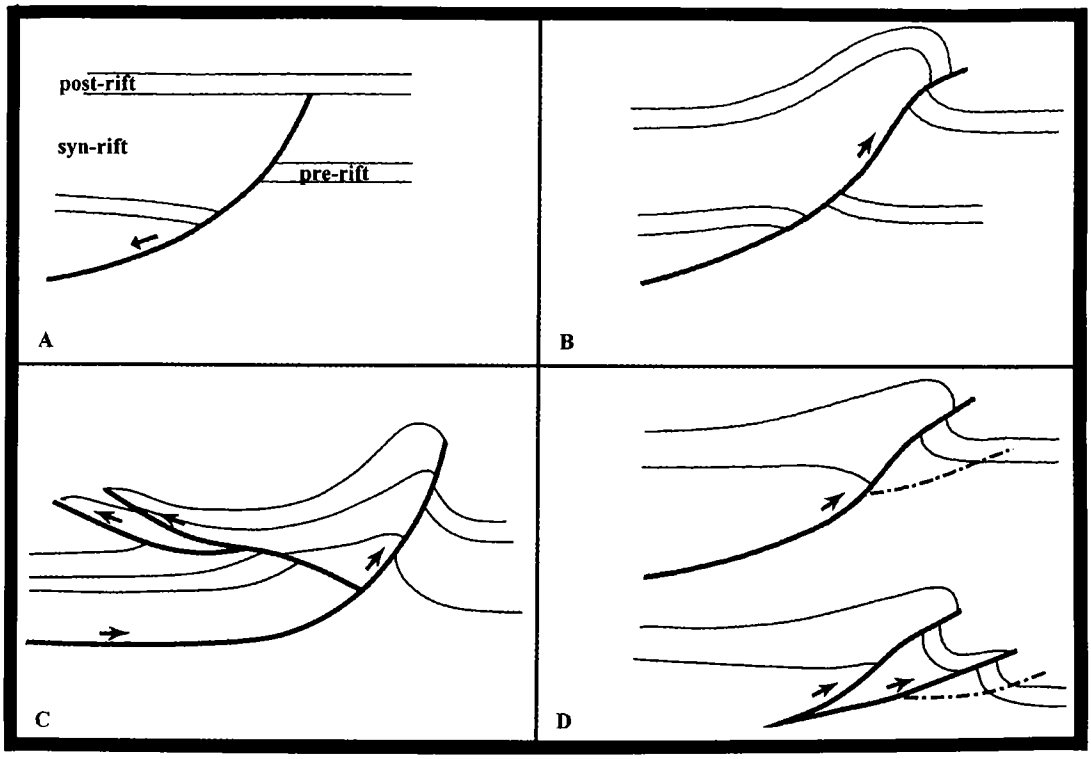


Figure 3. *A*—Initial geometry of asymmetric half-graben with basin-bounding listric normal fault. Diagram is modified after Williams and others (1989). In the case of the Arbuckle Mountains, the pre-rift sediments are not preserved; the syn-rift sediments include the Reagan through the Sycamore Formation; and post-rift sediments are not exposed in the uplift. *B*—Formation of rollover anticline in positive, contractional inversion; after Williams and others (1989). *C*—Backthrusting in positive inversion; after Bally (1984). Backthrusts form as room-accommodation features due to excessive bed length in the positive inversion of an asymmetric half-graben. *D*—Formation of footwall-shortcut thrust duplexes where the fault is too steep to completely invert, and where the footwall is composed of weak materials; after Hayward and Graham (1989).

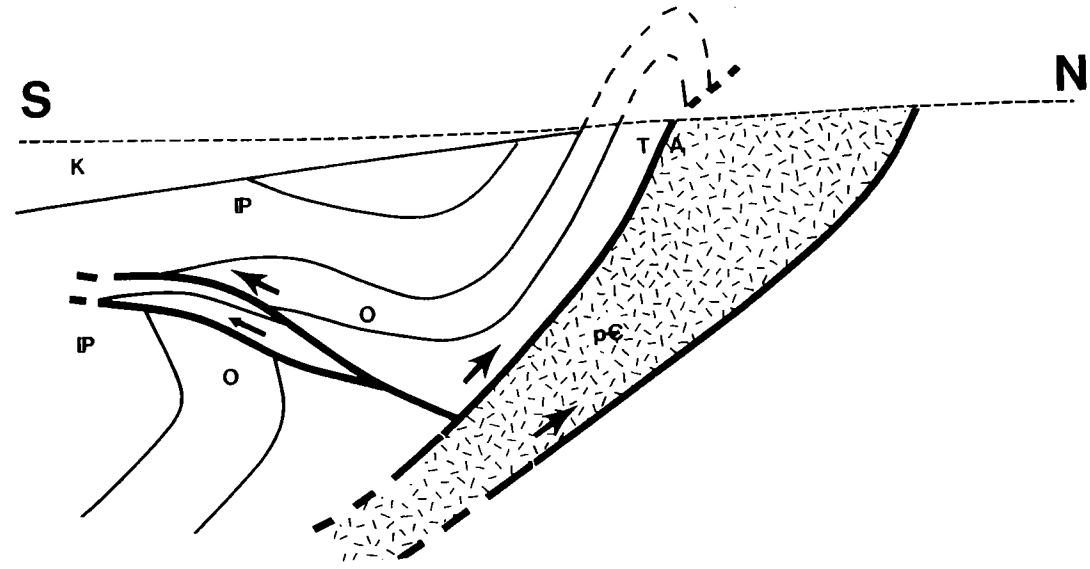


Figure 4. Diagrammatic cross section depicting the Sycamore Creek anticline and Cumberland–Ravia nappes as backthrusts formed during contractional inversion.

plained by the previous structural/tectonic models proposed for the area.

CONCLUSIONS

The data compiled for the Arbuckle region support the following conclusions:

1) The deformation in the region is the result of brittle deformation, with some pressure solution and only minor crystal plastic deformation. Brittle deformation mechanics strongly affects the styles of structures seen in the field area. All of the structures seen in the area developed in the brittle field.

2) Folding in the area is brittle flexural-slip, giving the appearance of local thrusting into the hinges of folds. This occurs on all scales of observation, and has been misinterpreted as the result of regional low-angle thrusting.

3) The tremendous variation of deformation style in the region is the result of contractional inversion during transpression. The apparently contradictory structures preserved in the Arbuckle uplift area fit the inversion model.

Significant work remains to fully test and evaluate the inversion model and to determine if the model is applicable to other problem areas in the region.

REFERENCES CITED

Bartlett, W. L.; Friedman, M.; and Logan, J. M., 1981, Experimental folding and fracturing of rocks under confining pressure. Part IX.—Wrench faults in limestone layers: Tectonophysics, v. 79, p. 255–277.

Bally, A. W., 1984, Tectonogenese et seismique reflection. Bulletin de la Societe Geologuique de France, v. 26, p. 279–286.

Booth, S. L., 1981, Structural analysis of portions of the Washita Valley fault zone, Arbuckle Mountains, Oklahoma. Shale Shaker, v. 31, p. 107–120.

Brewer, J. A.; Good, R.; Oliver J. E.; Brown, L. D.; and Kaufman, S., 1983, COCORP profiling across the southern Oklahoma aulacogen: overthrusting of the Wichita Mountains and compression within the Anadarko basin: Geology, v. 11, p. 109–114.

Brown, W. G., 1984, Washita Valley fault system: a new look at an old fault, *in* Technical proceedings of the 1981 American Association of Petroleum Geologists Mid-Continent Section regional meeting: Oklahoma City Geological Society, p. 68–80.

Brown, W. G.; Grayson, R. C.; Jamieson, W. H.; and Altum, J. T., 1985, Tectonism and sedimentation in the Arbuckle Mountain region, southern Oklahoma aulacogen: Baylor Geological Society, 44 p.

Carter, D. W., 1979, A study of strike-slip movement along the Washita Valley fault, Arbuckle Mountains, Oklahoma: Shale Shaker, v. 30, p. 80–108.

Cooper, M. A.; Williams, G. D.; de Gracaiansky, P. C.; Murphy, R. W.; Needham, T.; De Poar, D.; Stoneley, R.; Todd, S. P.; Turner, J. P.; and Ziegler, P. A., 1989, Inversion tectonics—a discussion, *in* Cooper, M. A.; and Williams, G. D. (eds.), Inversion tectonics: Geological Society of London Special Publication No. 44, p. 335–347.

Ferebee, C. D., 1991, Subsidence and basin development in the southern Oklahoma aulacogen: University of Tulsa unpublished M.S. thesis, 121 p.

Granath, J. W., 1988, Structural evolution of the Ardmore basin, Oklahoma; progressive deformation in the foreland of the Ouachita Collision: Tectonics, v. 8, p. 1015–1036.

Haas, E. A., 1981, Structural analysis of a portion of the Reagan fault zone, Murray County, Oklahoma: Shale Shaker, v. 31, p. 93–104.

Hayward, A. B.; and Graham, R. H., 1989, Some geometrical characteristics of inversion, *in* Cooper, M. A.; and Williams, G. D. (eds.), Inversion tectonics: Geological Society of London Special Publication No. 44, p. 17–40.

Hilliard, J. E., 1968, Estimation of microstructural properties in the presence of anisotropy, *in* Fulrath, R. M.; and Pask, J. A. (eds.), Ceramic microstructures: John Wiley and Sons, New York, p. 53–70.

Islam, Q.; and Nielsen, K. C., 1984, Detailed fault history in the east and central portions of the Arbuckle Mountains, Oklahoma [abstract]: Geological Society of America Abstracts with Programs, v. 16, no. 3, p. 87.

Morley, C. K., 1989, Extension, detachments, and sedimentation in continental rifts (with particular reference to East Africa): Tectonics, v. 8, p. 1175–1192.

Ramsay, J. G., 1967, Folding and fracturing of rocks: McGraw Hill, New York, 568 p.

Ramsay, J. G.; and Huber, M. I., 1987, Folds and fractures, *v. 2 of* Techniques of modern structural geology: Academic Press, New York, 307 p.

Tanner, J. H., 1967, Wrench fault movements along Washita Valley fault, Arbuckle Mountain area, Oklahoma: American Association of Petroleum Geologists Bulletin, v. 51, p. 126–141.

Tapp, B., 1991a, Deformation characteristics of the Arbuckle Group, *in* Johnson, K. S. (ed.), Arbuckle Group core workshop and field trip: Oklahoma Geological Survey Special Publication 91-3, p. 95–102.

_____1991b, Flower structure in the lower Arbuckle, *in* Johnson, K. S. (ed.), Arbuckle Group core workshop and field trip: Oklahoma Geological Survey Special Publication 91-3, p. 213–215.

_____1991c, Folding and thrusting in the lower Arbuckle, *in* Johnson, K. S. (ed.), Arbuckle Group core workshop and field trip: Oklahoma Geological Survey Special Publication 91-3, p. 216–217.

Wickham, J. S.; and Denison, R., 1978, Structural style of the Arbuckle region: Geological Society of America, South-Central Section, Guidebook for Field Trip No. 3 , 111 p.

Williams, G. D.; Powell, C. M.; and Cooper, M. A., 1989, Geometry and kinematics of inversion tectonics, *in* Cooper, M. A.; and Williams, G. D. (eds.), Inversion tectonics: Geological Society of London Special Publication No. 44, p. 3–16.

Wiltse, E. W., 1973, Surface and subsurface study of Southwest Davis oil field, Murray County, Oklahoma, *in* Ham, W. E. (ed.), Regional geology of the Arbuckle Mountains, Oklahoma: Oklahoma Geological Survey Special Publication 73-3, p. 57–63.

Significance of Air-Photograph Linears in the Basement Rocks of the Arbuckle Mountains

Rodger E. Denison
University of Texas at Dallas
Richardson, Texas

INTRODUCTION

Basement rocks in the Arbuckle Mountains can be divided on the basis of age and composition. These differences are the manifestation of the Cambrian rifting event that gave rise to the southern Oklahoma aulacogen. These basement-rock differences control every aspect of Paleozoic sedimentation and of structural style and direction.

For southern Oklahoma, Ham and others (1964) showed that the basement rocks were the controlling influence on later sedimentation and deformation. The Arbuckle Mountains were the critical area in defining this influence because the western area, the Arbuckle anticline, lay within the rifted zone, and the eastern Arbuckles lay just outside the rift. Many of the crucial structural and stratigraphic conclusions reported by Ham and others were based on observations made by W. E. Ham, on the basis of more than 25 years of experience and mapping in the Arbuckle Mountains (e.g., Ham and McKinley, 1954).

FRAMEWORK

The host rocks for Cambrian rifting are exposed in the core of the Tishomingo-Belton anticline (Fig. 1). These rocks are mostly massive Precambrian granitic rocks that yield ages between 1,350 and 1,400 Ma (million years) (Denison, 1973; Bickford and Lewis, 1979). There does not appear to be any definable regional structural grain, even in the gneisses. The massive granitic rocks are, however, cut by a variety of dikes that show a marked northwest strike (Denison, 1982).

In contrast, the Arbuckle anticline is cored by rhyolite of Cambrian age that represents the synrift filling of the aulacogen. The Cambrian igneous rocks were extruded or emplaced after major rifting had triggered partial melting at depth (see Gilbert and Denison, 1993, for a review). The two areas of exposed basement rocks are separated by a very unusual fault. The Washita Valley fault is the master fault of the Arbuckle Mountains. Tomlinson (1952) first documented that the fault plane has the shape of a propeller. Figure 2 shows that, in the east, the fault dips to the north, is up to the north, and has a direction of transport to the south. Westward along strike in the Arbuckle anticline area, the fault dips to the south, is up to the south, and has a direction of transport to the north. The hub of the propeller is marked by four points of no stratigraphic offset. Although Tomlinson made this judgment on the basis of field observations, later drilling confirmed this curious geometry (Ham and others, 1964; Brown, 1984; Huffman and others, 1978).

Determining the structural direction in the most complex and intensely deformed area in the central interior is best done by using regional data. I have chosen to use the strike of major regional faults to determine the late Paleozoic structural grain. Figure 3 shows the mean strike of faults that offset the basement at least 5,000 ft. The Washita Valley fault contributes substantially to the pronounced N60°W trend, considered to be the dominant late Paleozoic structural direction.

MEASUREMENT OF LINEARS

The Precambrian part of the Arbuckle Mountains was mapped by using topographic maps and air photos (shown in Ham, McKinley, and Johnson, 1990). During mapping, it was noted that there are numerous linears on the air photos that appeared to be systematic and to vary both in direction and density across the outcrop area (Fig. 4). If these were late Paleozoic tectonic linears, then perhaps they could be used to better understand the deformation and to define stress directions.

The linears were measured by using a clear overlay, on 1:20,000 air photos. The location of each linear was marked on the overlay, and the length and direction of each of the 2,173 linears were recorded. Curved linears were divided into a series of roughly straight segments. The total length of the linears is 447.8 mi.

Denison, R. E., 1995, Significance of air-photograph linears in the basement rocks of the Arbuckle Mountains, *in* Johnson, K. S. (ed.), Structural styles in the southern Midcontinent, 1992 symposium: Oklahoma Geological Survey Circular 97, p. 119–131.

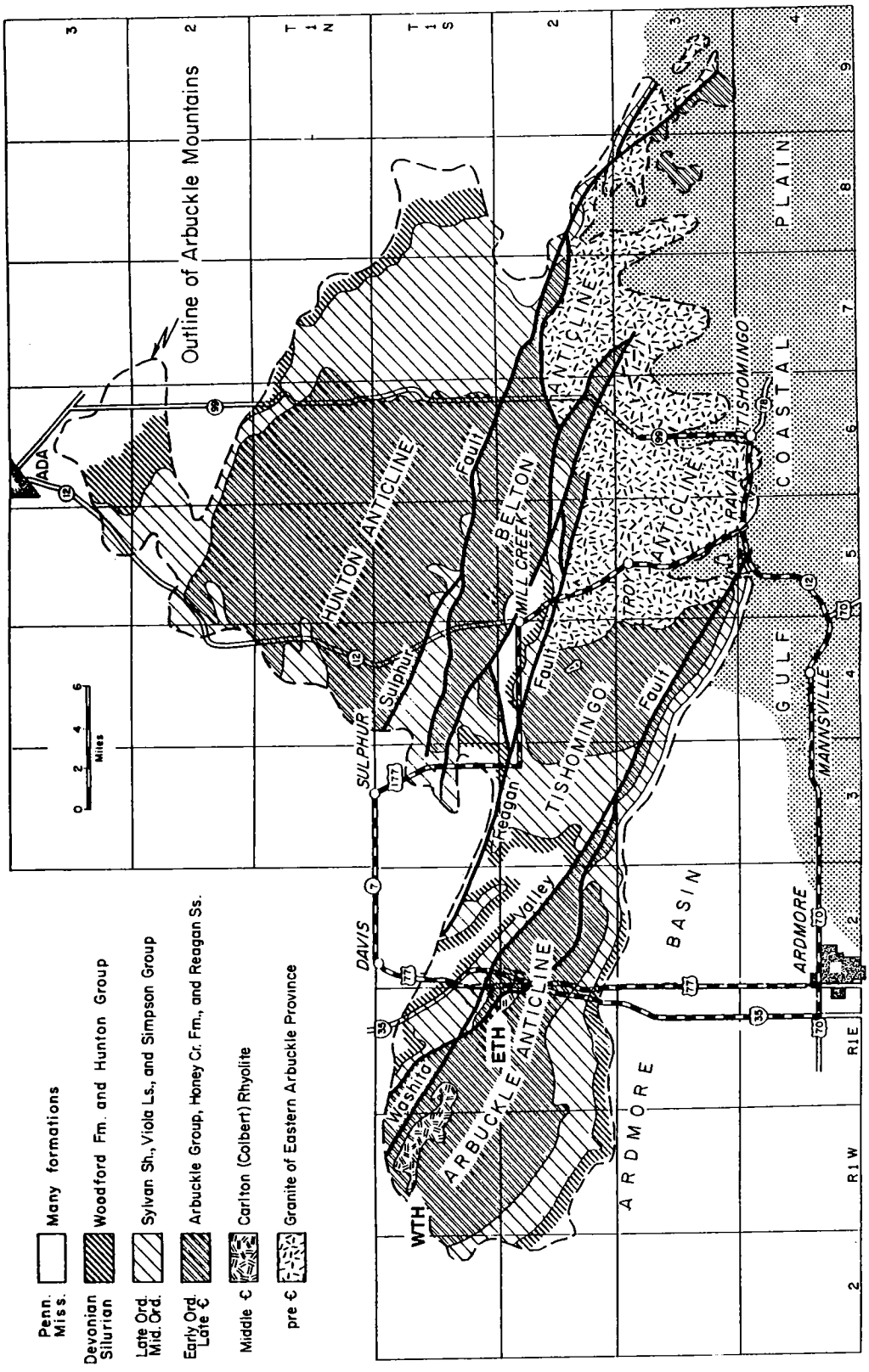


Figure 1. Simplified geologic map of the Arbuckle Mountains (modified from Ham, 1969). The Pennsylvanian Washita Valley fault marks the approximate Cambrian rift margin and separates the Arbuckle anticline from the Tishomingo-Belton anticline. The Cambrian rhyolite is exposed in the East Timbered Hills (ETH) and West Timbered Hills (WTH) of the Arbuckle anticline.

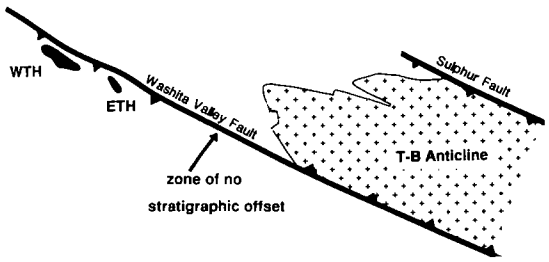


Figure 2. Schematic illustration of Tomlinson's (1952) propeller shape for the Washita Valley fault that separates the Precambrian rocks in the Tishomingo-Belton (T-B) anticline from the Cambrian rhyolites in the East and West Timbered Hills (ETH and WTH). The Washita Valley fault follows the original northern rift margin of the southern Oklahoma aulacogen. The configuration of the fault geometry has been confirmed by later drilling.

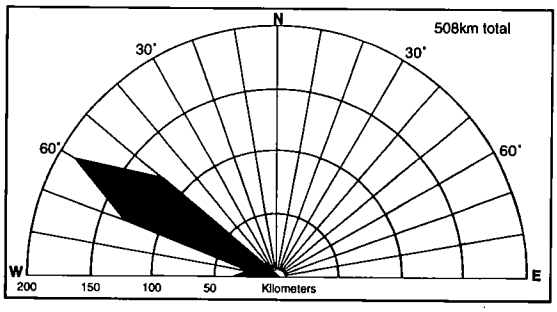


Figure 3. The orientation of late Paleozoic faults in the Arbuckle Mountain area, taken from Ham and others (1964, pl. II). All the measured faults offset the basement at least 5,000 ft at some point along strike.

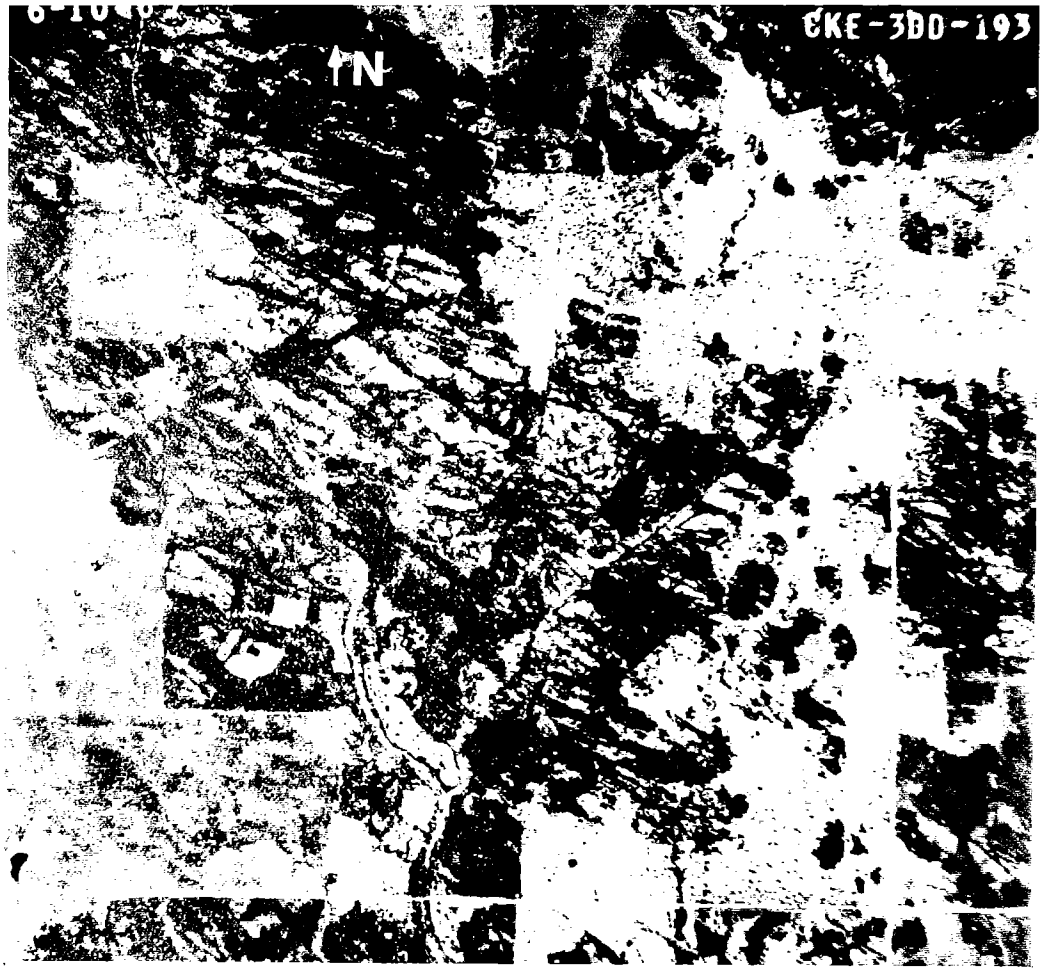


Figure 4. Air photo showing the conspicuous linears in massive Tishomingo Granite. The area is ~5 mi north of the aulacogen margin, with the photo centered in sec. 14, T. 2 S., R. 6 E., ~3 mi north of Ravia on Rock Creek. Photo width is ~3.5 mi. The cleared area without linears is underlain by a gravelly soil developed in Cretaceous time.

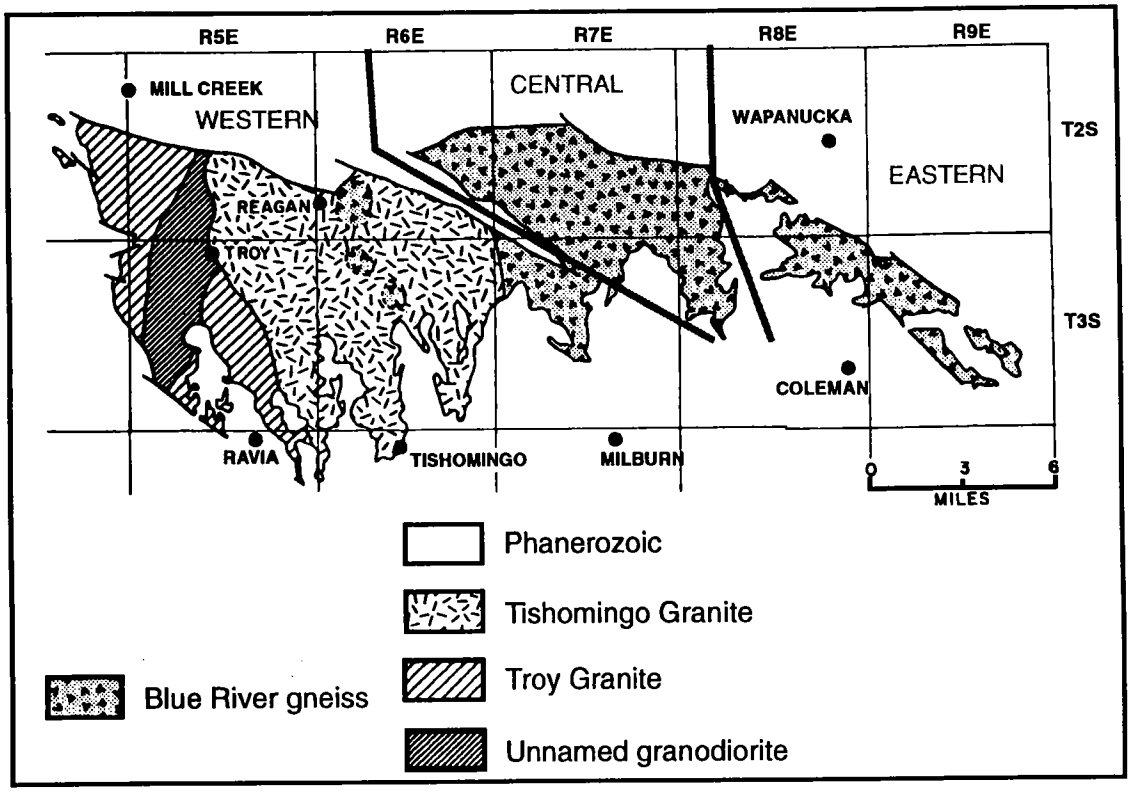


Figure 5. Precambrian rocks in the eastern Arbuckle Mountains. Each of the three major blocks (western, central, and eastern) shows a different distribution of air-photo linears, which is strongly influenced by proximity to the rift margin.

TISHOMINGO-BELTON ANTICLINE

A total of 1,907 individual linears was measured in the roughly 130 mi^2 of exposed Precambrian rocks in the eastern Arbuckle Mountains. The area is very flat because of Cretaceous peneplanation, and Cretaceous sandstones overlie the granites to the south (Fig. 1). The only systematic topographic relief is along present-day rivers and streams. The maximum relief is an elevation difference of ~160 ft, over a distance of 1,500 ft west of the town of Mill Creek in sec. 8, T. 2 S., R. 4 E. Ten to a few tens of feet of relief along streams is more typical. Only a small percentage of the Precambrian map area shown by Ham and McKinley (1954) actually contains exposed rock.

The main Tishomingo-Belton anticline is a wedge-shaped uplift with Pennsylvanian thrust faults dipping under the granitic mass both on the north and south (Ham and others, 1964). It plunges to the northeast and is covered unconformably by Cretaceous sandstones to the southeast. The uplift can be traced to the southeast for more than 80 mi with drill control, gravity, and magnetic data (Denison, 1989).

The Tishomingo Granite is the youngest major unit in the core of the anticline (Fig. 5). To the west it intrudes the Troy Granite, which in turn intrudes a granodiorite, the oldest western unit. To the east, the Tishomingo intrudes the Blue River gneiss (an informal name). This granitic gneiss is not in contact with western units, and the relative age relations cannot be determined. All units yield radiometric ages that are similar, within error.

The air-photo linears have at least two origins. Some are clearly late Paleozoic faults that can be traced into the Precambrian rocks. However, where the origin can be determined, the vast majority of linears appear to be due to mild topographic and vegetative differences caused by dikes cutting the massive granitic rocks.

All common dikes are fine grained and tend to form bouldery outcrops. The host granitic rocks disaggregate more readily and form a porous gravelly soil, commonly cleared for crops and grazing. The typical field expression of a dike is a line of boulders flanked by a well-grassed pasture with little or no outcrop. Because the bouldery dikes support a growth of trees and brush, they are conspicuous on air photos. The width of the dikes var-

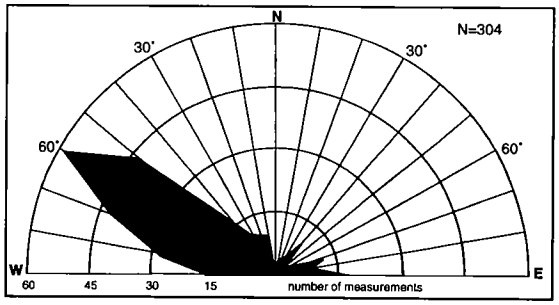


Figure 6. Strike direction of Precambrian and Cambrian diabase dikes cutting all major granitic units. A total of 304 dike directions was measured in the field.

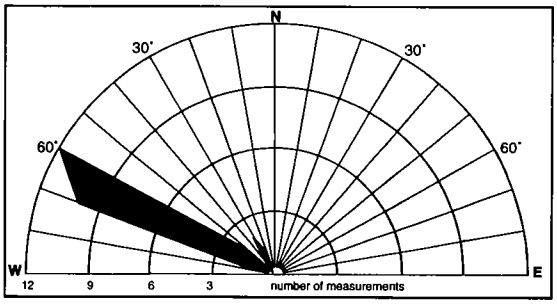


Figure 7. Strike direction of Cambrian rhyolite porphyry dikes cutting the Precambrian granitic units. The plot is based on air-photo and field measurements.

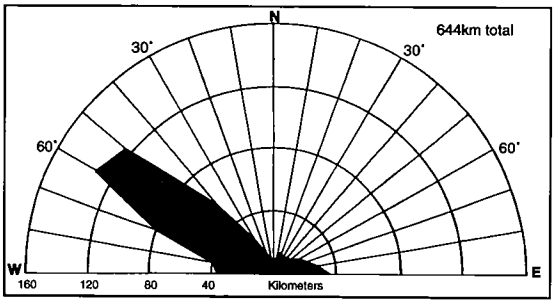


Figure 8. Strike direction of all air-photo linears in the eastern Arbuckle Mountains. The preferred N60°W direction reflects both the Cambrian rifting and late Paleozoic structural grain.

ies from a few inches to >100 ft. The largest ones can be traced for several miles in the field and on air photos and form mild topographic highs. Most dikes are vertical, or nearly so, where the dip can be determined.

There are perhaps other origins for the linears, but they are difficult to define. One example of a well-defined linear with an unusual origin is northeast of the town of Troy; on field checking, this "linear" was found to be an abandoned railroad line to an old gravel pit. The linear has a near-perfect N60°W strike and was not used in the data summary.

The majority of dikes are of four types: diabase, rhyolite, granite, and microgranite porphyry. There are also a small number of diorite and quartz diorite dikes; fewer than five were identified in the field. The diabases are of two ages: some are near the age of the host granitic rocks (1,350–1,400 Ma), and others are clearly Cambrian. The two diabase suites are petrographically indistinguishable and are difficult to date because of excess radiogenic argon. There is no meaningful way to estimate relative abundances. The diabase dikes mainly strike N60°W (Fig. 6). The distinctive brick-red rhyolite dikes are all of Cambrian age and are related to the Colbert Porphyry of the Arbuckle anticline. The rhyolite dike directions are essentially identical to those of the diabase (Fig. 7). The granite dikes are mostly local, rarely large, and show no systematic strike or dip. The microgranite porphyry dikes are distinctive in the field. Although not numerous, they are generally >10 ft wide, and some can be traced for several miles along strike. The microgranite dikes are conspicuous in the Troy Granite and the granodiorite, but have not been identified in the Tishomingo Granite or Blue River gneiss. These field relations indicate that the microgranite dikes are intermediate in the 1,350–1,400 Ma age range of the major granitic units. The strike of these dikes is the best evidence for an early zone of weakness. The plot of the dikes shows a profound N60°W preferred direction.

A total of 399.9 mi of linears was measured in the Tishomingo-Belton anticline (Fig. 8). The broad peak included N50°–60°W and is closely coincident with the dike and the late Paleozoic fault directions. About 60% of the linears are from areas underlain by the Troy and Tishomingo Granites and the granodiorite.

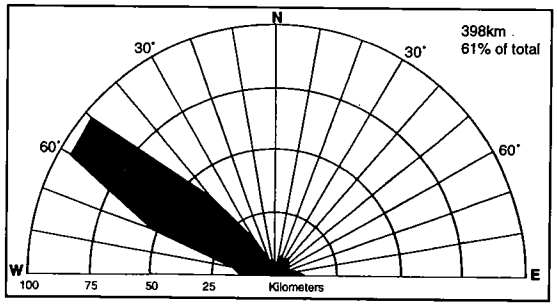


Figure 9. Strike direction of air-photo linears in the western block (Fig. 5) showing close agreement with the total linear analysis and the late Paleozoic structural grain.

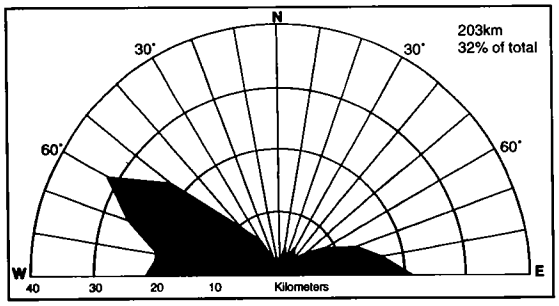


Figure 10. Strike direction of air-photo linears in the central block (Fig. 5). Note the addition of a due east peak to the still-dominant northwest direction.

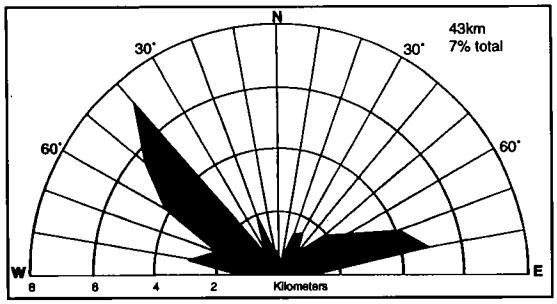


Figure 11. Strike direction of air-photo linears in the eastern block (Fig. 5). There is a shift to a conspicuous N40°W direction, with a secondary peak at N80°E. These peaks cannot be distinguished on the plot of total linears because of the longer and more numerous linears in the western block.

The strongly preferred northwest direction that characterizes the western Precambrian outcrop area is much less distinct in the eastern outcrop area. Here, where the anticline plunges beneath the Cretaceous, Ham and McKinley (1954) mapped late Paleozoic structures with well-defined northeast elements. The Precambrian linears were divided into three geographic segments shown in Figure 5.

The geographic separation brings out substantial differences in the strike of the linears. The western block (Fig. 9) mirrors the total Precambrian plot, because this block contains about 61% of the total linear length. The central block shows a strong N60°W peak and a secondary due east peak (Fig. 10). The eastern block is even more complicated, with a major N40°W peak and a secondary N80°E peak (Fig. 11). The more numerous western-block linears simply overpower these secondary central- and eastern-block peaks on the total plot.

There are well-developed joints in areas of good Precambrian exposure. Taylor (1915) identified two strong systems of nearly vertical joints in the eastern Arbuckles. The two sets strike N40°–70°W and N20°–50°E. White (1991) measured and analyzed the joints in several areas of excellent exposure of Precambrian rocks. These plots (Fig. 12) show inconsistency, even in nearby areas of the Tishomingo Granite. It must be concluded that these joints probably are not related to the air-photo linears. It is likely that these joints are cooling fractures dating from the time of crystallization or perhaps from initial uplift in the Precambrian. Because of the inconsistency, it is doubtful that they have a tectonic origin.

The vast majority of linears in the eastern Arbuckles are believed to be caused by dikes. This is based on the field observation that the dikes are most numerous in areas where the linears are most abundant and conspicuous. Specifically, the linears and dikes are most numerous near the edge of the aulacogen. Ham and others (1964) placed the aulacogen margin coincident with what was to be reactivated in the late Paleozoic as the Washita Valley fault. Near the fault, along Mill Creek northwest of the town of Ravia, the dikes are so numerous that they appear locally to present a substantial percentage of the exposed rocks. A well drilled near the aulacogen margin (Honeymon no. 1 Townsend, sec. 30, T. 5 S., R. 8 E.) penetrated 3,653 ft of base-

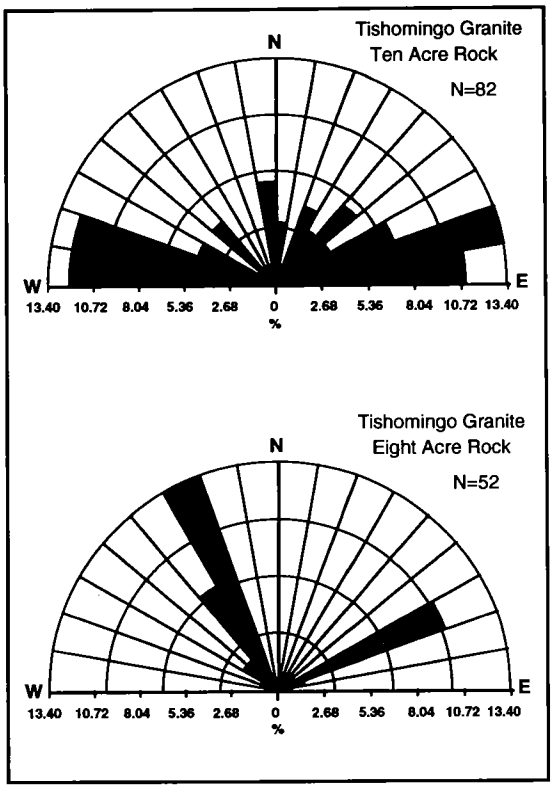


Figure 12. Joint direction in the Tishomingo Granite, measured by White (1991). The localities are <0.5 mi apart. The joints are interpreted here as cooling fractures formed at the time of crystallization.



Figure 13. Diabase dikes (dark rock) in the crushed-stone quarry south of Mill Creek (sec. 29, T. 2 S., R. 5 E.). The host rock is largely the Troy Granite. The quarry is ~5 mi north of the rift margin.

ment rock, of which 28% was diabase dikes in a granite host (Ham and others, 1964).

The Cambrian diabase dikes are therefore interpreted as the rift-related dike swarm that marks the aulacogen opening. The dikes are numerous 5 mi northeast of the aulacogen margin (Fig. 13). More than 10 mi northeast of the rift margin the dikes are rare, even in areas of exceptional exposure, and have lost the strongly preferred orientation, as seen in the eastern-block air-photo linears.

As noted, some of the linears are clearly late Paleozoic faults, because they can be traced into offsets in the sedimentary rocks. But these offsets are not common. The tectonic linears are believed to represent a small but uncertain number of the total air-photo linears in the Precambrian rocks.

The linears, and therefore the dikes, have a strong N60°W preferred orientation near the rift margin. For the origin of the secondary set of northeast-trending linears in the eastern block, one must look away from the southern Oklahoma aulacogen. The place to look, in my opinion, is to the southern rifted margin of the United States and the opening of the Ouachita depositional basin.

Thomas (1977) first showed the Ouachita opening as an irregularly shaped block, torn from the southern margin of the United States during the opening of the proto–Atlantic Ocean during the Cambrian. His later (Thomas, 1991) synthesis shows the rifted margin more accurately and documents the timing and sequence of events. An unpublished idea of J. H. Rosenfeld from 1981, independently proposed in modified form by Lowe (1985), made the torn block a substantial continental mass that came to rest offshore of the southern margin (Fig. 14). Rosenfeld's jigsaw block is most convenient in helping to explain (1) the sediment source in the Ouachita depositional basin and (2) the close timing of depositional and tectonic events separated by hundreds of miles along the sinuous strike of the Ouachita foldbelt.

It is possible that the northeast-trending dikes and air-photo linears observed in the eastern block of the Arbuckle Precambrian rocks are a reflection of the Ouachita opening. It is estimated that the rifted Ouachita margin lay some 75–100 mi to the east-southeast of the most easterly of the present Precambrian outcrops. The possibility that these dikes and linears do reflect Ouachita opening is evidence (the only evidence I know of) that the Cambrian Ouachita rift zone may have followed a much older zone of weakness. The evidence can be seen in at least one conspicuous, vertical, 40-ft-wide, quartz diorite dike (striking N20°E) that was described by Taylor (1915, p. 95). The quartz diorite is in turn cut by a younger diabase dike. The diabase may be of Cambrian or Precambrian age, but the quartz diorite is almost certainly near the age of the host granite gneiss. By analogy, just as the southern Oklahoma aulacogen margin inherited the zone of weakness shown in the Precambrian dike directions, so the Ouachita opening may follow a similar early weakness direction—much less distinct because it is much more distant.

ARBUCKLE ANTICLINE

The East and West Timbered Hills of the Arbuckle anticline (Fig. 1) are cored by the Colbert Porphyry of Cambrian age. The rhyolite crops out over about 5.7 mi^2 in the two areas, only about 4% of the total Arbuckle Mountain basement-rock outcrop area. These anticlinal cores are partly densely wooded and partly smooth grassy areas that show distinctive linears marked by more heavily wooded or brushy growth (Fig. 15). Diabase is not conspicuous on the outcrop, but is common as dikes and sills in a large West Timbered Hills quarry and in nearby wells. The strongly bedded character of the rhyolite flows may have encouraged sill injection rather than dike emplacement.

The rhyolite and diabase represent the final igneous episode that filled the aulacogen. There are two episodes of Cambrian dike injection. The rhyolites are considered to be younger than the diabase dike swarms in the Tishomingo area that signal the aulacogen opening, but obviously are older than the diabase dikes and sills that are the youngest igneous rocks. Because the rhyolites are postrifting, most air-photo linears are almost certainly tectonic in origin, formed during Pennsylvanian deformation (although an uncertain number could be caused by the youngest diabase dikes).

The core of the West Timbered Hills has a rhyolite outcrop of about 4.9 mi^2. In this small area, 188 linears having a total length of 34.2 mi were measured. The structure, considerably more complex than that of the smaller East Timbered Hills, is basically an asymmetric anticline, striking roughly N60°W with a steep northern flank. The Washita Valley fault dips south beneath the structure. The

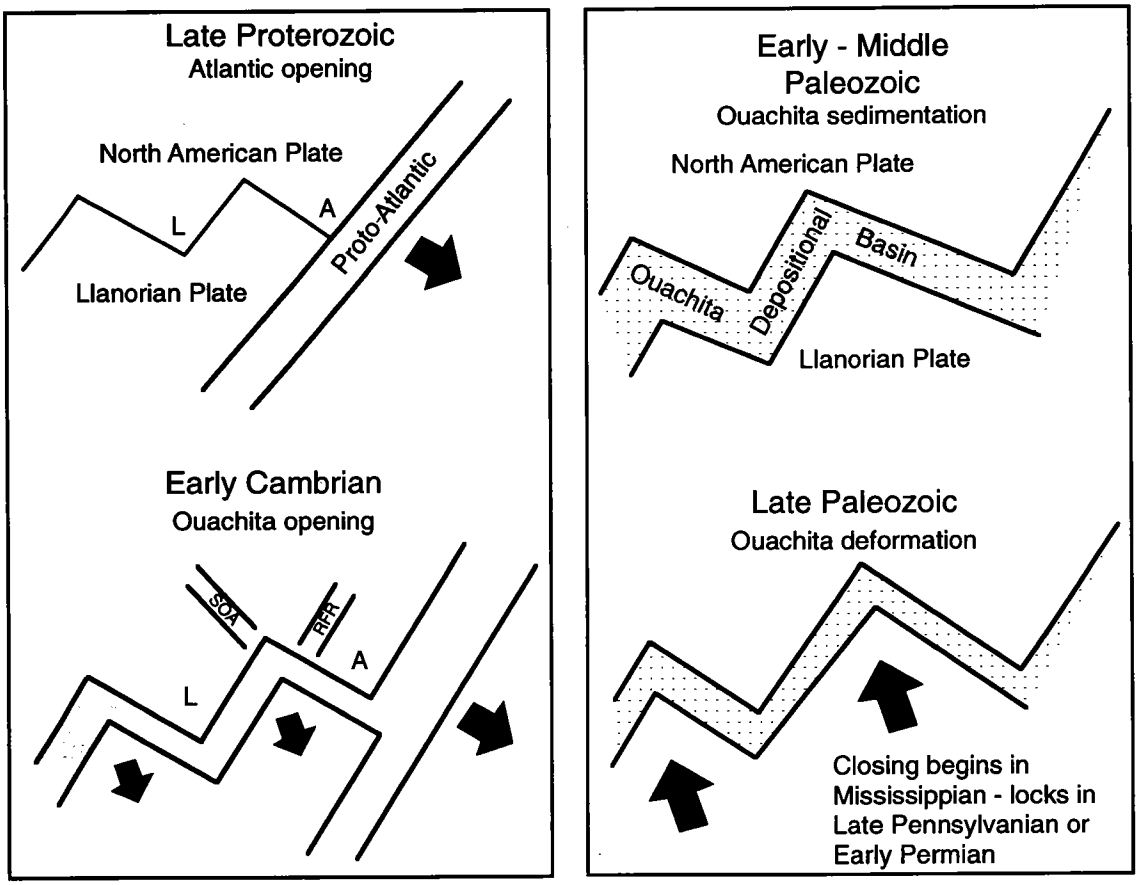


Figure 14. Simplified model of Ouachita depositional basin opening and closing, based on an unpublished idea of J. H. Rosenfeld. In the late Proterozoic, the proto-Atlantic opened. The Llanorian block separated from the southern craton margin in the Early Cambrian, and the southern Oklahoma aulacogen (SOA) and Reelfoot rift (RFR) formed on the foreland. The Alabama (A) and Llano (L) promontories set the basic shape of the Ouachita foldbelt (from Thomas 1977). During most of the Paleozoic, the failed Llanorian block sat outboard and supplied sediments to the Ouachita depositional basin. Closure began in the Mississippian, and the Llanorian block was reunited to the craton when sediments from the Ouachita depositional basin were thrust onto foreland-shelf sediments.

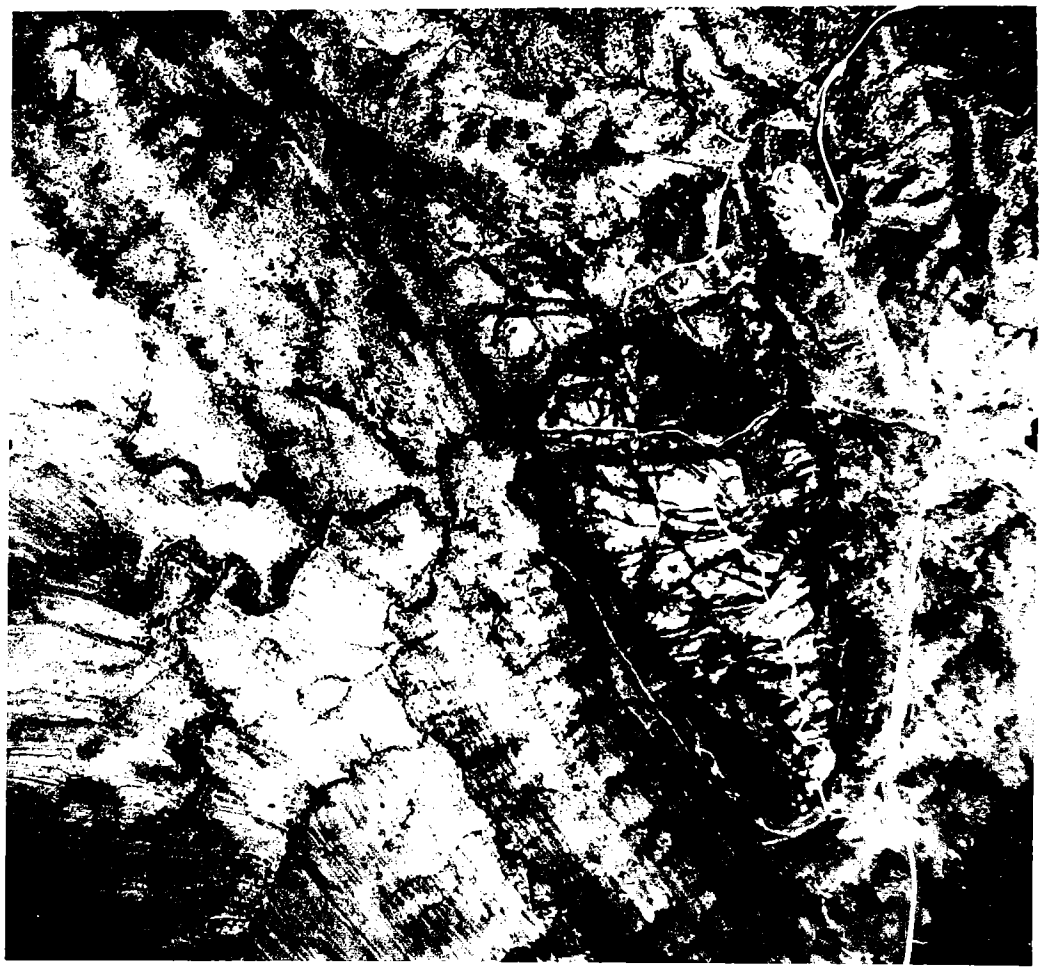


Figure 15. Air photo showing the well-defined linears in the Cambrian rhyolite of the East Timbered Hills. Photo is ~3 mi in wide and is centered in sec. 1, T. 2 S., R. 1 E.

rhyolite core is cut by several cross faults, as reflected in the offsets of the contact between the Reagan Sandstone (see Fig. 1) and the rhyolite.

The distribution of linears reflects the complexity in the West Timbered Hills (Fig. 16). The major peak is parallel to the anticlinal axis, and there are well-defined secondary peaks. A conjugate pair centered about the fold axis is obscure, if present. The peaks mirror the rather confused Pennsylvanian fault directions.

The East Timbered Hills are an asymmetric anticline with a south-dipping thrust fault on the northeast. The anticlinal axis strikes N35°W, well off the regional grain. The core has a rhyolite outcrop of only about 0.8 mi^2. In this small area, 78 linears with a total length of 13.3 mi were measured. The distribution represents the most unusual pattern of linears seen in the Arbuckle Mountains. Figure 17 shows the due east dominance, a secondary peak at N40°W, and a small peak at N60°W. No other area in the Arbuckle Mountains has such a strong due east peak, although the central block in the Precambrian (Fig. 10) has a secondary peak of this orientation.

The Washita Valley fault has been considered a major wrench fault with left-lateral displacement (Tanner, 1967; Wickham, 1978; Carter, 1979; Tapp, 1988; Granath, 1989). The East Timbered Hills could, therefore, be interpreted as a first-order drag fold off the major wrench fault. The secondary peak at N60°W would then be ascribed to the dominant half of a conjugate pair of the wrench-fault system. A pure wrench system requires the principal stress to be due east, and a transpressional system to be near N60°E.

This interpretation leaves the main due east linear peak unexplained. I have chosen to interpret the linears as a suite of small wrench faults (expressed as air-photo linears) with small movements on each fault. These small wrench faults are not caused by a major wrench system, but by compression normal to the N60°W structural direction and the critical lo-

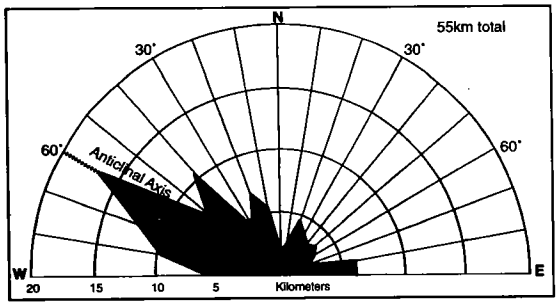


Figure 16. Strike direction of air-photo linears in the West Timbered Hills. The rather complex pattern has a major peak parallel to the fold axis and reflects Paleozoic fault directions. These are almost certainly Pennsylvanian tectonic linears.

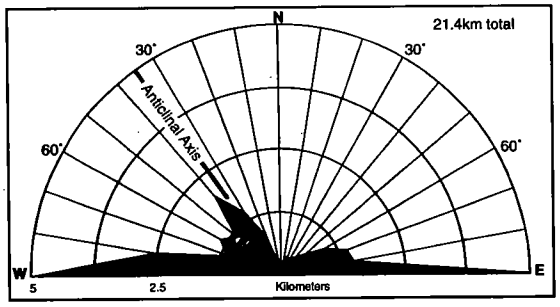


Figure 17. Strike direction of air-photo linears in the East Timbered Hills. The well-defined due east peak can be seen on the air photo (Fig. 15).

cation of the East Timbered Hills just west of the hub of Tomlinson's propeller fault.

The proposed evolution of the East Timbered Hills is shown in Figure 18. The northeast-transported fold is jammed against the massive Precambrian buttress of the eastern Arbuckles. The original fold is rotated clockwise from N60°W to N35°W. During rotation, a series of wrench faults (half of a conjugate pair) developed as the southeastern end of the fold encountered the buttress and was pinned by the propeller hub of zero stratigraphic offset along the Washita Valley fault. These wrench faults must have very little movement, because Ham and McKinley (1954) showed no offset of the Reagan/rhyolite contact and none can be seen on the air photos. Examination of air photos on the south flank of the East Timbered Hills shows that Arbuckle Group rocks do not show a well-developed, systematic fracture pattern. The exception is the Signal Mountain Formation, probably the "weakest" and least well exposed of the Arbuckle formations; the Signal Mountain shows a well-developed, closely spaced fracture network with strikes of N30°E and N90°E that can be interpreted as a conjugate pair centered on the fold axis. The N90°E-striking fractures appear dominant, but both sets are well developed.

INTERPRETATION OF LINEARS

Prior to quantitative analysis, the linears offered the possibility that they could be used to determine stress directions during Pennsylvanian deformation. This proved, in the interpretation here, to be impossible. The linears in the Precambrian are dominated by the strike of dikes intruded during two main periods of extension. The earlier dikes were emplaced during the igneous episode that gave rise to the host granitic rocks. These dikes are the earliest documentation of the structural direction that was to dominate southern Oklahoma geologic history for more than a billion years. The second dike suite was intruded during the Cambrian rifting event that signaled the opening of the southern Oklahoma aulacogen and the Ouachita depositional basin. The domination by dike-related linears is so complete that known Pennsylvanian tectonic linears appear lost. The linears in the Cambrian rhyolite of the East and West Timbered Hills are largely tectonic but not definitive. The East Timbered Hills are too close to the hub of the anomalous Washita Valley fault to be of regional signifi-

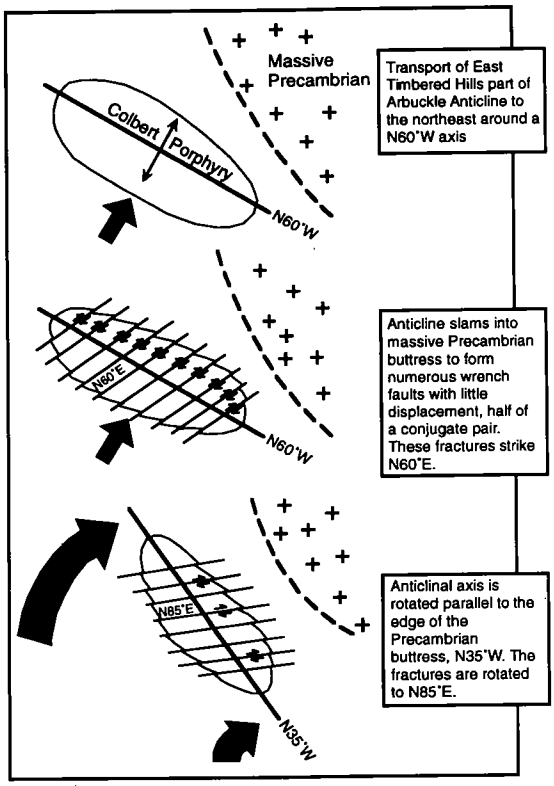


Figure 18. The proposed rotation of the East Timbered Hills in order to account for the anticlinal direction and linear peak.

cance. The West Timbered Hills linears form several well-defined peaks, but these cannot be uniquely interpreted.

Although the linear analysis does not offer definitive evidence for the nature of regional deformation in the Pennsylvanian, it does quantify and document the earliest structural grain that controls all later southern Oklahoma geologic events. The northeast-trending Precambrian linears hint of an early weakness direction that may have been utilized during the opening of the Ouachita basin in the Cambrian.

STRUCTURAL INTERPRETATION

There has been substantial disagreement concerning the driving force that gave rise to the most intensely deformed area in the central interior of the United States. Ham and others (1964) showed that the intense deformation was restricted to areas underlain by the rift-filling rhyolite—i.e., the aulacogen—an idea introduced later by Hoffman and others (1974). Observations in the Arbuckle Mountains were critical in reaching this conclusion.

The original opinions were essentially divided into strike-slip and dip-slip camps. The strike-slip explanation required that the faults steepen with depth. The fault steepening causes problems in cross-section balancing. The argument that sections across structures with substantial lateral motion normal to the plane of section need not balance is only partly true. No one has attempted to restore lateral movement along the fault and then balance the section.

Greatly improved seismic resolution at depth (e.g., Brewer and others, 1983) and carefully controlled cross sections (e.g., Petersen, 1983; Brown, 1984; Jacobson, 1984) have shown that the faults do not steepen with depth and there is substantial shortening across the basins. Tomlinson (1952) originally estimated 40% shortening across the Ardmore basin.

Because of these problems, transpression is now advocated by several workers to retain a strike-slip component, but still account for the obvious shortening normal to strike. Perry (1989) has provided a thoughtful analysis and review of structure in southern Oklahoma, with particular emphasis on the Arbuckle anticline. He concluded that the Washita Valley fault has ~2.7 mi of left separation, based on the offset of fold axes in the Arbuckle anticline area. The area is unfortunately close to the anomalous hub of the propeller fault. If there is a significant strike-slip component on the Washita Valley fault, then the propeller hub, with no stratigraphic offset where the fault changes dip from south to north, should be an area of intense and chaotic deformation. Ham and McKinley (1954) showed the hub area to be one of the least-faulted and least-deformed areas along the Washita Valley fault. Mapping in the hub area by Palladino (1986) and examination of air photos confirm this finding. The clockwise rotation of the East Timbered Hills, offered earlier in this paper as an explanation for linear and anticlinal orientation, would exaggerate apparent left-lateral offset.

Other estimates of the lateral offset through southern Oklahoma vary wildly, from much less than the amount of dip slip to 100 mi of left-lateral separation. Most of these estimates are based on apparent offsets of the thickness of a single stratigraphic unit (e.g., Tanner, 1967; Carter, 1979; McConnell, 1989). No study compares the thickness of adjacent stratigraphic units. For example, McConnell's (1989) analysis of the Hunton Group thickness across the Mountain View fault, which separates the Wichita-Criner uplift from the Anadarko basin, indicates 7–16 mi of left slip. Based on much less control than McConnell's data were, isopach thicknesses of the Sylvan and Woodford Shales (Amsden, 1980) that underlie and overlie the Hunton can be used to suggest, if anything, substantial right-lateral offset.

Piercing points are hard to come by in southern Oklahoma. The stratigraphic units all vary in thickness, generally parallel to regional structure (see Johnson and others, 1988). Structural complications make the accurate determination of stratigraphic thickness difficult. McConnell (1989) and Brown (1984), for example, have made a careful effort to correct for dip. Nonetheless, I reject any estimate of offset based on the analysis of a single stratigraphic unit. The fact is that analyses based on single-unit thickness have led to widely disparate estimates of the possible offset.

Possible inaccuracy in the estimation of offset does not mean that there is none, but instead that the determination is not simple. Rather than some of the more extravagant claims, the offset probably is no greater than the 7–16 mi estimated by McConnell (1989) along the Mountain View fault and no more than the 2.7 mi estimated by Perry (1989) along the Washita Valley fault. Because these and other estimates come from different faults, the total could add up to a tidy sum. There is such a large dip-slip offset on the major faults that—because many of these faults change strike—there must be, even in a "pure" dip-slip system, a substantial strike-slip component on segments of major faults (several miles of offset).

Any model for southern Oklahoma deformation must account for substantial shortening, the shift of deformation from south to north, and the general northeast vergence of major structures. Almost all more recent cross sections (e.g., Brewer and others, 1983; Brown, 1984; Jacobson, 1984; McConnell, 1989) are compatible with compression normal to the basin axis (directed N30°E). This interpretation does not preclude transpression. Indeed, the structural zone of weakness, developed in the Precambrian and mimicked during later events, is so profound that any northeast-directed movement

would certainly follow the established grain. Donovan (1988) suggested a displacement vector near N70°E to account for his interpretation of transpressional movement. It is not clear how the resulting transpression structures would differ from those developed during a N30°E-directed principal stress, given the established structural grain.

The curious geometry of the Washita Valley fault is difficult to explain, regardless of the deformational model called upon. It is very likely that the difference in sedimentary cover at the initiation of deformation played an important role. Basement rocks in the area that was to become the Tishomingo-Belton anticline probably stood more than 10,000 ft above those in the area of the Arbuckle anticline in mid-Pennsylvanian time (best shown by Ham, 1969). This disparity, coupled with the strong preexisting structural grain, may have caused the propeller-shaped rotation of the fault plane. Based on mapping in the hub area, Palladino (1986) interpreted the Washita Valley fault as two independent faults that appear as one, with the western fault slightly younger than the eastern fault. The appearance of a single fault is caused by a fortuitous level of erosion.

The tie between foreland deformation and the synchronous Ouachita collision is superficially appealing (Kluth and Coney, 1981; Granath, 1989). Exactly how the reuniting of the jigsaw block to the foreland (Fig. 14), or any model of Ouachita collision, is translated into a northeast-directed displacement vector in southern Oklahoma is not clear. I have contended (Denison, 1989) that an interrelation between Ouachita collision and foreland deformation, as attractive as it appears, is not proved and that the actual mechanics are difficult to explain. The foreland extension may well have been initiated by westward relative movement of northern Mexico, caused by the jostling of plates during the opening of the Ouachita basin. The subsequent southern Oklahoma shortening, in this interpretation, was caused by an eastward relative movement of Mexico during late Paleozoic deformation (Denison, 1982).

CONCLUSIONS

The majority of linears in the Precambrian of the Arbuckle Mountains reflect the strike direction of several suites of near-vertical dikes, some as old as 1,350–1,400 Ma and others of Cambrian age. The oldest dikes establish a zone and direction of weakness that was later reactivated during the Cambrian opening of the southern Oklahoma aulacogen and the intrusion of the younger dike swarm. Linears in the eastern Precambrian units have a substantial northeast component and may be in response to the distant Ouachita basin opening in the Cambrian. The potential contribution of late Paleozoic tectonic linears to total air-photo linears is overwhelmed by those caused by dikes. The linears in the Cambrian rhyolites of the Arbuckle anticline mostly have a tectonic origin, but cannot, in my opinion, be used to determine stress directions during Pennsylvanian deformation.

Southern Oklahoma, and particularly the Arbuckle Mountains, can be used to document one of the most remarkable and closely constrained examples of inheritance to be found. The intrusion of dikes 1,350–1,400 Ma ago established a location and direction of weakness that was later the focus of Cambrian rifting. Subsequent Paleozoic sedimentary facies and thicknesses were controlled by the aulacogen location. Finally, in the Pennsylvanian, more than a billion years after initial dike intrusion, the structural style and direction were completely dependent on a generous geological inheritance.

ACKNOWLEDGMENTS

The measurement of the linears took several months and was done nearly 20 years ago. The interpretation of their possible meaning took much longer. It has evolved because understanding of the relation between the Ouachita foldbelt and foreland structures has improved substantially. The concept of Ouachita basin opening by Bill Thomas has been pivotal in this improvement, and the outboard jigsaw block of Josh Rosenfeld seems to provide answers to otherwise difficult Ouachita problems. I have had long running disagreements and discussions with foreland and Ouachita workers who changed or tempered my own beliefs. John Wickham, Bill Thomas, George Viele, Nowell Donovan, Jerry Kendall, Bill Muehlberger, Bill Brown, Kasper Arbenz, and others have provided stimulating and sometimes spirited discussions on these problems that have caused me to question my own thinking (if only briefly). They are blameless for the interpretation presented in this paper. Gloria Eisenstadt and John Wickham reviewed the manuscript and made a number of worthwhile suggestions, some of which I actually heeded.

REFERENCES CITED

Amsden, T. W., 1980, Hunton Group (Late Ordovician, Silurian, and Early Devonian) in the Anadarko basin of Oklahoma: Oklahoma Geological Survey Bulletin 129, 136 p.

Bickford, M. E.; and Lewis, R. D., 1979, U–Pb geochronology of the exposed basement rocks in Oklahoma: Geological Society of America Bulletin, v. 90, p. 540–544.

Brewer, J. A.; Good, R.; Oliver, J. E.; Brown, L. D.; and Kaufman, S., 1983, COCORP profiling across the southern Oklahoma aulacogen: overthrusting in the Wichita Mountains and compression within the Anadarko basin: Geology, v. 11, p. 109–114.

Brown, W. G., 1984, Washita Valley fault system: a new look at an old fault, *in* Borger, J. G., III (ed.), Technical proceedings of the American Association of Petroleum Geologists, Mid-continent Section,

1981 regional meeting: Oklahoma City Geological Society, p. 68–80.

Carter, D. W., 1979, A study of strike-slip movement along the Washita Valley fault, Arbuckle Mountains, Oklahoma: Shale Shaker, v. 30, p. 80–108.

Denison, R. E., 1973, Basement rocks in the Arbuckle Mountains, *in* Ham, W. E. (ed.), Regional geology of the Arbuckle Mountains, Oklahoma: Oklahoma Geological Survey Special Publication 73-3, p. 43–46.

_____ 1982, Geologic cross section from the Arbuckle Mountains to the Muenster arch in southern Oklahoma and Texas: Geological Society of America Map and Chart Series MC-28R, 8 p.

_____ 1989, Foreland structures adjacent to the Ouachita foldbelt, *in* Hatcher, R. D., Jr.; Thomas, W. A.; and Viele, G. W. (eds.), The Appalachian-Ouachita orogen in the United States: Geological Society of America, The Geology of North America, v. F-2, p. 681–688.

Donovan, R. N., 1988, The southern Oklahoma aulacogen: a study in inheritance: American Association of Petroleum Geologists Annual Meeting Field Trip Guidebook, 72 p.

Gilbert, M. C.; and Denison, R. E., 1993, Basement rocks in the Wichita Mountains, *in* Reed, J. C., Jr.; Bickford, M. E.; Houston, R. S.; Link, P. K.; Rankin, D. W.; Sims, P. K.; and Van Schmus, W. R. (eds.), Precambrian: conterminous U.S.: Geological Society of America, The Geology of North America, v. C-2, p. 303–314.

Granath, J. W., 1989, Structural evolution of the Ardmore basin, Oklahoma; progressive deformation in the foreland of the Ouachita collision: Tectonics, v. 8, p. 1015–1036.

Ham, W. E., 1969, Regional geology of the Arbuckle Mountains, Oklahoma: Oklahoma Geological Survey Guidebook 17, 52 p.

Ham, W. E.; and McKinley, M. E., 1954, Geologic map and sections of the Arbuckle Mountains, Oklahoma: Oklahoma Geological Survey Map A-2, 1 sheet, scale 1:72,000.

Ham, W. E.; Denison, R. E.; and Merritt, C. A., 1964, Basement rocks and structural evolution of southern Oklahoma: Oklahoma Geological Survey Bulletin 95, 302 p.

Ham, W. E.; and McKinley, M. E. [1954]; revised by Johnson, K. S., 1990, Geologic map and sections of the Arbuckle Mountains, Oklahoma: Oklahoma Geological Survey Map GM-31, sheet scale 1:100,000.

Hoffman, P. F.; Dewey, J. F.; and Burke, K., 1974, Aulacogens and their genetic relations to geosynclines, with a Proterozoic example from Great Slave Lake, Canada, *in* Dott, R. H., Jr.; and Shaver, R. H. (eds.), Modern and ancient geosynclinal sedimentation: Society of Economic Paleontologists and Mineralogists Special Publication 19, p. 38–55.

Huffman, G. G.; Hart, T. A.; Olson, L. J.; Currier, J. D.; and Ganser, R. W., 1978, Geology and mineral resources of Bryan County, Oklahoma: Oklahoma Geological Survey Bulletin 126, 113 p.

Jacobson, M. I., 1984, The Harrisburg trough, Stephens County, Oklahoma; an update, *in* Borger, J. G., III (ed.), Technical proceedings of the American Association of Petroleum Geologists, Mid-continent Section, 1981 regional meeting: Oklahoma City Geological Society, p. 127–137.

Johnson, K. S.; Amsden, T. W.; Denison, R. E.; Dutton, S. P.; Goldstein, A. G.; Rascoe, B.; Sutherland, P. K.; and Thompson, D. M., 1988, Southern Midcontinent region, *in* Sloss, L. L. (ed.), Sedimentary cover—North American craton; U.S.: Geological Society of America, Geology of North America, v. D-2, p. 307–359.

Kluth, C. F.; and Coney, P. J., 1981, Plate tectonics of the Ancestral Rocky Mountains: Geology, v. 9, p. 10–15.

Lowe, D. R., 1985, Ouachita trough; part of a Cambrian failed rift system: Geology, v. 13, p. 790–793.

McConnell, D. A., 1989, Determination of offset across the northern margin of the Wichita uplift: Geological Society of America Bulletin, v. 101, p. 1317–1332.

Palladino, D. L., 1986, Structural analysis of a portion of the Washita Valley fault zone, Arbuckle Mountains, Oklahoma: Baylor University unpublished M.S. thesis, 150 p.

Perry, W. J., Jr., 1989, Tectonic evolution of the Anadarko basin region, Oklahoma: U.S. Geological Survey Bulletin 1866A, 19 p.

Petersen, F. A., 1983, Foreland detachment structures, *in* Lowell, J. D.; and Gries, R. (eds.), Rocky Mountain foreland basins and uplifts: Rocky Mountain Association of Geologists Guidebook, p. 65–77.

Tanner, J. H., III, 1967, Wrench fault movement along the Washita Valley fault, Arbuckle Mountain area, Oklahoma: American Association of Petroleum Geologists Bulletin, v. 51, p. 126–141.

Tapp, J. B., 1988, Structural styles in the Arbuckle Mountains, southern Oklahoma, *in* Hayward, O. T. (ed.), Geological Society of America Centennial Field Guide—South-Central Section, v. 4, p. 177–182.

Taylor, C. H., 1915, Granites of Oklahoma: Oklahoma Geological Survey Bulletin 20, 108 p.

Thomas, W. A., 1977, Evolution of the Appalachian-Ouachita salients and recesses from reentrants and promontories in the continental margins: American Journal of Science, v. 277, p. 1233–1278.

_____ 1991, The Appalachian-Ouachita rifted margin of the southeastern North America: Geological Society of America Bulletin, v. 103, p. 415–431.

Tomlinson, C. W., 1952, Odd geologic structures of southern Oklahoma: American Association of Petroleum Geologists Bulletin, v. 36, p. 1820–1840.

White, W. S., 1991, Analysis of fracture patterns in the Arbuckle anticline and Tishomingo granite regions, Arbuckle Mountains, Oklahoma: Texas Christian University unpublished M.S. thesis, 109 p.

Wickham, J. S., 1978, The southern Oklahoma aulacogen, *in* Structural style of the Arbuckle region: Geological Society of America South-Central Section, Field Trip Guidebook 3, p. 8–40.

The Collings Ranch Conglomerate of the Oklahoma Arbuckles: Its Origin and Tectonic Significance

Kevin Pybas, Ibrahim Cemen, and Zuhair Al-Shaieb
Oklahoma State University
Stillwater, Oklahoma

ABSTRACT.—The Collings Ranch Conglomerate, well exposed in the Turner Falls area of the Arbuckle Mountains in Oklahoma, mainly contains pebble- to boulder-size limestone fragments derived primarily from the Ordovician rocks of the Arbuckle and Tishomingo anticlines. The conglomerate was deposited in a relatively small basin, which we have named the Collings Ranch basin. It includes many characteristics of an alluvial-fan deposit, such as: (1) size of clasts ranging from pebble to boulder, (2) angularity of clasts, (3) poor sorting, (4) nearby source area, and (5) a red-colored silt to clay matrix. Measurements of the long-axis orientation of imbricated clasts indicate that predominant transport direction was from south to north, with some from north to south. The absence of distinguishable braided streams, as well as the rarity of fine sediments, indicates that deposits are primarily channel fill and sieve deposits in the proximal region of the fan.

The Collings Ranch basin is a divergent strike-slip (pull-apart) basin developed in response to left-stepping along the left-lateral Washita Valley fault zone. The Collings Ranch Conglomerate of the basin is folded into a relatively broad syncline and is intensely faulted, primarily by strike-slip faults associated by the Washita Valley fault zone, which has a main strand and a north strand in the Turner Falls area. About 2 mi east of Turner Falls, the south strand steps to the right and forms a small convergent (push-up) region which has caused thrusting of Arbuckle Group rocks over the Collings Ranch Conglomerate along the main strand.

The presence of both divergent and convergent zones along the Washita Valley fault zone suggests that it had substantial strike-slip movement during and after deposition of the Collings Ranch Conglomerate.

INTRODUCTION

One of the major structural features of southern Oklahoma is the Washita Valley fault zone. Wickham (1978) suggested that the fault was formed during the rifting stage of the southern Oklahoma aulacogen as a predominantly normal slip fault, and it was reactivated as a strike-slip fault during the deformation stage of the aulacogen during Pennsylvanian time. The deformation stage is recorded, along with other Pennsylvanian structural features and sedimentary rocks, by the Pennsylvanian Collings Ranch Conglomerate, exposed in the Turner Falls area of the Arbuckle Mountains (Figs. 1 and 2A).

The Collings Ranch Conglomerate is located on the northeastern flank of the most westerly fold (Arbuckle anticline) of the Arbuckle Mountains. It is situated in a northwest–southeast-trending basin which here is named the Collings Ranch basin. The conglomerate unconformably overlies steeply dipping Ordovician rocks on the north, and is bounded on the south by the through-going main strand of the Washita Valley fault zone.

Ham (1954) in a comprehensive study of the Collings Ranch Conglomerate, described the unit in detail and determined its age as Middle Virgilian, based on fossils. He proposed that the Collings Ranch Conglomerate was deposited in a graben and pointed out that most of the clasts in the conglomerate were derived from rocks exposed in the Arbuckle and Tishomingo anticlines. Wickham (1978), Brown (1984), Pybas and Cemen (1986,1987) proposed that the Collings Ranch Conglomerate was deposited as a result of left-lateral strike-slip movement along a bend in the Washita Valley fault in the Turner Falls area (Fig. 2A).

The main purpose of this paper is to reconstruct the Pennsylvanian tectonic-stratigraphic evolution of the Collings Ranch basin. This study is concerned especially with the detection of structural relationships between the Collings Ranch Conglomerate and the nearby Washita Valley fault zone. Therefore, we describe and interpret the

Pybas, Kevin; Cemen, Ibrahim; and Al-Shaieb, Zuhair, 1995, The Collings Ranch Conglomerate of the Oklahoma Arbuckles: its origin and tectonic significance, *in* Johnson, K. S. (ed.), Structural styles in the southern Midcontinent, 1992 symposium: Oklahoma Geological Survey Circular 97, p. 132–143.

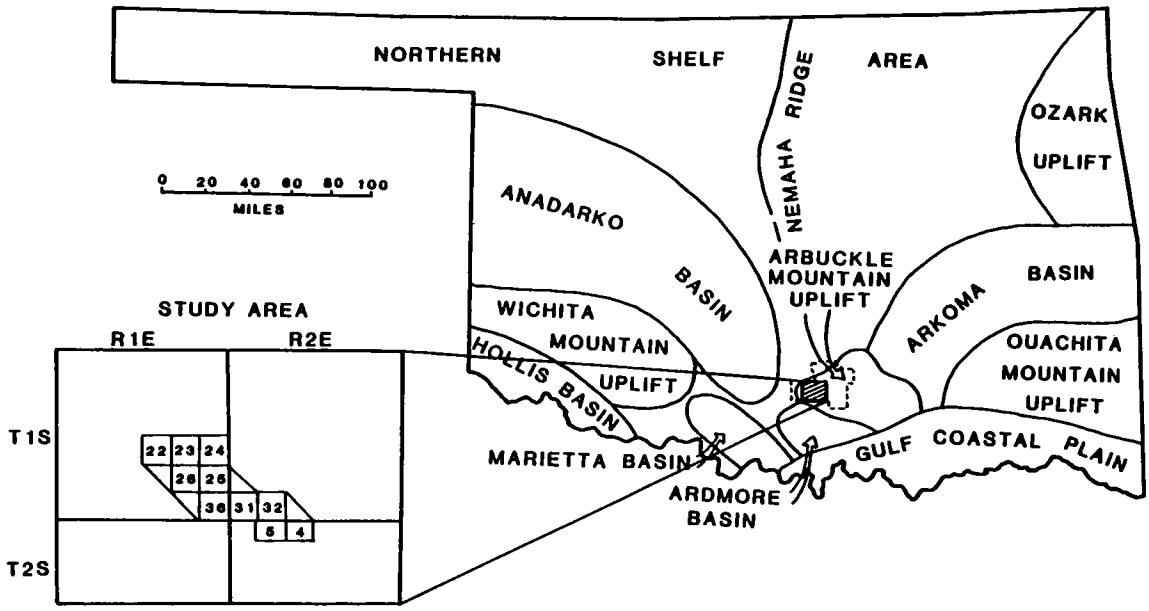


Figure 1. Tectonic map of Oklahoma. Enlargement in the bottom left shows the area of Figure 2A.

structural geology, lithology, clast content, sedimentary environments, petrology, and diagenesis of the Collings Ranch Conglomerate and its relationship with the Washita Valley fault zone. We have also compared the Collings Ranch basin with four other well-studied divergent strike-slip basins.

The various pre-Pennsylvanian rock units exposed in the Arbuckle Mountains are shown, in a generalized form, in the columnar section of Figure 3. Detailed descriptions of the formations are contained in papers by Dunham (1955), Fay (1969), and Ham (1973).

COLLINGS RANCH CONGLOMERATE

The Collings Ranch Conglomerate unconformably overlies pre-Pennsylvanian rocks in the Arbuckle Mountains. Exposed bedrock units beneath the conglomerate are the West Spring Creek Formation of the Lower Ordovician Arbuckle Group; Joins, Oil Creek, McLish, Tulip Creek, and Bromide Formations of the Middle Ordovician Simpson Group; and the Middle Ordovician Viola Limestone (Figs. 2 and 3).

We have measured and described 265 ft of the Collings Ranch Conglomerate (Fig. 4) in an incomplete section exposed along northbound Interstate 35. Ham (1954) estimated the restored thickness of the Collings Ranch Conglomerate to be 2,000–3,000 ft. The conglomerate has been penetrated by two oil wells. A well in the northwestern part of the basin encountered 900 ft of conglomerate; the second well penetrated 1,600 ft of conglomerate in the central part of the basin (Robert Allen, personal communication, 1987). The location of the second well is close to the area of maximum curvature of the left-stepping along the Washita Valley fault zone. This area is probably one of the deeper parts of the basin. Therefore, the restored thickness of the conglomerate is probably more than 1,600 ft, and may be as much as 3,000 ft, as suggested by Ham (1954).

Lithology and Clast Content

The Collings Ranch Conglomerate is a poorly sorted, subangular to subrounded, limestone-boulder conglomerate. It is well cemented and generally well stratified in thick, parallel-bedded layers. In exposures along Interstate 35, beds are separated by shear zones (Fig. 4). In the absence of shear zones, beds are distinguished by differences in clast size and the amount of matrix present. Imbricate structures are common throughout the conglomerate, but fossils are absent.

Rock fragments making up the conglomerate range from angular sand-sized grains to subangular boulders 3 ft in diameter. Boulders and cobbles generally constitute approximately 60–80% of the rock; the remainder is an interstitial matrix of pebble- and sand-size fragments bonded by a calcic cement. Hematite is distributed throughout the carbonate matrix; it is responsible for the predominantly dark-red color of the Collings Ranch Conglomerate, and it indicates deposition and diagenesis in subaerial conditions.

The oldest rock fragments in the Collings Ranch Conglomerate are Cambrian dolomites of the Butterly and Royer Formations. The most abundant identifiable rock fragments are from the Lower Ordovician McKenzie Hill, Cool Creek, Kindblade,

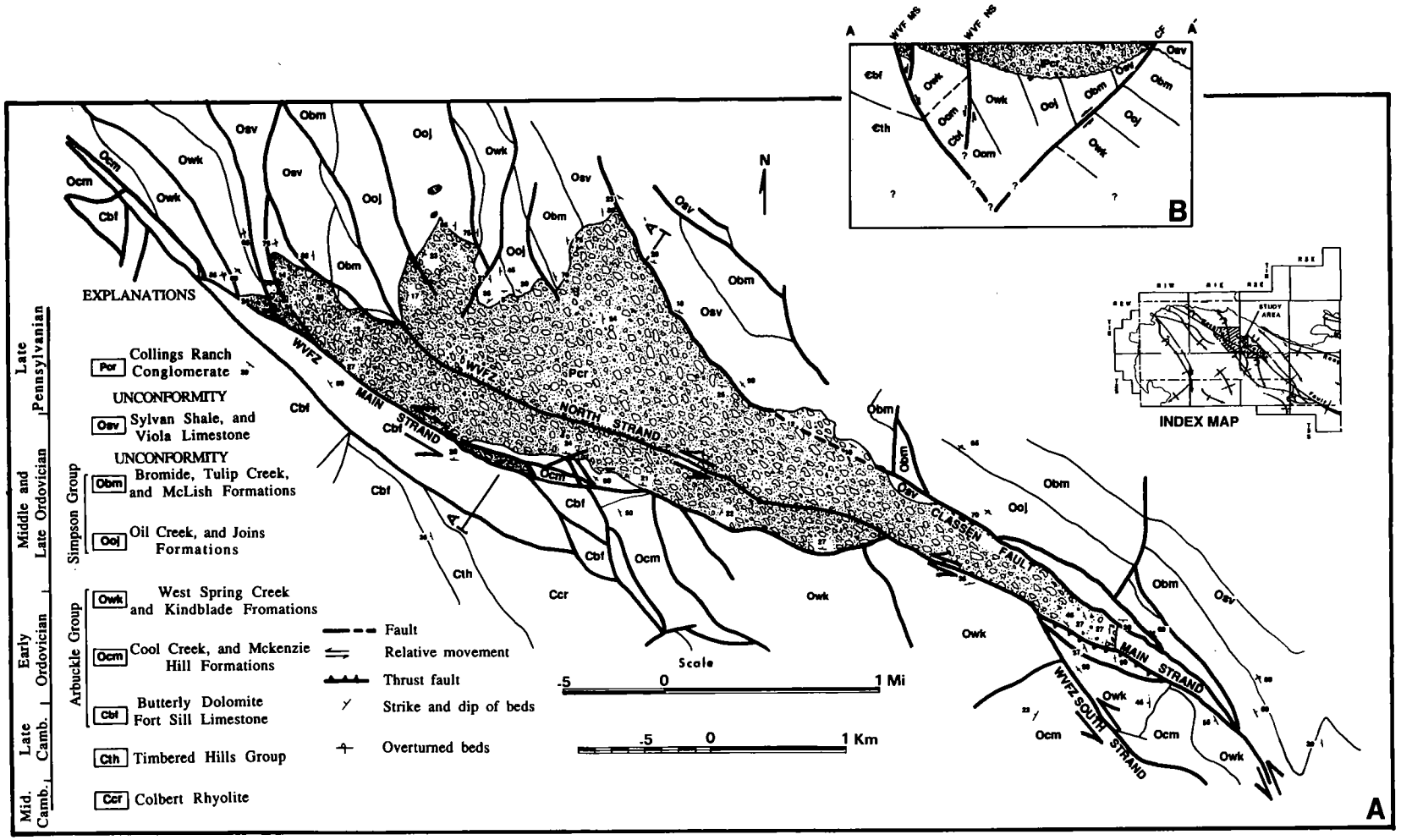


Figure 2. *A*—Geologic map of the Turner Falls area where the Collings Ranch Conglomerate is well exposed. The index map shows the major structural features of the western part of the Arbuckle Mountains and the location of the Turner Falls area. *B* (upper right)—Simplified cross section through the line A–A′. Abbreviations on map: WVFZ = Washita Valley fault zone. Abbreviations on cross section: WVFMS = Washita Valley fault zone, main strand; WVFNS = Washita Valley fault zone, north strand; CF = Classen fault.

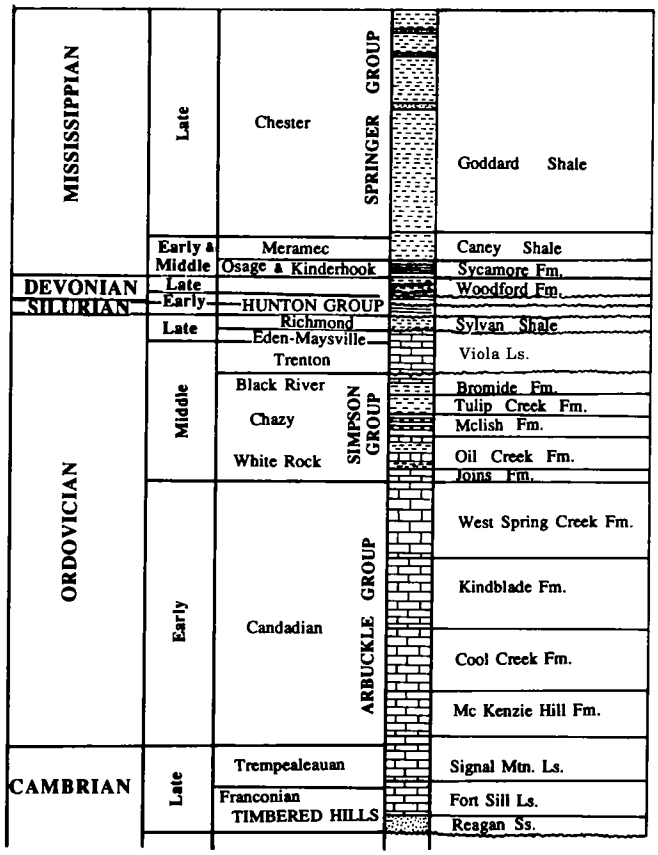


Figure 3. Generalized columnar section of the pre-Pennsylvanian rock units of the Arbuckle Mountains, Oklahoma.

and West Spring Creek Formations. Fragments of rocks younger than the Arbuckle Group are also present; they include fragments derived from the Middle Ordovician Simpson Group, and from the Upper Ordovician Hunton Group, Viola Limestone, and Sylvan Shale. Fragments of fine-grained dolomitic limestone, peloidal limestone, and algal or stromatolitic limestone are also abundant. The sources of these fragments were not identified.

Structural Geology

The main strand of the Washita Valley fault zone bounds the Collings Ranch Conglomerate on the south. The north strand of the fault zone cuts through the conglomerate. The two strands are almost vertical and join in the eastern part of the study area (Fig. 2A).

The geometry of the main strand suggests a left-stepover of segments of the Washita Valley fault zone. Therefore, we suggest, as did Wickham (1978), Brown (1984), and Pybas and Cemen (1986, 1987), that the Collings Ranch Conglomerate was deposited in a pull-apart basin which formed as a result of left-stepover along the Washita Valley fault zone.

The Collings Ranch Conglomerate is bounded on the northeast by the Classen fault and an unconformable contact with Ordovician rocks to the north and northeast. The Classen fault joins the main strand of the Washita Valley fault zone in the southeastern part of the study area (Fig. 2A). These faults are interpreted to merge in the subsurface within a negative flower-structure zone (Fig. 2B).

The unconformable contact between the conglomerate and underlying rocks is observed in the north-central part of the area of Figure 2A. It is also observed along the Interstate-35 road cuts, where the conglomerate overlies the faulted contact and is unconformable over the vertical beds of the Ordovician Viola Limestone (Fig. 5). This fault can be traced below the conglomerate to become the Classen fault, and is well exposed at an outcrop behind the Turner Falls Inn. At this outcrop, the conglomerate strikes 115° and dips 20° to the south, whereas the Viola Limestone strikes 130° and is approximately vertical. There, the Classen fault dips ~60° southwest. These observations suggest that the Classen fault controlled deposition of the Collings Ranch Conglomerate, which is interpreted to be an alluvial fan deposit.

In the southeastern part of the area (Fig. 2A), the main strand steps to the right and forms a small convergent (push-up) region that has thrust Arbuckle Group rocks (Fig. 2A, Owk) over the Collings Ranch Conglomerate along the main strand. The reverse separation is along the northern edge of a small (~1 × 0.5 mi) convergent (transpressional) zone. The area is delineated by reverse separation on the main strand and by left-lateral movement along the south strand of the Washita Valley fault zone (Figs. 2A and 6A).

Several small folds in the uplifted Arbuckle Group rocks are adjacent to the main strand. A stereonet plot of the trend and plunge of fold-axes (Fig. 6B) suggests that this folding occurred due to the movement which formed the zone of convergence, because the axial planes of these folds are roughly parallel to the strike of the main strand of the Washita Valley fault zone.

The Collings Ranch Conglomerate is folded into relatively broad, gently dipping, northwest–southeast-trending synclines and anticlines. An anticline and syncline pair is well exposed along Interstate 35 (Fig. 7). They are flexural-slip folds with well-developed shear zones containing rotated, but unbroken, clasts (Fig. 8). This suggests to us that the folds formed before lithification of the conglomerate and that they were contemporaneous with tectonism and deposition. If folding occurred after

lithification, broken conglomerate fragments would have been observed along the shear zones of the flexural-slip folds.

Depositional Environments

The Collings Ranch Conglomerate records unusual tectonic conditions, which permitted the erosion of limestone as pebbles, cobbles, and boulders, rather than by dissolution. This implies sharp uplift and high relief, best achieved along a fault scarp. These conditions could have prevailed along the Washita Valley fault zone during Pennsylvanian time. If so, the resulting conglomerate could be interpreted as an alluvial fan deposit. Indeed, the Collings Ranch Conglomerate includes many characteristics of alluvial fan deposits, such as: (1) size of clasts ranging from pebble to boulder, (2) angularity of clasts, (3) poor sorting, (4) nearby source area, and (5) silt to clay matrix with red color. The presence of red clay (hematite precipitate), and the absence of organic matter, suggest that sedimentation was in an oxidizing environment, not subject to reducing conditions.

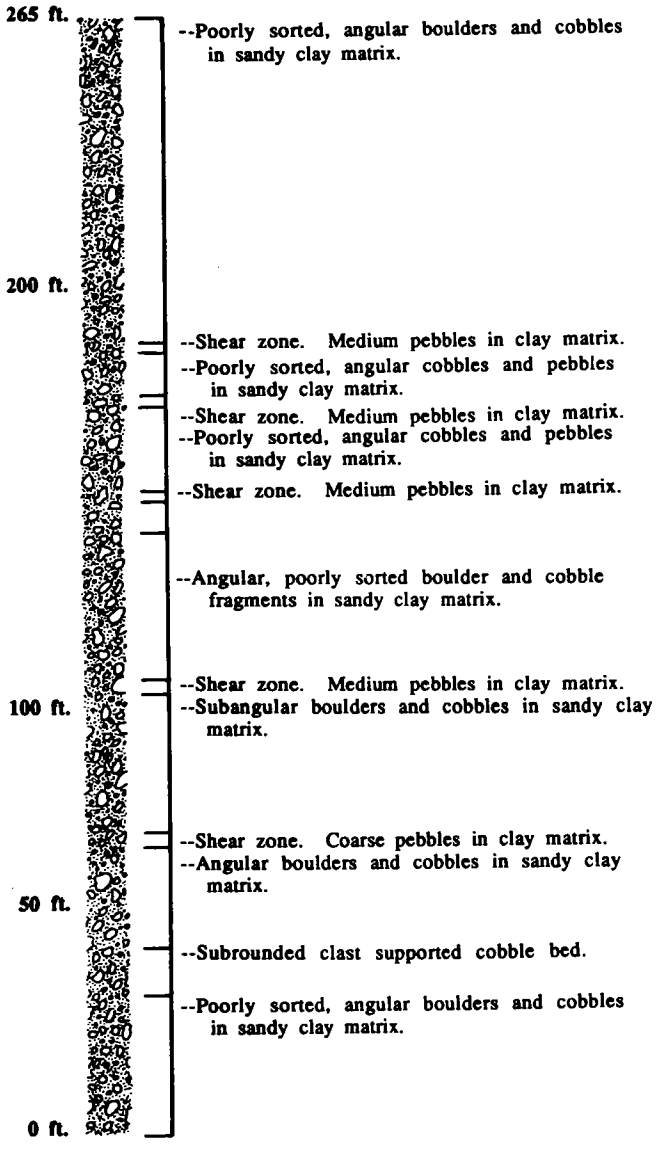


Figure 4. Incomplete measured columnar section of the Collings Ranch Conglomerate. The section was measured along I-35 northbound, east of the scenic-view point.

The Collings Ranch Conglomerate contains a limited suite of sedimentary structures, characteristic of alluvial fan deposits. Imbrication of the clasts is common, but cross-bedding is quite rare. Transport directions were inferred from a total of 143 measurements of the long-axis orientation of imbricated clasts at six localities (Fig. 9). The measured imbrications demonstrate a pattern of basin filling from the margins. The predominant transport direction was from south–southwest to north–northeast in the central part of the Collings Ranch basin, but it was generally from north to south in the eastern portion of the basin.

The absence of distinguishable braided streams, as well as the rarity of fine sediments, suggest that these are channel-fill and sieve deposits in the proximal region of the fan. It is possible that finer-grained, braided-stream deposits once existed but have since been eroded. However, the small size of the Collings Ranch basin, the nearby source area, and the likely arid climate probably precluded the development of braided streams.

Petrography and Diagenesis

In thin-section analysis, detrital quartz and chert were observed in addition to the lithologies described macroscopically. Limestone clasts comprise up to 85% of total constituents in the thin-sections analyzed (Table 1). They include micrite, dismicrite, biomicrite, sandy micrite, oosparite, pelsparite, biosparite, and sparite. Some of the limestone fragments have been extensively fractured in-situ and recemented with sparite. Diagenetic constituents include hematite, sparry calcite, dolomite, illite, and kaolinite. The majority of clasts show evidence of some degree of pressure solution. Sutured grain boundaries are common and they form as the result of extensive pressure solution. This suggests that post-depositional deformation other than compaction has influenced the Collings Ranch Conglomerate. This

deformation was probably associated with late movement along the Washita Valley fault zone.

Sparry calcite is both a cementing agent and a product of recrystallization of surrounding limestone grains. The large amount of spar is due to extensive pressure solution within the rock. In some instances, sutured grain boundaries are all that is left of what once were grains. The extensive pressure solution is probably a result of pre-cementation deformation associated with movements along the Washita Valley fault zone. The macroscopic effect of this deformation was seen in the flexural-slip



Figure 5. Angular unconformity between the Pennsylvanian Collings Ranch Conglomerate (CRC) and the underlying Viola Limestone and Bromide Formation. The Classen fault (CF) separates the Bromide Formation (B) from the Collings Ranch Conglomerate.

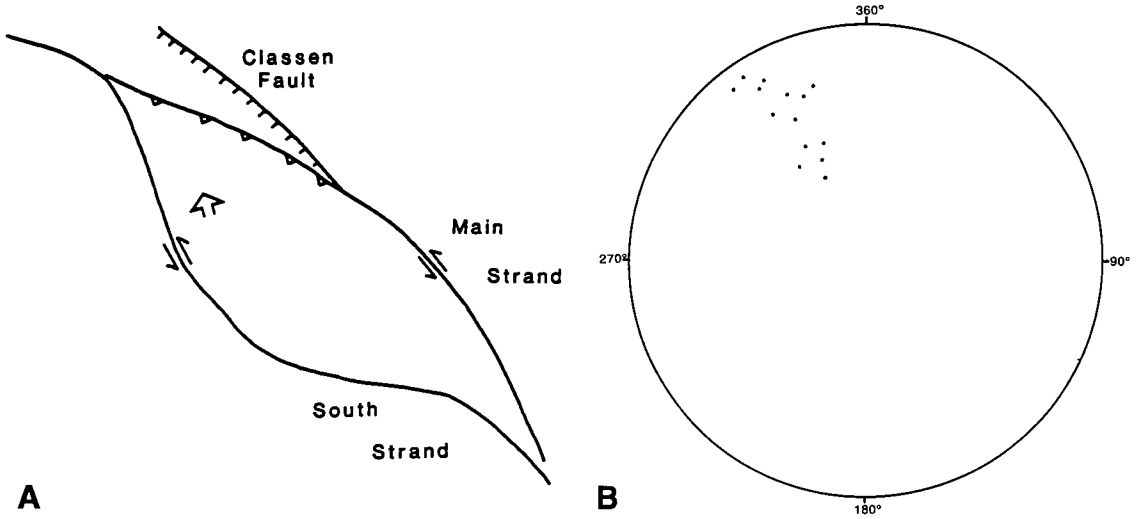


Figure 6. *A*—Sketch of the small uplifted area (push-up) along the Washita Valley fault zone. The main strand of the fault zone shows reverse separation, which brings the Arbuckle Group limestones over the Collings Ranch Conglomerate. Arrow shows the direction of block movement that produced the convergent zone. *B*—A stereonet plot of fold-axis orientations of the folds within the Arbuckle Group in the area of small convergence south of the main strand segment that has reverse separation (Fig. 2A). All of the trends are roughly parallel to the strike of the main strand, which is about N. 65° W.



Figure 7. An anticline (right) and syncline (left-center) pair along Interstate 35.

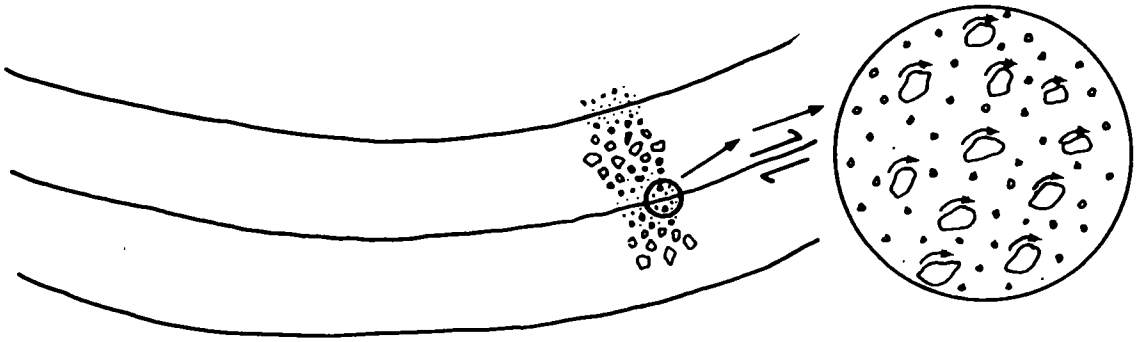


Figure 8. Sketch of a flexural slip fold showing shear zone with rotated, but unbroken, clasts.

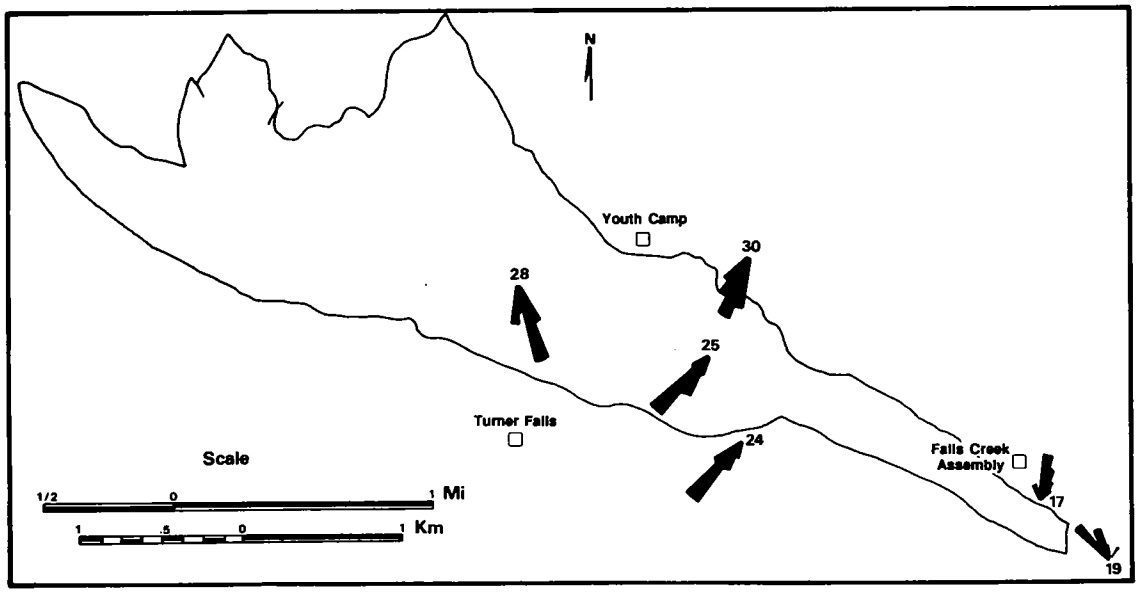


Figure 9. Paleocurrent directions at six locations within the Collings Ranch basin, based on a total of 143 long-axis orientations of clast imbrications.

TABLE 1. — MATRIX COMPOSITION OF COLLINGS RANCH CONGLOMERATE DETERMINED FROM THIN-SECTION POINT COUNTS OF 25 REPRESENTATIVE SAMPLES

Sample[a]	Detrital carbonate fragments (%)	Detrital chert fragments (%)	Detrital quartz fragments (%)	Authigenic carbonate cement (%)	Authigenic hematite (%)	Authigenic illite clay (%)
1	69	T[b]	T	22	8	—
2	55	1	1	35	8	—
3	76	T	2	18	3	—
4	70	2	1	19	7	T
5	75	—	—	19	6	—
6	82	T	1	14	—	2
7	65	1	2	25	7	—
8	72	2	3	17	6	—
9	65	2	2	23	8	—
10	66	1	2	24	7	—
11	68	3	2	19	8	—
12	88	T	T	4	7	—
13	81	1	T	12	5	—
14	64	—	T	30	5	—
15	70	—	—	23	7	—
16	60	—	T	30	9	—
17	91	—	T	6	2	T
18	77	—	1	17	5	—
19	78	—	T	14	7	—
20	75	1	1	16	7	—
21	70	1	2	18	9	—
22	72	—	4	17	7	—
23	57	T	5	27	10	—
24	58	—	7	26	9	—
25	65	—	4	24	7	—

[a]Matrix.
[b]T = trace.

folds of the Collings Ranch Conglomerate, which exhibit rotated but unbroken clasts along the shear zones.

Authigenic hematite observed in thin sections is both a grain-coating and a pore-filling cement (Table 1, Fig. 10). Hematite is also present along stylolites and sutured grain boundaries. Within the Collings Ranch Conglomerate, there are no distinct large areas of hematitic horizons, which suggests that sedimentation was quite steady. This is as expected, because rapid sedimentation and burial are typical of alluvial fan deposits.

Thin sections also contain authigenic dolomite. Well-defined zoned rhomboidal-carbonate grains, characteristic of dolomite, are present with hematite incorporated within the zone boundaries. However, staining indicates that the carbonate rhombohedra are calcitic and not dolomitic. These rhomboidal grains may have originally been dolomitic, but have since been dedolomitized.

No porosity could be identified in thin sections. If porosity is present in the Collings Ranch Conglomerate, it is probably as microporosity. The nonporous nature of the conglomerate may cause the formation to be a good caprock for oil trapped in underlying units.

Hematite precipitation was the earliest diagenetic event; it probably occurred under shallow-burial conditions in an oxidizing environment. Dolomite precipitation soon followed the hematite precipitation. Hematite incorporated within zone boundaries of the rhomboidal-carbonate grains indicate that dolomite precipitation began before the conclusion of hematite precipitation. Compaction and tectonic activity contributed to extensive dissolution of the carbonate fragments.

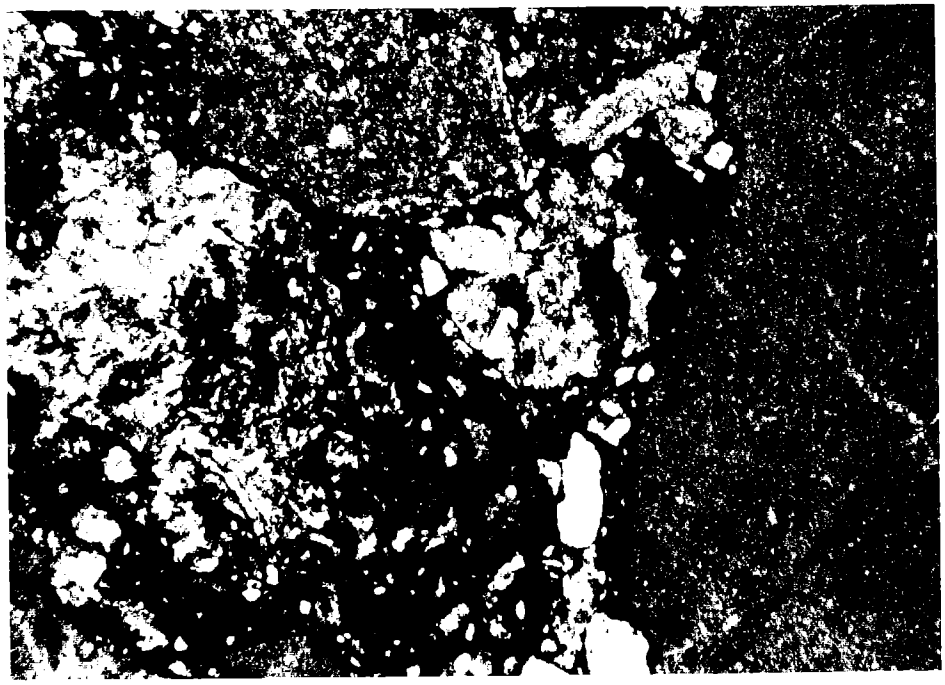


Figure 10. Photomicrograph showing authigenic hematite, both as grain-lining and pore-filling cement (×20, plane-polarized).

COMPARISON OF THE COLLINGS RANCH BASIN WITH OTHER STRIKE-SLIP BASINS

We have compared the structural and sedimentological characteristics of the Collings Ranch basin with other well-studied, divergent strike-slip basins of different sizes (Fig. 11). These basins are: the Devonian Hornelen basin in western Norway (Steel and Gloppen, 1980); the Miocene and Pliocene Furnace Creek basin of eastern California (Cemen and others, 1985; Cemen and Wright, 1988); the Miocene and Pliocene Ridge basin of southern California (Crowell, 1982); and the Pliocene Little Sulphur Creek basin of northern California (Nilsen and McLaughlin, 1985).

The Hornelen basin is bounded on the north and south by strike-slip faults (Fig. 11A). The northern fault is considered to have been a zone of major strike-slip movement that controlled sedimentation in the basin. The basin sediments form a broad east-plunging syncline, in which the synclinal axis is located close to the northern adge of the basin. The basin contains a cumulative sediment fill of 82,000 ft, and is ~40 mi long and 12 mi wide (Steel and Gloppen, 1980; Nilsen and McLaughlin, 1985).

The Furnace Creek basin is bounded by a major strike-slip fault zone to the north, the Furnace Creek fault zone which controlled sedimentation (Fig. 11B). The basin is ~30 mi long and ~10 mi wide (Cemen and Wright, 1988). The main sedimentary rock types in the basin are alluvial-fan conglomerate, sandstone, siltstone, mudstone, marl, and thin beds of freshwater limestone interbedded with siltstone. Gypsum and borate deposits are also present. The basin sediments are folded into broad anticlines and synclines, more or less parallel to the trend of the Furnace Creek fault zone (Cemen and others, 1985). The total thickness of sediments is >15,000 ft, about half of which was deposited during the early Pliocene at high sedimentation rates.

The Ridge basin is located between the San Andreas and San Gabriel faults in southern California (Fig. 11C). The basin developed as a stretched and sagged crustal wedge northeast of the San Gabriel fault, in the area where the fault has a curvilinear trace. It contains a cumulative sedimentary fill >23,000 ft thick, and the strata have been folded into broad asymmetric synclines and anticlines. The basin is ~20 mi long and 4–9 mi wide (Crowell, 1982).

The three Little Sulphur Creek basins were developed along the Maacama fault zone (Fig. 11D). The basins form part of a large number of Neogene nonmarine sedimentary basins of northern California. They extend along the Maacama fault zone for ~8 mi, and are bounded on the southwest by branching splays of the active right-lateral Maacama fault zone. The basins contain ~16,400 ft of sedimentary fill (Nilsen and McLaughlin, 1985).

This short summary of tectonic settings of the Hornelen, Furnace Creek, Ridge, and Little Sulphur Creek basins shows that these basins possess char-

acteristics similar to those of the Collings Ranch basin, despite important differences in age, size, and thickness of sedimentary-rock sequences. The Ridge and the three Little Sulphur Creek basins are especially similar to the Collings Ranch basin, although similarities also exist with the Hornelen and Furnace Creek basins.

The similarities between these basins can be summarized as follows:

1) All basins are elongate and parallel to the orientation of a major controlling strike-slip fault zone; in the Collings Ranch basin, it is the left-lateral Washita Valley fault zone.

2) Alluvial fan deposits are present along the margins of each basin. The alluvial fan deposits in the Hornelen, Furnace Creek, Ridge, and Little Sul-

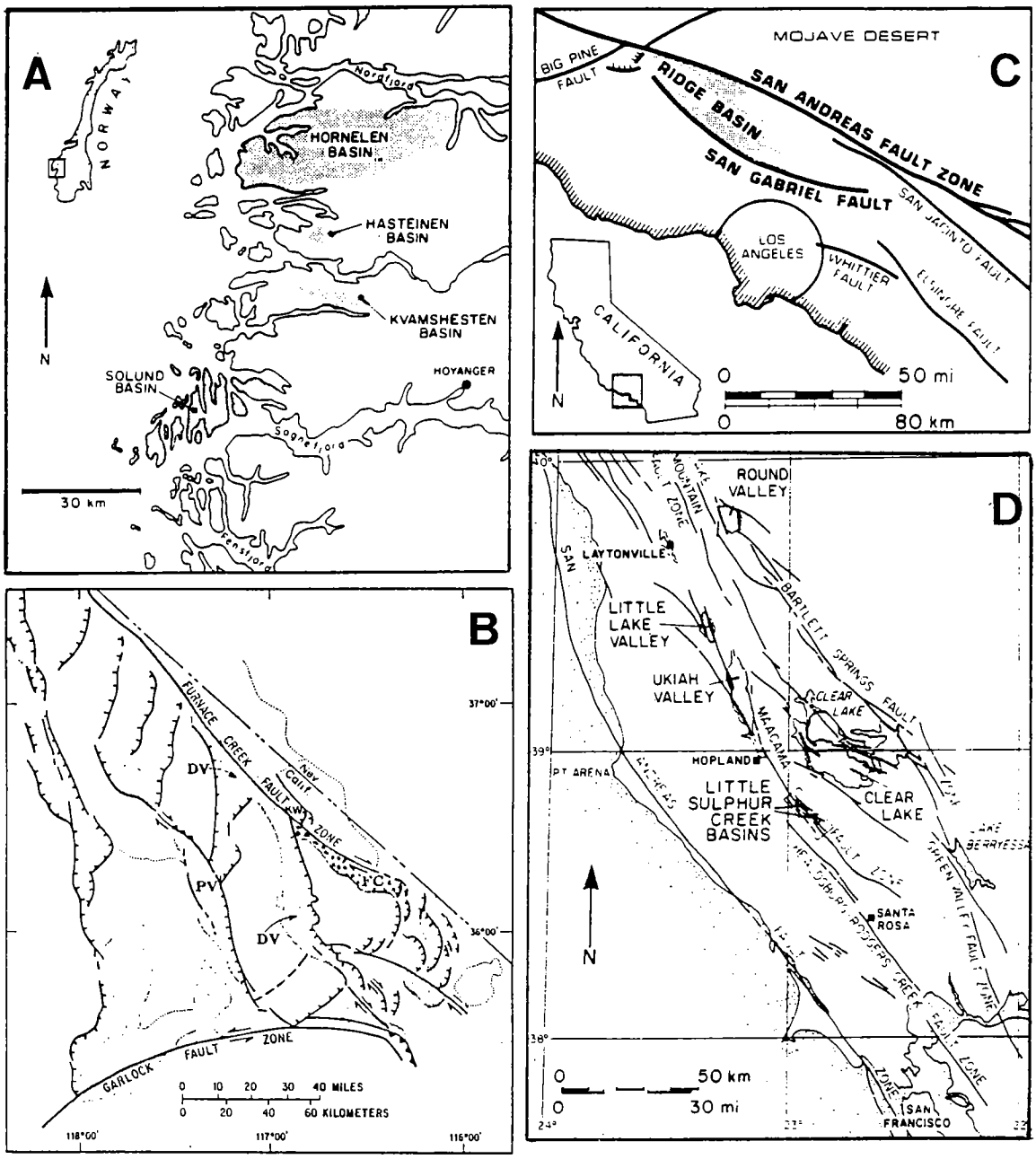


Figure 11. Index maps showing the locations of: *A*—Hornelen basin, *B*—Furnace Creek basin, *C*—Ridge basin, and *D*—three Little Sulphur Creek basins. Abbreviations in map *B:* DV = Death Valley; FC = Furnace Creek basin; PV = Panamint Valley.

phur Creek basins are more complex than those of the Collings Ranch basin, where alluvial fan deposits are the deposits present.

3) The basins were formed initially by extension, related to the lateral offset along the faults bounding the basin. In each basin, the major controlling strike-slip fault is through-going and forms a continuous bounding margin of the basin. The amount of left-lateral offset along the Washita Valley fault zone is probably greater than the length of the Collings Ranch basin, which is ~5 mi long. Estimates of the amount of left-lateral offset along the Washita Valley fault zone range from 3 mi (Ham, 1954) to 20 mi (Carter, 1979).

4) The sedimentary rocks in each basin were folded into broad anticlines and synclines, trending more or less parallel to the controlling fault of the basin. The Collings Ranch is also folded into broad synclines and anticlines.

5) Each basin has a length-to-width ratio of 3:1 to 5:1. For the Collings Ranch basin this ratio is 5:1.

SUMMARY AND CONCLUSIONS

It has been widely recognized that Pennsylvanian conglomerate units of southern Oklahoma record the deformation stage of the southern Oklahoma aulacogen. One of these conglomerates is the Late Pennsylvanian (Virgilian) Collings Ranch Conglomerate, which is well exposed in the Turner Falls area of the Arbuckle Mountains. The Collings Ranch Conglomerate is a limestone-cobble to -boulder conglomerate, derived primarily by erosion of Ordovician rocks from the Arbuckle and Tishomingo anticlines. The conglomerate was deposited in a divergent strike-slip basin that developed as a result of a left-stepping of the left-lateral Washita Valley fault zone. About 2 mi east of Turner Falls, right stepping along the south strand of the Washita Valley fault zone forms a small convergent (push-up) region which has caused Arbuckle Group rocks to be thrust over the Collings Ranch Conglomerate. The presence of both divergent and convergent zones along the Washita Valley fault zone suggests that the fault zone had substantial left-lateral strike-slip movement during, and probably after, deposition of the Collings Ranch Conglomerate.

The Collings Ranch Conglomerate is interpreted here as an alluvial fan deposit based on: (1) the size of clasts ranging from pebble to boulder; (2) the angularity of clasts; (3) poor sorting; (4) a nearby source area; and (5) a silt to clay matrix with red color. The clast imbrications measured suggest a pattern of basin filling from the margins. The predominant transport direction was from south–southwest to north–northeast in the central part of the Collings Ranch basin, but it was from north to south in the eastern part of the basin. The absence of distinguishable braided streams, as well as the rarity of fine sediments, indicate that deposition was accomplished primarily by channel fill and sieve deposits in the proximal region of the fan.

Hematite precipitation was the earliest diagenetic event which effected the Collings Ranch Conglomerate. It probably occurred under shallow-burial conditions in an oxidizing environment. Dolomite cementation soon followed the hematite precipitation. The nonpororous nature of the conglomerate may cause the formation to be a good caprock for oil trapped in underlying units.

The Collings Ranch basin has been compared with the Hornelen, Furnace Creek, Ridge, and three Little Sulphur Creek basins. This comparison has revealed that, despite important differences in age, size, thickness of basin fill, and regional geology, the Collings Ranch basin has a geometry and geologic history similar to other divergent strike-slip basins.

Characteristics that are common in the Collings Ranch and the other basins are:

1) Basins were formed adjacent to a significant strike-slip fault, with that fault forming the most prominent basin margin;

2) Basins were formed initially by extension;

3) Basin alignment is elongate and is parallel to the major controlling strike-slip fault;

4) The depositional environment along the basin margins is an alluvial fan; and

5) The basins are synclinal in overall structure, and the basin fill shows syndepositional structural features.

ACKNOWLEDGMENTS

This paper is mostly based on the M.S. thesis by Kevin Pybas, who did the field work in 1986 and 1987. We acknowledge the support provided by the Oklahoma Geological Survey for thesis fieldwork. Additional research in 1990 was carried out by ACS-PRF grant #22636-B8, awarded to Ibrahim Cemen. Acknowledgement is made to the donors of the Petroleum Research Fund, administered by the American Chemical Society, for the support of this research. Discussions, at various times, with James Helwig, Kristian Meisling, John Wickham, Nowell Donovan, and Bill Brown were very helpful. The final version of figures was drafted by Abdallà Azhari.

REFERENCES CITED

Brown, W. G., 1984, Washita Valley fault system—a new look at an old fault, *in* Boberg, J. G. (ed.), Proceedings of the American Association of Petroleum Geologists Mid-Continent Section meeting, p. 68–70.

Carter, D. W., 1979, A study of strike-slip movement along the Washita Valley fault, Arbuckle Mountains, Oklahoma: Shale Shaker, v. 30, p. 79–106.

Cemen, I.; Wright, L. A.; Drake, R. E.; and Johnson, F. C., 1985, Cenozoic sedimentation and sequence of deformational events at the southeastern end of the Furnace Creek strike-slip fault zone, Death Valley

region, California, *in* Biddle, K. T.; and Christie-Blick, N. (eds.), Strike-slip deformation, basin formation, and sedimentation: Society for Sedimentary Geology [SEPM] Special Publication 37, p. 127–141.

Cemen, I.; and Wright, L. A., 1988, Stratigraphy and chronology of the Artist Drive Formation, Furnace Creek basin, Death Valley, California, *in* Gregory, J. L.; and Baldwin, E. J. (eds.), Geology of the Death Valley region: South Coast Geological Society, Inc., Los Angeles, Annual Field Trip Guidebook 16, p. 77–87.

Crowell, J. C., 1982, The tectonics of Ridge basin, southern California, *in* Crowell, J. C.; and Link, M. H. (eds.), Geologic history of Ridge basin, southern California: Society for Sedimentary Geology [SEPM], Pacific Section, p. 25–42.

Dunham, R. J., 1955, Pennsylvanian conglomerates, structure, and orogenic history of Lake Classen area, Arbuckle Mountains, Oklahoma: American Association of Petroleum Geologists Bulletin, v. 39, p. 1–30.

Fay, R. O., 1969, Geology of the Arbuckle Mountains along Interstate 35, Carter and Murray Counties, Oklahoma: Ardmore Geological Society.

Ham, W. E., 1954, Collings Ranch Conglomerate, Late Pennsylvanian, in Arbuckle Mountains, Oklahoma: American Association of Petroleum Geologists Bulletin, v. 38, p. 2035–2045.

_____1973, Regional geology of the Arbuckle Mountains, Oklahoma: Oklahoma Geological Survey Special Publication 73-3, 61 p.

Ham, W. E.; McKinley, M. E.; and others, 1954 [revised by K. S. Johnson, 1990], Geologic map and sections of the Arbuckle Mountains, Oklahoma: Oklahoma Geological Survey Map GM-31, 1 sheet, scale 1:100,000.

Nilsen, T. H.; and McLaughlin, R. J., 1985, Comparison of tectonic framework and depositional patterns of the Hornelen strike-slip basin of Norway and the Ridge and Little Sulphur Creek strike-slip basins of California, *in* Biddle, K. T.; and Christie-Blick, N. (eds.), Strike-slip deformation, basin formation, and sedimentation: Society for Sedimentary Geology [SEPM] Special Publication 37, p. 79–103.

Pybas K.; and Cemen, I., 1986, Collings Ranch Conglomerate; an example of syndepositional deformation in an extensional strike-slip basin at the Arbuckle Mountains, Oklahoma [abstract]: Geological Society of America Abstracts with Programs, v. 18, no. 3, p. 260–261.

_____1987, Geology of the Turner Falls area, Arbuckle Mountains, Oklahoma: evidence for left-lateral strike-slip movement along the Washita Valley fault zone during the deformation stage of the southern Oklahoma aulacogen [abstract]: Geological Society of America Abstracts with Programs, v. 19, no. 3, p. 177.

Steel, R. M.; and Gloppen, T. G., 1980, Late Caledonian (Devonian) basin formation, western Norway: signs of strike-slip tectonics during infilling, *in* Ballance, P. F.; and Reading, H. G. (eds.), Sedimentation in oblique-slip mobile zones: International Association of Sedimentalogists Special Publication 4, p. 79–103.

Wickham, J. W., 1978, The southern Oklahoma aulacogen, *in* Wickham, J.; and Denison, R. (eds.), Field guide to the structural style of the Arbuckle region: Geological Society of America, South-Central Section, Guidebook for Field Trip No. 3, p. 8–41.

Geological Evolution of the Criner Hills Trend, Ardmore Basin, Oklahoma

J. Calvin Cooper
Houston, Texas*

ABSTRACT.—The complicated structural style of the Criner Hills trend and Ardmore basin documented by seismic profiles and densely spaced well penetrations results primarily from displacement and deformation above subhorizontal detachments deep within the basin. High angle faults have comparatively modest displacements. Substantial relative lateral shear, if present, must occur mainly across or below the major subhorizontal detachments. To a first approximation, the interference pattern of a simple succession of tectonic events is responsible for the present geometry.

A fold and thrust belt began to develop in the Late Mississippian; shortening progressed from southwest to northeast and continued until the early Atokan. Southwest verging folds and backthrusts are common. Progressive development of two major thrust sheets in the Criner Hills essentially corresponds with Wichitan phases I and II. Widespread erosion occurred over the entire trend.

During the Atokan, deformation was rooted in even deeper detachment levels. Rotation of fault blocks resulted in the simultaneous formation of compressional and extensional features. The evidence of Atokan extension is preserved in down-dropped blocks along the crest of the Criner Hills trend. Extension probably occurred in the Ardmore basin as well.

The region was buried during Desmoinesian and Missourian time. In Virgilian time, the preexisting fold-belt structures were reactivated and cross cut by a system of high-angle reverse faults related to basement shortening, perhaps with minor wrenching. Offsets of individual faults decrease from as much as 2,000 ft to zero within short distances, where fault offsets were transferred to other structures. This event caused uplift of the Criner Hills, reactivation of the present Criner fault as a backthrust, and broad folding of Pennsylvanian rocks associated with the Healdton–Hewitt–Lone Grove fault system. This shortening caused much of the Pennsylvanian section to be thrust out of the basin along low-angle detachments in the Springer shales.

Although evidence for strike-slip offset at higher levels along the Criner trend is minimal, this does not preclude relative strike-slip movement across subhorizontal detachments deep within the basin. It is probable that such a detachment underlies most of the Ardmore basin, and connects the Criner Hills with the Arbuckle anticline.

The Criner Hills and Ardmore basin is an area where elements of classic thrust tectonics blend with regional strike-slip faulting. In such a system, lateral offsets across steeply dipping faults are much less than offsets across gently dipping faults and high angle systems root into subhorizontal detachments.

INTRODUCTION

The Criner Hills trend is a structurally complicated uplift which separates the Ardmore basin from the Marietta basin in south-central Oklahoma (Fig. 1). For most of its surface exposure it appears as a low-relief, folded, and fault-bounded feature. Deformed lower Paleozoic carbonates are unconformably overlain by Pennsylvanian clastic units that were subsequently folded and faulted. Extensive unconformities, mapped on the surface, indicate that deformation occurred during Morrowan, Atokan, and late Missourian–Virgilian times, with mild rejuvenations in Permian and Cretaceous times. Subsurface data from well logs and seismic lines suggest that deformation of the Criner Hills trend began during Chesterian and continued throughout the Carboniferous. The present structural pattern resulted from the interaction of several phases of shortening with coeval extension. Cumulative uplift of the Criner Hills trend is more than 6 km (20,000 ft) relative to the Ardmore basin.

The uplift associated with the Criner Hills trend is really a collection of structural features. Individu-

*Present address: Milan, Italy

Cooper, J. C., 1995, Geological evolution of the Criner Hills trend, Ardmore basin, Oklahoma, *in* Johnson, K. S. (ed.), Structural styles in the southern Midcontinent, 1992 symposium: Oklahoma Geological Survey Circular 97, p. 144–160.

ally, none have much continuity along strike. Beyond the outcropping Criner Hills in Carter and Love Counties, Oklahoma (see maps in Jacobson, 1984; Granath, 1989; Perry, 1989), the trend continues in the subsurface to the northwest, and bifurcates into the Kirby, Fox–Graham, and Velma structures before it merges with the Washita Valley fault zone in Stephens County. To the southeast, as the trend traverses Love County, shortening across one of the major, shallow thrust sheets decreases and offset is transferred to a deeper thrust beneath the highly deformed intermediate-depth sheet which comprises most of the Enville structural complex. This trend continues in a complicated manner across Grayson County, Texas.

Data available for the Criner Hills trend and the Ardmore basin of south-central Oklahoma make it an outstanding place to constrain and unravel the

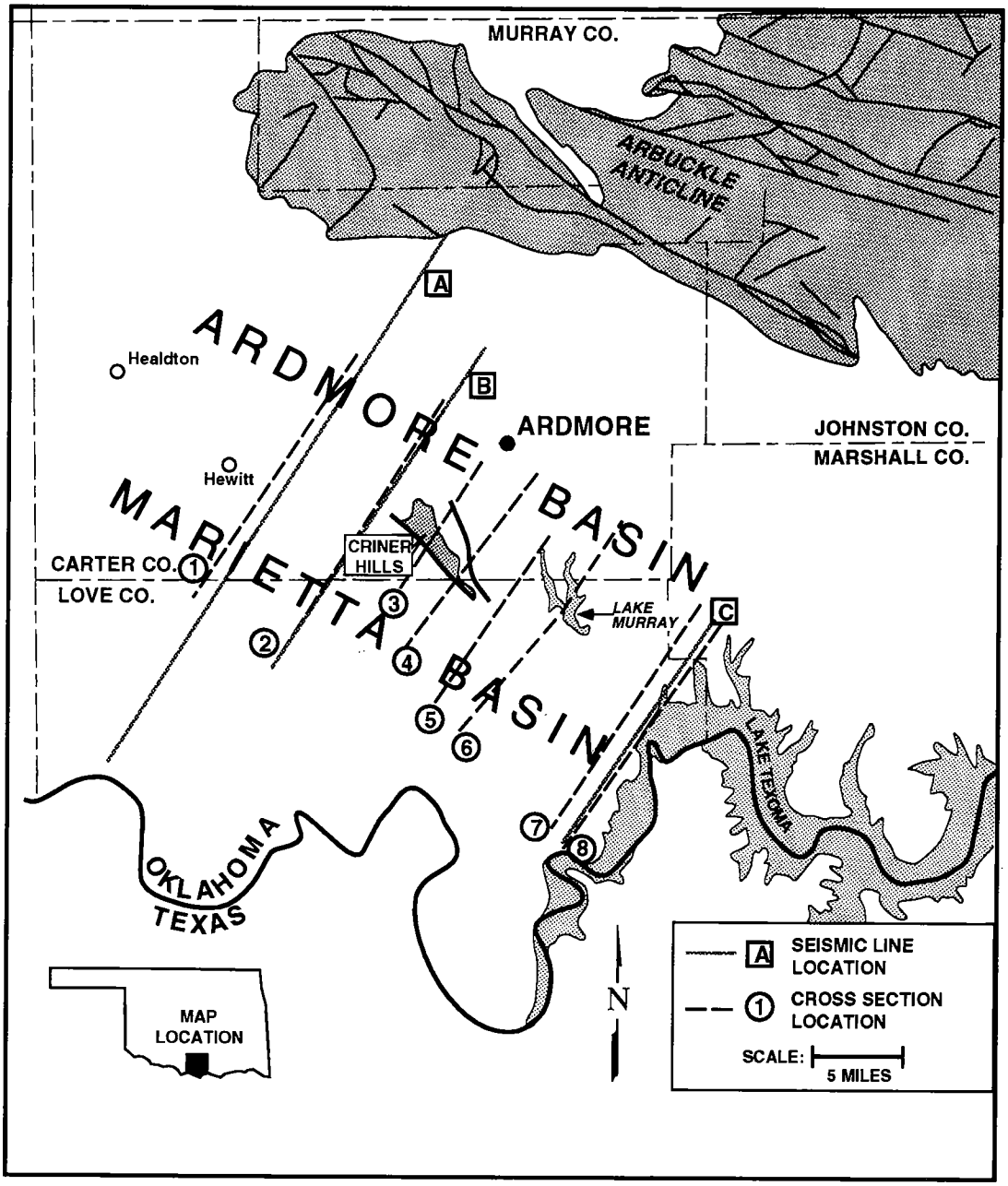


Figure 1. Generalized map showing the location of seismic lines and cross sections presented in this paper.

effects of complex deformation. It surely ranks among the most densely drilled areas on the planet, and borehole data are publicly available for the vast majority of the wells. Seismic lines of various vintages criss-cross the basin; unfortunately, most of these remain proprietary. Detailed studies of nearly every stratigraphic interval exist in public and private domains. Hundreds, if not thousands of earth scientists who have worked the basin are available to share their knowledge, even if it isn't published. Maps and cross sections are a bit more rare, but substantial amounts of material exist (e.g., Bullard, 1925; Frederickson, 1957; Lang, 1957; Westheimer, 1965; Denison, 1982).

This paper illustrates the geometry of the Criner Hills trend from the perspective of cross sections (Fig. 1). Key structural elements are first considered in their regional context based on a regional seismic line. Then progressing from the structurally simplest case, a series of cross sections shows how these key elements vary and interact along the trend.

All of the cross sections are simplified and reduced from those of a larger study that were constructed integrating well, seismic, and surface data. They were originally tied to structure maps at various time and depth levels that were generated from an extensive proprietary seismic and well data base covering the entire study area. Undoubtedly, these maps would help clarify the structural relationships described here. The maps also suggest leads and exploration concepts, so they have not been released for publication.

The text of this paper is mainly an effort to provide descriptions of the seismic interpretations and cross sections. Implications for the trend's structural evolution are considered. But even in this extremely data-rich basin, answers to many fundamental questions remain elusive.

STRATIGRAPHIC CONSIDERATIONS

The stratigraphy of the Criner Hills trend and the Ardmore basin is summarized in Figure 2. The depositional history is at least as complicated as the structural history. Those readers unfamiliar with the area should be assured that extensive research and numerous publications exist for nearly every stratigraphic interval. Johnson and others (1988) offers an excellent summary. Ham and others (1964) and Tomlinson and McBee (1959) provide a solid and detailed foundation for the correlations.

The stratigraphic section records a variety of depositional environments and the timing of structural events in the basin. All indications suggest a long and varied history. The basement rocks include Cambrian-age rhyolites, granites, and gabbros, presumably intruding, or lying unconformably above, the Precambrian Tishomingo Granite (Ham and others, 1964). From the onset of the Paleozoic Era, the study area, including the Marietta basin, was part of a gently subsiding trough known as the southern Oklahoma aulacogen in which more than 6,000 ft of Upper Cambrian and Lower Ordovician Arbuckle Group carbonates were deposited. Faulting and differential subsidence continued to play important roles throughout Arbuckle deposition. By Middle Ordovician time, a variety of clastic depositional systems represented by the Simpson Group were established in the basin. Gentle subsidence continued and more-homogeneous units were deposited until the Devonian, when differential uplift and erosion of the Hunton Group strata suggest segmentation of the aulacogen. Clastic foredeep sedimentation began in the

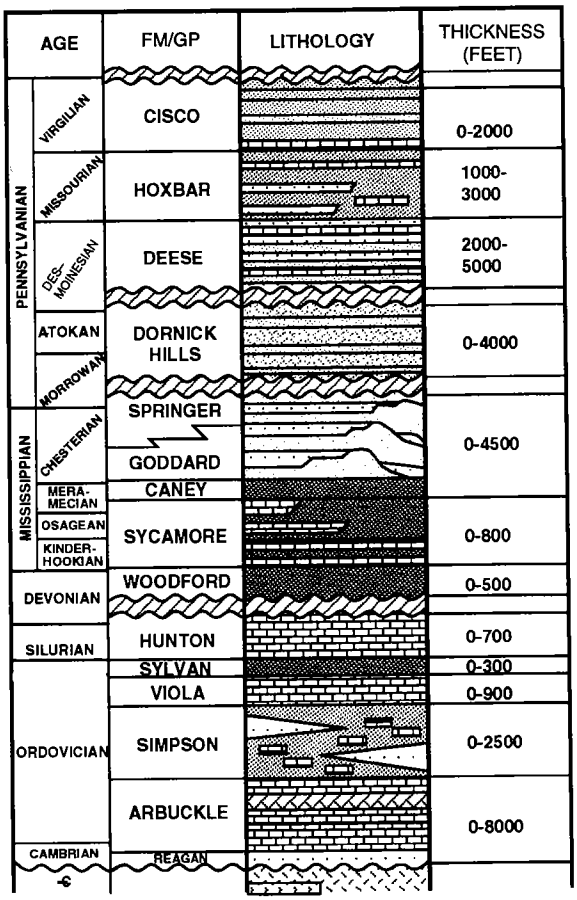


Figure 2. Simplified stratigraphic column for the Criner Hills and Ardmore basin as adopted for this paper. Cambrian and Precambrian basement rocks are not differentiated. Note that the Dornick Hills Group is Morrowan and Atokan in age. On cross sections (Figs. 3–6), the Morrowan part of the Dornick Hills Group is identified as Morrowan and is separated by an unconformity from the underlying Springer Formation. Strata identified as Dornick Hills on the cross sections are actually only the upper part of the Dornick Hills Group, which is largely Atokan in age.

Mississippian and continued throughout the Pennsylvanian. Relationships within the preserved Pennsylvanian section permit analysis of the structural history of the trend.

Three cycles of uplift and mountain building have been recognized in the uplifts bounding the southwest flank of the Ardmore basin based on the onlapping geometry of the Pennsylvanian section (Ham and Wilson, 1967). They are known as the Wichitan, second Wichitan, and Arbuckle orogenies and are, respectively, Morrowan, Atokan–early Desmoinesian, and Missourian–Virgilian in age. In the Ardmore basin, the pinchout of Springer sandstones (late Chesterian–early Morrowan) against the northeast Criner uplift has been cited as evidence that uplift associated with the formation of the Criner Hills mountain range began as early as late Mississippian time (Tomlinson and McBee, 1959). However, this uplift has not necessarily been distinguished from the Morrowan deformation. Seismic data, validated by boreholes in the Ardmore basin, also indicate that uplift and local erosion of the Goddard Formation (Chesterian) occurred during deposition of the middle, and possibly lower, Springer. However, over most of the Criner Hills trend, no record of Mississippian uplift is preserved due to erosion of that section below an Atokan unconformity. Events readily interpreted on structural highs and traditionally thought of as separate phases of deformation, now appear more like punctuated events within a continuum of deformation.

REGIONAL CROSS SECTION

Figure 3 is a line drawing constructed from a regional seismic profile (line A, Fig. 1) extending southwest–northeast from the Marietta basin across the Criner trend and the Ardmore basin to the southern part of the Arbuckle anticline. The section illustrates the variety of structural styles and the extent and timing of different deformational events. Multiple reactivated basement-involved thrusts dominate the picture. More shallowly detached thrusts are better developed in the Ardmore basin.

The general lack of structural deformation of Dornick Hills and younger rocks (post lower Desmoinesian) in the Marietta basin (segments A–B and B–C, Fig. 3) is in striking contrast to the substantial uplift and shortening that occurred in the Ardmore basin (segments C–D and D–E, Fig. 3). Generally, the structural picture becomes increasingly complex from southwest to northeast, and several phases of deformation reflected in the Criner trend and the Ardmore basin are not evident in the Marietta basin.

The profound unconformity surface, which developed in response to the Early Pennsylvanian compressional tectonics, obscures any evidence of the early evolution of both the structurally higher areas and the Marietta basin. Over wide areas, the erosional surface was not covered until the Desmoinesian. Note, however, that at the position of this cross section in the Marietta basin, Goddard, Springer, and lower Dornick Hills (Morrowan) are not preserved. In fact, it is not known whether or not any Chesterian rocks were deposited in the Marietta basin or above the higher structural elements of the Criner trend. The stratigraphically higher parts of the Springer Formation may have been restricted to the subsiding foreland of these thrust sheets. In any case, the regional plunge of the Marietta and Ardmore basins is to the southeast (possibly due to thrust loading of the advancing Ouachita front), and the thickness of sediments preserved generally increases in that direction. Morrowan sediments are preserved in the southeastern Marietta basin.

The Goddard and Springer shales act as highly efficient detachment levels, and there is a significant difference in structural style depending on whether or not they are present. In this respect, the difference between the Marietta basin and the Ardmore basin is evident. For the most part, Pennsylvanian strata are firmly attached to the underlying, strongly deformed pre-Pennsylvanian section on the west flank of the Criner trend and within the Marietta basin. By contrast, over much of the north and east flank of the trend, and in much of the Ardmore basin, Pennsylvanian strata are completely detached from the section originally below it.

Other detachments are equally important. Basement rocks are certainly involved in the thrust sheets (Fig. 3, well 23), and it seems likely that there is a major intra-basement detachment level whose position remains uncertain. The outcropping Arbuckle Group clearly has intraformational detachment levels, and at places it appears that a detachment occurs in the lower Simpson Group; but neither of these play a major role in regional structures.

While seismic lines provide essential data about the structural nature of the Criner Hills trend, they cannot possibly provide the entire picture. The display parameters of the seismic data tend to elongate structures horizontally, vertical beds cannot be imaged, and complexly faulted zones are rarely clear. Thick formations with particularly low velocities such as the Springer and Goddard Formations can wreak havoc with spatial visualizations of depth conversions. Sometimes, key relationships between deeper units, such as cut-offs, and their lateral extent are only vaguely constrained by data. Potentially important small faults are especially difficult to identify in carbonates with seismic data alone. Faults in the Arbuckle section known from well data, really can't be interpreted on the seismic. Therefore, the Arbuckle Group is likely to be much more internally deformed with low-angle faults than indicated by seismic data, and there is likely to be more deformation within the Arbuckle than shown on the cross sections in this paper. Fortunately, along the Criner Hills trend there is an enor-

mous amount of well data that can be integrated with the seismic data to expand and refine representations of the structural geometry.

Some geologists can hardly wait to name the latest nuance in structural styles. In this context, perhaps the Criner Hills trend may best be considered simply a mess; a wonderful, complicated mess with some characteristics of a sensible, predictable nature, but defiant of simple generalizations. It is a joy and a challenge to try to decipher it. Let's look at it in cross sections.

SERIAL GEOLOGIC CROSS SECTIONS

Figure 4 consists of seven serial cross sections across the Criner Hills trend, drawn to show depths (instead of time) and with no vertical exaggeration. The cross sections are arranged to permit a three-

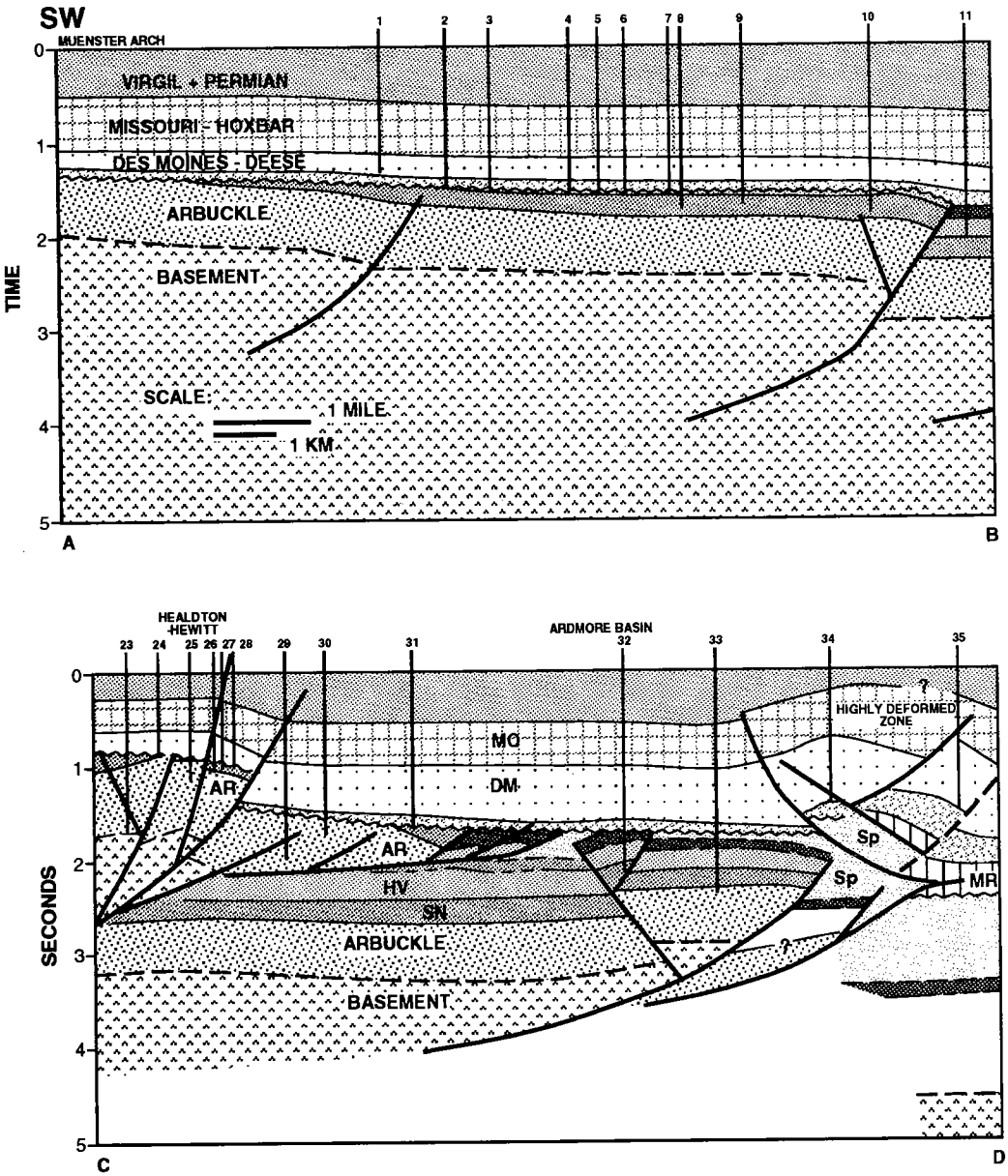


Figure 3 *(above and opposite page).* Line drawing of regional seismic line (Line A, Fig. 1) illustrated in four connecting segments (A–B, B–C, C–D, and D–E) across the Marietta basin, Criner Hills trend, and Ardmore basin. Numbered vertical lines indicate depth and location of well ties (see Appendix Table A1 for list of wells.) Vertical scale is two-way time in seconds; horizontal scale as illustrated. Patterns are identified in the figure.

dimensional visualization of the complex character of the trend.

The main structural elements of the Criner Hills trend, and their relationship to the Ardmore basin, should be more evident in section 1 (Fig. 4) than in the regional seismic line (Fig. 3). In its simplest form, the trend consists of two major basement-cored thrust sheets. They formed in latest Mississippian time, and subsequently were further deformed until Desmoinesian time, and then again in Virgilian time. The higher thrust sheet clearly shows evidence of a major backthrust (the Joiner City trend), and even the lower sheet suggests a backthrust style. Rocks of the Springer Formation are deformed along the leading edge of the higher thrust sheet (between wells 6 and 7), as well as in the deeper Ardmore basin (northeast of well 9).

Following tectonically quiescent Desmoinesian and Missourian Epochs, renewed compression and uplift in Virgilian time reactivated preexisting low-angle detachment surfaces and created the impression of major out-of-sequence thrusting. The frontal part of the higher thrust sheet (see well 5, section 1, Fig. 4) is now in a position considerably lower than

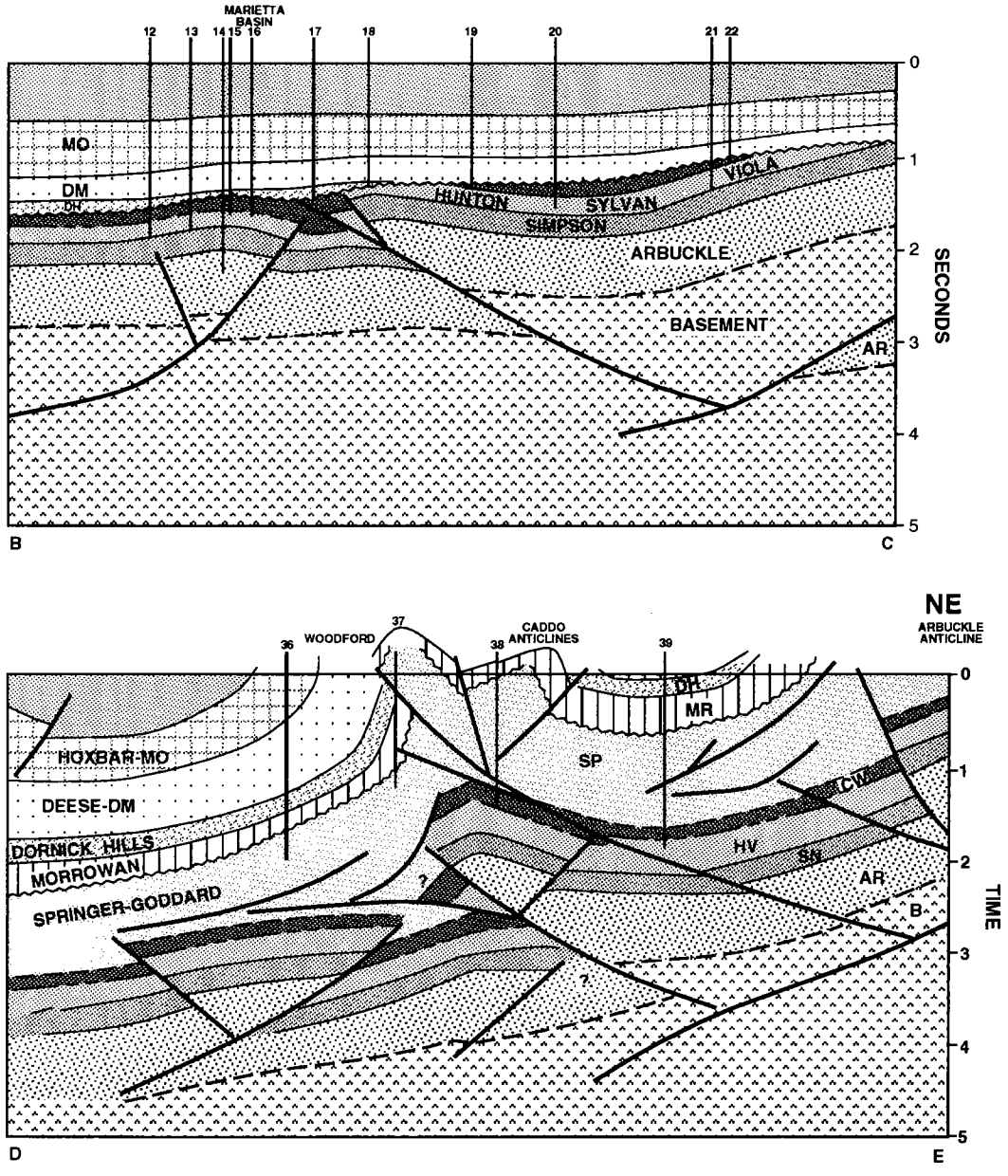


Figure 3 *(continued).*

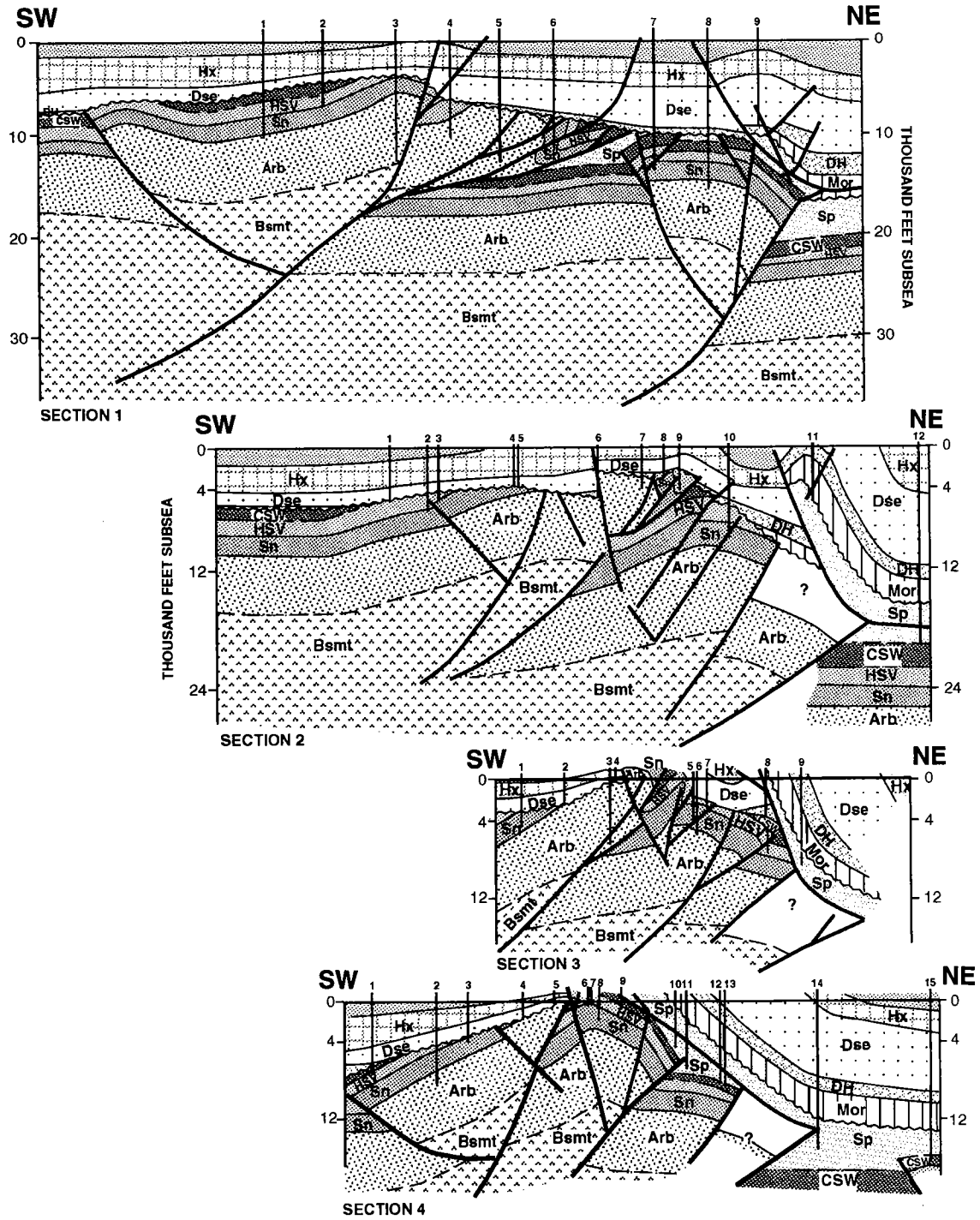


Figure 4 *(above and opposite page)*. Geologic cross sections of the Criner Hills trend. See text for discussion. No vertical exaggeration. Numbered vertical lines indicate depth and location of well ties (see Appendix Table A2 for lists of wells.) Bsmt = basement; Arb = Arbuckle; Sn = Simpson; HSV = Hunton, Sylvan, Viola; CSW = Caney, Sycamore, Woodford; Sp = Springer and Goddard; Mor = lower Dornick Hills Group (Morrowan); DH = upper Dornick Hills Group (Atokan); Dse = Deese Group; Hx = Hoxbar.

that of the rest of the thrust sheet. The Cottonwood Creek field fault block in the frontal part of the upper thrust sheet (well 5, section 1, Fig. 4) was an Early Pennsylvanian high, prior to the renewed compression in Virgilian time. In the Ardmore basin, Pennsylvanian clastic sequences were thrust

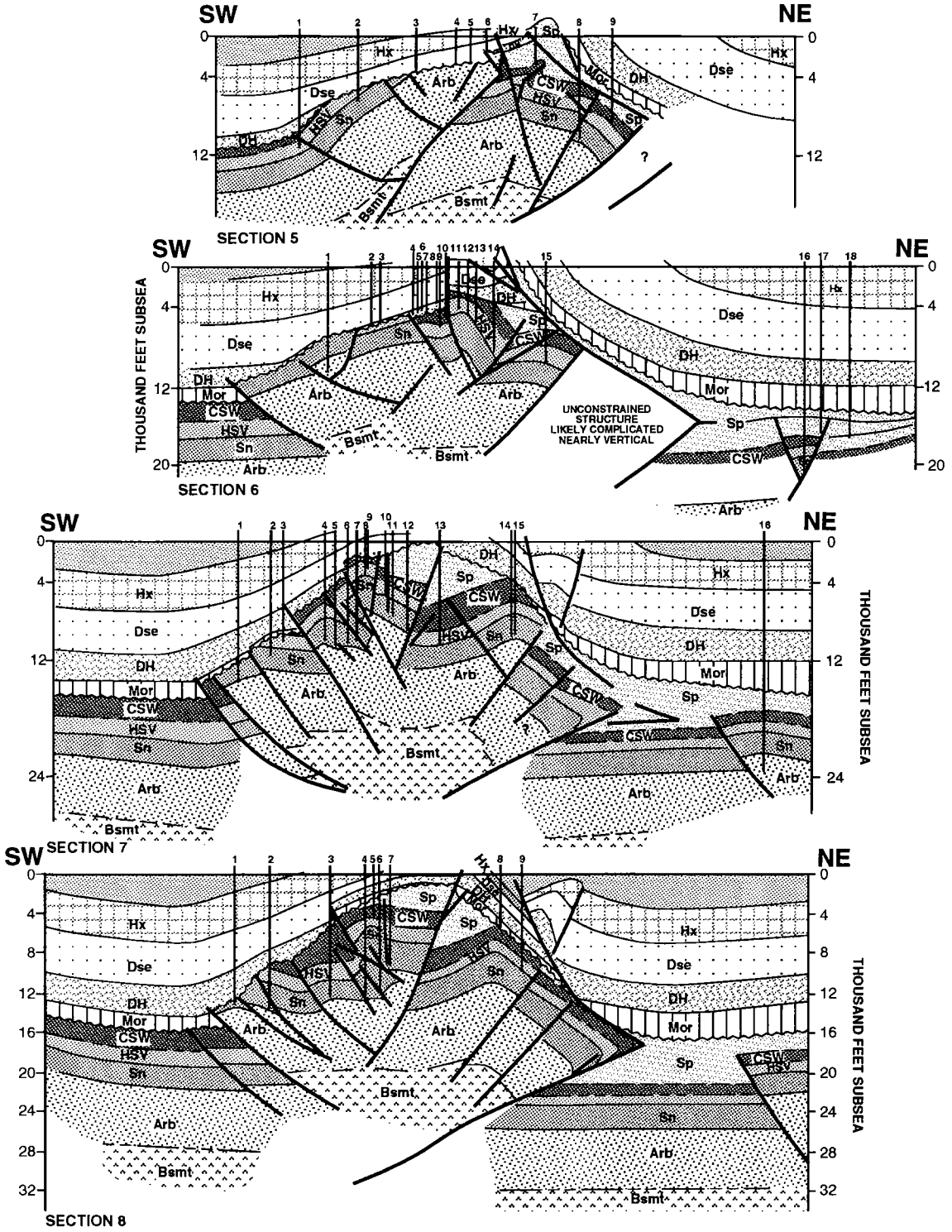


Figure 4 *(continued).*

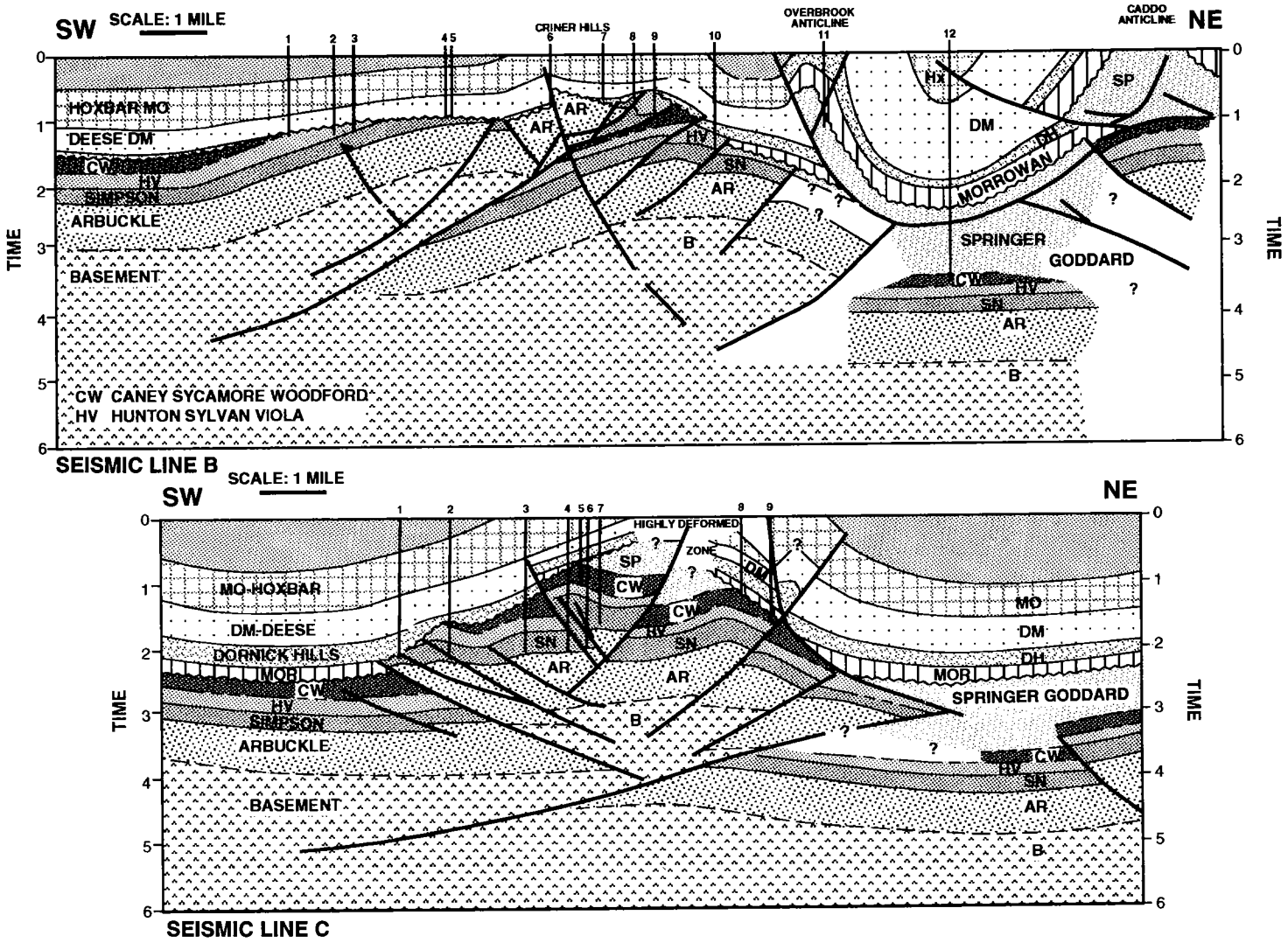


Figure 5. Geological interpretations of representative seismic profiles crossing the Criner Hills trend. Seismic-line B corresponds to section 2 of Figure 4. Seismic-line C corresponds to section 8 of Figure 4. Numbered vertical lines indicate the depth and location of well ties (see Appendix Table 2, sections 2 and 8.) Note that the top of the basement (dashed line) is a poorly constrained form line (i.e., based on the configuration of shallower markers.)

out of the basin, mostly detached within the Springer shales. Several of these structures are completely detached from underlying features.

In cross section 1, depth to basement can be actually constrained by projecting well data into the line at the position of well 3. However, elsewhere on these cross sections, the line indicating the top of the basement was drawn ~6,000 ft below the top of the Arbuckle, following the pattern of seismic reflectors; thus, it is merely a form line.

The second cross section (Fig. 4) is also northwest of the Criner Hills (Fig. 1). It corresponds to seismic data represented in seismic line B of Figure 5. Whereas the two major thrust sheets identified in section 1 that comprise the Criner uplift are easily discernible, the structure is more complex. Both sheets have clear imbrications, and a major Virgilian-age backthrust (the Criner fault, which is cut by well 6), offsets the entire structure. The Criner fault was also active in the Atokan–early Desmoinesian time, based on the offset pattern of deposition in that interval. Local normal faults along the crest of the Criner trend (e.g., West Brock field), were active into the Missourian Epoch, but there is no evidence for widespread regional extension at that time.

From the perspective of cross section 2, the Ardmore basin appears to be an enormous, squeezed syncline bounded by deep-seated, low-angle, basement-involved thrust faults. Certainly the Springer and Goddard shales act as excellent detachment levels within the Mississippian–Pennsylvanian section.

The subcrop pattern beneath the unconformity at the base of the Pennsylvanian suggests that two structural highs existed during early Pennsylvanian time: one along the Criner axis (near well 6), and another along the former crest of the lower thrust sheet (east of well 10). The crest of the lower thrust sheet has been rotated (clockwise as seen in cross section) by subsequent uplift, into a down-dip position. This clockwise rotation was partly caused by uplift and reverse displacement on the Criner fault, which is documented by a repeated section of upper Deese Chubbee sandstone in well 6 (section 2, Fig. 4). It is as if some structure were punching its way up from below. But displacement across the Criner fault is not enough to account for the entire rotation. One complication is that in this cross section it appears that the Criner fault had a normal offset during Dornick Hills and lower Deese deposition. Dornick Hills is preserved on both sides of the Criner fault. Normal offset is recorded in section 2, but not in section 3 and 4 updip where the Dornick Hills is missing by erosion and Deese (and even Hoxbar) strata lie directly on the Arbuckle Group.

Cross section 3 (Fig. 4) crosses the heart of the Criner Hills outcrop (Fig. 1) and incorporates detailed surface control and good well control. The Criner fault is a Late Pennsylvanian back thrust, and it offsets an even smaller width of the frontal part of the main upper thrust structure. There are no substantive data to show how the Criner fault connects at depth with other faults. The horizontal distance between the culminations of the two major thrust sheets continues to diminish from section 1 to 3. Whether this represents a change in relative shortening is problematic; the deeper level of erosion in this cross section obscures the relationship. Furthermore, if shortening occurred during deposition of upper Springer strata, the amount of post-Springer shortening could be overestimated. The northeast and southwest dip of the unconformity underlying Pennsylvanian strata increases dramatically between sections 1 and 3. The amount of shortening on the Criner edifice, with respect to the Ardmore basin, increases, and, correspondingly, there is a big increase in the amount of Pennsylvanian section backthrust out of the basin.

In section 4 (Fig. 4), the lower thrust sheet reaches its culmination, and is partially exposed on the surface. The Criner fault (dipping northeast between wells 5 and 6) clips only the leading edge of the upper thrust sheet.

On section 5 (Fig. 4), the apparent shortening between the upper thrust sheet and the lower thrust structure, is smaller than in the previous four sections. Although there has been significant uplift of the entire Criner structure, there is little deformation or offset of the sub-Pennsylvanian unconformity on the southwest flank compared to the northeast flank. Note the onlapping geometry of the Springer on the lower thrust structure, indicating a high and also providing further evidence that this block was affected by multiple phases of deformation (including, possibly, a Chesterian event, as documented in deeper parts of the Ardmore basin of section 6).

The lateral termination of the upper thrust sheet lies between cross sections section 5 and 6. The enormous changes associated with that termination are illustrated by a comparison of sections 5 and 6. Clearly, Early Pennsylvanian erosion removed much more of the Pre-Pennsylvanian section in cross section 5 than in cross section 6. There is significant expansion of the entire Dornick Hills Group, in contrast to sections 1–5, and Morrowan strata are preserved on the Marietta basin side of the uplift in section 6. In the Ardmore basin there is a corresponding expansion of the Goddard and Springer sections, and preservation of a preexisting structure (well 16, section 6, Fig. 4). Normal faulting during Dornick Hills deposition is indicated in cross section 6 by a down-dropped block to the left of center (see wells 4–9) (Grenville oil field). The configuration of this normal fault at depth is unresolved. The wide region between the interpreted structure and the deeper Ardmore basin (blank area, section 6, Fig. 4) is likely to be very complexly deformed with many vertical beds. This region was

at the front of a deforming wedge that was driven into the Ardmore basin, with possible wrenching.

Section 7 (Fig. 4) is the Enville trend (Reeves and others, 1959a,b). The structural style is more "upright" than that in previous sections. Note that the structurally highest segment of cross section 7 (wells 6–12) can be correlated to the high segment (wells 10–14) near the center of section 6. Mississippian rocks (CSW and Sp, Fig. 4) which are preserved on the uplift and thinner or absent on the flanks indicate that this uplift was a synclinal element during Mississippian time. Note that the relative elevation of the sub-Pennsylvanian unconformity suggests that this entire structure has been greatly uplifted over a narrow zone. On the Marietta basin side of the uplift, the sub-Pennsylvanian unconformity dips more steeply than in previous sections, and Morrowan strata are preserved on the flank of the uplift (wells 1–3). The relative thickness of pre-Pennsylvanian rocks and the sense of displacement of the sub-Pennsylvanian unconformity across the fault between wells 3 and 4 suggests that the fault was an Early Pennsylvanian normal fault that was reactivated as a reverse fault during Dornick Hills deposition. This block is in the same position (relative to the structurally highest block) as the normal-fault-bounded block in section 6 (wells 4–10) that has not been inverted.

The Late Pennsylvanian compression seen in section 6 (wells 7–11) is also reflected in section 7; it involves the same elements, but the offset is less and the uplifted area is wider. The Deese Group is substantially thinner across the top of this structure, and the Dornick Hills Group is not present in wells 6–12, suggesting that this was a high element during Deese deposition. This configuration is very similar to that of the uplift and Criner fault in section 2 (see well 6, section 2).

Section 8 (Fig. 4), which essentially follows seismic line C (Fig. 5), is very similar to section 7. As in sections 1–7, the geometry resembles that of a bivergent thrust sheet; it is mainly a northeasterly vergent thrust complex with southwesterly vergent backthrusts. How the various faults cut into basement is entirely conjectural. On the seismic profiles, intra-Arbuckle reflectors can only be vaguely correlated in the core of the structure.

Wells 1–3 of section 8 have no preserved Morrowan strata. Clearly a structural high existed at wells 1 and 2 during Dornick Hills deposition, but note that the Dornick Hills covers even the crest of the present structure, unlike in section 7. The inverted graben seen in sections 6 and 7 is also present in section 8. Although the structural high appears only modestly deformed in this cross section, in reality it is probably a much more complicated feature with highly deformed Springer shales. Wells 4–7 indicate that during Deese deposition a high (like the one in section 7) existed, but at a down-dip position as indicated by the preservation of some Dornick Hills and Morrowan strata.

SUMMARY OF STRUCTURAL STYLE

The structural style of the Criner Hills trend and the Ardmore basin is relatively easy to recognize, based on the cross sections described above. Its geologic evolution is summarized in Figure 6, which is based on cross section 1 in Figure 4.

- The entire area was progressively deformed from the Late Mississippian through the Pennsylvanian. The deformation phases included:
  1) Middle Chesterian compression, documented in the Ardmore basin (Fig. 4, sections 6 and 7);
  2) Morrowan through early Desmoinesian compression (probably in several phases);
  3) Atokan extensional collapse along structural highs, with intermediate block rotation;
  4) Virgilian, and possibly Missourian, uplift and high-angle faulting; and
  5) Permian, and even Cretaceous, minor rejuvenation of uplift.
- Deformation was predominantly compressional, with substantial shortening and associated uplift.
- Numerous detachment levels were involved including intra-basement detachments.
- Both high-angle and low-angle faulting were involved. Early Pennsylvanian compression was generally accomplished on low-angle detachment surfaces.
- A bivergent thrust style is common, ranging in scale from small structures (hundreds of feet) to entire thrust sheets (perhaps 6–8 mi).
- There are apparently deeper basement-detachment levels that were involved later in the deformation sequence.
- A southwest-to-northeast deformation sequence predominates, with later stage, deeper detachment levels giving the appearance of out-of-sequence thrusting along the Criner trend proper.
- Intermediate-depth blocks show evidence of rotation, as if twisted between deforming blocks. Depending on position, there are both normal faults (extension) and thrust faults (compression) within the overlying thrust sheet, resulting from the intermediate-block rotations. Normal faults are both subparallel and conjugate to fold trends.
- The frontal part of the Criner trend contains numerous folds with very steep frontal limbs. These may be related to blind thrusts.
- The vertical throw changes dramatically over short distances along high-angle faults, especially where displacement was transferred to a deeper thrust sheet.
- On seismic data, high-angle faults pass downward and into lower angle faults and, finally, subhorizontal detachments.
- Major faults cut across preexisting faults, but fault inversion and reactivation has also occurred.
- There is very little evidence of lateral (strike-slip) offset in the upper thrust sheets. Very little is

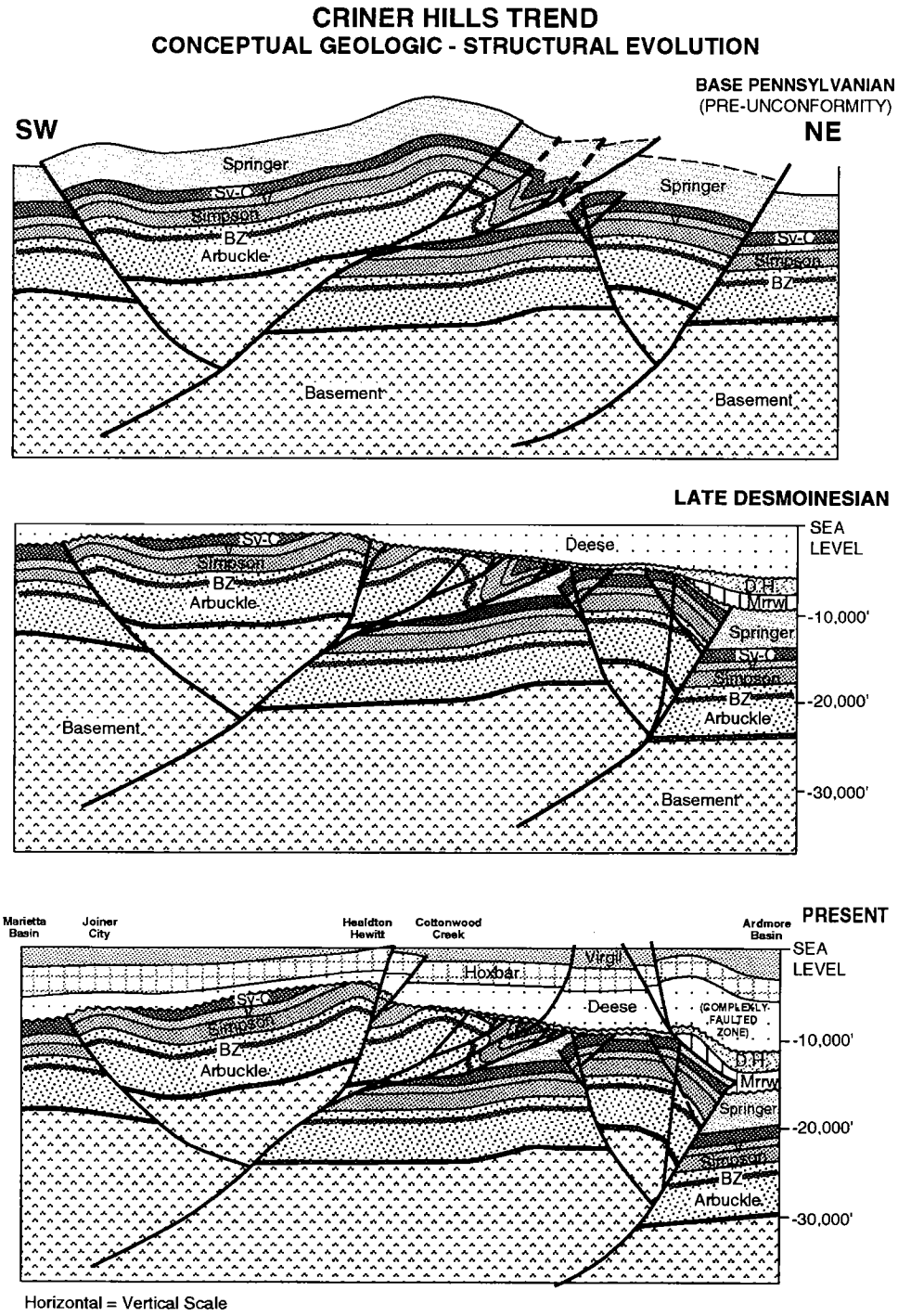


Figure 6. Generalized geologic cross section of the Criner Hills trend showing the major stages of structural development. These sections are based on section 1 of Figure 4. The lines representing the top of basement and the Arbuckle Group Brown zone are form lines (i.e., the configurations are based on the configuration of shallower markers.) BZ = Brown Zone in the Arbuckle; V = Viola; SV-C = Sylvan, Hunton, Woodford, Sycamore, Caney; Mrrw = lower Dornick Hills; DH = upper Dornick Hills. In the lowest cross section, the interval labeled Virgil also includes Permian-age rocks.

known about the relationship of the deepest thrust sheet to the basin.

The prevailing structural interpretation of the Ardmore basin concludes that the structural style results from regional left-lateral strike-slip faulting or transpressional wrench faulting (Ham and Wilson, 1967; Granath, 1989), although some have proposed that deformation was dominanted by right-lateral shear (Zolnai, 1991). The complicated structures have been labeled positive (and negative) flower structures (Harding and others, 1983; Harding, 1985). Recent efforts have attempted to determine the possible interference pattern of multiple events (Granath, 1989). In previous interpretations, the relative importance of thrust faulting was considered minor. The evidence presented here begs for a modification of the model.

Simply labeling the Criner Hills trend as a strike-slip, transpressional wrench-fault structure contributes little to the understanding of its structural evolution or to the ability to predict structural geometries. Although a quick glance at section 7 or 8 (Fig. 4) calls to mind a flower structure, it is extremely difficult to document lateral offsets of piercement points to illustrate any significant strike-slip motion within the Criner Hills trend and the Ardmore basin. Pre-Pennsylvanian subcrop maps and facies maps of Paleozoic strata constrain slip on major faults, such as the Healdton–Hewitt–Lone Grove fault, to less than 1 km, and are consistent with virtually none. Maps of the southern extension of the Criner Hills trend Ordovician Simpson Group facies indicate little possibility of strike-slip faulting (Remmer, 1988).

An unusually enormous data base exists to map various subsurface units in the Criner Hills trend. Careful mapping of data available to depths of 15,000 ft reveals that only minimal shear offsets are possible; this is especially true on the better known faults, such as the Healdton–Hewitt–Lone Grove system, the Kirby fault, or the Criner or Enville faults. By contrast, conservative estimates suggest that the shortening attributable to over-thrusting across individual faults (such as the sole thrust below the Cottonwood Creek structure) (Fig. 4, section 1) exceeds 4–5 mi.

Nevertheless, mega-regional basement studies such as aeromagnetic and gravity interpretations (Thompson and others, 1995), suggest that substantial left-lateral offset has occurred in the basement beneath the Ardmore basin.

In spite of some rather good seismic data, it is still difficult to map and understand the relationships of the faults deep in the Ardmore basin. Crustal shortening is predominant across the basin. However, it does seem clear that extensive subhorizontal detachments have played a major role in the structural evolution of the basin. Regional crustal strike-slip faulting would be a viable interpretation only if the strike-slip faults are subhorizontal over extensive areas.

If one accepts the argument for mega-regional-scale left-lateral deformation, then the structures in the Ardmore basin and the Criner Hills trend would seem to be an outstanding example of subhorizontal, basement-involved, regional, strike-slip faulting with co-existing compressional and extensional features. Little, if any, strike-slip offset would be expected to be observed at higher structural levels.

It should be immediately apparent that the deformation style of this area is remarkably similar to that of a classic fold and thrust belt in that as deformation progresses, successive major detachments are progressively deeper. Superimposed on the more classic fold-belt features are high-angle faults that have minor horizontal offset and that abruptly terminate and transfer their motion to other faults. These high-angle faults have been considered to be primary elements of positive flower structures in the past. Likewise, normal faults play an important role on the crests of structures. Entire preexisting structures have rotated in response to structures formed at great depths.

Taken singularly, the seismic lines and geologic cross sections presented above suggest that the Criner Hills trend is a particularly complex structural feature deserving the label "a mess." Evidence of substantial deformation is preserved, and the extensive record of boreholes and seismic lines makes simple interpretations untenable. However, when considered in terms of its major elements and progressive deformation, the Criner Hills trend begins to look like a sensible mess. Whatever mega-regional tectonic framework the trend belongs to, the facts indicate repeated deformation throughout the Pennsylvanian, which created a playground for geologists. Detailed studies of other "simple flower structures" worldwide will likely find that many of them are substantially more complicated than previously advertised; and that they have much in common with the Criner Hills trend and the Ardmore basin.

ACKNOWLEDGMENTS

This paper reports the results of a collaborative effort done with J. P. Blocher while we were employed by Shell Western E & P. Although the manuscript, cross sections, and seismic-line interpretations were all done by me following my employment with Shell, they are largely based on knowledge I gained while with the company. I am grateful to the management of Shell Western E & P for permitting me to present this work at the Norman conference and to publish it here. In particular, I thank W. F. Kiel for his original enthusiasm to have me give the paper when I was his employee, and his continued shepherding of the plan, following my separation from Shell.

The seismic lines used in construction of the line drawings in this paper are Shell proprietary data. I thank the outstanding teamwork of several "Con-

tinental Division" processing crews, whose high-caliber efforts permitted me to visualize potential solutions to the complicated geologic picture presented here. Original acquisition and ownership of the seismic data were by PGI and X-Mark. I am grateful to Marilyn Davies, Steve Tyrell, and Dick Nethers who, on behalf of the successors of PGI and X-Mark, permitted me to show the actual seismic lines at the Norman conference and to publish geological representations of the seismic lines. Chief geophysicist Mark Manion permitted their release on behalf of Shell. J. Kaspar Arbenz kindly reviewed the manuscript.

REFERENCES CITED

Bullard, F. M., 1925, Geology of Love County, Oklahoma: Oklahoma Geological Survey Bulletin 33, 77 p.

Denison, R. E., 1982, Geologic cross section from the Arbuckle Mountains to the Muenster arch, southern Oklahoma and Texas: Geological Society of America Map and Chart Series MC-28R, 8 p.

Frederickson, E. A., 1957, Geologic map of the Criner Hills area, Oklahoma: Oklahoma Geological Survey Map GM-4, scale 1:22,230.

Granath, J. W., 1989, Structural evolution of the Ardmore basin, Oklahoma: progressive deformation in the foreland of the Ouachita collision: Tectonics, v. 8, p. 1015–1036.

Ham, W. E.; and Wilson, J. L., 1967, Paleozoic epeirogeny and orogeny in the central United States: American Journal of Science, v. 265, p. 332–407.

Ham, W. E.; Denison, R. E.; and Merritt, C. A., 1964, Basement rocks and structural evolution of southern Oklahoma: Oklahoma Geological Survey Bulletin 95, 302 p.

Harding, T. P., 1985, Seismic characteristics and identification of negative flower structures, positive flower structures and positive structural inversion: American Association of Petroleum Geologists Bulletin, v. 69, p. 582–600.

Harding, T. P.; Gregory, R. F.; and Stephens, L. H., 1983, Convergent wrench fault and positive flower structure, Ardmore basin, Oklahoma, *in* Bally, A. W. (ed.), Seismic expression of structural styles—a picture and work atlas: American Association of Petroleum Geologists, Studies in Geology 15, v. 3, p. 4.2-13 to 4.2-17.

Jacobson, M. I., 1984, The Harrisburg trough, Stephens County, Oklahoma; an update, *in* Borger, J. G., III (ed.), Technical proceedings of the American Association of Petroleum Geologists Mid-Continent Section, 1981 regional meeting: Oklahoma City Geological Society, p. 127–137.

Johnson, K. S.; Amsden, T. W.; Denison, R. E.; Dutton, S. P.; Goldstein, A. G.; Rascoe, B., Jr.; Sutherland, P. K.; and Thompson, D. M., 1988, Southern Midcontinent region, *in* Sloss, L. L. (ed.), Sedimentary cover—North American craton; U.S.: Geological Society of America, Boulder, The Geology of North America, v. D-2, p. 307–359. [Reprinted as Geology of the southern Midcontinent, Oklahoma Geological Survey Special Publication 89-2, 1989, 53 p.]

Lang, R. C., III, 1957, The Criner Hills: a key to the geologic history of southern Oklahoma, *in* Kempf, J. H. (ed.), Criner Hills field conference guidebook: Ardmore Geological Society, p. 18–25.

Perry, W. J., Jr., 1989, Structural evolution of the southeastern portion of the Anadarko basin region, *in* Johnson, K. S. (ed.), Anadarko basin symposium, 1988: Oklahoma Geological Survey Circular 90, p. 77.

Reeves, C. C., Jr.; Probandt, W. T.; and Cullinan, T. A., 1959a, Southwest Enville—a development headache: Oil and Gas Journal, v. 57, no. 36, p. 110–113.

_____ 1959b, Southwest Enville: every well's a wildcat: Oil and Gas Journal, v. 57, no. 37, p. 256–260.

Remmer, R. H., 1988, An observation on strike slip movement in the Criner Hills, Love County, Oklahoma: Shale Shaker, v. 38, p. 14–15.

Thompson, T. L.; Howe, J. R.; Hawley, B.; and Gay, S. P., 1995 [this volume], Basement influence on the structural geology of southern Oklahoma inferred from residual aero-magnetic maps, *in* Johnson, K. S. (ed.), Structural styles in the southern Midcontinent, 1992 symposium: Oklahoma Geological Survey Circular 97, p. 13–14.

Tomlinson, C. W.; and McBee, W., 1959, Pennsylvanian sediments and orogenies of the Ardmore district, Oklahoma, *in* Petroleum geology of southern Oklahoma, v. 2: American Association of Petroleum Geologists, Tulsa, Oklahoma, p. 3–52.

Westheimer, J. M., 1965, Petroleum geology of Love County, *part 2 of* Geology and petroleum of Love County, Oklahoma: Oklahoma Geological Survey Circular 63, p. 48–77.

Zolnai, G., 1991, Continental wrench-tectonics and hydrocarbon habitat (2nd edition): American Association of Petroleum Geologists Continuing Education Course Note Series No. 30, Tulsa, Oklahoma.

APPENDIX

TABLE A1. — Wells Shown on Seismic Line A, Figure 3

Number	Well Name	Location	API Well Number
1	Jones No. 1 Auld	sec. 1, T. 7 S., R. 3 W.	
2	Phillips Thomas J-1	sec. 1, T. 7 S., R. 3 W.	
3	Phillips Hamilton B-1	sec. 31, T. 6 S., R. 2 W.	35-085-20492
4	Cox No. 1 Overstreet	sec. 31, T. 6 S., R. 2 W.	35-085-20908
5	Slawson No. 1-30 Kimbell	sec. 30, T. 6 S., R. 2 W.	35-085-20901
6	TXO No. B-1 Kimbell Trust	sec. 30, T. 6 S., R. 2 W.	35-085-20894
7	Anschutz 11-29 Vormac Trust	sec. 29, T. 6 S., R. 2 W.	35-085-20370
8	Jones No. 1 McNutt	sec. 29, T. 6 S., R. 2 W.	
9	Jones Prod. No. 1 Kimbell	sec. 20, T. 6 S., R. 2 W.	
10	Depco No. 1 Newell	sec. 17, T. 6 S., R. 2 W.	
11	Hadson No. 1-16 Smith	sec. 16, T. 6 S., R. 2 W.	
12	Quintana (Mulkay) No. 1 Sohio	sec. 3, T. 6 S., R. 2 W.	35-085-20593
13	Chevron No. 2 Easterwood	sec. 3, T. 6 S., R. 2 W.	
14	California No. 1 M. Walker	sec. 3, T. 6 S., R. 2 W.	35-085-07306
15	California No. 1 Wilson	sec. 3, T. 6 S., R. 2 W.	
16	California No. 1 C. Moore	sec. 34, T. 5 S., R. 2 W.	35-019-07315
17	Jones & Pellow No. 1 Monson	sec. 35, T. 5 S., R. 2 W.	35-019-21918
18	Lawrence No. 1 Monson	sec. 35, T. 5 S., R. 2 W.	35-019-01030
19	Nondorf No. 3-25 Sullivan	sec. 25, T. 5 S., R. 2 W.	35-019-22656
20	Tri-Pro No. 1 Godell	sec. 24, T. 5 S., R. 2 W.	35-019-23111
21	Tripledee No. 1 Smallwood	sec. 18, T. 5 S., R. 1 W.	35-019-22090
22	Tripledee No. 18-2	sec. 18, T. 5 S., R. 1 W.	35-019-22006
23	Jones No. 3 Wallace-Reed	sec. 6, T. 5 S., R. 1 W.	35-019-07961
24	Texas No. 3 Chubbee	sec. 5, T. 5 S., R. 1 W.	35-019-07947
25	Texas No. 6 Reynolds-Duke	sec. 5, T. 5 S., R. 1 W.	35-019-00385
26	Texaco No. 3 Payne	sec. 5, T. 5 S., R. 1 W.	35-019-07949
27	Bauman No. 1 Payne	sec. 5, T. 5 S., R. 1 W.	35-019-07940
28	Jedsco No. 1 Newman	sec. 32, T. 4 S., R. 1 W.	35-019-06348
29	CNG No. F1-32 Cottonwood Creek	sec. 32, T. 4 S., R. 1 W.	35-019-23711
30	CNG No. E1-32 Cottonwood Creek	sec. 32, T. 4 S., R.1 W.	35-019-23707
31	Carter No. 1 Smith	sec. 28, T. 4 S., R. 1 W.	35-019-00006
32	Cleary No. 1 Stubblefield	sec. 15, T. 4 S., R. 1 W.	35-019-30108
33	Lear No. 1 Martin	sec. 14, T. 4 S., R. 1 W.	35-019-22160
34	Texaco No. 1 Clendenin	sec. 11, T. 4 S., R. 1 W.	
35	Ingraham No. 1 Jones	sec. 1, T. 4 S., R. 1 W.	
36	Seaboard No. 3 Smith	sec. 19, T. 3 S., R. 1 E.	35-019-00128
37	Holden No. 1 Craighead	sec. 18, T. 3 S., R. 1 E.	35-019-21917
38	Winters No. 1 Scott	sec. 21, T. 3 S., R. 1 E.	
39	PSEC No. 1-9 Elmore	sec. 9, T. 3 S., R. 1 E.	35-019-23064

TABLE A2. — Wells Shown in Sections 1–8, Figure 4

Number	Well Name	Location	API Well Number
Section 1			
1	Frankfort No. 1 Parker	sec. 11, T. 5 S., R. 2 W.	
2	Apco No. 1 Selvidge	sec. 2, T. 5 S., R. 2 W.	35-019-21666
3	Conoco No. 1 Denny Smith	sec. 36, T. 4 S., R. 2 W.	35-019-20766
4	L. E. Jones No. 1 Austin	sec. 25, T. 4 S., R. 2 W.	35-019-23764
5	Mack No. 1 Hoffman	sec. 30, T. 4 S., R. 1 W.	35-019-23754
6	California No. 1 Price	sec. 20, T. 4 S., R. 1 W.	35-019-06332
7	Cleary No. 1 Stubblefield	sec. 15, T. 4 S., R. 1 W.	35-019-30108
8	Lear No. 1 Martin	sec. 14, T. 4 S., R. 1 W.	35-019-22160
9	Texaco No. 1 Clendenin	sec. 11, T. 4 S., R. 1 W.	
Section 2			
1	Tripledee No. 1 Norma	sec. 26, T. 5 S., R. 1 W.	35-019-22172
2	Blackwood & Nichols No. 1 Goddard	sec. 26, T. 5 S., R. 1 W.	35-019-00046
3	Samedan No. 1 Alford	sec. 26, T. 5 S., R. 1 W.	35-019-21803
4	Magnolia No. 1 Ickney-Wesley	sec. 24, T. 5 S., R. 1 W.	35-019-08000
5	Mid-Continent No. 1 Ickney Wesley	sec. 13, T. 5 S., R. 1 W.	35-019-07978
6	Turner No. 1 Worez	sec. 7, T. 5 S., R. 1 E.	35-019-00214
7	Chapman No. 1 McCarty	sec. 7, T. 5 S., R. 1 E.	35-019-21277
8	Simmons No. 1 Coffee	sec. 6, T. 5 S., R. 1 E.	35-019-30186
9	Sinclair No. 1 Coffee	sec. 5, T. 5 S., R. 1 E.	35-019-00374
10	Pan American No. 1 Hampton	sec. 32, T. 4 S., R. 1 E.	35-019-30357
11	Gulf Coast Western No. 1 Zeller	sec. 28, T. 4 S., R. 1 E.	35-019-00117
12	Northern Natural Gas 1-15 Herndon	sec. 15, T. 4 S., R. 1 E.	35-019-21710
Section 3			
1	Nelson Spain No. 1 Buck	sec. 32, T. 5 S., R. 1 E.	35-019-00073
2	Canco No. 1 Rox	sec. 28, T. 5 S., R. 1 E.	35-019-20175
3	Seaboard No. 1 Sutton	sec. 21, T. 5 S., R. 1 E.	35-019-00031
4	Producers No. 22 Clay	sec. 28, T. 5 S., R. 1 E.	35-019-30355
5	Holden No. 22-1 Sylvia	sec. 22, T. 5 S., R. 1 E.	35-019-07616
6	McCasland No. 1 McClure	sec. 15, T. 5 S., R. 1 E.	35-019-00272
7	McCasland No. 1 Kirby	sec. 15, T. 5 S., R. 1 E.	35-019-00093
8	Pan American No. B-1 Hedges	sec. 14, T. 5 S., R. 1 E.	35-019-07577
9	Huber No. 1 Hedges	sec. 11, T. 5 S., R. 1 E.	35-019-20172
Section 4			
1	Continental No. 1A Gant	sec. 16, T. 6 S., R. 1 E.	35-085-00063
2	Sinclair No. 1 Ewing	sec. 9, T. 6 S., R. 1 E.	35-085-00110
3	Nondorf No. 1 Keith	sec. 3, T. 6 S., R. 1 E.	35-085-20601
4	Dunlap No. 1 Hayes	sec. 2, T. 6 S., R. 1 E.	35-085-30111
5	Kingerly No. 1 Episcopal	sec. 2, T. 6 S., R. 1 E.	35-085-20822
6	Mack No. 1 Morris	sec. 35, T. 5 S., R. 1 E.	35-019-09309
7	Mack No. 1 Morris Arch	sec. 36, T. 5 S., R. 1 E.	35-019-07937
8	Compadre No. 1 Bourland	sec. 36, T. 5 S., R. 1 E.	35-019-22303
9	Sinclair No. 1 Bourland	sec. 36, T. 5 S., R. 1 E.	35-019-22514
10	Samedan No. 2 Frensley	sec. 25, T. 5 S., R. 1 E.	35-019-00204
11	Johnson No. 1 Martin	sec. 30, T. 5 S., R. 2 E.	35-019-20720
12	Western States No. 1 Davis	sec. 24, T. 5 S., R. 1 E.	35-019-30301
13	National No. 1 Van Eaton	sec. 17, T. 5 S., R. 2 E.	35-019-21964
14	CIG Exploration No. 1 Peddy	sec. 17, T. 5 S., R. 2 E.	35-019-21684
15	Signal No. 1 City Ardmore	sec. 4, T. 5 S., R. 2 E.	35-019-21126
Section 5			
1	Petroleum Texas No. 1 Roger	sec. 26, T. 6 S., R. 1 E.	35-085-20613
2	Blackwood & Nichols No. 1-23 Forbes	sec. 23, T. 6 S., R. 1 E.	35-085-00020
3	Skelly No. 1 Sykora	sec. 13, T. 6 S., R. 1 E.	35-085-00196

TABLE A2 *(continued).* — Wells Shown in Sections 1–8, Figure 4

Number	Well Name	Location	API Well Number
Section 5 (continued)			
4	Dunlap No. 1 Le Flore	sec. 13, T. 6 S., R. 1 E.	35-085-00103
5	Johnson & Thomas No. 1 Le Flore	sec. 18, T. 6 S., R. 2 E.	35-085-00086
6	Martin No. 1 Clark	sec. 7, T. 6 S., R. 2 E.	35-085-20076
7	Texas Pacific No. 1 Glasscock	sec. 6, T. 6 S., R. 2 E.	35-085-20276
8	Rodman No. 1-5 Stidham	sec. 5, T. 6 S., R. 2 E.	35-085-20618
9	Gulf No. 1 Overbrook State	sec. 32, T. 5 S., R. 2 E.	35-019-00015
Section 6			
1	Conoco No. 31-1 Riley	sec. 31, T. 6 S., R. 2 E.	35-085-20852
2	Sohio No. 1 Blake	sec. 32, T. 6 S., R. 2 E.	35-085-00547
3	Walker No. 1 Williams	sec. 29, T. 6 S., R. 2 E.	35-085-30108
4	Beard No. B-2 Conrad	sec. 29, T. 6 S., R. 2 E.	35-085-00539
5	Holden No. 54 Greenville	sec. 29, T. 6 S., R. 2 E.	35-085-00536
6	Holden No. 55 Greenville	sec. 29, T. 6 S., R. 2 E.	35-085-00537
7	Trice Pro No. 5 Hendon	sec. 28, T. 6 S., R. 2 E.	35-085-00523
8	Trice Pro No. 1 Hendon	sec. 28, T. 6 S., R. 2 E.	35-085-00527
9	Gilmer No. 11A Malone	sec. 20, T. 6 S., R. 2 E.	35-085-00487
10	Shermerhorn No. 1 Perry	sec. 21, T. 6 S., R. 2 E.	35-085-00019
11	Holden No. 21-1 Lane	sec. 21, T. 6 S., R. 2 E.	35-085-20594
12	Depco No. 1 Forbes	sec. 21, T. 6 S., R. 2 E.	35-085-20453
13	Depco No. 2-21 Forbes	sec. 21, T. 6 S., R. 2 E.	35-085-20701
14	Depco No. 1-21 Evans	sec. 21, T. 6 S., R. 2 E.	35-085-20550
15	Texaco No. 1 Forbes-Talbert	sec. 15, T. 6 S., R. 2 E.	35-085-20115
16	Pure No. 1 Resources Block	sec. 30, T. 5 S., R. 3 E.	35-019-01013
17	Cotton No. B-1 State Park	sec. 30, T. 5 S., R. 3 E.	35-019-22781
18	Cotton No. A-1 State Park	sec. 19, T. 5 S., R. 3 E.	35-019-22414
Section 7			
1	Pasotex No. 1 Brannan Unit 6	sec. 25, T. 7 S., R. 2 E.	35-085-00246
2	California No. 1 Sweet	sec. 24, T. 7 S., R. 2 E.	35-085-30128
3	British American No. B-1 Brannan	sec. 24, T. 7 S., R. 2 E.	35-085-00017
4	California No. 1 Green	sec. 13, T. 7 S., R. 2 E.	35-085-00254
5	Texaco No. B-1 Little-Green	sec. 18, T. 7 S., R. 3 E.	35-085-00271
6	Texaco No. 1 Little-Green	sec. 18, T. 7 S., R. 3 E.	35-085-00253
7	Texas No. 1 Green	sec. 18, T. 7 S., R. 3 E.	35-085-00249
8	Texaco No. 4 Green	sec. 18, T. 7 S., R. 3 E.	35-085-20468
9	Texaco No. 3 Green	sec. 18, T. 7 S., R. 3 E.	35-085-00280
10	Texas No. 1 Dexter	sec. 7, T. 7 S., R. 3 E.	35-085-00264
11	Texas No. 1 Spring	sec. 7, T. 7 S., R. 3 E.	35-085-00265
12	Cameron No. 1 Haynes		35-085-00021
13	Mapco No. 1 Carmon	sec. 5, T. 7 S., R. 3 E.	35-085-20698
14	Sinclair No. 1 Hefner	sec. 33, T. 6 S., R. 3 E.	35-085-00555
15	Sinclair No. 2 Hefner	sec. 33, T. 6 S., R. 3 E.	35-085-20377
16	Arkla No. 1-11 Cobb-Tipperary	sec. 11, T. 6 S., R. 3 E.	35-095-20138
Section 8			
1	Pasotex No. 1 J. & R. Brannon	sec. 25, T. 7 S., R. 2 E.	35-085-00245
2	Chevron No. 1 J. C. Brannon 3rd	sec. 30, T. 7 S., R. 3 E.	35-085-00189
3	Texaco No. 1 Westheimer-State	sec. 20, T. 7 S., R. 3 E.	35-085-30037
4	Marymac No. 1 Davis	sec. 17, T. 7 S., R. 3 E.	35-085-20886
5	Ware No. 1 Ruth	sec. 17, T. 7 S., R. 3 E.	35-085-20778
6	Texaco No. 1 Nobel	sec. 17, T. 7 S., R. 3 E.	35-085-30130
7	Texas No. 1 Baxter	sec. 17, T. 7 S., R. 3 E.	35-085-00252
8	Shell No. 1 Pershica	sec. 3, T. 7 S., R. 3 E.	35-085-00001
9	Texaco No. 1 Pershica	sec. 3, T. 7 S., R. 3 E.	35-085-30022

Oklahoma Geological Survey Circular 97, 1995

Thermal Evolution of the Harper Field, Central Basin Platform, Ector County, Texas

Jack G. Elam
Independent Geologist
Midland, Texas

ABSTRACT.—The structure of the Harper field in the Permian basin of West Texas illustrates the thermal nature of the symmetrical rifting process. In the Harper field, as well as in many others, the Permian Yates structural contours replicate those of the Ordovician Ellenburger. That is remarkable because the Harper structure was thermally uplifted during the Pennsylvanian, and the Yates sand was deposited 50 million years later during the subsequent Permian cooling cycle.

In the Elam rift model, the morphology developed during the thermal-uplift cycle is similar to that of the subsequent cooling cycle. It turns out that what the two periods of deformation have in common is episodic uncoupling of preexisting vertical fractures in the brittle crust. Thus, differential movement of basement blocks, in response to gravity after uncoupling, is similar whether the net movement of the crust is up or down.

The Elam dilational model of rifting has proven to be extremely helpful in locating anticlinoria in the Permian basin. Almost every single producing structure in symmetrical rift basins consists of mirror-image closures separated by crestal grabens.

Rift basins produce the majority of the hydrocarbons on our planet. The symmetry of the structures makes them easy to find, and they provide the perfect set of conditions for generating and entrapping hydrocarbons.

INTRODUCTION

The Harper field illustrates the evolution of a typical producing anticlinorium in the rifted Permian basin. Rifting of the earth's crust is caused by rising pods of greater heat flow within the mantle, and this thermal process yields symmetrical structures.

The Harper field is located on the central basin platform of the Permian basin of Texas ~10 mi west of Odessa (Fig. 1). It embraces ~35 mi^2 and produces from several pays from the shallow Permian San Andres Formation to the deep Ordovician Ellenburger Formation. Although the Permian basin is the sixth largest producing basin in the world, it is only partially exploited because its structural style is generally not well understood due to the failure on the part of geologists to differentiate between dilational and extensional processes. This failure is a consequence of use of planar structural models. Nowhere is this better illustrated than by the AAPG Memoir 46 (Tankard and others, 1989) titled *Extensional Tectonics and Stratigraphy of the North Atlantic Margins*. Within this massive tome, there is no illustration or model that takes into consideration the fact that our planet is a spheroid. I predict that there will be a significant upsurge in discovery rates in mature rift basins like the Permian and Anadarko when geologists begin to view deformation in three dimensions.

STRUCTURAL MODELS

The Permian basin is an ideal rift basin, and I propose that it be designated the type locality of rifting. Rifting is caused by rising pods of heat within the mantle. This increasing heat flow causes dilation, which is merely extension in three dimensions. The use of planar structural models has resulted in the failure to recognize that dilation and extension create completely different structural styles.

In order for a geologist to properly map the structures of a hydrocarbon-producing basin, his first step should be to develop a viable, three-dimensional structural model that is in accord with the hard well data. Unfortunately, planar thinking

Elam, J. G., 1995, Thermal evolution of the Harper field, central basin platform, Ector County, Texas, *in* Johnson, K. S. (ed.), Structural styles in the southern Midcontinent, 1992 symposium: Oklahoma Geological Survey Circular 97, p. 161–173.

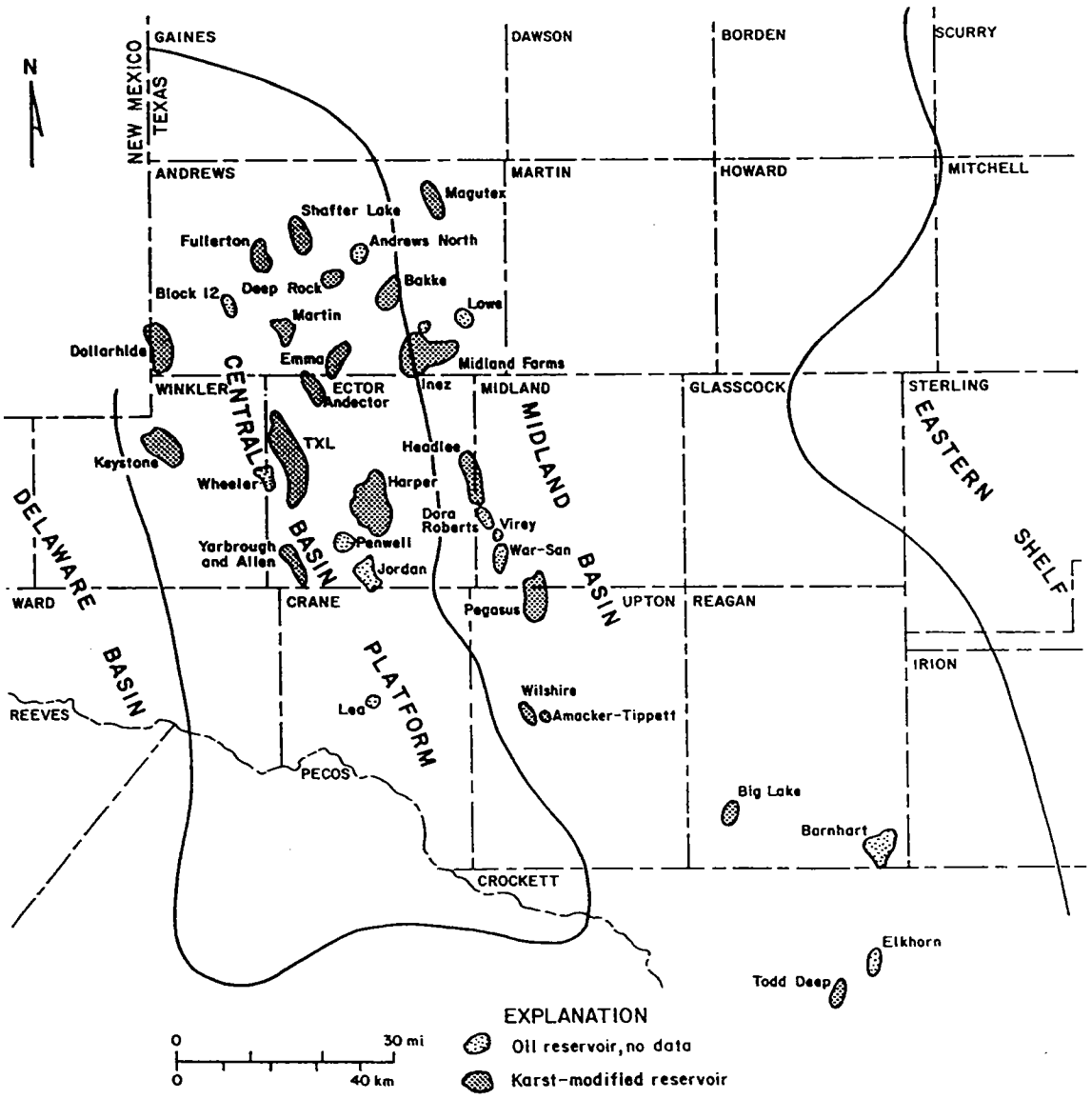


Figure 1. Location of Harper field and other major Ellenburger oil reservoirs. Reproduced from Galloway and others (1983).

and visualization persist even when two-dimensional structural models fail to work mechanically or fail to satisfy the subsurface data.

The Cloos Model

Hans Cloos (1930) may have been the first to recognize that dilation was extension in three dimensions. He inflated a balloon under a clay cake, creating the tilted fault-blocks morphology shown in Figure 2. Nevertheless, the significance of his discovery was ignored for many years, with disastrous results for our profession.

Anderson Stress Analysis

E. M. Anderson (1942) attempted to explain all faulting by showing what he thought to be the only three possible orientations of his principal stress axes ($P_1 > P_2 > P_3$), as shown in Figure 3. He did explain normal faulting (extension), thrust faulting (horizontal compression), and wrench faulting. His models and stress analysis techniques became embedded in the conventional wisdom in geology. Unfortunately, he overlooked fluid pressure, which causes most of the structural deformation in symmetrical rift basins.

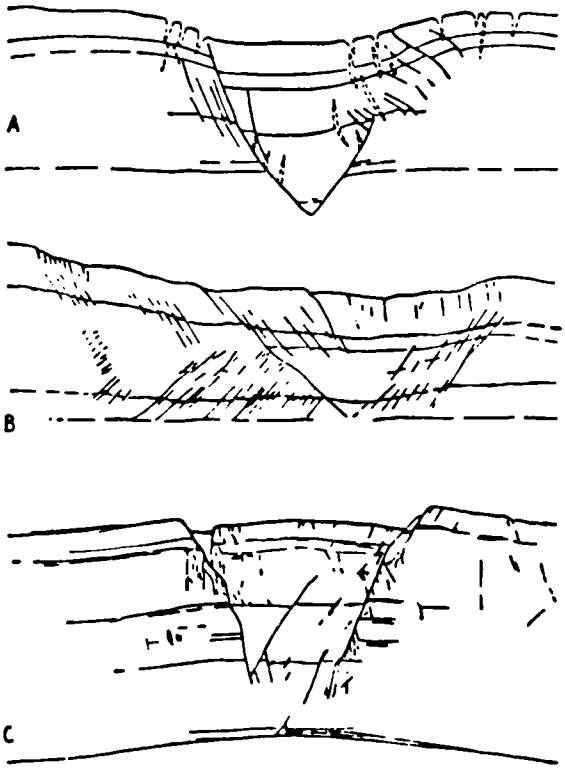


Figure 2. Cloos's (1930) experiments modeling normal faulting: (*A*) clay cake, (*B*) clay cake mounted on a rubber sheet, and (*C*) clay cake mounted on inflated balloon. The last diagram closely resembles the Elam rift model. Reproduced from DeSitter (1956).

The McKenzie Rift Model

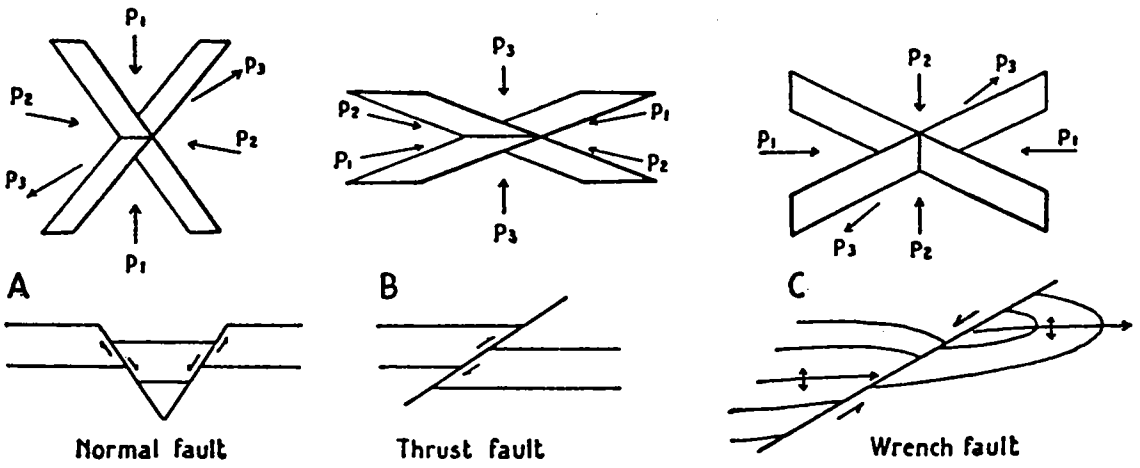
D. P. McKenzie (1978) proposed a 2-D model of rifting that quickly became accepted by most geologists. McKenzie believed that rifting was initiated by extensional thinning of the continental crust and lithosphere, although the mechanics of that process were not clear. He believed that this thinning caused a passive upwelling of the hot asthenosphere from below and the increased heat flow associated with rifting. McKenzie (1978) did not display a full rift model in his paper, so I have included two modified McKenzie rift models (Figs. 4,5) to permit a better viewing of his concepts.

Bally and Snelson

Next, let's consider Bally and Snelson's (1987) version of the McKenzie rift model (Fig. 4). Their model displays curved listric faults which are not commonly found, at least within the Permian basin. Although Bally and Snelson (1987) say rifting is an extensional process, their model actually displays uplift similar to that which occurs with dilation and thermal doming. There is no real need for extensional stresses, except possibly to create the curved listric faults.

Issler and Beaumont

Issler and Beaumont's (1989) interpretation of McKenzie's model (Fig. 5) treats rifting as a purely extensional process operative on a flat earth. They also rheologically treat the brittle crust as if it were ductile, and they also show an ocean basin developing over the rift without providing for a stress sys-



The origin of faults. P_1 = largest, P_2 = median, and P_3 = smallest principal stress.

Figure 3. Anderson's (1942) explanation of "all" faulting. He claimed that all faults could be explained using the three "possible" orientations of the principal stress axes. Reproduced from DeSitter (1956, p. 119).

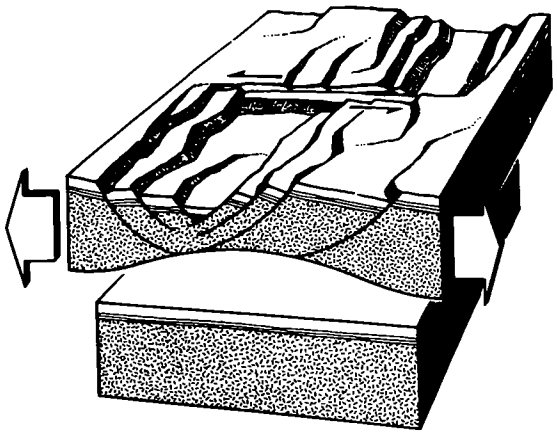


Figure 4. McKenzie (1978) rift model; from Bally and Snelson (1987). (Reprinted by permission from the Canadian Society of Petroleum Geologists.)

tem that could have created it. They have ignored the thermal expansion of the brittle crust associated with the increased heat flow that created the rifting. Had they integrated all their systems, they could have properly explained the "aulacogen" present at the crest of their rifted uplift.

Vierbuchen, George, and Vail Model

A most important and valuable rheological model of the earth was promulgated by Vierbuchen and others (1983) of the Exxon research lab (Fig. 6). However, they, too, treat the earth as if it really were "flat." In this model, the base of the brittle continental crust is ~15 km deep and the base of the underlying ductile crust is ~35 km deep at time (t) = 0 Ma. At t = 25 Ma, the brittle-ductile boundary is a bit shallower. Most significantly, their model shows that rising isotherms associated with rifting raise the boundaries between the various layers. That means that elevated temperatures alone may account for much or most of the crustal thinning associated with the rifting observed by McKenzie (1978). However, these researchers failed to emphasize the fact that as a consequence of thermal uplifts, the brittle crust may also be thinned by erosion.

In Figure 7, the earth's curvature has been incorporated into the Vierbuchen, George, and Vail rheological model. In this model, most or all of the features that McKenzie (1978) attributed to planar extension are explained by thermal uplift.

The Elam Rift Model of 1974

In reviewing the literature on rifting, preparatory to writing this paper on the Harper field, I retraced my thought processes in working out the thermal evolution of the Permian basin. Had I not commenced my research before 1978, I question whether I would have been able to overcome the conventional wisdom, i.e., planar modeling. That change to the 3-D perspective is far more difficult to do than most earth scientists realize. Only a handful of geologists still follow the teachings of Dallmus (1958) about the curvature of the earth.

Because rifting in the Permian basin was aborted early in the thermal cycle, the initial stages of rifting can be viewed in fine detail. The Ellenburger map (Figs. 8,9) permits working out of the structural evolution of this thermal uplift because there is enough deep-well control, and jammed electric-log cross sections permit a geologist to recognize the various episodes of thermal activity. Structural contours of the shallow Yates (Fig. 9) closely mimic those of the Ellenburger. As there is far more shallow-well control, this map provides guidelines for the deep Ellenburger contours. The contoured morphology in Figures 8 and 9 is quite different from that which most geologists have been visualizing, but it is very much in accord with my 1974 rift model (Fig. 10). The structure portrayed at the surface of Bally and Snelson's (1987) model (Fig. 4) is almost identical to that of the Elam dilational-rift model (Fig. 9), with one critical exception: the Bally and Snelson model shows the dip on the fault blocks steepening towards the crestal graben, whereas, in the Permian basin, the opposite sequence is true, at least on every anticlinorium I

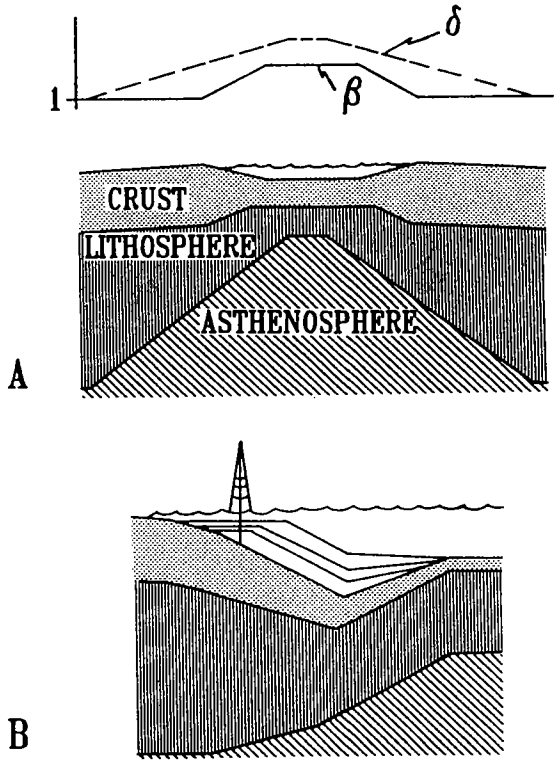


Figure 5. Modified McKenzie (1978) rift model; from Issler and Beaumont (1989).

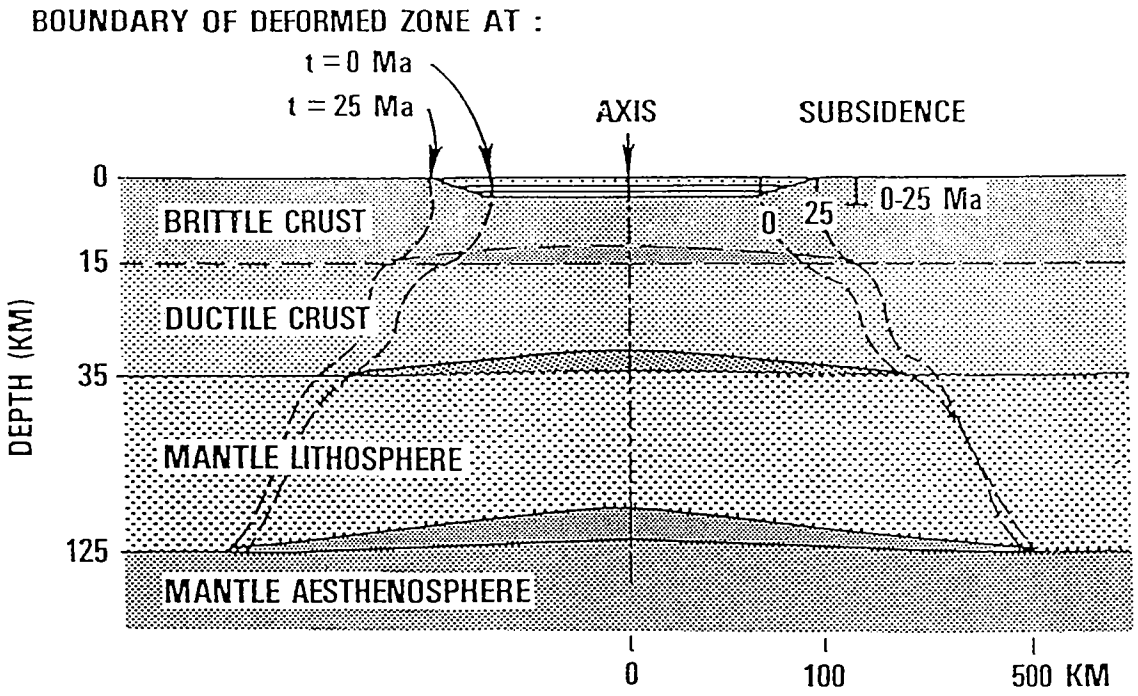


Figure 6. Vierbuchen, George, and Vail's planar rheological model; from Vierbuchen and others (1983). Note that this model allows for thinning of the brittle crust by an increasing heat flow.

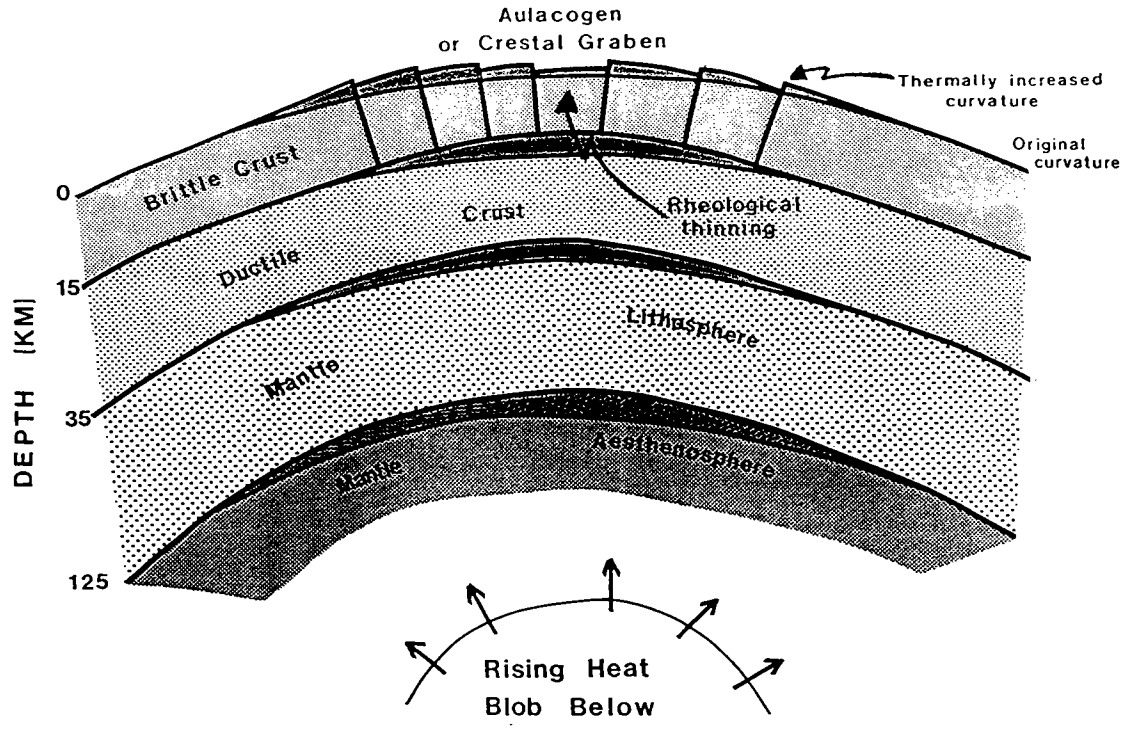


Figure 7. Rheological model modified from Vierbuchen and others (1983) to show the curvature of the earth.

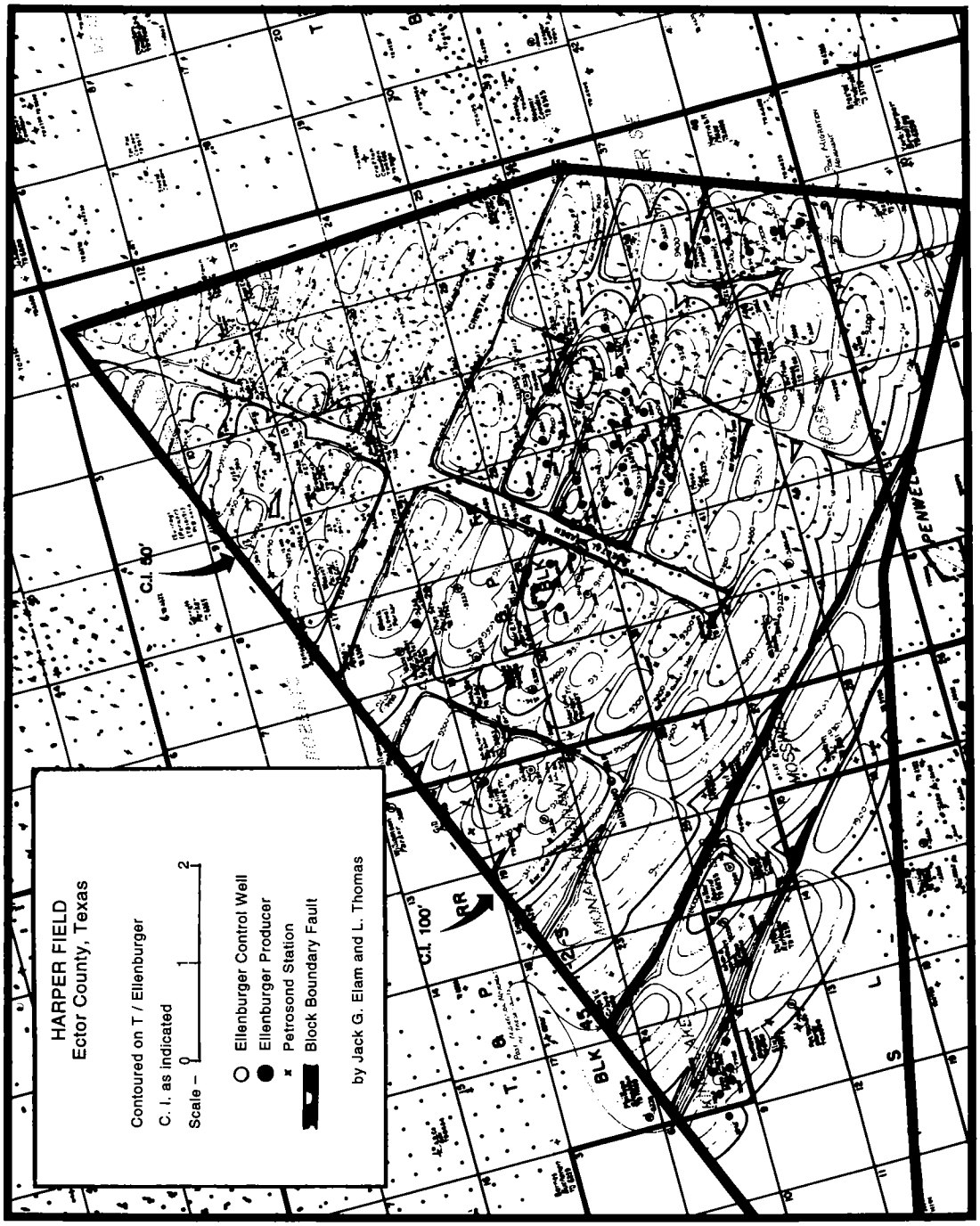


Figure 8. Structure contours on top of the Ordovician Ellenburger Group in Harper field, Ector County, Texas.

have mapped in detail. I am thankful that Woldegabriel and others (1990), in field mapping the Ethiopian rifting area (Fig. 11), described most of the rift phenomena present in the Permian basin.

In modeling rifting, I found that a valid explanation for vertical faulting was essential. Once that was resolved, everything else fell in place because most of the faulting in the Permian basin is the result of dilational pull-apart of the pervasive vertical-fracture system in the brittle crust and is not caused by shear stresses, as many geologists suggest.

Next to be modeled were the mechanics responsible for flattening of the tilt of the fault blocks (Fig.

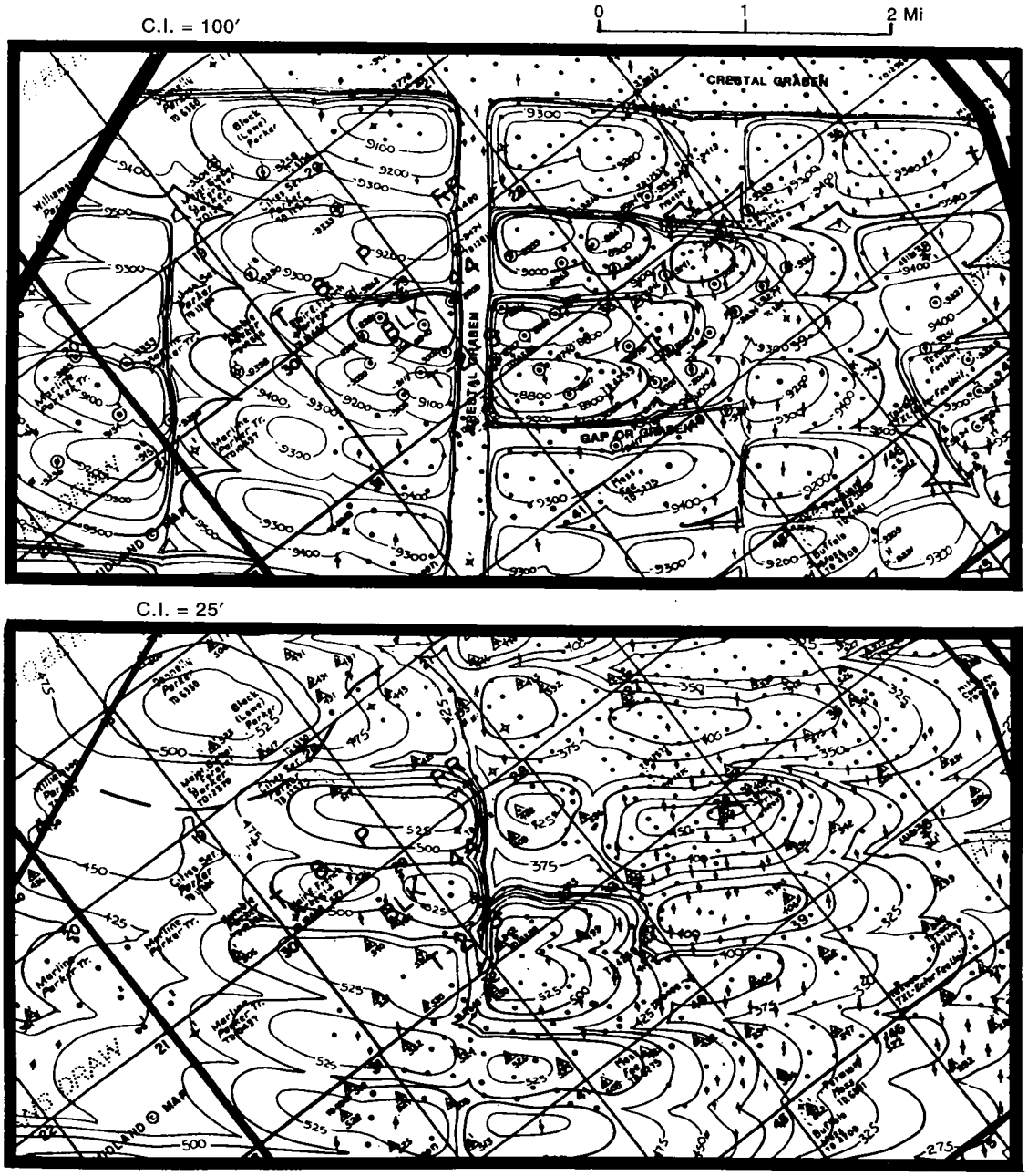


Figure 9. Structure contours of the Harper field, Ector County, Texas: upper map shows contours on top of Ellenburger Group (Ordovician); lower map shows contours on top of Yates Sandstone (Upper Permian).

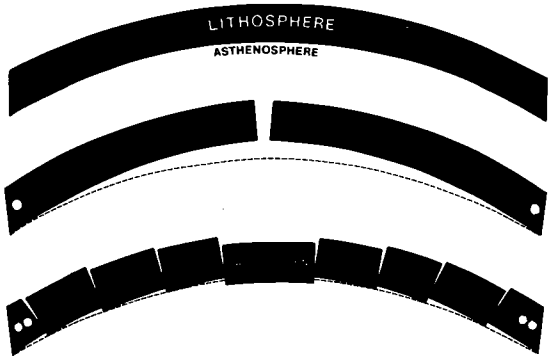


Figure 10. Elam's 1974 rift model (Elam, 1989). Several intermediate stages were later added. What turned out to be most significant were the gaps between the blocks; younger rocks are often found in these gaps within the Ellenburger Group.

10). In the real world, vertical faults and fractures converge toward the center of the earth. That means that the individual crustal blocks are wedge shaped. It is the downward convergence of the faults that is essential, if one is to adequately explain the stress systems associated with rifting.

When I constructed my model, I induced a 5° angle of tangency in the end blocks, and then preserved those tilts by inserting a second pin in them (Fig. 10). At that point, the remaining blocks were then allowed to settle downwards in response to gravity. In my 1974 model, I failed to take into consideration the coefficient of expansion of the brittle crust; therefore, I did not recognize that, with cooling and collapse, the tilted blocks would become recoupled well above their ultimate equilibrium position. After the initial recoupling, subsequent shrinkage of the brittle crust permitted the episodic uncoupling of the vertical fractures during the cooling cycle.

By overlooking that one step, though, my research was allowed to focus on another important geometric relationship, at least for an oil finder. As shown in my model, when the crust has finally returned to its original temperature, the blocks will have subsided to approximately original levels. However, the blocks now tilt away from the crestal graben or grabens (Fig. 10), but by that time the uplift should have entrapped hydrocarbons. The closure is provided by the crestal grabens which may be many hundreds of feet deep. Economically important is the fact that these flat-lying blocks are generally overlooked by explorationists, and narrow grabens, as in the Harper field, are particularly difficult to pick up on seismic sections.

THERMAL EVOLUTION OF THE PERMIAN BASIN

The Permian basin area experienced major episodes of thermal uplift during the late Precambrian and Carboniferous. The Carboniferous uplift was aborted early in the thermal cycle. There seldom are other structural overprints. This simple setting is so rare that the Permian basin should be designated as the *type locality of rifting.*

The first thermal cycle was associated with the opening of the Iapetus Sea in late Precambrian time (Fig. 12). The precursor Tobosa basin was a swale on the edge of the North American plate, located between two mantle plumes that I call the Llano

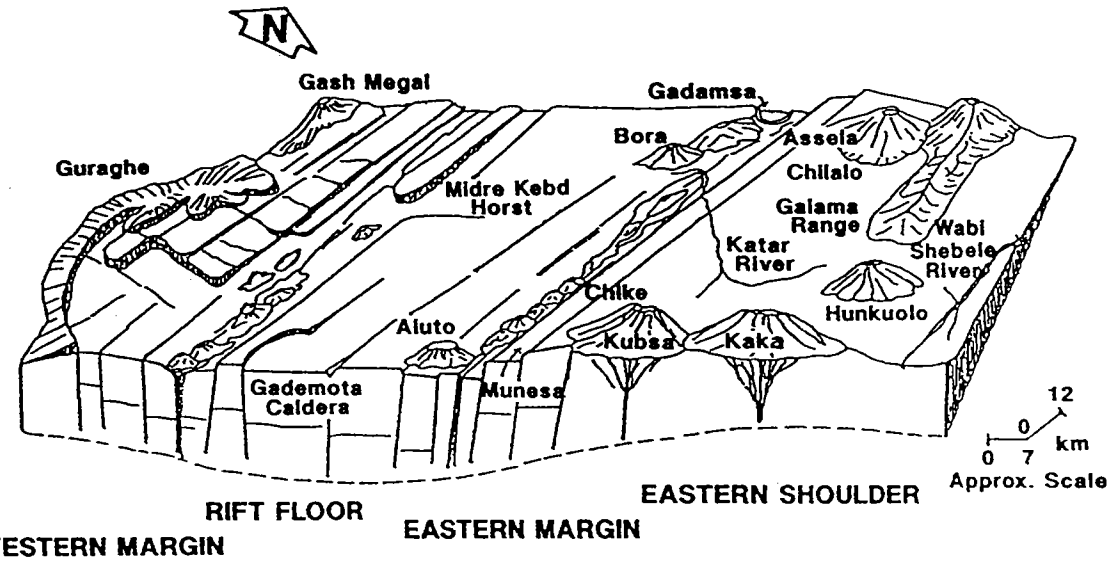


Figure 11. Block diagram across the Ethiopian rift, as shown by Woldegabriel and others (1990). This is the closest approach to the Elam rift model, although the curvature of the earth was ignored.

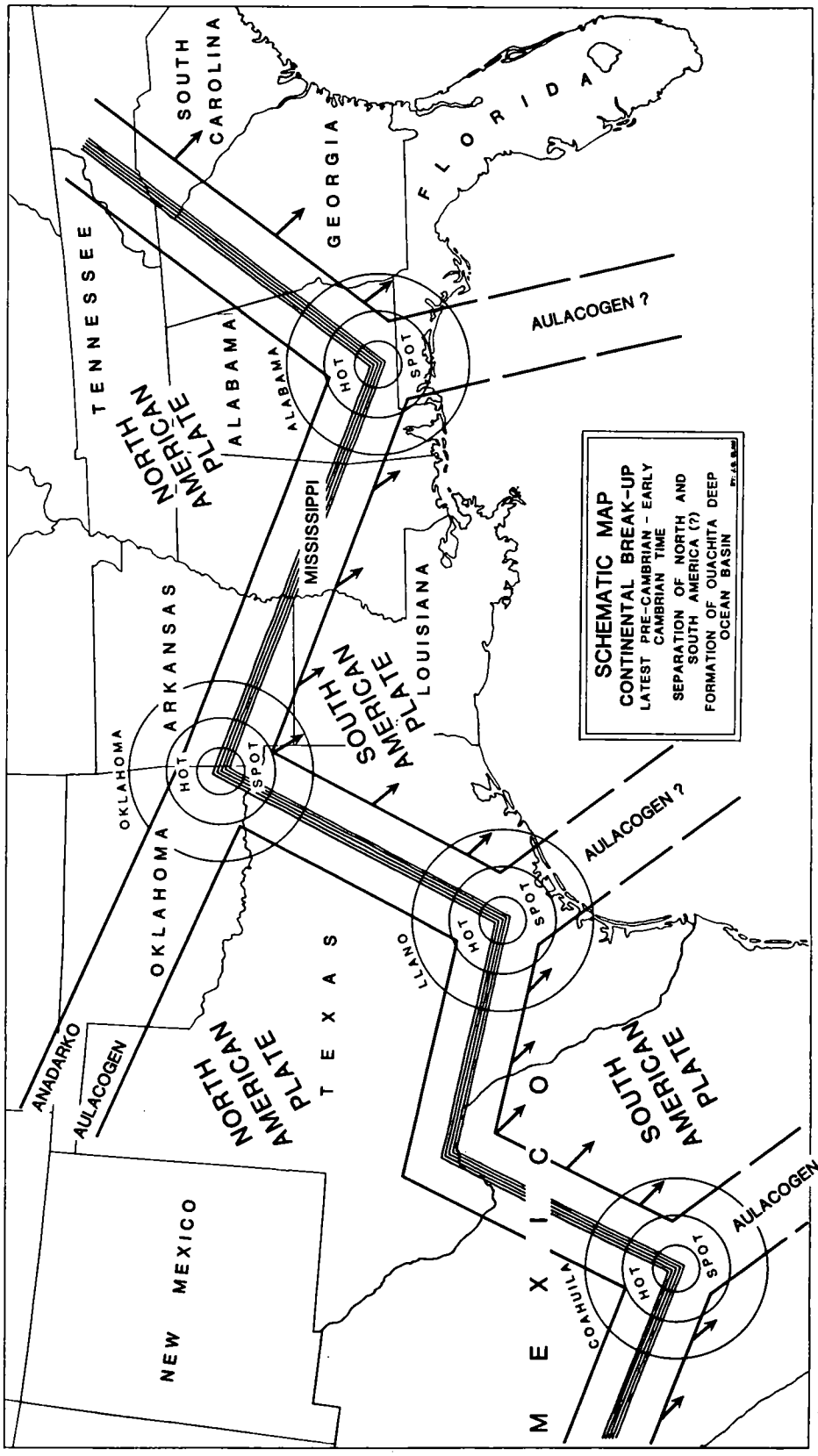


Figure 12. The opening of the Iapetus Sea in late Precambrian time.

and Coahuila hot spots. New oceanic crust was vertically emplaced all along the southern and eastern margins of the North American plate, and the Anadarko and Reelfoot aulacogens were formed during this thermal uplift (Fig. 12). However, there is no subsurface evidence to support the formation of a Delaware basin aulacogen or any other thermal uplifts in the Tobosa basin during the late Precambrian, as many allege. As the Tobosa basin cooled and subsided below sea level, Cambrian sandstones such as the Bliss and Hickory were deposited on the edges of the North American craton. By Ordovician time, the continental crust had cooled and subsided sufficiently so that thick Ellenburger shallow-water carbonates accumulated over much of the Tobosa basin. A similar depositional history, controlled by the same cooling curve, occurred all along the southern and eastern edge of the North American plate, facing the Iapetus Sea as far north as New York state.

The second thermal uplift cycle began in late Mississippian time, as evidenced by a gentle doming near the center of the Tobosa basin. As this thermal dome rose, its surface area increased more rapidly than the brittle crust expanded, creating a paucity of crustal material, and polygonal blocks started to develop. In places, ultramafic rocks were intruded into the gaps between blocks. The amount of permanent dilation was not great; with cooling, everything in the basin fit back into place. The polygonal blocks vary in size, but the largest one covers hundreds of square miles. Hydrocarbons migrated into the higher parts of the dome before the polygonal-block boundary faults became seals. Vertical offsets between the polygonal blocks may or may not have taken place as a consequence of the uncoupling and response to gravity. In places, the Simpson shales collapsed into the gaps. Thus, these block-boundary faults may or may not be impermeable barriers. Later, smaller discrete blobs of heat uplifted local areas of the crust and created anticlinoria with diverse orientations (Fig. 13).

Thermal Controls on Rifting

When plate-tectonic theory was first being promulgated, mantle plumes were considered to be the primary sources of heat flow within the mantle. Plumes are normally long-lived, and associated uplifts are clearly evident in the vicinity of the Hawaiian and Yellowstone hot spots, for example. However, in the Permian basin, the generalized heat source causing the rifting began to run out of energy fairly early. Local uplifting was caused later by smaller rising heat blobs. These smaller heat blobs were most evident in Dr. Jerry Shubert's UCLA Cray-computer simulation of mantle convection on our planet during the past many billions of years (personal communication). Although mantle plumes were clearly the primary thermal features in his simulation, many local heat blobs could be observed detaching themselves from the mantle plumes. The source of the heat for this convection is the earth's core, which is hotter than the surface of the sun. Today, seismic tomographers are in the process of tracing out many of these smaller rising heat blobs within the mantle.

Hydrocarbon Accumulations

As noted earlier, symmetrical rifting provides ideal conditions for the generation and entrapment of hydrocarbons. In a study of thermal maturity of the Tobosa basin, Dr. Walter Pitman of Lamont Observatory (personal communication) concluded that the depth of burial in the Tobosa basin was sufficient for the source rocks to commence generating hydrocarbons by Early Pennsylvanian time, even without making use of my newly recognized Pennsylvanian heat source. Furthermore, it is apparent that hydrocarbons accumulated early in this thermal dome as it commenced rising. As the Tobosa basin source rocks were being heated from below, both the porosity and permeability were being

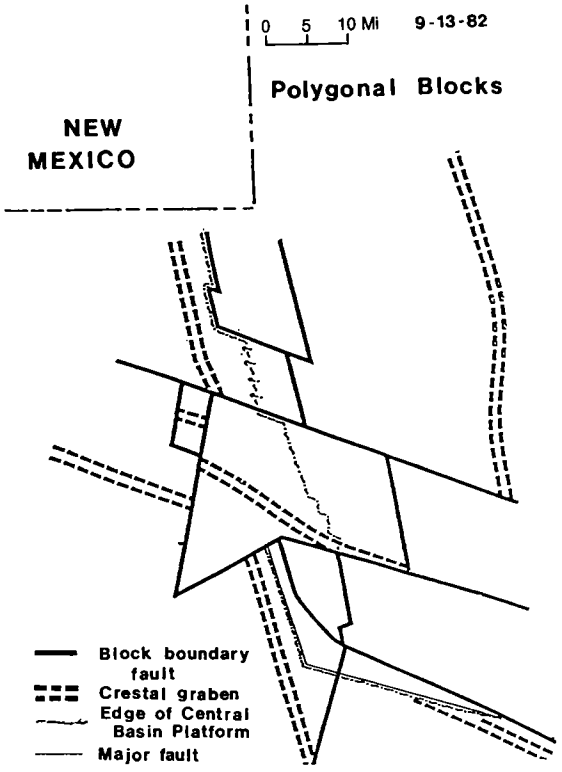


Figure 13. An example of the thermally developed polygonal blocks and discrete anticlinoria that were created at the crest of the Gomez Superdome. The anticlinorial crests are defined by the location of the crestal grabens. Anticlinoria have diverse orientations. The local stress systems that created the anticlinoria are a function of the shape of the intrusive bodies that raise the brittle crust.

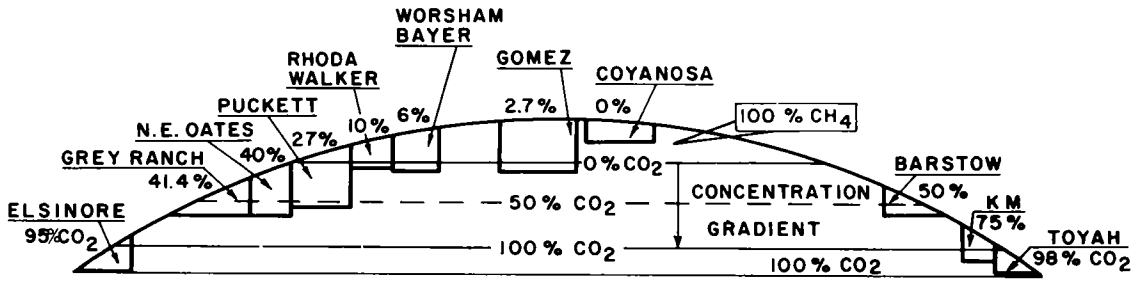


Figure 14. Schematic section of the Gomez Superdome, showing gas distribution within the Ordovician Ellenburger Group at that time. The CO_2 was initially driven out of the Ellenburger dolomite by the increased heat flow that also created the rifting. Heavier than methane, the CO_2 settled to the bottom of the Gomez Superdome. The structures located near the original crest of the superdome contain nearly 100% methane, whereas those around the edge contain nearly 100% CO_2.

dilationally enhanced. As a result of this dilational uplifting, the brittle carbonate reservoir rocks, such as the Devonian and Ellenburger, developed pressure sinks enhancing the movement of hydrocarbons out of the source rocks and into the reservoirs. Shortly after the polygonal blocks were formed, the various discrete producing anticlinoria were locally uplifted, apparently by lesser pods of greater heat flow within the overall heat blob. In some cases, the already-entrapped hydrocarbons remigrated into newly formed anticlinoria, but most commonly they remained in situ. The shape of the underlying intrusives controlled the local patterns of dilational failure of the ubiquitous preexisting vertical fractures. These heat blobs sometimes uplifted single polygonal blocks, as in the Harper area, but generally several blocks were uplifted. This caused the anticlinoria in the basin to have the very diverse orientations (Fig. 13) that many have attributed to wrench faulting. Most probably, the igneous bodies involved are sills at the base of the brittle crust. Remember that the crust can thin rheologically, so these sills are often found at lesser depths, and some have been drilled as legitimate seismic anomalies. (They were dry!)

On this rising thermal dome, which I call the Gomez Superdome, after the largest gas field at or near its original crest, the temperature eventually became hot enough so that CO_2 gas was driven out of the Ellenburger dolomite; but this gas generally remained within the Ellenburger reservoirs (Dr. Ian Kaplan, UCLA, personal communication). Methane was present at the top of the dome. The heavier CO_2 molecules settled into the lower reaches of the reservoir (Fig. 14). The column in this giant accumulation must have been at least 10,000 ft thick originally. Even after cooling and collapse, which allowed for considerable remigration into the newly developing anticlinoria, a generalized CO_2-concentration map still reveals part of the geometry of that original dome (Fig. 15). The Gomez Superdome covered several thousand square miles and probably trapped at least 100 Tcf of gas. Later-formed anticlinoria located near its original crest produce almost 100% methane, whereas fields around its edges produce large amounts of CO_2 from the Ellenburger (Figs. 14,15).

GEOPHYSICAL PROBLEMS

Although I have not examined any seismic data from the Harper field, data from many other areas reveal that even the most recent 3-D surveys may not define the actual morphology of the individual tilted fault blocks, unless the geophysicist knows what he is looking for. Near-surface velocity problems and great variations of velocity have to be overcome by stacking and computer processing, which tend to smooth out the structure and hide the fine detail. In the Permian basin, I have yet to see a 2-D seismic section that clearly defines the small second-order block faulting in the Harper field. However, I have recently heard from a reliable major-company source that their newest 3-D seismic reveals a tilted fault-block morphology, quite similar to that of the Harper field. Unfortunately, they didn't know what to make of it; but if that proves to be true, it will quickly change the exploration game. As of now, smoothed structures tend to be ignored by explorationists, but I believe that they can be properly visualized when one understands the processing involved.

THE HARPER ENIGMA

As mentioned earlier, the structure displayed on the shallow Yates structure-contour map in the Harper field almost appears to be an overlay of the Ellenburger structure-contour map (Fig. 9). This means that the stress systems operative during thermal uplifting appear to have been replicated millions of years later during the cooling cycle.

Given the now-described Elam rift model, I be-

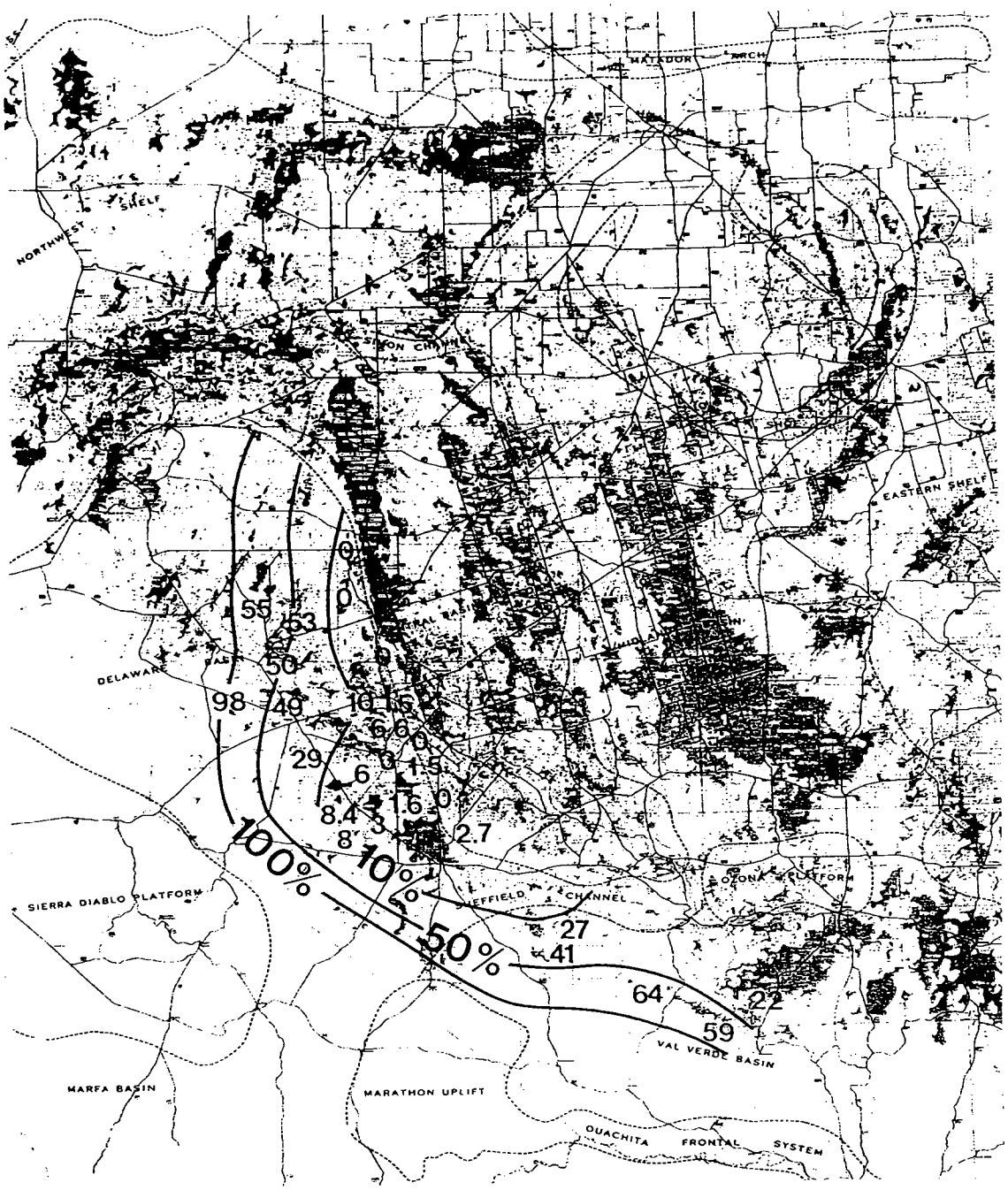


Figure 15. CO_2 concentration map. Figures are in wt% CO_2. Even though cooling and collapse greatly modified the Gomez Superdome, the CO_2-concentration map (Fig. 14) still reflects the morphology of the precursor dome.

lieve it has already provided the answers. During the dilational phase, fault offsets are caused by uncoupled vertical fractures. During thermal uplift, the basement expands, so that when the tilted blocks subside and are recoupled, they first come to rest well above their original level. As the brittle crust cools and contracts, the vertical fractures continue to uncouple and recouple. That cooling and collapse obviously continued for millions of years following the initial uplift. Thus, there is really no Harper field enigma; the heated and cooled brittle crust behave as it should in response to gravity, as was shown in my 1974 rift model.

There is a new telluric geophysical tool that can accurately measure true vertical depth, the PetroSonde (see Elam 1986,1990). These depth measurements were very important in validating my model. In every instance, the tilted fault block morphology came through loud and clear.

SUMMARY AND CONCLUSIONS

Although this paper has strived to emphasize 3-D modeling and visualization, there is another important point to be made. In many respects, the job of an exploration geologist in the Permian basin is similar to that of aircraft engineers who specialize in investigating plane crashes. For example, when Pan Am Flight 103 was destroyed by a bomb over Scotland a few years ago, the engineers were able to lay out all the many parts of the crashed plane, pinpoint the specific location of the suitcase that contained the explosive and pretty well estimate its size. We geologists surely ought to be able to match their capability in mapping out the "explosions" that created the producing anticlinoria because, with our contour maps, we are also laying out all the parts on the ground.

Certainly, the Harper field contour maps illustrate that it is not difficult when we use all the tools available. The tragedy is that many geologists have never been comfortable using stress analysis and structural mechanics to help them in contouring their structures. It is amazing that planar rift models have changed so little in the 34 years since Dallmus made his most significant contribution regarding the shape of our planet.

While the results of the new three-dimensional seismic have been sensational, I believe that 3-D visualization in geology may offer more long-term economic promise for our industry than even the 3-D seismology. In the rifted Permian basin, anyway, there are many partially developed anticlinoria, and most of them will remain under-exploited until geologists learn to view the earth using the right 3-D perspective.

REFERENCES CITED

Anderson, E. M., 1942, The dynamics of faulting and dyke formation with application to Britain: Oliver Boyd, Edinburgh and London, 206 p. [revised edition, 1951].

Bally, A. W.; and Snelson, S., 1987, Evolution of passive margins, *in* Foster, N. H.; and Beaumont, E. A. (eds.), Geologic basins I: American Association of Petroleum Geologists, Tulsa, p. 1–86.

Cloos, Hans, 1930, Zur experimentelle tektonik I, Die Naturwiessenschafter, v. 18, no. 34, p. 741–747.

Dallmus, D. F., 1958, Mechanics of basin evolution and its relation to the habitat of oil in the basin, *in* Weeks, L. G. (ed.), Habitat of oil: American Association of Petroleum Geologists, Tulsa, p. 883–931.

DeSitter, L. V., 1956, Structural geology: McGraw-Hill, New York, 552 p.

Elam, J. G., 1969, The tectonic style in the Permian basin and its relationship to cyclicity, *in* Elam, J. G.; and Chuber Stewart (eds.), Cyclic sedimentation in the Permian basin: West Texas Geological Society Publication No. 69-56, p. 55–79.

_____1986, New method helps to refine subsurface interpretations: World Oil, October 1986, p. 55–58.

_____1989, Hidden structures in the Permian basin, *in* Flis, J. E.; and others (eds.), Search for the subtle trap; hydrocarbon exploration in mature basins: West Texas Geological Society Publication 89-85, p. 191–198.

_____1990, New method helps to refine subsurface interpretations; Part 2—Theory: World Oil, June, 1990, p. 45–55.

Galloway, W. E.; Ewing, T. E.; Garrett, C. M., Jr.; Tyler, Noel; and Bebout, D. G., 1983, Atlas of major Texas reservoirs: University of Texas, Austin, Bureau of Economic Geology, 139 p.

Issler, D. R.; and Beaumont, Christopher, 1989, A finite element model of the subsidence and thermal evolution of extensional basins, *in* Naeser, N. D.; and McCulloh, T. H. (eds.), Thermal history of sedimentary basins: Springer-Verlag, New York, p. 239–267.

McKenzie, D. P., 1978, Some remarks on the development of sedimentary basins: Earth and Planetary Science Letters, v. 40, p. 25–32.

Tankard, A. J.; and Balkwill G. R. (eds.), 1989, Extensional tectonics and stratigraphy of the North Atlantic margins: American Association of Petroleum Geologists Memoir 46, 641 p.

Vierbuchen, R. C.; George, P. P.; and Vail, P. O., 1983, Thermal-mechanical rifting model, *in* Watkins, J. S; and Drake, C. L. (eds.), Studies in continental margin geology: American Association of Petroleum Geologists Memoir 34, p. 765–778.

Woldegabriel, G.; Aronson, J. L.; and Walter, R. C., 1990, Geology, geochronology and rift basin development in the central sector of the Main Ethiopia Rift: Geological Society of America Bulletin, v. 102, p. 439–458.

Connections Between Laramide Foreland Arches

Eric A. Erslev and Philipp Molzer*
Colorado State University
Fort Collins, Colorado

Both the Paleozoic southern Midcontinent and the Laramide Rocky Mountain orogenic belts of North America exhibit diverse structural orientations and complex interactions between basement-involved foreland structures. Tectonic models based entirely on either thrust-slip or strike-slip movement fail to explain the connections between the divergent structures in these orogens.

The importance and implications of connections between basement-cored structures are well demonstrated in the Laramide foreland of the western United States. On a large scale, Laramide structural highs (Fig. 1) are sinuous and continuous, defining the elliptical sedimentary basins of the Rocky Mountains. The basement highs are best described as *arches*, not as individual "uplifts." These arches anastomose, with individual basement highs splitting and merging into new highs. The geometries of the anastomosing arches more closely resemble the bifurcation of plate boundaries at triple junctions than the interference patterns generated by superimposed folding. Any model for Rocky Mountain tectonics must be able to explain the connections characteristic of this web of arches.

Several tectonic models for the Laramide orogeny explain the variety of Laramide structural orientations by hypothesizing multiple events to activate structures of different orientations at different times. But the continuous nature of these basement arches, and the lack of clear interference patterns, suggests that the diverse orientations of Laramide faults, folds, and arches may

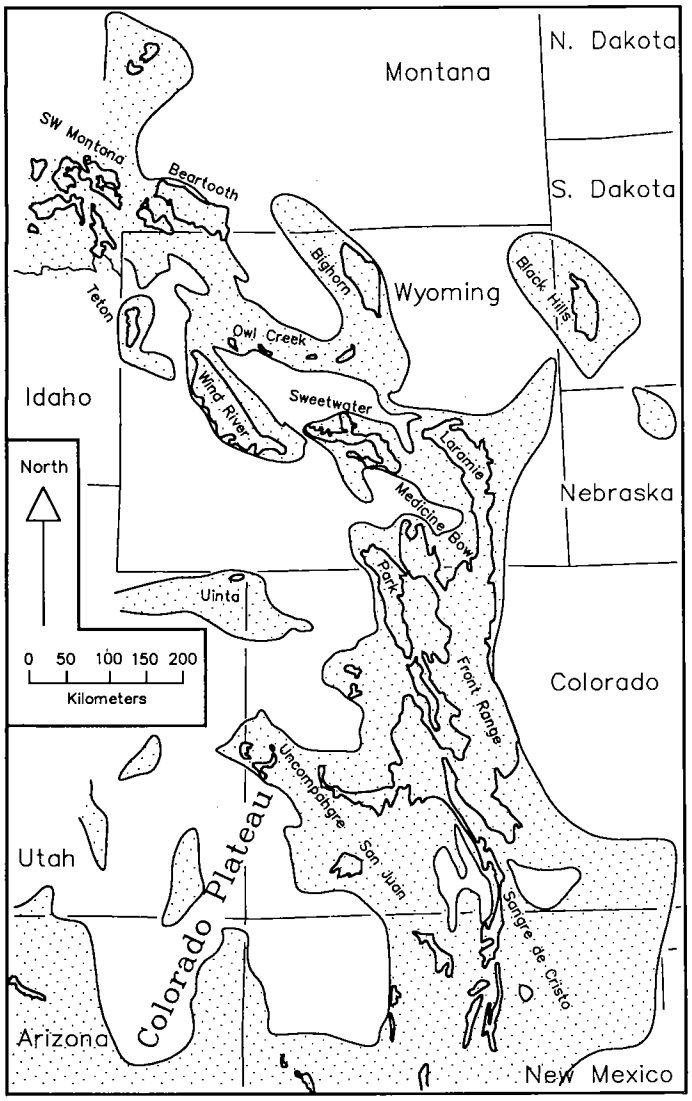


Figure 1. Generalized map of the Rocky Mountain foreland area (after MacLachlan and others, 1972). Exposed Precambrian crystalline rocks are outlined by thick lines, and Precambrian rocks above sea level are shown by dot pattern.

*Present address: E.G.&G. Rocky Flats, Golden, CO.

Erslev, E. A.; and Molzer, Philipp, 1995, Connections between Laramide foreland arches, *in* Johnson, K. S. (ed.), Structural styles in the southern Midcontinent, 1992 symposium: Oklahoma Geological Survey Circular 97, p. 174–177.

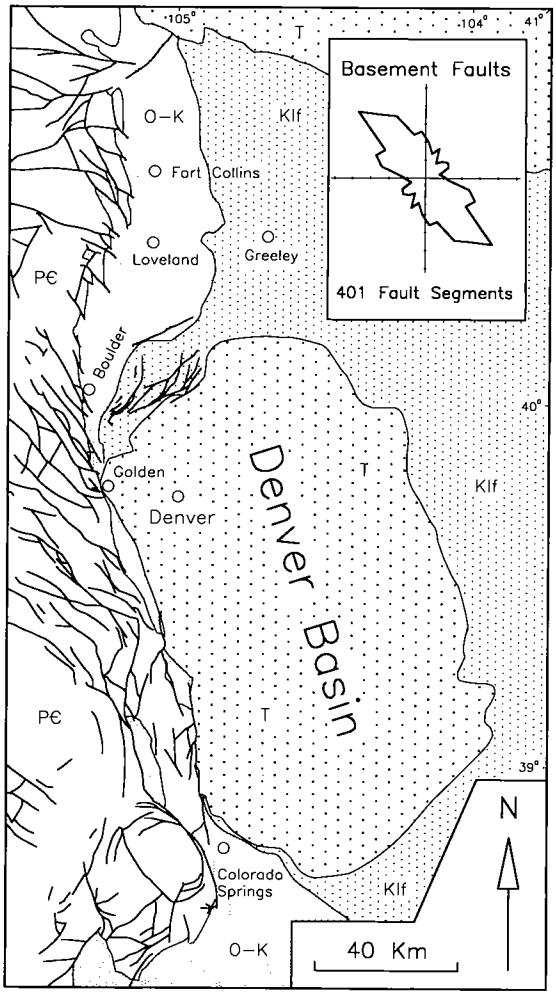


Figure 2. Geologic map of the northeastern Front Range (on left) and the adjacent Denver basin (after Tweto, 1979), with a rose diagram showing the orientations of basement-involved faults. Klf = Cretaceous Laramie and Fox Hills Formations.

have formed during a single, protracted event. One way to test these hypotheses is to determine the slip directions in mountain ranges that are oblique to the average trend of Laramide foreland structures. Models indicating a single phase of deformation predict a generally uniform convergence direction, regardless of arch trend, whereas multistage models predict multiple convergence directions oriented normal to the arch axes.

The eastern margin of the Front Range arch in Colorado (Fig. 2) is oblique to the northwest trend of most foreland faults, folds, and arches (Erslev, 1993). Despite the N4°W orientation of the contact between the Precambrian and Phanerozoic rocks, which parallels the arch axis, basement-involved faults (omitting gravitational detachment structures) predominantly strike to the northwest (see rose diagram inserted in Fig. 2) with a vector mean of N39°W. The obliquity of the fault strikes to the arch suggests that regional convergence may have been oblique, not normal, to the arch axis.

In the northeastern part of the arch, near Fort Collins, these faults dip from 65° to 20° to the northeast with predominantly thrust separations (Erslev and others, 1988). The development of highly altered gouge material in the fault zones prevents the direct measurement of the strike-slip component of motion on these faults. Adjacent slickensides (Fig. 3), however, clearly indicate northeast- and southwest-directed slip, consistent with regional convergence normal to these fault strikes and oblique to the Front Range arch axis.

The west-trending Owl Creek arch bordering the northern margin of the Wind River basin (Fig. 4) provides another test of these tectonic models. Faults exposed within the Owl Creek, Copper, Granite, and Casper Mountains all show a strong obliquity with the west-trending axes of these arches. On the basis of these oblique structural geometries, Paylor and Yin (1993) proposed oblique transpression in the western Owl Creek Mountains. Recent analyses of slickenline orientations from Copper Mountain (Fig. 5) and Casper Mountain

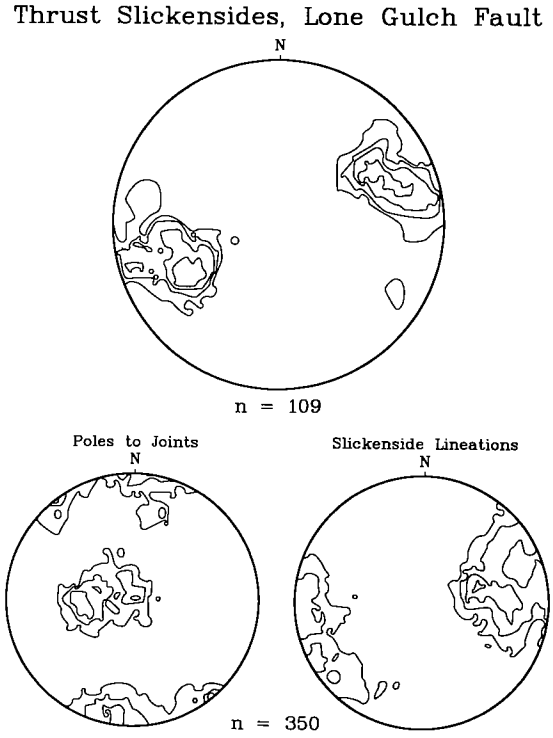


Figure 3. Slickenline directions from the Lone Gulch thrust fault (above) and from the slickensided joints in sandstones of the Dakota Group west of Fort Collins, Colorado (below). Contours at 1%, 3%, 6%, and 10%.

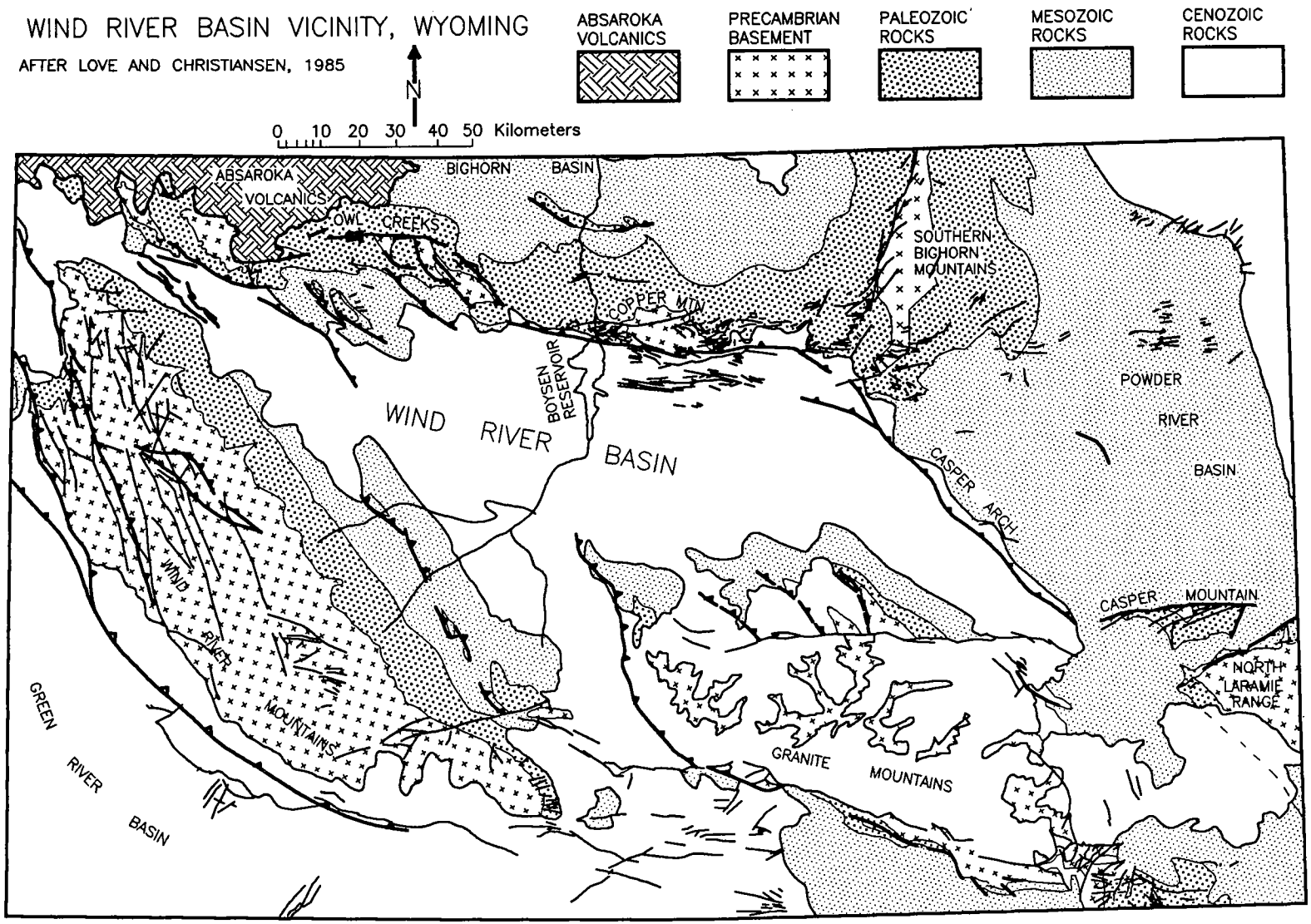


Figure 4. Generalized geologic map of the Wind River basin area, Wyoming (after Love and Christiansen, 1985).

(Molzer, 1993) confirm northeast-southwest shortening oblique to the west-trending arch axes. The northeast-southwest principal compression direction inferred from these fault studies is consistent with the northwest-southeast average orientation of Laramide faults, folds, and arches in Wyoming.

In conclusion, arch geometries, fault orientations, and fault-slip analyses support the concept of synchronous northeast-southwest shortening in an anastomosing system of foreland arches. The continuity of Laramide arches suggests direct linkages between the northeast- and southwest-directed master thrusts underlying the arches. The large-scale geometry of the arches suggests detachment folding where the arches form by crustal thickening and imbrication on ramps and pop-up structures. Basement rotations, crustal rheology (Ord and Hobbs, 1987), and geophysical evidence for an unbroken crust/mantle interface in Wyoming (Brewer and others, 1982; Hall and Chase, 1989) indicate that the master faults underlying the arches are listric, merging in a subhorizontal detachment in the lower crust. Southwest-directed faults (e.g., Wind River thrust) are probably back thrusts off the northeast-directed detachment. West- and north-trending basement arches probably form by oblique slip on lateral ramps connecting the northwest-trending arch culminations.

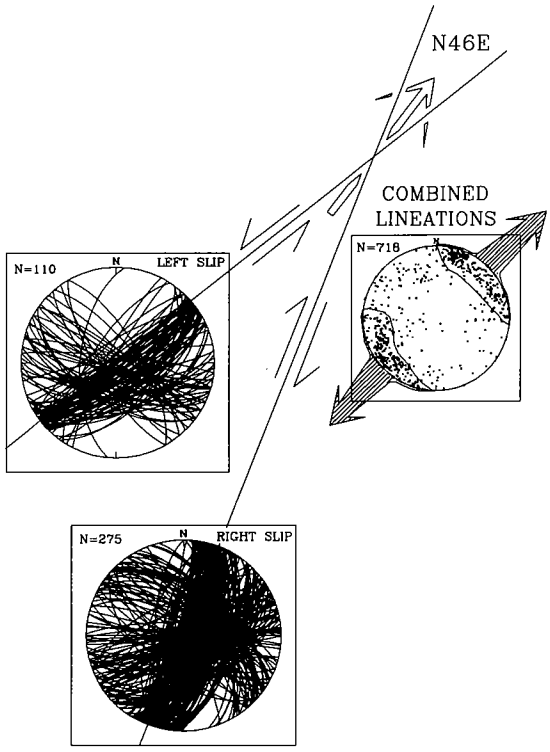


Figure 5. The conjugate geometry of minor high-angle conjugate strike-slip faults (left and below) and the overall geometry of all slickenlines (right) measured in the Copper Mountain area on the eastern Owl Creek arch, Wyoming (Molzer, 1993).

REFERENCES CITED

Brewer, J. A.; Allmendinger, R. W.; Brown, L. D.; Oliver, J. E.; and Kaufman, F., 1982, COCORP profiling in southern Wyoming, Part 1: Laramide structure: Geological Society of America Bulletin, v. 93, p. 1242–1252.

Erslev, E. A., 1993, Thrusts, back-thrusts and detachment of Rocky Mountain foreland arches, *in* Schmidt, C. J.; Chase, R.; and Erslev, E. A. (eds.), Laramide basement deformation in the Rocky Mountain foreland, western United States: Geological Society of America Special Paper 280, p. 339–358.

Erslev, E. A.; Rogers, J. L.; and Harvey, M., 1988, The northeastern Front Range revisited: compression and crustal wedging in a classic locality for vertical tectonics: Field Trip Guide for Geological Society of America 1988 Annual Meeting, p. 141–150.

Hall, M. K.; and Chase, C. G., 1989, Uplift, unbuckling, and collapse: flexural history and isostasy of the Wind River Range and Granite Mountains, Wyoming: Journal of Geophysical Research, v. 94, p. 17,581–17,593.

Love, J. D.; and Christiansen, A. C., 1985, Geologic map of Wyoming: U.S. Geological Survey Map, 1:500,000.

MacLachlan, J. C.; Blemis, H. C.; Holt, R. D.; Kleinkopf, M. D.; Lewis, C. J.; and Wilde, D. E., 1972, Configuration of the Precambrian rock surface, *in* Geologic atlas of the Rocky Mountain region: Rocky Mountain Association of Geologists, Denver, Colorado, p. 53.

Molzer, P. C., 1993, Oblique slip in east-west Laramide foreland arches: Colorado State University unpublished M.S. thesis, 156 p.

Ord, A.; and Hobbs, B. E., 1987, The strength of the continental crust, detachment zones and the development of plastic instabilities: Tectonophysics, v. 158, p. 269–289.

Paylor, E. D.; and Yin, A., 1993, Left-slip evolution of the north Owl Creek fault system, Wyoming, during Laramide shortening, *in* Schmidt, C. J.; Chase, R.; and Erslev, E. A. (eds.), Laramide basement deformation in the Rocky Mountain foreland, western United States: Geological Society of America Special Paper 280, p. 229–242.

Tweto, Ogden, 1979, Geologic map of Colorado: U.S. Geological Survey Map I-1416, scale 1:500,000.

The Slick Hills of Oklahoma and Their Regional Tectonic Setting

R. Nowell Donovan
Texas Christian University
Fort Worth, Texas

ABSTRACT.—The Slick Hills of southwestern Oklahoma are the exposed portion of the frontal fault zone, a region of intense Pennsylvanian deformation that is located between the contemporary Wichita uplift and the Anadarko basin. During the early Paleozoic, the area formed part of the southern Oklahoma aulacogen. A thick and structurally anisotropic sequence of thinly bedded rocks (mostly carbonates) was deposited on a thick suite of Cambrian igneous rocks, some of which are thickly layered. Subsequent Pennsylvanian deformation dismembered the aulacogen. The structural styles that developed reflect variation in isotropy between igneous basement (both within and without the aulacogen) and sedimentary cover. In essence, the cover was incrementally detached along numerous horizons of slippage, recording progressive phases of deformation, whereas strain in the more-massive basement rocks was resolved by large, discrete faults.

Various deformation signatures suggest a principal stress oriented approximately northeast-southwest. This direction is difficult to reconcile with more-or-less contemporary orogenic deformation in Oklahoma, but may reflect a reorientation of stress as a result of the final incorporation of the Laurentia plate within Pangea.

INTRODUCTION

The Slick Hills of southwestern Oklahoma are the exposed portion of the frontal fault zone, a region of intense Pennsylvanian deformation that is located between the contemporary Wichita uplift (to the south) and the Anadarko basin (to the north) (Fig. 1). The boundaries of the fault zone are the Meers fault, to the south, and the Mountain View–Bronxton fault system in the north. The Holocene fault scarp of the Meers fault is exposed for several miles in the Meers Valley: the Mountain View fault, like most of the frontal zone, is buried beneath a cover of Permian sedimentary rocks. This paper offers an overview of the structural geology of the Slick Hills and places them in a regional context.

STRATIGRAPHIC RELATIONSHIPS

The Slick Hills are the top of a partially exhumed land surface of Early Permian age, sharing this characteristic with the more-rugged Wichita Mountains to the south. This land surface resulted from a termination of the weathering processes as the climate became increasingly arid. Evidence for this interpretation includes datable Permian karst in Cambrian-Ordovician limestones, fossilized spheroidal weathering effects in granites, and contemporary caliche and evaporite precipitation in the enveloping Permian sediments (Donovan and others, 1992).

The oldest rock unit exposed in the Slick Hills is the Cambrian Carlton Rhyolite Group, which has a minimum measured thickness of ~3,600 ft on Bally Mountain (in the north part of the area; Fig. 2) (Ham and others, 1964). The rhyolite is a monotonous, thickly bedded sequence of lavas and subordinate pyroclastic deposits. Outcrops of the rhyolite in the Wichita uplift serve to establish stratigraphic continuity across the Meers fault; a stratigraphic separation across this fault of as much as 10,000 feet can be inferred.

By Late Cambrian time the rhyolites were eroded into a series of gentle hills with a minimum relief of 1,000 ft. An ~7,000-ft-thick sequence of Cambrian-Ordovician sedimentary rocks was deposited on this surface during a major transgressive event. The lowest stratigraphically defined units, the Reagan and Honey Creek Formations, together placed in the Timbered Hills Group, contain much siliciclastic detritus. However, limestones become

Donovan, R. N., 1995, The Slick Hills of Oklahoma and their regional tectonic setting, *in* Johnson, K. S. (ed.), Structural styles in the southern Midcontinent, 1992 symposium: Oklahoma Geological Survey Circular 97, p. 178–186.

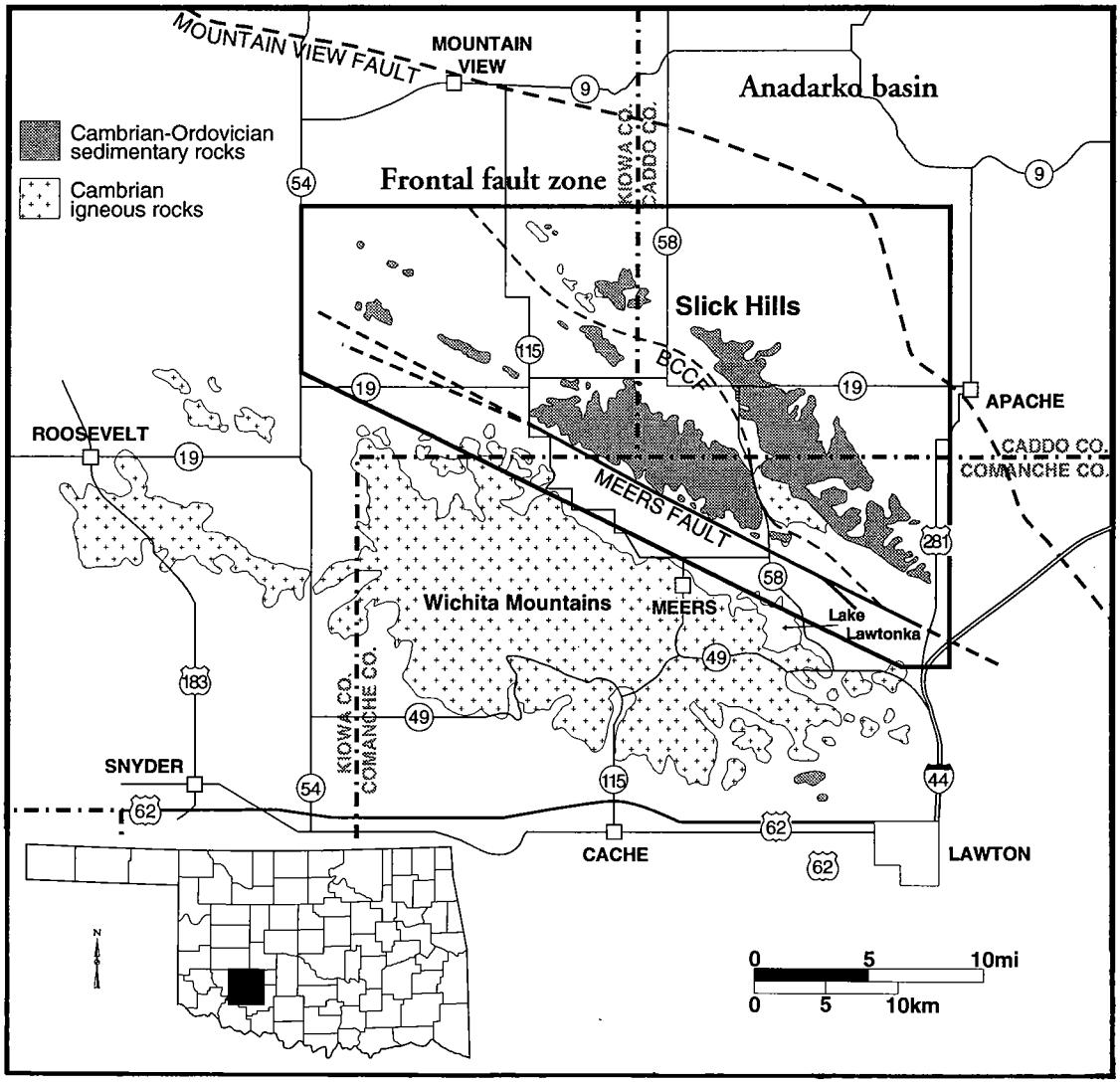


Figure 1. Location map showing relationship between Slick Hills and Wichita Mountains.

increasingly common toward the top of the Honey Creek, and the overlying Arbuckle Group is one of the world's thickest sequences of platform carbonates. Outcrops of Arbuckle strata form most of the Slick Hills; a thickness of >5,000 ft is exposed, although the topmost part of West Springs Creek Formation (topmost division of the Arbuckle) is not seen (Donovan, 1991). The Arbuckle is a lithologically homogeneous sequence of thinly bedded limestones with subordinate dolomites. Only fragments of the overlying section are exposed (Donovan and others, 1991), although the full Ordovician to Mississippian section characteristic of southern Oklahoma is known in the subsurface. With the exception of the basal Reagan Formation, the entire lower Paleozoic section is characterized by pronounced facies continuity and is dominated by carbonates.

REGIONAL TECTONIC SETTING

In a regional perspective, the lower Paleozoic section was deposited in the southern Oklahoma aulacogen. This aulacogen probably developed along a Precambrian zone of weakness that has existed for ~1.4 b.y. and, in today's coordinates, is oriented N60°W (i.e., 300°) (Denison and others, 1984). Cambrian reactivation of this weakness during a period of continental separation resulted in the emplacement of a complex bimodal suite of igneous rocks in the aulacogen (see Gilbert and Powell, 1988, for a review). The aforementioned

Carlton Rhyolite Group is apparently the topmost unit in this suite.

The Cambrian extensional event that accompanied this igneous activity is difficult to quantify, largely because of later cover (principally very thick Pennsylvanian and Permian sedimentary rocks), Pennsylvanian structural rejuvenation and overprinting, plus an incomplete understanding of the relationships and size of the various igneous units. A geologically reasonable model (McConnell and Gilbert, 1986; McConnell, 1990) suggests 17–21 km of crustal extension across the rift (i.e., along a N30°E trend).

The only exposed boundary of the rift is the Washita Valley fault complex in the Arbuckle Mountains. This structure juxtaposes Precambrian granite (presumed to be outside the northeastern margin of the aulacogen) and Colbert Rhyolite (the local equivalent of the Carlton Rhyolite). In the Wichita Mountains area, linear magnetic anomalies along the line of the Meers fault may indicate that this structure is a rejuvenated Cambrian fault (Purucker, 1986). However, as substantial outcrops of Cambrian igneous rocks are found on either side of the fault, its quantitative significance in the early evolution of the aulacogen is difficult to evaluate and may not be great. Apart from the two aforementioned faults, the architecture of the early rift phase of the aulacogen is poorly constrained. In the Slick Hills, a number of faults that trend north may record pre-Reagan but postrhyolite deformation. Thus, the minor Turtle Creek fault does not cut the lower Paleozoic sedimentary section, whereas there is equivocal geomorphic evidence suggesting that the larger Ketch Creek and Blue Creek Canyon faults may be earlier structures reactivated in the Pennsylvanian.

The significance of these north-trending structures is difficult to assess; a lineament analysis by Donovan and others (1987) in the Slick Hills detected a small north-south mode, and outcrop studies in the Wichitas (Schmidt, 1992) have detected a similarly oriented mode. The problem with these studies is that the fracture pattern can only be assigned a pre-Permian date. In an analysis of the Turtle Creek fault, Marchini (1986) thought that evidence of strike-slip motion along the fault suggested that the extension of the aulacogen involved stresses that were slightly oblique to the N60°W trend of the principal bounding faults.

The history of early Paleozoic sedimentation in the area is essentially that of a cooling and subsiding, passive continental margin adjacent to the Iapetus Ocean. The pattern of sedimentation across Texas, Oklahoma, and adjacent states involved an initial detrital and siliciclastic response to a major Late Cambrian (Franconian) transgression, followed by the gradual establishment of an immense carbonate platform that, by the end of Arbuckle Group deposition, covered much of the Laurentian plate (Ragland and Donovan, 1991). The result is a marked lithostratigraphic continuity that broke down to some extent during periods of regression, when clastic-system delivery tracks were operative, but otherwise was operative until the end of the Devonian.

The initiation of the early Paleozoic depocenter is well exposed in the Slick Hills, where the changes in facies in the Honey Creek, Fort Sill, and Signal Mountain Formations are consistent with a steadily increasing rate of sediment entrapment that reached a maximum during deposition of the Signal Mountain (McElmoyl and Donovan, 1993; Hosey and Donovan, 1993). Subsequent definition of the aulacogen is not seen so much in the development of distinctive facies, but rather in the extraordinary thickness of sediment that accumulated on the thermally weakened and subsequently flexed lithosphere of the aulacogen. Thus, lithostratigraphic units thicken by a factor of 3–4 times when traced into the aulacogen from the adjacent craton. This contrast in the rate of sediment accommodation was maintained even as the overall rate of accommodation declined across the entire shelf. Precise estimates of the rate of basin definition are difficult to arrive at in a section that is ~75% carbonate, because of long-term backstripping due to pressure solution of calcite under increasing confining pressure. This pressure solution resulted in ubiquitous bedding-parallel stylolites and related phenomena that may have removed ~25% of the lower parts of the carbonate section (Donovan and others, 1986b).

STRUCTURAL OVERPRINTING AND DISMEMBERMENT OF THE AULACOGEN

During the late Paleozoic, particularly during the Pennsylvanian Period, a major structural overprinting of the aulacogen took place, resulting in fragmentation of the basement into a complex of deep, rapidly subsiding basins and sharp uplifts. Both basins and uplifts are of similar size and shape: 20–50 mi across and elongated parallel to the aulacogen trend (N60°W). Length:breadth ratios are ~5:1. Although the overprinting affects an area up to 175 mi across (perpendicular to the aulacogen trend) and thus involves the ancient Precambrian basement, deformation is greatest above the original igneous foundation of the aulacogen. Definition of this new framework was essentially complete by the Early Permian.

Inversion of the uplifts was accompanied by syntectonic sedimentation. The present maximum stratigraphic separation, allowing for erosion of the lower Paleozoic section from the uplifts, is ~45,000 ft as measured between the projected top of the lower Paleozoic in the Wichita uplift and the top of the upper Paleozoic section in the adjacent Anadarko basin. The frontal fault zone carries most of the strain associated with this separation.

LATE PALEOZOIC STRUCTURAL IMPRINT ON THE SLICK HILLS

In the Slick Hills, two lithology-dependent structural styles are developed. In Blue Creek Canyon, the Carlton Rhyolite has been folded into a north-plunging asymmetric anticline that has a wavelength of ~0.5 mi and forms part of the hanging wall of the Blue Creek Canyon fault. Although the steep west-facing limb of the fold is intensely fractured, this fold maintains integrity even where dips exceed 40°. The fold is important as the most clearly exposed example of folded basement in the aulacogen.

In contrast to the rhyolite terrane, the overlying lower Paleozoic is intensely folded on a variety of scales from outcrop size to folds as much as 3 mi across. Most of these folds are true parallel folds, reflecting the character of the Arbuckle Group—a very thick, lithologically monotonous sequence of thinly bedded carbonates. Few beds in the Arbuckle Group exceed 3 ft in thickness, and there are very few shaly sequences: as a result, flexural slip is not concentrated at any particular décollement but is dispersed throughout the section, often utilizing insoluble residues concentrated along bedding-parallel stylolites. Although there is a tendency for folds in the most thinly bedded unit (the Signal Mountain Formation) to be of shorter wavelength, folds, in general, may be generated at any level in the section. Similarly, bedding-parallel faults are generated at numerous horizons (Marchini, 1986; Ragland and others, 1991). The result is that the lower Paleozoic section is incrementally detached from the underlying rhyolite along multiple horizons of flexural slip. The net effect of this behavior is that the Timbered Hills Group and the lower part of the Arbuckle Group tend to fold in accord with the underlying rhyolite, as for example in the Eastern Slick Hills, whereas upper parts of the section, above the Signal Mountain Formation, behave independently. No detachment at the rhyolite/sedimentary rock contact has been observed.

STRUCTURAL DETAILS

The Slick Hills are divided into East and West ranges by the Blue Creek Canyon fault (Fig. 2), a major reverse fault that has been downthrown to the southwest by 1,550–8,000 ft. Where exposed, the fault displays kinematic indicators (drag, sigmoidal shear arrays, slickensides) that suggest a component of left-lateral strike slip (Donovan and others, 1986a).

In a regional context, the Blue Creek Canyon fault is an oblique back thrust. The Eastern Slick Hills, as well as the structurally contiguous outliers in Bally and Zodletone Mountains, are the exposed part of the "pop-up" domain elevated by the fault. The structure of this domain is relatively simple: a mostly homoclinal sequence dipping at 15°–50° to the northeast. However, the section in the southern part of the Eastern Slick Hills is cut by two high-angle reverse faults, the Ketch Creek and Stony Point faults. Stratigraphic downthrow on both of these faults is to the southwest and decreases to the north. The Ketch Creek fault, which over much of its length cuts the Carlton Rhyolite, has a maximum observed throw of ~400 ft and dies out northward into a sequence of vertical fractures. The Stony Point fault, which cuts strata in the upper Arbuckle Group (specifically the Cool Creek and Kindblade Formations), has a maximum stratigraphic throw of ~3,000 ft and dies out northward into a highly asymmetric southwest-facing anticline. Stephenson (1990) has suggested that the fault flattens at depth and abuts the Meers fault in the subsurface to the southeast.

Only strata in the Arbuckle Group are found in the Western Slick Hills (Fig. 2). Deformation in this domain is an interplay between folds, faults, and pressure-solution cleavage. The most obvious deformation consists of numerous parallel folds that trend between N60°W and due north, averaging about N40°W. This folding is on a variety of scales, ranging from minor folds, with a wavelength of <3 ft, to folds with a width of 3 mi. More than 100 folds with a wavelength of >300 ft have been mapped (McConnell, 1983; Beauchamp, 1983; Marchini, 1986). These folds are essentially upright, although some are overturned by as much as 20°. Fold profiles usually are tight semichevrons. Adjacent to the Meers fault, some folds are isoclinal. Most folds are periclinal, except adjacent to the Blue Creek Canyon fault where a persistent northerly plunge is maintained (Donovan, 1986; Smith, 1991).

The section is cut by many steeply dipping bedding-parallel thrusts that have stratigraphic displacements, mostly down to the northeast, of as much as 2,500 ft. These faults may have their roots within the Arbuckle Group; only one, the Stumbling Bear thrust (Fig. 2), can convincingly be mapped throughout the entire length of the Western Slick Hills. Unlike the faults in the Eastern Slick Hills, none of these faults can be shown to cut igneous basement rock. Whereas most faults appear either to postdate folding or to be involved in the generation of folds, a few faults appear to predate some folds.

The third common indicator of strain takes the form of tectonic stylolites; in many cases, these are axial planar in orientation and clearly relate to the tightening of individual folds. However, close to the Meers fault, a regional fabric of spaced pressure solution is developed. In addition, many fault planes display evidence of intense pressure-solution cleavage, either in the form of left-lateral sigmoidal shear zones (McCoss and Donovan, 1986) or as a simple compressional fabric.

All the structures described so far are compressional in origin; in addition, the area is cut by nu-

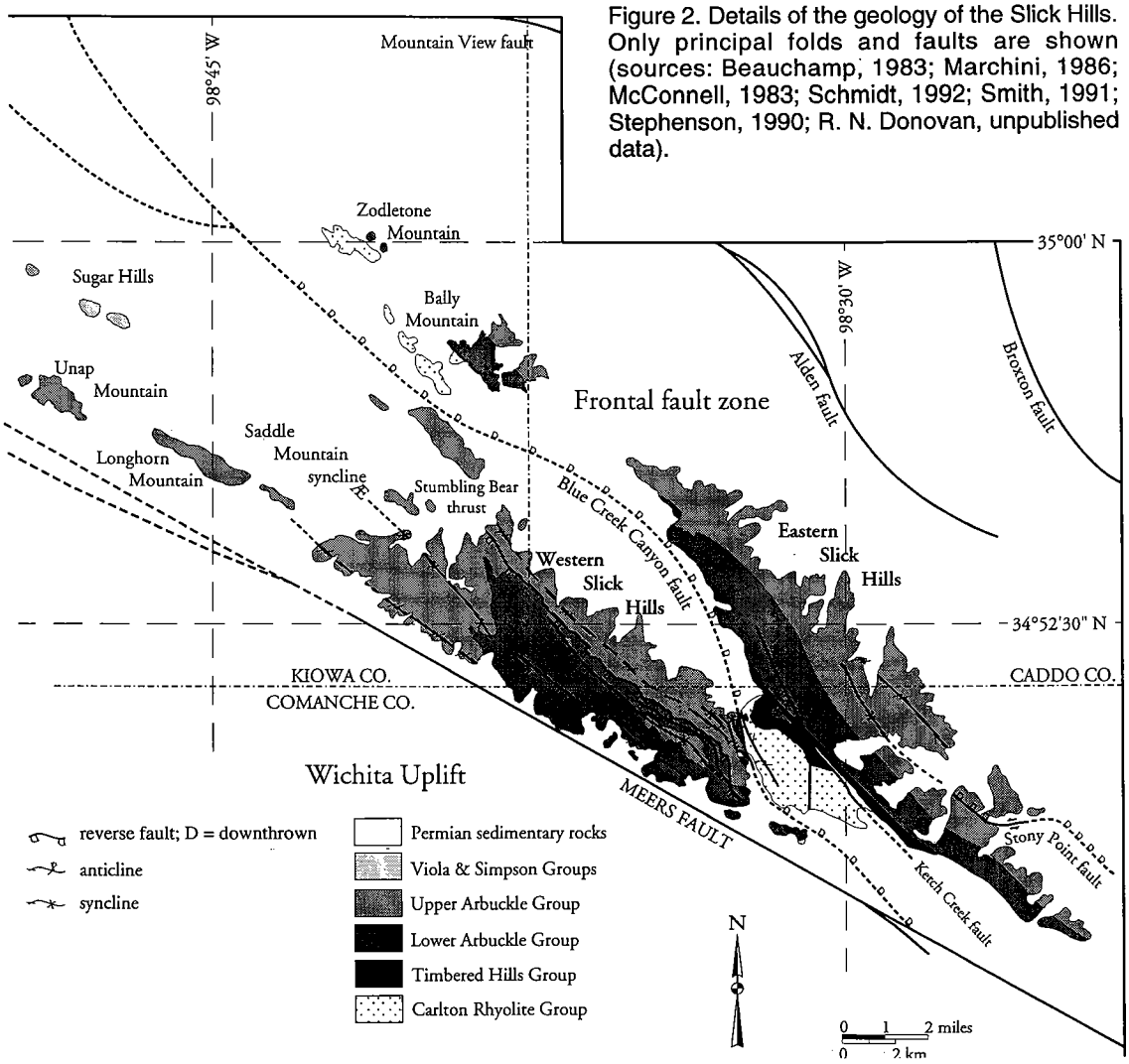


Figure 2. Details of the geology of the Slick Hills. Only principal folds and faults are shown (sources: Beauchamp, 1983; Marchini, 1986; McConnell, 1983; Schmidt, 1992; Smith, 1991; Stephenson, 1990; R. N. Donovan, unpublished data).

merous brittle fractures, often seen as calcite veins. These tensional structures are of several ages and origins. Many are related to deformation associated with individual folds; some predate the development of bedding-parallel stylolites. However, there is a pronounced regional pattern that can be detected both in the field and by Landsat analysis (Donovan and others, 1987; Stephenson, 1990; Schmidt, 1992). The principal fracture mode is oriented approximately N40°–50°E. This pervasive pattern clearly postdates the principal compressional features described above and, for the most part, predates the Early Permian unconformity surface.

STRUCTURAL ANALYSIS OF LATE PALEOZOIC DEFORMATION IN THE SLICK HILLS

The Slick Hills have a maximum relief of ~500 ft; they thus record no more than ~10% of the total vertical (i.e., stratigraphic) separation between the Wichita uplift and the Anadarko basin. The scale of this late Paleozoic (principally Pennsylvanian) deformation is truly extraordinary; at the end of the Mississippian, the base of the Arbuckle Group was at a depth that reasonably can be estimated at 12,000–14,000 ft. By the Early Permian, this horizon was ~40,000 ft below the surface in the Anadarko basin and can be estimated to have been as much as 5,000 ft above the present level of erosion in the Wichita uplift. In addition, deep seismic profiling (Brewer, 1982) indicates a considerable overhang of the frontal fault zone. Simple geometric considerations indicate that within the frontal fault zone there has been a crustal shortening perpendicular to the fault-zone trend, on the order of 1:2. This contrasts with a figure of ~1:1.2 in the adjacent uplift and basin.

Not surprisingly, the limited outcrop of the Slick Hills displays evidence of considerable shortening

in the form of tight folds, with axial-plane dips in excess of 50°, and areas of intense pressure solution. High-angle reverse faults, including the very large back-thrust displacement on the Blue Creek Canyon fault, attest to both compression and vertical accommodation.

Several authors (e.g., Donovan and others, 1989) have noted that the Slick Hills display kinematic indications of left-lateral strike slip. On the basis of subsurface piercement points, McConnell (1989) has suggested that the ratio of left-lateral strike-slip to dip-slip movement across the frontal fault zone is between 1.4:1 and 3:1, although the data are not well constrained. In the Slick Hills, McCoss and Donovan (1986) showed that the principal evidence for strike-slip movement includes fault drag, sigmoidal pressure-solution arrays, and the orientation of folds. McCoss and Donovan applied a geometric technique developed by McCoss (1986), noting a clockwise orientation of fold axes from the Meers fault. They suggested that this indicated that a left-lateral transpressive-stress regime had controlled deformation in the Slick Hills. In addition, they identified second-order left-lateral faults in the Western Slick Hills which they interpreted as Riedel shear fractures. However, adjacent to the Meers fault they described folds that are subparallel to the fault. Folds in this domain are upright and isoclinal, and it is in this domain that recent work has uncovered regional pressure-solution evidence that is oriented 10°–20° clockwise to the Meers fault. A reasonable interpretation of these field relationships is that the Meers fault demarcates a profound lithological contrast between rocks that could easily deform by flexural slip (the Arbuckle Group), and those that could not (in this case, gabbros and granites of the Wichita uplift). As a result of this lithological contrast, early-formed folds in the Slick Hills were tightened and rotated into near parallelism with the Meers fault. Once the folds had become isoclinal and parallel to the fault, further strain could be accommodated only by regional pressure solution. In this respect, it is pertinent to note that Donovan and others (1989) reported evidence that progressive rotation of folds has taken place in this area.

This analysis highlights two facets of the Pennsylvanian deformation: first, the extreme isotropy contrast between the basement and the sedimentary cover and, second, the importance of preexisting fault trends. Thus, where blocks of homogeneous basement are juxtaposed by faults that parallel the aulacogen trend (as, for example, in the eastern Arbuckle Mountains), strain is likely to be resolved into discrete vertical and strike-slip components, whereas deformation in the markedly anisotropic Arbuckle Group proceeded incrementally, involving both rotation and tightening (Fig. 3).

As noted previously, the pervasive fracture patterns that cut the Slick Hills were imprinted late in the history of late Paleozoic deformation. The most likely timing for this period of brittle fracture is during late stages of the uplift that would eventually expose the present level of the Slick Hills during the Early Permian. The orientation of these fractures (N40°–50°E) is not orthogonal to the aulacogen trend (N60°W), but is compatible with the displacement vector for compression calculated by McCoss and Donovan (1986) (Fig. 4).

REGIONAL CONTEXT OF PENNSYLVANIAN DEFORMATION

The frontal fault zone displays the greatest amount of Pennsylvanian strain in southern Oklahoma. The results of this ongoing study in the Slick Hills are similar to those of studies in the Arbuckle Mountains in that they highlight the importance of compression oriented approximately northeast-southwest. The style of deformation in these two major areas of inversion is similar, as are the orientations of the various strain indicators.

In general, there are four sets of ideas (reviewed in McConnell, 1989) concerning the finite stress that was responsible for Pennsylvanian deformation in southern Oklahoma: (1) pure compression and shortening, with a maximum compressive stress oriented perpendicular (i.e., trending N30°E) to the trend of the preexisting structural framework; (2) left-lateral strike slip, which in a pure system would require a maximum compressive stress trending about N80°E; (3) compression (as above) followed by left-lateral strike slip (as above); and (4) left-lateral transpression (the interpretation favored here). In the Slick Hills, various kinematic indicators suggest a maximum compressive stress oriented northeast-southwest.

The difference between 3 and 4 may be an artifact of uplift related to the isotropy differences between the massive igneous basement (both within and without the Cambrian aulacogen) and the thinly bedded sedimentary cover (Fig. 3). The closer to the surface that basement-cutting N60°E faults came, the greater would be the tendency for strain energy to be concentrated along such faults (and resolved into compressional and strike-slip increments), rather than expended throughout the bulk of the anisotropic sedimentary section.

In a regional context, the Wichita uplift and Anadarko basin can be thought of as a vast overturned fold whose orientation (N60°E) is controlled by preexisting structural weaknesses. A similar assumption can be made for the Criner uplift, Ardmore basin, Arbuckle uplift, etc. Given the crustal weakness of the underlying Cambrian crust, the concentration of strain above and adjacent to the old aulacogen is not unexpected, nor is it surprising that the Pennsylvanian stress system may have been slightly oblique to the existing framework. What is more difficult to explain is the cause of the stress vectors.

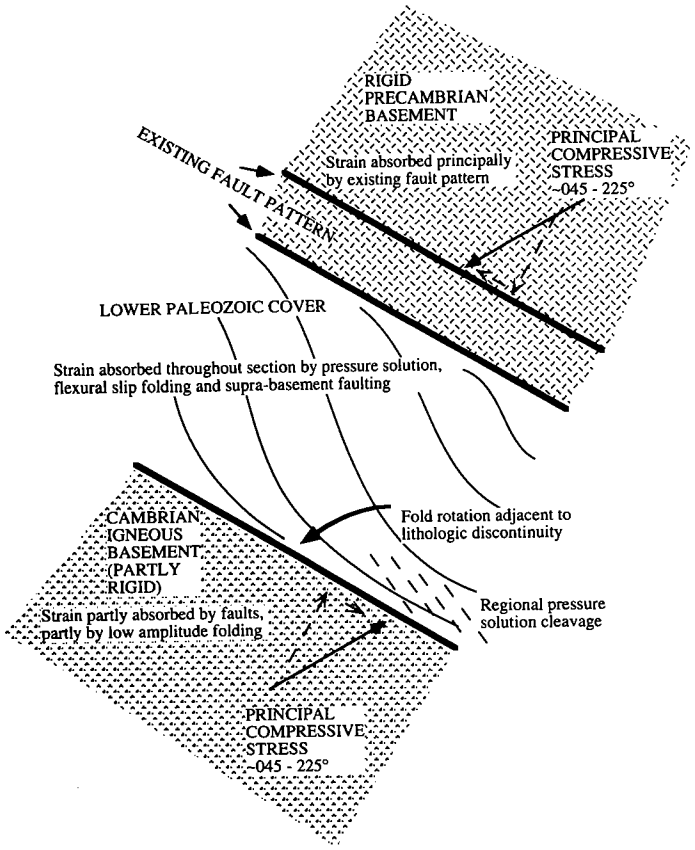


Figure 3. Schematic representation of relationships between structural style and rock type in the southern Oklahoma aulacogen.

During the late Paleozoic, the southern section of the Iapetus Ocean finally closed when Gondwana and associated microplates rotated clockwise and collided with the southern part of Laurentia. This gradual collision is recorded by the increasingly younger timing of deformation shown by the Ouachita-Marathon orogene as it is traced toward Mexico. The general coincidence of this deformation with dismemberment of the aulacogen has generally been taken to indicate a linkage between the two. However, it is difficult to reconcile the likely stress vectors of the two deformations by comparing the styles of deformation. Although, as noted above, there is some dispute as to the relative importance of strike slip and left-lateral slip associated with deformation within the aulacogen area, it seems clear that a vector oriented approximately northeast-southwest was required to generate the structures observed. This trend is at variance with what is required to generate the Oklahoma Ouachita Mountains, which are the geographically proximal part of the orogene. Furthermore, it is not clear that the precise timing of deformational events in the two areas coincides.

It is suggested that the final closure of the Iapetus Ocean was the last event in the encirclement of the Laurentian plate by collisional and/or convergent margins during the assembly of Pangea. This event may well have have had large consequences for the reorientation of stress. Within this context, the admittedly spectacular crustal shortening displayed in the aulacogen area (as well as the contemporary events associated with the development of the Ancestral Rockies) can be seen as a relatively minor response by zones of weakness within an otherwise-stable cratonic block.

ACKNOWLEDGMENTS

The financial support of the Mobil Foundation and the Charles B. Moncrief Chair is appreciated. I thank Randy Hosey for his help in drafting Figures 1 and 2.

REFERENCES CITED

Beauchamp, W. H., 1983, The structural geology of the southern Slick Hills, Oklahoma: Oklahoma State University unpublished M.S. thesis, 117 p.

Brewer, J. A., 1982, Study of southern Oklahoma aulacogen, using COCORP deep seismic profiles, *in* Gilbert, M. C.; and Donovan, R. N. (eds.), Geology of the eastern Wichita Mountains, southwestern Oklahoma: Oklahoma Geological Survey Guidebook 21, p. 31–39.

Denison, R. E.; Lidiak, E. G.; Bickford, M. E.; and Kisvarsanyi, E. B., 1984, Geology and geochronology of Precambrian rocks in the central interior region of the United States: U.S. Geological Survey Professional Paper 1241-C, 20 p.

Donovan, R. N., 1986, Geology of the Slick Hills, *in* Donovan, R. N. (ed.), The Slick Hills of southwestern Oklahoma—fragments of an aulacogen?: Oklahoma Geological Survey Guidebook 24, p. 1–12.

_____ 1991, The Arbuckle Group—an aide de memoire, *in* Johnson, K. S. (ed.), Arbuckle Group core workshop and field trip: Oklahoma Geological Survey Special Publication 91-3, p. 199–208.

Donovan, R. N.; Ragland, D. A.; Rafalowski, M. B.; Collins, K.; Tsegay, T.; McConnell, D.; Marchini, D.; Beauchamp, W.; and Sanderson, D. J., 1986a, Geological highlights of the Blue Creek Canyon area: Oklahoma Geological Survey Guidebook 24, p. 84–91.

Donovan, R. N.; Ragland, D. A.; and Shaefer, D., 1986b, Geology of the Cook Creek road cut: Oklahoma Geological Survey Guidebook 24, p. 100–105.

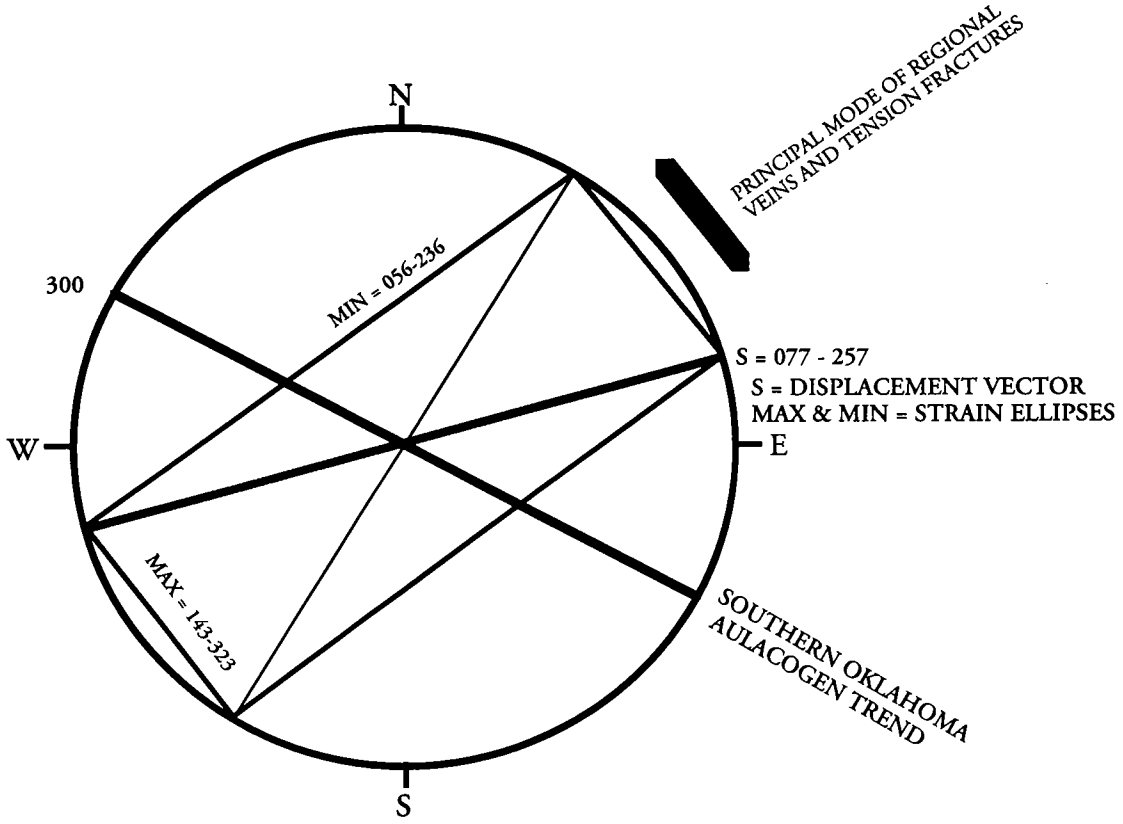


Figure 4. Orientation of displacement vectors and strain-ellipse axes in Slick Hills. Data sets used include fold orientations, sigmoidal-shear arrays, and fracture-pattern data (number of fractures measured is 1,350). Compressional data from McCoss and Donovan (1986), fractures and veins from R. N. Donovan (unpublished data). Note the close agreement among different types of data.

Donovan, R. N.; Morgan, K.; Marchini, W. R. D.; Wilhelm, S.; and Bridges, S., 1987, Lineaments in the Slick Hills, southwestern Oklahoma—an application of remote sensing technology: American Association of Petroleum Geologists, Southwestern Section, Transactions, p. 74–79.

Donovan, R. N.; Marchini, W. R. D.; McConnell, D. A.; Beauchamp, W.; and Sanderson, D. J., 1989, Structural imprint on the Slick Hills, southern Oklahoma, *in* Johnson, K. S. (ed.), Anadarko basin symposium, 1988: Oklahoma Geological Survey Circular 90, p. 78–84.

Donovan, R. N.; Busbey, A. B.; Bridges, S. S.; Collins, K.; Ditzell, C.; Jenkins, D.; and Wilhelm, R., 1991, On three outcrops of the Simpson Group in the northwestern part of the Slick Hills, southern Oklahoma, *in* Johnson, K. S. (ed.), Late Cambrian–Ordovician geology of the southern Midcontinent, 1989 symposium: Oklahoma Geological Survey Circular 92, p. 85–97.

Donovan, R. N.; Busbey, A. B.; Elmore, R. D.; and Engels, M. H., 1992, Oil in Permian karst in the Slick Hills of southwestern Oklahoma, *in* Johnson, K. S.; and Cardott, B. J. (eds.), Source rocks in the southern Midcontinent, 1990 symposium: Oklahoma Geological Circular 93, p. 198–209.

Gilbert, M. C.; and Powell, B. N., 1988, Igneous geology of the Wichita Mountains, southwestern Oklahoma: Geological Society of America, South-Central Section, Centennial Field Guide, p. 109–126.

Ham, W. E.; Denison, R. E.; and Merritt, C. A., 1964, Basement rocks and structural evolution of southern Oklahoma: Oklahoma Geological Survey Bulletin 95, 302 p.

Hosey, Randy; and Donovan, R. N., 1993, The geological significance of the boundary between the Fort Sill and Signal Mountain Formations in the Lower Arbuckle Group (Cambrian): Geological Society of America Abstracts with Programs, v. 25, no. 1, p. 14–15.

Marchini, W. R. D., 1986, Transpression, an application to the Slick Hills, SW Oklahoma: Queen's University unpublished Ph.D. thesis, Belfast, 286 p.

McConnell, D. A., 1983, The mapping and interpretation of the structure of the northern Slick Hills, southwest Oklahoma: Oklahoma State University unpublished M.S. thesis, 131 p.

_____ 1989, Constraints on magnitude and sense of

slip across the northern margin of the Wichita uplift, southwest Oklahoma, *in* Johnson, K. S. (ed.), Anadarko basin symposium, 1988: Oklahoma Geological Survey Circular 90, p. 85–96.

_____ 1990, Cambrian extensional tectonics and magmatism within the southern Oklahoma aulacogen: Tectonophysics, v. 174, p. 147–157.

McConnell, D. A.; and Gilbert, M. C., 1986, Calculations for Cambrian extension of the southern Oklahoma aulacogen, *in* Gilbert, M. C. (ed.), Petrology of the Cambrian Wichita Mountains igneous suite: Oklahoma Geological Survey Guidebook 23, p. 11–20.

McCoss, A. M., 1986, Simple constructions for deformation in transpression/transtension zones: Journal of Structural Geology, v. 8, p. 715–718.

McCoss, A. M.; and Donovan, R. N., 1986, Application of a construction for determining deformation in zones of transpression to the Slick Hills in southern Oklahoma, *in* Donovan, R. N. (ed.), The Slick Hills of southwestern Oklahoma—fragments of an aulacogen?: Oklahoma Geological Survey Guidebook 24, p. 40–44.

McElmoyl, Courtney; and Donovan, R. N., 1993, A transgression-regression event during the deposition of the Upper Cambrian Honey Creek Formation in the southern Oklahoma aulacogen: Geological Society of America Abstracts with Programs, v. 25, no. 1, p. 38.

Purucker, Michael, 1986, Interpretation of an aeromagnetic survey along the Wichita frontal fault zone: Oklahoma Geological Survey Guidebook 23, p. 129–136.

Ragland, D. A.; and Donovan, R. N., 1991, Sedimentology and diagenesis of the Arbuckle Group in outcrops of southern Oklahoma, *in* Johnson, K. S. (ed.), Arbuckle Group core workshop and field trip: Oklahoma Geological Survey Special Publication 91-3, p. 9–29.

Ragland, D. A.; Smith, S. S., and Donovan, R. N., 1991, Parallel folds and the Thatcher Creek Member in Blue Creek Canyon, *in* Johnson, K. S. (ed.), Arbuckle Group core workshop and field trip: Oklahoma Geological Survey Special Publication 91-3, p. 263–266.

Schmidt, K. W., 1992, Orientation and age of fractures in the Wichita Mountains and Slick Hills of southwestern Oklahoma: Texas Christian University unpublished M.S. thesis, 44 p.

Smith, S. S., 1991, Parallel fold styles in the Blue Creek Canyon area of the Slick Hills, southwestern Oklahoma: Texas Christian University unpublished M.S. thesis, 96 p.

Stephenson, M. D., 1990, Mapping and structural analysis of the the southeastern Slick Hills, Comanche County, Oklahoma: Texas Christian University unpublished M.S. thesis, 123 p.

Structural Framework of the Meers Fault and Slick Hills Area, Southwestern Oklahoma, Based on Magnetic Data

Meridee Jones-Cecil
U.S. Geological Survey
Denver, Colorado

R. Nowell Donovan
Texas Christian University
Fort Worth, Texas

Lee-Ann Bradley
U.S. Geological Survey
Denver, Colorado

ABSTRACT.—Aeromagnetic, ground-magnetic, and paleomagnetic data provide insight into the structure of the Meers fault and the fault's role in the evolution of the Frontal Wichita fault system of southwestern Oklahoma. Quantitative analyses of digital aeromagnetic data from the Lawton area included locating maximum horizontal gradients and modeling three regional profiles. In addition, models of ground-magnetic profiles provide detailed structural information about the Meers fault zone, including: (1) apparent splaying and a left-stepping offset of the Meers fault northwest of the fault segment that was reactivated in the Quaternary, (2) the presence of a dikelike body along ~12 km of the reactivated part of the fault, and (3) dragging and truncation of a wedge of magnetic basement at the junction between the Blue Creek Canyon (BCC) fault and the Meers fault by later motion on the BCC fault. The splays and left step are spatially associated with both older Cambrian structures and a back-thrust fault in the Frontal Wichita fault system. The dikelike body could be either a dike (of Cambrian? age) or a horse block (emplaced during Pennsylvanian? faulting). Though the magnetic data cannot resolve the origin of these features, we consider their implications to the structural history of the Meers fault.

Models of the ground-magnetic data constrain the dip of the Meers fault in the area of the dikelike body to be nearly vertical down to at least 0.5 km depth. In addition, the models identified secondary basement faults that were reactivated during the Quaternary. To minimize assumptions, the models incorporated paleomagnetic data from unoriented core that penetrated the dikelike body, and magnetic-susceptibility measurements of the principal rock types in the area.

Northeast of the Meers fault, a comparison of mapped folds and faults of the pre-Permian sedimentary rocks with folding and faulting interpreted from the magnetic data shows that structure in the basement rocks reflects many of the larger near-surface features. However, significant discrepancies between the magnetic data and the surface or subsurface geology do exist. The greatest discrepancy is in the western Slick Hills, where folds and faults in the overlying Cambrian–Ordovician carbonate rocks have slightly different orientation and a distinctly shorter wavelength than the underlying structures in the magnetic basement. Some of the difference in the wavelength of the features is probably due to a difference in rigidity between the crystalline and sedimentary rocks. Near the Meers fault, folds are subparallel to the fault. This subparallelism of fold axes supports the concept that the BCC and Meers faults were transpressive faults that bounded the western Slick Hills. The overturning and truncation of beds near the BCC fault, and the apparent truncation of the wedge of magnetic basement in the junction between the two faults, imply that motion on the BCC fault postdates formation of these structures. Another discrepancy between the magnetic and geologic data is in the location of the BCC fault between Blue Creek Canyon and Bally Mountain. Contrary to its previously inferred location, the magnetic and drill-hole data imply that the BCC fault either bends or terminates in this area. If it terminates, a subparallel fault west of Bally Mountain continues to the northwest.

Jones-Cecil, Meridee; Donovan, R. N.; and Bradley, Lee-Ann, 1995, Structural framework of the Meers fault and Slick Hills area, southwestern Oklahoma, based on magnetic data, *in* Johnson, K. S. (ed.), Structural styles in the southern Midcontinent, 1992 symposium: Oklahoma Geological Survey Circular 97, p. 187–207.

INTRODUCTION

Geologic Setting

The Meers fault is the southernmost fault in the Frontal Wichita (FW) fault system, which is an anastomosing network of faults that separates the Amarillo–Wichita uplift to the south from the Anadarko basin to the north (Fig. 1). Along most of its length, the Meers fault trends 300°, but this trend becomes more northerly to the northwest where the fault divides and intersects the Mountain View fault. The tectonic history of the FW fault system and surrounding area began ~1,400 Ma (million years ago) with intrusions, including dikes that now trend 300°, in the basement exposed in the northern Arbuckle Mountains (Denison, 1982). The Precambrian–Cambrian failed rifting that formed the southern Oklahoma aulacogen (Gilbert, 1982) paralleled this trend in the weakened basement. The mafic rocks of the Glen Mountains Layered Complex were first to be intruded in the rift, followed by intrusion of the Roosevelt Gabbros and possibly extrusion of the Navajoe Mountain Basalt–Spilite Group on both sides of the rift (Ham and others, 1964). Structural inversion of the aulacogen in Cambrian time brought the gabbros to the surface; the Meers Quartzite was probably deposited at that time (Gilbert, 1982). Subsequently, the Carlton Rhyolite Group was extruded over the area and sill-like granite bodies of the Wichita Granite Group were intruded between the rhyolite and the gabbros. Ham and others (1964) suggested that the Meers fault may have been a rift-bounding fault on the northern side of the aulacogen, which was active prior to extrusion of the rhyolite. Subsidence, which began later in the Cambrian and continued through the Early Mississippian, was due at least in part to thermal cooling of the rift-related igneous rocks. A thick sequence of mainly carbonate rocks accumulated over the aulacogen and in the Anadarko basin in response to the subsidence (Feinstein, 1981). The aulacogen was dismembered in the Late Mississippian to Early Permian, coincident with, and possibly related to, the plate collision that formed the Ouachita Mountains. Faulting within the FW fault system and downwarping of the Anadarko basin began in earnest during this time (Perry, 1989), resulting in at least 12 km of vertical separation across the Frontal Wichita fault system (Johnson, 1989). The presence of both compressive and transcurrent structural features in the FW fault zone and in other parts of the aulacogen is cited as evidence that the late Paleozoic deformation was a transpressive tectonic event (McConnell, 1983; Donovan and others, 1989).

Following the dismemberment, most of the Amarillo–Wichita uplift and Anadarko basin were covered by a veneer of upper Paleozoic sedimentary rocks that are progressively younger to the northwest. In the area of the Wichita Mountains these rocks are Early Permian in age. The Permian cover that remains in the area seriously impedes geological investigations of the underlying Pennsylvanian and older structures.

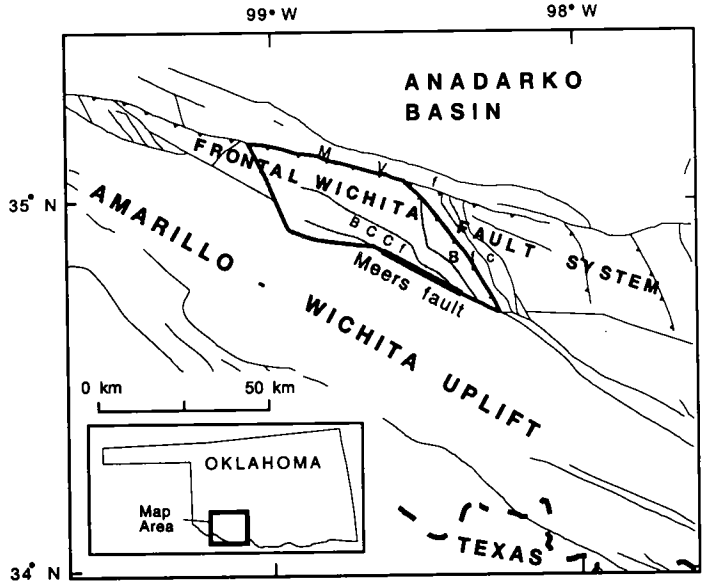


Figure 1. Map of major faults in and surrounding the Frontal Wichita fault system (modified from Chenoweth (1983)). Lines are faults. Bold line is outline of Lawton segment (McConnell, 1987,1991). Wide bold line is the segment of the Meers fault with Quaternary scarp. Teeth on upthrown side of reverse faults. MVf = Mountain View fault. BCCf = Blue Creek Canyon fault. Bfc = Broxton fault complex. Shading indicates the aeromagnetic survey area shown in Figure 3.

History of the Meers Fault

The role of the Meers fault as a persistent tectonic element in the southern Midcontinent began as early as rifting in the Cambrian. The peak of activity on the Meers fault occurred during Late Mississippian and Pennsylvanian time as oblique slip consisting of left-lateral and, ~2 km of down-to-the-north, vertical offset. Minor reactivation of the Meers fault has occurred twice since then. The first reactivation is suggested by deposition of the Post Oak Conglomerate during Permian. Donovan and others (1982, 1989) described breccia containing large boulders of limestone in the Post Oak Conglomerate south of the Meers fault. The boulders were probably derived from an uplifted source area northwest of the Meers fault, implying a minor reversal in the sense of

vertical motion. A long gap in the sedimentary record extends from Permian to Quaternary time. The next suggestion of reactivation is based on the offset of a middle to late Pleistocene topographic ridge and a valley wall (Kelson and Swan, 1990). Several tens or hundreds of thousands of years later, between 2,900 and 3,400 years ago, late Quaternary movement occurred. This was followed by the most recent reactivation, ~1,050 years ago (Kelson and Swan, 1990). The Quaternary reactivation consisted of both left-lateral and up-to-the-north movement (Ramelli and Slemmons, 1986; Ramelli and others, 1987; Crone and Luza, 1990; Kelson and Swan, 1990), and resulted in the formation of a 26-km-long, nearly straight fault scarp. Low sun-angle photography has revealed splays and short subparallel scarps at either end of the continuous straight scarp, suggesting the total length of Quaternary faulting was 37 km (Ramelli and Slemmons, 1986; Ramelli and others, 1987).

The purpose of this paper is to present a structural interpretation of the Meers fault and adjacent features based on aeromagnetic and ground-magnetic data, and to compare these interpretations with surface and subsurface geologic data. In our analysis, we draw principally on our previous work (Donovan, 1986; McCoss and Donovan, 1986; Donovan and others, 1989; Jones-Cecil and Crone, 1989; Jones-Cecil, 1990; Bradley and Jones-Cecil, 1991; Stephenson and Donovan, 1991; Donovan and others, 1993; Jones-Cecil, 1995a; Jones-Cecil and Robbins, in press). In addition, we summarize the results of new ground-magnetic surveys and additional magnetic-susceptibility measurements that are discussed in greater detail elsewhere (Jones-Cecil, 1995b).

GEOMETRY AND SENSE OF MOTION OF THE MEERS FAULT

The straightness of the reactivated segment of the Meers fault is atypical of frontal Wichita faults and led early workers to interpret the fault to be nearly vertical at depth (Harlton, 1951,1963,1972; Ham and others, 1964). In contrast, the interpretations of COCORP deep seismic-reflection profiles (Brewer, 1982; Brewer and others, 1983) and seismic-refraction studies (Chang and others, 1989) that crossed the Meers fault northwest of the reactivated segment suggest that the dip of the Meers fault is similar to the 30–40° SW dip of the Mountain View fault. However, reprocessing of the COCORP data led to a possible reconciliation of the two interpretations. When reprocessed, the deep seismic-reflection data indicate a southwest dip on the Meers fault of >70° (Lemiszki and Brown, 1988). Unequivocal in the interpretation of the seismic data is the moderate southwest dip of the Mountain View fault, which is the largest basinward fault in the FW fault system (Brewer, 1982; Brewer and others, 1983).

A large component of left-lateral strike slip has been inferred for the Meers fault during late Paleozoic faulting, as well as during Quaternary reactivation, though the ratio of strike-slip to dip-slip motion is uncertain. As much as 120 km of left-lateral displacement in Pennsylvanian time has been proposed for a megashear system which contains the FW fault system (Budnik, 1987), although the amount of displacement across any one fault in the zone would be less. Studies of individual faults have yielded more conservative estimates for the strike-slip component. For example, by palinspastically restoring isopachs, McConnell (1989a,b) estimated reverse- to lateral-slip ratios of 1.1:1 to 4.3:1, with an east–northeast slip-vector orientation (or 1:3 to 1.3:1, with an east–west slip vector), along WNW- and NW-trending sections of the Mountain View fault, respectively. In addition, two studies have addressed the sense of Quaternary motion on the Meers fault. Ramelli and Slemmons (1986) and Ramelli and others (1987) measured a range of ratios of lateral to vertical slip of 2:1 to 4:1 along the western part of the Quaternary fault scarp. Kelson and Swan (1990) measured ratios of late Quaternary lateral to vertical slip of 1.3:1 to 1.4:1 in ponded alluvial deposits.

MAGNETIC DATA

Because the basinward part of the FW fault system contains petroleum, abundant drill-hole information is available in some areas. Close to the Meers fault, however, drill holes are scarce. Between the Blue Creek Canyon (BCC) fault and the Meers fault, structural interpretations are mainly based on surface geologic mapping and the analysis of exposed structures. Magnetic data provide information about the structure of the magnetic basement, or of igneous rocks at depth that are the source of the magnetic anomalies. Because of the heterogeneous distribution of magnetic minerals and their possible alteration, particularly in fault zones, it is commonly difficult to match lithologies with values of magnetic susceptibility. However, many of the igneous rocks in the aulacogen are exposed, which allowed us to measure directly the magnetic susceptibility of rocks at more than 40 sites throughout the study area. From these measurements we can generally correlate exposed rock types and magnetic susceptibilities. In addition, we measured the magnetic susceptibility of core from three Oklahoma Geological Survey drill holes that penetrated igneous rocks at ~61 m depth adjacent to the Meers fault (Bradley and Jones-Cecil, 1990; Jones-Cecil, 1995b). The sedimentary rocks we measured were essentially nonmagnetic. In the igneous rocks, granite and rhyolite had lower magnetic susceptibilities than mafic igneous rocks, except for zones L–N of the Glen Mountains Layered Complex (Fig. 2). The distinction among various remaining mafic rocks was less clear, although the suscep-

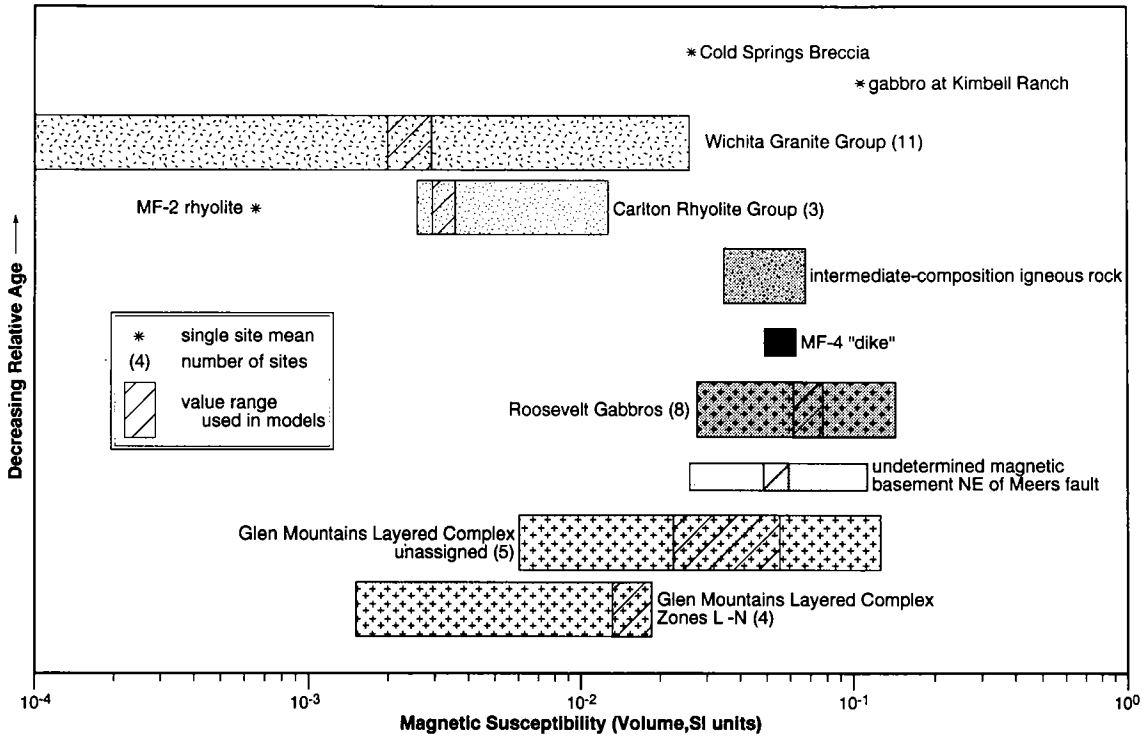


Figure 2. Ranges of magnetic susceptibility for site medians of major igneous-rock types in study area. Median site magnetic-susceptibility values for sedimentary rocks: 7×10^{-4} (SI) or less. Gabbro at Kimbell Ranch—gabbroic intrusion into Carlton Rhyolite Group east of Blue Creek Canyon. MF-2 rhyolite—rhyolite at bottom of Oklahoma Geological Survey (OGS) drill hole northeast of Meers fault. MF-4 "dike"—diorite and gabbro from bottom of OGS drill hole southwest of Meers fault. Undetermined magnetic basement—values used in magnetic models for magnetic basement northeast of the Meers fault (all but model for profile F used values in cross-hatched range). Cold Springs Breccia—microdiorite intrusion into Glen Mountains Layered Complex and Roosevelt Gabbros, dated as youngest of igneous rocks.

tibilities of the unassigned Glen Mountains Layered Complex were generally lower than the later-stage mafic intrusions. The susceptibility of the mafic igneous rock from the drill hole immediately south of the Meers fault (MF-4 "dike," Fig. 3) was in the susceptibility range of the Roosevelt Gabbros.

All of the magnetic susceptibilities used to represent major rock types in the magnetic models were in the range of the measured susceptibilities, except for the buried magnetic basement northeast of the Meers fault. A gabbro at Kimbell Ranch intrudes the Carlton Rhyolite Group and appears to be of limited areal extent northeast of the Meers fault. Unless it extends over a large area at depth, the Kimbell gabbro is an unlikely source for the long-wavelength magnetic anomalies north of the Meers fault. Possible sources for these anomalies include a large extent of the tholeiitic basalt of the Navajoe Mountain Basalt–Spilite Group, encountered in the Stanolind no. 1 Perdasopfy well (Fig. 3) north of the Meers and BCC faults (Ham and others, 1964), the Glen Mountains Layered Complex, or the Roosevelt Gabbros. As shown in Figure 2, the magnetic-susceptibility values used to model the undetermined magnetic basement northeast of the Meers fault were similar to values for most of the exposed mafic rocks.

Two sets of magnetic data at different scales were used in this study. A regional data set was digitized from an aeromagnetic map of the Lawton area (U.S. Geological Survey, 1975; Jones-Cecil, 1995a). Figure 3 shows the northern part of the digital aeromagnetic map. In addition, 12 ground-magnetic profiles as much as 4 km long provided more detail of the Meers fault zone (Jones-Cecil, 1995b). The profiles were spaced along a 38-km-long section of the fault that included the section that was reactivated in the Quaternary. Three regional profiles, taken from the original contoured map (U.S. Geological Survey, 1975), were modeled to examine structures to the north of the Meers fault. First we will discuss the aeromagnetic and ground-magnetic data as they pertain to the Meers fault, and then we will discuss the interaction of the Meers fault with adjacent structures.

The Meers Fault

Aeromagnetic Signature

Calculation and mapping of high horizontal gradients from the digitized aeromagnetic data provide a quantitative means to identify juxtaposition of rocks that have contrasting magnetic properties. This juxtaposition can be caused by faulting, igneous intrusion, or tilting of depositional boundaries. Major alignments of high horizontal gradients from Jones-Cecil (1995a) are superimposed on the map in Figure 3, excluding gradients within the Wichita uplift unrelated to the Meers fault. With the exception of the high gradients on the northeastern side of the high northeast of the Blue Creek Canyon fault, caused by the tilted unconformity between the Carlton Rhyolite Group and the Reagan Sandstone, high horizontal gradients in the area probably correspond to faults or intrusive boundaries.

The high horizontal gradients associated with the Meers fault help to identify details of faulting in magnetic basement. The apparent splaying of the Meers fault ~8 km northwest of the end of the Quaternary rupture is one of the most notable features (Fig. 3). In this area, magnetic basement north of the Meers fault is brought near the surface by a fan-shaped pattern of faults commonly associated with splays. The shallowness of magnetic basement in the area bounded by the splays is confirmed by drill holes northeast of the Meers fault that bottom in igneous rocks at elevations above sea level (McConnnell, 1987). The splays are spatially associated with a major N–S-trending structural boundary to the south (Jones-Cecil, 1995a) and with a backthrust in the FW fault system that merges with the Meers fault in this area. The structural boundary has been mapped as an inferred fault (Coffman and others, 1986) that separates the primarily granitic rocks in the eastern Wichita uplift from the older Glen Mountains Layered Complex in the central Wichita uplift. The structural boundary is expressed on the aeromagnetic map as an alignment of magnetic highs and a boundary across which regional magnetic anomalies change in intensity and frequency (Jones-Cecil, 1995a). In addition, a large positive gravity anomaly is centered over and elongated along the structural boundary (Robbins and Keller, 1992; Jones-Cecil and Robbins, in press). The magnetic anomaly associated with the main trace of the Meers fault steps ~2 km to the left across the structural boundary, and, west of the boundary, the trend of the Meers fault curves to a more northerly direction.

The geometry of the apparent splays and left step of the Meers fault is similar to the geometries observed in strike-slip fault zones and/or predicted by models. The splays are similar to those mapped at the ends of strike-slip fault zones (Price and Cosgrove, 1990, p. 139–145). King and Nábělek (1985) predict that an array of higher-order faults is produced at bends or terminations of strike-slip fault zones. Finally, the left step is similar to a dilatational jog in a pure strike-slip fault system (Sibson, 1986).

However, the Meers fault is different from these models in several respects. First, the Meers fault has a clear vertical component of slip in addition to the strike-slip component. Secondly, faulting probably did not occur in homogeneous rock. A gravity high along the structural boundary (Robbins and Keller, 1992; Jones-Cecil and Robbins, in press) indicates the presence of a large, dense body at depth that may have altered the local stress field during faulting. Finally, the interaction of a backthrust that has been mapped as a fork of the Meers fault (Havens, 1977; McConnell, 1987) could also be a factor in the splaying. The overall picture suggested by magnetic and gravity data indicates that the zone of splaying and the left step formed where a preexisting structure influenced the geometry of the Meers fault.

As first pointed out by Purucker (1986), dikelike bodies that are parallel to, and immediately south of, the Meers fault are evident on the aeromagnetic map. There is a narrow, discontinuous dikelike body along the northwest 12 km of the reactivated portion of the Meers fault. Several of the ground-magnetic profiles cross this dikelike body and provide further detail.

Finally, the aeromagnetic map provides insight into the structure where the BCC fault converges with the Meers fault. Magnetic basement is relatively shallow in this zone of convergence and appears to have been dragged between the Meers and Blue Creek Canyon faults and truncated by the BCC fault.

Ground-Magnetic Signature

Models of 12 ground-magnetic profiles provide details about structural relationships in and near the Meers fault. General features observed on the aeromagnetic maps are reinforced by the ground-magnetic profiles, including the splays northwest of the Quaternary fault scarp and the narrow dikelike body along part of the fault. In addition, analysis of the ground-magnetic data gives insight into the attitude of the Meers fault to depths of about 0.5 km and provides details about secondary strands of the fault that were reactivated in the Quaternary. The magnetic profiles were modeled using the computer program SAKI (Webring, 1985), which includes an inversion function that varies the location and/or magnetic susceptibility of the modeled bodies to decrease the root mean square error between the calculated response curve and the observed data. Once a gross match of model to observed data is made, the inversion function refines the model.

Modeling of potential-field data is inherently non-unique; that is, more than one model can

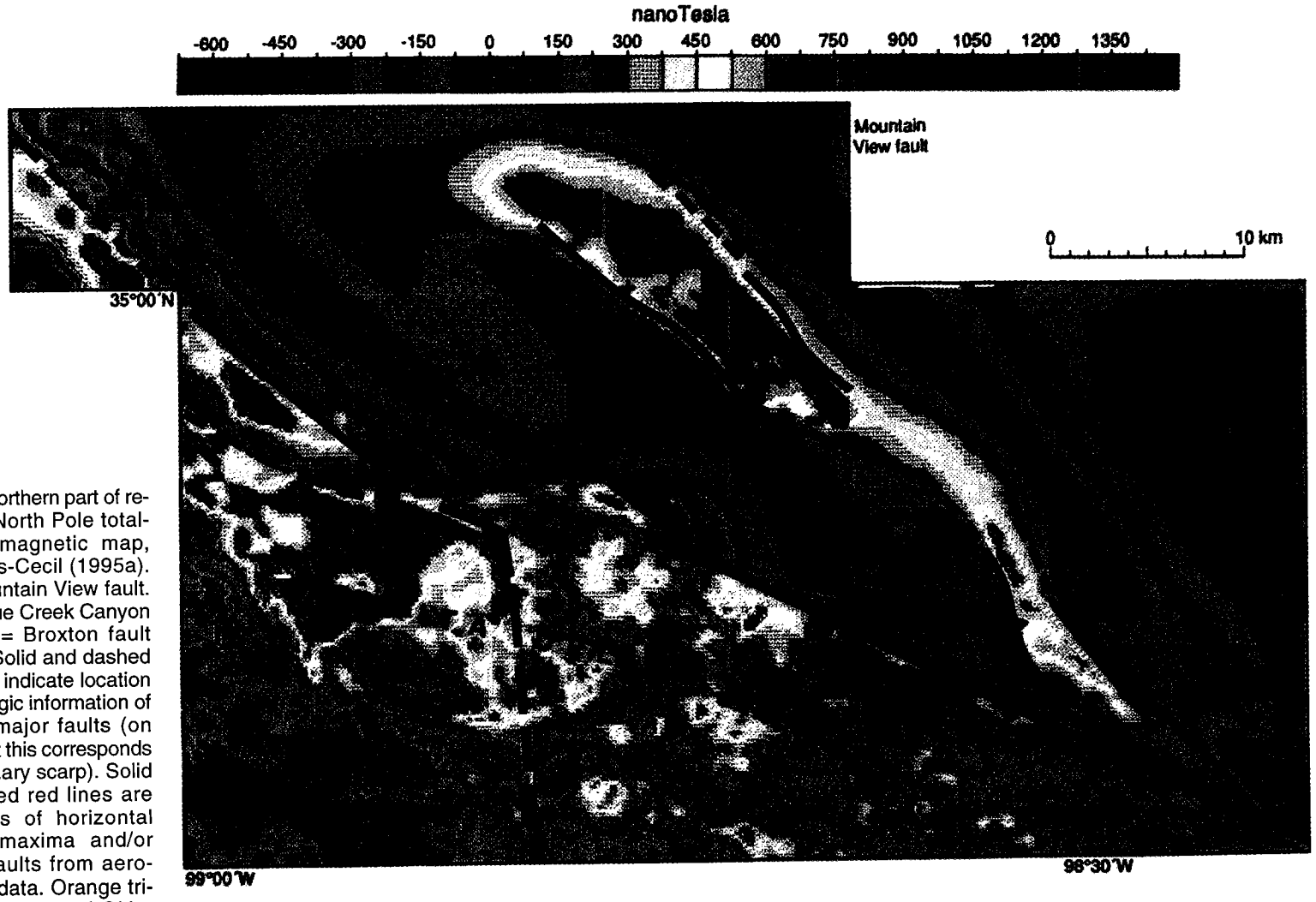


Figure 3. Northern part of reduced-to-North Pole total-field aeromagnetic map, from Jones-Cecil (1995a). MVf = Mountain View fault. BCCf = Blue Creek Canyon fault. Bfc = Broxton fault complex. Solid and dashed black lines indicate location from geologic information of selected major faults (on Meers fault this corresponds to Quaternary scarp). Solid and dashed red lines are alignments of horizontal gradient maxima and/or inferred faults from aeromagnetic data. Orange triangle is location of Oklahoma Geological Survey drill holes.

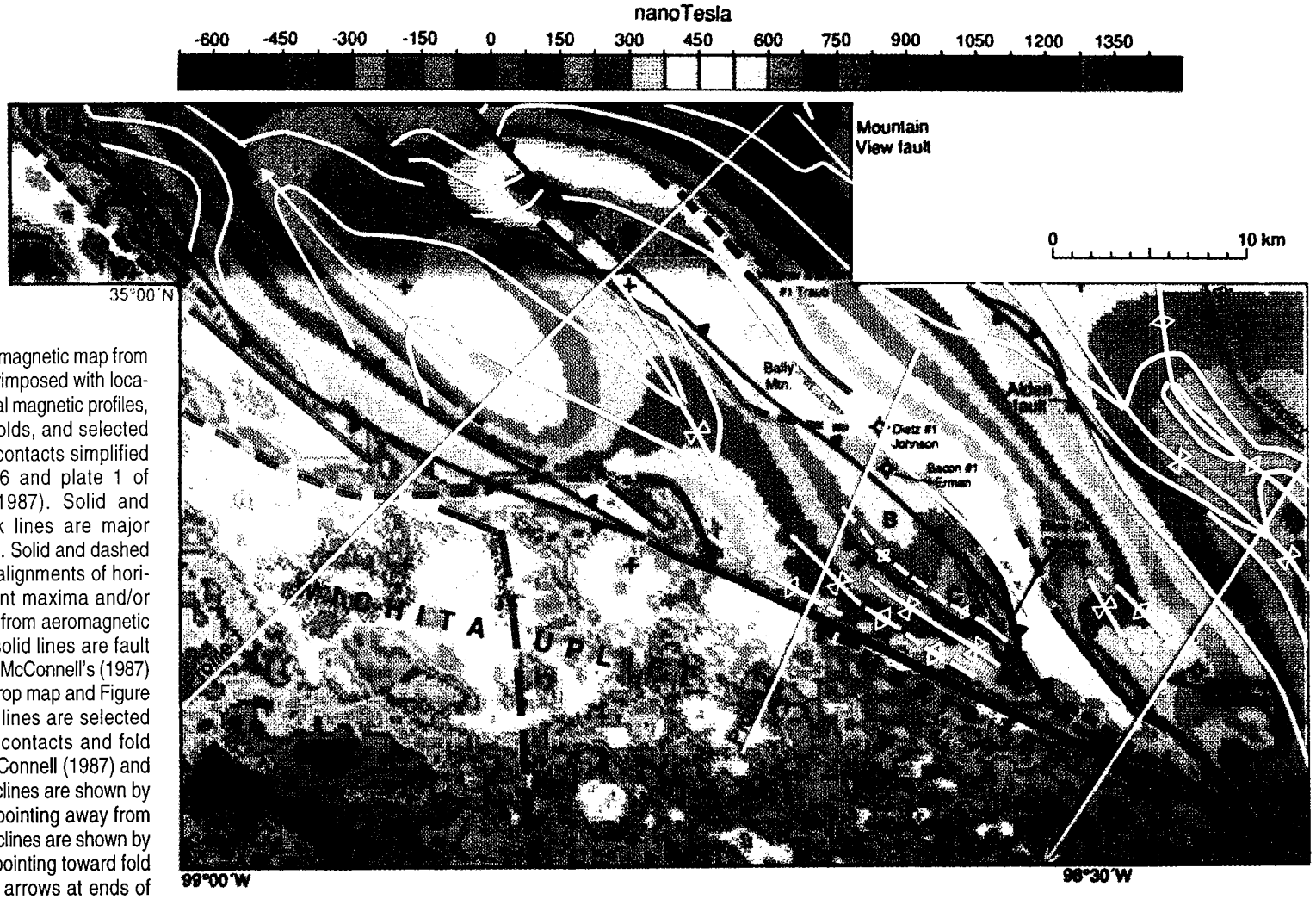


Figure 8. Aeromagnetic map from Figure 3 superimposed with locations of regional magnetic profiles, faults, large folds, and selected stratigraphic contacts simplified from Figure 6 and plate 1 of McConnell (1987). Solid and dashed black lines are major mapped faults. Solid and dashed red lines are alignments of horizontal gradient maxima and/or inferred faults from aeromagnetic data. Green solid lines are fault locations from McConnell's (1987) Permian subcrop map and Figure 6. Thin white lines are selected stratigraphic contacts and fold axes from McConnell (1987) and Figure 6. Anticlines are shown by open arrows pointing away from fold axes; synclines are shown by open arrows pointing toward fold axes. Closed arrows at ends of fold axes denote direction of plunge. Straight blue lines are regional magnetic profile lines. Teeth on upthrown side of faults.

(Figure 8 is placed here to minimize color-reproduction costs.)

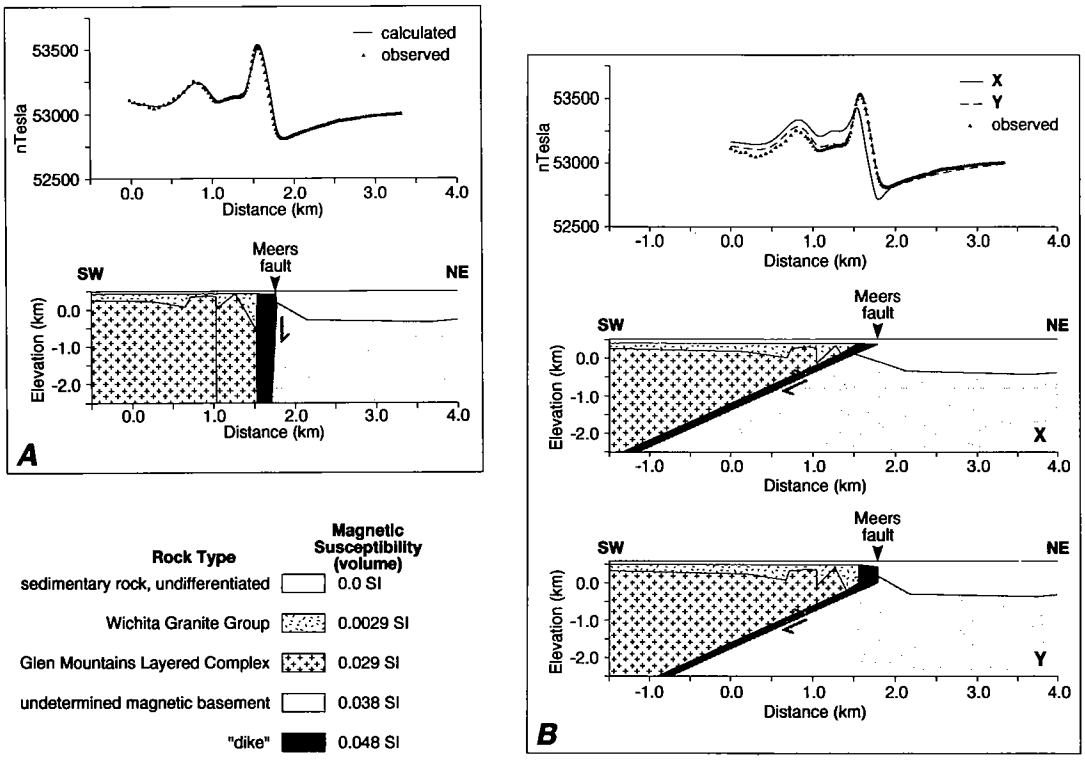


Figure 4. Ground-magnetic profile D (see Fig. 5 for location). Elevation relative to sea level. Arrows adjacent to faults in models show relative vertical movement. *A*—Best-fit model using a 285° declination and −15.6° inclination for remanent direction for the dikelike body. *B*—Models testing constraint on dip angle by changing geometry of bodies from model in *A*. Upper model X—45° SW dip of Meers fault. Lower model Y—close fit of the anomaly associated with the dikelike body for a simplified geometry of an overturned Meers fault. Near-vertical dip of Meers fault is well constrained only within approximately the upper 0.5 km.

match the observed data. However, geologic data can be used to constrain the range of possibilities. In this study, magnetic-susceptibility values in the models were based on the values we measured for the major rock types. In addition, measurements of magnetic susceptibility and remanent magnetization on cores of igneous rocks from three Oklahoma Geological Survey drill holes adjacent to the Meers fault provided key information about the dikelike body and the adjacent igneous rocks. Because the core was unoriented, we could only measure the inclination of the remanent magnetization, which averaged −15.6° for the dioritic/gabbroic rock from the dikelike body. Demagnetization of the paleomagnetic samples showed this inclination, for the most part, to be uncontaminated by drilling-induced magnetization. The remanent magnetization was probably acquired during either Cambrian cooling/tectonism or during late Paleozoic tectonism; both Cambrian and late Paleozoic pole positions for North America indicate shallow inclinations at the site. Therefore, we tested a range of possible declinations in models of a pilot profile, and chose a Middle to Late Cambrian declination of 285° (see Jones-Cecil, 1995b). The remanent component of magnetization was less than half the total magnetization; thus, the remanent contribution was of secondary importance. However, by including an intensity and direction for the remanence, the resulting models are more accurate. We have tried to minimize the assumptions in the modeling of the ground-magnetic data, by using measured magnetic susceptibilities and inclinations of the remanent component of magnetization. However, we refer to the models in this paper as "preferred" models to acknowledge the non-uniqueness of any magnetic model.

The preferred model for profile D (Fig. 4) was used to evaluate how well the magnetic data could constrain the dip of the Meers fault at depth and to illustrate the non-uniqueness of the magnetic models. At profile D, the dikelike body is narrow and can be modeled as a very simple, nearly rectangular body (Fig. 4). The best fit for the Meers fault is near vertical. By changing the dip of the dikelike body to 45° to the SW, and varying the depth at which this dip begins, the near-vertical dip of the dikelike body only needs to extend to ~0.5 km below the

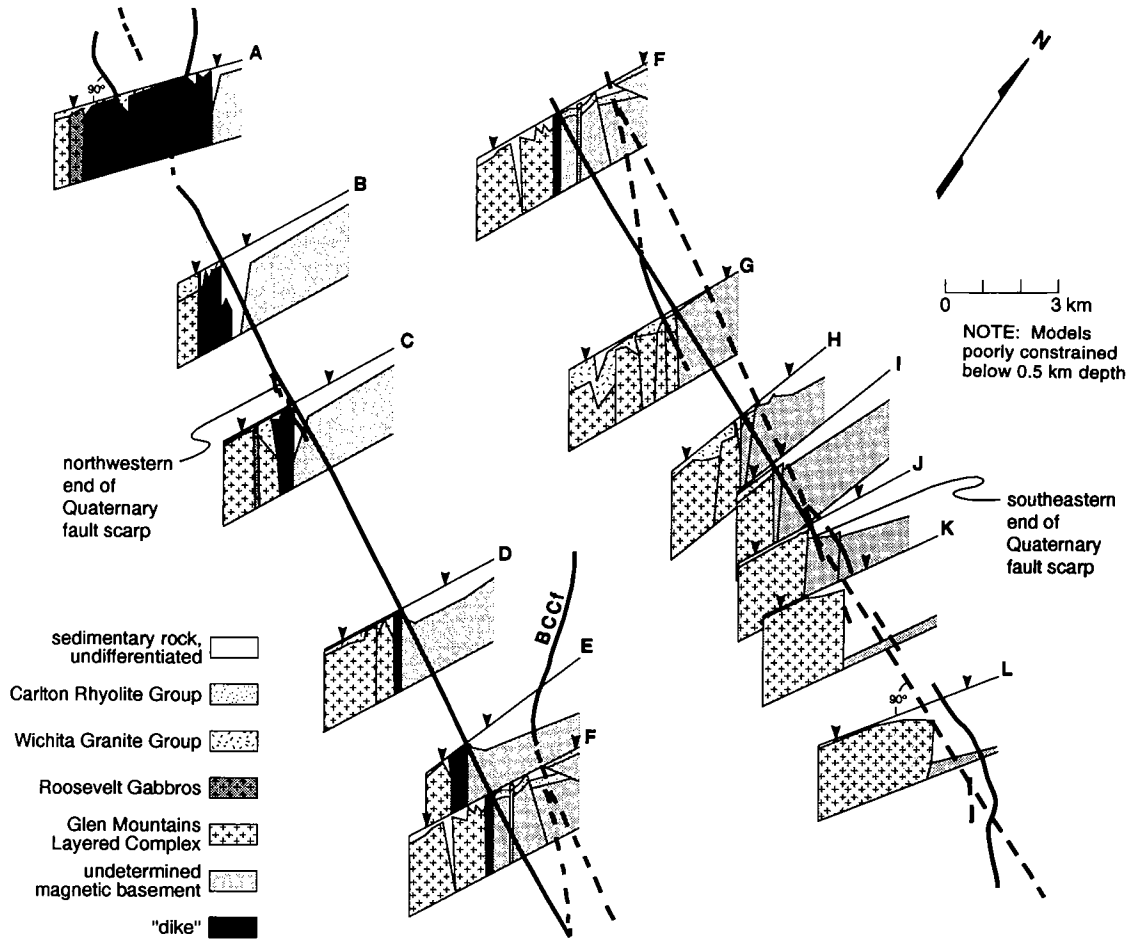


Figure 5. Oblique view of ground-magnetic models across the Meers fault. Scale applies in all dimensions. For range of magnetic-susceptibility values, refer to Figure 2. Arrowheads denote endpoints of measured magnetic profile. Northwest of Quaternary fault scarp, fault location determined from aeromagnetic map. Faults are shown as bold lines and dashed lines where inferred. BCCf = Blue Creek Canyon fault. Subparallel faults near profile C and southeast of profile J are from Ramelli and Slemmons' (1986) and Ramelli and others' (1987) interpretations of low sun-angle photographs. Other faults are from Harlton (1951,1963,1972).

surface to closely match the observed data. Thus, magnetic modeling of profile D suggested a near-vertical dip to the Meers fault, but could not resolve this dip with much certainty below 0.5 km depth.

Figure 5 is a composite of the preferred models for the 12 ground-magnetic profiles. Blocks of rock with different magnetic susceptibility are separated by faults, intrusive contacts, or contacts between igneous and sedimentary rocks. Faults that offset the upper surface of a body have been extended linearly through the body, even though they do not separate adjacent blocks of different susceptibility at depth. The simplified geometries in the models tend to emphasize vertical structures; because the resolution of the magnetic models is poorly constrained at depth, it is unrealistic to introduce shallowly dipping features at depth unless required by other geophysical or drill data. For simplicity, rhyolite was rarely modeled on top of the undetermined magnetic basement, although the Carlton Rhyolite Group is exposed at several locations northeast of the Meers fault. Because the susceptibility for the rhyolite is more than an order of magnitude less than that of the undetermined magnetic basement, the effect of omitting the rhyolite is to slightly decrease the depth to the more magnetic basement.

In most cases, the location of faults in the ground-magnetic models corresponds well to the mapped faults shown in Figure 5. The models show apparent basement control of several of the splays reactivated during Quaternary faulting. For example, in model C, an offset in basement rocks corresponds to a splay south of the main fault trace. In model G, the basement fault south of the Meers fault clearly

corresponds to the splay that was mapped by Harlton (1972), Ramelli and Slemmons (1986), and Ramelli and others (1987). The secondary faults mapped by Ramelli and Slemmons (1986) at the south end of the Quaternary fault scarp have no magnetic expression, which implies that they may be confined to the sedimentary section.

The narrow dikelike body is well defined in profiles C–F, but the magnetic data show that it does not extend as far southeast as magnetic profile G. In models A and B, bodies of similar susceptibility, but much wider, are present adjacent to the Meers fault. The possible presence of fault slivers in profile C suggests that the Meers fault splays inferred from the aeromagnetic map may begin as far southeast as the northwestern end of the Quaternary fault scarp.

Resolution of the origin of the dikelike body could help determine if the Meers fault is a Precambrian–Cambrian rift-related feature. The body could represent a horse block dragged into the Meers fault by Cambrian or, more likely, Pennsylvanian faulting. Alternatively, if the dikelike body was intruded along the preexisting Meers fault, the fault would most likely be Cambrian in age, because there is no evidence of post-Cambrian igneous activity in the region. Petrographic analysis of core from the Oklahoma Geological Survey drill hole ~18 mi southwest of the Meers fault indicates that this body is composed of highly altered diorite and hornblende gabbro (Collins, 1992). It is not clear if the presence of two rock types in 7.6 m of core is the result of faulting that juxtaposed different source rocks or is the result of compositional differentiation within a cooling dike. The presence of two overlying conglomerates that have different degrees of alteration in this drill hole, and in another drill hole ~180 m to the southwest, would suggest a Cambrian age for the dike if the lower, highly altered and sheared conglomerate is Upper Cambrian Reagan Sandstone. The upper conglomerate would correspond to Post Oak Conglomerate. Unfortunately, the pervasive alteration in the drill core and the limited extent of drilling make it difficult to determine the age of the dikelike body and its role in the evolution of the Meers fault.

Profiles F–I cross the area where the Meers and the BCC faults converge. The model for profile F, for the most part, incorporates data from the Oklahoma Geological Survey drill holes regarding depths and susceptibilities. In order to model the shorter-wavelength features northeast of the Meers fault, it was necessary to use rhyolite susceptibility values measured at outcrops rather than the lower susceptibility measured on the core. We allowed the inversion function to compute the susceptibility of unknown magnetic basement northeast of the Meers fault. In addition, the inversion function was used to find the best fit for the dip of the BCC fault, which was 50° to the NE. This dip is close to the 45° dip reported by Donovan (1982) for the southern part of the BCC fault. The model for profile F includes several faults between the Meers and BCC faults, implying that the basement rock wedge inferred from the aeromagnetic map may include slivers of brittlely deformed basement rock.

In summary, the aeromagnetic and ground-magnetic data provide detailed information about the geometry of the upper part of the Meers fault. The splays of the Meers fault northwest of the Quaternary fault scarp are near a major structural boundary in the Wichita uplift and near a mapped fork of the Meers fault. A left step and change in trend of the Meers fault is present where it crosses the structural boundary. A 12-km-long dikelike body is immediately south of a part of the reactivated Meers fault. Detailed models of ground-magnetic profiles reveal the control that basement faults had in the location of Quaternary faulting. A near-vertical dip is the best-fit attitude for the Meers fault, yet even with the control provided by the paleomagnetic data, the near-vertical dip cannot be well constrained below ~0.5 km depth using the ground magnetic data. This near-vertical dip is extended to the upper few kilometers by regional magnetic models (Figs. 9–11).

RELATIONSHIP OF THE MEERS FAULT TO ADJACENT STRUCTURES

North of the Meers fault, in the area including the Slick Hills, a thick sequence of Cambrian, Ordovician, and Lower Permian sedimentary rocks overlies all but a few outcrops of igneous basement. A comparison of the structures in the magnetic basement north of the Meers fault with the structures in the overlying sedimentary section provides insight into the timing and development of the Meers fault, with respect to adjacent structures.

Structures in the Slick Hills

The Slick Hills are part of the Lawton segment, which is a parallelogram with approximately 70- and 25-km diagonals (McConnell, 1989a,b). The long sides of this parallelogram are defined by the Meers fault on the south–southwest and the Mountain View fault on the north–northeast. The short sides are defined by the Broxton fault complex on the east–northeast and a more N-trending segment of the Meers fault on the west–southwest (Fig. 1). The boundary formed by the NNW-trending Broxton fault complex is a series of SW-dipping reverse faults and associated hanging-wall folds.

The Blue Creek Canyon Fault

The Slick Hills are divided by the BCC fault into two approximately equal parts—the eastern and western Slick Hills (Fig. 6). Going from southeast to northwest, the main trace of the BCC fault trends a few degrees clockwise of the Meers fault (Figs. 1, 6). In Blue Creek Canyon, the fault turns sharply

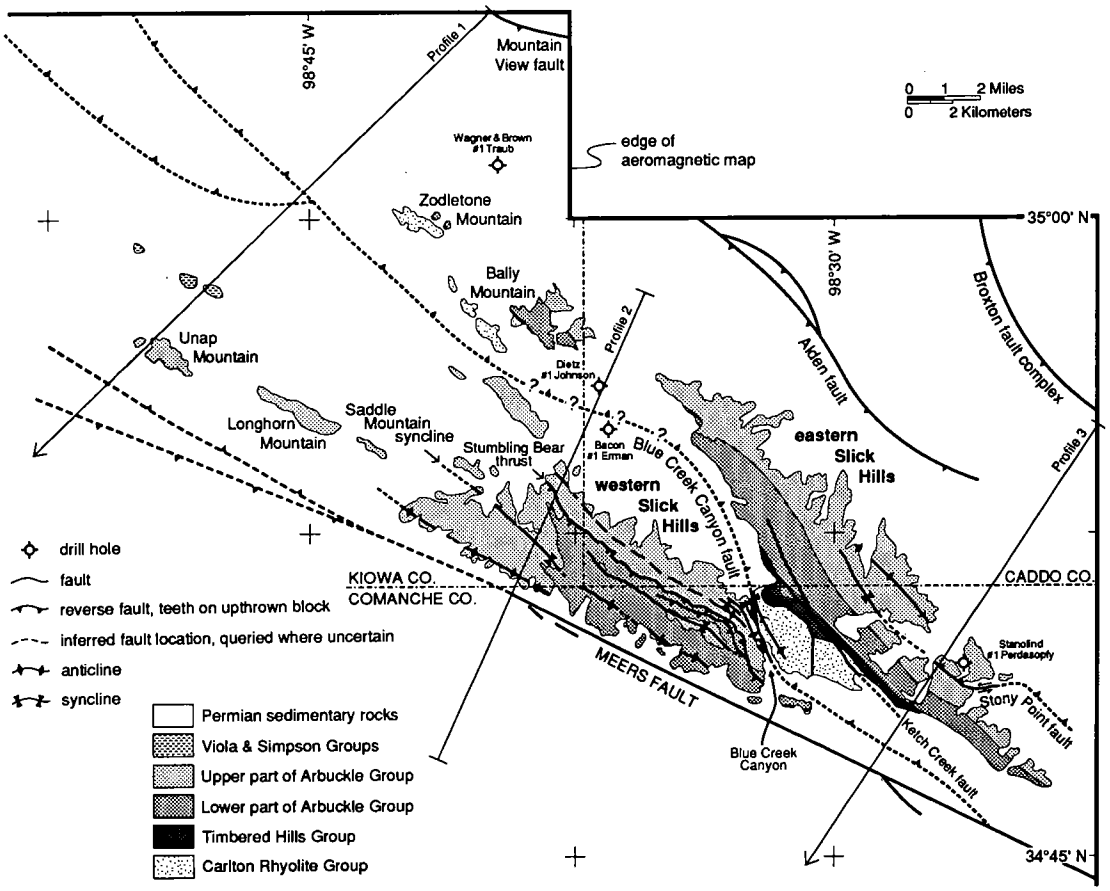


Figure 6. Location of large faults, folds, and rock groups in the Slick Hills, and regional magnetic profiles. Secondary faults south of the Meers fault are simplified from Ramelli and Slemmons' (1986) and Ramelli and others' (1987) interpretations of low sun-angle photographs. Fault locations outside the Slick Hills are from McConnell (1987). The bend in the Blue Creek Canyon fault south of Bally Mountain is based on aeromagnetic horizontal gradient maxima and data from the Bacon no. 1 Erman and Dietz no. 1 Johnson drill holes. Queried segment of fault indicates location of possible end of BCC fault and tear fault south of Bally Mountain in an alternate interpretation.

northward for ~3.25 km. North of the canyon, it resumes a more northwesterly trend, and it eventually splays and apparently terminates a short distance south of the Mountain View fault. The fault is exposed only along the N–S section in Blue Creek Canyon, where it is clearly a steep E-dipping reverse fault with variable stratigraphic displacement averaging ~800 m down to the west. Small-scale structures, principally the drag of bedding and en echelon pressure-solution cleavage arrays, suggest a component of left-lateral motion on the fault (Donovan, 1986). To the northwest, in the vicinity of Bally Mountain, the fault has as much as 2,200 m of throw. In essence, the BCC fault can be viewed as an oblique back thrust in the FW fault system that elevates the eastern Slick Hills block in a direction opposite to the regional downthrow to the northeast.

The Eastern Slick Hills

A thickness of as much as 1.1 km of Carlton Rhyolite Group is exposed in the eastern Slick Hills. The rhyolite is cut by diabase dikes and at least one small basic intrusion (the Kimbell gabbro, Figs. 2,7). Overlying the Carlton Rhyolite Group are basal siliciclastics and carbonate rocks of the Timbered Hills and Arbuckle Groups, respectively (Fig. 7). The overall structure of the eastern Slick Hills is that of a homocline that dips 20–45° NE. The trend of the large structures in this block is compatible with a maximum compressional stress that was oriented ~055°.

In the southeast part of the eastern Slick Hills, the simple homoclinal geometry is complicated by several folds and faults. In Blue Creek Canyon, a large N-plunging anticline that clearly involves

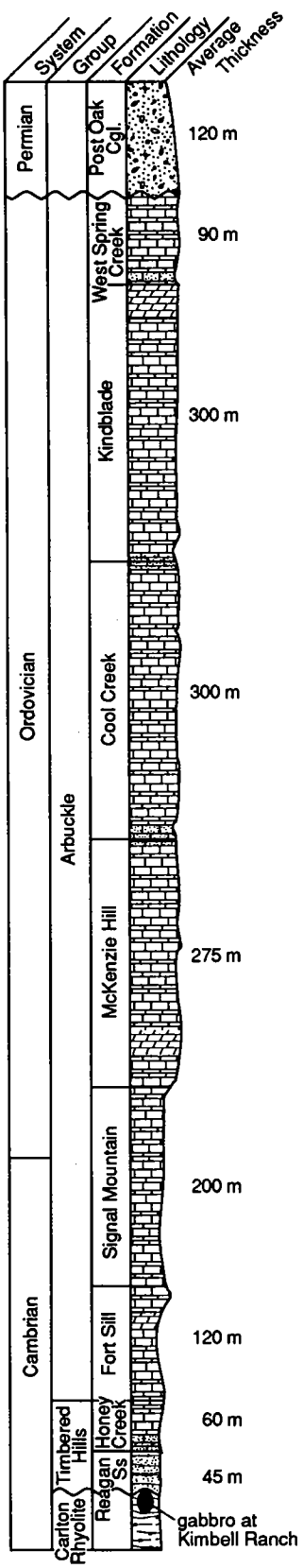


Figure 7 (left). Simplified stratigraphy of the Slick Hills (modified from Donovan, 1986). Gabbro at Kimbell Ranch is the gabbroic intrusion in the Carlton Rhyolite Group east of Blue Creek Canyon. Standard stratigraphic symbols.

Carlton Rhyolite Group reverses the regional northeast dip of the section adjacent to the BCC fault. In addition, there are two faults that have a down-to-the-west displacement similar to that of the BCC fault (Fig. 6). The Ketch Creek fault offsets the Carlton Rhyolite Group and has a maximum throw of ~160 m. East of the Ketch Creek fault, the Stony Point fault offsets the upper part of the Arbuckle Group and has a maximum throw of ~325 m (Stephenson and Donovan, 1991). Both faults die into a series of splays and small folds to the northwest.

Northeast of the eastern Slick Hills, subsurface drill-hole and seismic data (McConnell, 1989a,b; Stephenson and Donovan, 1991) show that the regional northeast homoclinal dip continues as far as the northwest boundary of the Lawton segment beneath an increasing thickness of Permian rocks. The depth to basement varies considerably along strike to the northwest. Immediately northwest of Blue Creek Canyon, the Carlton Rhyolite Group is well below the surface, whereas to the northwest, on Bally and Zodletone Mountains, as much as 1.1 km of the Carlton Rhyolite Group is exposed. The depth to basement correlates with the dip of the homocline; where basement is deeper, the dip is shallower. Farther to the northwest, the basement plunges NW toward the Mountain View fault as the throw on the BCC fault becomes negligible.

The Western Slick Hills

Most outcrops in the western Slick Hills consist of highly deformed rocks of the Arbuckle Group. However, a very small inlier of Carlton Rhyolite and Timbered Hills Groups is exposed at the extreme southeastern edge of the western Slick Hills between and near the junction of the Meers and BCC faults. The principal structure in the western Slick Hills is the Stumbling Bear thrust (Fig. 6), a major SW-dipping fault that ramps across the middle of the Arbuckle Group. It has a maximum stratigraphic displacement of ~650 m, and it juxtaposes strata of the McKenzie Hill and Kindblade Formations of the Arbuckle Group.

Northeast of the Stumbling Bear thrust, deformation consists primarily of semi-chevron parallel folds with variably steep axial surfaces. In a few places, the folds have vertical to slightly overturned limbs. Some of the folds exhibit pressure-solution cleavage in their hinge areas, indicating a high degree of strain associated with the folding. Most of the folds trend NW, face to the NE, and generally have wavelengths of ~400 m.

Folds with comparable geometry are also present southwest of the Stumbling Bear thrust. Within 1–2 km of the Meers fault, the folds are tighter, and, in some cases, are both upright and isoclinal. A regional pressure-solution cleavage, that is not necessarily parallel to the axial planes of the folds, indicates a continuation of strain and possible rotation of fold axes in this tightly folded terrain. In addition to the folding and cleavage, additional shortening was caused by thrust faulting that approximately follows vertical or steeply dipping bedding. As much as 370 m displacement has been measured on such faults, but this style of faulting is present on both small and large scales. Many faults are the sites of narrow zones of intense pressure-solution cleavage. Commonly, the cleavage is sigmoidal, which is consistent with deformation that would be caused by a left-lateral transpressive stress (McCoss and Donovan, 1986).

McCoss and Donovan (1986) noted that the fold axes in the western Slick Hills consistently trend a few degrees north of the strike of the Meers fault, and suggested that this orientation was consistent with deformation by a compressive stress oriented 055°. This stress orientation would have induced a component of left-lateral motion along the Meers fault.

At the western end of the western Slick Hills is the Saddle Mountain syncline, a large fold with a wavelength of >1.6 km (Fig. 6). This fold is similar in style and character to several folds that are present in the subsurface to the northwest (McConnell, 1989a,b; Fig. 8 [p. 193]). All of these folds plunge gently northwest. Regional magnetic profile 1 crosses two of these folds (Figs. 6,8,9). Based on interpretations of proprietary seismic-reflection data, these folds appear to be associated with back-thrusting of the BCC fault and a fork of the Meers fault that mimics the BCC fault in trend and sense of displacement.

In summary, the western Slick Hills block tilts to the northwest and is bounded on the northeast by the BCC fault, on the southwest by the Meers fault, and on the northwest by the Mountain View fault. The block is the footwall of both the Meers and Blue Creek Canyon faults. This simple picture is complicated greatly by folding and faulting. No part of the Frontal Wichita fault system shows more evidence of shortening, especially in the part of the block adjacent to the Meers fault. Analysis of stress vectors indicates that movement on the Meers fault probably had a component of left-lateral strike slip.

Comparison of Surface Structures with Magnetically Determined Basement Structures

Structural analysis based on surface geology in the study area is constrained by limited exposures in some critical areas. For example, there is no exposure of the Meers fault in pre-Permian rocks, the BCC fault is only exposed along a short part of its length in an area where its trend is anomalous, and pre-Permian rocks are poorly exposed in the structurally complex area where the Blue Creek Canyon, Meers, and Ketch Creek faults converge. This general lack of exposure makes it difficult to assess the degree of coupling between the sedimentary and underlying igneous rocks. The aeromagnetic data allows a glimpse beneath the nonmagnetic sedimentary section northeast of the Meers fault.

Problems in Relating Geologic and Magnetic Data

Aside from the non-uniqueness of magnetic models, an inherent problem in interpreting the magnetic data northeast of the Meers fault is that we have few direct magnetic-susceptibility measurements of basement rocks beneath the sedimentary rocks. We have susceptibility measurements of the Carlton Rhyolite Group at two localities in the Blue Creek Canyon area, and measurements of the Kimbell gabbro, which intrudes the Carlton Rhyolite Group. We do not have measurements for the Navajoe Mountain Basalt–Spilite Group, which was encountered at a depth of 2.6 km in the Stanolind no. 1 Perdasopfy drill hole (Figs. 6,8). Finally, we do not know the basement-rock type or types beneath the Slick Hills that produce(s) the large magnetic highs. Thus, we make two simplifying assumptions about the magnetic basement: (1) it is generally homogeneous and has susceptibilities similar to those of the undetermined magnetic basement in the ground-magnetic models, and (2) it has negligible remanent magnetization. Clearly, the validity of our interpretations depends on the correctness of these assumptions.

Possible scale-related incompatibilities exist between the surface mapping and the aeromagnetic surveying. As depth to magnetic basement increases, short-wavelength features become subdued. Thus, unless the basement is shallow, short-wavelength features are not apparent in the magnetic data. To minimize the effects of basement depth, we compare only large folds and major faults in the sedimentary section with basement structures. In addition, some short-wavelength features have been artificially introduced into the aeromagnetic data set by errors in flight-line location. The flight paths of the magnetic survey were oriented E–W, so location errors produced small east–west zigzags of individual contours (see zigzags north and east of intersection of profile 2 and the Meers fault in Fig. 8). If the flight-line-location errors are large, they could obscure subtle E–W-trending structures, but they would have less impact on more N-trending features. Fortunately, few surface features are oriented E–W, and the subsurface features generally trend NW.

Aside from the effect that depth of magnetic basement has on the observed wavelength of structures, it is reasonable to expect shorter wavelength structures in the sedimentary rocks than in the underlying basement rocks due to the lower rigidity and greater anisotropy of the sedimentary rocks. The style of deformation in the sedimentary rocks is consistent with low rigidity and high anisotropy. Ubiquitous parallel folds are dominantly flexural slip folds. Folding was principally controlled by anisotropy imparted by bedding in the Arbuckle carbonate rocks. As a result of the folding, much of the western Slick Hills is characterized by belts of steep and vertical bedding. In addition, pressure solution that reduced the volume of the carbonate rocks was responsible for further shortening. The volume of rock removed by pressure solution is difficult to quantify, but appears to be considerable in the southern part of the western Slick Hills, close to the Meers fault. Some of the faulting in the sedimentary rocks is internal; that is, it does not involve the basement. The stratigraphically lowest potential décollement horizons are shale beds in the Reagan Sandstone, although no décollement has been observed in these horizons. In several parts of the western Slick Hills, some reverse faults flatten into the most thinly bedded part of the Signal Mountain Formation (Arbuckle Group). In addition, bedding-parallel thrust faults have been reported in thinly bedded units at higher levels in the Arbuckle

Group (Donovan and Ragland, 1991). Tight parallel folds, flexural slip folds, pressure solution, and décollement horizons would be unlikely in a rigid, homogeneous basement rock.

It is difficult to directly assess the rigidity and homogeneity of the basement rocks because little igneous basement is exposed north of the Meers fault. However, the Carlton Rhyolite Group is folded at one locale (Fig. 6), indicating that it is not too rigid to fold. On the east side of the BCC fault, the Carlton Rhyolite Group forms the core of a N-plunging, open, asymmetric anticline. In the rhyolite, the limbs of the anticline dip ~40° and ~12°, respectively (Fig. 6). Farther to the northwest at Bally Mountain, the Carlton Rhyolite Group is not folded, but simply tilted 20–45° NE, consistent with the overlying sedimentary section. Thus, in two places, structures in the Carlton Rhyolite Group appear to be coupled with large structures in the overlying sedimentary rocks. There is no exposure of basement rocks in the western Slick Hills where short-wavelength folding, pressure solution, and internal faulting have been observed in the sedimentary rocks.

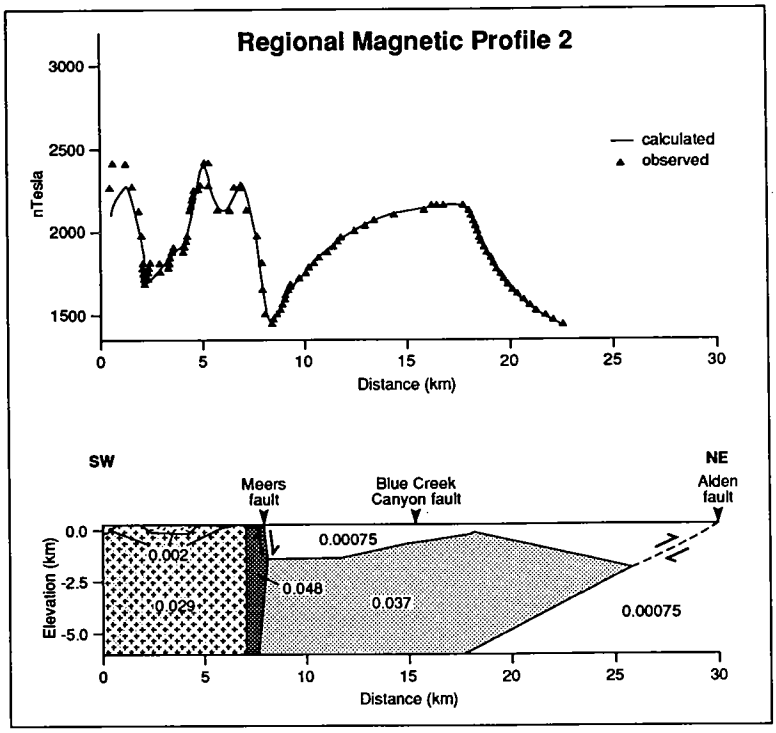


Figure 9. Magnetic profile 2 based on aeromagnetic data (U.S. Geological Survey, 1975), above, and preferred model, below. Elevation relative to sea level. See Figure 8 for location of profile. Location of fold axes (using symbols shown in Fig. 8) and faults (arrowheads) are from McConnell (1987) and are shown above model. Arrows adjacent to faults in model show relative vertical movement. Magnetic-susceptibility values (SI) are superimposed on bodies in the model. Refer to Figures 2, 4, and 5 for lithologic symbols.

Figure 8 superimposes the major faults and large folds from Figure 6, as well as selected features from McConnell's subsurface map (1987), onto the aeromagnetic map. Large structural features in the sedimentary section correlate well with inferred features in the underlying magnetic basement in most areas. The greatest differences are in the western Slick Hills, between Blue Creek Canyon and the Meers faults, and in the eastern Slick Hills, northeast of the BCC fault from Bally Mountain northwestward.

Correlation of Geology and Magnetics along the Blue Creek Canyon Fault

Where exposed in Blue Creek Canyon, the mapped trace of the BCC fault agrees well with the location of the high horizontal gradients calculated from the aeromagnetic data. Harlton's (1963,1972) inferred continuations of the BCC fault southeast of Blue Creek Canyon are only weakly suggested by the aeromagnetic data (Fig. 8). Ground-magnetic profile F (Fig. 5) clearly shows a fault that corresponds to this southeastward continuation of the BCC fault. Uplift of magnetic basement on the northeastern side of the BCC fault is well-expressed in profile F, and the preferred model shows the BCC fault as a reverse fault dipping ~50° NE. The vertical separation in the model is 980 m, which is comparable to the 800-m separation reported by Stephenson and Donovan (1991). Ground-magnetic profile G (Fig. 5) crosses a splay south of the Meers fault that could be a further continuation of the BCC fault; the preferred model includes a basement fault that correlates with this splay. Models for profiles H and I include a basement fault that corresponds to Harlton's (1963) inferred more northerly continuation of the BCC fault, but evidence for the fault is absent in profile G, which implies that the more northerly continuation may be incorrect.

The BCC fault is not exposed northwest of Blue Creek Canyon, but has been mapped on the basis of drill-hole information and nearby exposures of igneous rocks (Havens, 1977; McConnell, 1987). Its

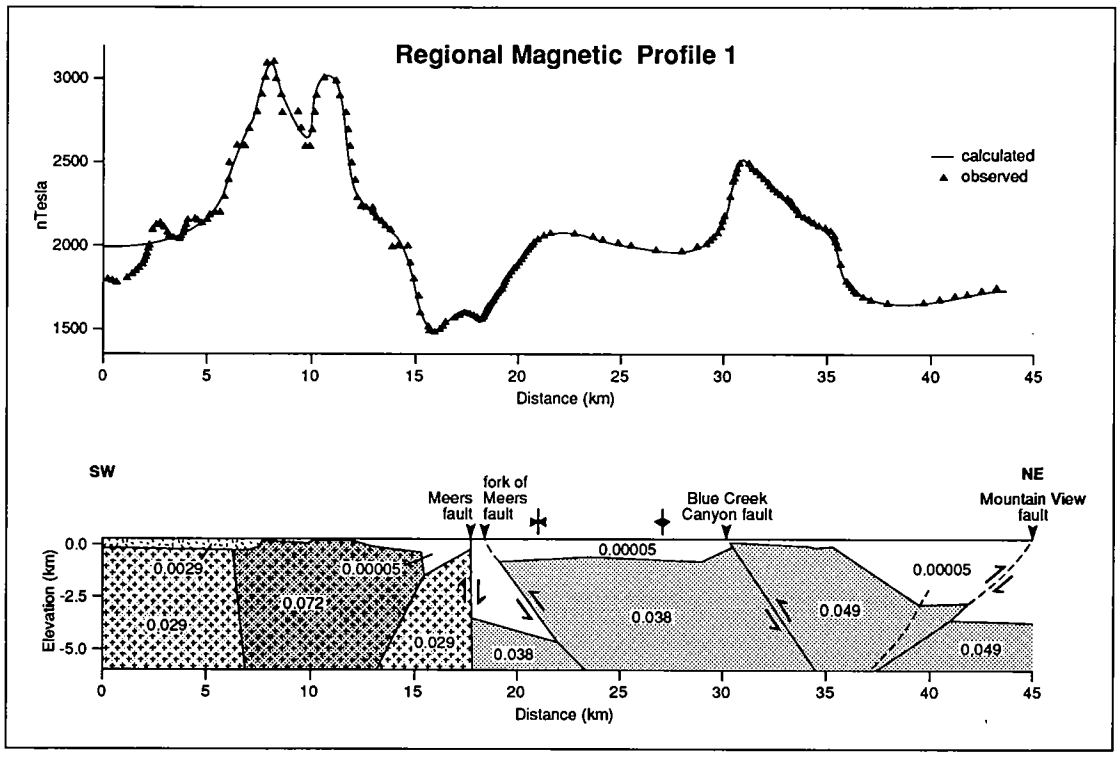


Figure 10. Magnetic profile 1 based on aeromagnetic data (U.S. Geological Survey, 1975), above, and preferred model, below. Elevation relative to sea level. See Figure 8 for location of profile. Location of fold axes (using symbols shown in Fig. 8) and faults (arrowheads) are from McConnell (1987) and are shown above model. Arrows adjacent to faults in model show relative vertical movement. Magnetic-susceptibility values (SI) superimposed on bodies in the model. Refer to Figures 2, 4, and 5 for lithologic symbols.

mapped location does not correspond with the magnetic expression of the BCC fault. The magnetic data show the magnetic high northeast of the BCC fault (referred heretofore as the Blue Creek Canyon uplift) continues in a more northerly direction northwest of Blue Creek Canyon, and then curves westward immediately south of Bally Mountain (Figs. 6,8). Drill-hole data are consistent with this bend. The Bacon no. 1 Erman drill hole, north of the previously inferred trace of the BCC fault, bottomed in the Arbuckle Group rather than rhyolite at 46 m, as expected north of the fault and along strike of the Carlton Rhyolite Group (McConnell, 1987). Farther to the northwest, and along strike of the Arbuckle Group rocks, the Dietz no. 1 Johnson drill hole bottomed in granite wash (representing the unconformity on top of igneous basement) at 39 m. If the fault follows the magnetic trend, the Bacon no. 1 Erman drill hole would be south of the fault where Arbuckle Group rocks would be expected, and the Dietz no. 1 Johnson drill hole would be north of the fault where evidence of igneous basement would be expected, as shown in Figures 6 and 8. Maximum horizontal gradients are absent near profile line 2 (Fig. 8). Using bodies with identical magnetic susceptibility on either side of the BCC fault, the model of profile 2 (Fig. 9) shows no vertical displacement on the BCC fault in this saddle between Blue Creek Canyon and Bally Mountain. However, this lack of vertical displacement does not preclude some strike-slip offset through this area, or the possibility of vertical displacement if, in fact, the BCC fault juxtaposes basement rocks of different susceptibilities. Alternate interpretations include: (1) the BCC fault ends between Blue Creek Canyon and Bally Mountain (does not curve westward), a subparallel fault southwest of Bally Mountain continues to the northwest, and the south end of the magnetic high at Bally Mountain corresponds to a tear fault; or (2) the BCC fault has a very shallow NE dip that produced the apparent offset between the surface fault trace and the location in magnetic basement at depth. We reject the second alternative because it does not readily explain the drill-hole data.

Northwest of Bally Mountain, the location of the BCC fault from McConnell (1987) and Havens (1977) is ~0.5 km northeast of the maximum hori-

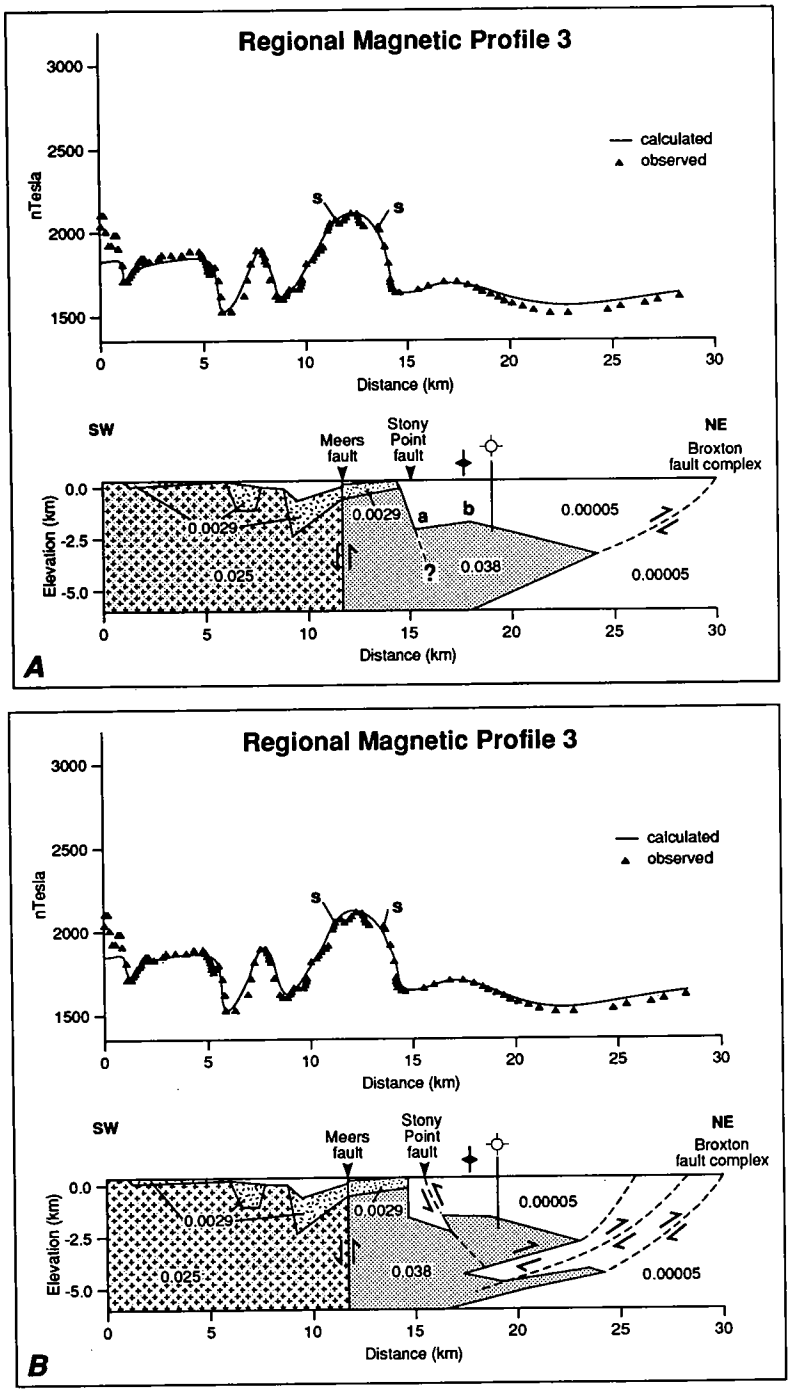


Figure 11. Magnetic profile 3 based on aeromagnetic data (U.S. Geological Survey, 1975) and preferred models. Elevation relative to sea level. Location of fold axes (using symbols shown in Fig. 8) and faults (arrowheads) from McConnell (1987) are shown above model. Arrows adjacent to faults in models show relative vertical movement. Magnetic-susceptibility values (SI) are superimposed on bodies in the models. Refer to Figures 2, 4, and 5 for lithologic symbols. Drill-hole symbol and depth of drill hole are shown on the models at the along-strike location. *A*—Model is based on simplified geometries. *B*—Model is based on simplification of the Stephenson and Donovan (1991) cross section interpreted from seismic and drill-hole information. The similarity of the calculated curves for the different geologic models shown in *A* and *B* illustrates the non-uniqueness of potential-field models. Nevertheless, the gross geometry of the source bodies is similar in the two models.

zontal gradients calculated from the aeromagnetic data. Some of this discrepancy could be due to poor exposure and drill-hole control, and the resultant uncertainty in the fault's location. However, where the BCC fault is shown to divide into two strands near magnetic profile 1, drill-hole control is good, and the two data sets clearly disagree. One possible reconciliation between the interpretations is suggested by McConnell's (1987) extended cross section H–H', which is ~6 km southeast of profile 1. He shows the BCC fault as a series of closely spaced back-thrust faults, rather than as a single fault. The magnetic data may define the location of the southwesternmost strand in the fault zone. We modeled

the BCC fault as a back thrust in Figure 10, based on proprietary seismic data in this area.

The aeromagnetic data show that the location of the BCC fault northwest of Blue Creek Canyon may need to be revised. Between Blue Creek Canyon and Bally Mountain, the aeromagnetic data can be satisfied by either a bend in the fault that is consistent with drill-hole information, or a termination of BCC fault and a subparallel fault continuing to the northwest from west of Bally Mountain. Models of the ground-magnetic data suggest the possible southeastward continuation of the BCC fault between Blue Creek Canyon and the Meers fault.

Correlation of Geology and Magnetics in the Eastern Slick Hills

Northeast of the BCC fault, many of the geologic structures mapped in the eastern Slick Hills correspond to structures in the magnetic basement that are modeled in profiles 1–3 (Figs. 9–11).

From Bally Mountain northwestward, the large fold in sedimentary rocks in the hanging wall of the BCC fault plunges NW. The shape of the contours on the aeromagnetic map resemble the concave-to-the-southeast shape of contours of the subcrop map of the base of the Permian (Fig. 8). In addition, modeling of profile 1 shows a 35° NE dip of basement rocks, which is consistent with dips measured on outcrops near Bally Mountain, and is similar to the dips in McConnell's (1987) two cross sections near profile 1. To define the Mountain View fault as a moderately SW-dipping thrust fault offsetting basement, the preferred model includes a triangular fault block of basement rock in the hanging wall of the Mountain View fault. The presence of a second fault in this area is suggested by Ham and others (1964, pl. 1). In the preferred model, the top of magnetic basement in the footwall of the Mountain View fault is ~4 km deep. Five kilometers southeast of profile 1, the depth to basement is >6.3 km in the Wagner and Brown no. 1 Traub drill hole (McConnell, 1987). Decreasing depth to basement to the northwest in the footwall of the Mountain View fault is consistent with the increase in magnetic intensity along the regional strike between the Traub well and the northern boundary of the map in Figure 8; however, the rapid change in depth to basement suggests the presence of another fault or incorrect assumptions in the model.

The strength of the anomaly associated with the Blue Creek Canyon uplift is difficult to resolve, particularly northwest of Bally Mountain. The magnetic susceptibility of the basement rock within the uplift that was used in the preferred model for profile 1 (0.049 SI) is almost four times higher than the Carlton Rhyolite Group median susceptibility measured at Bally Mountain (0.013 SI, Jones-Cecil, 1995a). The homoclinal NE dip across the Bally Mountain area and the presence of Carlton Rhyolite Group close to the BCC fault preclude the presence of a conformable substrate more magnetic than the Carlton Rhyolite Group that could produce this magnetic high. Perhaps a body similar to the Kimbell gabbro, but of greater areal extent, intruded the Carlton Rhyolite Group and is present below the rhyolite outcrops. The near-horizontal body in the model of profile 1 is suspect, however, because the Carlton Rhyolite Group dips to the northeast in outcrop, and there is no evidence of any igneous intrusions that postdate tilting of the rhyolite. A smaller linear high immediately southwest of the Carlton–Timbered Hills contact northeast of Bally Mountain contributes to the intensity of the magnetic high. Because the linear high follows the strike of the rhyolite and the overlying sedimentary rocks, the causative body is probably conformable with the Carlton Rhyolite Group, which implies that it is either a sill-like intrusion or a more magnetic layer in the rhyolite.

Southeast of Bally Mountain, the general NE homoclinal dip in the central part of the eastern Slick Hills is modeled as a 13° NE dip of the upper surface of magnetic basement in profile 2 (Fig. 9). This shallow dip is consistent with the greater depth to igneous basement in the vicinity of the profile, as discussed above. The Alden fault and the low-susceptibility sedimentary rocks beneath the thrust fault were easily modeled.

Profile 3 crosses the eastern Slick Hills in the southeast in an area of structural complexity (Fig. 6). It crosses the Stony Point fault, (a back thrust subparallel to and northeast of the BCC fault in the sedimentary rocks), and the extension of an anticline northeast of and parallel to the Stony Point fault (Fig. 11A,B). The synclinal feature labeled "a" in the model in Figure 11A corresponds to the thick section of sedimentary rocks in the footwall of the Stony Point fault. The anticline modeled in the magnetic basement and labelled "b" (Fig. 11A) corresponds to the anticline mapped at the surface. The Stanolind no. 1 Perdasopfy well is <1 km southeast of profile 3, and its location projected along strike is shown in Figure 11A,B. In the Stanolind well, the Navajoe Mountain Basalt–Spilite Group, likely a strong magnetic source rock, was encountered at 2.6 km depth (or ~2.2 km below sea level). The depth to the top of the basalt-spilite corresponds to the approximate top of the magnetic body in both models in Figure 11. The Stony Point fault could not be recognized from the magnetic data, indicating that it probably offsets only nonmagnetic sedimentary rocks. However, Figure 11B shows a second magnetic model that is based on Stephenson and Donovan's interpretation (1991) of seismic and drill-hole data near magnetic profile 3. Clearly the magnetic data can support their interpretation, and the gross geometry of the underlying magnetic bodies approximates the distribution of the magnetic basement in the model in Figure 11A.

McConnell (1987) compiled drill-hole information for much of the area surrounding the Slick

Hills, and his subcrop map of the rocks beneath the Permian unconformity shows an anticline/syncline pair at the northeast end of profile 3. The fold pair is not apparent on the aeromagnetic map, nor was it needed in the preferred model for profile 3. The absence of this fold pair in the magnetic data is consistent with McConnell's (1987) inference that the anticline could not have a basement core, based on a constant thickness of Cambrian and Ordovician rocks and the geometry of the Mountain View fault.

Detailed structures in the Blue Creek Canyon uplift crossed by profile 3 were not modeled because they contributed little to the overall magnetic signature of the basement uplift. This implies that there is only minor displacement across the BCC and Ketch Creek faults because of the small variation in the magnetic high of the uplifted block. Displacement on the BCC and the Ketch Creek faults could cause the southwest and northeast shoulders, respectively ("s," Fig. 11), of the high in the observed magnetic data between the Meers and Stony Point faults.

Correlation of Geology and Magnetics in the Western Slick Hills

The correlation of geology and magnetics in the western Slick Hills varies by geographic area. Correlation is generally good in the area northwest of the western Slick Hills. However, in the western Slick Hills there appears to be some decoupling between sedimentary rocks and the underlying basement. Geologic information is poor in the juncture zone between the Meers and BCC faults southeast of Blue Creek Canyon, so the magnetic data provide new insight into the relationship between these faults.

Northwest of the western Slick Hills, McConnell's subcrop map shows an anticline/syncline fold pair in the sedimentary rocks in the footwall of the BCC fault, north of the splays at the northwest end of the Quaternary scarp of the Meers fault. The location of the syncline roughly corresponds to the location of Havens' (1977) Rainy Mountain syncline. The pattern of magnetic contours over these folds is similar to the pattern of formational contacts on the subcrop map, although the magnetic data suggest doubly plunging fold axes rather than the singly plunging features shown on the subcrop map. The model of profile line 1 (Fig. 10) shows that the axes of the folds in the sedimentary rocks are close to the axes of similar, subdued structures in basement rock.

Profile 1 crosses three faults on McConnell's subcrop map—the Meers fault, a northeast fork of the Meers fault, and the BCC fault. All three faults are modeled in Figure 10, as well as the Mountain View fault, which is northeast of the profile. Using the inversion function in the SAKI modeling program, the best fit for the dip of the Meers fault was near vertical. Because the northeast fork and the BCC fault appear to be back-thrusts in proprietary seismic data, the magnetic model has incorporated NE dips for these faults. However, the magnetic data alone do not constrain the faults to be back thrusts. On McConnell's subcrop map (1987), and on maps of Ham and others (1964) and Havens (1977), the northeast fork of the Meers fault splits off of the main fault near the splays at the northwest end of the Quaternary fault scarp. North of the splays, the depth to magnetic basement increases abruptly (Figs. 3,8). The abrupt change in basement depth and the difference in dip direction of the Meers fault and the northeast fork challenge the interpretation of simple forking of the Meers fault/back thrust on the aforementioned maps.

In the western Slick Hills, folds and faults in the Cambrian and Ordovician sedimentary rocks can be mapped in detail because of excellent exposure. However, these Arbuckle Group rocks are covered by largely undeformed Permian rocks close to the Meers fault and the BCC fault, except in Blue Creek Canyon. Consequently, exposed Arbuckle Group rocks are limited to the southern flank of a moderate-wavelength apparent fold pair, similar in magnetic-contour pattern to the fold pair observed northwest of the western Slick Hills ("B" and "C," Fig. 8). These structures in the magnetic basement are termed "apparent" because we have not constructed a magnetic model across them—profile line 2 crosses only the edge of the apparent anticline. The Saddle Mountain syncline is west of the apparent anticline in the magnetic basement and has no obvious magnetic expression. However, the Saddle Mountain syncline is approximately in line with the Rainy Mountain syncline and its magnetic equivalent to the northwest. There is no magnetic expression of the Stumbling Bear thrust, which suggests that it soles in the sedimentary rocks. The aeromagnetic map shows what appear to be a short-wavelength fold pair or faults immediately west of and parallel to the BCC fault ("D," Fig. 8). This is an example of magnetic basement involvement in much shorter wavelength folding or faulting than is seen elsewhere below the sedimentary rocks. The apparent short-wavelength folds are northwest of the exposed Arbuckle Group rocks and are not aligned with any of the large folds shown in Figure 8. However, the apparent basement folds are aligned with smaller folds mapped immediately west of the BCC fault in Blue Creek Canyon (Fig. 6) and are parallel to the more southerly trend of the Stumbling Bear thrust as it approaches Blue Creek Canyon.

In the central part of the western Slick Hills, the general trend of the large mapped folds and the fault follows the trend of the magnetic contours (Fig. 8). However, closer to the Meers fault the trend of large folds approaches parallelism with the Meers fault trend and diverges from the trend of the magnetic contours. This divergence implies decoupling between the sedimentary rocks and the

underlying basement and possible rotation of sedimentary fold axes into subparallelism with the Meers fault.

The junction between the BCC and Meers faults is mostly covered by undeformed Permian sedimentary rocks, except for a small inlier of Carlton Rhyolite Group and rocks of the Timbered Hills and Arbuckle Groups. (Note that the preferred model for ground-magnetic profile F [Fig. 5] shows the edge of a faulted block of Carlton Rhyolite Group at the surface in this juncture zone.) The curved magnetic contours on the aeromagnetic map could be interpreted as elevated basement rocks that were caught and dragged between the two faults. The Upper Cambrian Reagan Sandstone is missing between the Carlton and Timbered Hills Groups, implying that this area was a topographic high during deposition of the Reagan Sandstone. This paleorelief could be responsible for the high magnetic intensity in the juncture zone. Nonetheless, the curvature of the juncture zone and its truncation by the BCC fault suggest dragging between two faults with strike-slip components of motion. The truncation of the dragged basement by the BCC fault implies that the last motion occurred on the BCC fault.

The change in trend of the large fold axes and faults relative to the orientation of the magnetic contours, and the absence of magnetic expression of the Stumbling Bear thrust, suggest that the large folds and faults did not always act in concert with the long-wavelength basement structures. The rotation of fold axes into near-parallelism with the Meers fault may be due to a component of left-lateral slip on the Meers fault under the 055° maximum compressive stress direction proposed by McCoss and Donovan (1986). Geologic mapping of overturned fold limbs and the truncation of folds at the BCC fault indicate that the folds formed before left-lateral slip occurred on the BCC fault (Donovan and others, 1989). McConnell's suggestion (1983) that the western Slick Hills were in a transpressive region bounded by the Meers and BCC faults could explain the rotation of the fold axes and faults relative to basement structures and the drag of basement rocks between the two faults. The rotation could be the response of the less competent sedimentary rocks to strike-slip motion on the bounding faults. The truncation of folds and of the basement drag feature are both consistent with late phase left-lateral motion on the BCC fault.

CONCLUSIONS

The aeromagnetic and ground-magnetic data provide a view of igneous basement structures within a part of the FW fault system that has been difficult to image seismically and is obscured by overlying sedimentary rocks. By limiting the assumptions in the modeling of ground-magnetic data, the dip of the Meers fault can be well constrained to near vertical within 0.5 km depth. Below this, the model is not well constrained, but the best fit to the data is a near-vertical dip to at least 2.5 km depth. A comparison of the magnetic and geologic data from mapping and drill holes shows a general agreement with many of the interpreted structures. In several cases, specific areas of disagreement provide information about the interaction of the sedimentary and basement rocks, and suggest some space and time relationships among the faulting and folding events in the study area.

In general, there is agreement between mapped and magnetically defined locations of the Meers fault. The magnetic data show apparent splaying and a left step of the Meers fault northwest of the Quaternary fault scarp that are only suggested by geologic data as a fork in the Meers fault. The splays and left step are near a back thrust, a large gravity high in the Wichita uplift, and a major structural boundary that is evident in both the magnetic basement and the surface geology. The genetic relationships among these features is uncertain, although their spatial association suggests that one or more of them may have influenced the location of the apparent splays and left step. A 12-km-long dikelike body in the subsurface along part of the Quaternary Meers fault scarp may be a Cambrian(?) intrusion along the fault or a horse block carried up into the fault zone during Pennsylvanian(?) faulting. Some of the fault splays mapped in the field or from low sun-angle photography correspond to basement faults in models of the ground-magnetic profiles. The models for profiles at the southeastern termination of the Quaternary fault scarp did not show basement faults that correspond to previously mapped splays. This suggests that the splays may be secondary features which do not extend below the sedimentary rocks.

The magnetic expression of the BCC fault agrees closely with the mapped trace of the fault in Blue Creek Canyon. To the northwest, between Blue Creek Canyon and Bally Mountain, the magnetic gradient associated with the BCC fault is northeast of the previously inferred fault location. This difference could be due to a bend in the fault, or the termination of BCC fault, and the presence of a subparallel fault west of Bally Mountain and connected to the BCC fault by a tear fault south of Bally Mountain. The lack of significant vertical displacement in the model of the magnetic profile across the BCC fault and drill holes that encountered unexpected rock units in the area between Blue Creek Canyon and Bally Mountain imply that the mapped extent and location of the fault should be reexamined. Northwest of Bally Mountain, the gradient related to the BCC fault is southwest of the fault's mapped location. This difference could be due to the presence of a series of closely spaced back-thrust faults. The magnetic gradient could reflect the southwest edge of the series, and the fault mapped could be a more northeastward fault in the series.

A comparison between the structures mapped in the sedimentary rocks and the magnetic basement shows that most large structures are present in both. However, a difference between the fold orientations in the western Slick Hills and the orientation of magnetic contours implies that the less competent sedimentary rocks are probably decoupled from the basement rocks. Because of the near parallelism of folds near the Meers and BCC faults to the fault trends, this decoupling likely occurred during transpression that caused left-lateral strike-slip movement on the Meers and BCC faults.

Finally, the crosscutting relationships based on geologic data and the interpretation of the magnetic data help define the temporal relationship between movement on the Meers fault and development of adjacent structures. Geologic relationships indicate that movement on the BCC fault postdated folding in the western Slick Hills. In the juncture zone between the BCC and the Meers faults, magnetic basement may be high due to paleorelief inherited from Cambrian time, but the apparent truncation of the high by the BCC fault suggests that movement on the BCC fault was the last movement to affect magnetic basement in this zone.

ACKNOWLEDGMENTS

We thank all of the many property owners who gave us access to their land and extended us hospitality. In particular, we thank the owners and proprietors of the Kimbell, Hillary, and Thomas Ranches. We are also grateful to Randall Hosey for assistance in drafting.

REFERENCES CITED

Bradley, Lee-Ann; and Jones-Cecil, Meridee, 1991, Density and magnetic susceptibility measurements of rocks in the Wichita uplift and Slick Hills, southwestern Oklahoma: U.S. Geological Survey Open-File Report 91-269, 31 p.

Brewer, J. A., 1982, Study of southern Oklahoma aulacogen, using COCORP deep seismic-reflection profiles, *in* Gilbert, M. C.; and Donovan, R. N. (eds.), Geology of the eastern Wichita Mountains, southwestern Oklahoma: Oklahoma Geological Survey Guidebook 21, p. 31–39.

Brewer, J. A.; Good, R.; Oliver, J. E.; Brown, L. D.; and Kaufman, S., 1983, COCORP profiling across the southern Oklahoma aulacogen—overthrusting of the Wichita Mountains and compression within the Anadarko basin: Geology, v. 11, p. 109–114.

Budnik, R. T., 1987, Late Miocene reactivation of Ancestral Rocky Mountain structures in the Texas Panhandle—a response to basin and range extension: Geology, v. 15, p. 163–166.

Chang, W.-F.; McMechan, G. A.; and Keller, G. R., 1989, Wave field processing of data from a large-aperture seismic experiment in southwestern Oklahoma: Journal of Geophysical Research, v. 94, no. B2, p. 1803–1816.

Chenoweth, P. A., 1983, Principal structural features of Oklahoma: Penn Well Publishing Co., Tulsa, Oklahoma, scale 1:506,880.

Coffman, J. D.; Gilbert, M. C.; and McConnell, D. A., 1986, An interpretation of the crustal structure of the southern Oklahoma aulacogen satisfying gravity data, *in* Gilbert, M. C. (ed.), Petrology of the Cambrian Wichita Mountains igneous suite: Oklahoma Geological Survey Guidebook 23, p. 1–10.

Collins, D. S., 1992, A petrographic study of igneous rock from three drill holes near the Meers fault, Oklahoma: U.S. Geological Survey Open-File Report 92-411, 25 p.

Crone, A. J.; and Luza, K. V., 1990, Style and timing of Holocene surface faulting on the Meers fault, southwestern Oklahoma: Geological Society of America Bulletin, v. 102, p. 1–17.

Denison, R. E., 1982, Geologic cross section from the Arbuckle Mountains to the Muenster arch, southern Oklahoma and Texas: Geological Society of America Map and Chart Series MC-28R, 8 p., scale 1:250,000.

Donovan, R. N., 1982, Geology of Blue Creek Canyon, Wichita Mountain area, *in* Gilbert, M. C.; and Donovan, R. N. (eds.), Geology of the eastern Wichita Mountains, southwestern Oklahoma: Oklahoma Geological Survey Guidebook 21, p. 65–77.

_____(ed.), 1986, The Slick Hills of southwestern Oklahoma—fragments of an aulacogen?: Oklahoma Geological Survey Guidebook 24, 112 p.

Donovan, R. N.; and Ragland, D. A., 1991, Turner Falls: tufa, travertine and bedding-parallel thrusts, *in* Johnson, K. S. (ed.), Arbuckle Group core workshop and field trip: Oklahoma Geological Survey Special Publication 91-3, p. 223–224.

Donovan, R. N.; Babaei, A.; and Sanderson, D. J., 1982, Stop 10—Blue Creek Canyon, *in* Gilbert, M. C.; and Donovan, R. N. (eds.), Geology of the eastern Wichita Mountains, southwestern Oklahoma: Oklahoma Geological Survey Guidebook 21, p. 148–153.

Donovan, R. N.; Marchini, W. R. D.; McConnell, D. A.; Beauchamp, W.; and Sanderson, D. J., 1989, Structural imprint on the Slick Hills, southern Oklahoma, *in* Johnson, K. S. (ed.), Anadarko basin symposium, 1988: Oklahoma Geological Survey Circular 90, p. 78–84.

Donovan, R. N.; White, S. W.; Morgan, K. M.; and Stephenson, M. D., 1993, Distribution and orientation of Arbuckle Group fracture patterns in the Slick Hills and Arbuckle Mountains, southern Oklahoma: an analogy for fractured Arbuckle reservoirs, *in* Johnson, K. S.; and Campbell, J. A. (eds.), Petroleum-reservoir geology in the southern Midcontinent, 1991 symposium: Oklahoma Geological Survey Circular 95, p. 206–207.

Feinstein, Shimon, 1981, Subsidence and thermal history of southern Oklahoma aulacogen—implications for petroleum exploration: American Association of Petroleum Geologists Bulletin, v. 65, p. 2521–2533.

Gilbert, M. C., 1982, Geologic setting of the eastern Wichita Mountains, with a brief discussion of unresolved problems, *in* Gilbert, M. C.; and Donovan, R. N. (eds.), Geology of the eastern Wichita Mountains, southwestern Oklahoma: Oklahoma Geologi-

cal Survey Guidebook 21, p. 1–30.

Ham, W. E.; Denison, R. E.; and Merritt, C. A., 1964, Basement rocks and structural evolution of southern Oklahoma: Oklahoma Geological Survey Bulletin 95, 302 p.

Harlton, B. H., 1951, Faults in the sedimentary part of the Wichita Mountains of Oklahoma: American Association of Petroleum Geologists Bulletin, v. 35, p. 988–999.

_____1963, Frontal Wichita fault system of southwestern Oklahoma: American Association of Petroleum Geologists Bulletin, v. 47, p. 1552–1580.

_____1972, Faulted fold belts of southern Anadarko basin adjacent to frontal Wichitas: American Association of Petroleum Geologists Bulletin, v. 56, p. 1544–1551.

Havens, J. S., 1977, Reconnaissance of the water resources of the Lawton Quadrangle, southwestern Oklahoma: Oklahoma Geological Survey Hydrologic Atlas 6, 4 sheets, scale 1:250,000.

Johnson, K. S., 1989, Geologic evolution of the Anadarko basin, *in* Johnson, K. S. (ed.), Anadarko basin symposium, 1988: Oklahoma Geological Survey Circular 90, p. 3–12.

Jones-Cecil, Meridee, 1990, Ground-magnetic profiles across the Meers fault, SW Oklahoma—Quaternary reactivation of a Late Paleozoic fault zone [abstract]: Geological Society of America Abstracts with Programs, v. 22, no. 7, p. A18.

_____1995a, Total-field aeromagnetic and derivative maps of the Lawton area, southwestern Oklahoma: U.S. Geological Survey GP-998-A, 2 sheets, scale 1:100,000.

_____1995b, Structural controls of Holocene reactivation of the Meers fault, southwestern Oklahoma, from magnetic studies: Geological Society of America Bulletin, v. 107, p. 98–112.

Jones-Cecil, Meridee; and Crone, A. J., 1989, Constraints on the Anadarko basin–Wichita uplift boundary interpreted from aeromagnetic data, *in* Johnson, K. S. (ed.), Anadarko basin symposium, 1988: Oklahoma Geological Survey Circular 90, p. 228–232.

Jones-Cecil, Meridee; and Robbins, S. L. [in press], Bouguer and isostatic residual gravity anomaly and derivative maps of the Lawton area, southwestern Oklahoma: U.S. Geological Survey GP-998-B, 3 sheets, scale 1:100,000.

Kelson, K. I.; and Swan, F. H., 1990, Paleoseismic history of the Meers fault, southwestern Oklahoma, and implications for evaluations of earthquake hazards in the central and eastern United States, *in* Weiss, A.W. (compiler), Proceedings of the seventeenth water reactor safety information meeting: U.S. Nuclear Regulatory Commission NUREG/CP–0105, v. 2, p. 341–365.

King, G. C. P.; and Nábělek, J., 1985, Role of fault bends in the initiation and termination of earthquake rupture: Science, v. 228, p. 984–987.

Lemiszki, P. J.; and Brown, L. D., 1988, Variable crustal structure of strike-slip fault zones as observed on deep seismic reflection profiles: Geological Society of America Bulletin, v. 100, p. 665–676.

McConnell, D. A., 1983, The mapping and interpretation of the structure of the northern Slick Hills, southwest Oklahoma: Oklahoma State University unpublished M.S. thesis, 131 p.

_____1987, Paleozoic structural evolution of the Wichita uplift, southwest Oklahoma: Texas A&M University unpublished Ph.D. dissertation, 219 p.

_____1989a, Constraints on magnitude and sense of slip across the northern margin of the Wichita uplift, southwest Oklahoma, *in* Johnson, K. S. (ed.), Anadarko basin symposium, 1988: Oklahoma Geological Survey Circular 90, p. 85–96.

_____1989b, Determination of offset across the northern margin of the Wichita uplift, southwest Oklahoma: Geological Society of America Bulletin, v. 101, p. 1317–1332.

McCoss, A. M.; and Donovan, R. N., 1986, Application of a construction for determining deformation in zones of transpression to the Slick Hills in southern Oklahoma, *in* Donovan, R. N. (ed.), The Slick Hills of southwestern Oklahoma—fragments of an aulacogen?: Oklahoma Geological Survey Guidebook 24, p. 40–44.

Perry, W. J., Jr., 1989, Tectonic evolution of the Anadarko basin region, Oklahoma: U.S. Geological Survey Bulletin 1866-A, 19 p.

Price, N. J.; and Cosgrove, J. W., 1990, Analysis of geologic structures: Cambridge University Press, Cambridge, England, 502 p.

Purucker, Michael, 1986, Interpretation of an aeromagnetic survey along the Wichita frontal fault zone, *in* Gilbert, M. C. (ed.), Petrology of the Cambrian Wichita Mountains igneous suite: Oklahoma Geological Survey Guidebook 23, p. 129–136.

Ramelli, A. R.; and Slemmons, D. B., 1986, Neotectonic activity of the Meers fault, *in* Donovan, R. N. (ed.), The Slick Hills of southwestern Oklahoma—fragments of an aulacogen?: Oklahoma Geological Survey Guidebook 24, p. 45–54.

Ramelli, A. R.; Slemmons, D. B.; and Brocoum, S. J., 1987, The Meers fault—tectonic activity in southwestern Oklahoma: U.S. Nuclear Regulatory Commission NUREG/CR-4852, 25 p.

Robbins, S. L.; and Keller, G. R., Jr., 1992, Complete Bouguer and isostatic residual gravity maps of the Anadarko basin, Wichita Mountains, and surrounding areas, Oklahoma, Kansas, Texas, and Colorado: U.S. Geological Survey Bulletin 1866-G, 11 p, 2 pl., scale 1:1,000,000.

Sibson, R. H., 1986, Earthquakes and lineament infrastructure: Philosophical Transactions of the Royal Society of London, v. A317, p. 63–79.

Stephenson, M. D.; and Donovan, R. N., 1991, Pennsylvanian deformation in the eastern Slick Hills, southwestern Oklahoma [abstract]: Geological Society of America Abstracts with Programs, v. 23, no. 4, p. 97–98.

U.S. Geological Survey, 1975, Aeromagnetic map of the Wichita Mountains area, southwestern Oklahoma: U.S. Geological Survey Open-File Report 75-16, 1 sheet, scale 1:62,500.

Webring, Michael, 1985, SAKI—a FORTRAN program for generalized linear inversion of gravity and magnetic profiles: U.S. Geological Survey Open-File Report 85-122, 108 p.

Oklahoma Geological Survey Circular 97, 1995

Structural Development of the Nemaha Tectonic Zone in Kansas

Pieter Berendsen and Kevin P. Blair
Kansas Geological Survey
Lawrence, Kansas

ABSTRACT.—The Nemaha tectonic zone, which includes the Nemaha uplift and the zone of complex faulting to the east and west, is considered to be an integral part of the Keweenawan-age Midcontinent rift system. The Nemaha tectonic zone was part of the rift-flanking basin filled with a considerable thickness of clastic sedimentary rocks on the east flank of the central rift valley. During late-stage compression of the rift, the Nemaha tectonic zone was uplifted and the clastic sedimentary rocks were eroded and redeposited in structurally controlled basins in eastern Kansas and western Missouri. NW-trending faults, some of which are of regional significance, intersect the Nemaha tectonic zone and may predate NE-trending structures. The NW-trending faults probably acted as accommodation zones during the development of the rift, and gave rise to the orthogonal block pattern that is characteristic of pre-Pennsylvanian rocks in this region.

Structural and stratigraphic studies have shown that the Nemaha tectonic zone remained a positive feature throughout much of the Paleozoic. Many of the structures in the Nemaha tectonic zone, such as en echelon faults, rhombic grabens and horsts, antithetic fault systems, propeller and scissor faults, are characteristic of wrench environments. The geometry and orientations of the observed structures imply left-lateral deformation of the Nemaha tectonic zone.

INTRODUCTION

The NE-trending Nemaha tectonic zone is 400 mi long and extends from near Omaha, Nebraska, through eastern Kansas, to Oklahoma City, Oklahoma (Fig. 1). In Kansas, we define the Nemaha tectonic zone to include the Nemaha uplift and the zones of complex faulting on the east and west sides of the uplift.

Before 1917, the Nemaha anticline was recognized as a post-Mississippian anticlinal feature of great length, occupying the position of what we now refer to as the Humboldt fault zone. As a result of drilling activity, it was recognized that granite occurred at relatively shallow depths along the trace of the anticline. In areas farther to the west the granite was directly overlain by rocks of Pennsylvanian age. Moore and Haynes (1917) proposed to name this uplifted ridge the "Nemaha Granite Mountains." Other terms, such as the Nemaha anticline, Nemaha granite ridge, or simply granite ridge, have also been applied to the uplift in older literature. Faults along the steep eastern flank of the uplift were described by a number of authors (Moore, 1936; Jewett and Abernathy, 1945; Jewett, 1949). The fault bounding the uplift on the east side in northern Kansas and southern Nebraska was called the Humboldt fault by Condra (1927), but the name has since been applied to the fault throughout Kansas. More recent studies (Berendsen and others, 1989) show that the Humboldt fault may be best described as a complex zone of anastomosing faults separating a series of blocks generally stepped down to the east, and should therefore be referred to as the Humboldt fault zone. Compound vertical offset of basement rocks across the Humboldt fault zone is as much as 2,000 ft. Faults on the west side of the uplift are less well defined, and vertical offset is generally up to a few hundred feet.

The Nemaha tectonic zone is broken up into orthogonal blocks by a series of regularly spaced NW-trending faults. Some of these are regional structures that can be traced for hundreds of miles. Examples are the Fall River, Chesapeake, and the Bolivar–Mansfield tectonic zones. In central Kansas, the individual NW-trending faults are ~10 mi in length. Vertical displacement on these faults is generally less than a few hundred feet (Berendsen and Blair, 1986).

In this paper we will discuss the Nemaha tectonic zone in some detail and attempt to convince the reader that the zone is not only a complex struc-

Berendsen, Pieter; and Blair, K. P., 1995, Structural development of the Nemaha tectonic zone in Kansas, *in* Johnson, K. S. (ed.), Structural styles in the southern Midcontinent, 1992 symposium: Oklahoma Geological Survey Circular 97, p. 208–214.

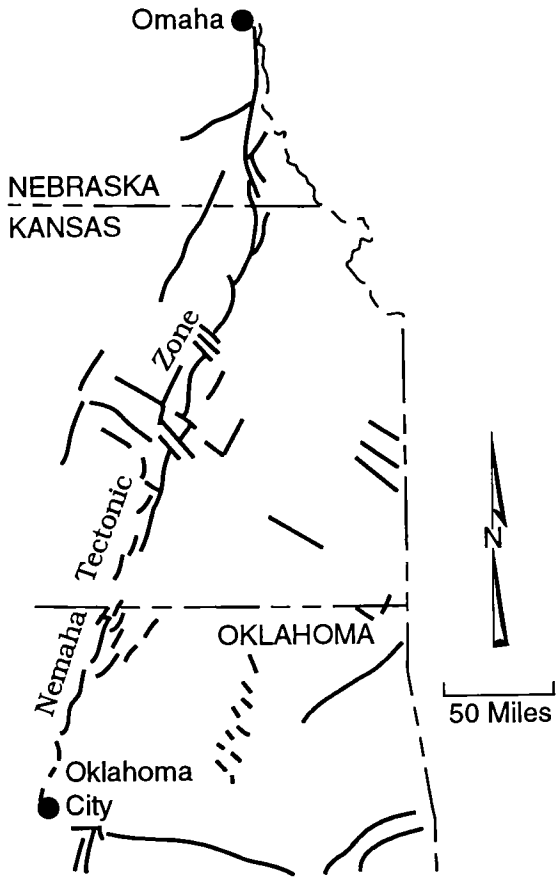


Figure 1. General trend of the Nemaha tectonic zone in Nebraska, Kansas, and Oklahoma.

ture, but that it also has a complex tectonic history that can be traced at least as far back as early Paleozoic time. We believe that the structure is even older and is an integral part of the Midcontinent rift system, which was active at 1,100 Ma (million annum).

DEFINITION OF THE NEMAHA TECTONIC ZONE

The Nemaha tectonic zone is ~50 miles wide in northern Kansas and narrows considerably to the south (Fig. 2). The eastern boundary, or Humboldt fault zone, follows a more or less straight NNE-trending path from eastern Nemaha County in the north to eastern Sumner County in the south (Fig. 2). The western boundary trends in a southwesterly direction from Washington County into Riley County, and then gradually changes to a direction parallel to the Humboldt fault zone (Fig. 2). Consequently, the zone narrows to around 10 mi in central Kansas, where it consists basically of only the Humboldt fault zone. The zone is less clearly defined at its southern end near the Oklahoma border.

The Abilene anticline (Fig. 3), extending southward from Marshall into Riley County (Barwick, 1928), and its northern extension into Nebraska (the Barneston anticline of Condra and Upp [1931]), is part of the Nemaha uplift. The Abilene anticline appears to be a narrow horst in Marshall County near the Nebraska state line. The regional Bolivar–Mansfield fault system in Missouri (McCracken, 1971) can be traced in a northwesterly direction into Kansas (Fig. 3), and is believed to extend into Riley and Washington Counties, where it coincides with the SW-trending margin of the Nemaha uplift. Notwithstanding the fact that early-exploration drill holes all encountered granite upon reaching the basement, the uplift is underlain by a variety of Proterozoic rocks: 1,630–1,800 Ma granitic rocks, 1,100 Ma mafic rocks, and slightly younger clastic sedimentary rocks.

Farther to the south, the Nemaha tectonic zone is characterized by a series of prominent highs that were recognized long ago, and resulted in the naming of the Nemaha anticline as a geologic structure. They include the Burns and Elmdale domes, and the Boyer, Chelsea, Chesney, Oil Hill, Robinson, Shumway, and Wilson domes, which are part of the well-known El Dorado anticline or dome (Fig. 3). Additional unnamed highs are present along the trend of the Nemaha tectonic zone.

Besides the Bolivar–Mansfield tectonic zone, two other regional NW-trending tectonic zones are important. They are the Chesapeake and the Fall River tectonic zones (Fig. 3). The former is mapped in western Missouri (McCracken, 1987) and can be traced into eastern Kansas. The latter is more pronounced and crosses the Nemaha tectonic zone in central Kansas (Fig. 3) and continues north of the Central Kansas uplift (Berendsen and Blair, 1986).

The depth to the Precambrian basement along the trend increases to the south. In Marshall and Nemaha Counties (northern Kansas), depth to the basement is as little as 600 ft. Depth to the basement on top of the El Dorado dome (southern Kansas) is ~2,800 ft.

Major deformation of the Nemaha tectonic zone was coeval with the Ouachita orogeny. During this time, considerable thicknesses of Paleozoic and older sedimentary rocks, and possibly igneous rocks, were removed from the uplift. Along the higher parts of the uplift, Pennsylvanian rocks as young as the Lansing–Kansas City Group directly overlie the Precambrian basement.

STRUCTURAL STYLES ALONG THE TREND

The Humboldt fault zone trends in a north–northeasterly direction and parallels other rift-related structures farther to the west. Structurally, the Humboldt fault zone occupies a similar position as major rift-related faults along the Midcontinent rift in Nebraska, Iowa, Minnesota, Michigan, and Wisconsin. Therefore, we believe that the Humboldt fault zone, and other structures that delineate

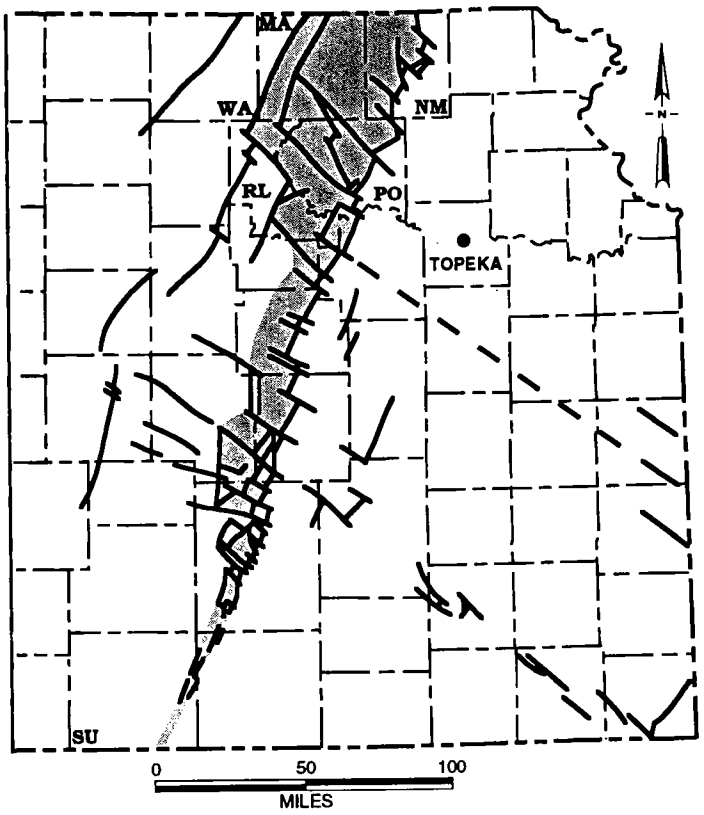


Figure 2. The Nemaha tectonic zone (shaded) in Kansas. NM = Nemaha County, MA = Marshall County, WA = Washington County, RL = Riley County, PO = Pottawatomie County, SU = Sumner County.

the Nemaha tectonic zone, are at least 1,100 Ma old. During the last few years, deep seismic reflection surveys in the Lake Superior region have shown that the rift system extends to great depths, estimated by Behrendt and others (1988) to be in excess of 30 km.

It is useful to review the structure of the rift in the Lake Superior area, because of the similarity of the rocks and structures in Kansas. Woelk and Hinze (1991) used reprocessed COCORP (Consortium for Continental Reflection Profiling) data from northeastern Kansas to suggest homogeneity for structural style and tectonic evolution along the length of the rift.

Interpretation of GLIMPCE (Great Lakes International Multidisciplinary Program on Crustal Evolution) seismic data by Cannon and others (1989) shows that normal faulting played a major role in the subsidence of a deep, asymmetrical, central graben. In addition, it is interesting that the asymmetry of the central graben changes along the trend of the rift. Differences in the rate of extension along the rift may have created accommodation zones and given rise to the segmented nature of the structure (Cannon and others, 1989). Eventually, tectonic inversion resulted in uplift and reactivation of the original normal faults as high-angle reverse faults with throws of 5 km or more in places (Cannon and others, 1989). A considerable amount of rock was thus removed in the later stages of rifting.

Normal and high-angle reverse faults are also common along the trend of the Nemaha tectonic zone. As the name implies, the Humboldt fault zone in most places consists of a number of down-to-the-east faults separating individual fault blocks. Cumulative vertical movement across the Humboldt fault zone is as much as 2,600 ft in places. Interpretation of a seismic-reflection profile over the trace of the Humboldt fault zone in Nemaha County by Steeples (1989) indicates a high-angle reverse fault with a throw exceeding 1,500 ft. Several reverse faults were interpreted by Woelk and Hinze (1991) in an east–west reprocessed COCORP seismic-reflection profile across the central rift basin in the northern tier of counties in Kansas. Reverse displacements on nearby minor faults, such as those associated with the en echelon anticlines of the Alma trend in the Forest City basin east of the Humboldt fault zone (Fig. 3), are known directly from drilling.

As is the case in the Lake Superior region, the Nemaha tectonic zone is broken up into a number of segments by NW-trending faults that probably acted as accommodation zones. The NW-trending faults are quite regularly spaced on the order of 10 mi. They are most pronounced where they cross the Humboldt fault zone, and are generally difficult to trace into the basins on either side. Where they cross the Humboldt fault zone, the faults show apparent translational movement up to ~8 mi, and vertical displacement up to ~1,500 ft (Berendsen and Blair, 1986). Some of the faults are parts of the regional NW-trending structures, such as the Bolivar–Mansfield and the Fall River tectonic zones. Both the NNE- and NW-trending faults along the Nemaha tectonic zone bound uplifts from which Paleozoic sedimentary rocks were removed by erosion (Berendsen and Blair, 1986).

TIMING OF DEFORMATIONAL PROCESSES

Positive aeromagnetic (Yarger and others, 1981) and gravity (Kansas Geological Survey, 1982) anomalies, as well as the presence of mafic rift-related igneous rocks at the Precambrian-basement surface (Bickford and others, 1979), reveal the position of the central rift valley in Kansas. Inasmuch

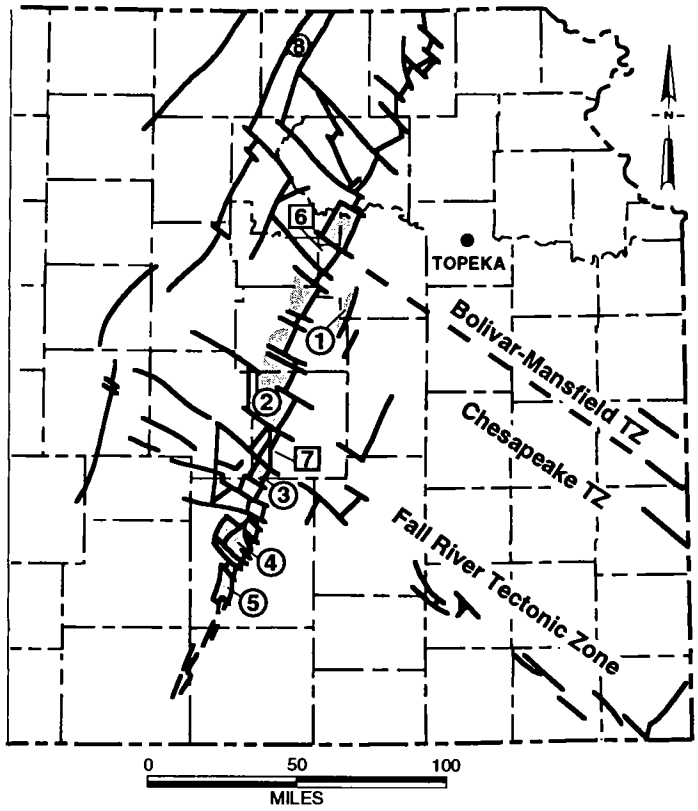


Figure 3. Nemaha tectonic zone in Kansas. Circled numbers denote domes or uplifts, squares denote downdropped blocks. (1) Alma trend. (2) Elmdale dome. (3) Burns dome. (4) El Dorado anticline. (5) Augusta anticline. (6) Wabaunsee County low. (7) Cedar Creek syncline. (8) Abilene anticline. Shaded areas denote general outlines of domes.

as Woelk and Hinze (1991) argued for homogeneity in structural style and evolution along the length of the rift, one might expect clastic-filled flanking basins to have developed on either side of the central graben when extensional processes waned and thermal collapse took place (Cannon and others, 1989). Clastic sedimentary rocks are present in the Salina basin to the west of the central rift valley, and are also preserved in down-dropped blocks along the trace of the central rift valley in Marshall, northern Pottawatomie, and northern Riley Counties (Fig. 2). However, east of the central rift valley, clastic sedimentary rocks occur in only a few places. Instead, basement rocks of the Nemaha tectonic zone are, for the most part, granitic. If rift development in Kansas took a similar course as farther north, one might expect clastic sedimentary rocks to have been deposited over the Nemaha tectonic zone.

We hypothesize that Precambrian clastic sedimentary rocks were indeed deposited over the Nemaha tectonic zone, but that the zone has been a positive feature throughout most of its geologic history. It has always been assumed that lower Paleozoic rocks were also deposited over the Nemaha tectonic zone. It was shown by Berendsen and others (1992) that the Nemaha tectonic zone, as far south as the central part of the state, is underlain by granitic basement rocks and was a positive element in Middle Ordovician time. If, during Late Cambrian–Early Ordovician time, several miles of combined Arbuckle carbonate and Precambrian clastic sedimentary rocks were eroded from the uplift, we might expect to see evidence in the form of conglomerates, clastic wedges, or some other indication of large-scale, extensive erosion in the Forest City basin east of the uplift.

East of the Humboldt fault zone, in eastern Kansas and western Missouri, several dozen drill holes (Fig. 4) record penetrations of up to 1,000 ft of pre-Paleozoic clastic sedimentary rocks. None of these holes penetrated the entire clastic section. Interpretation of potential-field geophysical data indicate that large amounts of pre-Paleozoic clastic sedimentary rocks are preserved in what appear to be, and in places can be shown to be, fault-bounded sedimentary basins within a largely granitic terrane (Berendsen and Blair, 1991). The rocks in these basins are described as being conglomerate, sandstone, shale, arkose, schist, slate, and phyllite. Well cuttings from two drill holes in Vernon County, Missouri, each of which penetrated >1,000 ft of clastic sedimentary rocks, were described by Skillman (1948). Our interpretation of Skillman's (1948) descriptions indicate that some of the clastics may have been derived from mafic igneous rocks. In Allen County, Kansas, close to 1,500 ft of "sandstone conglomerate varying slightly in color and carbonate content, and in size of grains up to ¾ inch in diameter" was reported by Haworth and Bennett (1908). The cuttings that we have examined over the years show that most of the pre-Paleozoic clastic rocks are unmetamorphosed to slightly metamorphosed. We think that it is likely that Keweenawan clastic sedimentary rocks were deposited in the rift-flanking basins east of the central rift valley. They were subsequently eroded from the Nemaha tectonic zone area in pre-Paleozoic time and deposited in eastern Kansas and western Missouri. The Nemaha tectonic zone must have been a positive element in Precambrian time, prior to deposition of the Reagan Sandstone and the Arbuckle carbonate rocks.

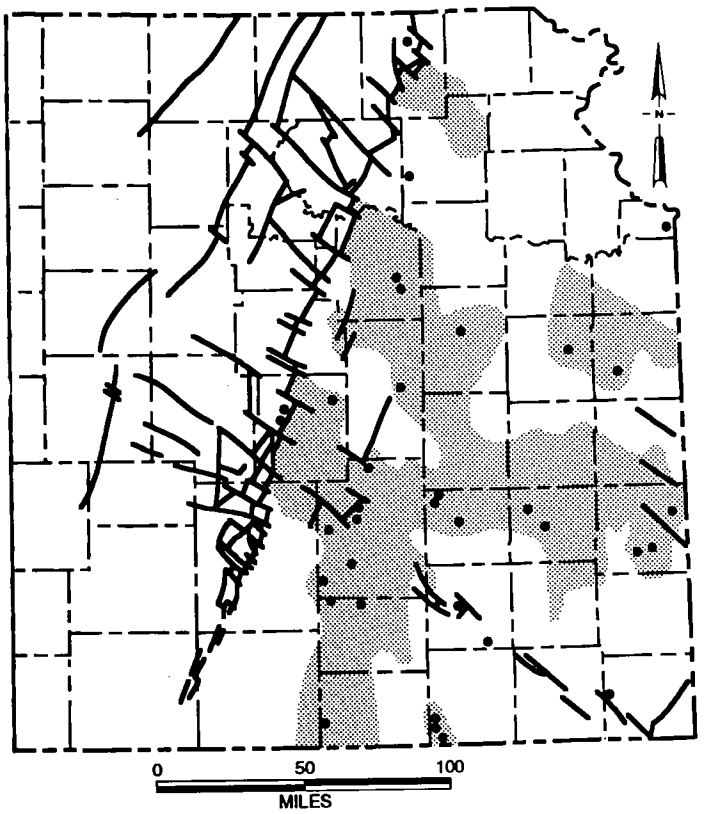


Figure 4. Location of drill holes (solid dots) and interpreted areas (stippled pattern) of pre-Paleozoic clastic rocks in Kansas.

Most of the Nemaha tectonic zone remained a positive element during Cambrian time, but may have been inundated during the Early Ordovician (Chenoweth, 1968). During deposition of the Chattanooga Shale (Late Devonian–Earliest Mississippian time), parts of the Nemaha tectonic zone were again exposed at the surface, as evidenced by the presence of oolites and oxidized shale in the section (M. W. Lambert and J. H. Doveton, personal communication). Little is presently known about the history of the Nemaha tectonic zone during Mississippian time.

To summarize, we believe that large parts of the Nemaha tectonic zone were above sea level during much of pre-Mississippian time. This leads us to question the existence of the North Kansas basin, which was named by Rich (1933) and reportedly encompassed all of northeastern Kansas and adjacent parts of Nebraska.

The major period of Paleozoic folding and faulting that can be documented was coeval with the Ouachita orogeny, starting in latest Mississippian time and extending into the Pennsylvanian (Merriam, 1963). Wrenching was imposed on older established structures, and is most apparent along the Nemaha tectonic zone. According to Wilcox and others (1973), the basement is invariably involved in the deformation. En echelon structures, such as the Alma anticline (Fig. 3), pull-apart basins, or rhomb-shaped grabens and horsts, present in this area are commonly associated with horizontal slip along faults (Aydin and Nur, 1982). Antithetic-fault systems, and propeller and scissor faults (faults along which the throw is reversed), are other observed structures that are common in wrench environments. The geometry and orientation of the structures observed imply left-lateral motion on faults associated with the Nemaha tectonic zone (Berendsen and Blair, 1986).

A number of domes and anticlines are recognized along the trend of the Nemaha tectonic zone. They include, from north to south, the Elmdale, Burns, El Dorado, Augusta, and several unnamed domal structures (Fig. 3). Adjacent to the domes are downdropped blocks, of which the Cedar creek syncline (Fig. 3) is the most pronounced. The Cedar Creek syncline is at the intersection of the NW-trending Fall River tectonic zone and the Nemaha tectonic zone. A structural-contour map on top of the Arbuckle Group (Berendsen and Blair, 1986) shows that the elevation difference between the Cedar Creek syncline and the top of the Elmdale dome to the north is on the order of 2,000 ft. Arbuckle Group rocks are absent from the very top of the dome, and progressively younger rocks are absent from progressively larger areas on the flanks of the dome. No Mississippian rocks are present on the dome, implying post-Mississippian erosion. In the Cedar Creek syncline to the south, the full section of Mississippian rocks is present. In the basins to the east and west, Mississippian rocks are unconformably overlain by ~350 ft of Pennsylvanian Cherokee Group rocks. In the Cedar Creek syncline, Cherokee Group rocks are recognized based on electric-log expression similar to that of the Cherokee Group farther to the east. But here, an additional 250 ft of sandstone, siltstone, shale, and possibly coal is present below the Cherokee Group. These rocks are not recognized anywhere else in Kansas. Their lithology and stratigraphic position suggest that they may be Desmoinesian or possibly Atokan in age and that the Cedar Creek syncline moved downward in post-Mississippian time.

Down-dropped blocks also occur at the intersection of the NW-trending Bolivar–Mansfield tectonic zone and the Nemaha tectonic zone (Fig. 3), as well as in other locations. Adjustments on structures resulting from stresses generated by the Late Missis-

sippian to Early Pennsylvanian Ouachita orogeny occurred throughout the region, but the exact timing of movement on individual structures is difficult to reconstruct. Where data are available, similar analysis may give clues about the timing of deformation along the trend.

A NW-trending zone of NW-trending en echelon faults affect rocks of Permian age (Council Grove and Chase Groups) on top of the Elmdale dome. Their geometry indicates right-lateral movement in a wrenching environment, possibly in response to northeast-directed stresses from the uplift of the Marathon Mountains (W. F. Wilson, personal communication) or the result of stresses generated by the Laramide orogeny in Late Cretaceous time.

CONCLUSION

The 400-mi-long, NNE-trending Nemaha tectonic zone is an integral part of the Midcontinent rift system. The complex history of folding and faulting of the Nemaha tectonic zone started with the opening of the 1,100 Ma old Midcontinent rift system. The zone was a positive feature throughout much of the Proterozoic and Paleozoic. The Humboldt fault zone, bounding the Nemaha tectonic zone on the east, may be compared to the Keweenaw fault which bounds the Midcontinent rift on the east on the Keweenaw Peninsula in Michigan, where Proterozoic rift-related rocks are exposed. In Kansas, Proterozoic rift-related, mostly clastic sedimentary rocks were removed from the Nemaha tectonic zone by erosion prior to the onset of Paleozoic time. We believe that they were transported to the south and east and are preserved in structurally controlled basins in eastern Kansas and western Missouri. NW-trending faults, some of which may predate the NNE-trending faults, cut the rift, and acted as accommodation zones. Stresses associated with orogenic activity were mostly transmitted through the basement, and resulted in differential movement on these two sets of faults. Extension, followed by compression, characterized the stress regime during the Keweenawan. Wrench movements, in response to oblique stress, characterized the tectonic regime during much of the Paleozoic.

We believe that the Nemaha tectonic zone was a positive feature during much of the Paleozoic up to Mississippian time. Good evidence indicates that large portions of the Nemaha tectonic zone, especially in central and northern Kansas, were also exposed during Middle Ordovician and Late Devonian time. At other times, the zone may have been a swell on the sea floor.

Many major sequences of rock may not have been deposited to the full thickness seen in adjacent basins; hence, post-Mississippian movement on the Humboldt fault zone may be considerably less than the several thousand feet that has been previously assumed.

REFERENCES CITED

Aydin, A.; and Nur, A., 1982, Evolution of pull-apart basins and their scale independence: Tectonics, v. 1, no. 1, p. 91–105.

Barwick, J. S., 1928, Salina basin of north-central Kansas: American Association of Petroleum Geologists Bulletin, v. 12, p. 77–199.

Behrendt, J. C.; Green, A. G.; Cannon, W. F.; Hutchinson, D. R.; Lee, M.; Milkereit, B.; Agena, W. F.; and Spencer, C., 1988, Crustal structure of the Midcontinent rift system—results from GLIMPCE deep seismic reflection profiles: Geology, v. 16, p. 81–85.

Berendsen, P.; and Blair, K. P., 1986, Subsurface structural maps over the Central North American rift system (CNARS), central Kansas, with discussion: Kansas Geological Survey, Subsurface Geology Series 8.

_____1991, Interpretive subcrop map of the Precambrian basement in the Joplin 1° × 2° quadrangle: Kansas Geological Survey, Subsurface Geology Series 14, 10 p.

Berendsen, P.; Blair, K. P.; and Newell, K. D., 1989, Structural aspects of the Midcontinent rift system in Kansas: Transaction volume of the 1989 AAPG Midcontinent section meeting, Oklahoma City: Oklahoma City Geological Society, 26 p.

Berendsen, P.; Doveton, J. H.; and Speczik, S., 1992, Distribution and characteristics of a Middle Ordovician oolitic ironstone in northeastern Kansas based on petrographic and petrophysical properties: a Laurasian ironstone case study: Sedimentary Geology, v. 76, p. 207–219.

Bickford, M. E.; Harrower, K. L.; Nusbaum, R. L.; Thomas, J. J.; and Nelson, G. E., 1979, Preliminary geologic map of the Precambrian basement rocks of Kansas: Kansas Geological Survey Map M-9, scale 1:500,000.

Cannon, W. F.; Green, A. G.; Hutchinson, D. R.; Lee, M.; Milkereit, B.; Behrendt, J. C.; Halls, H. C.; Green, J. C.; Dickas, A. B.; Morey, G. B.; Sutcliffe, R.; and Spencer, C., 1989, The North American Midcontinent rift beneath Lake Superior from GLIMPCE seismic reflection profiling: Tectonics, v. 8, p. 305–332.

Chenoweth, P. A., 1968, Early Paleozoic (Arbuckle) overlap, southern Mid-Continent, United States: American Association Petroleum Geologists Bulletin, v. 52, p. 1670–1688.

Condra, G. E., 1927, The stratigraphy of the Pennsylvanian System in Nebraska: Nebraska Geological Survey Bulletin 1, 2nd series, 291 p.

Condra, G. E.; and Upp, J. E., 1931, Correlation of the Big Blue Series in Nebraska: Nebraska Geological Survey Bulletin 6, 2nd series, 76 p.

Haworth, E.; and Bennett, J., 1908, General stratigraphy, *in* Haworth, E., Special report on oil and gas: Kansas Geological Survey, Lawrence, p. 57–160.

Jewett, J. M., 1949, Oil and gas in eastern Kansas with special reference to developments from 1944 to 1948: Kansas Geological Survey Bulletin 77, 308 p.

Jewett, J. M.; and Abernathy, G. E., 1945, Oil and gas in

eastern Kansas: Kansas Geological Survey Bulletin 57, 244 p.

Kansas Geological Survey, 1982, Bouguer gravity-anomaly map of the Nemaha uplift region: Map NU-7, scale 1:1,000,000.

McCracken, M. H., 1971, Structural features of Missouri: Missouri Geological Survey and Water Resources, Report of Investigations 49, 99 p.

_____1987, Pre-Pennsylvanian paleogeologic map of Missouri: Missouri Department of Natural Resources, Division of Geology and Land Survey, OFM-87-237-GI, Contribution to the Tectonic Atlas No. 1.

Merriam, D. F., 1963, The geologic history of Kansas: Kansas Geological Survey Bulletin 162, 317 p.

Moore, R. C., 1936, Carboniferous rocks of North America: Report of the XVI International Geologic Congress, 1933, p. 593–617.

Moore, R. C.; and Haynes, W. P., 1917, Oil and gas resources of Kansas: Kansas Geological Survey Bulletin 3, 391 p.

Rich, J. L., 1933, Distribution of oil pools in Kansas in relation to pre-Mississippian structure and areal geology: American Association Petroleum Geologists Bulletin, v. 17, p. 793–815.

Skillman, M. W., 1948, Pre-Upper Cambrian sediments of Vernon County, Missouri: Missouri Department of Business and Administration, Division of Geological Survey and Water Resources, Report of Investigations 7, 17 p.

Steeples, D. W., 1989, Structure of the Salina–Forest City interbasin boundary from seismic studies, *in* Steeples, D. W. (ed.), Geophysics in Kansas: Kansas Geological Survey Bulletin 226, p. 31–52.

Wilcox, R. E.; Harding, T. P.; and Seely, D. R., 1973, Basic wrench tectonics: American Association of Petroleum Geologists Bulletin, v. 57, p. 74–96.

Woelk, T. S.; and Hinze, W. J., 1991, Model of the Midcontinent rift system in northeastern Kansas: Geology, v. 19, p. 277–280.

Yarger, H.; Robertson, R.; Martin, J.; Ng, K.; Sooby, R.; and Wentland, R., 1981, Aeromagnetic map of Kansas: Kansas Geological Survey Map M-16, scale 1:500,000.

Neotectonic Relations of the Nemaha Uplift in Oklahoma

Kenneth V. Luza
Oklahoma Geological Survey
Norman, Oklahoma

ABSTRACT.—The Nemaha uplift, which is common to the states of Oklahoma, Kansas, and Nebraska, is ~670 km long and 20–40 km wide. In Oklahoma, the uplift developed mainly during the Pennsylvanian Period as a number of small crustal blocks that were raised sharply along a generally north-trending axis. The uplifted crustal blocks typically are 5–8 km wide and 8–32 km long and are bounded by faults on the east and/or west side.

The Oklahoma City, Lovell, Garber, and Crescent uplifts are several discontinuous blocks elevated along a fault zone that extends in a northwesterly direction from Oklahoma City. Another fault zone, the McClain County fault zone, intersects the Oklahoma City uplift in southern Oklahoma County. This fault zone trends south-southwest and terminates against the Pauls Valley uplift in Garvin and southern McClain Counties.

Fine- to medium-grained clastic rocks of Permian age overlie the Nemaha uplift structures in central Oklahoma. Except for a few localities, surface geologic relations offer very little insight into understanding the structural relations associated with the Nemaha uplift. Only in northern Kansas and southeastern Nebraska is a fault exposed at the surface; this is locally referred to as the Humboldt fault.

Oklahoma is one of the most active seismic areas in the southern Midcontinent. From 1897 to 1992, more than 940 earthquakes are known to have occurred in Oklahoma. Of the ~50 earthquakes that are located in Oklahoma each year, only one or two, on the average, are reported as felt. Prior to 1962, all earthquakes in Oklahoma, 59, were either known from historical accounts or from seismograph stations outside the State. From 1962 through 1976, after the first seismographs were installed in late 1961, 70 additional earthquakes were added to the earthquake data base. In 1977, the statewide network of seismograph stations greatly improved earthquake detection and location. From 1977 through 1992, more than 810 additional earthquakes were located in Oklahoma, mostly of magnitudes <2.5.

The pre-1977 earthquake data, when combined with the 1977–92 data, define a 40-km-wide by 145-km-long earthquake zone that extends northeastward from near El Reno toward Perry (Noble County). Correlation of historical and recent earthquake activity with known structural features remains unclear. The El Reno–Perry trend appears to cut diagonally across the Nemaha uplift structures at about a 30° angle. The southern end of this trend appears to be more active than the middle and northern parts. The recent and historic earthquake data seem to support this observation.

A majority of Oklahoma's earthquakes have occurred within a 135-km-long by 40-km-wide zone situated between Canadian County and the south edge of Garvin County. The southern end of this trend closely parallels the McClain County fault zone, which is about 40 km wide and 60 km long.

INTRODUCTION

King (1951), Hadley and Devine (1974), and others have categorized the geologic regions of the United States into tectonic provinces. The largest of these tectonic provinces is the central stable province, which extends from the western margin of the Appalachian Plateau to the eastern edge of the Rocky Mountain uplift, and from the Gulf Coastal Plain to northern Canada. Compared to the Appalachian tectonic province, the central stable region has had little tectonic activity since Late Pennsylvanian time. The historical record of faulting and seismicity has been limited, with a notable exception being the area of New Madrid, Missouri, including adjacent areas in Kentucky, Tennessee, and Illinois.

Luza, K. V., 1995, Neotectonic relations of the Nemaha uplift in Oklahoma, *in* Johnson, K. S. (ed.), Structural styles in the southern Midcontinent, 1992 symposium: Oklahoma Geological Survey Circular 97, p. 215–230.

Nevertheless, the entire region is so large that despite the broad-scale picture of relative historical stability, there is, within it, considerable geologic diversity and sufficient seismic history to require a moderate seismic classification for the Nemaha uplift region.

The Nemaha uplift, which is common to the states of Oklahoma, Kansas, and Nebraska, is ~670 km long and 20–40 km wide. The Midcontinent geophysical anomaly extends southward from Minnesota across Iowa and the southeastern corner of Nebraska and probably terminates in central Kansas. A number of moderate-sized earthquakes—magnitude ≥5—have occurred along or west of the Nemaha uplift.

The Oklahoma Geological Survey, in cooperation with the geological surveys of Kansas, Nebraska, and Iowa, conducted a five-year investigation of the seismicity and tectonic relations of the Nemaha uplift and associated geologic features in the Midcontinent (Fig. 1). This investigation, which began in October 1976, was intended to provide data to be used to design nuclear-power plants. However, the information is also being used to design better large-scale structures, such as dams and high-use buildings, and to provide the necessary data to evaluate earthquake-insurance rates in the Midcontinent.

Oklahoma progress summaries for fiscal years 1977, 1978, 1979, 1980, and 1981 were published as NUREG/CR-0050 (Luza and others, 1978), NUREG/CR-0875 (Luza and Lawson, 1979), NUREG/CR-1500 (Luza and Lawson, 1980), NUREG/CR-2439 (Luza and Lawson, 1981), and NUREG/CR-3109 (Luza and Lawson, 1983), respectively. A final project report was prepared by the state geological surveys of Iowa, Nebraska, Kansas, and Oklahoma (Burchett and others, 1983) and published as NUREG/CR-3117.

GEOLOGY

Regional Geology

The Midcontinent region contains a number of structural features (Fig. 1). The tectonic events vary in age from formation of the oldest basement rock at 1.3 Ga (billion years ago), through the Paleozoic and ending with the close of the Permian, at ~225 Ma (million years ago). Included are at least 30 separate tectonic events in the Paleozoic, of which 14 are regionally significant (Ham and Wilson, 1967). The regional Paleozoic disturbances are chiefly of Ordovician, Silurian, Devonian, Mississippian, and Pennsylvanian age. All these disturbances are epeirogenic except those of the Pennsylvanian and Early Permian, which are orogenic in southern Oklahoma and in the craton-bordering Ouachita system.

Over most of the central craton, the Paleozoic tectonic record is characterized generally by episodes of marine sedimentation—which were terminated by episodes of uplift, gentle folding, and erosion—and partly by the overlap of younger strata upon unconformable surfaces. The Salina and Forest City basins, which contain 1,200–3,000 m of strata, are examples of relatively shallow intracratonic basins.

Along the southern border of the craton, north of the Ouachita system, is the Arkoma basin, which contains as much as 7,500 m of strata. A transverse belt, locally called the Wichita-Amarillo trend, as well as the Arbuckle Mountains, developed in middle Paleozoic time. This area is one of intense folding and uplift associated with longitudinal faults at least 640 km long with vertical displacements of at least 4,500 m. North of the Wichita Mountains is the Anadarko basin, which was the site of almost continuous deposition from Late Cambrian through Permian time. The thickest sedimentary sections are estimated to be >13,700 m.

Another structural feature, the Nemaha uplift, developed mainly during the Pennsylvanian Period as a number of small crustal blocks were raised sharply along its axis. The crustal blocks making up the Nemaha uplift typically are 5–8 km wide and 8–32 km long and are bounded by faults on the east and/or west side (Huffman, 1959). Only in northern Kansas and southeastern Nebraska is a fault exposed at the surface; this is locally referred to as the Humboldt fault.

Middle Pennsylvanian (Desmoinesian) strata overlie Devonian or older units on many of the raised blocks that make up the Nemaha uplift in Oklahoma. The missing rock record over these blocks has contributed to a more generalized structural-history interpretation than, perhaps, is desired. A generalized map of pre-Pennsylvanian rocks in Oklahoma is shown in Figure 2. The greatest thickness of Mississippian strata, 6,000 m, is in the Ouachita province. The strata are characterized by alternating beds of sandstone and shale of Meramecian age. In western Oklahoma, within the Anadarko basin, Mississippian units are primarily carbonate rocks from 450 m to >1,000 m thick. In northern Oklahoma, the Chesterian and/or Meramecian units have been removed by pre-Pennsylvanian erosion. The remaining Meramecian or Osagean rocks are principally cherty carbonate units ranging in thickness from 60 to 180 m. Morrowan and Atokan rocks are absent over north-central Oklahoma. Middle and upper Desmoinesian strata were probably the first units deposited over the uplifted Nemaha fault blocks since the Mississippian.

Subsurface Geology

Except for a few localities, surface geologic relations offer very little insight into understanding the structural relations associated with the Nemaha uplift. Therefore, to gain a better understanding of the geologic and tectonic history of the Nemaha uplift, a series of structure-contour maps of key stratigraphic horizons was constructed. The area

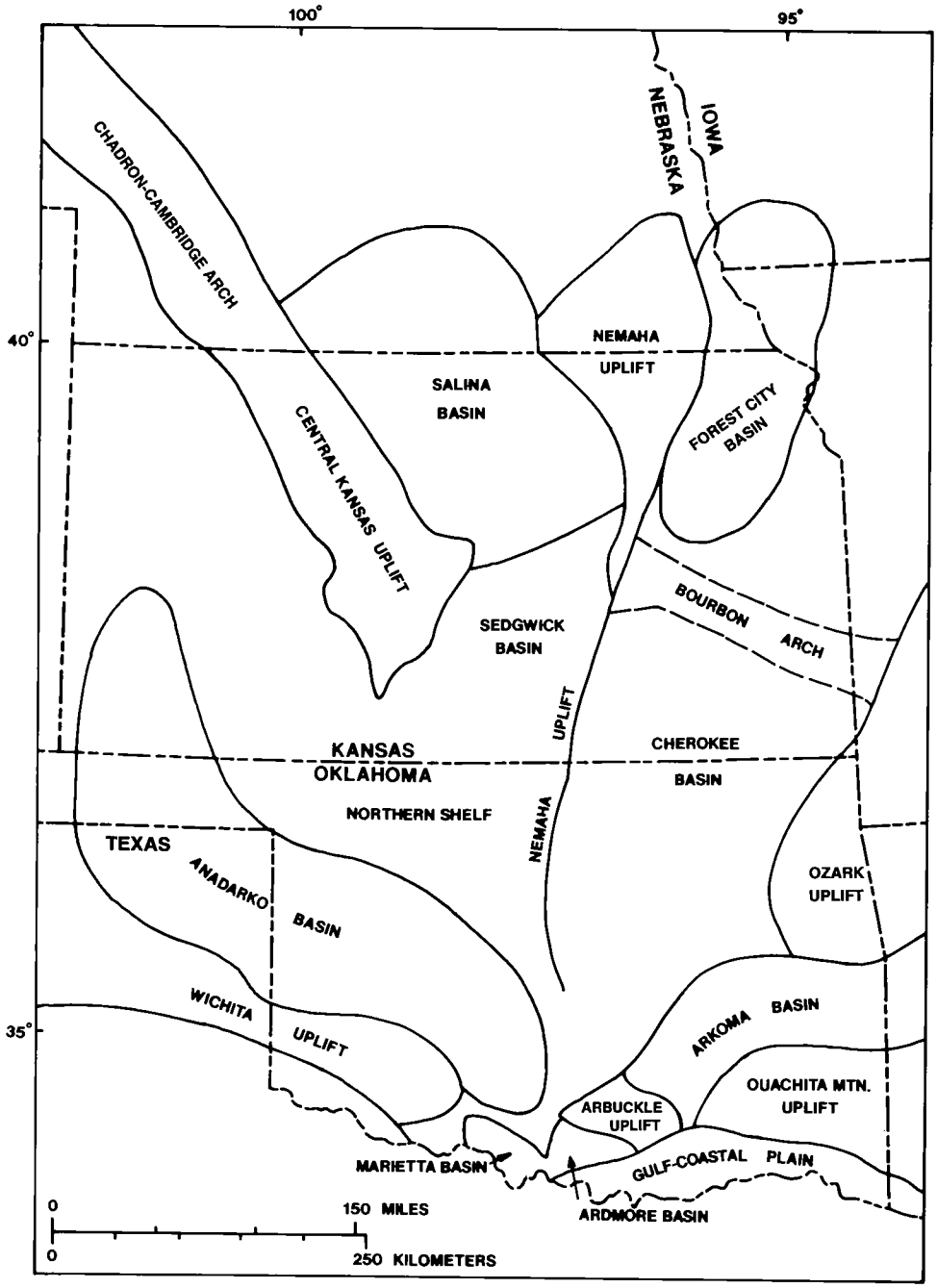


Figure 1. Major geologic and tectonic provinces of the Midcontinent.

contoured was expanded to include all of the area within the Enid and Oklahoma City 1° x 2° Quadrangles.

Three horizons were selected for structure-contour mapping: the top of the Viola Group (Late Ordovician), the base of the Pennsylvanian, and the top of the Oswego Limestone (Middle Pennsylvanian) (Fig. 3). These units were selected because they have been penetrated by a large number of boreholes and because they are easily recognizable on electric logs.

The term "Viola" (now Viola Springs Formation) was applied by Taff (1902) to limestones that crop out near the former village of Viola, Johnston Coun-

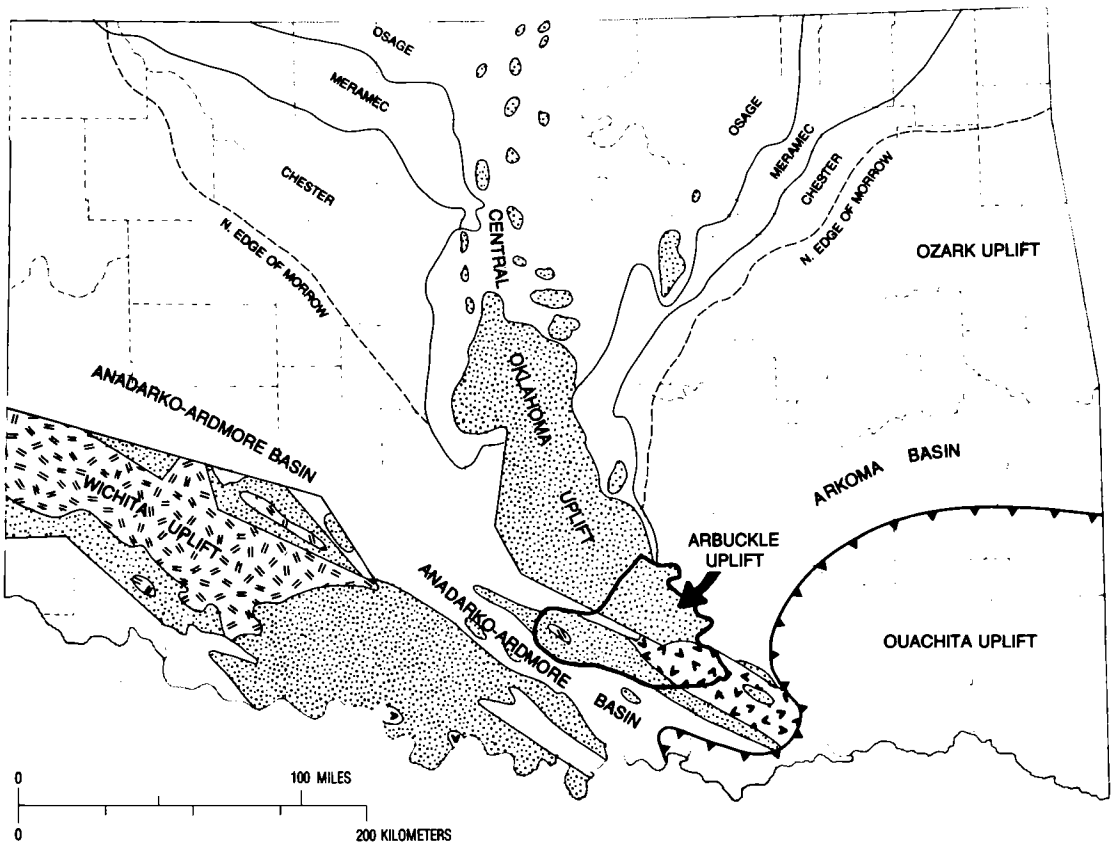


Figure 2. Pre-Pennsylvanian paleogeologic map of Oklahoma (exclusive of the Panhandle) showing rocks below the Pennsylvanian in the subsurface (modified from Jordan, 1962). Random-dot pattern denotes Devonian through Upper Cambrian rocks; pattern in Wichita uplift region denotes Middle Cambrian igneous rocks; V pattern in Arbuckle uplift region represents Precambrian granite.

ty, Oklahoma. Subsequent work by Wengerd (1948) subdivided the Viola into four lithologic members and gave formation rank to an overlying limestone, the Fernvale, now called the Welling Formation (Amsden, 1979). The Viola Springs Formation consists of dense, fine-grained, cherty, even-bedded limestone. The overlying Welling is a coarsely crystalline, fossiliferous limestone that rests disconformably on the Viola Springs Formation. For this project, the structure-contour map represents the top of the Viola Group, which includes the Welling Formation as well as the underlying Viola Springs Formation, because these two units are most often grouped together on drillers' logs (Fig. 4).

The Viola conformably overlies the Simpson Group. The Sylvan Shale, which consists of light-gray to gray-green, slightly calcareous, pyritic shale, rests conformably on top of the Viola Group. Regional isopach studies by Huffman (1959) and others indicate a maximum thickness of 450 m for the Viola in the Anadarko-Ardmore basins. The Viola has been removed by erosion in northern Oklahoma and along the uplifted features associated with the Nemaha uplift.

The structure map of the base of Pennsylvanian strata represents an unconformable surface (Fig. 5). Most of the Upper Mississippian strata were eroded prior to Pennsylvanian deposition. The principal geologic formations that basal Pennsylvanian sedimentary rocks rest upon include the Hunton Group, the Woodford Shale, the Mayes Limestone, and the Caney Shale. These Ordovician and older formations generally occur beneath the Pennsylvanian in the major uplifted areas, such as the Oklahoma City uplift. The pre-Pennsylvanian unconformity surface is relatively flat and therefore generally reflects pre-Pennsylvanian structure (Pulling, 1979).

The top of the Oswego Limestone (Middle Pennsylvanian) was also chosen as a reference horizon because it is continuous laterally in north-central Oklahoma, is easily recognizable on electric logs, and is most often reported on Oklahoma completion cards.

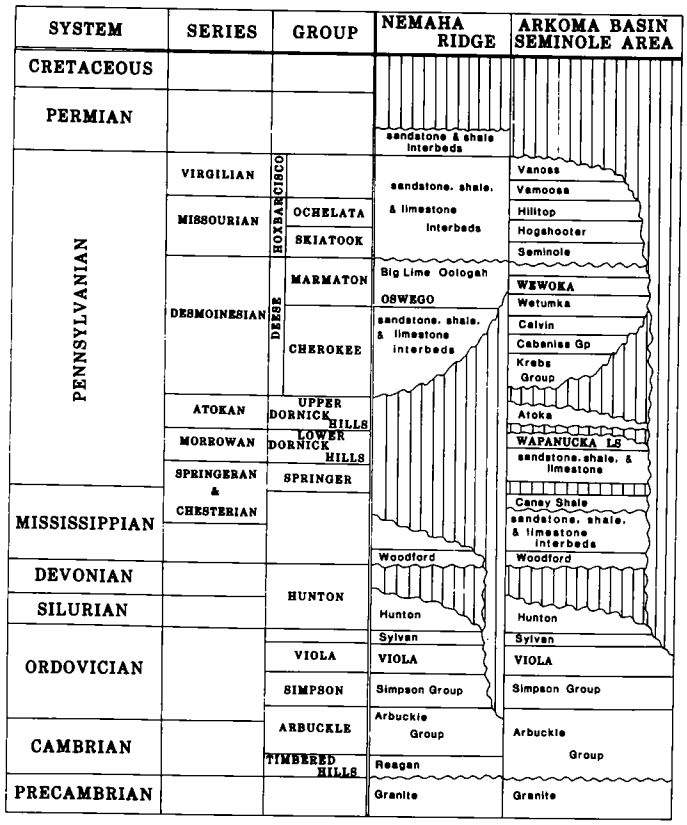


Figure 3. Generalized subsurface geologic section for north-central Oklahoma.

The Oswego Limestone is the lowermost formation of the Marmaton Group. It is equivalent to the Fort Scott Formation and is an informal subsurface name widely used in Oklahoma. The Oswego is fairly uniform in thickness (15–25 m) and gradually thins southeastward, where it interfingers with interbedded sandstones and shales of the Wewoka Formation. The top of the Wewoka is herein used as a mapping horizon principally in Pottawatomie and Seminole Counties. In the southeastern part of the area, the top of the Wapanucka Limestone is used as a mapping horizon because it is the youngest widespread limestone in the Arkoma basin (Fig. 6).

The structure-contour maps (Figs. 4–6) reveal essentially two complex fault patterns, of which the westernmost is due to the Nemaha uplift. This structure consists of a number of discontinuous, raised crustal blocks, such as the Oklahoma City, Lovell, Garber, and Crescent uplifts, that are typically 5–8 km wide and 8–32 km long. The blocks are generally bounded by near-vertical faults on the east side that are downthrown to the east. These features form a fault zone that extends from Oklahoma City in a northwesterly direction to T. 18 N., R. 3 W. In this region, the orientation of the fault zone becomes north-northeast and extends northward through Kansas and terminates in southeastern Nebraska. The southern end of the Nemaha uplift is believed to be the Oklahoma City uplift and its associated faults. Another fault zone, the McClain County fault zone, intersects the Oklahoma City uplift in southern Oklahoma County. This fault zone, which is composed of a number of subparallel faults and is thought to be temporally related to the Nemaha faults, trends south-southwest and terminates against the Pauls Valley uplift in Garvin and southern McClain Counties.

The second major complex fault pattern occurs in the east-central part of the study area. This feature was named the Wilzetta fault by Cole (1969), Pulling (1979), and others, probably after the Wilzetta oil field that was discovered in 1934 and located in T. 13 N., R. 5 E., in southeastern Lincoln County. The Wilzetta fault extends north-northeast diagonally across Pottawatomie, Lincoln, and western Creek Counties. This fault zone marks the westward extension of the Seminole-Cushing uplift, which trends in a north-northeast direction and plunges northward away from the Pauls Valley uplift (Pulling, 1979).

The Seminole-Cushing uplift may have originated in Middle Devonian time, when a major epeirogeny occurred. The general uplift from the northeast may have given rise to southeastward dip in the Hunton and older rocks. Major folding took place during the Wichita orogeny in post-Mississippian, pre-Desmoinesian time. The formation of northeast-trending structures, such as the Wilzetta fault, is probably related to the Wichita orogeny. Renewed movement along the Wilzetta fault and slight uplift of the Seminole-Cushing uplift occurred during the deposition of Cherokee Group strata and afterward (Pulling, 1979).

The Nemaha uplift in northern Oklahoma, in Grant, Kay, Garfield, and Noble Counties, is composed of a number of discontinuous raised blocks that occupy a northeast-trending zone. This zone, ~50 km wide in northern Kay County, narrows southwestward until it is <10 km wide in northern Kingfisher County. In northern Kingfisher County, the Nemaha fault zone trends southeastward toward Oklahoma City (Fig. 4). Koff's (1978) study of the Oklahoma City uplift, the southernmost extension of the Nemaha uplift, and its associated fault features suggests that a number of the Nemaha-related faults were developed in pre-Mississippian

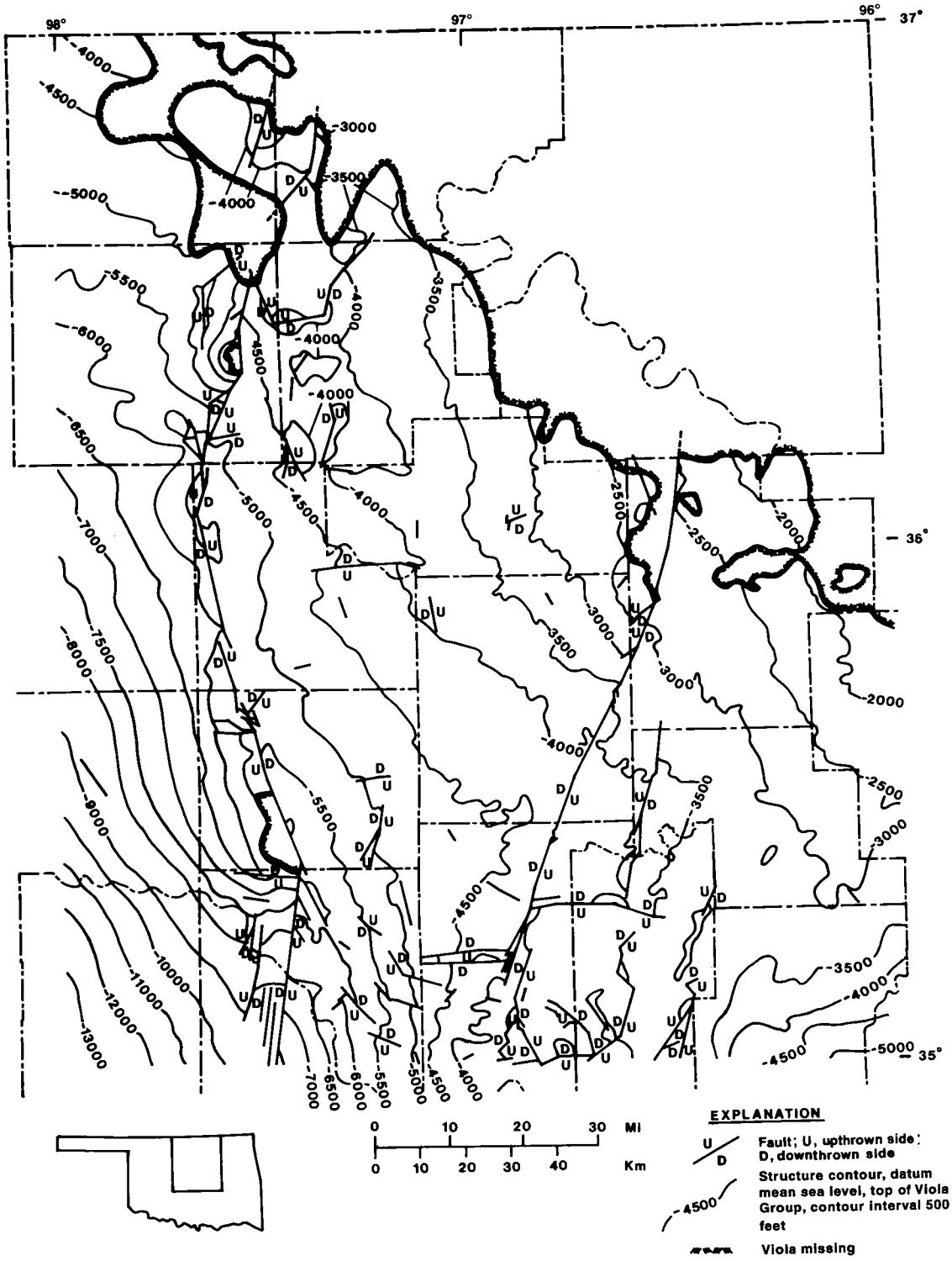


Figure 4. Structure-contour map on top of Viola Group in north-central Oklahoma (modified from Luza and Lawson, 1983).

time. Many of these faults exhibit both increasing and decreasing displacements from early to late Paleozoic time. However, the displacement for most of the Oklahoma City faults took place between the end of Devonian (Hunton) time and the end of Middle Pennsylvanian (Oswego) time.

In central Oklahoma, particularly near the axis of the Nemaha uplift, the basement-rock surface slopes gently southward. It is ~1,200 m below the land surface near the Kansas border and is ~2,400 m deep near Oklahoma City. The most systematic basement-rock studies that embrace the Nemaha uplift area were done by Denison (1966,1981), who examined and described samples from more than 220 wells that penetrated Precambrian rocks in adjoining parts of Oklahoma, Kansas, Missouri, and Arkansas. Twenty-five isotopic-age determinations were made on 20 samples of basement rocks from wells and outcrops.

Denison (1981) classified the northeastern Oklahoma basement rocks into the following four units: (1) Washington Volcanic Group, (2) Spavinaw Granite Group, (3) Osage Microgranite, and (4) Central Oklahoma Granite Group. There are few borehole penetrations into basement rock in central Oklahoma. Therefore, basement-rock lithologies, contact relations, and structural interpretations in the vicinity of the Nemaha uplift are highly interpretive. Regional contact relations suggest that the Central Oklahoma Granite must have been intruded into several kilometers of overlying rock, namely the Washington Volcanic Group. The intruded rocks are not present above the Central Oklahoma Granite in the vicinity of the Nemaha uplift. Perhaps this region was uplifted in late Precambrian to Early Cambrian time. Subaerial erosion probably was a primary factor that contributed to the removal of the overlying volcanic units before Middle Cambrian deposition of sediments. Perhaps zones of weakness, which developed from the initial uplift (late Precambrian to Early Cambrian), were reactivated during the Early Pennsylvanian orogeny to form the main axis of the Nemaha uplift.

EARTHQUAKE SEISMOLOGY

Introduction

Prior to about 1950, the few seismographs that operated in the states adjacent to Oklahoma were not sensitive enough to detect most earthquakes originating in the State. Only written records, usually found in local newspapers and diaries, of humans having felt earthquakes are available. Some of the larger felt earthquakes were listed in the "Seismological Notes" column bimonthly bulletin of the Seismological Society of America. A more complete listing appeared, beginning about 1929, in the annual publication *United States Earthquakes*.

The first Oklahoma seismographs became operational in December 1961. The stations were located at the Jersey Research Co.'s (now Exxon) Leonard Earth Sciences Observatory near Leonard in southern Tulsa County and at the U.S. Air Force Advanced Research Projects Agency's Wichita Mountains Seismological Observatory in Comanche County. The Leonard Earth Sciences Observatory has been designated by the international station abbreviation TUL since 1961; it is now operated as the Oklahoma Geological Survey's Oklahoma Geophysical Observatory. The Air Force installation in Comanche County, designated by the abbreviation WMO, was designed and operated primarily to detect and distinguish between distant earthquakes and distant underground nuclear tests. WMO closed in 1971, after several years of sharply curtailed activity. Both WMO and TUL seismographs made excellent recordings of P waves from distant earthquakes, but they partially filtered out high-frequency waves characteristic of nearby earthquakes.

In 1964, Eysteinn Tryggvason, professor at the University of Tulsa, compiled historical information on Oklahoma earthquakes, primarily from *United States Earthquakes* and Kalb (1964). This study led to the development of a formula used to assign a local Richter magnitude (ML) to some of the historical earthquakes on the basis of the size of the area in which they were felt. Tryggvason also searched the TUL short-period seismic records of January 1962 through September 1963 and found 10 Oklahoma earthquakes. The seismograms from WMO and seismograph stations in other states were used to make location determinations of the 10 events. TUL seismogram trace amplitudes were also used to determine approximate local Richter magnitudes (ML). Jerry Docekal's (1970) extensive study of earthquakes of the Midcontinent provided more details of the felt effects of many Oklahoma shocks.

A program was established in 1970 to reduce information on Oklahoma earthquakes to a standard 80-column computer format. The TUL short-period (SP) seismograms were searched for regional events (Oklahoma and vicinity). Of the few that were found, some were located with the aid of arrival times at other stations, such as FAV (Fayetteville, Arkansas), LUB (Lubbock, Texas), GOL (Golden, Colorado), and ALQ (Albuquerque, New Mexico). Others were located by using the TUL records alone, with the distance to the epicenter being determined by the interval between S and P phases, and the direction of movement by the ratio of the north-south and east-west motion of the S waves.

A near-vertical-motion short-period seismograph sensitive to high frequencies was added at TUL in April 1972. This improvement enabled the detection of many more regional earthquakes. However, most of these additional events could not

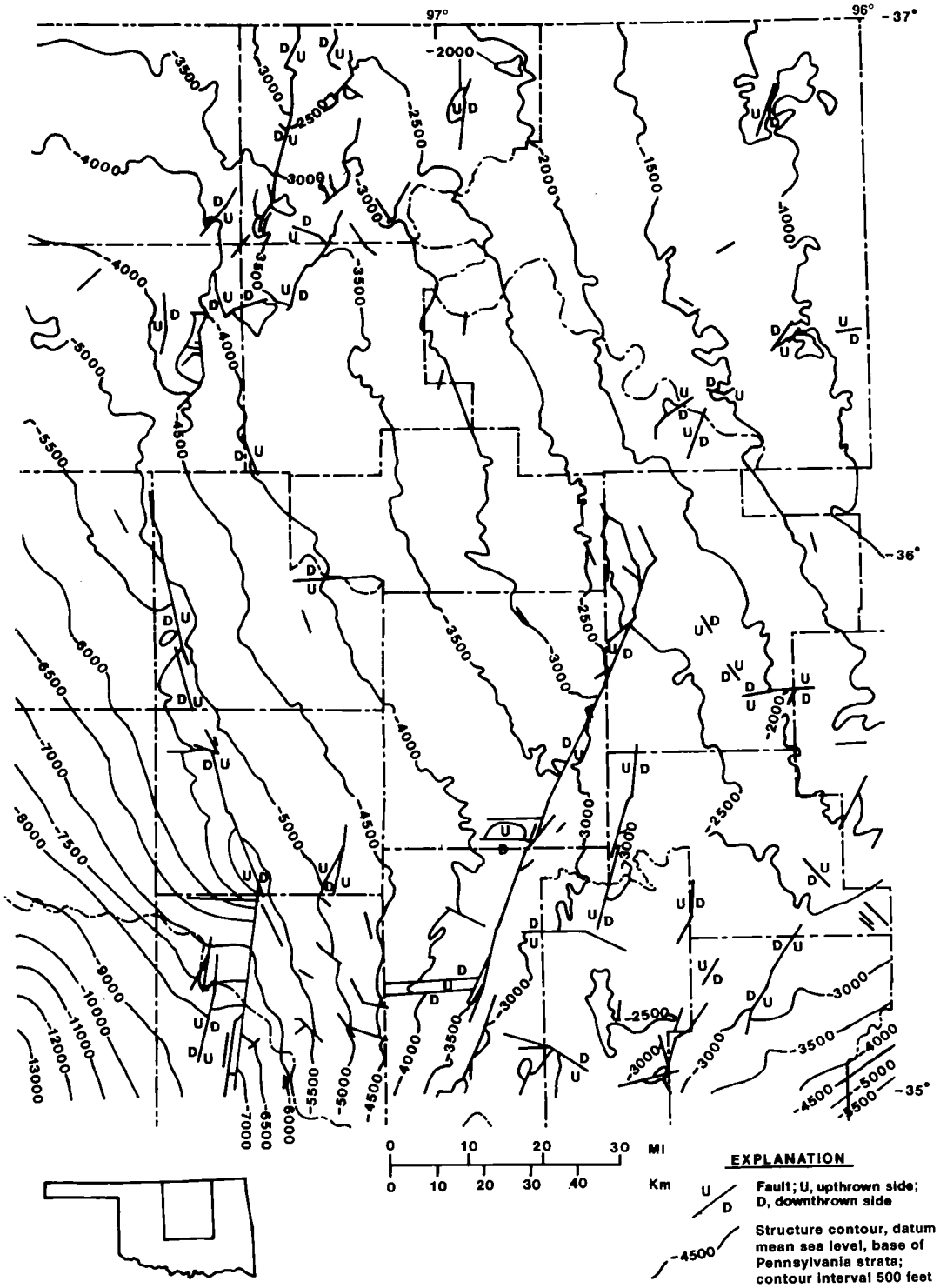


Figure 5. Structure-contour map on base of Pennsylvania strata in north-central Oklahoma (modified from Luza and Lawson, 1983).

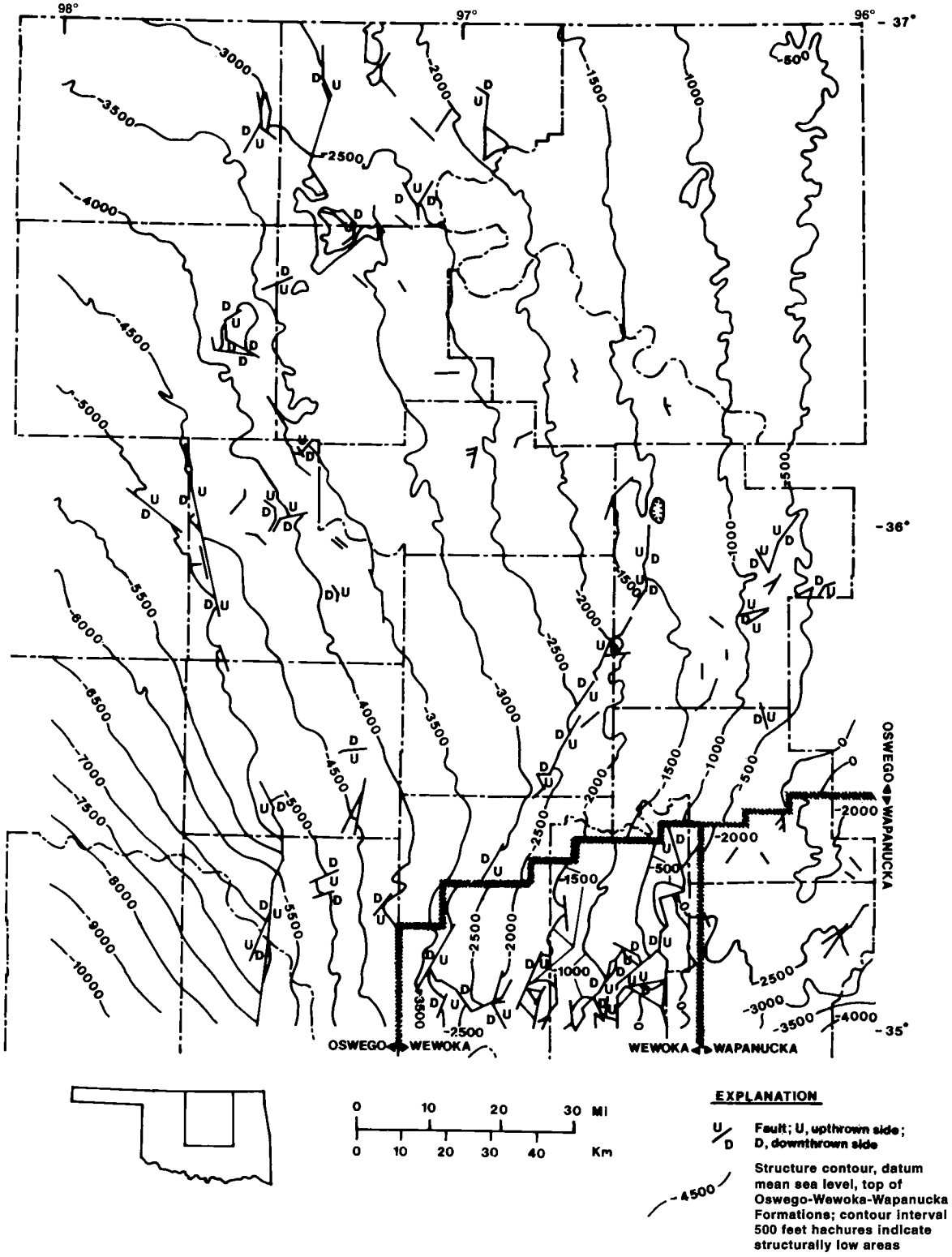


Figure 6. Structure-contour map on top of the Oswego Limestone, Wewoka Formation, and Wapanucka Limestone in north-central Oklahoma (modified from Luza and Lawson, 1983).

be located other than specifying their distance from TUL.

In the early 1970s, TUL became the established source of information to the seismological community for Oklahoma earthquakes and some nearby earthquakes. The Observatory became one of about 50 agencies throughout the world that report epicenters directly to the International Seismological Centre in Newbury, England, for publication in its monthly bulletin and semiannual catalog. In 1975, the Observatory began officially to furnish the National Oceanic and Atmospheric Administration (NOAA) with data on earthquakes felt in Oklahoma for the annual publication of *United States Earthquakes*.

The University of Oklahoma, the Oklahoma Geological Survey, and the U.S. Nuclear Regulatory Commission (NRC) started a cooperative program in 1976 to study seismicity of the Nemaha uplift and other areas of Oklahoma. The Observatory staff began a program to computerize the accumulated earthquake catalog, which included compiling data from published and unpublished reports with data held on magnetic tape for complete or selected printing whenever needed. By the middle of 1977, the Observatory was operating a five-station network, and by 1978 nine stations were operating. These additional seismograph stations have tremendously improved earthquake detection and location accuracy in Oklahoma, as well as in the adjacent states. These improvements are reflected by the large increase in locatable Oklahoma earthquakes. The Oklahoma seismograph network is recording and locating about 50 Oklahoma earthquakes per year, as compared to previous years, such as 1974, when only four earthquakes were located.

Instrumentation

A statewide network of 12 seismograph stations is used to locate earthquakes in Oklahoma (Fig. 7). The Oklahoma Geological Survey Observatory station, TUL, located near Leonard, Oklahoma, in southern Tulsa County, records 15 continuous seismic signals from sensors located at five stations. The data are recorded, analyzed, and archived on a GSE digital seismic system provided by the Defense Advanced Research Projects Agency/Nuclear Monitoring Research Office.

Signals are digitized by two Geotech RDAS (remote data acquisition system) units at either 36,000 or 1,200 24-bit samples per second. The RDAS then applies digital anti-alias filtering to eliminate frequencies too high for the final sampling rate. After one to three digital filtering and resampling stages, the RDAS produces 40, 60, or 10 24-bit samples per second. The samples are time-tagged by RDAS clocks locked to very low frequency Omega Navigation/Time signal receivers. The signals are passed by RS422 serial links to an AST 386/25 RTDS (real-time data server) computer, which has a Lynx™ real-time UNIX-like operating system. The partially processed signals are passed by ethernet to a Sun Sparc 1+ UNIX workstation with 40 megabytes of memory, two 660-megabyte disks, and two 2.3-gigabyte Exabyte™ tape drives. All of the data from the most recent two to three days are retained on disk. Each day, data from the preceding day (167 million bytes) are automatically archived onto Exa-

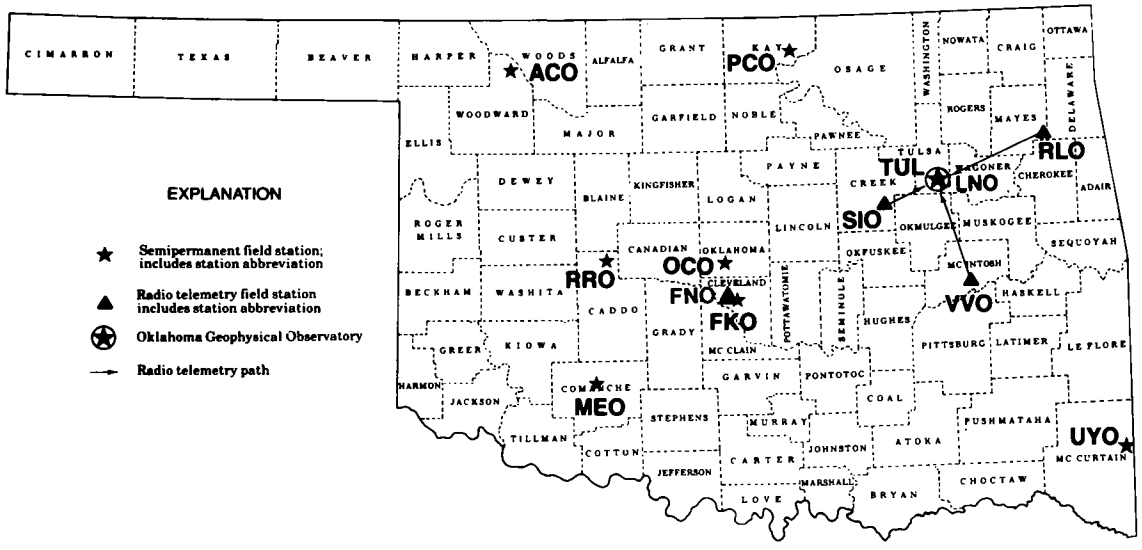


Figure 7. Active seismograph stations in Oklahoma, 1992.

byte™ tape. All Oklahoma earthquakes, and other selected events, are placed in named de-archive directories on a 900-megabyte disk attached to a Sun 3/50 computer belonging to Lawrence Livermore National Laboratories. The de-archive directories are remote mounted, by way of the ethernet, by the Sun Sparc 1+ workstation. An Oracle™ data base on the Sun Sparc 1+ keeps track of every second of data on the permanent archive tapes, the last two or three days' data on disk, and data in the de-archive directories. Data analysis is done by Teledyne-Geotech and Science Applications International Corporation software on the Sparc 1+ workstation.

The digital-system signals are from six sensors in the TUL vault; from three sensors in a borehole on the Observatory property (station LNO); and from single sensors located at Rose Lookout (RLO) in Mayes County, at the Bald Hill Ranch near Vivian (VVO) in McIntosh County, and at the Jackson Ranch near Slick (SIO) in Creek County.

TUL has three short-period (vertical, north-south, east-west) Geotech GS-13 seismometers. These seismometers produce signals that are digitized at 40 samples per second. Signals from a Geotech KS-54,000 three-component broadband seismometer, located at the bottom of a 120-m-deep borehole, are digitized at 20 samples per second. Three one-sample-per-second long-period signals are derived by the workstation from the broadband signals. The short-period and broad-band signals are particularly useful in determining the wave-arrival direction for Oklahoma earthquakes.

The LNO station has a Geotech 20171A seismometer in a 4.5-m-deep borehole and two Geotech 23900 (a deep-hole version of the 20171A) seismometers at 432- and 748-m depths in a borehole that is 1 m away from the 4.5-m-deep hole. The LNO equipment is provided and partially supported by Lawrence Livermore National Laboratories. The three LNO signals are digitized by a second RDAS near the borehole and recorded and archived at 60 samples per second. This approach allows recording of higher-frequency waves than is possible with the 40-sample-per-second data. The higher frequencies are particularly prominent in nearby (Oklahoma and adjacent areas) earthquakes. At frequencies above 10 Hz, the high-frequency background noise produced by wind and cultural activity is almost absent at the 748-m-deep sensor. It is particularly important for recording signals from smaller Oklahoma earthquakes, which are very difficult to see on seismograms from near-surface seismometers.

RLO, VVO, and SIO have Geotech S-13 seismometers in shallow tank vaults. The seismic signals are amplified and used to frequency-modulate an audio tone that is transmitted to TUL with 500-mW FM transmitters at various frequencies in the 216–220-mHz band. The signals are received by antennas on a 40-m-high tower at TUL, the tones are discriminated to produce a voltage that is proportional to the remote seismometer voltage, and the voltages are digitized at 40 samples per second by the vault RDAS. The operation of RLO, VVO, and SIO is partially supported by the NRC. A fourth radio-telemetry station, FNO, was installed in central Oklahoma on April 28, 1992. The seismometer, a Teledyne Geotech S-500, is located at the bottom of a 30-m-deep borehole, ~7 km northeast of the Oklahoma Geological Survey's building. A discriminator converts the audio-signal frequency fluctuations to a voltage output. The voltage output is amplified and recorded by a Sprengnether MEQ-800 seismograph recorder (located in a display case at the Survey) at 60 mm/min trace speed.

In the TUL vault, seven additional seismometers produce analog recordings on paper-drum recorders. Eleven such recordings are produced, five of which are the proper frequencies to record some aspect of nearby earthquakes. Each of the single-sensor stations, RLO, VVO, and SIO, produces one paper recording. There are no LNO paper records. The paper records are used as a digital-system backup and to scan for earthquakes faster than is possible on computer screens.

In addition to the digital and analog seismographs at the Observatory, there are seven volunteer-operated seismographs. Each consists of a Sprengnether S-13 short-period vertical-motion-sensing seismometer; five are situated in shallow tank vaults, one in an abandoned mine shaft (station MEO), and one in a large-diameter, hand-dug, shallow water well (station UYO). The seismometer signal runs through 60–550 m of cable in surface PVC conduit to the volunteer's house or other building. Each volunteer has a Sprengnether MEQ-800B timing system, amplifier-filter, and drum recorder, which records 24 h of seismic trace at 1 mm/min in a spiral path around the paper on the drum. The times are set by a time-signal radio receiver tuned to the National Institute of Standards and Technology and high-frequency radio station WWV. The volunteers mail in the seismograms weekly, or more often, upon request.

Data Reduction and Archiving

Seismic traces from the TUL vault vertical seismometer (TUL sz), the deepest-borehole short-period vertical seismometer of station LNO (LNO/sz1), and one radio-telemetry site (usually VVO) are displayed on a 19-in. monitor on the Sun Sparc 1+. The data are processed through 0.4–4.0-Hz digital band-pass filters and are displayed in 90-min segments. A fourth, long-period vertical trace is displayed, but it records only waves from distant earthquakes. The 90-min traces are fuzzy lines with spikes showing signals above the noise. Distant

earthquakes of magnitude ≥5.0 are usually identifiable by the shape of the spike and the following long-period surface waves. Other spikes represent local or regional earthquakes or quarry blasts. There are from 10 to 30 recordable quarry blasts each weekday, two to five on Saturday, and one or two on Sunday.

The monitor display is zoomed on a 60-s segment surrounding each spike, and the event is identified by its appearance. If it is a P wave from a distant earthquake, the display is zoomed to 15 s, and the arrival time, frequency, amplitude, and polarization (direction) are measured, calculated, and recorded for transmission to international data centers.

If a spike is identified as a possible near or regional earthquake, nine traces are displayed on the monitor (TUL sz, sn, se; LNO sz1, sz2, sz3; RLO sz; VVO sz; SIO sz). They are then filtered and unfiltered repeatedly to enhance and identify the phases. One set of filters, developed at NORESS (Norwegian Experimental Seismic System), has been described by Mykkeltveit and others (1990). By using the time interval between phases, the distance can be determined; the direction is determined from polarization (using the TUL vault vertical, north-south, and east-west signals). The distance and direction give an approximate location, which is then improved by incorporating arrival times from remote sites RLO, VVO, and SIO. At this point, a short press release is issued from the Oklahoma Geological Survey offices at Norman. Paper seismograms are also searched for regional and local earthquakes. Some small earthquakes are initially spotted on only the digital system or on only the paper seismograms.

The next stage is de-archiving digital data from the nine short-period records (listed in the preceding paragraph). These are put in a permanent named disk file and indexed in the on-line Oracle™ data base.

Each three months, paper seismograms from all volunteer stations and from Observatory seismograms are carefully searched for local earthquakes. Arrival times are measured and added to those already determined from the digital system. As many as two or three additional earthquakes may be found. These are de-archived from Exabyte™ tapes for digital-system analysis.

The depth to the hypocenter for most Oklahoma earthquakes is unknown. In almost all Oklahoma events, the stations are several times farther from the epicenter than the likely depth of the event. This situation makes the locations indeterminate at depth, which usually requires that the hypocenter depth be restrained to an arbitrary 5 km for purposes of computing latitude, longitude, and origin time. All available evidence indicates that no Oklahoma hypocenters have been deeper than 15–20 km.

Catalog

A desktop computer system, including linked HP-9825T and HP-9835A computers, hard and flexible disks, and printers, is used to calculate and catalog local earthquake epicenters. Arrival times, signal durations, and various signal amplitudes are entered into a location program. After each location is finalized, it is entered into an Oklahoma earthquake catalog. This catalog is used to produce lists (by date, by county, by latitude-longitude rectangle, and several other choices) and to produce maps with a six-color Hewlett-Packard 7975A plotter. Any earthquake within Oklahoma, or within about 100–200 km of Oklahoma's borders, is considered a local earthquake.

The catalog contains date, origin time, county, intensity, magnitude, location, focal depth, and references. Each earthquake is sequentially numbered. The numbering system is compatible with the system used for the "Earthquake Map of Oklahoma" (Lawson and others, 1979) and subsequent additions (Lawson and Luza, 1980–90,1993; Lawson and others, 1991,1992).

The date and time are given in UTC (Coordinated Universal Time, formerly Greenwich Mean Time). The first two digits refer to the hour on a 24-h clock. The next two digits refer to the minute, and the remaining digits are the seconds. To convert to local Central Standard Time, subtract 6 h.

Earthquake magnitude is a measurement of energy and is based on data from seismograph records. There are several different scales used to report magnitude. The Oklahoma Geological Survey uses three magnitude scales, which are mbLg (Nuttli), m3Hz (Nuttli), and MDUR (Lawson). Each magnitude scale was established to accommodate specific criteria, such as the distance from the epicenter, as well as the availability of certain seismic data.

For earthquake epicenters located 11–222 km from a seismograph station, Otto Nuttli developed the m3Hz magnitude scale (Zollweg, 1974). This magnitude is derived from the following expression:

$$\text{m3Hz} = \log(A/T) - 1.63 + 0.87 \log(\Delta),$$

where A is the maximum center-to-peak vertical-ground-motion amplitude sustained for three or more cycles of Lg waves, near 3 Hz in frequency, measured in nanometers; T is the period of the Lg waves measured in seconds; and Δ is the great-circle distance from epicenter to station measured in kilometers.

In 1979, St. Louis University (Stauder and others, 1979) modified the formulas for m3Hz. This modification was used by the Observatory beginning January 1, 1982. The modified formulas had the advantage of extending the distance range for measurement of m3Hz out to 400 km, but also had the disadvantage of increasing m3Hz by about 0.12

units compared to the previous formula. Their formulas were given in terms of log(A) but were restricted to wave periods of 0.2–0.5 s. In order to use log(A/T), we assumed a period of 0.35 s in converting the formulas for our use. The following equations result:

(epicenter 10–100 km from a seismograph)
$$m3Hz = \log(A/T) - 1.46 + 0.88 \log(\Delta)$$
(epicenter 100–200 km from a seismograph)
$$m3Hz = \log(A/T) - 1.82 + 1.06 \log(\Delta)$$
(epicenter 200–400 km from a seismograph)
$$m3Hz = \log(A/T) - 2.35 + 1.29 \log(\Delta).$$

Otto Nuttli's (1973) earthquake magnitude, mbLg, for seismograph stations located between 55.6 and 445 km from the epicenter, is derived from the following equation:

$$mbLg = \log(A/T) - 1.09 + 0.90 \log(\Delta).$$

Where seismograph stations are located between 445 and 3,360 km from the epicenter,

$$mbLg = \log(A/T) - 3.10 + 1.66 \log(\Delta),$$

where A is the maximum center-to-peak vertical-ground-motion amplitude sustained for three or more cycles of Lg waves, near 1 Hz in frequency, measured in nanometers; T is the period of Lg waves measured in seconds; and Δ is the great-circle distance from epicenter to station measured in kilometers.

The MDUR magnitude scale was developed by Lawson (1978) for earthquakes in Oklahoma and adjacent areas. It is defined as

$$MDUR = 1.86 \log(DUR) - 1.49,$$

where DUR is the duration or difference, in seconds, between the Pg-wave arrival time and the time the final coda amplitude decreases to twice the background-noise amplitude. Before 1981, if the Pn wave was the first arrival, the interval between the earthquake-origin time and the decrease of the coda to twice the background-noise amplitude was measured instead. Beginning January 1, 1982, the interval from the beginning of the P wave (whether it was Pg, P*, or Pn) to the decrease of the coda to twice the background-noise amplitude was used.

EARTHQUAKE DISTRIBUTION

Of the ~50 earthquakes that are located in Oklahoma each year, only one or two earthquakes, on the average, are reported as felt. Prior to 1962, all earthquakes in Oklahoma, 59, were either known from historical accounts or from seismograph stations outside the State. From 1962 through 1976, after the first seismographs were installed in late 1961, 70 additional earthquakes were added to the earthquake data base. In 1977, expanding the statewide network of seismograph stations greatly improved earthquake detection and location. From 1977 through 1992, more than 790 additional earthquakes were located in Oklahoma, mostly of magnitudes <2.5.

The earthquake epicenter data reveal at least two seismic trends worthy of discussion. These trends are located in north-central Oklahoma and along the eastern margin of the Anadarko basin.

North-Central Oklahoma

Prior to the installation of the statewide earthquake-station network, more than half of the known Oklahoma earthquakes occurred in Canadian County. After the El Reno earthquake of 1952, magnitude 5.5 (mb), no earthquakes were reported for this region until 1978.

The pre-1977 earthquake data and the 1977–92 earthquake data are shown in Figure 8, as well as the location of the Nemaha uplift. A 40-km-wide and 145-km-long earthquake zone extends northeastward from near El Reno toward Perry (Noble County). Most of the earthquakes have occurred in the vicinity of the El Reno–Mustang area, which has been the site of numerous earthquakes since 1908.

The correlation of historical and recent earthquake activity to known structural features remains unclear. Some faults that cut pre-Pennsylvanian rocks are shown in Figure 8; these data were compiled from Wheeler (1960), Jordan (1962), Luza and Lawson (1983), and unpublished reports. The El Reno–Perry trend appears to cut diagonally across the Nemaha uplift structures at about a 30° angle. The southern end of this trend appears to be more active than the middle and northern parts. Both the recent and historic earthquake data seem to support this observation.

Anadarko Basin

More than 350 located earthquake events have taken place in the Anadarko basin since 1897. A majority of the Anadarko basin earthquakes have occurred within a 135-km-long by 40-km-wide zone between Canadian County and the south edge of Garvin County. More than 90% of the earthquakes within this zone have taken place since 1977 (Fig. 9). The southern end of this trend closely parallels the McClain County fault zone (sometimes referred to as the central Oklahoma fault zone) that is about 40 km wide and 60 km long.

Only a few earthquakes are known to have occurred in the shelf and deep portions of the basin. The Amarillo-Wichita uplift and associated fault zone are seismically very quiet, as compared to McClain, Garvin, and Canadian Counties. Perhaps when the stress along the frontal fault zone is periodically relieved, as by a substantial break such as the Meers fault, the region may experience very low seismic activity for a considerable time.

DISCUSSION

It is not clear what the earthquake activity between El Reno and Perry represents. The zone may be the result of a coincidental plot of earthquake

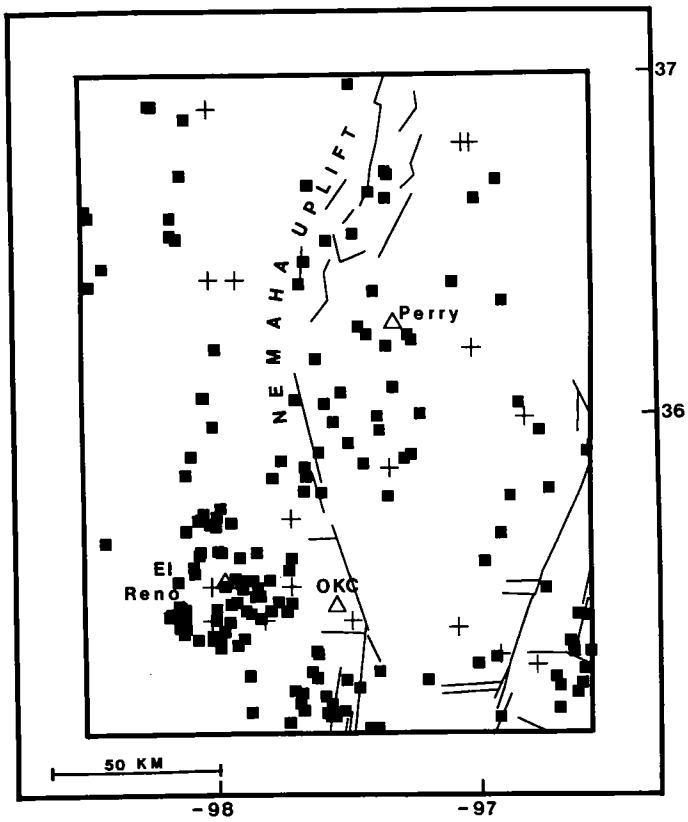


Figure 8. Distribution of pre-1977 earthquake epicenters (+) and post-1977 earthquake epicenters (■) in north-central Oklahoma. Open triangles show city locations: OKC, Oklahoma City. A solid line indicates a fault; structure is generalized.

epicenters, and/or it may be related to some unknown northeast-trending structure(s). There do not appear to be any major Paleozoic structures in the vicinity of the zone. Perhaps the earthquake activity is related to a northeast-trending Precambrian structure.

The Canadian County earthquakes appear to coincide with the transition boundary between the shelf and Anadarko basin. This transition zone appears to coincide with early Paleozoic faults that probably were initiated when the Anadarko basin began to develop in Middle Cambrian time. However, most of these structures are not present in late Paleozoic rocks. Joe Hayden's (1985) gravity study in western Canadian County and vicinity suggests that the Anadarko basin is not in isostatic equilibrium. If the Anadarko basin is still undergoing some form of isostatic adjustment, earthquake activity near the basin margin may occur.

The earthquake activity between Norman and Pauls Valley is closely associated with the McClain County fault zone and related structures. This fault zone consists of many subparallel faults that have created a number of fault blocks within the zone. Small adjustments between fault blocks may be producing some of the earthquakes in this region.

The seismic network has a 50% probability of locating ≥1.6 magnitude earthquakes and a 90% probability of locating a ≥2.0 magnitude earthquake. The network has exceeded the NRC's original objective for the location of ≥2.5 magnitude earthquakes.

Prior to 1977, Oklahoma had about 129 known earthquakes. From 1977 through 1992, more than 810 additional earthquakes were located in Oklahoma, mostly of magnitudes <2.5. The seismic network has enabled the Oklahoma Geological Survey to identify areas not previously known to be seismically active. For example, most of the earthquakes between Norman and Pauls Valley would have gone undetected if the network had not been operational.

Good progress has been made toward the identification of earthquake-prone areas in Oklahoma. Earthquake-source mechanisms, focal-depth determinations, and fault-plane solutions remain elusive. It will take several years of locating small-magnitude earthquakes and deeper and larger-magnitude earthquakes before specific earthquake-generating structures can be identified. Apparently many of the earthquake-generating structures are deeply buried.

REFERENCES CITED

Amsden, T. W., 1979, Welling Formation, new name for Upper Ordovician unit in eastern Oklahoma (formerly called "Fernvale"): American Association Petroleum Geologists Bulletin, v. 63, p. 1135–1138.

Burchett, R. R.; Luza, K. V.; van Eck, O. J.; and Wilson, F. W., 1983, Seismicity and tectonic relationships of the Nemaha uplift and Midcontinent geophysical anomaly (final project summary): U. S. Nuclear Regulatory Commission NUREG/CR-3117, 33 p.

Cole, J. G., 1969, Cherokee Group, east flank of the Nemaha Ridge (parts 1 and 2): Shale Shaker Digest VI, p. 75–99.

Denison, R. E., 1966, Basement rocks in adjoining parts of Oklahoma, Kansas, and Arkansas: University of Texas, Austin, unpublished Ph.D. dissertation, 292 p.

_____ 1981, Basement rocks in northeastern Oklahoma: Oklahoma Geological Survey Circular 84, 84 p.

Docekal, Jerry, 1970, Earthquakes of the stable interior, with emphasis on the Midcontinent: University of Nebraska, Lincoln, unpublished Ph.D. dissertation, v. 1, 169 p.; v. 2, 332 p.

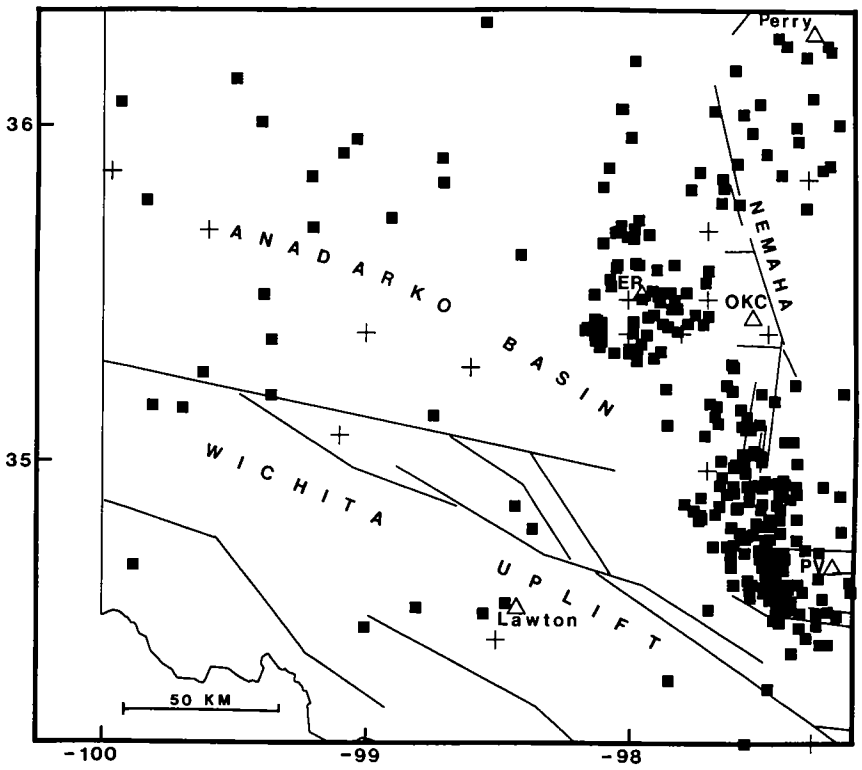


Figure 9. Distribution of pre-1977 earthquake epicenters (+) and post-1977 earthquake epicenters (■) in the Anadarko basin and vicinity. Open triangles show a city location: PV, Pauls Valley; ER, El Reno; OKC, Oklahoma City. A solid line indicates a fault; structure is generalized.

Hadley, J. B.; and Devine, J. F., 1974, Seismotectonic map of the eastern United States: U.S. Geological Survey Miscellaneous Field Studies Map MF-620, 8 p., 3 sheets.

Ham, W. E.; and Wilson, J. L., 1967, Paleozoic epeirogeny and orogeny in the central United States: American Journal of Science, v. 265, p. 332–407.

Hayden, J. M., 1985, A gravity and magnetic investigation of a microseismically active area in central Oklahoma: University of Oklahoma unpublished M.S. thesis, 175 p.

Huffman, G. G., 1959, Pre-Desmoinesian isopachous and paleogeologic studies in central Midcontinent region: American Association of Petroleum Geologists Bulletin, v. 43, p. 2541–2574.

Jordan, Louise, 1962, Geologic map and section of pre-Pennsylvanian rocks in Oklahoma: Oklahoma Geological Survey Map GM-5, scale 1:750,000.

Kalb, Bill, 1964, Earthquakes that shook Oklahoma: Orbit Magazine—The Sunday Oklahoman, Oklahoma City, September 27, p. 4–7.

King, P. B., 1951, The tectonics of middle North America east of the Cordilleran system: Princeton University Press, Princeton, New Jersey, 203 p.

Koff, L. R., 1978, Tectonics of the Oklahoma City uplift, central Oklahoma: University of Oklahoma unpublished M.S. thesis, 64 p.

Lawson, J. E., Jr., 1978, A preliminary duration magnitude scale for local and regional earthquakes recorded at Oklahoma seismograph stations: Oklahoma Geological Survey Observatory Open-File Report, 14 p.

Lawson, J. E., Jr.; and Luza, K. V., 1980, Oklahoma earthquakes, 1979: Oklahoma Geology Notes, v. 40, p. 95–105.

_____ 1981, Oklahoma earthquakes, 1980: Oklahoma Geology Notes, v. 41, p. 140–149.

_____ 1982, Oklahoma earthquakes, 1981: Oklahoma Geology Notes, v. 42, p. 126–137.

_____ 1983, Oklahoma earthquakes, 1982: Oklahoma Geology Notes, v. 43, p. 24–35.

_____ 1984, Oklahoma earthquakes, 1983: Oklahoma Geology Notes, v. 44, p. 32–42.

_____ 1985, Oklahoma earthquakes, 1984: Oklahoma Geology Notes, v. 45, p. 52–61.

_____ 1986, Oklahoma earthquakes, 1985: Oklahoma Geology Notes, v. 46, p. 44–52.

_____ 1987, Oklahoma earthquakes, 1986: Oklahoma Geology Notes, v. 47, p. 65–72.

_____ 1988, Oklahoma earthquakes, 1987: Oklahoma Geology Notes, v. 48, p. 54–63.

_____ 1989, Oklahoma earthquakes, 1988: Oklahoma Geology Notes, v. 49, p. 40–48.

_____ 1990, Oklahoma earthquakes, 1989: Oklahoma Geology Notes, v. 50, p. 68–76.

_____ 1993, Oklahoma earthquakes, 1992: Oklahoma

Geology Notes, v. 53, p. 51–62.
Lawson, J. E., Jr.; DuBois, R. L.; Foster, P. H.; and Luza, K. V., 1979, Earthquake map of Oklahoma, earthquakes shown through 1978: Oklahoma Geological Survey Map GM-19, 15-page text, scale 1:750,000.
Lawson, J. E., Jr.; Luza, K. V.; and Moss, Dan, 1991, Oklahoma earthquakes, 1990: Oklahoma Geology Notes, v. 51, p. 50–61.
Lawson, J. E., Jr.; Luza, K. V.; Brown, R. L.; and Moss, Dan, 1992, Oklahoma earthquakes, 1991: Oklahoma Geology Notes, v. 52, p. 48–59.
Luza, K. V.; and Lawson, J. E., Jr., 1979, Seismicity and tectonic relationships of the Nemaha uplift in Oklahoma, part II: U.S. Nuclear Regulatory Commission, NUREG/CR-0875, 81 p.
_____ 1980, Seismicity and tectonic relationships of the Nemaha uplift in Oklahoma, part III: U.S. Nuclear Regulatory Commission, NUREG/CR-1500, 70 p.
_____ 1981, Seismicity and tectonic relationships of the Nemaha uplift in Oklahoma, part IV: U.S. Nuclear Regulatory Commission NUREG/CR-2439, 52 p.
_____ 1983, Seismicity and tectonic relationships of the Nemaha uplift in Oklahoma, part V: U.S. Nuclear Regulatory Commission NUREG/CR-3109, 115 p.
Luza, K. V.; DuBois, R. L.; Lawson, J. E., Jr.; Foster, P.; and Koff, L., 1978, Seismicity and tectonic relationships of the Nemaha uplift in Oklahoma: U.S. Nuclear Regulatory Commission, NUREG/CR-0050, 67 p.
Mykkeltveit, Svein; Ringdal, Frode; Kvaerna, Tormad; and Alewine, R. W., 1990, Application of regional arrays in seismic verification: Seismological Society of America Bulletin, v. 80, p. 1777–1801.
Nuttli, O. W., 1973, Seismic wave attenuation and magnitude relations for eastern North America: Journal of Geophysical Research, v. 78, p. 876–885.
Pulling, D. M., 1979, Subsurface stratigraphic and structural analysis, Cherokee Group, Pottawatomie County, Oklahoma: Oklahoma City Geological Society, Shale Shaker, v. 29, no. 6, p. 124–137; v. 29, no. 7, p. 148–158.
Stauder, W.; Hermann, R.; Singh, S.; Reidy, D.; Perry, R.; and Morrissey, Sean-Thomas, 1979, Central Mississippi Valley Earthquake Bulletin: First Quarter 1979, no. 19, 50 p.
Taff, J. A., 1902, Description of the Atoka Quadrangle (Indian Territory): U.S. Geological Survey Atlas, Folio 79, 8 p.
United States Earthquakes, Annual publication of: U.S. Dept. of Commerce, Coast and Geodetic Survey, 1928 through 1968; NOAA National Ocean Survey for 1969; NOAA Environmental Data Service for 1970–72 and U.S. Dept. of Commerce, NOAA, and U.S. Dept. of Interior, Geological Survey, for 1973 to present.
Wengerd, S. A., 1948, Fernvale and Viola limestones of south-central Oklahoma: American Association of Petroleum Geologists Bulletin, v. 32, p. 2183–2253.
Wheeler, R. R., 1960, The structural map of the Midcontinent from Denver to the east Texas Gulf Coast: Dallas, Texas, scale 1 in. = 6 mi. (Central series [consisting of 3 sheets] covers Oklahoma from T. 24 N., southward into north Texas.)
Zollweg, J. E., 1974, A preliminary study of the seismicity of the central United States, 1963–1974: St. Louis University unpublished undergraduate paper, 15 p.

PART II

ABSTRACTS AND SHORT REPORTS RELATED TO POSTER PRESENTATIONS

Structural Analysis of the Potato Hills, Ouachita Mountains, Oklahoma

Mark W. Allen
EnecoTech, Inc.
Tulsa, Oklahoma

Structural relationships in the Potato Hills (Fig. 1) have been controversial for more than 60 years. The Potato Hills have been interpreted as a window in the Windingstair thrust sheet (Miser, 1929) and as a window in the Jackfork Mountain thrust sheet (Miller, 1955; Roe, 1955; Arbenz, 1968). Detailed mapping, seismic interpretation, and analysis of several key well logs provide the basis for reinterpretation of structural relationships in the Potato Hills. Interpretations are based on data from three key areas and cross section A–A' (Figs. 1,2). In the northeastern area, mapping and subsurface control indicated that the North Potato Hills thrust was intersected and offset by the South Potato Hills thrust (Allen, 1991). In the western Potato Hills, the South Potato Hills thrust was found to continue westward (Allen, 1992), intersecting a minor back thrust (Fault A in Fig. 1), rather than "curving" to the northeast as previously mapped. In the northwestern Potato Hills, the North Potato Hills thrust was mapped extending to the northwest (Allen, 1994a) and not "curving" to the southwest.

Subsurface structure (Fig. 2, from Allen, 1994b) is based on the analysis of electric and sample logs and seismic interpretation. Analysis of the cross section reveals several items: (1) the North and South Potato Hills thrusts are definitely not the same fault; (2) a basal detachment separates lower Paleozoic strata from the Mississippian Stanley Group; (3) the Stanley Group is in fault contact with the underlying Pennsylvanian Jackfork Group; (4) tectonic evolution of the area resulted from north-directed horizontal translation on the basal detachment resulting in the formation of the imbricate thrust faults that exist in the Potato Hills; and (5) the lack of folded thrust faults indicates that the imbricate faults formed out-of-sequence from north to south (Allen, 1994b).

The window hypothesis for the Potato Hills was based on the assumption that the North Potato Hills thrust and the South Potato Hills thrust were one fault (called the Potato Hills thrust) that had been folded and eroded through exposing lower Paleozoic strata. Based on my mapping (Allen, 1991, 1992, 1994a) showing that the faults are separate faults and that the major thrust faults are not folded by sub-thrust stacking (Allen, 1994b), the window hypothesis is invalid. The Potato Hills are the surface expression of an imbricate-fan thrust system that developed from north-directed translation on a basal detachment.

REFERENCES CITED

Allen, M. W., 1991, Structural analysis of the northeastern Potato Hills, Ouachita Mountains, Oklahoma: Oklahoma Geology Notes, v. 51, p. 188–197.

_____ 1992, Structural analysis of the western Potato Hills, Ouachita Mountains, Oklahoma: Oklahoma Geology Notes, v. 52, p. 173–183.

_____ 1994a, Analysis of the North Potato Hills thrust: its importance to the interpretation of the Potato Hills, Ouachita Mountains, Oklahoma: Shale Shaker, v. 44, p. 75–78.

_____ 1994b, Subsurface structural geology of the Potato Hills, Ouachita Mountains, Oklahoma: Oklahoma Geology Notes, v. 54, p. 100–108.

_____ 1994c, Structural analysis and tectonic history of the Potato Hills, Ouachita Mountains, Oklahoma, *in* Suneson, N. H.; and Hemish, L. A. (eds.), Geology and resources of the eastern Ouachita Mountains frontal belt and southeastern Arkoma basin, Oklahoma: Oklahoma Geological Survey Guidebook 29, p. 253–261.

Arbenz, J. K., 1968, Structural geology of the Potato Hills, Ouachita Mountains, Oklahoma, *in* Cline, L. M. (ed.), A guidebook to the geology of the western Arkoma basin and Ouachita Mountains: Oklahoma City Geological Society Guidebook, AAPG/SEPM Annual Meeting Field Trip, p. 109–121.

Miller, B. W., 1955, Geology of the western Potato Hills, Pushmataha and Latimer Counties, Oklahoma: University of Oklahoma unpublished M.S. thesis, 55 p.

Miser, H. D., 1929, Structure of the Ouachita Mountains of Oklahoma and Arkansas: Oklahoma Geological Survey Bulletin 50, 30 p.

Roe, N. C., 1955, Geology of the eastern Potato Hills, Pushmataha and Latimer Counties, Oklahoma: University of Oklahoma unpublished M.S. thesis, 63 p.

Allen, M. W., 1995, Structural analysis of the Potato Hills, Ouachita Mountains, Oklahoma, *in* Johnson, K. S. (ed.), Structural styles in the southern Midcontinent, 1992 symposium: Oklahoma Geological Survey Circular 97, p. 233–235.

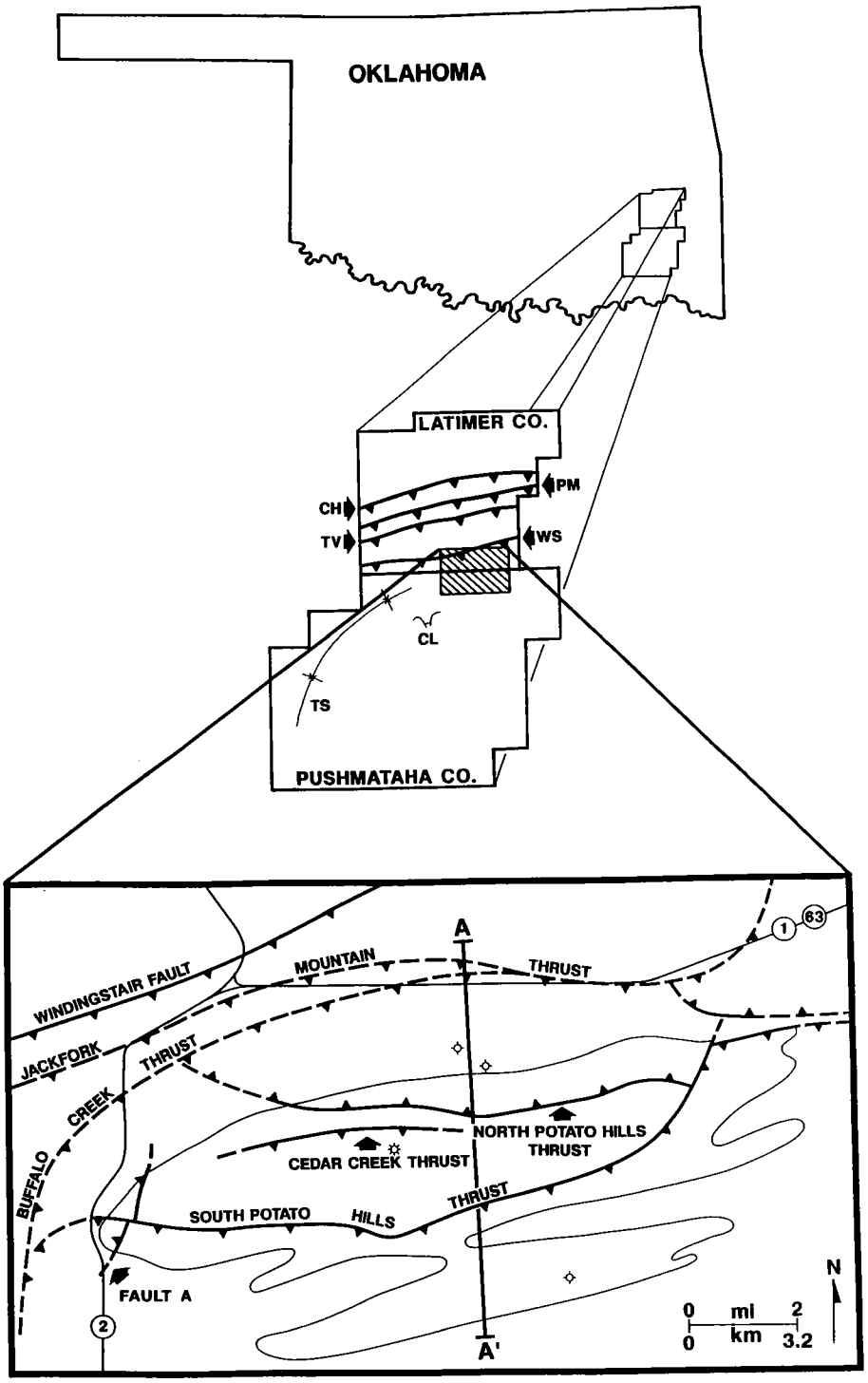


Figure 1. Potato Hills location map (Allen, 1994c). See Figure 2 for cross-section A–A'. CH = Choctaw fault, PM = Pine Mountain fault, TV = Ti Valley fault, WS = Windingstair Fault.

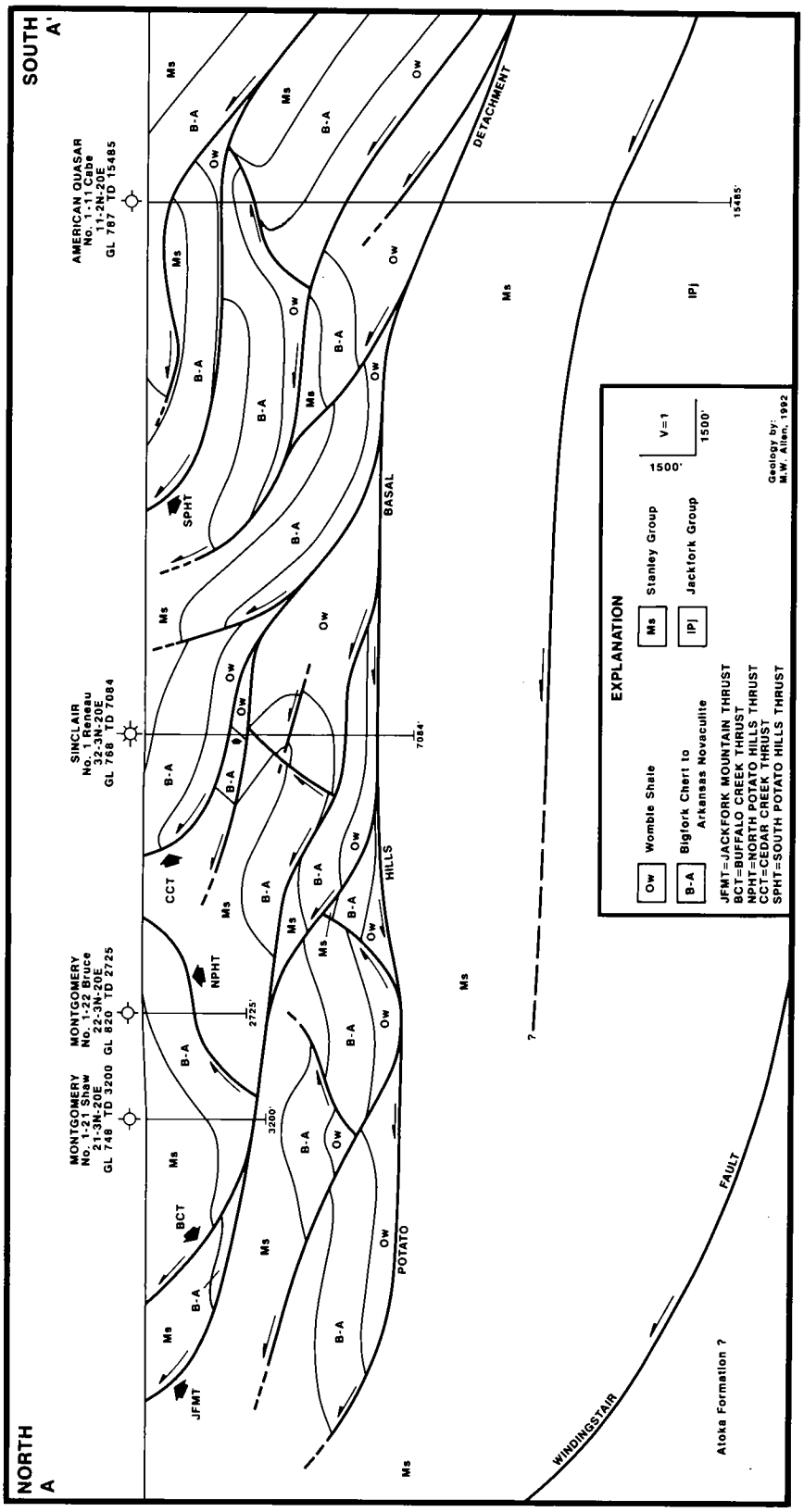


Figure 2. Structural cross section through the Potato Hills based on interpretation of seismic data, electric and sample logs, and surface geology. See Figure 1 for location of cross section and wells.

Reconnaissance Study of Womble Formation, Broken Bow Uplift

Steve Erickson
Independent Geologist
Robbinsdale, Minnesota

Bryan Tapp
University of Tulsa
Tulsa, Oklahoma

INTRODUCTION

The Ordovician Womble Formation crops out in the Black Knob region, and in the Broken Bow uplift of the Ouachita Mountains, but has received little study since the early part of the century. It contains predominantly fine-grained sandstones and shales (psammites) that have been metamorphosed to lowest greenschist grade, and have been recently interpreted as having accumulated in an accretionary prism (Houseknecht and Kacena, 1983). In this reconnaissance study we attempt to interpret the provenance, structural style, and tectonic setting of the Womble Formation.

Previous Work

The first description of rocks in the Womble Formation was made near Black Knob Ridge by Taff (1902), who used the term Stringtown Shale for the pre-Mississippian black shale underlying the Bigfork Chert. Purdue (1909) split the unit into two shales, the lower Ouachita Shale and the upper Stringtown Shale. Miser (1918) discontinued the use of the terms and introduced the term Womble Formation for the rocks between the Blakely Sandstone and the Bigfork Chert near the town of Womble, Arkansas (now Normal, Arkansas). The formation name and description were used by Honess (1923) in mapping the Broken Bow uplift, and by Hendricks and others (1937) in mapping the Black Knob Ridge. Later workers (Pitt, 1955; Dunagan, 1974; Hubert, 1984) combined the Womble with other formations in the area for mapping, due to limited outcrops and inaccurate description of the Womble Formation in Oklahoma. The purpose of this study is to determine if the Womble Formation is a mappable unit in the core area of the Ouachitas, and to attempt to place it into the stratigraphic and structural history of the region.

FIELD STUDY

Reconnaissance mapping was carried out in the winters of 1987–88 and 1988–89. In the field area, the Womble Formation was distinguished from the Bigfork Chert and Blakely Sandstone based on bedding thickness and composition. The Womble has generally thicker beds, from 4 in. to 5 ft thick, consisting mostly of medium-grained psammites. Chert beds are rare in the Womble Formation, and are usually bounded by thicker sandstone beds.

Unoriented samples were collected where the lithology was determined to be the most important feature, and where the bedding planes were obscured or undetermined. Oriented samples were collected where bedding and cleavage could be determined in the field. Oriented samples were collected for description of cleavage, and to attempt kinematic interpretation of transport direction during deformation.

Strike and dip of both bedding and cleavage were measured where present. Bedding orientation in the field area is uniform, plotting as a moderately well-defined cluster on stereographic projection (Fig. 1A). The area contains relatively few small folds, whose hinges are nearly horizontal and may be related to local thrust faults. Cleavage orientation is relatively uniform across the field area, and plots as a moderately well-defined cluster on stereographic projection (Fig. 1B). Cleavage is easily recognized in the field. It occurs at a low angle relative to bedding, in the hinges of folds where the cleavage takes on an axial planar orientation. The relationships between folds, cleavage, and bedding suggest that all developed in a single deformation event. The cross-cutting, multiphase deformation events seen in Silurian age rocks in the Broken Bow uplift (Feenstra and Wickham, 1975; Nielsen, 1982) are not apparent within the field area.

Erickson, Steve; and Tapp, Bryan, 1995, Reconnaissance study of Womble Formation, Broken Bow uplift, *in* Johnson, K. S. (ed.), Structural styles in the southern Midcontinent, 1992 symposium: Oklahoma Geological Survey Circular 97, p. 236–239.

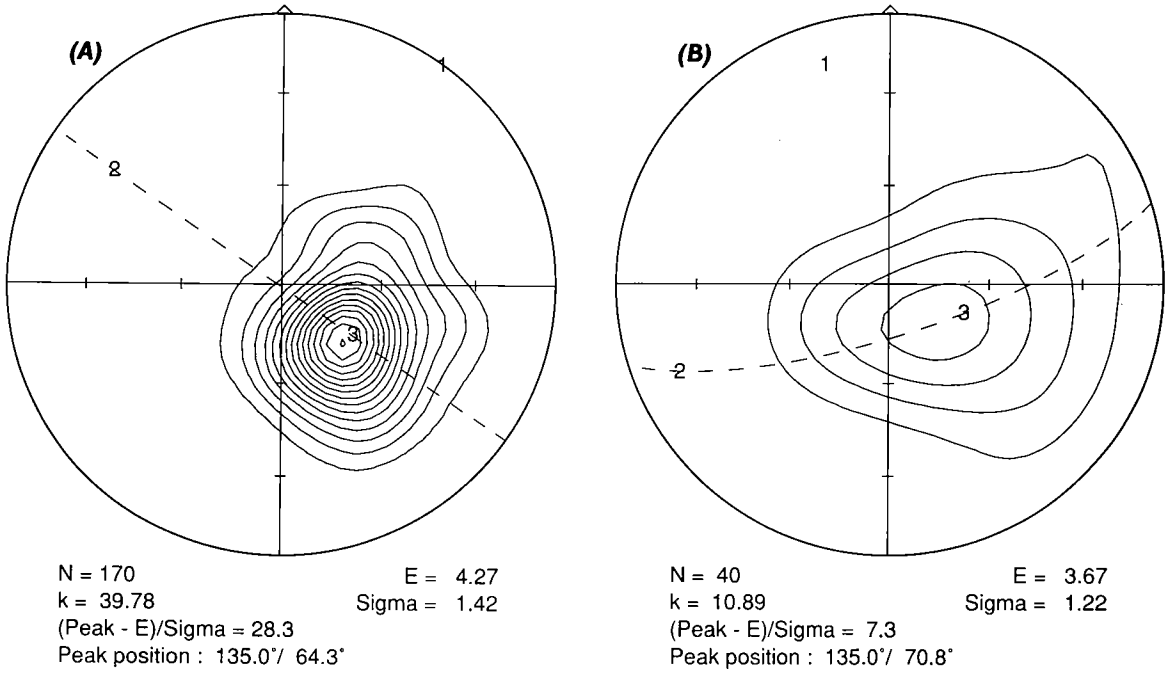


Figure 1. Contoured plot of bedding (*A*) and cleavage (*B*) orientation data; both figures show a moderately well-defined cluster, indicating a single deformation event for this region of the uplift.

The most striking features seen in the field are several low-angle thrust faults, present both within the body of the Womble Formation and at the contacts of the Womble with the Bigfork Chert and the Blakely Sandstone (Erickson, 1990). Seven distinct thrust faults were located in the field; however, the faults could not be traced laterally. The thrust faults dip to the north, and may have transport directions to the south, although the kinematics are unclear and the interpreted transport direction is based on only a few slickenside measurements and rotational markers. Each location where the contacts with both the overlying Bigfork and underlying Blakely are well exposed shows evidence of thrust faulting. This has led us to conclude that the formational contacts in the study area are thrust contacts rather than depositional contacts, and that stratigraphic thickness measurements and detailed stratigraphic reconstructions of the Womble in the study area are impossible. The Bigfork chert was found to be clearly in thrust contact with the Womble at three different locations. At two of these, the Womble was thrust over Bigfork cherts (Erickson, 1990).

The diabase sill reported in the Womble by Honess (1923) was closely examined in the field. Several lines of evidence suggest that this feature is not a Mesozoic sill. The contacts do not show any indication of contact metamorphism. The contacts of the sill are thrust contacts, and the body shows evidence of transportation along the thrusts (Erickson, 1990). Thin-section examination shows that the sill has been deformed, and it possesses a weak disjunctive cleavage with the same orientation as the cleavage in the surrounding rock. Although the textures in the rock support the conclusion that the feature is a sill, the cleavage and nature of the contacts suggest that it was incorporated into the Womble during the tectonic event that formed the cleavage and thrusts present in the study area.

PETROLOGY AND PETROGRAPHY

Samples collected in the field were brought back to the lab for hand-specimen and thin-section description, X-ray diffraction, and microprobe work. Polished slabs were stained using Alizarin Red-S, and described through a binocular microscope using color, composition, grain shape, grain orientation, grain size, sorting, fabric, grain-to-grain contact, and matrix. Fifty samples were selected for thin-section study, using point counts of 250 grains (Erickson, 1990). Samples with 50% or more clay were analyzed using standard X-ray methods. The results of these studies are briefly described below.

Cleavage and Metamorphic Grade

Pressure solution was observed in most samples, and is the dominant mechanism of cleavage formation. The cleavage is a rough, anastomosing disjunctive cleavage. No high-grade metamorphic

minerals, textures, or relic textures were observed in these samples, except as lithic fragments. The Womble has not been exposed to temperatures or pressures above lower greenschist. The schistose nature of the Womble Formation, described as a field characteristic, is due entirely to disjunctive cleavage, and much of the local quartz accumulations may be the result of quartz dissolution along the disjunctive cleavage.

Grain Types and Provenance

Quartz grains are the most common type of grain observed in the psammites. Most of the quartz is monocrystalline, without undulose extinction; although some grains do show undulose extinction due to post-depositional deformation along cleavage traces. Lithic fragments are the second most common type of grain, with polycrystalline quartz and recrystallized quartz grains being most common. Many of the polycrystalline quartz rock fragments appear to be metamorphic in origin. Sedimentary rock fragments of sandstones, claystones, and carbonates are present in many samples. Clasts were determined to be sedimentary, if individual grains could be seen within the clast boundaries. Chlorite was observed in many thin sections, as detrital clasts and as an authigenic mineral. Most of the authigenic chlorite occurs as very small grains that are aligned parallel with the cleavage trace in thin section, and is easily distinguished from detrital chlorite. Detrital biotite is also seen in some slides. Muscovite occurs as an authigenic mineral. Metamorphic rock fragments and igneous rock fragments are found in many samples. Metamorphic rock fragments are mostly schists containing biotite, chlorite, and muscovite or quartz. Igneous rock fragments include fragments of plutonic rocks and volcanic rocks. Individual feldspar grains are uncommon relative to the quartz and lithics. Most of the feldspar is sodic plagioclase, and microprobe data show them to be albite (Erickson, 1990).

The point-count data are plotted on a quartz-feldspar-lithic fragment diagram (Fig. 2) to show the provenance of the Womble Formation. The data indicate a recycled-orogen provenance, specifically a foreland-uplift provenance (Dickinson and Suczek, 1979).

TECTONIC SETTING

Houseknecht and Kacena (1983) described an accretionary model for the development of the Ouachita Mountains and the Arkoma basin. The field and petrologic data we collected suggest that this might be a reasonable interpretation since the Womble shows a tectonic provenance, with overall thrust contacts similar to that of the Shimanto belt, Japan (Taira and others, 1988), and the incorporation of a sill early in the accumulation/deformation phase of the Womble Formation.

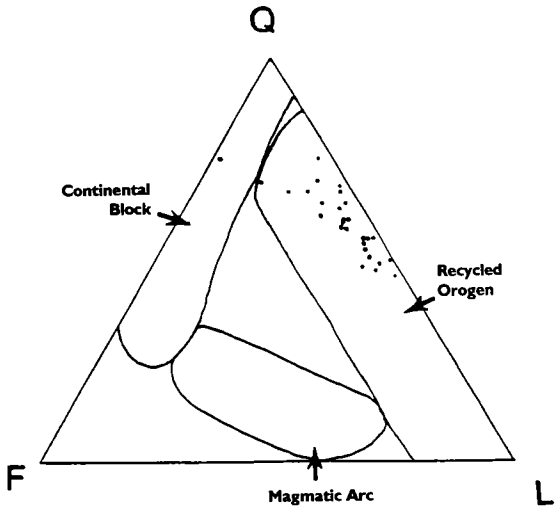


Figure 2. Quartz-feldspar-lithic fragment plot of point-count data from thin sections. These points fall within the "recycled orogen" area of Dickinson and Suczek (1979).

CONCLUSIONS

Data collected in this reconnaissance study support the following conclusions:

1) Metamorphism is only to lower-greenschist grade. No high-grade metamorphic minerals, textures, or fabrics were found, except as detrital fragments. Grains in the psammites are mostly monocrystalline quartz, lithic fragments such as polycrystalline quartz, shale, igneous and metamorphic rock fragments, including chlorite schist.

2) The Womble Formation is in fault contact with the Bigfork Chert in the field area. This can be demonstrated by the sheared and distorted beds lying between the two formations, the nonconformable relationship between the beds in the area, and, in two locations, Womble overlying Bigfork Chert. Thrust faults are the most significant structural features found in the area.

3) The detrital composition of the sediments in the Womble matches the recycled-orogen provenance, supporting the accretionary-prism model for the rocks in the region.

REFERENCES CITED

Dickinson, W.; and Suczek, C., 1979, Plate tectonics and sandstone compositions: American Association of Petroleum Geologists Bulletin, v. 63, p. 2164–2182.

Dunagan, J. F., 1976, Geology of the Lower Ordovician rocks of the Choctaw anticlinorium, southeastern Oklahoma: University of Oklahoma unpublished M.S. thesis, 46 p.

Erickson, S. G., 1990, A reconnaissance mapping of the Womble Formation along the Glover River, McCurtain County, Oklahoma: University of Tulsa

unpublished M.S. thesis, 85 p.
Feenstra, R.; and Wickham, J., 1975, Evolutions of folds around Broken Bow uplift, Ouachita Mountains, southeastern Oklahoma: American Association of Petroleum Geologists Bulletin, v. 59, p. 974–985.
Hendricks, T. A.; Knechtel, M. M.; and Bridge, J., 1937, Geology of the Black Knob Ridge, Oklahoma: American Association of Petroleum Geologists Bulletin, v. 21, p. 1–29.
Honess, C. W., 1923, Geology of the southern Ouachita Mountains of Oklahoma: Oklahoma Geological Survey Bulletin 32, pt. 1, 278 p.
Houseknecht, D. W.; and Kacena, J. A., 1983, Tectonic and sedimentary evolution of the Arkoma foreland basin, *in* Houseknecht, D. W. (ed.), Tectonic-sedimentary evolution of the Arkoma basin and guidebook to deltaic facies, Hartshorne sandstone: Society of Economic Paleontologists and Mineralogists, Midcontinent Section Meeting Guidebook, v. 1, 119 p.
Hubert, L. M., 1984, Structure and lithologic variation in the central core of the Broken Bow uplift, Ouachita Mountains, Oklahoma: University of Texas at Dallas unpublished M.S. thesis, 112 p.
Miser, H. D., 1918, Manganese deposits of Arkansas, *in* Contributions to economic geology: U.S. Geological Survey Bulletin 660, p. 59–122.
Nielsen, K. C. (ed.), 1982, Structural styles of the Ouachita Mountains, southeastern Oklahoma: Program in Geosciences, The University of Texas at Dallas, 72 p.
Pitt, W. D., 1955, Geology of the core of the Ouachita Mountains of Oklahoma: Oklahoma Geological Survey Circular 34, 34 p.
Purdue, A. H., 1909, The slates of Arkansas, with a bibliography of the geology of Arkansas by J. C. Branner: Arkansas Geological Commission, Little Rock, 170 p.
Taff, J. A., 1902, Description of the Atoka Quadrangle [Indian Territory]: U.S. Geological Survey Geologic Atlas, Folio 79, 8 p.
Taira, A.; Katto, J.; Tashiro, M.; Okamura, M.; Kodama, K., 1988, The Shimanto belt in Shikoku, Japan—evolution of Cretaceous to Miocene accretionary prism: Modern Geology, v. 12, p. 5–46.

Structural and Stratigraphic Framework of the Wapanucka Formation (Pennsylvanian), Southeastern Oklahoma

Victoria L. French and Robert C. Grayson, Jr.
Baylor University
Waco, Texas

Surface exposures of the Wapanucka Formation (Pennsylvanian) occur in a northeast–southwest-trending belt along the frontal Ouachita Mountains and on the northeastern margin of the Arbuckle Mountains. The formation is present in the subsurface throughout most of the Arkoma basin, where the unit is a proven gas reservoir (Fig. 1). Exploitation of this resource will be enhanced through detailed knowledge of its structural and stratigraphic framework.

Accumulation and subsequent deformation of the Wapanucka occurred in three overlapping stages: (1) deposition on a passive margin, (2) burial and normal faulting associated with the development of the Arkoma (foreland) basin, and (3) thrusting along the southern margin of the basin. In the Ouachita Mountains, the Wapanucka (Morrowan) consists primarily of spiculite, spiculitic limestone, bioclastic and oolitic calcarenite, algal-micritic limestone, and shale. These lithologies occur in several shoaling sequences separated by flooding events. The shallow-shelf and shelf-margin regimes, which existed on a ramp-like passive margin, persisted through deposition of the overlying Spiro Formation (Atokan).

The predominantly north–south transitional nature of Wapanucka shoaling sequences can be established from study of exposures along the frontal Ouachita Mountains and of core from the Arkoma basin (Fig. 2). The southernmost exposures of Wapanucka consist largely of shale and spiculite, with a few thin allodapic calcarenites. Measured sections located on more northerly imbricates, and cores from the sub-Choctaw thrust, record a shallower marine environment characterized by shoaling sequences that contain significant amounts of algal-micritic and spiculiferous limestone. Along the northeastern margin of the Arbuckle Mountains, the Wapanucka consists almost entirely of shallow-shelf carbonates. Northwestward, within the Arkoma basin, the Wapanucka exhibits shallow-shelf, shoaling characteristics, as observed in cores from the Chiles dome field. Geographically restricted oolitic shoaling sequences suggest deposition on local highs; they are indicative of a continuation of shallowing conditions to the north and west with respect to exposures along the northern part of the frontal Ouachita Mountains. The transitional nature of the facies indicate deposition on a ramp-like shelf rather than on a shelf with a sharp shelf break (Fig. 3).

Intraformational conglomerates within the Wapanucka and Spiro suggest that normal faulting, associated with the advancing thrust system and incipient subsidence of the Arkoma basin, had begun during Morrowan and early Atokan time. Increasing rates of subsidence led to establishment of the Arkoma (foreland) basin, tilting of the northern margin of the basin, and increased normal faulting. In the western Arkoma basin, the relationship between the Wapanucka and overlying Atoka is complex and was controlled, in part, by penecontemporaneous faulting. Regional correlation suggests that the Wapanucka–Atoka Formation boundary represents a flooding event across a faulted surface, which resulted in localized erosion and truncation of the Wapanucka.

Further emplacement of Ouachita thrust sheets cratonward carried the Wapanucka to the surface in the frontal Ouachita Mountains. In addition, the subsurface Wapanucka is displaced by blind thrusts in the southern Arkoma basin. Resultant structural traps produce from Wapanucka strata at the Pittsburgh, South Blanco, and Wesley fields (Fig. 1). Gas is produced from beneath the Choctaw fault in the Pittsburg field and from multiple thrust-faulted reservoirs in the South Blanco field. Farther north in the Arkoma basin, the Wapanucka is a vi-

French, V. L.; and Grayson, R. C., Jr., 1995, Structural and stratigraphic framework of the Wapanucka Formation (Pennsylvanian), southeastern Oklahoma, *in* Johnson, K. S. (ed.), Structural styles in the southern Midcontinent, 1992 symposium: Oklahoma Geological Survey Circular 97, p. 240–243.

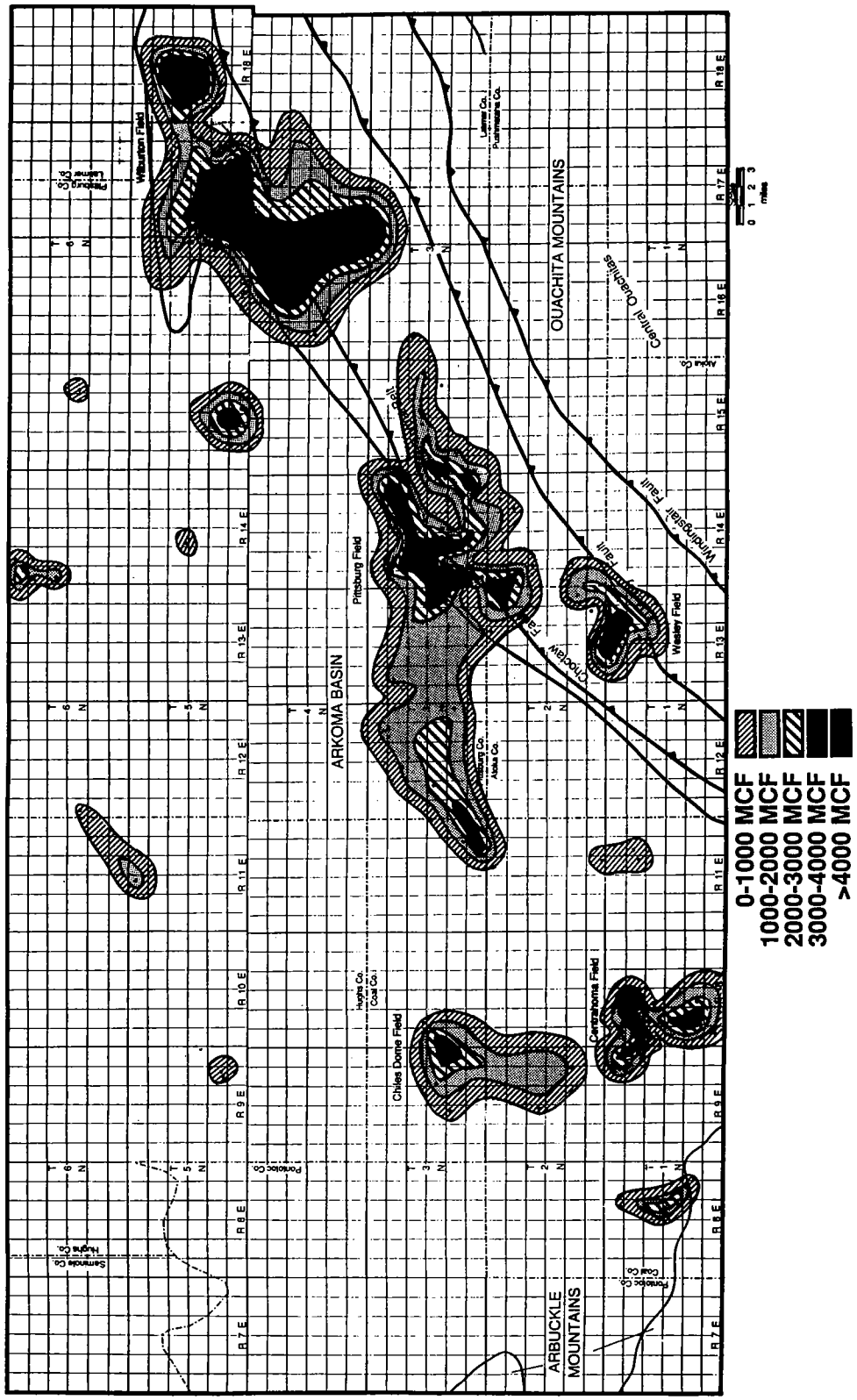


Figure 1. Map showing initial-production flow from the Wapanucka Formation in major fields within the Arkoma basin and frontal Ouachita Mountains. In the Wilburton field area, initial-production flow is from Spiro/Wapanucka combined.

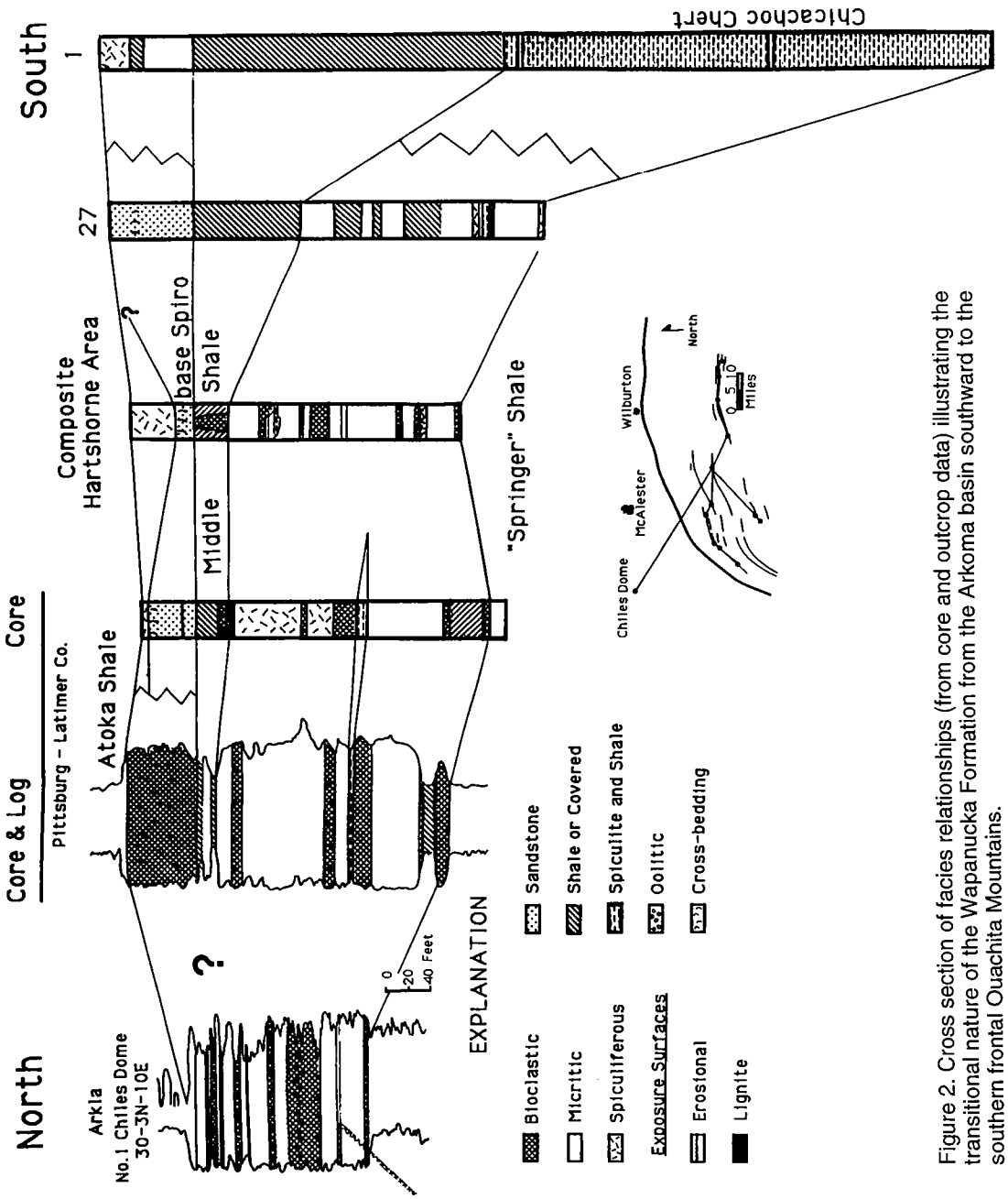


Figure 2. Cross section of facies relationships (from core and outcrop data) illustrating the transitional nature of the Wapanucka Formation from the Arkoma basin southward to the southern frontal Ouachita Mountains.

able gas reservoir in the Chiles dome and Ashland fields. Similar undiscovered hydrocarbon traps likely exist. Following termination of thrusting, the area has remained relatively stable. Further structural and stratigraphic studies concerning the Wapanucka Formation are likely to produce additional information leading to the discovery of new hydrocarbon accumulations.

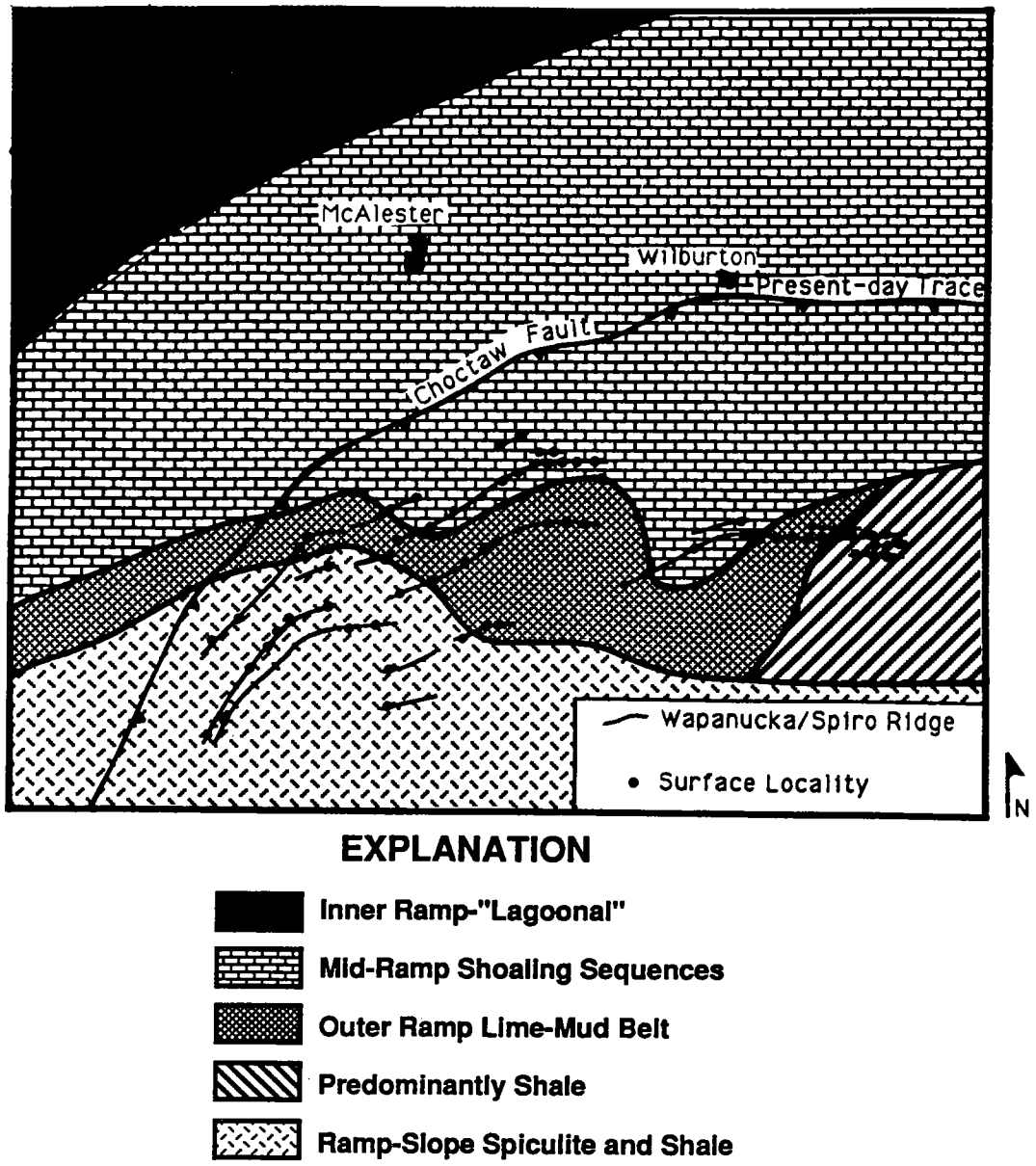


Figure 3. Diagrammatic map illustrating generalized Wapanucka facies belts developed on a ramp-like depositional surface.

Relationships of Southern Midcontinent Structures to a Postulated Late Precambrian Transcontinental Fault

Gary L. Kinsland
University of Southwestern Louisiana
Lafayette, Louisiana

ABSTRACT.—Kinsland (1982) pointed out that a remarkable pattern match could be attained by cutting a national gravity map from Florida to Montana, and shifting the portions by about 800 km. Such an action implies a fault termed the North American transcontinental transform fault (NATTF). Information uncovered in attempts to deny or confirm the existence of such a fault has not been conclusive; rather, it has illuminated the coincidence of many southern continental-basement features (e.g., central Kansas uplift, southern "termination" of the Midcontinent rift, northeastern boundary of the Arkoma basin, southern termination of the Reelfoot rift, eastern "termination" of the Ouachitas, and the Mississippi slate belt) with the trace of the fault. Consideration of the NATTF as a possible causal element in the development of these features would lead to different interpretations of their histories and consequently to different interpretations of resource potentials. A stepwise developmental scenario for the central North American basement presented here counters the objections most often raised to this hypothesis.

INTRODUCTION

Kinsland (1982) presented an interpretation, based primarily on the filtered gravity data of Hildenbrand and others (1982), which implied a strike-slip fault extending northwesterly from the southeastern United States through Montana. Kinsland (1986) published the most comprehensive representation of the evidence relating to this proposal to date. The current report contains some of the previously published evidence (especially that which relates to the structure of the southern Midcontinent) and much evidence not previously presented. In this short note only a few of the figures can be published; consequently, the most important ones are included, and synopses of the evidence contained in the others, along with references to their origins, are enumerated. Certainly this is a radical proposal, the acceptance of which would necessitate changing many ideas about North American continental structure and evolution. At the end of this note, after presenting the evidence for terminations and offsets of features along this line, I enumerate evolutionary steps which could lead to a basement that is faulted as I suggest.

CORRELATIONS, TRUNCATIONS, AND COLINEARS

Figure 1A is filtered gravity data from Hildenbrand and others (1982). In Figure 1B these data have been cut and offset, implying right-lateral offset of ~800 km. The cut is a single cut along a small circle (see Kinsland 1986); however, it is understood that any such faulting would occur over a zone tens of kilometers wide and would not perfectly fit a smooth curve. Particularly note that the offset juxtaposes the signature from the area of the present-day Ouachitas with the signature from the present-day Appalachians and the pattern of the Midcontinent rift (MCR) in Kansas with that in the area of the Hartville uplift in Wyoming.

Similar cutting and offset of the composite Magnetic Anomaly Map of the United States (U.S. Geological Survey, 1982) also produces a pattern match across the cut. In particular, the anomaly of the Hartville uplift, unusually narrow and linear for Laramide uplifts, is matched with the narrow, linear anomaly of the MCR.

The map of the vertical gravity gradients of North America (Arkani-Hamed and Urquhart, 1990) also correlates after being offset. One striking new pattern, continuous across the offset map, arises—a roughly SSW-striking band of anomalies from Hudson's Bay down to the Black Hills, thence across the fault into western Montana and on through Idaho to western Arizona. The northern part is the signature of the Trans-Hudsonian Collisional Belt. Is the southern part related? Correlations may be seen on the unoffset and offset reduced-to-the-pole magnetic anomalies of North

Kinsland, G. L., 1995, Relationships of southern Midcontinent structures to a postulated late Precambrian transcontinental fault, Arkansas, *in* Johnson, K. S. (ed.), Structural styles in the southern Midcontinent, 1992 symposium: Oklahoma Geological Survey Circular 97, p. 244–248.

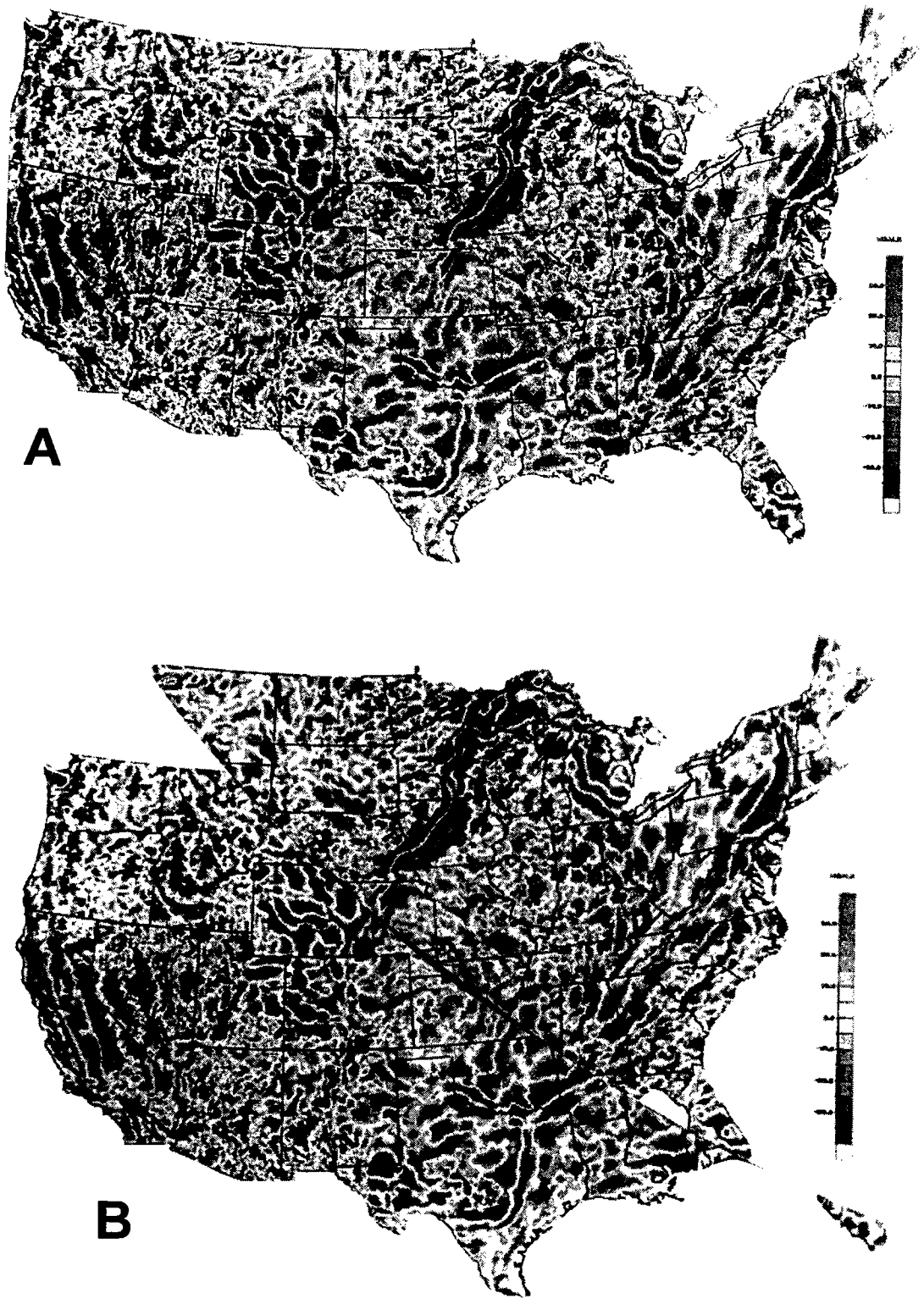


Figure 1. *A*—Filtered gravity data: cutoff wavelengths of 250 km (short wavelengths passed), reproduced from the color map of Hildenbrand and others (1982). *B*—The map shown in *A*, cut and recombined so as to imply a left-lateral strike-slip fault of ~800 km offset.

America map (Arkani-Hamed and Urquhart, 1990). Here, too, an anomaly apparently related to the Trans-Hudsonian Collisional Zone is continuous across the fault after offset.

The proposed fault superimposed on the horizontal gravity gradient map of Hildebrand (1985) truncates the Reelfoot rift and MCR. On the ratio map (magnetization-contrast/density-contrast) of Hildenbrand (1985), the proposed fault truncates four anomalies: the Reelfoot rift, the MCR, and two distinct low-ratio zones between the rifts.

The proposed fault runs NW–SE, almost exactly through the northwestern corner of Arkansas (Fig. 1B) and is colinear with a NW-trending "zone of abrupt basement dislocation" in Mississippi and Arkansas (Woods and Addington, 1973).

In Yarger's (1985) figures 11, 13, and 14, the proposed fault (zone) would enter Kansas from the south at ~95.5° and exit in the north at ~101°. Such a fault would, in figure 11, parallel the central Kansas uplift, cross (without offsetting) the Humboldt fault, and divide the state into a northeastern part with N–S-trending basement contours and a southwestern part with E–W-trending contours. In his figures 13 and 14, note that the dense bands of magnetic lineations possibly related to the rift are not colinear across the proposed fault.

A POSSIBLE EXPLANATION

1. I suggest that in the late Precambrian much of the continental interior was age layered. Underneath Kansas and Wyoming (as well as elsewhere), >2.5 b.y. (billion-year-old) rocks underlay 1.9 b.y. rocks, which in turn underlay 1.6–1.3 b.y. rocks. Certainly some of the younger rocks of the Midcontinent were intrusive into the older rocks, but the boundaries between major units were roughly horizontal, with younger units (sedimentary, extrusive, and/or overthrust) on top. This situation persists today in some places (see seismic section from Pratt [1988] and Fig. 2).

2. The Precambrian continent was fundamentally fractured, with predominant directions being NW–SE and NE–SW. These fractures persist today (see lineament map by Thomas [1976] and Proceedings of the International Conferences on Basement Tectonics, vols. 1–7). How these fractures were formed, I do not know; however, I suggest they are maintained through time and are propagated upwards and outwards by earth tides.

3. About 1.1 billion years ago, the MCR was propagated into Kansas, roughly following NE–SW fractures with segments of the rift offset along NW–SE fractures—successive southwestern segments being less well-developed than segments to the NE.

4. Late Precambrian–early Paleozoic opening of the Iapetian Sea occurred with rifts along NE–SW fractures and transform faults along NW–SE fractures. This is well documented in many studies of the Paleozoic continental margin of eastern North America.

5. I suggest that at this time (late Precambrian–early Paleozoic) a major NW–SE-trending transform fault developed northwestward (facilitated by the preexisting continental fracture pattern) from the eastern continental margin, cutting completely through the continent. This I call the North American transcontinental transform fault (NATTF) (Kinsland, 1984). At this time the eastern margin of North America would have been a rift passive margin (RPM) from Canada to Alabama, a major transform passive margin (TPM) from Alabama through Mississippi into Arkansas, and RPM from Arkansas into Texas (Kinsland, 1984,1986).

6. I suggest that this fault offset the incipient southwesternmost segment of the MCR to become what is now the Hartville uplift (Fig. 2). It offset the southwestern extension of the Reelfoot rift to a position nearly opposite the MCR. It also offset the Iapetian RPM, which is now underneath the Ouachita and Appalachian Mountains. This ~800 km of offset could have occurred in about 20 million years, with relative plate motion rates of 4 cm/year.

7. In the area of the MCR, some sediments had probably been deposited, but not all of the Rice Formation. In the area of the Hartville uplift, an immature rift probably existed in the shallower Precambrian rocks (1.6–1.3 b.y.). Underneath this immature rift, the rift faulting continued downward into older Precambrian rocks (more than 2.5–1.9 b.y.). A "rift pillow" (a deep magma chamber that supplies magma for rift volcanoes) existed within the older rocks and extended underneath what is today the Hartville uplift (Fig. 2).

8. Subsequent erosion combined with differential vertical movement across the NATTF, major regional uplift in Wyoming, and local Laramide uplifts, have created at the surface (or in subcrop beneath younger sediments) a Precambrian basement with a variety of ages at the top. Today in Kansas, the subcropping Precambrian surrounding the MCR is about 1.6–1.3 b.y., with clear evidence of erosion as Precambrian mesozonal rocks subcrop adjacent to Paleozoic sedimentary rocks. At the Hartville uplift, the younger Precambrian rocks which would contain the proposed immature rift are gone. What remains is the Hartville uplift, composed of older Precambrian rocks containing a multiply reactivated NE–SW-trending Precambrian fault system (Snyder, 1991). Beneath the Hartville uplift, a dense rift pillow may be present (Fig. 2) that could account for some of the gravity anomaly associated with the Hartville uplift. The linear magnetic anomaly of the Hartville uplift could also be largely accounted for by the same rift pillow raised above the Curie depth by Laramide uplift, and/or by mafic intrusions sourced from the rift pillow below, few, if any, of which are exposed at the present-day surface (Humphris and Kinsland, 1992). (This proposed southwesternmost MCR segment may never have developed to the stage charac-

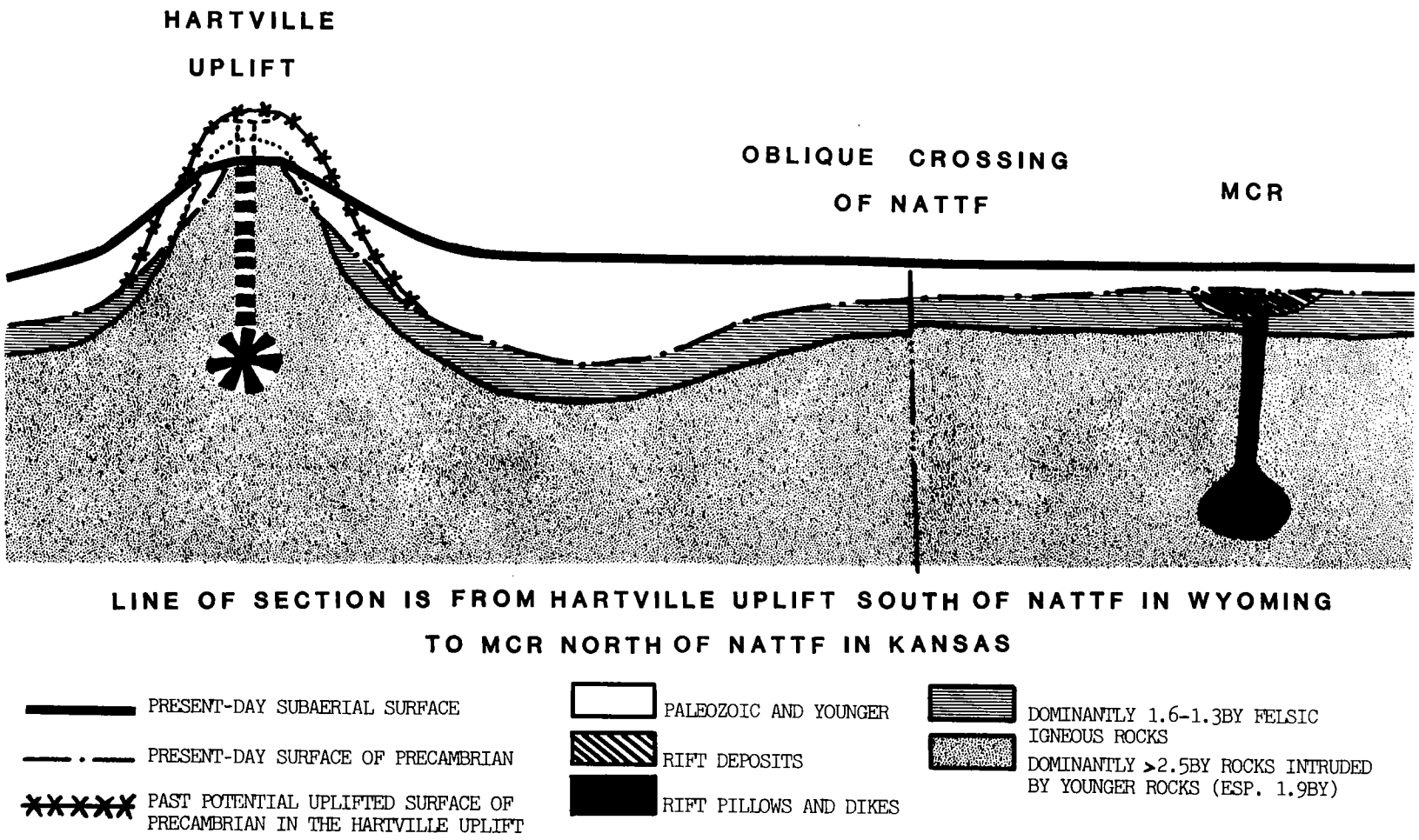


Figure 2. Diagrammatic, hypothetical cross section from the Hartville Uplift in Wyoming to Midcontinent Rift (MCR) in Kansas. The cross section is subparallel to the proposed fault and obliquely crosses it somewhere in southern Nebraska. This cross section illustrates how a proposed rift pillow and dike in the Hartville uplift could have been an extension of the MCR intrusives even though the MCR intrusives are surrounded by 1.6–1.3 b.y. rocks and the uppermost Precambrian rocks at the Hartville uplift are largely >2.5 b.y.

terized by lava flows fed from the rift pillow.) (See Fig. 2.)

9. Carboniferous deformation in Kansas resulted in the Nemaha ridge which parallels the MCR and crosses the NATTF. Perhaps the MCR discontinuity in the crust concentrated stresses, causing minor propagation of fractures into the adjacent unrifted crust SW of where the MCR had been cut off by the NATTF (Kinsland, 1989). This fracturing may have been aided by the near-coincidence of the offset southwest end of the Reelfoot rift fracture system.

10. Late Paleozoic collision along the Eastern continental margin resulted in formation of the Ouachita and Appalachian Mountains over the RPMs, and the buried deformed belt underneath Mississippi along the TPM. Perhaps collision against such a major offset of the RPM resulted in propagation of a fault southeastward into the colliding landmass. This could explain the major geological and geophysical discontinuity in southern Florida, which is colinear with the Bahamas fracture zone and the NATTF. Continental material southeast of the RPMs was not part of North America until this collision; i.e., the NATTF did not offset rocks and geophysical anomalies southeast of the RPMs. The alignment of anomalies southeast of the RPMs in the reconstructions may be attributable to similarities in subsequent tectonic processes at similar distances from the late Precambrian–early Paleozoic RPMs.

GENERAL COMMENTS

I presented some remarkable coincidences and a fault idea which might explain them. This idea is not new; I arrived at it when I first saw the filtered gravity map of Hildenbrand and others (1982), and subsequently found that Sam Carey (1976) had considered it years before. Since that time I have found many features coincident with the fault. Some are discussed here, and many others are in the references listed here.

I cannot "prove" that the fault which I call the North American transcontinental transform fault exists. Whether one can "prove" that it does not exist may depend upon how strongly one believes in current models of continental crustal structures and evolution. Models are used to interpolate separate geologic data to form maps and cross sections with the result that current maps and cross sections are reflections of current models.

I ask only that you consider the evidence presented here, and the idea of the NATTF when forming models and making maps in your own area. Perhaps this different idea will help explain some data with which you have been struggling.

REFERENCES CITED

Arkani-Hamed, J.; and Urquhart, W. E., 1990, Reduction to the Pole of the North American magnetic anomalies: Geophysics, v. 55, no. 2, p. 218–225.

Carey, S. W., 1976, The expanding Earth, developments in geotectonics, no. 10: Elsevier Science Publishers, Amsterdam, p. 377–380.

Hildenbrand, T. G., 1985, Magnetic terranes in the central United States determined from the interpretation of digital data, *in* Hinze, W. J. (ed.), The utility of regional gravity and magnetic anomaly maps: Society of Exploration Geophysicists, p. 248–266.

Hildenbrand, T. G.; Simpson, R. W.; Godson, R. H.; and Kane, M. F., 1982, Digital colored residual and regional Bouguer gravity maps of the conterminous United States with cut-off wavelengths of 250 km and 1000 km: U.S. Geological Survey Geophysical Investigations Map GP 953-A.

Humphris, D. D.; and Kinsland, G. L., 1992, Possibilities of similar rift histories for the central North American rift system in Kansas and the Hartville uplift in Wyoming, *in* Mason, R. (ed.), Proceedings of the 5th International Conference on Basement Tectonics, Ontario, Canada, August 1987: International Basement Tectonics Association Publication No. 7, p. 341–351.

Kinsland, G. L., 1982, Transcontinental transform?: American Geophysical Union, Spring Meeting Program and Abstracts, p. 49.

_____1984, Basement structure of the Gulf Coast: interpretation of gravity anomalies supported with structural, magnetic and seismic data, *in* White, B. R. (ed.), Proceedings: Gulf Coast Association of Geological Societies Annual Meeting, Shreveport, Louisiana, vol. 34, p. 85–94.

_____1986, Transcontinental transform fault across North America, *in* Riad S.; and Baars, D. L. (eds.), Proceedings of the 5th International Conference on Basement Tectonics, Cairo, Egypt, October 16–18, 1983: International Basement Tectonics Association Publication No. 5, p. 267–284.

_____1989, The North American transcontinental transform fault—a case where mega-regional geophysical investigations influence Kansas exploration strategies: Geophysics in Kansas, p. 297–301.

Pratt, Thomas, 1988, Proterozoic layered sequence: EOS, Transactions American Geophysical Union, v. 69, no. 17, cover and caption.

Thomas, G. E., 1976, The crustal fracture system of North America and its possible origin, *in* Hodgson, R. A.; Gay, S. P., Jr.; and Benjamins, J. Y. (eds.), Proceedings of the First International Conference on the New Basement Tectonics: The Utah Geological Association, Salt Lake City, p. 537–549.

U.S. Geological Survey, 1982, Composite magnetic anomaly map of the conterminous United States: U.S. Geological Survey Map GP-954A.

Woods, R. D.; and Addington, J. W., 1973, Pre-Jurassic geologic framework, northern gulf basin: Gulf Coast Association of Geological Societies Transactions, vol. 23, p. 179–195.

Yarger, H. L., 1985, Kansas basement study using spectrally filtered aeromagnetic data, *in* Hinze, W. J. (ed.), The utility of regional gravity and magnetic anomaly maps: Society of Exploration Geophysicists, p. 213–232.

Wapanucka Formation (Morrowan): Facies and Fractures, Frontal Ouachita Mountains

Darrell L. Mauldin
Phillips Petroleum Co.
Bellaire, Texas

Robert C. Grayson, Jr.
Baylor University
Waco, Texas

INTRODUCTION

Gas discoveries in the frontal Ouachita Mountains are attributable to structural and stratigraphic relationships within the overthrust belt. Although most gas production has been from the Spiro sandstone, the Wapanucka limestone (Morrowan) has locally proven to be a gas reservoir.

Fractures in Wapanucka limestones are commonly related to the lithology and are important factors for gas production. For example, the Amoco no. 1 Zipperer had a production test of 48.8 MMcfgd (million cubic feet of gas per day) from fractured Wapanucka limestone. Commingling gas from the Wapanucka and the Spiro, this well has produced 21.7 Bcfg (billion cubic feet of gas) from August 1988 to February 1992. Also, portions of the Pittsburg field produce from fractured micritic limestone (Montgomery, 1989).

Three Wapanucka facies are potential hydrocarbon reservoirs. These are those shallow shelf deposits that contain: oolites, phylloid algae, and in situ sponges with scattered sponge spicules. The oolitic and phylloid-algal facies might contain primary or diagenetic porosity, whereas the sponge boundstone and spiculitic-limestone facies could develop significant fracture porosity in certain structural configurations. Thus, mapping the surface extent of the fractures and facies is significant because well control and seismic data do not provide this kind of information.

STRATIGRAPHY

The Arkoma basin was depositionally part of a broad, stable shelf, the Arkoma shelf, along a passive continental margin. Depositional patterns on this shelf varied greatly during the Chesterian, Morrowan, and early Atokan time (Sutherland, 1988). The Wapanucka Formation is the only predominantly shallow-marine unit exposed in the now-deformed Ouachita mobile belt.

The Wapanucka Formation is underlain by a thick shale section that presumably spans the Mississippian/Pennsylvanian boundary in the frontal Ouachitas. The upper part of this shale is informally called "Springer" and is lithologically indistinguishable from thick shale intervals within the lower Wapanucka Formation (Grayson, 1980). The Wapanucka Formation is overlain by the Atoka Formation, which is predominantly shale with some sandstone lenses in the frontal Ouachitas. According to Grayson (1980), the Wapanucka Formation in the frontal Ouachitas consists of four members (one of which is formally named): an upper sandstone-limestone member, a middle shale member, a lower limestone member, and the Chickachoc Chert which is laterally equivalent, in part, to the lower limestone member. The upper sandstone-limestone member at the surface is considered to be equivalent to the Spiro sandstone in the Arkoma basin subsurface, although some workers consider the Spiro sandstone to be the basal sandstone of the Atoka Formation (Lumsden and others, 1971; Grayson, 1980). This paper uses the informal subsurface nomenclature: Wapanucka or Wapanucka limestone refers to the lower limestone member and/or Chickachoc Chert; sub-Spiro shale refers to the middle shale member; and Spiro, Spiro sandstone, and Spiro limestone refer to the upper sandstone-limestone member.

Thick successions of repetitive subtidal-carbonate sequences that include platform, platform-margin, and shelf-slope facies characterize the Wapanucka Formation in outcrop. Shelf-margin deposits (Fig. 1) consist of bioclastic shelf bars capped by oolites and local intertidal-beach deposits. Upper-shelf facies are demosponge boundstones with local foram-peloid packstones, and mounds of phylloid algae. Upper shelf-slope deposits are mostly tubular-algal (*Donezella*) boundstones (Mauldin, 1995). The lower shelf slope is represented by the Chickachoc Chert. The Chickachoc is generally highly frac-

Mauldin, D. L.; and Grayson, R. C., Jr., 1995, Wapanucka Formation (Morrowan): facies and fractures, frontal Ouachita Mountains, *in* Johnson, K. S. (ed.), Structural styles in the southern Midcontinent, 1992 symposium: Oklahoma Geological Survey Circular 97, p. 249–258.

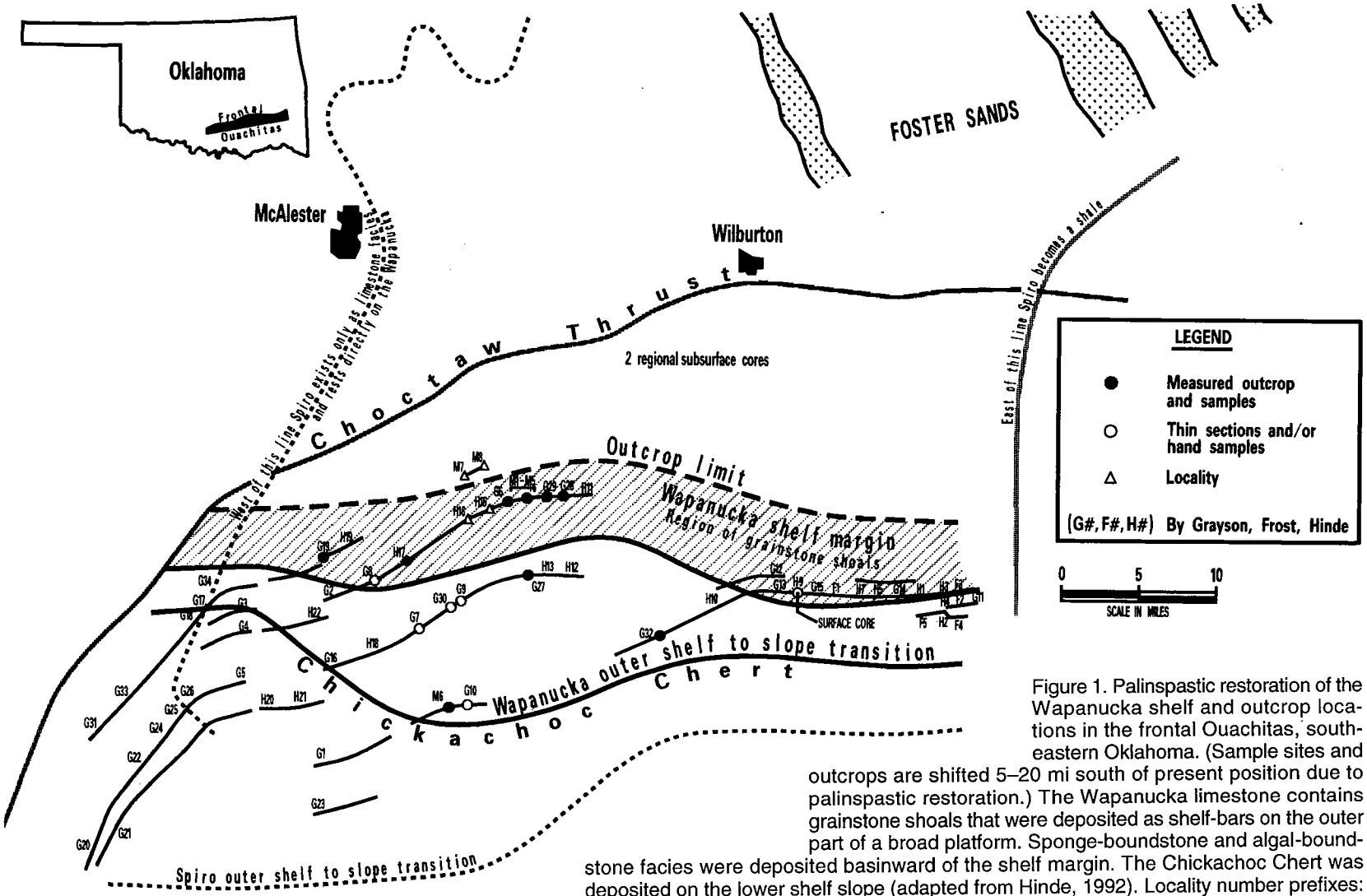


Figure 1. Palinspastic restoration of the Wapanucka shelf and outcrop locations in the frontal Ouachitas, southeastern Oklahoma. (Sample sites and outcrops are shifted 5–20 mi south of present position due to palinspastic restoration.) The Wapanucka limestone contains grainstone shoals that were deposited as shelf-bars on the outer part of a broad platform. Sponge-boundstone and algal-boundstone facies were deposited basinward of the shelf margin. The Chickachoc Chert was deposited on the lower shelf slope (adapted from Hinde, 1992). Locality number prefixes: M-numbers denote localities described in this study. H-numbers are from Hinde (1992); F-numbers are from Frost (1981); G-numbers are from Grayson (1980).

tured where shale is not abundant; the chert may therefore have some reservoir potential. The Chickachoc Chert consists mostly of spiculite (alternating layers of shale and transported spicules).

The Wapanucka limestone is overlain by an extensive shale called the middle shale in outcrop (Grayson, 1980) and usually referred to as the sub-Spiro shale by subsurface workers. This shale represents a fine-clastic influx that choked out carbonate production in the Ouachita region. The Spiro sandstone represents renewed shallow-shelf conditions in which sand and sandy limestones accumulated as shelf-bar deposits (Hinde, 1992). However, some Spiro facies are very similar to those that occur in the Wapanucka. The Wapanucka and Spiro sandstone are the only rigid rocks that are laterally extensive and, therefore, likely to contain economically significant fractures.

REGIONAL TECTONIC HISTORY

The frontal Ouachita Mountains in southeastern Oklahoma contain several imbricate-thrust outcrops of the Wapanucka limestone and overlying Spiro sandstone. These rocks have numerous fractures and faults created by compressional, thin-skinned deformation as thrust sheets were pushed toward the surface. However, this is only one of the tectonic events that led to fracturing of the Wapanucka in the complexly structured Ouachita thrust belt. Several episodes of stress are recorded by calcite-healed fractures in the Wapanucka that formed at different times. Small cross-cutting fractures have different types of calcite mineralization, and some of these fractures occurred after others, as evidenced by a second generation of calcite cutting across a healed fracture.

Major structures in the frontal Ouachitas and Arkoma basin that could have had an affect on Wapanucka fracturing include: basement-involved high-angle faults (normal and reverse), foreland-style thrusts, and folds (Montgomery, 1989). Normal faults were created by the breakup of the preexisting North American continent, accompanied by development of a system of rift arms and faults that reached far into the cratonic interior (Arbenz, 1989). These basement faults experienced several minor episodes of rejuvenation before major reactivation in the Early Pennsylvanian (Montgomery, 1989). The Wapanucka and Spiro were deposited on the passive margin at the southern edge of the North American plate (Houseknecht, 1986).

Early and Middle Atokan flexural downwarping of the southern margin of the shelf and down-to-the-south syndepositional normal faults were caused by subduction of the North American plate beneath either an island arc or another continental plate (Houseknecht, 1986; Sutherland, 1988). This continental collision resulted in the formation of a collisional orogenic belt, known as the Ouachita system. An allocthonous belt of older Paleozoic deep-water deposits were thrust northward onto the outer continental shelf. Foreland thrusting occurred in the Late Atokan and Desmoinesian (Houseknecht, 1986). The Ouachita Mountains and Arkoma basin contain a broad zone of compressional surface structures, with narrow upright anticlines separated by broad synclines. The frontal zone of the Ouachita Mountains in southeastern Oklahoma consists of numerous imbricate thrust sheets that repeat the Wapanucka and/or Chickachoc Chert and Spiro sandstone between the Choctaw and Ti Valley thrust faults. These thrust sheets are stacked in multilevel duplexes, and the strata within the thrust sheets are complexly folded (Arbenz, 1989). The continental collision may have also reactivated some of the older normal faults as high-angle reverse faults.

FRACTURE CLASSIFICATION

The AGI *Glossary of Geology* (1980) defines "fracture" as "a general term for any break in a rock, whether or not it causes displacement, due to mechanical failure by stress. Fractures include cracks, joints and faults." Kulander and others (1990) added, "any physical discontinuity in a rock caused by stresses exceeding the rock's strength." Pollard and Aydin (1988) suggested the word "'joint' be restricted to those fractures with field evidence for dominantly opening displacements. Joints are the most common result of brittle fracture of rock . . . and play an important role in the transport of fluids." In Wapanucka exposures, most fractures cannot be definitely classified, owing to the fact that most fracture faces are obscured by weathering, mineralization (mainly calcite), or soil. Because plumose structures are the most common and generally the only texture recognized, most fractures in this study are interpreted as joints. Surface ornamentation such as plumose structure is usually present on regional fractures (Kulander and others, 1979), although it is rarely observed or recognized in some outcrop studies (Lorenz and Finley, 1991).

Smooth, continuous, and planar fracture faces are common in the Wapanucka and are also characteristic of joints (Pollard and Aydin, 1988). Slickensides could be found on most fault planes. Horizontal fractures were not recorded as such unless they had slickensides. Without slickensides they would be hard to differentiate from bedding planes.

OUTCROP FRACTURES AND RESERVOIR POTENTIAL

Fracturing in the frontal Ouachitas can be assessed at surface locations, but comparison to Wapanucka reservoir fractures is difficult because of the lack of subsurface data. The abundance of fractures observed in Wapanucka exposures is evidence of how hydrocarbons could exist in the subsurface. They could be the reservoir, or they could

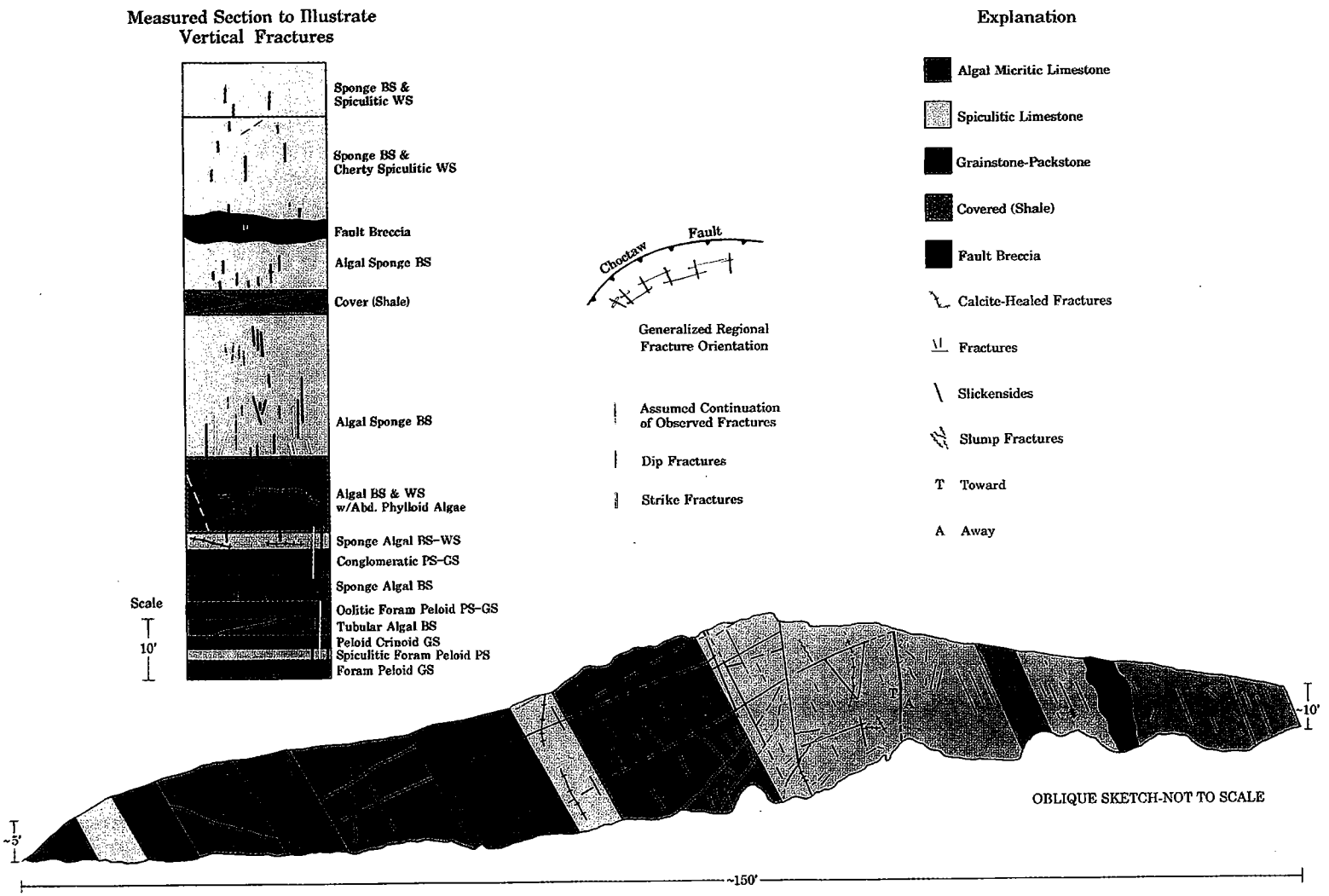


Figure 2. Typical outcrop of the Wapanucka limestone along Limestone Ridge (locality G28), with numerous fractures, including two identified as faults. Most fractures are perpendicular to bedding, but because of the orientation of the outcrop, the dip fractures could not be illustrated cutting through the beds; however, this is shown in the stratigraphic column.

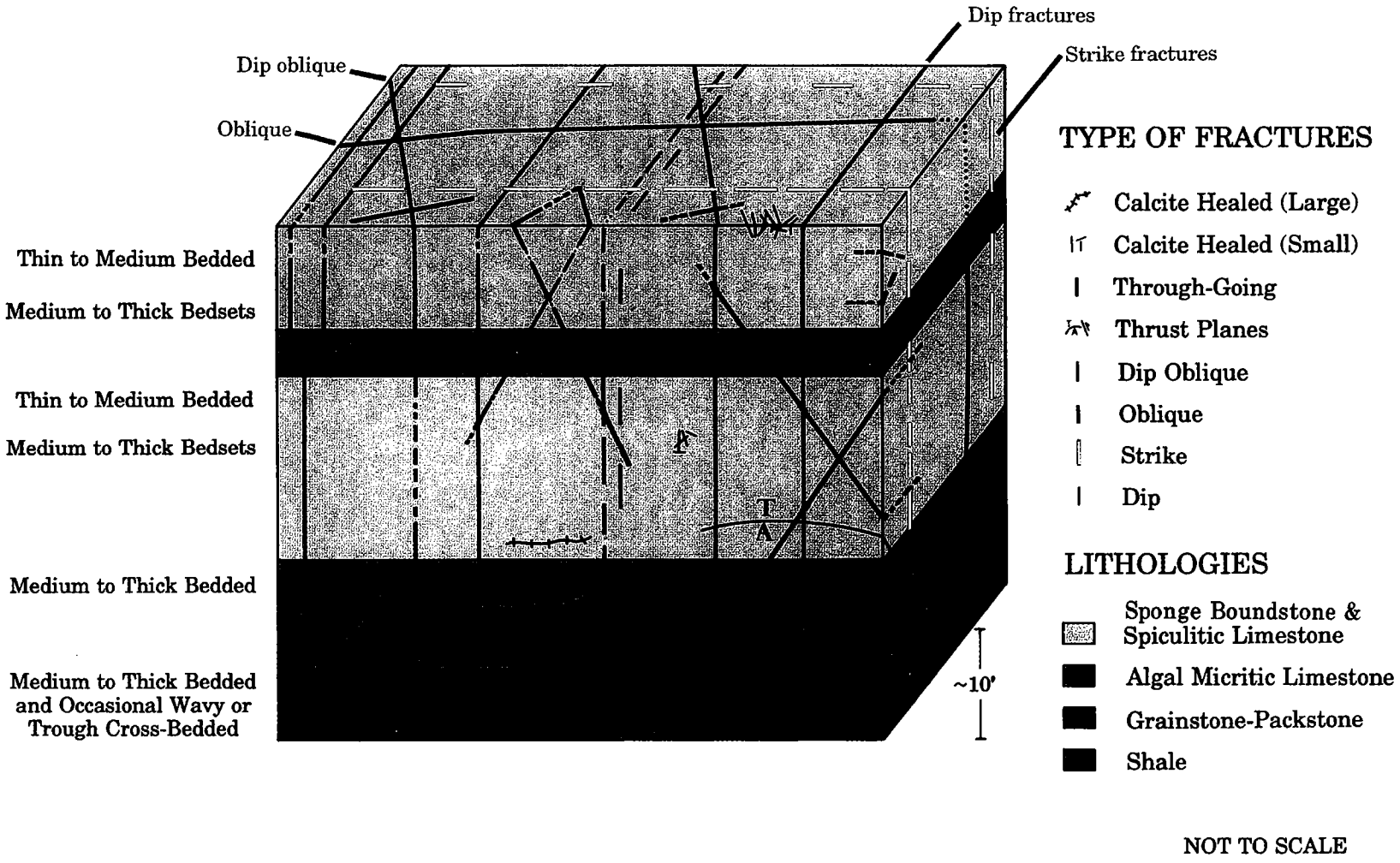


Figure 3. A schematic representation of lithology, bedding, and fractures in the Wapanucka limestone. Most fractures in the frontal Ouachitas are dip and strike fractures that cut perpendicular to bedding. Some regions contain numerous fractures oriented oblique to dip. Fracture abundance is probably influenced by lithology and/or bed thickness. Fractures are more abundant in the sponge-boundstone and spiculitic-limestone facies, which are generally more thinly bedded than other facies.

greatly enhance the permeability. Wapanucka limestone reservoirs are probably fracture controlled, but vugs and primary pores undoubtedly contribute to production (Suneson and Campbell, 1990). In the Arkoma basin subsurface, where the Spiro or Foster sandstone rest unconformably on the Wapanucka limestone, hydrocarbons could migrate from the porous sandstones into the Wapanucka. Fractures in the Arkoma basin, north of the Choctaw fault (Melton, 1929), have orientations similar to the dip fractures (perpendicular to strike) found in this study. Other fracture orientations developed in the frontal Ouachitas may also exist in the subsurface Arkoma basin. In outcrop, many of the large fractures are open, but most of the smaller ones are mineralized. However, the smaller fractures could remain open in the subsurface, depending on the fluid phases present during the history of the rock (Lorenz and others, 1991).

Fracture Morphology

Abundant fractures in the Wapanucka resulted from a complex postdepositional history of burial, tectonism, uplift, and erosion. The first fractures probably occurred in Atokan time, when regional down-to-the-south normal faults were created by tectonic and sediment loading associated with the advancing Ouachita thrust system (Houseknecht, 1986). Experts disagree on what events have the most effect on fracturing, but fracture orientation in the frontal Ouachitas indicates that fracturing was strongly affected by regional thrusting. Most macrofractures are perpendicular to bedding (Fig. 2, top left) and are either perpendicular (dip fractures) or parallel (strike fractures) to the Choctaw fault (see sketch in the center of Fig. 2). Dip and strike fractures are represented in Figure 3 by the red and yellow lines, respectively. The strike fractures are parallel to the inferred direction of maximum horizontal compression. Strike-fractures can be common in the subsurface despite the absence of flexure, and they are commonly important contributors to reservoir permeability (Lorenz and others, 1991).

In the Hartshorne area, numerous fractures are oblique to dip (green lines in Fig. 3), commonly oriented approximately NNW to NW as a possible consequence of the change of strike of the Choctaw fault in this area. To the east, the fault's orientation is mostly east–west, but near measured section G6 it turns toward the southwest (see Fig. 1 at the "aw" in "Choctaw"). Dip-oblique fractures are likely more abundant than might be inferred from outcrops, because this type of fracture is difficult to detect without bedding plane exposures, which are not common in Wapanucka outcrops.

In the frontal Ouachitas, most major thrust faults that affected the Wapanucka are located in the underlying shale; however, many minor thrusts are visible in the Wapanucka limestone. A few of these have obvious displacement, but most were recognized by the presence of slickensides or fault gouge. In outcrop, faults that are approximately parallel to strike are barely visible as gouge (approximately 2–6 in. thick). These faults resemble and could be mistaken for thin shale beds; however, they climb gradually and cut across limestone beds in an arcuate shape that is characteristic of thrust faults. Thrusts and other faults are commonly evident as zones of closely spaced, randomly oriented, small fractures or brecciated zones. A fault breccia (1–3 ft thick) consists of calcite-cemented fragments of adjacent beds, and occurs in the upper part of the Wapanucka at locality G28 (Fig. 2). (Abundant calcite in subsurface samples could be an indication of a fault.) Thrust faults in the middle shale (sub-Spiro shale) repeat or overturn the Spiro sandstone, independently of the Wapanucka limestone (Frost, 1981; Hinde, 1992).

Literature that addresses the orientation of subsurface Wapanucka fractures confirms that the subsurface fractures strike parallel to the Choctaw fault, analogous to many of the outcrop fractures. The Chitty Scott no. 1-30, in Pittsburg County, had an initial production of 6.7 MMcfd at 540 psi flowing pressure in fractured Wapanucka limestone. A frac-finder log of one of the wells in the area showed 74 ft of fractures and an east-west fracture trend, parallel to the Choctaw fault (Bleakley, 1980). In the Pittsburg field, imbricate thrusts repeat the Wapanucka–Spiro interval five or more times, and each individual imbricate slice (especially of the Wapanucka) is potentially productive (Montgomery, 1989). In this field, many wells have reserves >3 Bcfg. Most wells drilled in the structurally low areas were either dry holes or marginal wells due to the absence of porosity (Richardson, 1987). Greater reservoir enhancement may occur along the crestal portions of the structure due to tectonic fracturing.

Fracture Size, Spacing, and Relation to Lithology

The algal micritic-limestone unit (tubular algal boundstone in Fig. 2) in the middle part of the Wapanucka at locality G28 contains mostly irregular calcite-healed fractures. They have a random, chaotic orientation and are discontinuous. Adjacent, but different, lithologies may have been fractured at different times and with different fracture patterns (Nickelsen and Hough, 1967). This algal micrite has a fracture spacing ranging from 0.5 to 3.0 ft. Fractures do not appear to be capable of enhancing reservoir permeability because the fractures have been sealed with calcite. Also, these fractures terminate within the algal micrite unit, which has few bedding planes; therefore, fluid communication between fractures does not appear possible. However, because the outcrop surface is two-dimensional, it is impossible to determine if the fractures are connected in a third dimension. One of the cores exam-

ined for this study had irregular calcite-cemented fractures in micritic limestone and was from a well with excellent production. This core also contained abundant microfractures which, though observed in outcrops, were not recorded. The microfractures in the core are straight, 1–3 in. long, and either perpendicular or parallel to bedding. These microfractures may be the key to the production, because, unlike the larger irregular fractures, the small fractures are not calcite healed. Alternatively, production in this well could be enhanced by open fractures perpendicular to bedding that were poorly represented in the core because they are parallel to the axis of the borehole.

Locality G29 (Fig. 1), an abandoned quarry near Hartshorne, Oklahoma, contains abundant fractures in the thin-bedded sponge-boundstone and spiculitic-limestone unit near the top of the Wapanucka. Some strike-fracture planes (parallel to strike) are spaced as closely as 1–2 ft and are as much as approximately 20 ft by 40 ft in extent. The latter two dimensions might be greater, but some of the fracture plane is covered or has slumped to the quarry floor.

Numerous dip fractures (perpendicular to bedding) also occur in this sponge-rich limestone. Fractures commonly occur in groups. Fractured areas 20–40 ft wide are separated by areas 20–40 ft wide that are relatively fracture free. The fractured areas contain large fractures spaced ~6 ft apart. Many small dip fractures occur between the larger fractures, with an average spacing of ~3 ft and lengths of 1–6 ft. The long fractures normally range from 10 ft long, with terminations at bedding planes, to 40 ft long, where they cut completely through the sponge-boundstone and spiculitic limestone. Typically, at most outcrops, roughly half of the fractures terminate at bedding planes and the other half are longer. The long fractures in this quarry appear to die out in the Middle Shale Member above the sponge facies. Very few extend into the underlying micritic algal boundstone. As fractures frequently terminate at these micritic algal units, these units may be significant permeability barriers in the subsurface.

Throughout the frontal Ouachitas, large fractures (≥15 ft long) cut across several rock types and do not appear to be affected by lithology (Fig. 3). However, some fractures in one facies might not continue through the adjacent rock unit. Three long fractures near the center portion of locality G28 (Fig. 2) cut continuously through the sponge facies, but not through the other facies. Most fractures continue through shales <6 in. thick, but terminate in thicker shales (Fig. 3), especially if the shales are thicker than 3 ft. This might be expected because fracture terminations are common at contacts with more ductile beds (Stearns and Friedman, 1972). Subsurface Wapanucka shales that are 0.5–3 ft thick may not be permeability barriers because of fracturing. However, shales >3 ft thick may be considered permeability barriers because fractures were not observed to cut through them.

The fact that fractures are more abundant in the sponge-boundstone and spiculitic-limestone facies may be attributed to their thin bedding and hardness. Generally, thinner bedded units have more closely spaced fractures (Lorenz and others, 1991), and more brittle lithologies have more abundant fractures (Mallory, 1977). The sponge-boundstone and spiculitic facies appear to be the most brittle, and often contain abundant secondary chert, which is very brittle.

Spacing of dip fractures (perpendicular to strike) was measured at outcrops that haven't been dynamited, localities M6, M7, and M8 (Fig. 1). Locality M6 (Fig. 1) consists almost entirely of micritic tubular algal boundstone deposited on the outer portion of the Wapanucka platform. Fracture spacing was measured over a lateral distance of ~1,500 ft on a mound-shaped limestone outcrop (Fig. 4). It could be an algal (*Donezella*) mud mound, or its shape could have resulted from recent erosion. Because of the lack of bedding in this massive tubular algal boundstone, it is impossible to tell if the morphology is depositional or erosional, or if it is due to the fact that this anticline is plunging eastward. The fractures at this location are mostly grouped in sets ~200 ft across separated by 200-ft intervals that are, for the most part, devoid of large fractures. Most fractures cut entirely through the mound, which is ~20 ft thick. These fracture sets usually contain pairs of dip fractures, whereas the distance between fracture pairs ranges from 15 to 25 ft. The mound tapers to only 6 ft thick in the eastern 300 ft of the outcrop. Here, most dip fracture pairs cut through the entire 6 ft of limestone. Spacing between pairs is about 20–30 ft in the eastern portion, and fractures are approximately 3–6 ft apart in each pair (Fig. 4). In the far western part of this outcrop, where bedding is obvious, few fractures are observed, but more of the outcrop is obscured by soil and vegetation.

Fractures are well exposed ~18 mi west-southwest of Wilburton (Fig. 1) on the north limb of a tightly folded syncline just north of a snakehead anticline along the Choctaw thrust (Fig. 5). In the palinspastic restoration (Fig. 1), localities M7 and M8 are plotted about 7 mi south of the present site of the Choctaw fault. Sixteen dip fractures occur across 70 ft of outcrop (Fig. 6) in a 20-ft-thick exposure of medium-bedded Wapanucka limestone on the north side of the syncline (Fig. 6). Most fractures extend through the entire 20 ft of this fossil-rich limestone. Most of these macrofractures were spaced 6–8 ft apart; a few were spaced ~3 ft apart. Although extensive cover precluded measurement of stratigraphic intervals and definite identification of litho-facies, outcrops measured nearby contain Wapanucka shelf-margin and related deposits

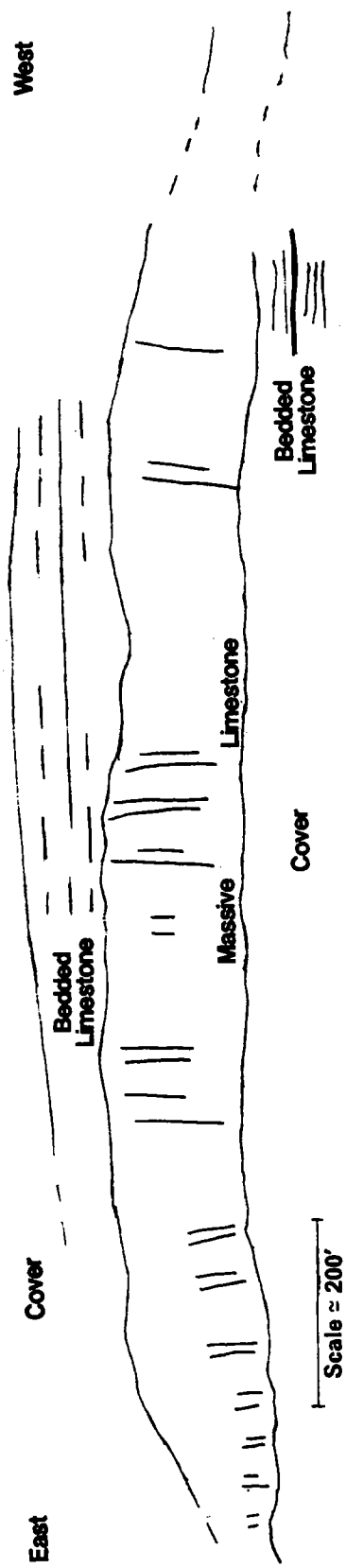


Figure 4. Fracture spacing in outcrop of the Wapanucka limestone. Dip fractures in an algal micritic-limestone (mostly tubular algal boundstone) at locality M6. The mound shape of the outcrop may be (1) depositional (i.e., an algal bioherm), (2) the result of recent erosion, or (3) structural. This outcrop is on the south limb of an anticline that plunges below the surface to the east. (The thickest portion of the massive limestone is ~20 ft.)

(grainstones, packstones, and sponge boundstones). Fractures, with the characteristics observed at this outcrop, could permit hydrocarbon communication between grainstone units in the subsurface.

No detailed measurements of fractures in the Spiro were made; however, based on observations at approximately 30 outcrops, fractures are more abundant in the limestone facies of the Spiro than in the sandstones, and silica- and/or calcite-cemented sandstones generally contain more fractures than the porous, weakly cemented sandstones. As in the Wapanucka, dip fractures and strike fractures are the most abundant fracture types in Spiro limestones. At Hartshorne Lake and localities G34 and G33, ~50% of the observed fractures are dip fractures and 30% are strike fractures. The remaining 20% are evenly divided between oblique fractures (in all facies) and irregular calcite-healed fractures (primarily in micritic limestones). This distribution of fracture types is essentially the same as distribution in Wapanucka limestones.

In contrast to the Spiro limestone which has abundant dip fractures at locality G34, the top of the Wapanucka has sets of orthogonal fractures oriented obliquely to dip and strike. These could be younger fractures related to near-surface phenomena (Lorenz and others, 1991), or may be evidence that dip fractures did not travel through the 48 ft of sub-Spiro shale between the Wapanucka and the Spiro. Due to lack of exposure, it is impossible to determine if the shale is fractured, or if it ever contained fractures that extended from the Wapanucka to the Spiro. In the cores studied, the sub-Spiro shale had some microfractures but no large fractures; perhaps because shales behave plastically (Nolte, 1988), which hinders fracture penetration (Lorenz and others, 1991). The thickness of the sub-Spiro shale could be an important factor for Wapanucka hydrocarbon accumulations. Fracture communication between the Wapanucka and the more-porous Spiro sandstone could possibly enhance the reservoir potential of the Wapanucka. This would be more likely to occur in regions of the subsurface where the sub-Spiro shale is thin or missing.

SUMMARY

Fracturing is believed to be of major importance to reservoir potential of the Wapanucka limestone. Numerous fractures in the frontal Ouachitas cut perpendicular to bedding. Most of these are oriented perpendicular to strike (dip fractures) or parallel to strike (strike fractures) (Fig. 3).

Fractured reservoirs of the Wapanucka Formation might be found in the sponge-boundstone and spiculitic-limestone facies because it has a high fracture density, as does the Chickachoc Chert. The sponge-boundstone and spiculitic-limestone facies was deposited on the upper Wapanucka shelf adjacent to the shelf margin. The Chickachoc Chert is the most basinward Wapanucka shelf deposit and should be recognizable on seismic sections due to its considerable difference in lithology from other Wapanucka facies.

Fracturing might create communication between porous segments of oolitic facies or phylloid-algal mounds. Oolites were formed on the shelf margin, usually capping bioclastic shelf bars. Phylloid-algal facies were deposited as

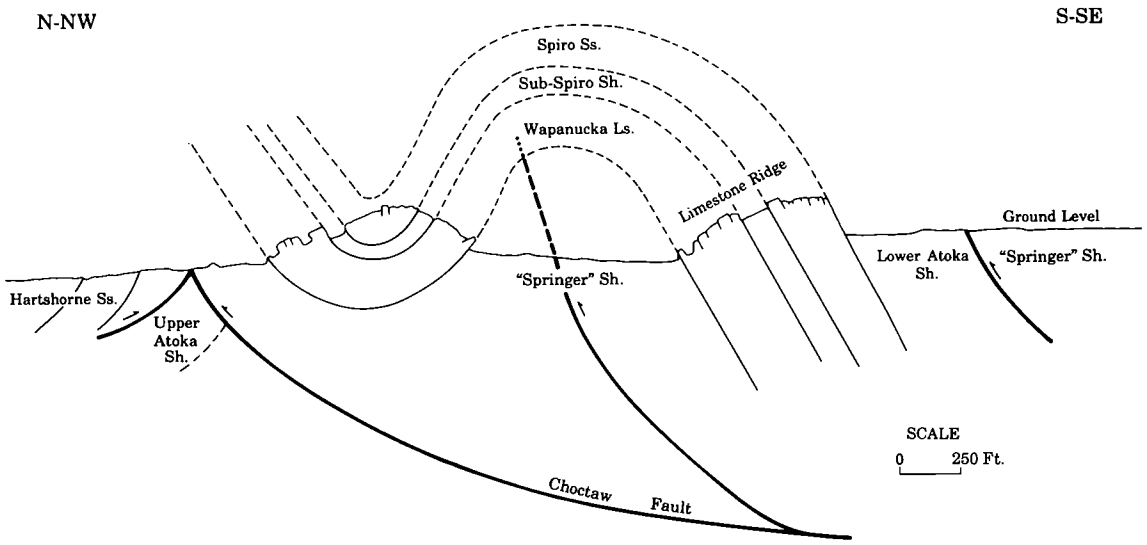


Figure 5. Cross section across Limestone Ridge ~18 mi west-southwest of Wilburton (near the "a" in Choctaw in Fig. 1). The syncline was identified by the presence of south-dipping Wapanucka limestone on the north side of the ridge and north-dipping Wapanucka limestone on the south side of the ridge and by Spiro sandstone and limestone in middle of the ridge.

shoals or boundstone mounds adjacent to the shelf margin, and may contain shelter porosity. The location of oolite and phylloid-algae deposits may be indicated on isopach maps by thick anomalies. Paleotopographic highs on top of the Springer shale, if not obscured by compaction, might also be indications of these favorable Wapanucka facies, because oolites and phylloid algae were probably deposited on local highs.

ACKNOWLEDGMENTS

Sincere appreciation is expressed to Phillips Petroleum Co. for sponsoring some drafting for this paper, and to Chip Feazel for his useful suggestions, discussion, and editing. Thanks, also, to Helen Farrell for her helpful suggestions.

REFERENCES CITED

Arbenz, J. K., 1989, The Ouachita system, *in* Bally, A. W.; and Palmer, A. R. (eds.), The geology of North America—an overview: Geological Society of America, The Geology of North America, v. A, p. 371–396.

Bates, R. L.; and Jackson, J. A. (eds.), 1980, Glossary of geology: American Geological Institute, Falls Church, Virginia, 749 p.

Bleakley, W.B., 1980, Hamilton tackles Arkoma basin completions: Petroleum Engineer International, April, p. 64–71.

Frost, R. W., 1981, The stratigraphy and distribution of the Wapanucka Formation in the Red Oak/Wilburton area of eastern Latimer County, Oklahoma: Baylor University unpublished senior thesis, 83 p.

Grayson, R. C., Jr., 1980, The stratigraphy of the Wapanucka Formation (Lower Pennsylvanian) along the frontal margin of the Ouachita Mountains, Oklahoma: University of Oklahoma unpublished Ph.D. dissertation, 319 p.

Hinde, L. K., 1992, Stratigraphy and structural styles of the Spiro Formation, frontal Ouachita Mountains, southeastern Oklahoma: Baylor University unpublished M.S. thesis, 100 p.

Houseknecht, D. W., 1986, Evolution from passive margin to foreland basin: the Atoka Formation of the Arkoma basin, south-central U.S.A., *in* Allen, P. A.; and Homewood, P. (eds.), Foreland basins: International Association of Sedimentologists, Special Publication 8, p. 327–332.

Houseknecht, D. W.; Woods, M. O.; and Kastens, P. H., 1989, Transition from passive margin to foreland basin sedimentation, Field Trip No. 15: the Atoka Formation of the Arkoma basin, Arkansas and Oklahoma, *in* Vineyard, J. D.; and Wedge, W. K. (compilers), Geological Society of America Field Trip Guidebook: Missouri Department of Natural Resources, Division of Geology and Land Survey, Special Publication 5, p. 121–174.

Kulander, B. R.; Barton, C. C.; and Dean, S. L., 1979, The application of fractography to core and outcrop fracture investigations: U.S. Department of Energy, Morgantown Energy Technology Center, Report METC/SP-79/3, 174 p.

Kulander, B. R.; Dean, S. L.; and Ward, B. J., Jr., 1990, Fractured core analysis: interpretation, logging, and use of natural and induced fractures in core: American Association of Petroleum Geologists Methods in Exploration Series 8, 88 p.

Lorenz, J. C.; and Finley, S. J., 1991, Regional fractures II: fracturing of Mesaverde reservoirs in the Piceance basin, Colorado: American Association of Petroleum Geologists Bulletin, v. 75, p. 1738–1757.

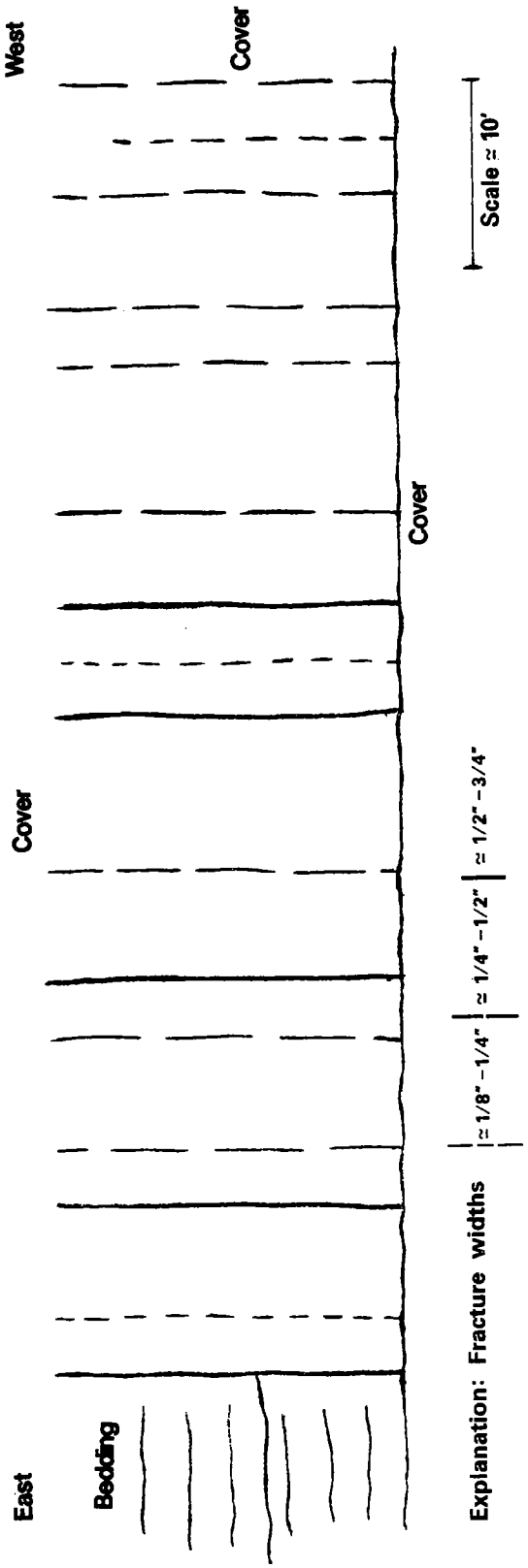


Figure 6. Fracture spacing measured along a strike fracture face (parallel to the Choctaw fault) at locality M8. Most of these are dip fractures (perpendicular to strike), except for a few that are slightly oblique. Runoff, from the slope above, probably has some effect on the fracture widths. All of the fractures are open, except for microfractures which were not recorded. Since the Wapanucka beds are usually tilted in the Ouachitas and southern Arkoma basin, most boreholes should intersect numerous Wapanucka fractures if this type of fracture spacing exists in the subsurface.

Lorenz, J. C.; Teufel, L. W.; and Warpinski, N. R., 1991, Regional fractures I: a mechanism for the formation of regional fractures at depth in flat-lying reservoirs: American Association of Petroleum Geologists Bulletin, v. 75, p. 1714–1737.

Lumsden, D. N.; Pitman, E. D.; and Buchanan, R. S., 1971, Sedimentation and petrology of Spiro and Foster sands (Pennsylvanian), McAlester basin Oklahoma: American Association of Petroleum Geologists Bulletin, v. 55, p. 254–266.

Mallory, W. W., 1977, Oil and gas from fractured shale reservoirs in Colorado and northwest New Mexico: Rocky Mountain Association of Geologists Special Publication 1, 38 p.

Mauldin, D. L., 1995, Depositional relationships, facies, and fractures in the Wapanucka limestone, frontal Ouachita Mountains, southeastern Oklahoma: Baylor University unpublished M.S. thesis.

Melton, F. A., 1929, A reconnaissance of the joint-systems in the Ouachita Mountains and central plains of Oklahoma: Journal of Geology, v. 37, p. 729–746.

Montgomery, S. L., 1989, Drilling the deep Arkoma; Part 1, New depths, new possibilities, *in* Cain, D. L. (ed.), Petroleum frontiers: Petroleum Information Corp., v. 6, no. 1, 42 p.

Nickelsen, R. P.; and Hough, V. N. D., 1967, Jointing in the Appalachian Plateau of Pennsylvania: Geological Society of America Bulletin, v. 78, p. 609–630.

Nolte, K. G., 1988, Application of fracture design based on pressure analysis: Society of Petroleum Engineers Production Engineering, v. 3, p. 31–42.

Pollard, D. D.; and Aydin, A., 1988, Progress in understanding jointing over the past century: Geological Society of America Bulletin, v. 100, p. 1181–1204.

Richardson, W. E., 1987, Pittsburg field complex opportunities for additional well locations: Oil and Gas Journal, v. 85, p. 64–66.

Stearns, D. W.; and Friedman, M., 1972, Reservoirs in fractured rock, *in* King, R. E. (ed.), Stratigraphic oil and gas fields—classification, exploration methods, and case histories: American Association of Petroleum Geologists Memoir 16, p. 82–106.

Suneson, N. H.; and Campbell, J. A., 1990, Ouachitas need more exploratory drilling: Oil and Gas Journal, v. 88, p. 65–69.

Sutherland, P. K., 1988, Late Mississippian and Pennsylvanian depositional history of the Arkoma basin area, Oklahoma and Arkansas: Geological Society of America Bulletin, v. 100, p. 1787–1797.

Structural Interpretations of the Arkoma Basin–Ouachita Mountains Transition Zone, Southeastern Oklahoma: A Review

Neil H. Suneson
Oklahoma Geological Survey
Norman, Oklahoma

INTRODUCTION

The differences between Arkoma basin geology and Ouachita Mountain geology in Oklahoma are stratigraphic and structural. Strata exposed north of the trace of the Choctaw fault, which is the leading thrust of the Ouachita fold-and-thrust belt and the "traditional" boundary between the Arkoma basin and Ouachita Mountains (Fig. 1), are mostly upper Atokan to Desmoinesian deltaic sandstones and mudstones. In contrast, strata immediately south of the fault are Morrowan to lower Atokan shallow-water carbonates and sandstones overlain by deep-water turbidite sandstones and mudstones. At the surface, the area north of the trace of the Choctaw fault is mostly characterized by few faults and broad, open folds. To the south, isoclinal folds, overturned strata, and closely spaced imbricate faults characterize the structural geology.

The transition from lower Atokan turbidites to upper Atokan deltaic strata occurs in the footwall of the Choctaw fault. However, the exact nature of this stratigraphic transition is difficult to establish because several different interpretations of the structural geology of the Arkoma basin–Ouachita Mountains transition zone (also located in the footwall of the fault) have been published.

On the surface, "simple" Arkoma basin structural geology locally grades into "complex" Ouachita Mountains geology. North of the trace of the

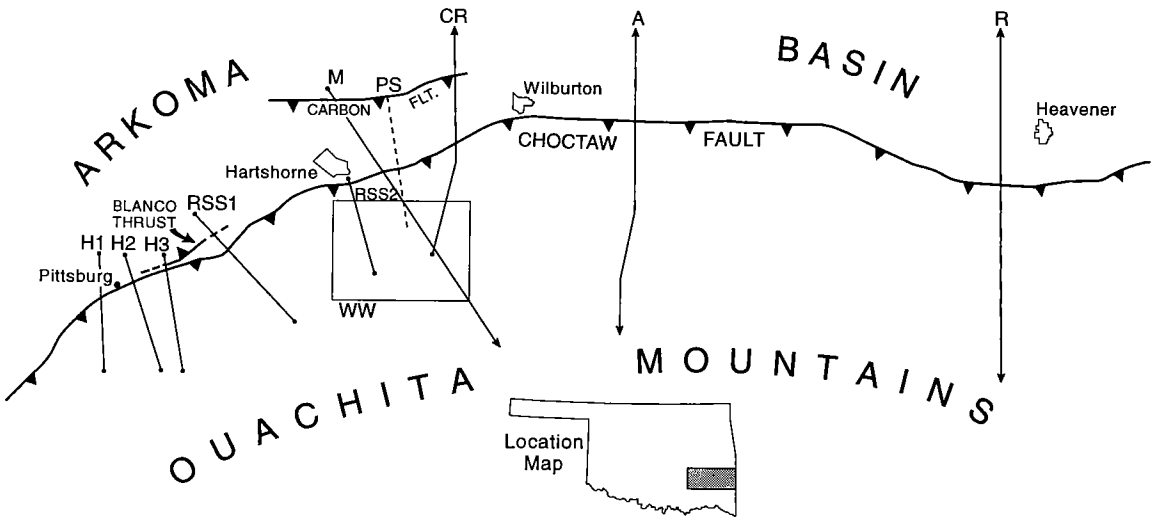


Figure 1. Generalized tectonic map of the Ouachita Mountains frontal belt and adjacent Arkoma basin, showing location of geologic and geographic features referred to in the text and location of "modern" cross sections and study areas. Arrows indicate those cross sections that extend beyond the frontal belt. Cross-section labels and sources: A—Arbenz (1989a); H1, H2, H3—Hardie (1988); M—Milliken (1988); CR—Camp and Ratliff (1989); RSS1, RSS2—Reeves and others (1990); PS (approximate location)—Perry and Suneson (1990) and Perry and others (1990); R—Roberts (1992); area WW—Wilkerson and Wellman (1993).

Suneson, N. H., 1995, Structural interpretations of the Arkoma basin—Ouachita Mountains transition zone, southeastern Oklahoma: a review, *in* Johnson, K. S. (ed.), Structural styles in the southern Midcontinent, 1992 symposium: Oklahoma Geological Survey Circular 97, p. 259–263.

Choctaw fault, tight, isoclinal folds are locally present and pass into more-open folds. Similarly, some areas south of the fault contain relatively open folds. The same lack of distinction between "simple" Arkoma basin geology and "complex" Ouachita Mountains geology holds true in the subsurface of the footwall of the Choctaw fault, where both styles are complexly interwoven.

The purpose of this paper is to review recent ideas on the subsurface geology of the Ouachita Mountains frontal belt near the trace of the Choctaw fault in southeastern Oklahoma. Most, if not all, of the papers that have been published on the structural geology of the Arkoma basin–Ouachita Mountains transition zone (simply called the "transition zone" in the remainder of this paper) resulted from increased gas-exploration activities beginning in 1986 (Suneson and Campbell, 1990; Suneson and others, 1991) and the discovery of significant new gas reserves. Most of the recent studies are based on new seismic-reflection data, and some incorporate surface geology and new well data. Of particular interest are (1) the interpretation of the northern frontal belt as a triangle zone, (2) the importance of blind imbricate thrust faults and duplex structures, and (3) the nature of a basal décollement that floors the compressional structures of the Arkoma basin and Ouachita Mountains.

PREVIOUS INTERPRETATIONS

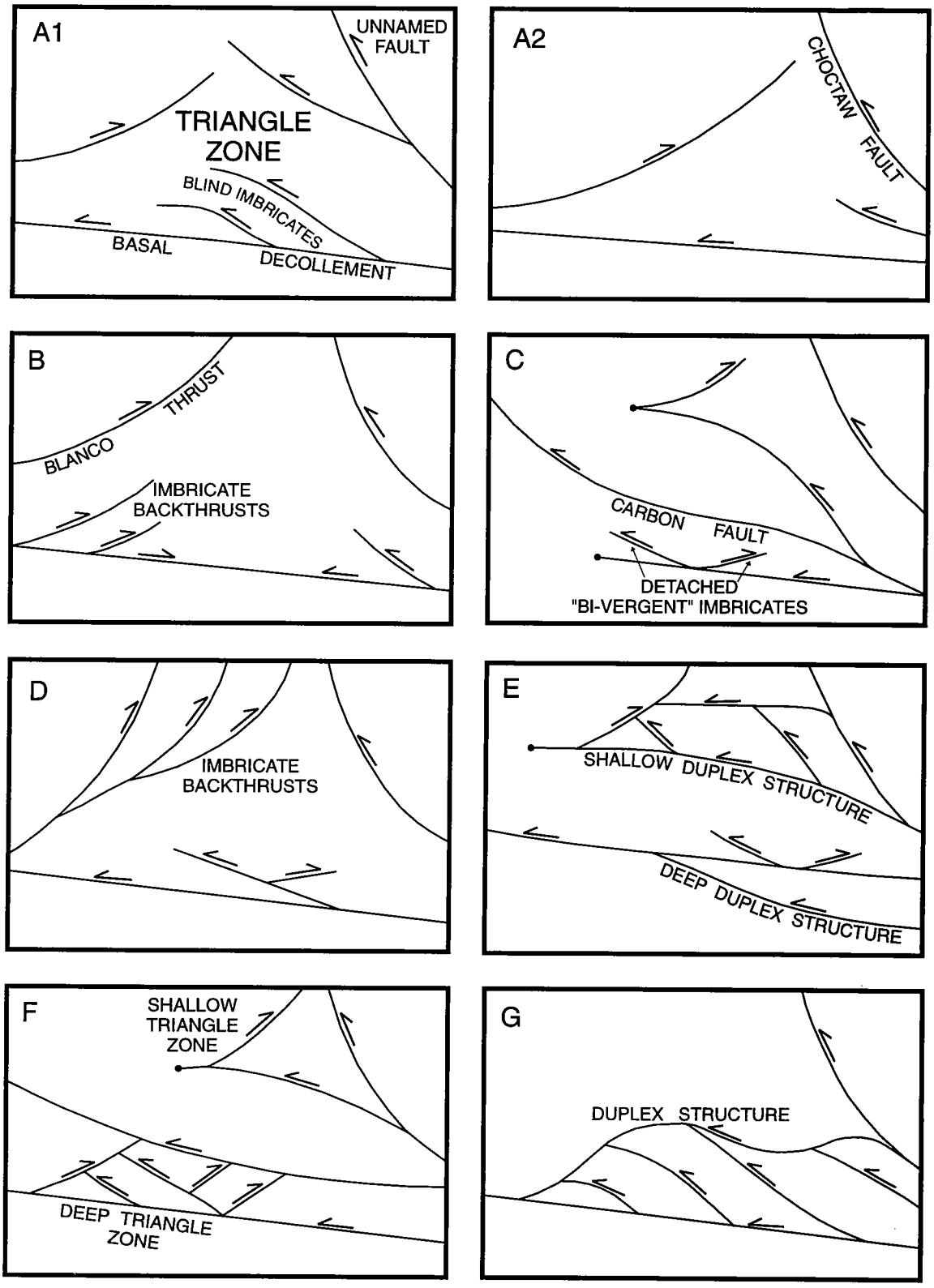
Modern studies of the structural geology of the northern edge of the Ouachita Mountains frontal belt began with a classic paper by Arbenz (1984). Although he did not focus on the frontal belt, Arbenz (1984, p. 83) clearly recognized (1) south-directed thrusts in the Arkoma basin (triangle zone); (2) blind imbricate thrusts extending basinward from the leading edge of the main part of the exposed fold-and-thrust belt; and (3) a deep, mostly bedding-parallel décollement that serves as the root of the imbricate thrusts and extends far into the basin (Fig. 2-A1). The décollement gradually rises northward; the footwall consists mainly of preorogenic (Cambrian to Devonian) shallow-water strata to the south and Middle Pennsylvanian deep- to shallow-water clastic strata to the north. No previous papers on the structural geology of the transition zone (referenced in Arbenz, 1984) recognized these three key elements. These ideas were developed more fully and applied to the transition zone in Oklahoma in later publications (Arbenz, 1989a,b) (Fig. 1, line A; Fig. 2-A2).

Subsequent studies have built on the concepts introduced by Arbenz and have incorporated electric-log and seismic data. Hardie (1988) first applied the term "triangle zone" to characterize the structural geology of the northern edge of the Ouachita fold-and-thrust belt (Fig. 2-B). Based on surface mapping, Hardie (1988) identified the Blanco thrust fault as the basinward roof of a relatively thick triangle zone; the trace of this fault extends to the southwest and northeast, but is parallel to bedding, and its position can only be inferred. Based on electric-log analysis and surface mapping, Hardie (1988) drew three cross sections (lines H1, H2, and H3, Fig. 1) that showed blind imbricate thrusts and backthrusts and north-directed overturned folds beneath the Choctaw fault. He also mapped a basal décollement at the base of the Pennsylvanian (base of the "Springer" Formation) that extended basinward from the Choctaw fault. Hardie (1988) suggested that the sense of movement on the northern part of the décollement was to the south; this interpretation is unique among modern frontal-belt structural analyses. A significant feature of Hardie's (1988) study is that he attempted to balance his cross sections.

Milliken's (1988) regional study of Ouachita structure included his interpretation of one seismic line across the northern part of the Ouachita Mountains frontal belt (Fig. 1, line M). His cross section (Fig. 2-C) shows a thin triangle zone floored by a high-level north-directed imbricate thrust fault. Deeper small-displacement imbricate thrust faults and backthrusts form what he termed "detached bivergent imbricates"; Milliken interpreted these to be beneath a major, midlevel décollement located in the Middle Pennsylvanian Atoka Formation (Fig. 2-C). This décollement gradually deepens southward beneath the imbricate thrust faults in the frontal belt. Milliken (1988) suggested that the décollement does not extend basinward beneath the folds of the Arkoma basin; rather, it surfaces as the Carbon fault.

On the basis of surface mapping, seismic data, and closely spaced well control, Camp and Ratliff (1989) published a computer-balanced cross section across the transition zone near Wilburton, Okla-

Figure 2 *(opposite page)*. Schematic cross sections showing styles of faulting and major geologic features in the subsurface of the Arkoma basin–Ouachita Mountains transition zone. Choctaw fault and basal décollement are located in the same place in each cross section, except where noted. North is to left. *A1*—Arbenz (1984): note triangle zone, blind imbricates, and basal décollement; Choctaw fault not present. *A2*—Arbenz (1989a). *B*—Hardie (1988): note imbricate backthrusts and surface expression of roof of triangle zone (Blanco thrust). *C*—Milliken (1988): note "detached bi-vergent" imbricates, tip of basal décollement, and floor and roof thrusts of triangle zone. *D*—Camp and Ratliff (1989): note imbricate backthrusts. *E*—Reeves and others (1990): note shallow and deep duplex structures and higher level of basal décollement. *F*—Perry and others (1990): note passive roof duplex and shallow and deep triangle zones. *G*—Roberts (1992): note absence of triangle zone and presence of thick duplex structure.


A1
UNNAMED FAULT
TRIANGLE ZONE
BLIND IMBRICATES
BASAL DECOLLEMENT
A2
CHOCTAW FAULT
B
THRUST
BLANCO
IMBRICATE BACKTHRUSTS
C
CARBON FAULT
DETACHED "BI-VERGENT" IMBRICATES
D
IMBRICATE BACKTHRUSTS
E
SHALLOW DUPLEX STRUCTURE
DEEP DUPLEX STRUCTURE
F
SHALLOW TRIANGLE ZONE
DEEP TRIANGLE ZONE
G
DUPLEX STRUCTURE

homa (Fig. 1, line CR). They identified a thick triangle zone floored by blind imbricate thrust faults and backthrusts and a deep north-directed décollement that climbs from Mississippian shales in the south to Middle Pennsylvanian strata beneath the folds of the Arkoma basin (Fig. 2-D). Their cross section also shows imbricate backthrusts splaying off the roof backthrust of the triangle zone.

A field-trip guidebook to the western frontal belt of the Ouachita Mountains by Suneson and others (1990) contains several cross sections of the northern frontal belt. One of these is by Reeves and others (1990, fig. 12) (Fig. 1, line RSS1), and it shows a thin triangle zone floored by two north-directed duplex structures. A relatively shallow major décollement separates the duplex structures (Fig. 2-E). Unlike other interpretations of subsurface frontal-belt structure in which the décollement typically overlies Mississippian to Morrowan strata, Reeves and others (1990) suggested that the deep décollement is in lower Atokan strata. A second cross section (Reeves and others, 1990, fig. 13) (Fig. 1, line RSS2) shows a complex series of blind imbricates and associated small-displacement backthrusts similar to the "detached bi-vergent imbricates" of Milliken (1988).

Perry and Suneson (1990) interpreted a seismic line south of Hartshorne, Oklahoma (Fig. 1, line PS), and showed a shallow triangle zone overlying a deeper triangle zone or "passive roof duplex." The deep zone, which consists of one north-directed imbricate thrust fault and two south-directed backthrusts, was interpreted to have moved basinward while the roof sequence remained relatively stationary, thus requiring a south-directed roof thrust. A deep décollement that climbed northward from Upper Devonian–Lower Mississippian strata to Middle Pennsylvanian strata was shown not to extend beyond the line of cross section. This interpretation was revised in a subsequent publication (Perry and others, 1990), as a result of reprocessing the original seismic data. The deep triangle zone was reinterpreted as consisting of (1) two north-directed imbricates, (2) a floor thrust (basal décollement) that extends north beyond the line of the cross section, and (3) a north-directed roof thrust that gradually rises northward within the Atoka Formation and extends beyond the line of cross section (Fig. 2-F).

Most modern cross sections through the northern part of the Ouachita Mountains frontal belt in Oklahoma have been drawn between Wilburton and Pittsburg; this is where most recent gas-exploration activity has occurred and where subsurface data (electric logs, seismic studies) are available. Roberts (1992), however, has interpreted the structure of the frontal belt near Heavener, Oklahoma, on the basis of seismic data and sparse well control. His cross section (Fig. 1, line R) does not show a shallow south-directed thrust and triangle zone; rather, he has suggested that the folds exposed on the surface in this part of the southern Arkoma basin are the result of an underlying duplex structure (Fig. 2-G). He also showed a basal décollement in the lower part of the Atoka Formation extending far into the basin.

The Gale-Buckeye thrust system (Wilkerson and Wellman, 1993) lies south of the Arkoma basin–Ouachita Mountains transition zone (Fig. 1, area WW); however, it may have important implications for the structural geology of the frontal belt. On the basis of closely spaced seismic lines (1–2 mi apart) and good well control, Wilkerson and Wellman (1993) drew nine cross sections across the Gale-Buckeye imbricate structure. Although outside their study area, they suggested that (1) a thin triangle zone is present, (2) the floor thrust of the triangle zone is the roof thrust of a duplex structure, and (3) blind imbricates are present near the base of the duplex structure. With regards to the Gale-Buckeye structure, they document the importance of transverse structures (oblique ramps, tear fault) to thrust geometry and relate them to basement structural trends and suggest that the system is backward stepping.

DISCUSSION

New interpretations of the transition from "complex" Ouachita Mountains-style structural geology to "simple" Arkoma basin-style geology are based on recently acquired and processed seismic data, closely spaced wells with electric-log data, and, to a lesser extent, surface geology. Many features typical of the leading edge of thrust belts elsewhere in the world have been recognized in the Ouachita Mountains frontal belt in Oklahoma. For example, imbricate thrusts, triangle zones, duplex structures, backthrusts, and a basal décollement have been described in many recent studies.

However, many questions remain, as evidenced by some of the "unique" interpretations of the available data. (1) Are parts of the basal décollement south-directed, as suggested by Hardie (1988)? (2) Is the basal décollement exposed at the surface, and/or is it underlain by small-displacement imbricates, as suggested by Milliken (1988)? (3) Is there surface or seismic evidence for imbricate backthrusts off the south-directed roof backthrust over the triangle zone, as suggested by Camp and Ratliff (1989)? (4) Is the shallow (lower Atokan) décollement proposed by Reeves and others (1990) as extensive as the more commonly held décollement within the Upper Mississippian–lower Morrowan? (5) How common are "passive roof duplexes" and multiple triangle zones, as pictured by Perry and others (1990)? (6) What is the evidence for triangle zones, and can the unusually thick section and anticlinal structure observed at the surface in the transition zone be more simply explained by duplex structures, as suggested by Roberts (1992)? (7) What is the effect of transverse and basement

structures, as documented by Wilkerson and Wellman (1993), on the structural geology of the transition zone?

The answers to these questions will come from reinterpretations of (1) existing and new, improved seismic data; (2) electric-log data, especially dipmeter data; and (3) existing and new surface geologic maps. These new data will not only allow geologists to better understand one of the major fold-and-thrust belts in North America, but will help them develop existing gas fields and discover new gas fields in the Arkoma basin and Ouachita Mountains.

ACKNOWLEDGMENTS

Comments by Bill Perry (U.S. Geological Survey, Denver) and a review by Ibrahim Cemen (Oklahoma State University, Stillwater) greatly improved an early version of the manuscript.

REFERENCES CITED

Arbenz, J. K., 1984, A structural cross section through the Ouachita Mountains of western Arkansas: Arkansas Geological Commission Guidebook 84-2, p. 76–84.

_____ 1989a, Ouachita thrust belt and Arkoma basin, *in* Hatcher, R. D., Jr.; Thomas, W. A.; and Viele, G. W. (eds.), The Appalachian-Ouachita orogen in the United States: Geological Society of America, The Geology of North America, v. F-2, p. 621–634.

_____ 1989b, The Ouachita system, *in* Bally, A. W.; and Palmer, A. R. (eds.), The geology of North America—an overview: Geological Society of America, The Geology of North America, v. A, p. 371–396.

Camp, W. K.; and Ratliff, R. A., 1989, Balanced cross section through Wilburton gas field, Latimer County, Oklahoma: implications for Ouachita deformation and Arbuckle (Cambro-Ordovician) exploration in Arkoma basin [abstract]: American Association of Petroleum Geologists Bulletin, v. 73, p. 1044.

Hardie, W. E., 1988, Structural style of the frontal thrust belt of the Ouachita Mountains, southern Pittsburg County, Oklahoma: Oklahoma Geology Notes, v. 48, p. 232–246.

Milliken, J. V., 1988, Late Paleozoic and early Mesozoic geologic evolution of the Arklatex area: Rice University, Houston, unpublished M.S. thesis, 259 p.

Perry, W. J., Jr.; and Suneson, N. H., 1990, Preliminary interpretation of a seismic profile across the Ouachita frontal zone near Hartshorne, Oklahoma: Oklahoma Geological Survey Special Publication 90-1, p. 145–148.

Perry, W. J., Jr.; Agena, W.; and Suneson, N. H., 1990, Preliminary reinterpretation of the Ouachita frontal zone near Hartshorne, Oklahoma, based chiefly on seismic reflection data: U.S. Geological Survey Circular 1060, p. 82.

Reeves, D. L.; Schreiner, W. P.; and Sheffield, T. M., 1990, Stop 6—New State Mountain (Amoco 1-5 Rosso Unit): Oklahoma Geological Survey Special Publication 90-1, p. 37–40.

Roberts, M. T., 1992, Shelf to basin transect, eastern Oklahoma: Shreveport Geological Society Guidebook, May 27–29, 1992, unnumbered pages.

Suneson, N. H.; and Campbell, J. A., 1990, Ouachitas need more exploratory drilling [original title: Oil and gas exploration in the western Ouachita region, Oklahoma]: Oil and Gas Journal, v. 88, no. 15, p. 65–69; no. 16, p. 85–87.

Suneson, N. H.; Campbell, J. A.; and Tilford, M. J., 1990, Geology and resources of the frontal belt of the western Ouachita Mountains, Oklahoma: Oklahoma Geological Survey Special Publication 90-1, 196 p.

Suneson, N. H.; Brown, D. P.; and Mycek-Memoli, A. C., 1991, Update of Ouachita Mountains frontal belt exploration and development: Oklahoma Geology Notes, v. 51, p. 84–97.

Wilkerson, M. S.; and Wellman, P. C., 1993, Three-dimensional geometry and kinematics of the Gale-Buckeye thrust system, Ouachita fold and thrust belt, Latimer and Pittsburg Counties, Oklahoma: American Association of Petroleum Geologists Bulletin, v. 77, p. 1082–1100.

Evidence for Recurrent Left-Lateral Deformation from the Vicinity of the Depew Field, Creek County, Oklahoma

Dorothy L. Swindler
University of Tulsa
Tulsa, Oklahoma

ABSTRACT.—The Depew field and study area are in T. 15 N., R. 8 E., in southwestern Creek County in east-central Oklahoma. Structural features and relative timing were interpreted from subsurface structure and isopach maps, well-log cross sections, and published surface maps.

En echelon, right-stepping normal faults in the Vamoosa Formation (Virgilian) trend about N. 30° W. (~45° to the fault zone), indicating the presence of a primary fault oriented about N. 15° E. at depth. The orientations of other faults, uplifts, and depressions mapped in the subsurface closely match those predicted by left-lateral physical and mathematical models with the maximum compressive stress oriented about N. 30° W. The similarity between mapped and predicted orientations of structural features indicates that little rotation has occurred and that horizontal displacement along the primary fault is minimal.

Faults identified on the Viola structure map, and trends in thickness anomalies of the Arbuckle Group, Sylvan Shale, and Atoka Formation, correspond to model-predicted shear orientations. Both the Sylvan Shale and Dutcher sandstone (Atokan) are thin over the Depew uplift and thick in adjacent depressions. This indicates that left-lateral deformation occurred before and/or during Sylvan Shale deposition, and during Atoka Formation deposition. The en echelon faults at the surface indicate that left-lateral deformation also occurred at some time after deposition of the Vamoosa Formation (Virgilian).

The evidence for recurrent deformation in a left-lateral stress regime, and the absence of prominent structural trends that do not fit the left-lateral fault model, is interpreted as an indication that the orientation of the primary fault was the dominant influence on the structural evolution of the study area, rather than regional tectonic forces. Regional forces are interpreted to have affected the area by inducing movement along the primary fault and by influencing the sense and amount of displacement along secondary faults whose orientations were largely determined by the orientation of the primary fault at depth.

Swindler, D. L., 1995, Evidence for recurrent left-lateral deformation from the vicinity of the Depew field, Creek County, Oklahoma, *in* Johnson, K. S. (ed.), Structural styles in the southern Midcontinent, 1992 symposium: Oklahoma Geological Survey Circular 97, p. 264.

Stratigraphy and Structural Styles of the Lower Stanley Tuffs: Northwest Flank of the Broken Bow Uplift, McCurtain County, Oklahoma

Charles A. O. Titus and Thomas E. Legg
Tex-Con Oil and Gas Co.
Houston, Texas

ABSTRACT.—The Tenmile Creek Formation (lower Stanley Group) crops out along the flanks of the Broken Bow uplift and represents a structurally complex area where conventional seismic methods are unable to delineate subsurface structure. The "unconventional" method of geologic mapping and interpretation represents the most appropriate approach with which to identify oil and gas prospects in this structural regime. Within the lower Tenmile Creek Formation, two separate and distinct volcaniclastic tuff couplets—the upper and lower Mud Creek and the Hatton and Beavers Bend—represent the only reliable time-stratigraphic markers. By utilizing standard geologic field-mapping techniques, the position of the tuffs in the stratigraphic section was determined, and their resultant structural expression mapped.

Differentiation of the tuffs is based on grain size, matrix composition, lapilli type, and color. The Hatton and Beavers Bend tuff couplet represents the lowest stratigraphic expression of the tuff sequence. This tuff couplet lies ~900 ft above the Arkansas Novaculite, and its gross thickness is 180 ft. The upper and lower Mud Creek tuff couplet is stratigraphically 350 ft above the Hatton and Beavers Bend tuff couplet and has a gross thickness of 200 ft.

The 730-ft (gross) tuff interval usually deforms structurally as a single lithic unit, demonstrating south-verging, tight-to-closed, overturned, concentric folds. The south-verging folds change to a vertical (nonvergent) fold attitude northwest of the Broken Bow uplift. Where the folds are tight, the concentric fold detaches from the Arkansas Novaculite, but where the tuff-defined folds are open, the tuffs and the Arkansas Novaculite deform uniformly without major detachment surfaces. Although the two tuff couplets generally deform in unison, detachment surfaces are locally observed between them. Tear faults (caused by lateral ramps?) are common, but do not have a preferred offset direction within the tuff interval.

The surface-mapping project delineated a prospective tuff-defined anticlinorium that was tested in 1985 by the Sohio no. 1-7 Weyerhaeuser well. The targeted Arkansas Novaculite was encountered at a drilled depth of 2,467 ft, and total depth was reached at 6,721 ft in the Blaylock Sandstone. Dipmeter analysis from the borehole confirmed the structural styles observed in the surface-mapping program.

INTRODUCTION

The northwest flank on the Broken Bow uplift is dominated by the "middle and lower" Tenmile Creek Formation of the lower Stanley Group. This part of the Ouachita flysch sedimentary section is thin- to medium-bedded sandstone and siltstone beds in a predominantly shale lithology. Correlation within this part of the stratigraphic section is only possible with the well-developed time-stratigraphic volcaniclastic tuff units found near the base of the formation. The steeply dipping attitude of the beds, resulting from one of the major detachments within the Ouachita facies, hinders definition of any underlying hydrocarbon prospect (or structure) by seismic exploration methods. Thus, an obvious method for delineating a structure containing hydrocarbon-prospective reservoirs (Arkansas Novaculite, Bigfork Chert, and Blaylock Sandstone) is to conduct a detailed surface-mapping survey. Establishing the stratigraphic and structural relations of the lower Stanley tuffs to the Arkansas Novaculite–Bigfork section would generate a drillable prospect. The volcaniclastic tuff mapping program investigated ~400 mi^2 centered in the northwest part of McCurtain County (Fig. 1). This area extends

Titus, C. A. O.; and Legg, T. E., 1995, Stratigraphy and structural styles of the lower Stanley tuffs: northwest flank of the Broken Bow uplift, McCurtain County, Oklahoma, *in* Johnson, K. S. (ed.), Structural styles in the southern Midcontinent, 1992 symposium: Oklahoma Geological Survey Circular 97, p. 265–276.

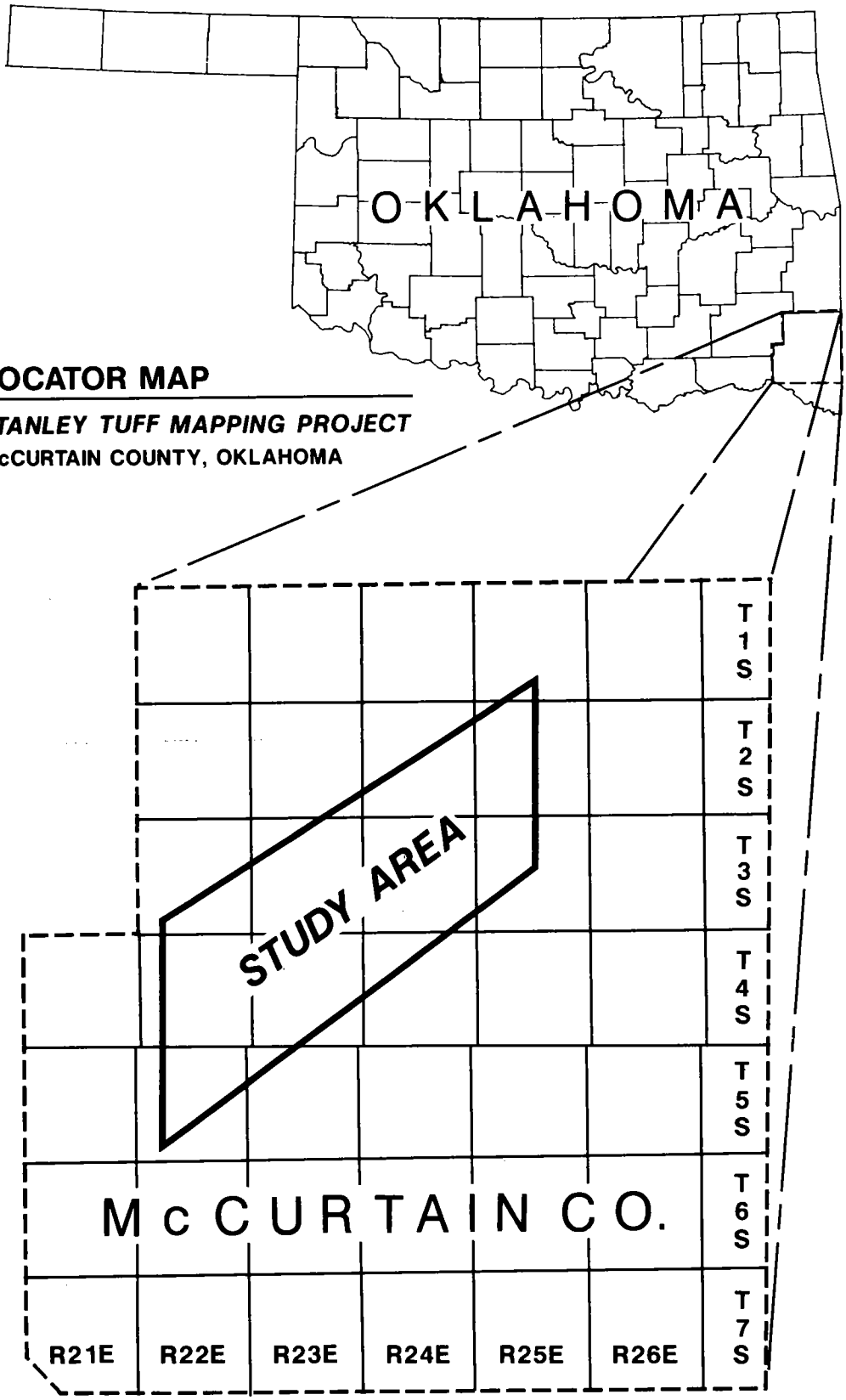


Figure 1. Location of the study area in the Ouachita Mountains (McCurtain County) of southeastern Oklahoma.

from the Tenmile Creek Formation/Cretaceous onlap boundary to the Cross Mountains anticlinorium to the northeast and from the Arkansas Novaculite outcrop to the southeast flank of the Bethel syncline.

PREVIOUS WORK

The occurrence of tuffs in the Stanley Group was first reported by Miser (1920) and Miser and Purdue (1929), who suspected that there were three to five tuff beds in the Caddo Gap and DeQueen Quadrangles (Arkansas). Miser named the most prominent of these beds the Hatton Tuff lentil. Honess published a geologic map of the southeast Oklahoma Ouachitas in 1923 showing the locations of the more prominent tuff outcrops. However, owing to the complex structures, Honess was not able to determine whether there was more than one tuff horizon. Honess stated that when he "observed or tried to measure a section or part of a section of the Stanley tuffs, or any other part of the Stanley for that matter, save for bottom beds or the extreme top, it was not known whether the measured section was the bottom or top of the series." Consequently, the tuffs are undifferentiated on his map.

Neim (1971) studied the lower Stanley stratigraphy and noted there are at least four mappable tuff sequences interbedded with marine graywackes and shales in the lower 1,600 ft of the Stanley Group. These are, in ascending order, the Beavers Bend, Hatton, and lower and upper Mud Creek tuffs. The tuff sequences are important because they are time-stratigraphic horizons, exhibit distinctive lithologies, and are relatively consistent around the periphery of the Broken Bow uplift.

Neim (1971) and Miser and Purdue (1929) both suggested a southern volcanic source for the tuff sequences. Neim postulated the possibility of a northeastern continuation of the buried metamorphic interior belt southeast of the Luling overthrust front in Texas. Miser and Purdue considered a possible island-arc setting, referred to as "Llanoria," situated to the south of the present-day outcropping Ouachitas. These statements were based on the observations of tuff thickness, grain-size trends, paleocurrent indicators, and Mississippian paleogeography. R. L. Nicholas (1982, personal communication to Thomas Uphoff) suggested that the volcanic terrane encountered by two wells in the area of the Sabine uplift was the source of the Stanley tuffs. The area is believed to have been a volcanic arc associated with a north-dipping subduction zone.

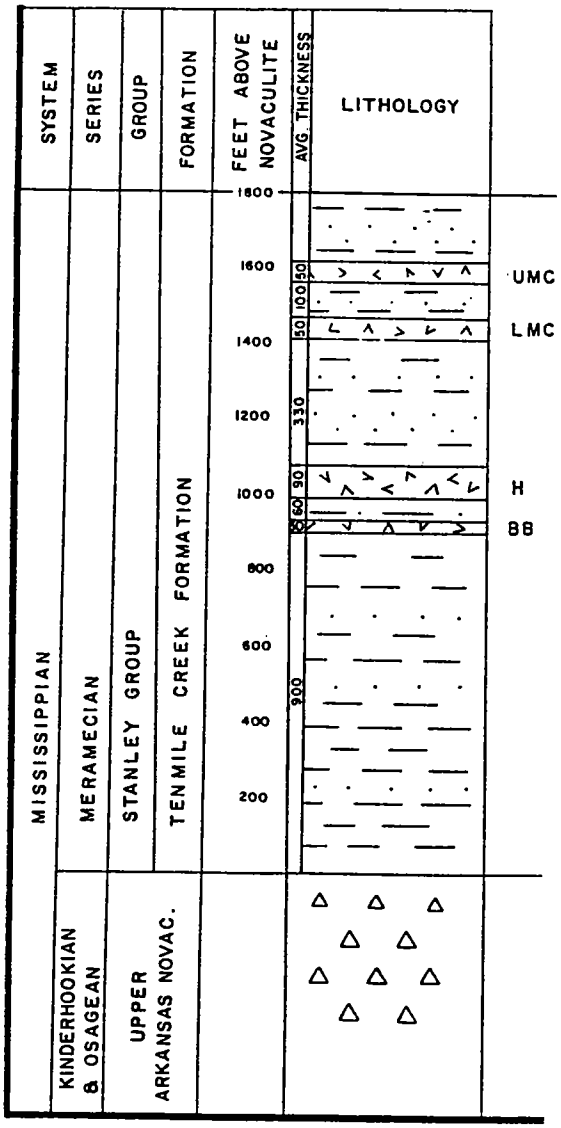


Figure 2. Stratigraphic column of lower part of Stanley Group showing position of four tuff beds: UMC = upper Mud Creek tuff, LMC = lower Mud Creek tuff, H = Hatton tuff, BB = Beavers Bend tuff.

FIELD METHODOLOGY

The field-mapping program was conducted between January and May, 1983. The program utilized Honess's (1923) "Geologic map of the southern Ouachita Mountains in southeastern Oklahoma" as a guide to identified tuff outcrops. The extensive Weyerhaeuser road network provided partial access to 70% of the tuff localities. Orthophotographs taken in 1980 were used for orientation in the field and for mapping bases. Color stereoscopic pairs (1977) were also utilized to trace the stratigraphically defined tuff couplets across the somewhat inaccessible countryside. The stereoscopic interpretation complemented the field-mapped tuff interpretation, and many outcrop-pattern ambiguities were resolved by the stereopairs (i.e., complex faulting, fold detachments, etc.). Stereoscopic interpretations in areas of limited field

mapping were later field checked for accuracy and lithologic delineation.

STRATIGRAPHY

The Stanley Group is divided into three formations that are, in ascending order, the Tenmile Creek, Moyers, and Chickasaw Creek (Fig. 2). Total estimated thickness of the Stanley Group in the study area averages 10,000 ft. The dominant lithologies of the Stanley are fine-grained graywackes, subgraywackes, feldspathic sandstones, and gray to black shales. Tuffs are minor in abundance, but are invaluable for mapping and stratigraphic work.

The four tuffs identified in the mapping program all occur in the lower 1,600 ft of the Tenmile Creek Formation. The tuffs represent the only mappable horizon within the lower part of the Stanley Group. The "tuffs" are actually volcanic sandstone, since they have been transported and deposited by marine currents (Neim, 1971). Graywacke sandstones in the area of investigation are "tufflike" in appearance but, upon closer examination, represented reworked tuff material. Only those units that clearly are tuffs were mapped in this study.

The tuffs are rhyodacitic in composition and are predominantly represented by four pyroclastic components: (1) devitrified shards and volcanic dust, (2) devitrified pumice lapilli, (3) crystals of feldspar and quartz, and (4) rare volcanic-rock fragments (Neim, 1971). Neim also described the upper and lower Mud Creek tuffs as composites of massive and bedded crystal tuff and the Hatton and Beavers Bend tuffs as bedded and massive pumiceous vitric tuff. All of the tuffs are fine grained and vitric near their tops.

Beavers Bend Tuff

The four tuffs usually are observed as two couplets in the field: the Beavers Bend and Hatton couplet and the upper and lower Mud Creek couplet. The lowest unit of the tuff sequence is the Beavers Bend tuff. The Beavers Bend tuff is 930 ft above the Arkansas Novaculite and 60 ft below the overlying Hatton tuff, as measured in its type section on Rattlesnake Bluff (SW¼ sec. 10, T. 5 S., R. 25 E.) along the Mountain Fork River in the Beavers Bend State Park. The average thickness of section between the Arkansas Novaculite and the Beavers Bend tuff is 900 ft, as stated by Neim (1971) and as verified several times during this mapping project. The thickness of the lowermost tuff averages 30 ft near the Broken Bow uplift, but gradually decreases to ~15 ft northwest of the uplift, within the northwestern part of McCurtain County. The Beavers Bend tuff exhibits a crystal-enriched basal zone several inches thick, but is predominantly massive, pumiceous, and vitric, with large euhedral and broken feldspar and quartz crystals suspended in a very fine-grained matrix. The pumice lapilli are flattened along bedding planes and altered to a "yellowish-green" 1*M* muscovite (Neim, 1971). The sequence displays an upward fining of the feldspar crystals, until no visible feldspar crystals are observed.

Hatton Tuff

The Hatton tuff is approximately 45–75 ft above the Beavers Bend tuff. The clastic interval between the two tuffs is composed of thin sandstone and shale beds. The Hatton tuff is the most prominent of all of the lower Stanley tuffs. Its thickness ranges from 60 ft in northwestern Arkansas to 120 ft in southeast Oklahoma. Within the mapped area, the Hatton thickness averages 90 ft. The Hatton is a vitric tuff, characteristically containing abundant flattened, green lapilli of devitrified pumice in a light- to medium-gray ash matrix. The unique and characteristic green lapilli are most numerous in the upper part of the tuff lentil.

Lower Mud Creek Tuff

The uppermost tuff couplet is represented as the lower and upper Mud Creek. The Mud Creek tuff couplet contains a much higher percentage of feldspar crystals, which enables distinguishing them from the lower tuff couplet. The lower Mud Creek tuff is approximately 310–370 ft above the Hatton tuff and is separated from it by shales and graywackes. The upper Mud Creek tuff is 100 ft above the lower Mud Creek tuff; they are separated by typical Stanley shales and graywackes. The lower Mud Creek is a crystal tuff ranging in thickness from 20 to 60 ft and averaging 50 ft. The basal section of the lower Mud Creek tuff consists of poorly sorted, euhedral to broken feldspar crystals and coarse ash in a light-gray matrix. The entire sequence grades upward to a more vitric zone. Locally, weathered boulders of the Mud Creek tuff are nearly 80% feldspar crystals. Near the base of the lower Mud Creek tuff, shale rip-up clasts are locally contained within the tuff unit and are up to 10 in. long by 5 in. thick.

Upper Mud Creek Tuff

The upper Mud Creek tuff is similar to the lower Mud Creek tuff and also is ~50 ft thick. Layers in the upper tuff contain well-developed gray-black lapilli that are 0.25–0.5 in. in diameter. The color of the lapilli in the upper Mud Creek (gray-black) and Hatton (green) is an important field criterion in distinguishing between the upper and lower tuff couplets.

The published type section for the upper and lower Mud Creek tuff is ~1.5 mi south of Mt. Herman along U.S. 259 in the SW¼NE¼ sec. 20, T. 3 S., R. 24 E. (Neim, 1971). Neim described the southeast tuff exposure at this site as the upper Mud Creek and the northwest tuff outcrop as the lower Mud

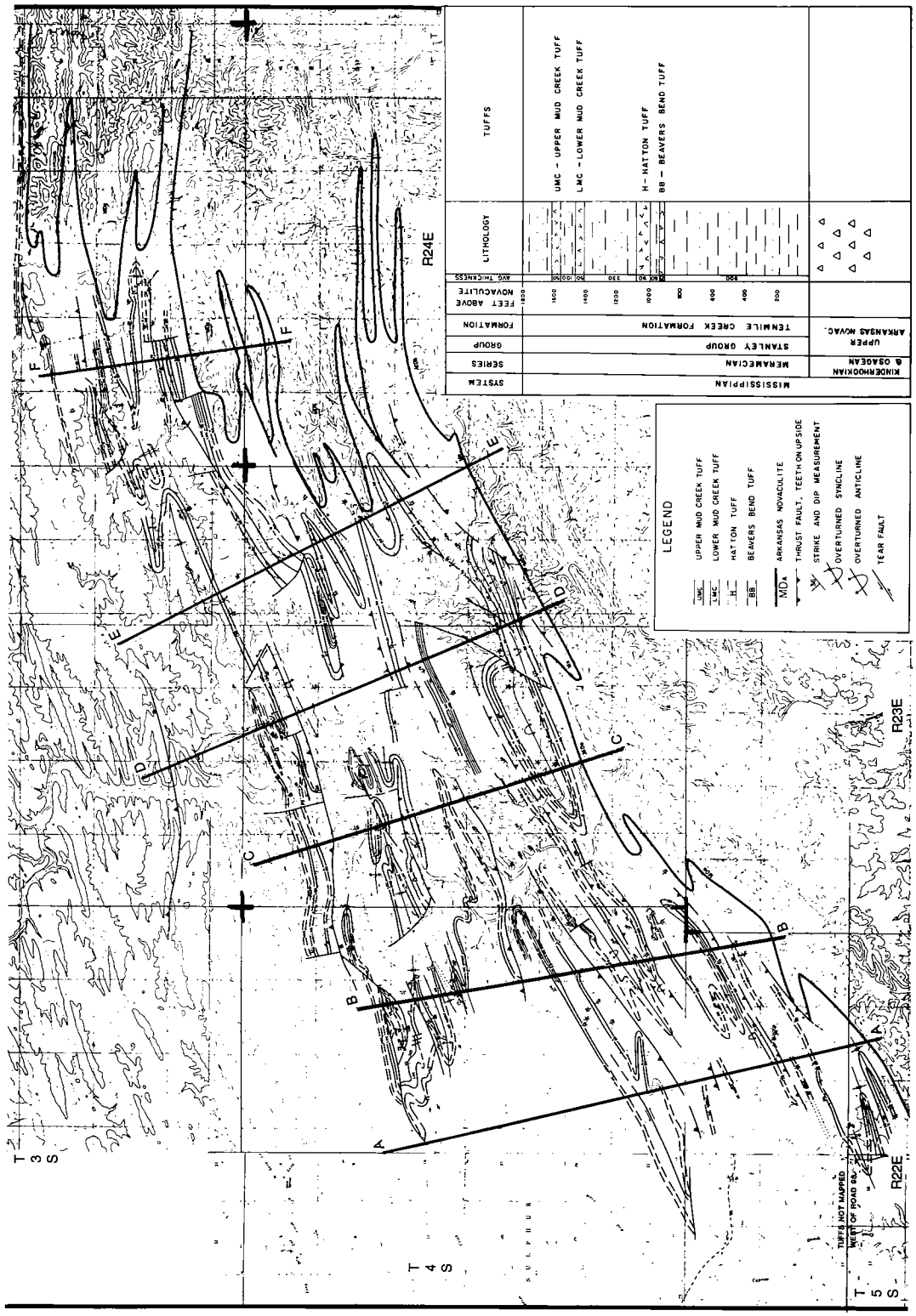


Figure 3. Geologic map of lower Stanley tuff beds on north flank of Broken Bow uplift.

Creek tuff. After detailed examination of this type section, doubts were raised about the nature of the described stratigraphic section because of the observation of apparent faulting between the upper and lower Mud Creek tuffs. Significant cleavage development is observed in the Stanley shales adjacent to the northern tuff exposure (Neim's lower Mud Creek tuff), whereas the southern fault block has no cleavage adjacent to the southern exposed tuff (Neim's upper Mud Creek tuff). Verification of the suspected high-angle fault was documented by use of vitrinite-reflectance data. The vitrinite data averaged 2.65% R_o for the southern, noncleaved fault block, whereas the northern fault block had an average vitrinite-reflectance value of 4.36% R_o. (The high-angle reverse fault probably formed during the late stage of the Ouachita orogeny and is associated with the Broken Bow uplift event.) To resolve the Mud Creek tuff "type section" question, further field study identified a complete lower Stanley tuff sequence (Beavers Bend tuff through upper Mud Creek tuff) in N½ sec. 29, T. 3 S., R. 24 E., and in secs. 6 and 7, T. 4 S., R. 23 E. Although the quality of outcrops at these new locations is not as good as those in road cuts or stream cuts, the section is quite workable.

STRUCTURE

The tuffs of the lower Stanley Group on the northwest flank of the Broken Bow uplift are a time-stratigraphic interval that has undergone intense structural deformation. The geologic map of the outcropping tuff units (Fig. 3) shows the structural complexity of the lower Tenmile Creek section of the Stanley Group. In general, the tuff units ex-

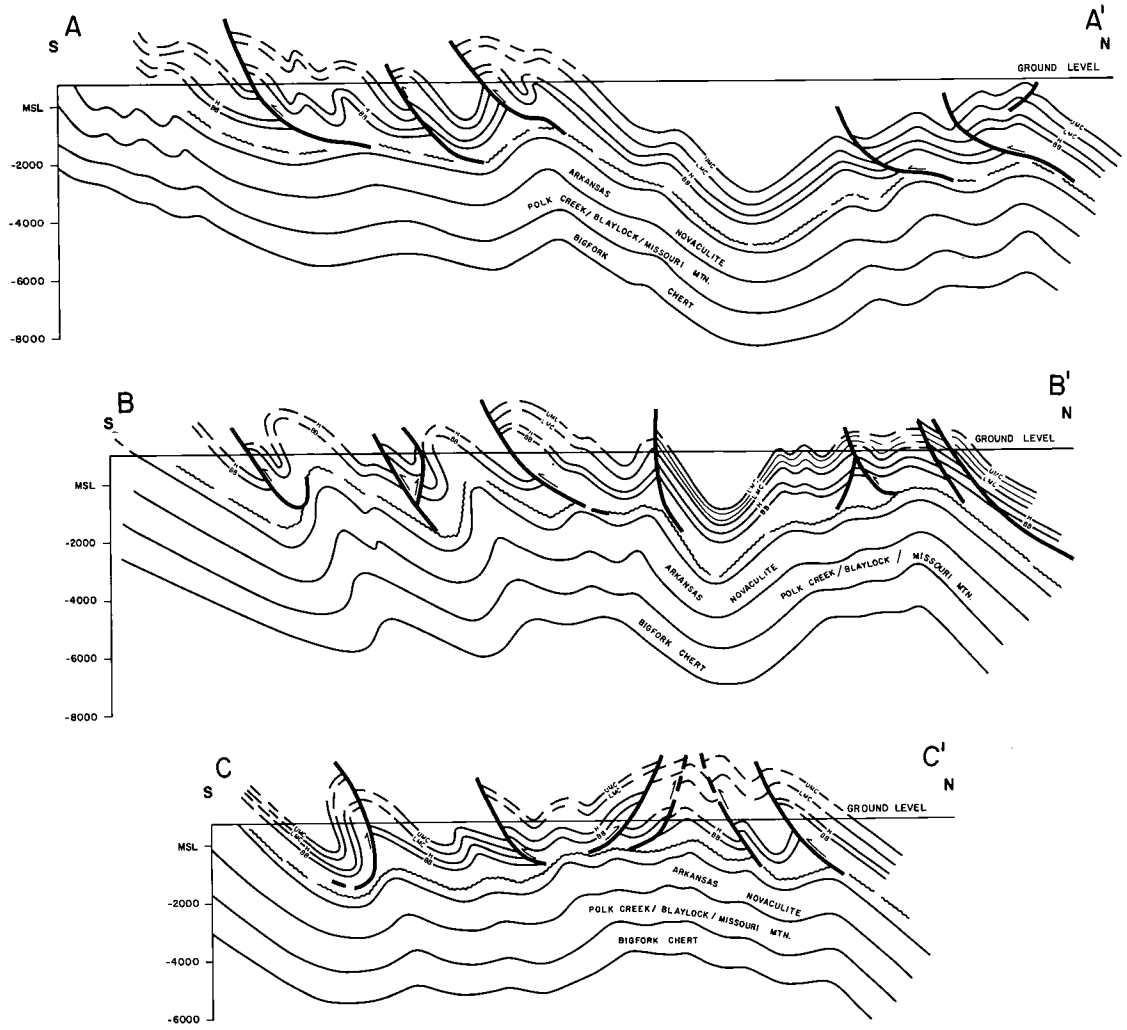


Figure 4 *(above and opposite page).* Cross sections A–A' through F–F' showing lower Stanley tuffs (location of cross sections shown in Fig. 3).

hibit south-verging, tight to closed, overturned concentric-fold geometries as the dominant structural style near the boundary of the Broken Bow uplift, as defined by outcrops of the Arkansas Novaculite. The vergence of the folds decreases to near zero (vertical fold attitude) as the distance increases away (northwestward) from the uplift. The general strike of the tuff beds and resultant structures mimic the strike along the northwest flank of the Broken Bow uplift (N65°E). Locally, tear faults (lateral ramps) break the tuff outcrop belt with offsets of 200 ft. Where tear faults are associated with well-developed thrust faults, the displacements are 2,000–3,000 ft. No preference is noted between left-lateral or right-lateral movement along the tear faults. A series of cross sections (Fig. 4) was constructed perpendicular to the structural strike in an attempt to demonstrate a down-plunge view across the prominent anticlinorium centered in sec. 7, T. 4 S., R. 23 E.

Concentric Folding

The concepts of concentric folding and structural lithic units must be integrated in order to better understand the complex structures present at the tuff stratigraphic level. The tuff-defined folds are concentric. Where the folds are tighter, volume problems arise within the core of the fold. The volume problem may be resolved by increased folding and/or faulting of less-competent strata within the core of the fold. Both of these responses to tightening were observed in the mapped area. The concentric fold may also detach from the folding strata where the volume problem can no longer be addressed by increased folding or faulting. When the

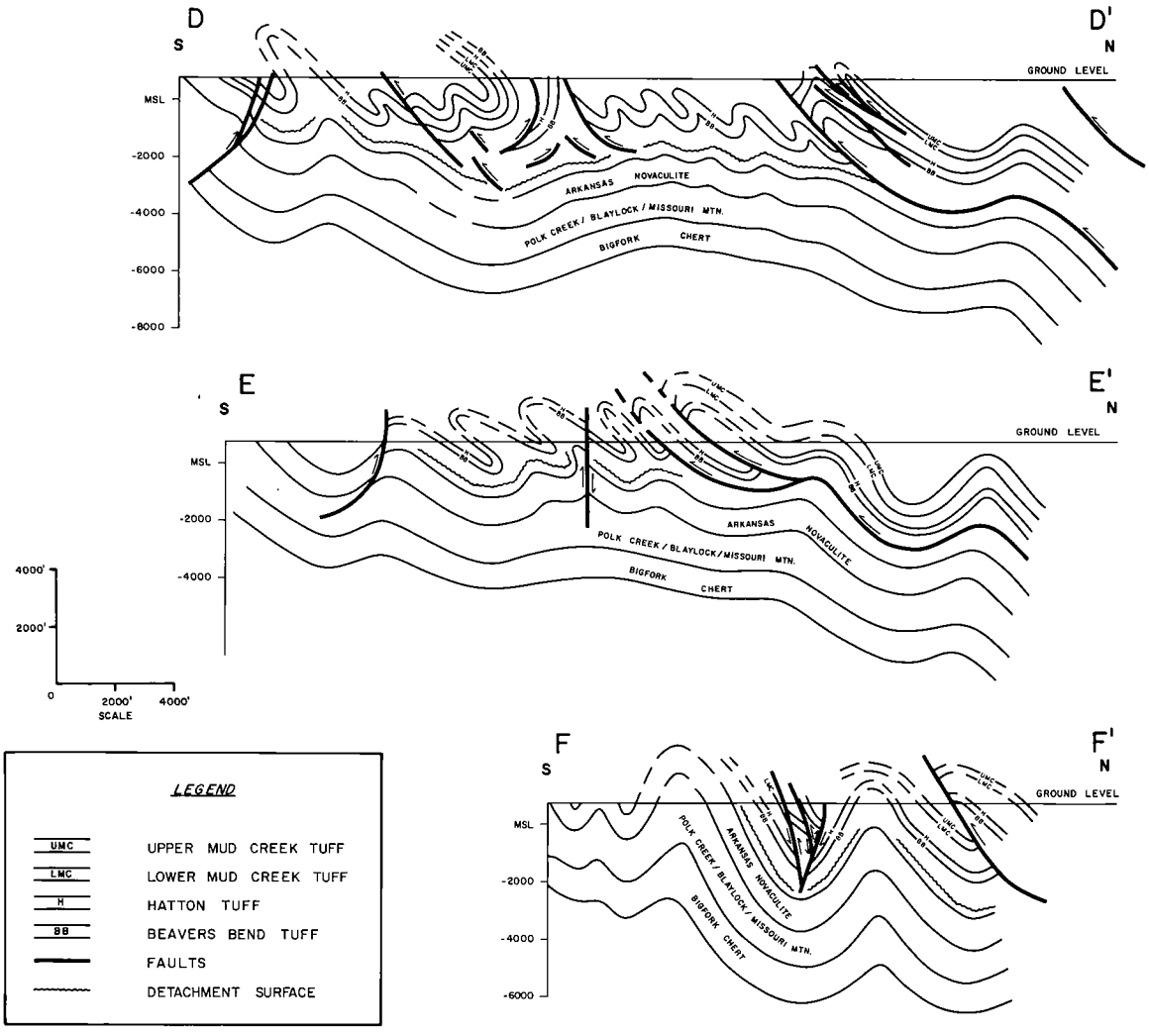
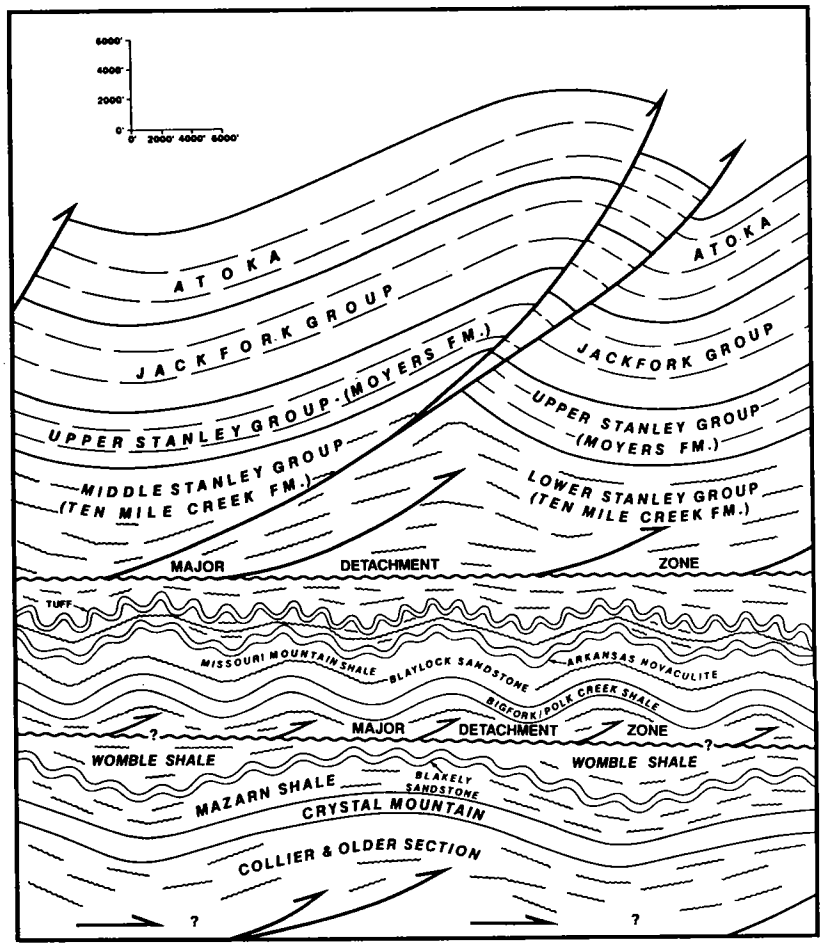


Figure 4 *(continued).*



BASAL OUACHITA THRUST ZONE

AGE	FORMATION	STRUCTURAL LITHIC UNIT THICKNESS			OBSERVED FOLD WAVELENGTH OF MEMBERS	COMMENTS (Nomenclature from Currie etal, 1962)
PENN.	ATOKA	UPPER UNIT	24,000'±	17,000'±	COMPLICATED BY THRUST FAULTS	DOMINANT MEMBER(S)
MISSISSIPPIAN	JOHN'S VALLEY SH.					
	JACKFORK SS.					
	UPPER STANLEY					
						DETACHMENT SURFACE
	MIDDLE STANLEY			7000'	1-100'	INCOMPETENT MEMBER
	LOWER STANLEY					
				BOUNDARY ZONE		
DEV.	VOLCANICLASTIC TUFF SECTION &LOWER FLYSCH	MIDDLE UNIT	3400'+	400'	1000-1500'	CONFORMING MEMBER TO ARKANSAS NOVACULITE
						DETACHMENT ZONE
	UPPER NOVACULITE			600'	2000'±	DOMINANT CONFORMING MEMBER
	NOVACULITE SHALE					MINOR DETACHMENT ZONE IN MIDDLE MEMBERS
	LAMINATED ZONE					
	PINETOP CHERT					CONFORMING MEMBER TO UPPER NOVACULITE
	MISSOURI MTN. SH.					
SIL.	UPPER BLAYLOCK					
	LOWER BLAYLOCK			400'	5-20'	DETACHMENT ZONE IN MIDDLE - LOWER BLAYLOCK SS.
ORDOVICIAN	POLK CREEK SH.			1000'±	10,000'±	DOMINANT MEMBER
	BIGFORK CHERT					
	UPPER WOMBLE SH.					
	?		?	BOUNDARY ZONE		? ? ?
	LOWER WOMBLE SH.	LOWER UNIT	3500'+	2500'±?	1-100'±	INCOMPETENT MEMBER
	BLAKELY SS.					
	MARZARN SH.					
						DETACHMENT ZONE
	CRYSTAL MTN. SS.			1000'±?	30,000'±?	? DOMINANT MEMBER ?
	COLLIER SH.			1000'±?	1-100'±	INCOMPETENT MEMBER

Figure 5. Diagrammatic section of postulated structural lithic units and fold wavelengths in the Ouachita facies in and near Broken Bow.

fold detaches, the detachment zone is representative of a type of décollement surface. The tuff couplets appear to detach within the lower Tenmile Creek Formation, ~300 ft above the Arkansas Novaculite. The Arkansas Novaculite does not appear to be directly involved in the tighter folds expressed by the tuffs. Where the tuff folds are more open, the tuffs and the lower, competent Arkansas Novaculite do appear similarly deformed.

Fold detachments can and do occur between the two tuff couplets; this response may be due in part to dip slip along a low-angle thrust. Such detachments, best observed at the northernmost Mud Creek tuff couplet exposure, are shown in cross sections D–D′ and F–F′ (Fig. 4), where the tightly folded upper couplet is detached from the lower couplet. Although this detachment is recognized (cross section D–D′), the occurrence of the detachment is limited to localities where the Mud Creek couplet is tightly folded to produce a detachment surface. Dip-slip movement along bedding planes within concentric folds provides the mechanics for subsequent "independent" folding to generate the nonparallel outcrop pattern of the tuff couplets observed along the western edge of the mapped area.

Structural Lithic Units

A structural lithic unit is defined as a set of beds containing one or more dominant members whose thickness and physical properties determine the wavelength of the resultant fold (Currie and others, 1962). Included within this "unit" can be other competent members (of lesser thickness) and incompetent beds that conform to the fold style of the dominant controlling member(s). Within the lower Tenmile Creek Formation, the tuff interval (400-ft gross thickness) is treated as the one and only competent member that responds as a structural lithic unit upon folding and deformation. The mapped tuff section has a fold wavelength of 1,500–2,000 ft, whereas the enclosing, thin- to medium-bedded (0.1–10.0 ft thick), noncompetent siltstones and shales have a 10–200-ft fold wavelength.

Examination of the regional geologic map for the southern Ouachita Mountains in southeastern Oklahoma by Honess (1923) reveals characteristic fold wavelengths for the lower "starved-basin" sedimentary section (Devonian and older strata) and, in part, for the overlying flysch section (Mississippian and Pennsylvanian). Figure 5 shows the dominant, competent structural lithic units within the Ouachita facies and their respective detachment surfaces. One of the key points is the overall relation of the lower Stanley tuffs to the Arkansas Novaculite and the significant detachment within the lower Stanley Group; this detachment is a boundary between two distinct and independent deformation styles observed in the core area and in the synclinal foldbelt of the Ouachita Mountains. The lower Stanley detachment is confirmed by proprietary drilling results and is observed in seismic data. Detailed mapping from aerial photographs readily reveals this major detachment surface.

Arkansas Novaculite Structure

The original purpose of the tuff-mapping project was to delineate a closed structure (i.e., a drillable hydrocarbon prospect) at the Arkansas Novaculite–Bigfork Chert stratigraphic level. Based on field measurements, observations, and structural relations between the tuff and Arkansas Novaculite, an Arkansas Novaculite structure map (Fig. 6) was constructed from the cross sections (Fig. 3). The Arkansas Novaculite structure shows a series of long, narrow anticlines and synclines, trending approximately N65°E along the northwest flank of the Broken Bow uplift. Toward the northern extent of the uplift and along the Cross Mountains, the beds strike east. As expected, the Arkansas Novaculite maintains a structural style in the subsurface that is similar to that observed in outcrops.

The geologic map of the stratigraphically differentiated lower Stanley tuff units confirmed a large anticlinorium centered in sec. 18, T. 4 S., R. 23 E., as suggested by previous mapping (Honess, 1923). The novaculite structure map also reflects a large closed structure in the same area. Cross sections A–A′ through D–D′ also demonstrate this closed structure (Fig. 4).

RESULTS OF EXPLORATORY DRILLING

On the basis of the results of the tuff mapping project, the SOHIO no. 1-7 Weyerhaeuser well (sec. 7, T. 4 S., R. 23 E., in McCurtain County) was designed as a conceptual test of the Arkansas Novaculite, Blaylock Sandstone, and Bigfork Chert fractured reservoir within the tuff-defined anticlinorium. The rank wildcat reached a total depth of 6,721 ft on June 25, 1985, in the Blaylock Sandstone. Results showed a south-verging, overturned fold incorporating the Arkansas Novaculite, Missouri Mountain Shale, and the upper Blaylock Sandstone. The fold is detached in the overlying lower Tenmile Creek Formation and in the middle of the Blaylock Sandstone, as interpreted from dipmeter analysis, SCAT (Fig. 7). The structural style of the tuff units within the mapped area, and especially of the outcropping Arkansas Novaculite, coincided with the structure seen from the well results. However, the well had no gas shows, and the potential reservoirs were tight (calcite-healed fractures). The SOHIO no. 1-7 Weyerhaeuser well was plugged and abandoned on July 1, 1985.

ACKNOWLEDGMENTS

The writers express their appreciation to the Tex-Con Oil and Gas Co. (formerly Sohio Petroleum Co.) for permission to publish this paper. The writers also acknowledge the contributions of nu-

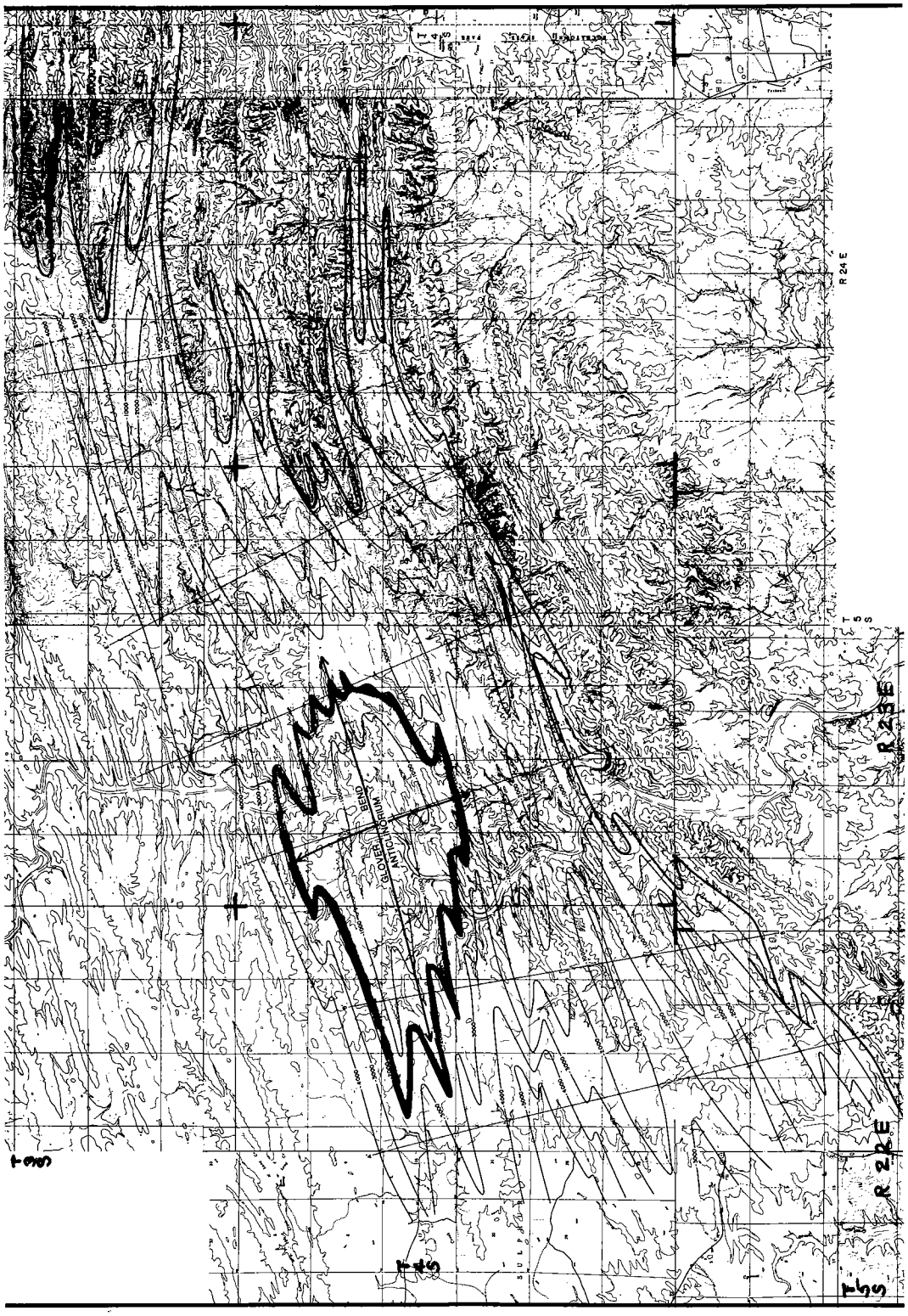


Figure 6. Structure map on top of the Arkansas Novaculite: contour interval 1,000 ft; all elevations below sea level.

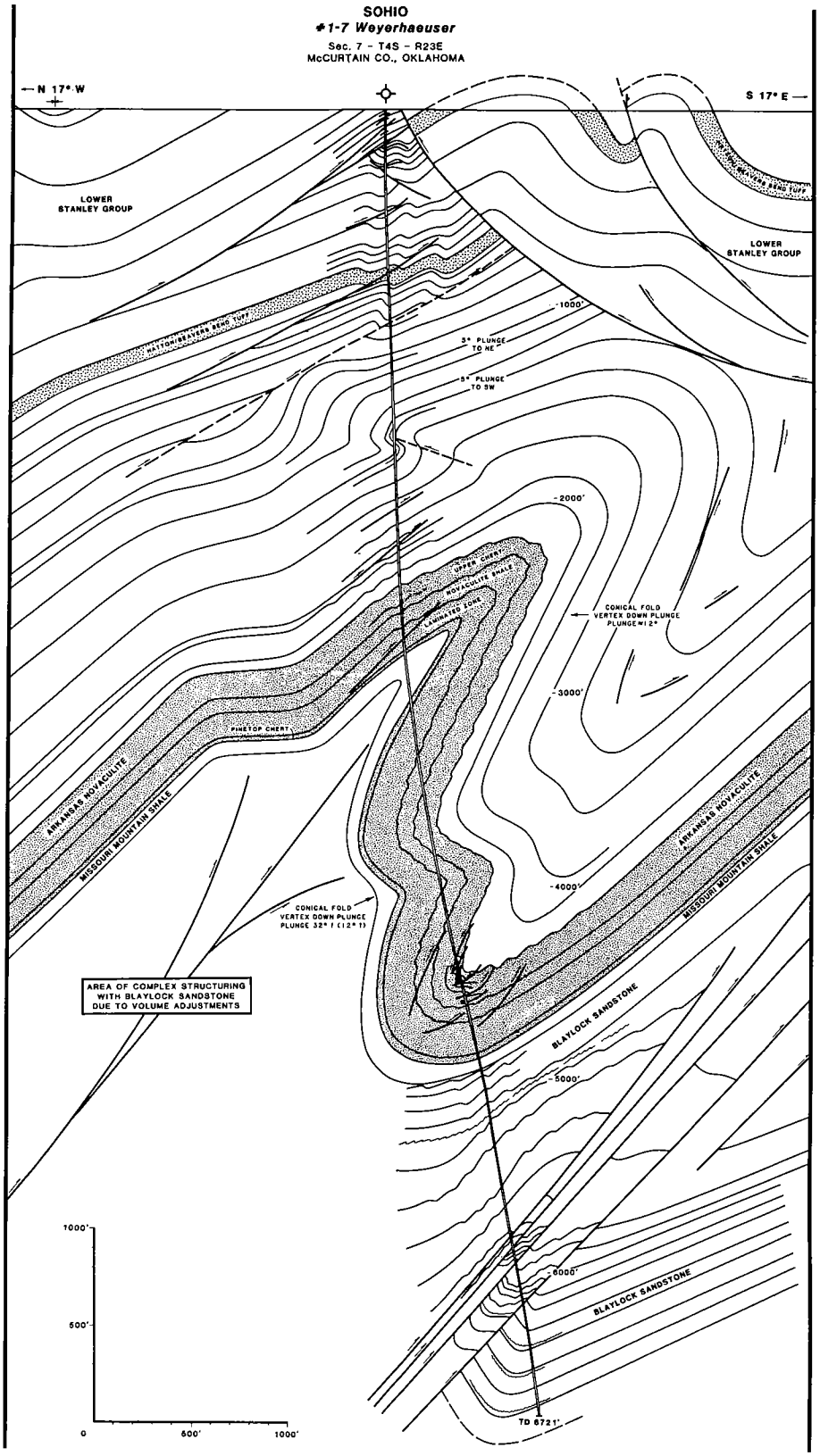


Figure 7. Geologic cross section of the Sohio no. 1-7 Weyerhaeuser (Allison, 1985).

merous coworkers at Sohio (Dallas) who assisted with the field-mapping project.

REFERENCES CITED

Allison, M. L., 1985, Cross section of the Sohio Weyerhaeuser #1-7, McCurtain County, Oklahoma: Sohio Petroleum Co. report, 1 plate.

Currie, J. B.; Patnode, H. W.; and Trump, R. P., 1962, Development of folds in sedimentary strata: Geological Society of America Bulletin, v. 73, p. 655–674.

Honess, C. W., 1923, Stratigraphy, structure, and physiographic history, *in* Geology of the southern Ouachita Mountains of Oklahoma: Oklahoma Geological Survey Bulletin 32, 278 p.

Miser, H. A., 1920, Mississippian tuff in the Ouachita Mountain region [abstract]: Geological Society of America Bulletin, v. 31, p. 125–126.

Miser, H. A.; and Purdue, A. H., 1929, Geology of the DeQueen and Caddo Gap Quadrangles, Arkansas: U.S. Geological Survey Bulletin 808, 195 p.

Neim, A. R., 1971, Stratigraphy and origin of tuffs in the Stanley Group (Mississippian), Ouachita Mountains, Oklahoma and Arkansas: University of Wisconsin unpublished Ph.D. dissertation, 150 p.

Surface to Subsurface Study of the Northwest Plunge of the Arbuckle Anticline

Christopher P. Saxon*
Baylor University
Waco, Texas

Outcrops of the northwestern part of the Arbuckle uplift can be divided into three segments: (1) the area containing the Colbert Creek, Pickens, and Lick Creek anticlines, (2) the Garrison Creek anticline, and (3) the major Arbuckle anticline. These areas are separated by two exposed faults, the Garrison Creek and Washita Valley faults. Each area displays a different exposed stratigraphy and structural style (Fig. 1). First-order folds are broadest in the Arbuckle anticline and become progressively smaller and tighter across the Garrison Creek anticline and into the Colbert Creek, Pickens, and Lick Creek area. Displacement is greater on the Garrison Creek fault (Kindblade against Hunton) than on the Washita Valley fault (Cool Creek on Kindblade).

Based on observed deformational style, the exposed northwestern edge of the Arbuckle anticline is interpreted to be a fault-bend fold. Major slip occurred on the Arbuckle thrust, which remains buried but is well documented by well data (Brown, 1984). The Garrison Creek fault and Washita Valley fault are back-limb imbricates to the Arbuckle thrust. The subcrop trace of the Garrison Creek fault turns to the north–northwest and links

*Present address: University of Oklahoma, Norman.

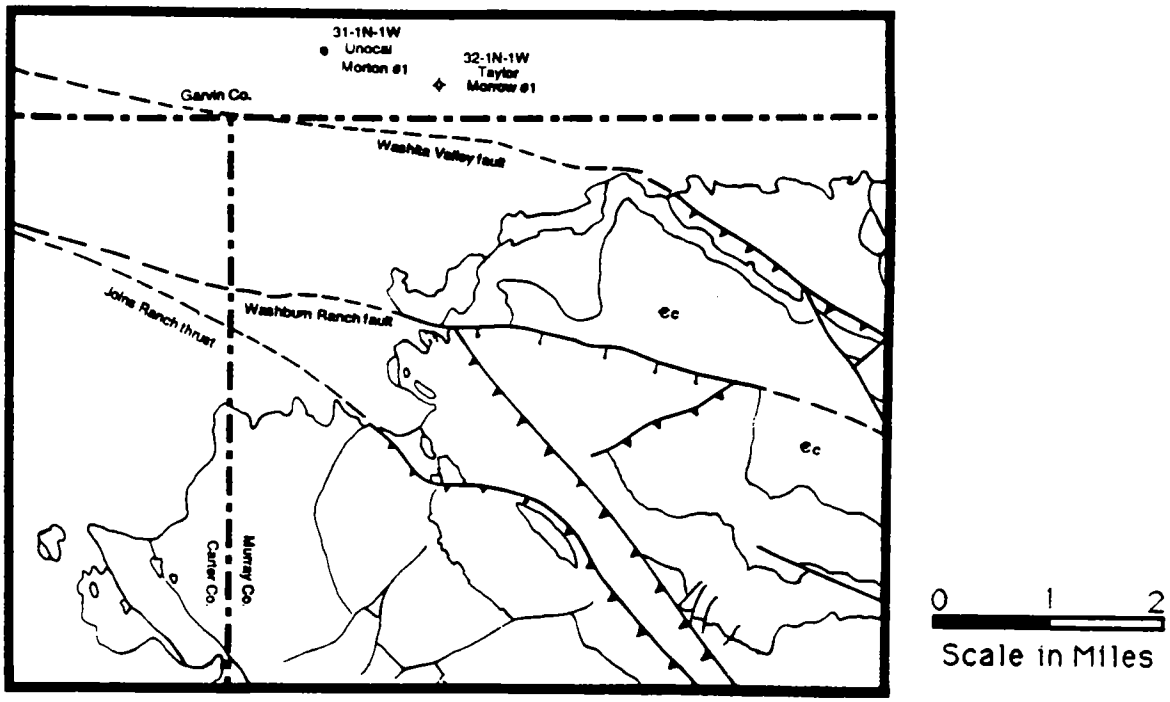


Figure 1. Pre-Pontotoc subcrop trace of faults along the northwest plunge of the Arbuckle anticline. Note the Washita Valley fault must subcrop south of the Unocal and Taylor wells. The Washburn Ranch fault truncates older compressional features.

Saxon, C. P., 1995, Surface to subsurface study of the northwest plunge of the Arbuckle anticline, *in* Johnson, K. S. (ed.), Structural styles in the southern Midcontinent, 1992 symposium: Oklahoma Geological Survey Circular 97, p. 277–279.

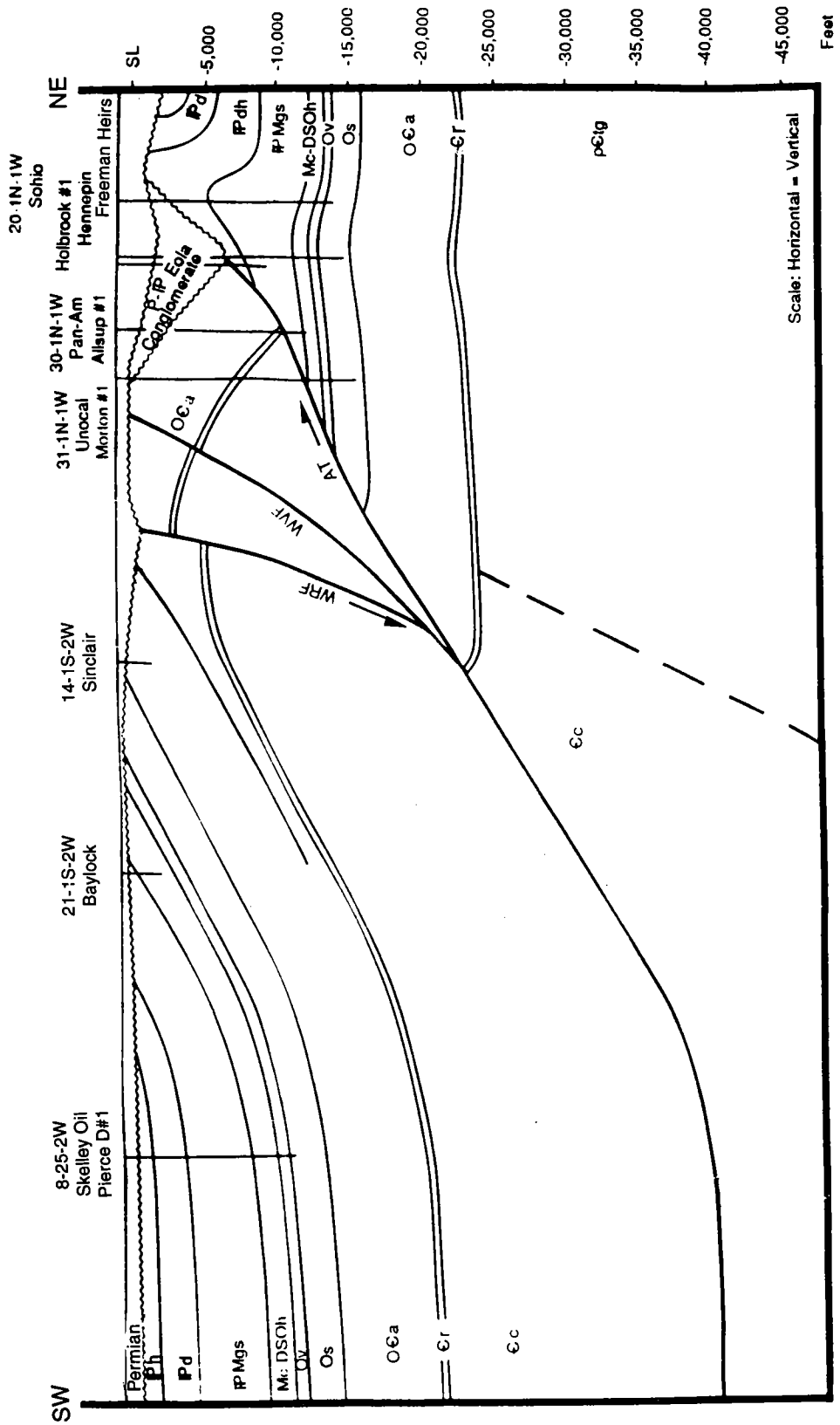


Figure 2. True scale NE–SW cross section (perpendicular to B-axis) across the buried NW Arbuckle anticline. Note the normal displacement of the Washburn Ranch fault (WRF) and its topographic expression on the unconformity at the base of the Permian. WVF = Washita Valley fault; AT = Arbuckle thrust.

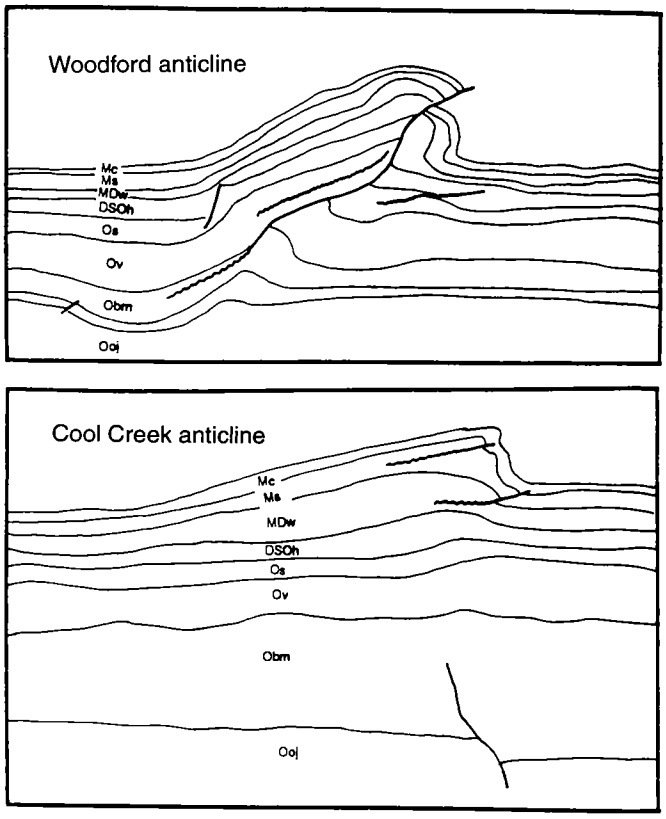


Figure 3. Down-plunge constructions of the Woodford and Cool Creek anticlines on the southern flank of the Arbuckle anticline. Note the deformation mechanisms, such as bedding planar detachments and fault-bend folding.

with the leading edge of the Arbuckle thrust. This serves to compartmentalize the SE Hoover block to the east and the Garrison Creek block to the west. The subcrop trace of the Washita Valley fault is approximately E–W, and displacement decreases from east to west. The northern location is constrained by the Unocal Morton (sec. 31, T. 1 N., R. 1 W.) and Taylor Morrow (sec. 32, T. 1 N., R. 1 W.) wells (Fig. 1), which do not encounter the Washita Valley fault but do encounter the Arbuckle thrust.

The Washburn Ranch fault reflects a period of postcompressional extension. The Washburn Ranch fault has an E–W surface trace which turns to the northwest in the subsurface, paralleling the trend of the buried uplift. Displacement increases to the northwest and appears to correspond to a change in structural style of the Arbuckle anticline, from that of a fault-bend fold to that of a fault-propagation fold (Fig. 2). On the surface, the Washburn Ranch fault clearly truncates compressional folds and thrusts. In the map pattern, onlapping syntectonic conglomerates make an embayment to the south of the Washburn Ranch fault. Cross sections constructed down plunge indicate that the conglomerates fill a half-graben formed by the down-to-the-southwest motion of the Washburn Ranch fault (Fig. 2). The conglomerate fill of this half-graben is overlain by Permian red beds to the northwest, providing an upper time constraint on the extensional movement of the Washburn Ranch fault. As displacement increases to the northwest, the size of the graben and amount of infilling conglomerate increase. Where Washburn Ranch fault extends into the Eola area, the displacement is on the order of several thousand feet. The resulting "beheaded" basement block could be misinterpreted as a "flower" structure on seismic data.

Based on the presence of parallel folding, detachments, small-scale incipient triangle zones, and bedding-parallel slip in outcrops along the southern end of the Arbuckle anticline, the Woodford and Spring Creek anticlines are interpreted to be back-limb thrusts (Fig. 3). Previous workers (Ham and others, 1954) have tended to map prominent Arbuckle Group fractures as faults, and merged them with unrelated faults in younger rocks, despite the fact that the fault must cut across unbroken contacts or that the ensuing fault had a variable sense and amount of displacement.

REFERENCES CITED

Brown, W. G., 1984, Washita Valley fault system: a new look at an old fault, *in* Technical Proceedings of the 1981 American Association of Petroleum Geologists Mid-Continent Section regional meeting: Oklahoma City Geological Society, p. 68–80.

Ham, W. E.; McKinley, M. J.; and others, 1954 [revised by K. S. Johnson, 1990], Geologic map and sections of the Arbuckle Mountains, Oklahoma: Oklahoma Geological Survey Map GM-31, 1 sheet, scale 1:100,000.

Significance of Fault Dip to Angle of Bedding in Determination of Structural Styles: Examples from Southern Oklahoma

Christopher P. Saxon
University of Oklahoma
Norman, Oklahoma

The literature on structural geology of southern Oklahoma contains a myriad of interpretations of structural styles, many in extreme variance with one another. Although large amounts of northeast-southwest shortening exist across the major basins and uplifts, many authors classify the regional style of deformation as strike-slip because many faults are reported as having a high angle of dip (near-vertical to vertical dip). Additionally, many authors report the presence of normal faults on the crests or flanks of large folds, leading them to conclude that the dominant structural style involves differential vertical uplift or strike-slip faulting, or a combination of the two. The significance of the shortening

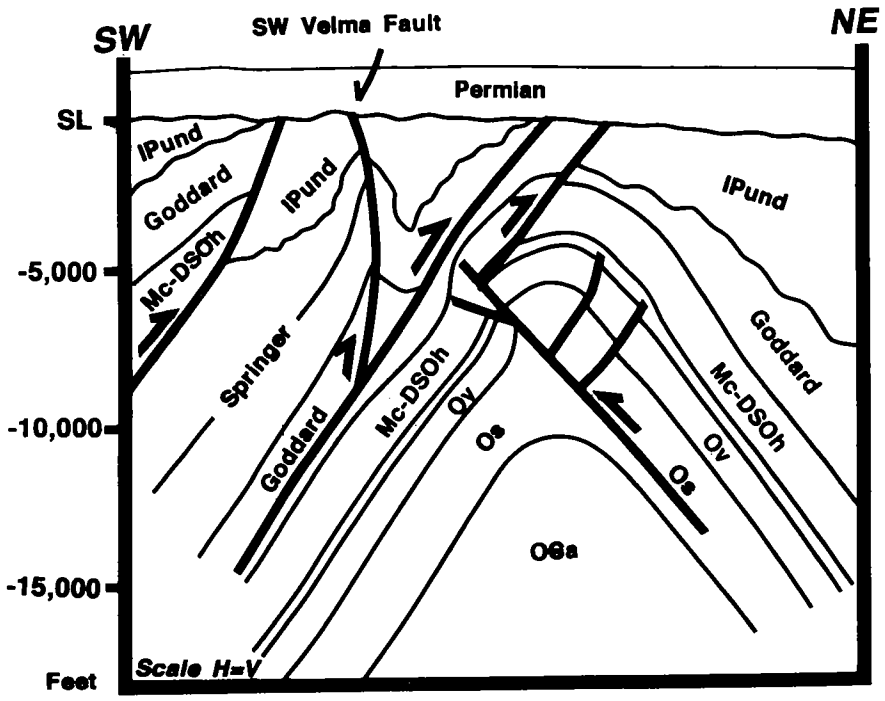


Figure 1. Structural cross section across the Southwest Velma field. Well control has been removed from the original illustration for clarity. Note the dominant style of thrusting along thrusts that detach within the sedimentary section. The beds that the faults detach into are located in areas of steep dip on a large Arbuckle-cored fold. Thrusts that ramp at low angle from the bedding-planar detachment (Southwest Velma fault) appear as high-angle and even normal faults in boreholes. IPund = Pennsylvanian, undifferentiated; Mc-DSOh = Mississippian Caney–Devonian-Silurian-Ordovician Hunton; Ov = Ordovician Viola; Os = Ordovician Simpson; OCa = Ordovician-Cambrian Arbuckle. (Modified from Hicks, 1956.)

Saxon, C. P., 1995, Significance of fault dip to angle of bedding in determination of structural styles: examples from southern Oklahoma, *in* Johnson, K. S. (ed.), Structural styles in the southern Midcontinent, 1992 symposium: Oklahoma Geological Survey Circular 97, p. 280–282.

accommodated by folding and the relationship of folding to faulting have not been well documented in southern Oklahoma. Most of the literature addresses fault slip only and then usually in only one direction. This paper proposes that in the assessment of structural style, the dip angle of the fault, as compared to the dipping sedimentary section, and its spatial and temporal relationship to the geometry of the dominant structural features (major folds as well as faults) should be the primary consideration in assessing interpretations of structural style.

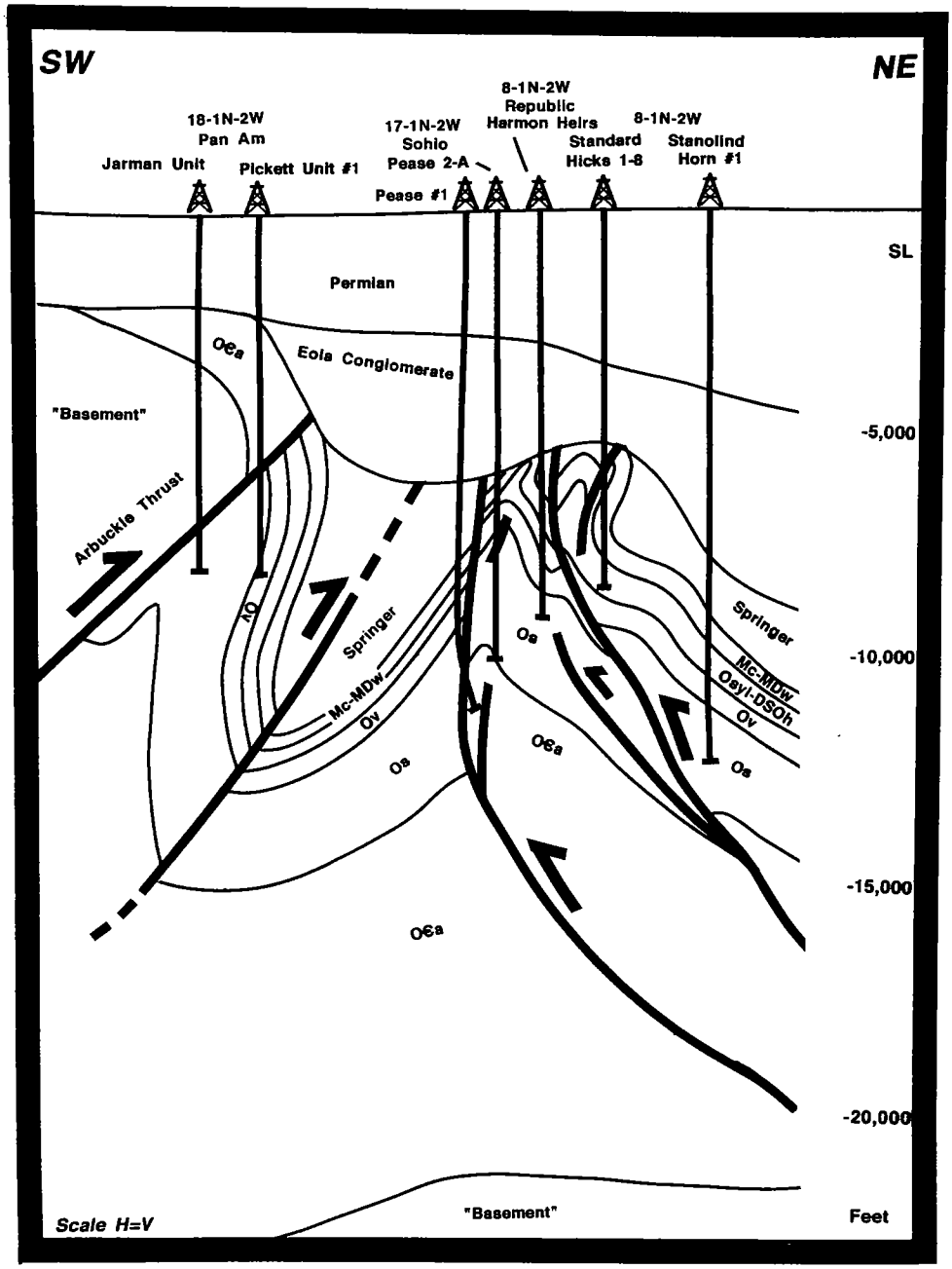


Figure 2. Structural cross section across the Eola anticline. The overturned thrust in the Arbuckle Group contributed to the "peeling back" of the thrusts near the crest of the structure. In assessing structural style and tectonic history, note which faults and folds contain the greatest amount of shortening (i.e., the Arbuckle thrust and the Eola anticline) and which faults and folds are of subsidiary importance (i.e., the overturned thrust).

Faults that now have a steep dip, but are at a low angle to bedding, either have been rotated into place or represent local crowding conditions as a result of larger-scale folding processes. Additionally, faults that show an apparent sense of normal offset may be thrust faults that have been overturned. Examination of the regional style of deformation—by means of properly oriented, closely spaced, one-to-one scale cross sections—is crucial to the assessment of structural style.

Figure 1 is a cross section across the Southwest Velma field. This cross section depicts an anticlinal fold in the Arbuckle Group, above which numerous subsidiary structures occur above detachments. The subsidiary folds have vergence across either flank of the fold and follow the type example of a "ping-pong" structure noted in the Wyoming foreland (Brown, 1988). Note the West Velma anticline, which is a subsidiary thrust-cored anticline on the southwest limb of the Arbuckle Group-cored fold. The Southwest Velma fault is a back-limb imbricate to a cross-crestal detachment that is cut by the Permian unconformity. Near its ramp, the Southwest Velma fault appears as a steep-dipping normal fault, especially in the numerous well logs that have been made through this productive reservoir (logs not shown in Fig.1 for clarity); however, the Southwest Velma fault becomes a bedding-planar to sub–bedding-planar fault as it detaches in the Goddard shales.

Figure 2 is a structural cross section across the Eola anticline in the footwall of the Arbuckle thrust. The Sohio Pease no. 1 well intersected a steeply dipping to overturned reverse fault that appears as a normal fault on the electric log (upper Simpson into Arbuckle). The Standard Hicks no. 1-8 well also intersected an apparent normal fault on the hanging wall of the overturned thrust. These two wells could be misinterpreted as defining an element of extension superimposed across an area of dominant shortening. Note, however, that the abundant well control shows that these faults are flanked by areas of steep dip, overturned folds, major crustal shortening, and numerous detachments. In assessing the tectonic significance of various structures, the faults and folds that accommodate the greatest amounts of shortening or extension (depending on regional style) should be considered as having the most significance. In Figure 2, the Arbuckle thrust places basement rock against Simpson Group strata and generates severe footwall folding. On the Eola anticline, folding takes up more shortening than does the overturned thrust. Furthermore, if the overturned thrust were interpreted as a normal fault, the extension (heave) would be insignificant compared to the shortening present in the Eola anticline.

REFERENCES CITED

Brown, W. G., 1988, Deformation style of Laramide uplifts in the Wyoming foreland, *in* Schmidt, C. J., and Perry, W. J., Jr. (eds.), Interaction of the Rocky Mountain foreland and the Cordilleran thrust belt: Geological Society of America Memoir 171, p. 1–25.

Hicks, I. C., 1956, Geology of the Southwest Velma field, Stephens County, Oklahoma, *in* Petroleum geology of southern Oklahoma, volume 1: American Association of Petroleum Geologists, Tulsa, p. 244–259.

Structural Control of the Reagan and Mill Creek Faults on the Sedimentary Environments of the Deese Conglomerate, Arbuckle Mountains, Southern Oklahoma

Craig Stafford, Ibrahim Cemen, and Zuhair Al-Shaieb
Oklahoma State University
Stillwater, Oklahoma

ABSTRACT.—The Desmoinesian Deese conglomerate is exposed in the Mill Creek syncline area between the Reagan and Mill Creek fault zones. The conglomerate contains rounded to well-rounded clasts of Ordovician to Devonian carbonates eroded from the Arbuckle Mountains. Interbedded with the conglomerates are beds of fossiliferous limestone, brown shale, and sandstone.

The Deese conglomerate is interpreted as a coastal-plain alluvial fan, or possibly a fan-delta complex, that received sediments from highlands to the south, southeast, east, and northeast. Transport directions were derived from field measurements of imbricated clast orientation. The presence of glauconite in many samples is a good indication of marine lithofacies. Channel-dominated facies were deposited in the coastal alluvial fan or fan delta while, in deeper parts of the basin, fine-grained clastic rocks and limestones were deposited.

The highly elevated areas necessary for formation of these fans were probably formed by strike-slip movement along the Reagan and Mill Creek fault zones. Therefore, the basin in which the Deese conglomerate was deposited can be classified as a strike-slip basin formed between two strike-slip faults.

INTRODUCTION

Pennsylvanian conglomerates within the Arbuckle Mountains are direct evidence of the deformation stage of the southern Oklahoma aulacogen (Fig. 1). This stage consisted of numerous orogenic pulses related to the collision of the North American plate with the southern continental land mass (Sadd, 1986). Ham and Wilson (1967) suggest that there were at least six individual episodes of Pennsylvanian tectonism in the Mid-continent. These episodes occurred in pre-Morrowan, pre-Atokan, early Desmoinesian, early Missourian, early Virgilian, and late Virgilian times.

Wickham (1978) proposed that the northwest-trending high-angle faults of the Arbuckle Mountains (Fig. 1) were formed during the rifting stage of the southern Oklahoma aulacogen as predominantly normal faults, and were reactivated as strike-slip faults during the deformation stage of the aulacogen in Pennsylvanian time. Two of these faults are the Mill Creek and Reagan faults. The Desmoinesian Deese Group (Fig. 2) was deposited between the Reagan and Mill Creek faults in the Mill Creek syncline, ~3 mi south of the town of Sulphur in Murray County (Figs. 1 and 3). Therefore, the Deese conglomerate records the nature of movement along the two fault zones during the Desmoinesian.

The main purpose of this paper is to describe the structural control of the Reagan and Mill Creek fault zones on sedimentation patterns of the Desmoinesian Deese conglomerate. Therefore, the relationship between fault zones, lithofacies, sedimentary environments, and petrography of the Deese conglomerate will be discussed.

Figure 2 is a generalized stratigraphic section of the Mill Creek syncline area. The stratigraphic framework of the sedimentary rocks in the Arbuckle Mountain region is discussed in detail by Maxwell (1931), Gilbert (1952), McKinley (1954), and Glaser (1965).

DEESE CONGLOMERATE

The Deese conglomerate consists of pebble- to boulder-size clasts. The clasts are mostly limestone, but pebble-size chert clasts are also present in some areas. Outcrops of the conglomerate are rare, and, where present, they are small lenses between shale or fine-sand layers. A partial section (Fig. 4) was measured in NW¼NW¼NE¼ SW¼ sec. 26, T. 1 S., R. 3 E. (see Fig. 3). The limestone clasts are subrounded to rounded, although some angular ones

Stafford, Craig; Cemen, Ibrahim; and Al-Shaieb, Zuhair, 1995, Structural control of the Reagan and Mill Creek faults on the sedimentary environments of the Deese conglomerate, Arbuckle Mountains, southern Oklahoma, *in* Johnson, K. S. (ed.), Structural styles in the southern Midcontinent, 1992 symposium: Oklahoma Geological Survey Circular 97, p. 283–287.

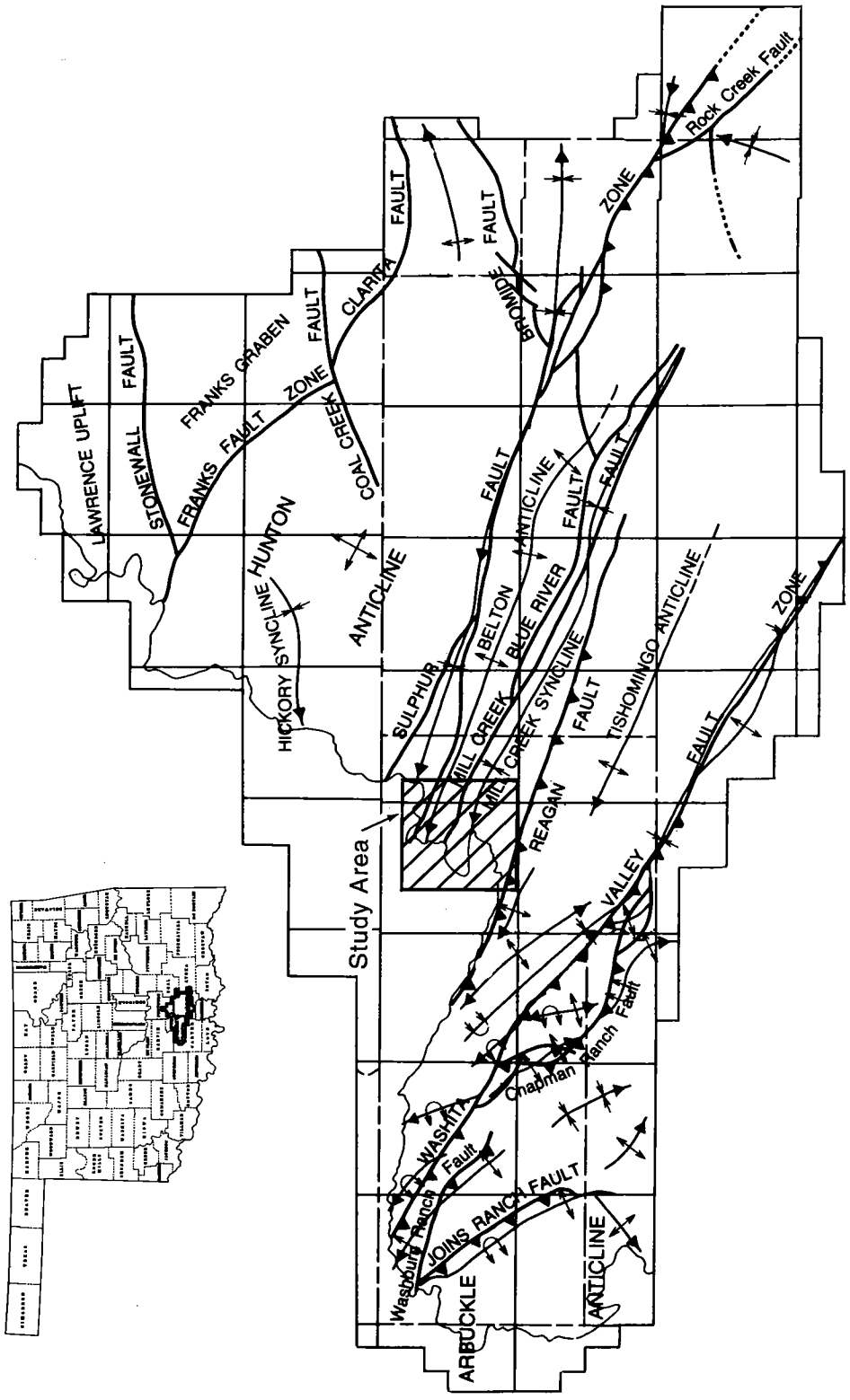


Figure 1. Index map of the Arbuckle Mountains showing the study area and principal structural features (modified from Ham and McKinley, 1954).

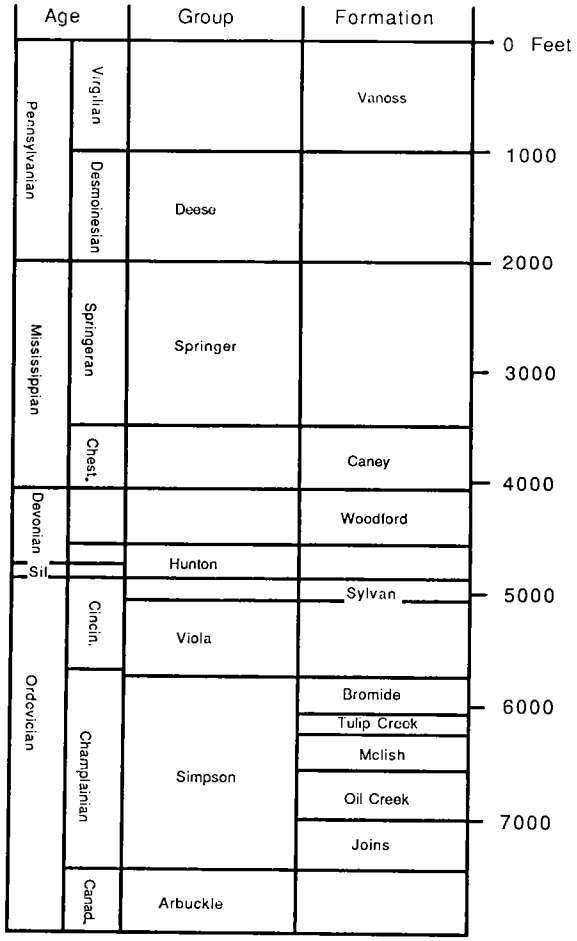


Figure 2. General stratigraphic section of the Sulphur area, Murray County, Oklahoma (modified from Williams, 1985).

are also present. However, the chert clasts are very angular; this suggests that the Deese conglomerate was derived from a nearby source area.

Determination of the source formation of each clast observed in the field would be extremely difficult. However, the limestone clasts generally appear to be very similar to the Cambrian and Ordovician carbonate-rock units exposed in adjacent areas. Some chert clasts with dolomite rhombs are similar to the cherts of the Early Ordovician Cool Creek Formation. In fact, one chert fragment that contains ~27% dolomite, along with a trace of zircon, is compositionally identical to the chert found in the Cool Creek Formation (M. D. Allison, personal commmunication, 1992).

Based on measured orientations of 72 imbricate clasts (Fig. 5) in sec. 26 and 27, T. 1 S., R. 3 E., the conglomerate was transported from source areas to the south and the northeast. Furthermore, this also suggests that the clasts may have been derived from uplifted blocks of the Reagan fault, to the south, and of the Mill Creek fault, to the north.

Also associated with the conglomerate are two separate limestone facies, which are present in secs. 26 and 34, T. 1 S., R. 3 E. These limestones are lithologically different and are separated stratigraphically by a shale and a conglomerate. The lower limestone contains more than 50% echinoderm plates, ossicles, and fragments, suggesting a mound or bioherm typical of a shallow-water environment. The upper limestone contains only about 10% fossils, but almost half of the fossils are planktonic foraminifera, suggesting a deeper-water environment.

Evidence of pressure solution is rare in the samples examined under a petrographic microscope. However, sutured grain boundaries of a few clasts were observed. The presence of glauconite in many samples is an indication of a marine depositional environment.

Thin-section analysis revealed that the sand and mud (silt and clay) sized terrigenous constituents in the matrix consist mostly of quartz, feldspar, and chert grains. The quartz ranges in amount from 0 to 38% of the matrix. Two separate types of quartz grains are present. The very angular–angular grains appear to be from a nearby source area, since they show very little rounding due to transportation. These quartz grains probably were derived from Tishomingo Granite that was exposed close to the site of deposition. Rounded to well-rounded quartz grains are possibly reworked fragments of older sediments. These probably were derived from sandstones in the West Spring Creek or Oil Creek Formations. Plagioclase–feldspar, present in trace amounts, probably was derived from the Tishomingo Granite to the south.

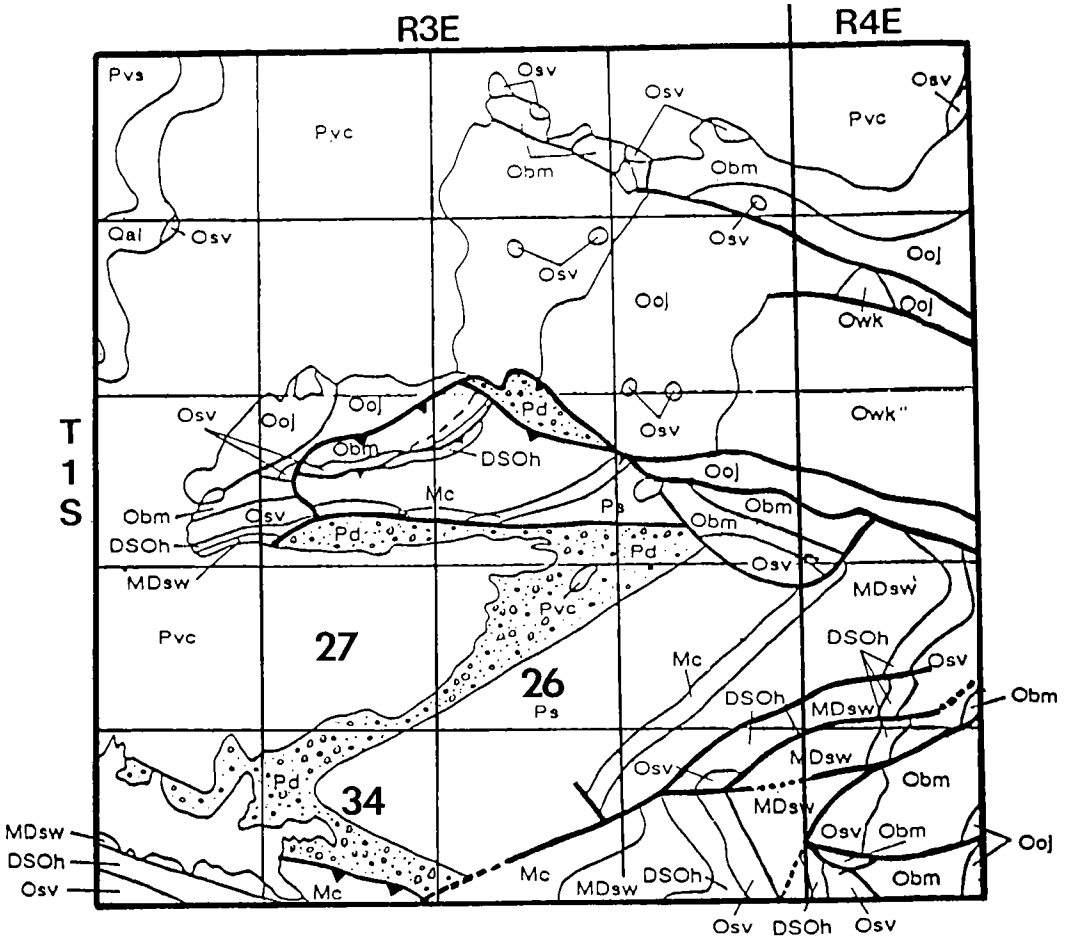
CONCLUSIONS

The field observations and microscopic analysis carried out during this study suggest that the Deese conglomerate was probably deposited in a coastal alluvial-fan or a fan-delta environment (Stafford, 1993). Fine-grained clastics and limestones were deposited in deeper parts of the basin. Paleocurrent measurements indicate that the conglomerate was transported from elevated areas to the south, southeast, east, and northeast. The elevated source areas probably were formed by possible strike-slip movement along the Reagan and Mill Creek fault zones. A similar mechanism was suggested by Wickham (1978) for the other Pennsylvanian basins of the Arbuckle Mountains during the deformation stage of the southern Oklahoma aulacogen. Therefore, the Deese Conglomerate basin can be classified as a strike-slip basin formed between two strike-slip faults. This geometry suggests that the strike-slip movement along the Mill Creek fault zone was a right-lateral, strike-slip movement, whereas along the Reagan fault zone it was a left-lateral.

The presence of the limestones between the conglomerates suggests that movement along the two fault zones was not continuous and that periods of tectonic activity were probably separated by periods of relative tectonic quiescence.

ACKNOWLEDGMENTS

This paper is based on M.S. thesis research by Craig Stafford, who did the field work in 1990 and the petrographic analyses in 1991. We acknowledge the funding provided by Union Oil Co. and a Larry Murphy Scholarship. Additional support was provided, in part, by ACS-PRF Grant No. 22636-B8, awarded to Ibrahim Cemen. Acknowledgment for partial support is also made to the donors of the Petroleum Research Fund, administered by the American Chemical Society. Discussions at various times with Kenneth Johnson, Nowell Donovan, and M. D. Allison were also helpful.



Qal - ALLUVIUM
Pvs/Pvc - VANOSS GROUP
Pd - DEESE GROUP
Ps - SPRINGER FORMATION
Mc - CANEY SHALE
MDsw - SYCAMORE LIMESTONE, WELDON LIMESTONE, WOODFORD SHALE
DSOh - HUNTON GROUP
Osv - SYLVAN SHALE & VIOLA GROUP
Obm - BROMIDE, TULIP CREEK & McLISH FORMATIONS
Ooj - OIL CREEK & JOINS FORMATIONS
Owk - WEST SPRING CREEK & KINDBLADE FORMATIONS
CONTACTS
FAULTS
FAULTS - INFERRED
FAULTS - THRUST

Figure 3. Simplified geologic map of study area (modified from Ham and McKinley, 1954).

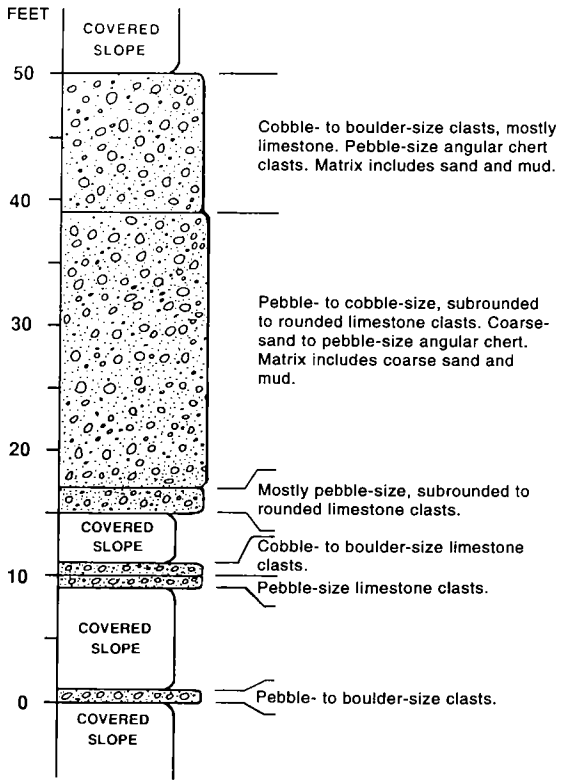


Figure 4. Incomplete measured columnar section of the Deese conglomerate. All clasts are limestone, unless otherwise noted. The matrix is sandy. Bedding planes are difficult to determine. The dip used to calculate bed thickness was 36°. Upper and lower contacts are hidden under covered slope.

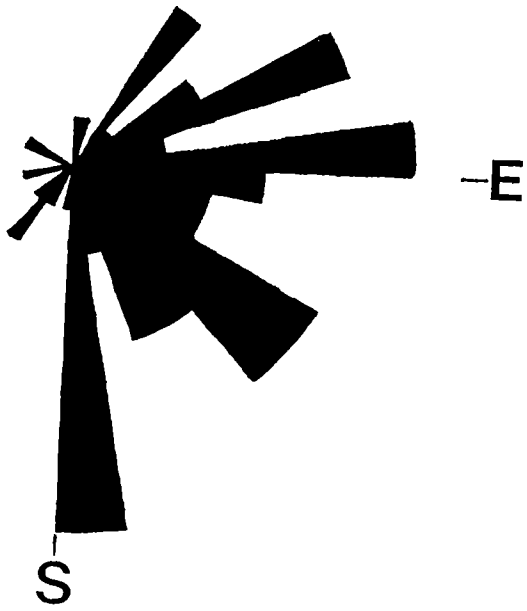


Figure 5. Rose diagram showing orientation of imbricate pebble- and cobble-size clasts in the Deese conglomerate, Murray County, Oklahoma. The long-axis trend and plunge of 72 imbricate clasts were measured. The dominant plunge of clasts is to the south, southeast, east, and northeast, indicating source areas to the south–southeast and east–northeast.

REFERENCES CITED

Gillert, M. P., 1952, The geology of the Simpson Group on the northeast flank of the Arbuckle Mountains, Oklahoma: University of Oklahoma unpublished M.S. thesis, 76 p.

Glaser, G. C., 1965, Lithostratigraphy and carbonate petrology of the Viola Group (Ordovician), Arbuckle Mountains, south-central Oklahoma: University of Oklahoma unpublished Ph.D. dissertation, 197 p.

Ham, W. E., 1969, Regional geology of the Arbuckle Mountains, Oklahoma: Oklahoma Geological Survey Guidebook 17, 52 p.

Ham, W. E.; and Wilson, J. L., 1967, Paleozoic epeirogeny and orogeny in the central United States: American Journal of Science, v. 265, p. 322–407.

Ham, W. E.; McKinley, M. E.; and others, 1954 [revised by K. S. Johnson, 1990], Geologic map and sections of the Arbuckle Mountains, Oklahoma: Oklahoma Geological Survey Map GM-31, 1 sheet, scale 1:100,000.

Maxwell, R. A., 1931, The Hunton Formation of the Arbuckle Mountains: University of Oklahoma unpublished M.S. thesis, 36 p.

McKinley, M. E., 1954, The geology and petrology of the Arbuckle and Timbered Hills Groups in the southeastern Arbuckle Mountains, Oklahoma: University of Oklahoma unpublished M.S. thesis, 200 p.

Pruatt, M. A., 1975, The southern Oklahoma aulacogen: a geophysical and geological investigation: University of Oklahoma unpublished M.S. thesis, 62 p.

Sadd, J. L., 1986, Petrology and geochemistry of the Buckhorn asphalt (Desmoinesian), Arbuckle Mountains, Oklahoma: University of South Carolina unpublished Ph.D. dissertation, 155 p.

Stafford, Craig, 1993, Stratigraphy, sedimentary environments and petrology of the Deese conglomerate in the Chickasaw National Recreation area: implications concerning structure of the Sulphur and Mill Creek fault zones, southern Oklahoma: Oklahoma State University unpublished M.S. thesis, 70 p.

Wickham, J. W., 1978, Arbuckle breccias, conglomerates, and the Washita Valley fault zone, *in* Field guide to the structural style of the Arbuckle region: Geological Society of America, South-Central Section Meeting, p. 100–102.

Williams, D. B., 1985, Structure and geochemical study of the south Sulphur asphalt deposits, Murray County, Oklahoma: Shale Shaker, v. 36, p. 182–196.

Surface Structures in Permian Strata of Southwestern Oklahoma as Indicators of Deep-Seated Structures

Kenneth S. Johnson
Oklahoma Geological Survey
Norman, Oklahoma

INTRODUCTION

Permian strata in southwestern Oklahoma overlie and mantle deep-seated structures that were developed mainly during Pennsylvanian tectonic activity. Surface mapping of the Blaine Formation and associated Permian strata shows that a number of faults, flexures, and folds, with vertical displacement of less than several hundred feet, overlie similar deep-seated structures with several thousand feet of relief. Structures in outcropping Permian strata result from late-stage tectonic adjustments along preexisting (Pennsylvanian) structures and/or from differential compaction of thick-versus-thin sequences of sedimentary layers on either side of deep-seated faults or basement-rock highs.

From north to south across southwestern Oklahoma (Fig. 1), the three major structural provinces are the Anadarko basin, which contains as much as 40,000 ft of Paleozoic strata; the west-northwest-trending Wichita uplift, which is covered by about 1,000–3,000 ft of uppermost Pennsylvanian–Lower Permian strata in the study area; and the Hollis basin, which typically has 6,000–12,000 ft of Paleozoic strata. The veneer of outcropping Permian sedimentary rocks responded passively to forces deeper in the crust and mantle. Stresses on these strata were mostly vertical, because block faulting and broad folding are the only results observed and at no place do the structures contain evidence of compression.

About 50 faults or flexures have been mapped in the Upper Permian Blaine Formation and associated strata in southwestern Oklahoma (Carr and Bergman, 1976; Havens, 1977). All faults are presumed to be normal; the several faults where fault planes can be observed are known to be normal, with fault-plane dips of about 60–65°. It is likely that most, or all, of the surface structures overlie similar deep-seated structures, but subsurface data are not available to prove this relation at all sites. On the other hand, additional deep-seated structures (other than those overlain by known surface faults, flexures, and folds) must also exist, but their presence would not be indicated on the outcrop if the structure has not been active since deposition of outcropping Permian strata.

Following is a discussion of four surface structures and their relation to known deep-seated structures. These structures are (1) the outcropping Sentinel fault zone, overlying the Mountain View fault; (2) the north Plainview flexure, overlying a basement fault on the Wichita uplift; (3) the Duke flexure zone, overlying the Burch fault zone; and (4) the Louis fault zone, overlying a horst in the SW Duke oil field.

SENTINEL FAULT ZONE

The Sentinel fault zone (Fig. 1) comprises seven faults that cut outcropping Permian strata and strike mainly west-northwest (Carr and Bergman, 1976). All faults are presumed normal and probably dip about 60–65°. They are 1–5 mi long and have throws of 20–115 ft, mainly down to the north.

The Sentinel fault zone overlies and parallels a major zone of thrust faults (Fig. 2) that separate the Wichita uplift from the Anadarko basin (Harlton, 1963; Ham and others, 1964). In the lowest part of the Anadarko basin, several miles to the north, the basement-rock surface is 20,000–40,000 ft lower than over the Wichita block. This vertical displacement is the result of crustal subsidence beneath the basin throughout the Paleozoic, accentuated mainly by Pennsylvanian and Early Permian thrusting of the Wichita block upward and somewhat northward. The main deep-seated thrust fault in this system is called the Mountain View fault.

Figure 2, the pre-Permian part of which is generalized from several cross sections by Harlton (1963), shows the basic relations of these deep-seated thrust faults to surface faults and flexures in the Sentinel fault zone. Permian strata were deposited unconformably on a subhorizontal or gently sloping surface that extended across the nearly dormant thrust zone. Subsequently, late-tectonic adjustments along the ancient thrust faults, or differential compaction of Paleozoic sedimentary rocks on either side of the thrust faults, were transmitted as differential vertical movements to the basal Per-

Johnson, K. S., 1995, Surface structures in Permian strata of southwestern Oklahoma as indicators of deep-seated structures, *in* Johnson, K. S. (ed.), Structural styles in the southern Midcontinent, 1992 symposium: Oklahoma Geological Survey Circular 97, p. 288–292.

mian strata and to the overlying rocks, which failed by means of normal faults or monoclinal flexures displaced down on the north.

NORTH PLAINVIEW FLEXURE

At Plainview, in the central part of the Wichita uplift, a double-plunging syncline (Fig. 1) is the surface expression of a deep-seated graben. The north and south flanks of the Plainview syncline are sharply defined by 4-mi-long monoclinal flexures (Carr and Bergman, 1976) across which beds are displaced vertically as much as 150 ft. Outcropping strata in the Blaine Formation dip 25–65° toward the synclinal axis across both flexures in narrow belts about 100–200 ft wide. At several places the flexed beds are faulted. To the east and west, both flanks of the fold grade into gentle flexures where dips are only 60–120 ft/mi.

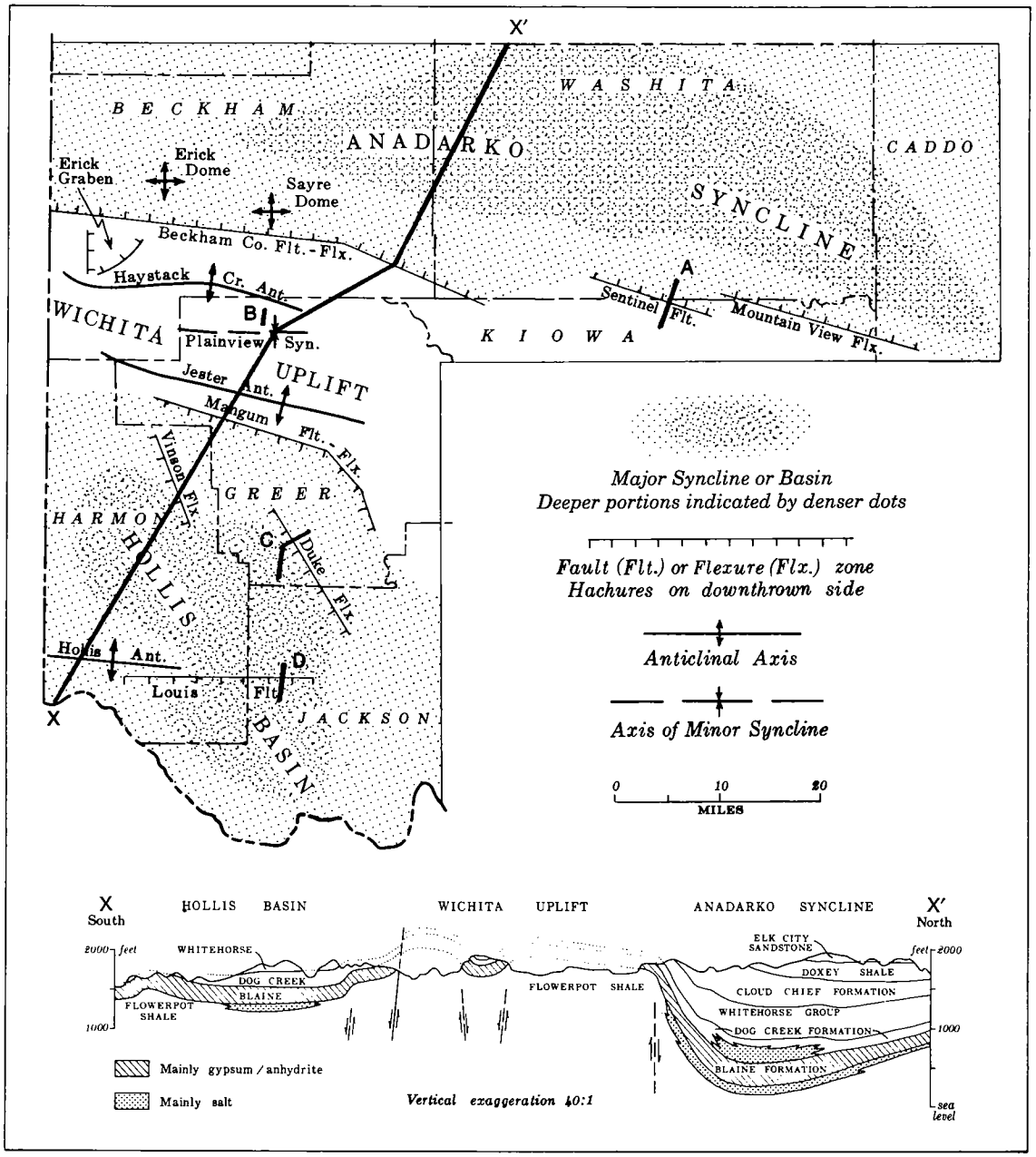


Figure 1. Map and cross section (X–X') showing surface and shallow-subsurface structural features in Permian strata of southwestern Oklahoma. Cross sections A, B, C, and D are shown in Figures 2, 3, 4, and 5, respectively.

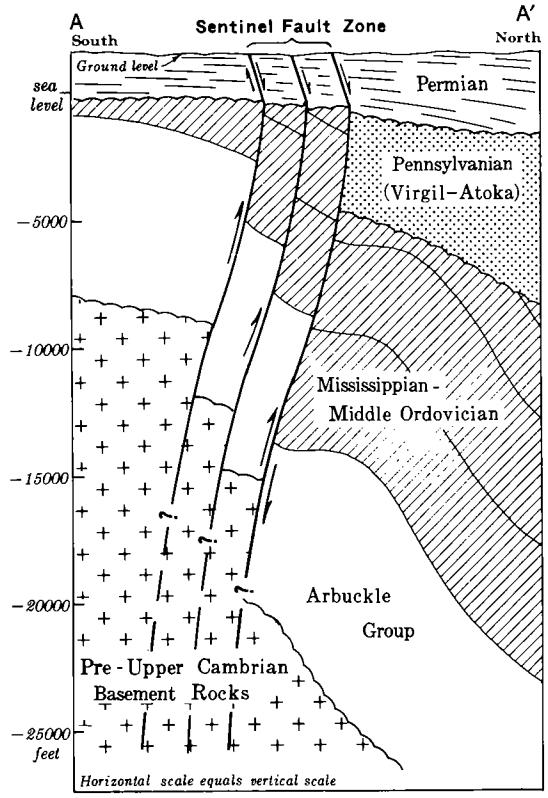


Figure 2. Schematic cross section A showing relation of the Sentinel fault zone to the deep-seated Mountain View fault zone that separates the Wichita uplift (south) from the Anadarko basin (north). Subsurface data from Harlton (1963).

The north Plainview flexure is the surface expression of a normal fault that extends down into granitic basement rock (Fig. 3). The O. P. Russel no. 1 Falkner, located 800 ft south of the surface flexure, was drilled through the fault plane between 1,625 and 1,885 ft below ground level, while drilling in the lower Wellington anhydrite (Blazenko, 1964, p. 70). Trigonometric calculations using these data show that the fault plane dips ~65° to the south. As this fault has a constant throw of ~150 ft from the surface down to a depth of ~1,700 ft, there is little doubt that it also cuts basement rock, which is but several hundred feet below the Wellington. The sharpness of rock failure decreases upward; what is undoubtedly a deep-seated fault passes upward into a flexure. Presumably the south Plainview flexure is also the surface expression of a normal fault originating in basement rock, and the two normal faults therefore bound a graben.

Faulting of sedimentary rocks beneath the flanks of the Plainview syncline occurred entirely after deposition of the outcropping Blaine Formation and overlying Dog Creek Shale, for those formations are the youngest units affected; also, the vertical displacement across the fault is the same at the surface as it is near the base of the sedimentary-rock column. However, the faults may overlie zones of weakness where pre-Permian basement-rock faults were reactivated after being dormant during Permian deposition. Clearly, the surface structure results from tectonics, and not differential compaction.

DUKE FLEXURE ZONE

The Duke flexure zone is a 16-mi-long zone comprising two flexures and one fault, en echelon, all of which are downthrown to the west-southwest (Fig. 1) (Havens, 1977). Beds are displaced vertically as much as 250 ft across the 1- to 2-mi-wide zone, and they dip as steeply as 40° where arched over the monoclinal folds. The Duke flexure zone separates a broad platform on the northeast from the Hollis basin's principal low area several miles to the southwest.

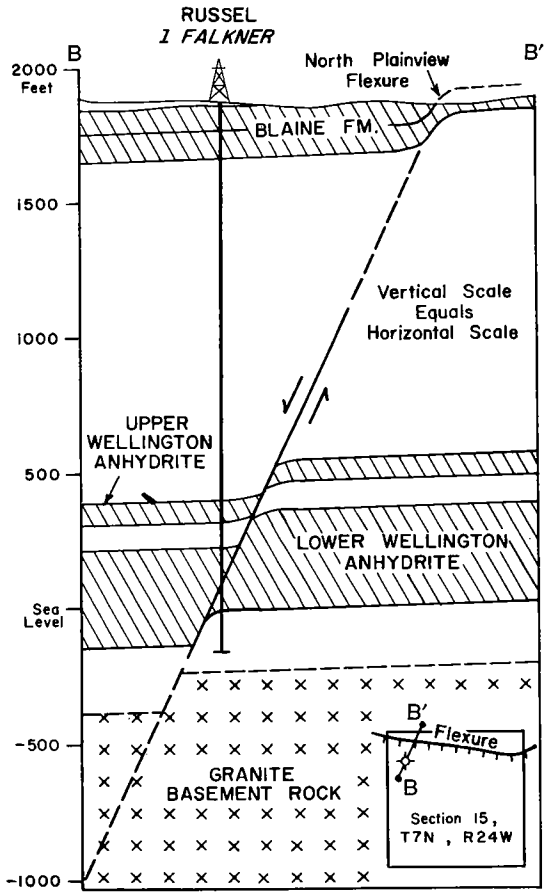


Figure 3. Cross section B showing the north Plainview flexure to be the surface expression of a deep-seated normal fault.

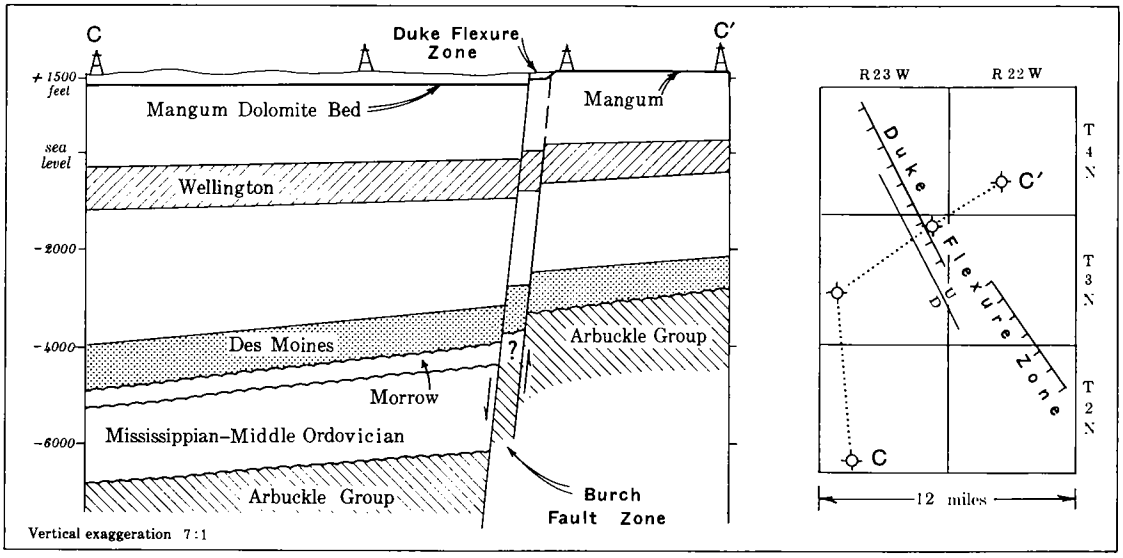


Figure 4. Schematic cross section C showing relation of the Duke flexure zone to the deep-seated Burch fault zone on the east side of the Hollis basin. Subsurface data from Sears (1951, fig. V).

Flexures and the fault in the Duke flexure zone are surface expressions of deep-seated faults along the Burch fault zone (Fig. 4) in the vicinity of the NE Duke oil field. In all probability the surface flexures pass downward into faults where the beds are definitely ruptured. Major movement along the Burch fault zone during Early and Middle Pennsylvanian time produced a minimum throw of 2,000 ft, and a thick sequence of Ordovician through Lower Pennsylvanian strata was eroded from the upthrown block (Sears, 1951; Jordan, 1962) before deposition of Middle Pennsylvanian (Desmoinesian/Strawn) beds. Slight adjustments along this zone of crustal weakness persisted for some time after the Blaine Formation was deposited, and these adjustments caused beds now at the surface to be flexed and ruptured. Some vertical displacement of the Blaine probably resulted from differential compaction of underlying strata on either side of the deep-seated faults, but such displacement is believed small compared to the throw that probably was induced tectonically.

LOUIS FAULT ZONE

The Louis fault zone is a major east-trending fault zone located on the south flank of the Hollis anticline in the Hollis basin. It is 2–3 mi wide, overlies a zone of Pennsylvanian structural weakness, and extends 20 mi across parts of Harmon and Jackson Counties (Fig. 1) (Havens, 1977). The fault zone consists of eight main faults and two minor faults, all presumably normal. Individual faults are 2–8 mi long and have throws of 20–100 ft.

Surface faults in the eastern half of the fault zone are 2–5 mi long (Havens, 1977) and bound a horst raised 20–40 ft above adjacent parts of the basin (Fig. 5). They strike east, are 1–2 mi apart, and are downthrown away from the higher central block. The horst is in a direct line with the east-plunging Hollis anticline, which is located farther west (Fig. 1). Laing (1964) showed seismic evidence of a major horst affecting lower and middle Paleozoic rocks in the SW Duke oil field, directly beneath the surface-mapped horst. His subsurface data provide an excellent example of the coincidence of surface and deep-seated structures (Fig. 5). Major uplift of the deep-seated horst resulted from post-Morrowan and pre-Desmoinesian normal faulting. Following probable intermittent movement during Late Pennsylvanian and Early Permian time, the horst was again slightly raised after deposition of Blaine and Dog Creek strata; rock failure was along those zones of weakness that had yielded earlier.

SUMMARY

Surface faults and flexures, with vertical displacements of 20–150 ft, overlie similar deep-seated structures with several thousand feet of relief. Pennsylvanian orogenies caused most of the relief of the subsurface structures, but gentler vertical movements during or after Late Permian (Blaine Formation) deposition induced still more structural relief and caused minor deformation of outcropping strata. This tectonic history is known to be true for the major structural provinces (Wichita uplift and the Anadarko and Hollis basins), as well as for many smaller structures where subsurface data are available. Deep-seated structures other than those overlain by surface folds and faults must also exist, but their presence would not be indicated if the

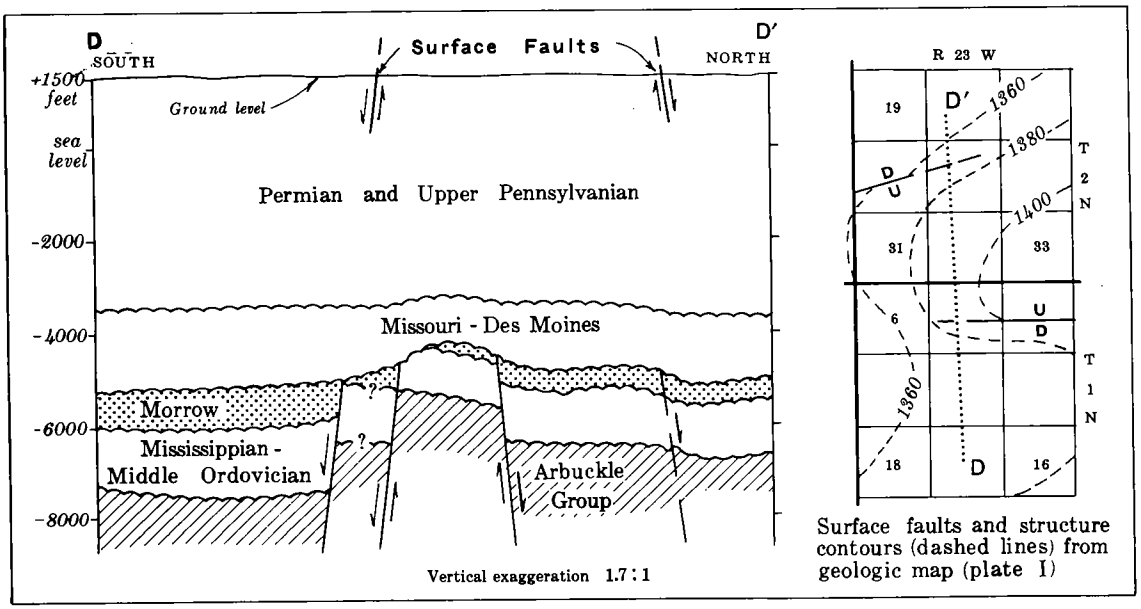


Figure 5. Schematic cross section D over the east part of the Louis fault zone showing relation of surface structure to a deep-seated horst in the SW Duke field. Surface structure contours on the outcropping Blaine Formation. Subsurface data from Laing (1964, fig. 11).

structure has been inactive since deposition of outcropping rocks.

Considering the data available on geology of southwestern Oklahoma, it is impossible to imagine any large surface structure that dies out at depth and is not underlain by a somewhat-similar structure in underlying Paleozoic and basement rocks (except where underlying Permian salts have been dissolved to produce dissolution/collapse structures in overlying strata). The veneer of Permian sedimentary layers responded passively to forces deeper in the crust and mantle. Stresses were mostly vertical, for block faulting and broad folding are the only results observed, and at no place is there evidence of horizontal compression affecting the Blaine Formation. Structures in these strata resulted from a combination of tectonic adjustments and differential compaction of underlying sedimentary units. Tectonic adjustments consisted of minor late-orogenic pulses, or slight renewed movement, along zones of earlier crustal weakness; the displacement across faults decreases upward, and some of the faults grade upward into monoclinal flexures. Differential compaction of sedimentary layers on either side of deep-seated faults probably caused some of the vertical displacement across surface structures. The age of surface structures is uncertain. Faulting and folding certainly occurred after outcropping Permian rocks were deposited, but how long after is unknown, inasmuch as younger strata do not overlie these structures.

REFERENCES CITED

Blazenko, E. J., 1964, Geology of the South Erick gas area, Beckham and Greer Counties, Oklahoma: Oklahoma City Geological Society, Shale Shaker, v. 15, p. 53–78.

Carr, J. E.; and Bergman, D. L., 1976, Reconnaissance of the water resources of the Clinton Quadrangle, west-central Oklahoma: Oklahoma Geological Survey Hydrologic Atlas 5, 4 sheets, scale 1:250,000.

Ham, W. E.; Denison, R. E.; and Merritt, C. A., 1964, Basement rocks and structural evolution of southern Oklahoma: Oklahoma Geological Survey Bulletin 95, 302 p.

Harlton, B. H., 1963, Frontal Wichita fault system of southwestern Oklahoma: American Association of Petroleum Geologists Bulletin, v. 47, p. 1552–1580.

Havens, J. S., 1977, Reconnaissance of the water resources of the Lawton Quadrangle, southwestern Oklahoma: Oklahoma Geological Survey Hydrologic Atlas 6, 4 sheets, scale 1:250,000.

Jordan, Louise, 1962, Geologic map and section of pre-Pennsylvanian rocks in Oklahoma, showing surface and subsurface distribution: Oklahoma Geological Survey Map GM-5, scale 1:750,000.

Laing, W. E., 1964, Southwestern Oklahoma—a geophysical case history of a basin: Geophysics, v. 29, p. 968–984.

Sears, J. M., 1951, The Hollis basin, southwestern Oklahoma: Oklahoma City Geological Society, Shale Shaker, v. 2, p. 4–16.

Imaging of Basement-Block Configuration in the Wichita Mountain Frontal Zone

Roger A. Young
University of Oklahoma
Norman, Oklahoma

ABSTRACT.—The Wichita Mountain Frontal Zone lies between the Anadarko basin and the Wichita uplift in southern Oklahoma. It is characterized by a complex style of basement deformation inherited from multiple episodes of tectonism. Rifting of the southern Oklahoma aulacogen in the Early Cambrian established the basement-block boundaries which were the locus of movement during compression in the Pennsylvanian. This accordion action generated a history of relative block movements.

A measure of these basement movements can be read from the surface geology, but it is primarily the geophysical signatures of the blocks themselves that have established the current picture of basement configuration. This paper compares the seismic appearance of major basement features as seen on three reflection surveys from the 1980s, and provides a framework for further analysis. The principal geological target was different for each survey, and acquisition and processing were designed accordingly. As a result, major features have somewhat different signatures on different surveys.

COCORP LINE 2A AND 5/5A, 1981

The COCORP surveys of the early 1980s focused on the regional structure of the southern Oklahoma aulacogen, particularly the nature of the boundaries between the Wichita uplift and the Anadarko and Hardeman basins (Fig. 1) (Brewer and others, 1983). The former boundary consists of several faults, the principal ones being the Mountain View fault and the Meers fault which bracket the Wichita Mountain frontal zone (Fig. 1).

Acquisition of the COCORP data employed a large seismic-array aperture of 10.05 km that insured wide-angle reflections would image the major faults of the frontal zone. A reverberatory train of reflections on line 2A extends to 5 s (seconds) traveltime, and is interpreted to dip 30–40° southward. This feature was identified as the trace of the Mountain View fault by Brewer and others (1983). The trace of the Mountain View fault was also identified on line 5/5A (Brewer and others, 1983). Taken together, these traces (small, straight arrows in Fig. 1) fix the location of the Mountain View fault. A second band of reflections on line 2A between 0.5–1.5 s dips northward from a point just north of the Meers fault (curved arrow, Fig. 1) and was interpreted by Brewer and others (1983) to be a listric thrust fault above the Chester (Mississippian) horizon. Strong reflections from the deep Anadarko basin appear at 3–4 s and possible indications of sedimentary layering beneath the hanging wall of the Mountain View fault are seen at 5–6 s. A detailed picture of the frontal zone is not possible due to the large group spacing (~0.1 km) and the low sweep frequency (8–40 Hz). Moreover, line 2A was shot at an angle of ~30° to the direction of dip of the frontal zone; consequently, reflections from the side obscure the image directly beneath the line.

UNIVERSITY OF TEXAS LINE, 1985

A very large aperture of 90 km (Fig. 1) was employed in 1985 by the University of Texas at Dallas and El Paso (UTD/UTEP) to examine the crustal and upper-mantle structure beneath the Wichita uplift and the Anadarko basin (Chang and others, 1989). The survey was designed to acquire very wide-angle to normal-incidence reflections as well as refractions. Two fixed-receiver spreads, each 45-km long, were combined into a single-shot supergather. Prestack migration reveals a possible upper-mantle reflector (Chang and others, 1989), but resolution of crustal features, such as the faults identified on the COCORP data, is difficult due to the small number of shots acquired. However, modeling traveltimes of principal refractions and reflections (Hsueh, 1991) produced a layered crustal model of considerable complexity. Reflections from

Young, R. A., 1995, Imaging of basement-block configuration in the Wichita Mountain frontal zone, *in* Johnson, K. S. (ed.), Structural styles in the southern Midcontinent, 1992 symposium: Oklahoma Geological Survey Circular 97, p. 293–296.

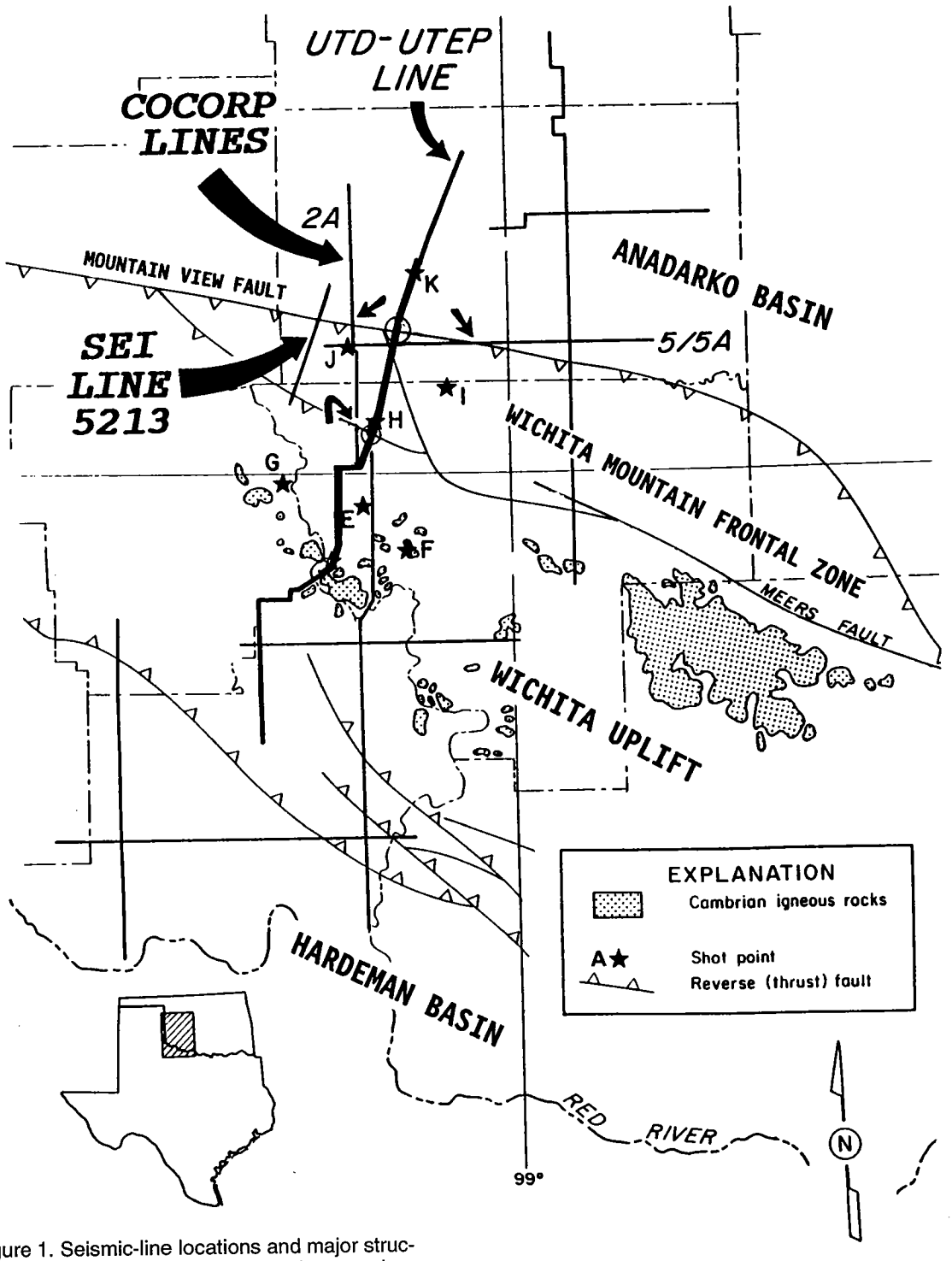


Figure 1. Seismic-line locations and major structural features in the southern Oklahoma aulacogen. UTD–UTEP line is bold; SEI line 5213 and COCORP lines 2A and 5/5A are labeled. All other seismic lines are COCORP lines. Small arrows and circles locate intersections of seismic lines with major faults (see text for explanation). (After Chang and others, 1989.)

the Mountain View fault itself—seen on the COCORP lines—were not identified by Hsueh on the University of Texas data.

By reviewing broadside shot records recorded in the middle of the aperture (shots F, G, I, and J, Fig. 1), and end-on shots recorded on the northern half of the aperture (shots E and H, Fig. 1), I have identified a strong band of reflections in the UTD/UTEP data which dip southward and correspond to the trace of the Mountain View fault on COCORP line 2A. This band extrapolated to the surface (large open circle, Fig. 1) is very close to the subcrop location of the Mountain View fault given by Ham and others (1964). In addition, this Mountain View fault location lies between the corresponding fault locations on COCORP lines 2A and 5/5A (small, straight arrows, Fig. 1). The UTD/UTEP data also show a band of reflections corresponding to the feature identified by Brewer and others (1983) as a listric thrust fault above the Chester. Surface projections of this feature from the COCORP line (curved arrow, Fig. 1) and the UTD/UTEP line (small open circle, Fig. 1) are very close to each other.

SEISMIC EXCHANGE, INC., 1989

The most recent dataset examined focuses on the structure of the frontal zone itself. The Wichita Mountain Front Project of Seismic Exchange, Inc. (SEI) consists, in part, of some three dozen short, 2-D lines across the frontal zone between Lawton and the Oklahoma/Texas border. These lines were shot parallel to local dip by examining gravity and magnetic maps which reveal approximate positions of block boundaries (Schneider, 1991). Line SEI 5213 lies several miles west of, and roughly parallel to, COCORP line 2A (Fig. 1).

Line SEI 5213 was shot with a small group spacing (0.0167 km), high sweep frequency and large bandwidth (8–72 Hz), and high fold (240, nominal), all of which contribute to much higher resolution in the first 3 seconds than on COCORP line 2A. Several processed versions of SEI 5213 have been released by SEI: final stack, DMO final stack, DMO migration, and a prestack migration. The trace of the Mountain View fault is not a prominent feature of SEI line 5213, in contrast to its prominence on COCORP line 2A. However, it is apparent down to ~2.3 s and appears to have much the same dip as on COCORP line 2A. The weakness of this event downdip can be attributed to the smaller acquisition aperture of the SEI survey, which was needed to enhance shallower features.

Considerably more layering detail beneath the Mountain View fault is seen on SEI 5213 than on COCORP line 2A. In addition, the north-dipping band on COCORP line 2A, identified as a listric fault above the Chester horizon, is very strong on SEI 5213 and can be traced down to 0.4 s, where it overlies crystalline basement. However, the high-amplitude, multicycle nature of this event suggests that it is a reverberation within Lower Pennsylvanian units rather than a reflection from a listric fault.

There are three principal reasons for the greater detail in the SEI data compared to the COCORP data. (1) Higher dominant frequency in the SEI data than in the COCORP data yields greater resolution between events. (2) Diffracted energy is imaged by SEI, but not by COCORP. Diffractions reside principally in the high frequencies and are, therefore, quite noticeable on the SEI stacked section. Diffraction energy interferes with reflection images, but the strongest diffractions help locate small faults bounding basement blocks beneath the Paleozoic sediments. The processing step of migration—which collapses diffractions to a point on the fault—produces sharp images of these small faults. The COCORP line 2A, on the other hand, used a lower-frequency source, lost high frequencies to receiver array attenuation, and was processed to emphasize crustal features beneath the small faults. (3) By shooting perpendicular to local strike, the SEI data record fewer reflections from outside the recording plane.

The SEI line 5213 presents an excellent opportunity to clarify the small-scale basement-block configuration within the Wichita Mountain frontal zone. Preliminary analysis at the University of Oklahoma finds basement faults dipping both north and south, and fault displacement of overlying strata as young as Pennsylvanian. One subsidiary fault—which crops out ~1 mi south of the Mountain View fault subcrop location—displays relative motion that is up on the Anadarko basin (north) side. This same sense of motion (up on the north) has also been observed in Holocene strata along the outcrop trace of the Meers fault (Crone and Luza, 1990).

Future investigation at the University of Oklahoma of these exciting new data will feature interpretation of a number of adjacent dip lines using interactive workstation software to determine a tectonic history consistent with a three-dimensional picture of the basement configuration.

ACKNOWLEDGMENTS

The author is grateful to Seismic Exchange, Inc., for permission to use SEI line 5213, and to Mr. James Booher for his assistance in obtaining the data. Dr. G. R. Keller kindly provided unpublished thesis material.

REFERENCES CITED

Brewer, J. A.; Good, R.; Oliver, J. E.; Brown, L. D.; and Kaufman, S., 1983, COCORP profiling across the southern Oklahoma aulacogen: overthrusting of the Wichita Mountains and compression within the Anadarko basin: Geology, v. 11, p. 109–114.

Chang, Wen-fong; McMechan, G.; and Keller, G. R., 1989, Wave field processing of data from a large-aperture seismic experiment in southwestern Okla-

homa: Journal of Geophysical Research, v. 94, p. 1803–1816.

Crone, A. J.; and Luza, K. V., 1990, Style and timing of Holocene surface faulting on the Meers fault, southwestern Oklahoma: Geological Society of America Bulletin, v. 102, p. 1–17.

Ham, W. E.; Denison, R. E.; and Merritt, C. A., 1964, Basement rocks and structural evolution of southern Oklahoma: Oklahoma Geological Survey Bulletin 95, 302 p.

Hsueh, Fu-Jen, 1991, Application of ray trace modeling to a large scale seismic experiment in Oklahoma: University of Texas, El Paso, unpublished M.S. thesis, 55 p.

Schneider, R. E., 1991, Exploring the Wichita Mountain front—with new parameters: Proceedings of the Continuing Education Program, Geophysical Society of Oklahoma City, February, p. 1–22.

Structure, Timing, and Tectonic Interpretation of Ancestral Rocky Mountain Deformation within Central New Mexico

William C. Beck and Charles E. Chapin
New Mexico Bureau of Mines and Mineral Resources
Socorro, New Mexico

On the basis of stratigraphic relationships, Kottlowski (1960), Kottlowski and Stewart (1970), Baars (1982), and Siemers (1983) have interpreted the modern-day Joyita Hills (Fig. 1, north-central Socorro County, New Mexico) as the location of a late Paleozoic, north-trending positive element (the Joyita uplift). Detailed geologic mapping and structural analysis of the Joyita Hills (Beck and Chapin, 1991) indicate two normal-fault trends were active during ancestral Rocky Mountain (late Paleozoic) tectonism. Restoration (accomplished by removing regional dip, determined from all post-ancestral Rocky Mountain strata) defines the faults as north-striking, west-dipping normal faults (Fig. 2A), and northwest-striking, southwest-dipping normal faults (Fig. 2B). These fault trends bound the Joyita uplift on the west and south, respectively, and define the uplift as a north-trending structural element. Restored fault striae indicate that fault displacements were predominantly dip slip. However, north-striking normal faults show a component of left slip (striae rake ~63° southward).

Faults in both sets were reactivated during younger deformation, with the exception of one of the north-striking faults (Fig. 3). Arkosic clastics of the syntectonic Bursum Formation (Permian) are anomalously thick and coarse grained in the hanging wall of this fault, and were apparently deposited along the exposed fault scarp. In the footwall, Madera (Pennsylvanian) and Bursum (Permian) strata are thin. The Madera is thin due to erosion and the Bursum is thin due to nondeposition and/or erosion. Both the fault and offset strata are overlain by anomalously thin, unfaulted strata of the Abo Formation (Permian), which thickens to both the east and west. This fault is interpreted to be a buried ancestral

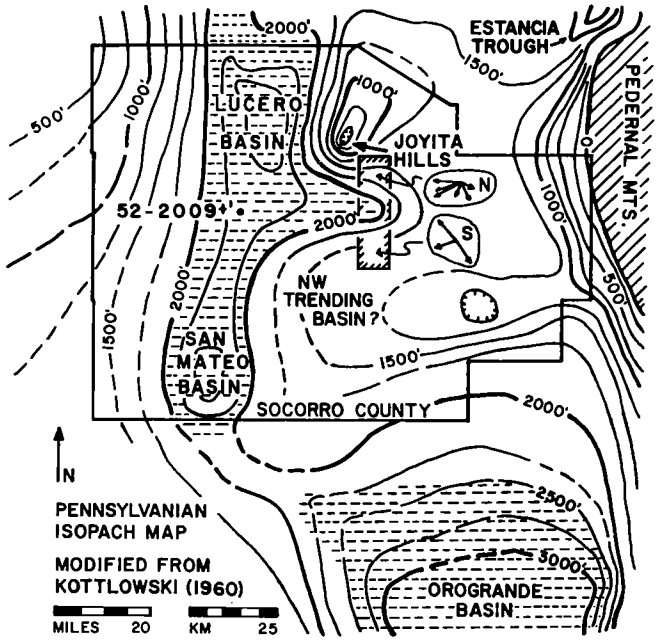


Figure 1. Modified Pennsylvanian isopach map superimposed with early Wolfcampian paleocurrent directions from Altares (1990). Hachured box (in middle) outlines the location of Altares' (1990) field area. Paleocurrent directions (vector means), labeled N and S, are from the north and south parts of Altares' field area; length of each vector is proportional to vector magnitude. Drill-core data (Krewedl, 1974; Chapin, unpublished core log; control point number 52, Kottlowski, 1960) documents stratigraphic thickness of Pennsylvanian rocks to be >2,000 ft at location labeled 52-2009+, and indicates that the Lucero and San Mateo basins are one continuous, north-trending basin.

Beck, W. C.; and Chapin, C. E., 1995, Structure, timing, and tectonic interpretation of ancestral Rocky Mountain deformation within central New Mexico, *in* Johnson, K. S. (ed.), Structural styles in the southern Midcontinent, 1992 symposium: Oklahoma Geological Survey Circular 97, p. 297–300.

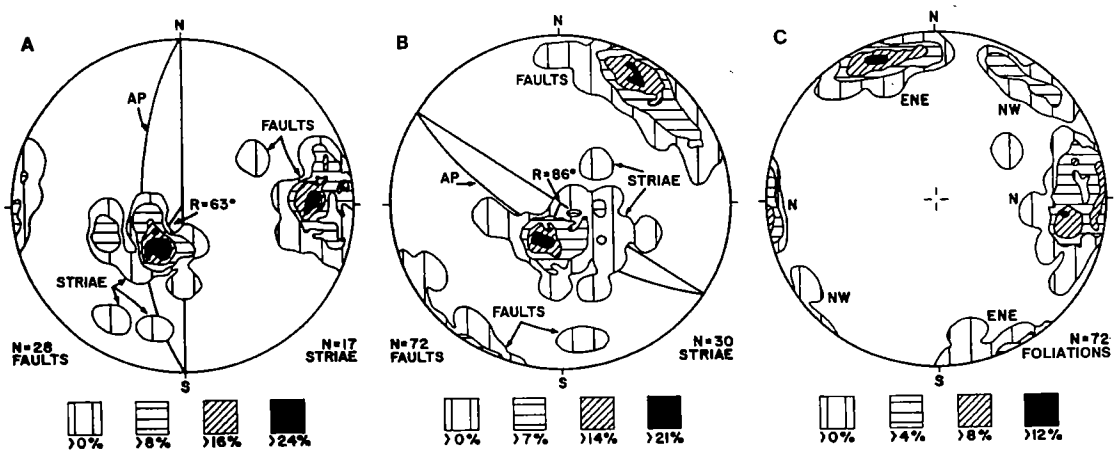


Figure 2. Structural data from the Joyita Hills. Lower-hemisphere, equal-area projections of composite poles to fault planes and fault striae (A and B) and poles to foliations (C), contoured at specified intervals per 1% area. AP = average fault plane; R = approximate angle of rake of fault striae. *A*—North-striking ancestral Rocky Mountain normal faults and contained striae. *B*—Northwest-striking ancestral Rocky Mountain normal faults and contained striae. *C*—Proterozoic, gneissic to mylonitic foliations, which strike north (N), east–northeast (ENE), and northwest (NW).

Rocky Mountain fault that has not been reactivated.

Analysis of basement fabrics within the Proterozoic core of the Joyita Hills reveals three preferred orientations (ENE, N, and NW) of gneissic to mylonitic foliations (Fig. 2C). Two of these orientations (N and NW) are comparable to orientations of the late Paleozoic faults (Fig. 2A,B). Direct field observation shows that north-striking mylonites and foliations have been reactivated by the younger, north-striking brittle faults (Fig. 3). The comparable orientation of both northwest-striking foliations (Fig. 2C) and brittle faults (Fig. 2B) is also thought to represent reactivation, although evidence for this has not yet been observed in the field.

The Pennsylvanian isopach map and paleocurrent data reflect the influence of the foregoing fault trends and help delineate uplift margins (Fig. 1). A mineral-exploration hole midway between the San Mateo and Lucero basins (Fig. 1) cored 2,009 ft of Pennsylvanian strata (Krewedl, 1974; Chapin, unpublished core log). This indicates that the San Mateo and Lucero basins were parts of one continuous, north-trending basin. An arm extending southeastward from the modified San Mateo/Lucero basin bounds the Joyita uplift on the south and southwest. Paleocurrent data from early Wolfcampian Bursum strata (Altares, 1990), superimposed on the Pennsylvanian isopach map, indicate that the southeast-trending arm of the San Mateo/Lucero basin may have been more extensive than originally defined by Kottlowski (1960) (Fig. 1). Altares' (1990) field area spans the north–south dimension of the arm. Paleocurrent data north of the arm indicate paleoflow directions to the west, southwest and south; i.e., basinward with respect to the arm. Paleocurrent data south of the arm, however, also show paleoflow directions to the west, southwest, and

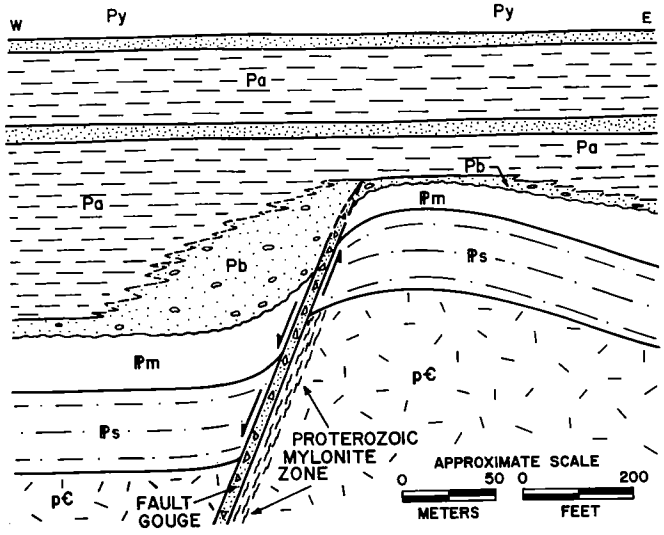


Figure 3. Generalized cross section across a north-striking, ancestral Rocky Mountain normal fault that has not been reactivated. Cross section has been restored to its post-ancestral Rocky Mountain orientation by removing 30° of down-to-the-west rotation about a N35°E horizontal axis (net rotation from younger deformation). Py = Yeso; Pa = Abo; Pb = Bursum; IPm = Madera; IPs = Sandia; p€ = Proterozoic basement. Fault and contacts dashed where obscured.

south, indicating that the axis of the arm lay farther to the southwest. Isopachs between the San Mateo/Lucero basin and the Orogrande basin to the southeast are poorly defined, due to a paucity of control points. However, the combination of the southeast-trending arm of the San Mateo/Lucero basin, paleoflow directions to the west, southwest, and south, and a southeast-trending trough between the southern end of the San Mateo/Lucero basin and the northern end of the Orogrande basin, suggests that the two basins were connected during the late Paleozoic.

The late Paleozoic structures associated with the Joyita uplift are comparable, in both orientation and

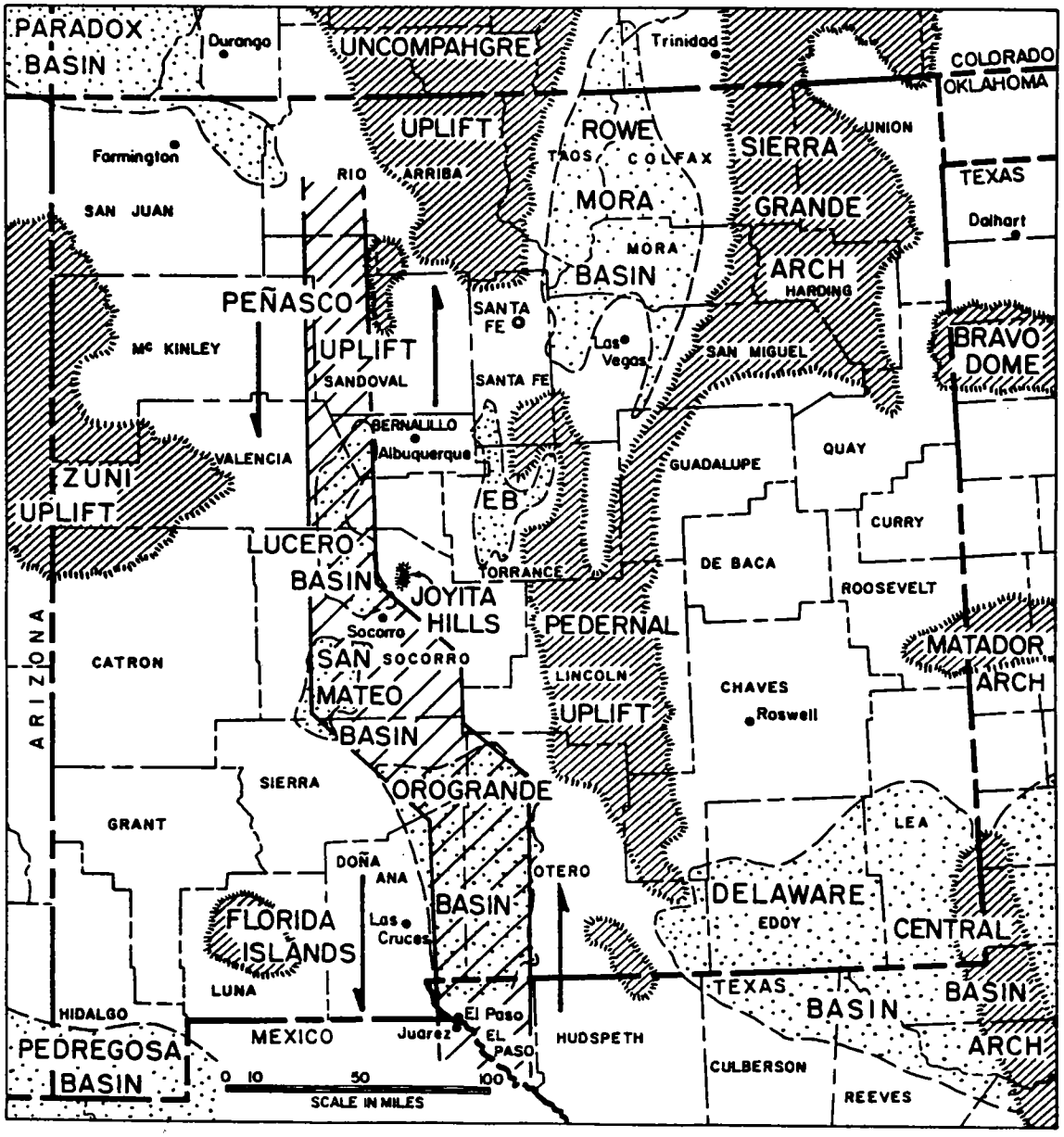


Figure 4. Pennsylvanian paleogeographic map (from Kottlowski and Stewart, 1970) with inferred late Paleozoic, north-trending, left-lateral wrench zone (diagonal lines) in central and southern New Mexico superimposed. The Sierra Nacimiento area is coincident with the Peñasco uplift of Kottlowski and Stewart (1970). North-trending basins (San Mateo/Lucero and Orogrande basins) developed within principal zones of left-lateral shear. The inferred northwest-trending basin connecting the southern end of the San Mateo/Lucero basin and the northern end of the Orogrande basin is envisaged as a rhomb-graben at the stepover between two left-lateral, left-stepping, shear zones.

sense of offset, to those associated with late Paleozoic uplifts to the north (Sierra Nacimiento; Baars, 1982) and the south (Sacramento Mountains; Pray, 1961). In addition, deformation within these three areas was approximately synchronous: new fusulinid data (*Schwagerina* and *Triticites* fauna; identifications courtesy of D. A. Myers, personal communication, 1990,1991) from the syntectonic Bursum Formation date the dominant phase of deformation within the Joyita uplift as early Wolfcampian. Baars (1982) documented several episodes of displacement along the Nacimiento fault during ancestral Rocky Mountain deformation. The latest occurred after Madera deposition and before Abo deposition. Pray (1961) also concluded that ancestral Rocky Mountain deformation within the Sacramento Mountains was Late Pennsylvanian to early Wolfcampian. The comparable structural styles and nearly synchronous timing of deformation indicates that, during ancestral Rocky Mountain tectonism, a large area of the crust in New Mexico experienced a similar deformational history. The San Mateo/Lucero and Orogrande basins are aligned in a north-trending, left-stepping en-echelon pattern. The two basins were probably connected by a southeast-trending "channel" at the stepover. Bounding structures are high-angle to vertical normal faults, with north-striking faults showing a component of left slip (Fig. 2). Geometric and kinematic analyses, when integrated with isopach, paleocurrent, and biostratigraphic data, indicate that a north-trending, divergent, left-lateral wrench zone was active in central New Mexico during the late Paleozoic (Fig. 4).

REFERENCES CITED

Altares, T., III, 1990, Stratigraphic description and paleoenvironments of the Bursum Formation, Socorro County, New Mexico: New Mexico Institute of Mining and Technology unpublished M.S. thesis, 189 p.

Baars, D. L., 1982, Paleozoic history of the Albuquerque trough: implications of basement control on Rio Grande rift: New Mexico Geological Society Guidebook 33, p. 153–157.

Beck, W. C.; and Chapin, C. E., 1991, Structural data from the Joyita uplift: implications for ancestral Rocky Mountain deformation within central and southern New Mexico: New Mexico Geological Society Guidebook 42, p. 183–190.

Kottlowski, F. E., 1960, Summary of Pennsylvanian sections in southwestern New Mexico and southeastern Arizona: New Mexico Bureau of Mines and Mineral Resources Bulletin 66, 187 p.

Kottlowski, F. E.; and Stewart, W. J., 1970, The Wolfcampian Joyita uplift in central New Mexico: New Mexico Bureau of Mines and Mineral Resources Memoir 23, Part I, 31 p.

Krewedl, D. A., 1974, Geology of the central Magdalena Mountains, Socorro County, New Mexico: University of Arizona unpublished Ph.D. dissertation 128 p.

Pray, L. C., 1961, Geology of the Sacramento Mountains escarpment, Otero County, New Mexico: New Mexico Bureau of Mines and Mineral Resources Bulletin 35, 144 p.

Siemers, W. T., 1983, The Pennsylvanian system, Socorro region, New Mexico: stratigraphy, petrology, depositional environments: New Mexico Geological Society Guidebook 34, p. 147–155.